Food Engineering Series

Series Editor: Gustavo V. Barbosa-Cánovas

Helen S. Joyner *Editor*

Rheology of Semisolid Foods

Springer

Food Engineering Series

Springer's *Food Engineering Series* is essential to the Food Engineering profession, providing exceptional texts in areas that are necessary for the understanding and development of this constantly evolving discipline. The titles are primarily reference-oriented, targeted to a wide audience including food, mechanical, chemical, and electrical engineers, as well as food scientists and technologists working in the food industry, academia, regulatory industry, or in the design of food manufacturing plants or specialized equipment.

More information about this series at http://www.springer.com/series/5996

Helen S. Joyner
Editor

Rheology of Semisolid Foods

Springer

Editor
Helen S. Joyner
School of Food Science
University of Idaho
Moscow, ID, USA

ISSN 1571-0297
Food Engineering Series
ISBN 978-3-030-27133-6 ISBN 978-3-030-27134-3 (eBook)
https://doi.org/10.1007/978-3-030-27134-3

© Springer Nature Switzerland AG 2019
This work is subject to copyright. All rights are reserved by the Publisher, whether the whole or part of the material is concerned, specifically the rights of translation, reprinting, reuse of illustrations, recitation, broadcasting, reproduction on microfilms or in any other physical way, and transmission or information storage and retrieval, electronic adaptation, computer software, or by similar or dissimilar methodology now known or hereafter developed.
The use of general descriptive names, registered names, trademarks, service marks, etc. in this publication does not imply, even in the absence of a specific statement, that such names are exempt from the relevant protective laws and regulations and therefore free for general use.
The publisher, the authors, and the editors are safe to assume that the advice and information in this book are believed to be true and accurate at the date of publication. Neither the publisher nor the authors or the editors give a warranty, express or implied, with respect to the material contained herein or for any errors or omissions that may have been made. The publisher remains neutral with regard to jurisdictional claims in published maps and institutional affiliations.

This Springer imprint is published by the registered company Springer Nature Switzerland AG
The registered company address is: Gewerbestrasse 11, 6330 Cham, Switzerland

Contents

Part I Semisolid Food Rheology

Introduction: Measuring Rheological Properties of Foods 3
Haotian Zheng

Overview: Semisolid Foods 31
Juzhong Tan

Rheological Testing for Semisolid Foods: Traditional Rheometry 63
Judith K. Whaley, Catherine Templeton, and Mohammad Anvari

LAOS (Large Amplitude Oscillatory Shear) Applications for Semisolid Foods 97
Gamze Yazar, Ozlem Caglar Duvarci, Merve Yildirim Erturk, and Jozef L. Kokini

Semisolid Food Tribology 133
Helen S. Joyner

Structuring Semisolid Foods 167
Juzhong Tan

Rheological Properties of Yogurt: Effects of Ingredients, Processing and Handling 203
Stephanie Clark, Minto Michael, and Karen A. Schmidt

Sensory and Oral Processing of Semisolid Foods 231
Tugba Aktar, Rituja Upadhyay, and Jianshe Chen

Relationships Among Semisolid Food Microstructures, Rheological Behaviors, and Sensory Attributes 249
Mitchell Culler

Part II Case Studies

The Impact of Formulation on the Rheological, Tribological, and Microstructural Properties of Acid Milk Gels 275
Maryam Baniasadidehkordi and Helen S. Joyner

Relationships Among Acid Milk Gel Sensory, Rheological, and Tribological Behaviors 323
Maryam Baniasadidehkordi and Helen S. Joyner

Using Human Whole Saliva to Better Understand the Influences of Yogurt Rheological and Tribological Behaviors on Their Sensory Texture 349
Maryam Baniasadidehkordi and Helen S. Joyner

Index 399

Contributors

Tugba Aktar Faculty of Engineering, Food Engineering Department, Alanya Alaaddin Keykubat University, Antalya, Turkey

Mohammad Anvari Tate & Lyle, PLC, Hoffman Estates, IL, USA

Maryam Baniasadidehkordi School of Food Science, University of Idaho, Moscow, ID, USA

Jianshe Chen Food Oral Processing Laboratory, School of Food Science and Biotechnology, Zhejiang Gongshang University, Hangzhou, People's Republic of China

Stephanie Clark Department of Food Science and Human Nutrition, Iowa State University, Ames, IA, USA

Mitchell Culler University of Massachusetts, Amherst, MA, USA

Ozlem Caglar Duvarci Food Science Department, Purdue University, West Lafayette, IN, USA

Department of Chemical Engineering, Izmir Institute of Technology, Izmir, Turkey

Helen S. Joyner School of Food Science, University of Idaho, Moscow, ID, USA

Jozef L. Kokini Food Science Department, Purdue University, West Lafayette, IN, USA

Minto Michael School of Food Science, Washington State University, Pullman, WA, USA

Karen A. Schmidt Food Science Institute, Kansas State University, Manhattan, KS, USA

Juzhong Tan Department of Food Science, Rutgers, The State University of New Jersey, New Brunswick, NJ, USA

Catherine Templeton Tate & Lyle, PLC, Hoffman Estates, IL, USA

Rituja Upadhyay Food Oral Processing Laboratory, School of Food Science and Biotechnology, Zhejiang Gongshang University, Hangzhou, People's Republic of China

Judith K. Whaley Tate & Lyle, PLC, Hoffman Estates, IL, USA

Gamze Yazar Food Science Department, Purdue University, West Lafayette, IN, USA

School of Food Science, University of Idaho, Moscow, ID, USA

Merve Yildirim Erturk Food Science Department, Purdue University, West Lafayette, IN, USA

Haotian Zheng Animal Science Department, Leprino Foods Dairy Innovation Institute, California Polytechnic State University, San Luis Obispo, CA, USA

About the Editor

Helen S. Joyner is an Associate Professor at the University of Idaho in the School of Food Science. Her research focuses on rheological and tribological behavior of food products, with the goal of determining relationships between structure, mechanical/friction behavior, and sensory texture. She has over ten years of experience in evaluation of rheological and tribological behaviors of fluid, semisolid, and solid food products. Her current focus is on dairy products, although she has worked with many other products, including bread, sauces, gels, and emulsions. While her lab focuses on fundamental rheology research, Dr. Joyner also works on applied research with industry, as well as provides contract testing services for a wide variety of food products.

Dr. Joyner teaches graduate and undergraduate courses in Food Engineering, Food Quality Management, Evaluation of Dairy Products, and Food Rheology. She is an active member of the Institute of Food Technologists, the American Dairy Science Association, and the Society of Rheology, and has served in multiple volunteer roles for these organizations. She is currently the faculty advisor for the Washington State University/University of Idaho/Washington State University Idaho Milk Processor's Association product development team and Collegiate Dairy Product Evaluation team.

Dr. Joyner has won multiple awards for her research and teaching, as well as for her involvement in professional societies, including the North Carolina State University CALS Outstanding Young Alumna Award, the North American Colleges and Teachers of Agriculture Teaching Award of Merit, the Journal of Texture Studies Rising Stars in Texture Award, and the Institute of Food Technologists Dairy Foods Division Outstanding Volunteer Award.

Part I

Semisolid Food Rheology

Introduction: Measuring Rheological Properties of Foods

Haotian Zheng

1 The Evolution of Rheology Through History

Rheology as a discipline has a long history that includes multiple major milestones. Understanding how the understanding of rheology and the precision and accuracy of rheological methods has evolved over time provides a framework of the scope of rheology as a specific discipline. Specifically, this historical background provides the origins of the development of major rheological theories, equations and instrumental devices used in measuring rheological properties. Some introductory level equations are introduced in the following sections of this chapter for the purpose of understanding the necessary fundamental concepts. More details are provided in the subsequent topical chapters, in which the fundamental theories and equations are explained. The milestones mentioned in this section may be considered classic examples for illustrating the methodology and research involved in rheology. Moreover, examples of applications of each milestone to the food industry are provided to allow the reader to interpret major rheological theories in terms of their use in the food industry. A more detailed history of rheology may be found in The Rheology Handbook (Mezger 2014).

Rheology is the science that describes deformation and flow behaviors of materials. Rheology models summarize the physical responses (rheological parameters) under a certain deformation stress or a flow driving force. These parameters (1) reflect processability of crude, or semi-processed or processed food materials, (2) determine physical stability (phase separation rate) of manufactured food products, and (3) describe textural properties of food materials and reveal their sensory attributes. Therefore, rheological parameters and models are essential elements in the food industry for designing processing lines, selecting operational equipment such

---

H. Zheng (✉)
Animal Science Department, Leprino Foods Dairy Innovation Institute,
California Polytechnic State University, San Luis Obispo, CA, USA
e-mail: hazheng@calpoly.edu

H. S. Joyner (ed.), *Rheology of Semisolid Foods*, Food Engineering Series,
https://doi.org/10.1007/978-3-030-27134-3_1

as flow systems and filtration membranes, predicting the physical shelf life of food products, designing formulations for achieving a targeted structure, and predicting sensory attributes.

The term “rheology” was only coined and became a dedicated subject of study in the twentieth century, although rheological research for describing material deformation and flow behaviors was conducted as early as the fifteenth century. One of the first rheological researchers, Leonardo de Vinci, illustrated accurate hydrodynamic and aerodynamic phenomena, such as the flow behavior of air under bird wings and other flying instruments in the 15th and 16th centuries. In 1687, Isaac Newton discovered the relationship between flow resistance and flow velocity; also, he hypothesized the existence of “internal friction of fluids” which is considered a basic law of fluid mechanics and hydrodynamics. In the same year, two brothers, Jacob and Johann Bernoulli defined the theory of elasticity and improved the understanding of hydrodynamic flow and efflux behavior. This theory is still used in the characterization of physical features of fluids and solids. In 1738, Johann Bernoulli’s son Daniel Bernoulli described the mathematical relationship between tubular flow behavior and flowing pressures. This relationship is known as the Bernoulli equation, which is used today for computing flow velocity of flowable food materials via flow pressure measurements, including static pressure, pressure due to gravity, and dynamic stagnation pressure. Moreover, hydrodynamic cavitation, which can be calculated using the Bernoulli equation, is considered an innovative process for food sterilization: it may induce cellular inactivation by pressure fluctuations. As the generation of cavities is flow pressure dependent, the Bernoulli equation is the key base knowledge for achieving and controlling the dedicated cavitation effects (Gogate 2011).

In 1839 and 1840, Gotthilf Hagen and Jean Poiseuille designed the first capillary viscometers for characterizing flow behaviors of water, blood, and other low-viscosity fluids. Capillary viscometers are traditional tools for characterizing fluid and semisolid materials; however, this tool has limitations for application in the modern food industry, such as the tubular pinch effect and stick-slip effect. Furthermore, it cannot used for measuring shear-sensitive food materials, as the shear rates in capillary viscometers are quite high (Rao 1977). The mathematical relationships concerning fluid flow behaviors in a capillary tube was consolidated by Gustav Wiedemann and published in 1856 as the Hagen-Poiseuille equation, relating fluid viscosity, volumetric flow rate, pressure drop, length of the tube, and radius of the cross section of the capillary tube. The Hagen-Poiseuille equation plays a critical role in food process engineering; among other uses, it has been used for modeling the permeate flux in the ultrafiltration process of skimmed milk in hollow fibers (Chiang and Cheryan 1986). It is also useful for calculating pressure drop in pipes, and thus sizing pumping equipment.

In 1851, Georges Stokes, the founder of modern concepts of flow dynamics, used “falling-ball” experiments to develop Stokes’ Law, a measure of resistance to flow under gravitational forces. In a dispersion system, Stokes’ Law models the relationship between buoyancy forces, flowing (creaming or falling) particle diameter, velocity of the flowing particle, and viscosity of the continuous phase. Particle creaming or sedimentation velocity may be computed using Stokes' Law; therefore, this law is widely used in the food industry for predicting or characterizing the physical stability of emulsion- or suspension-based food products (Maher et al. 2011; Taherian et al. 2008).

The understanding of material viscoelastic behaviors notably increased in the nineteenth century. In 1867–1868, James Maxwell presented "Maxwellian behavior" using viscoelastic liquids. This is considered the first explanation of viscous behavior displayed by solids; the model comprises a spring (elastic component) and dashpot (viscous component) in series, indicating that elastic and viscous behaviors are sequential. Maxwellian behavior in nonlinear oscillatory flow is found in gel-like food materials such as mayonnaise-like emulsions (Hemar and Horne 2000). In 1874, Oskar Meyer presented the Kelvin-Voigt model, one of the first models to summarize the viscoelastic behavior of solids. Generated from oscillatory tests, the model consists of a spring (elastic component) and dashpot (viscous component) in parallel, indicating that these elements react simultaneously to an applied torque or deformation. The Burgers model, developed in 1935, is a derivative model of both the Maxwell model and Kelvin-Voigt model. The Burgers model may be used to characterize the transient viscoelastic properties of solid foods such as cheeses and dairy foams (Karaman et al. 2016; Sharma et al. 2017; Zhao et al. 2015). In 1880, the world's first report on shear-thinning materials was presented by T. Schwedoff, in which he showed that the viscosities of castor oil and gelatin-gel solutions changed as a function of rotational speed of a concentric cylinder system. Shear-thinning flow behavior is one of the key physical features of many food products including ketchup, applesauce, and dairy foods. Accordingly, shear-dependent behavior has been extensively studied and modeled for a wide variety of food systems (Dervisoglu and Kokini 1986; Tárrega et al. 2004). In 1883, the shear-thickening effect was observed by Osborne Reynolds, who also described and discriminated laminar and turbulent flows using the dimensionless Reynolds number. Interestingly, in area of food science and technology, the Reynolds number has been traditionally used to describe flow behaviors of Newtonian and shear-thinning fluids. A specifically modified Reynolds number that properly fit the behavior of shear-thickening food materials was reported only in 2010 and used to model flow behaviors of starch paste and starch–polysaccharide complex paste systems (Ptaszek 2010). The Reynolds number can also be used in heat transfer calculations, as flow regime is a major factor in heat transfer rate. Thus, it is a critical factor in heat exchanger design (Rozzi et al. 2007); Researchers also observed that the Reynolds number affected the fouling rate of whey protein in tubular heat exchangers, likely due to the difference in flow behavior at different flow profiles (Belmar-Beiny et al. 1993).

In 1905, Albert Einstein contributed the Einstein equation in which the viscosity of suspension systems was explained as a function of the viscosity of continuous phase and the volume fraction of the containing particles. This equation opened a door for the exploration of how microstructure of suspension-based food matrices impacts their stability and functionality. A century later, a third-order expansion of the Einstein equation showed better estimation of apparent viscosity of complex food suspension containing hydrocolloid texturizer and green peas (Chakrabandhu and Singh 2005). The Einstein equation may be also used as tool for predicting viscosity during design of reduced-fat food emulsions (Chung et al. 2013). Around 1913, when the first symposium on “the viscosity of colloids” took place in London, the viscosity of liquid and semisolid materials was considered a material constant which was calculated from measured raw data using the Hagen-Poiseuille equation. Shortly after this symposium, Eugene Bingham defined “viscoplastic liquids” using the Bingham model, and the concept of “yield value” was introduced for discriminating naturally flowable liquids in 1916. Around 1923–1925, A. de Waele and Wolfgang Ostwald reported the famous “power law” model, which expressed the mathematical relationship between shear rate and shear stress for a shear-thinning flow behavior without a yield stress. Currently, this model is one of the most widely used tools for characterizing rheological properties of food materials, for food processing pipeline design, and for food structure design (Sablani and Shayya 2003; Shaker et al. 2000; Verheul et al. 1998; Wu et al. 2013). In 1924, Heinrich Hencky, studying viscoelastic effects, defined Hencky strain, or true strain accounting for deformation of the object, and Hencky strain rate. In viscoelastic food materials such as cheeses, the Hencky strain at the fracture point is thought to be one of the most common instrumental parameters associated with oral textural attributes. Therefore, it was included in a model for predicting textural sensory properties of cheeses, including oral crumbliness, oral firmness, and oral stickiness (Wium et al. 1997). In 1926, Winslow Herschel and Ronald Bulkley modeled flow curves in which “yield point” was considered. In recent decades, the Herschel-Bulkley model is often found in published semisolid food research and is commonly used for designing process parameters (Nindo et al. 2007; Vélez-Ruiz and Barbosa-Cánovas 1998; Gonçalves et al. 2017; Ramaswamy and Basak 1991).

During the last 70 years, due to the advancement of instrumentation and the applications of rheology concepts for solving real-life industrial problems, rheology underwent fast and extensive development. In 1959, N. Casson developed another model to explain flow behavior containing a yield point. Both the Herschel-Bulkley and Casson models are widely used for characterizing the physical nature of semisolid food products; the fit is often compared between the two models (Dervisoglu and Kokini 1986; Gajo et al. 2017; Ramaswamy and Basak 1991). Moreover, an interesting engineering approach showed that the Casson model may be used for computing yield point (yield stress) from experimental data, then the calculated yield stress may be used to generate a better fit to the Herschel-Bulkley model (Tárrega et al. 2004). In 1968, Pierre Carreau introduced the concepts of zero-shear viscosity and infinite-shear viscosity. These concepts are part of a rheological means for describing food structural breakdown (Javanmard et al. 2018), and the zero-shear viscosity is a key rheological parameter that defines the bulk physical nature of a food material. It has also been associated with several sensory attributes including adhesiveness and cohesiveness (Kealy 2006; Nakauma et al. 2011; Selway and Stokes 2013). Additionally, the change of zero-shear viscosity during storage has been used in characterization of shelf life physical stability of yogurt (Lobato-Calleros et al. 2014).

Many scientific instruments have been commercialized, and the measuring methods and systems have been standardized since the 1950s. In 1951, the first rheometer was invented by Karl Weissenberg; the instrument was designed to perform both rotational and oscillatory tests. In 1954, the Haake Company was likely the first commercial manufacturer to launch a rotational viscometer as a product. In 1961, Brookfield Company manufactured a viscometer in which the tests were carried out by pneumatic drive. In 1980s, DIN (Deutsches Institut für Normung, translated as "German Institute for Standardization") standards for the geometry of cylinder systems used in rheometers were published. In the period between 1970s and 1980s, several companies introduced rheometers, including the Rheometrics Company, which became part of TA Instruments in 2002; the Bohlin Company, which became part of Malvern Instruments in 2003; and the Physica Company, which changed its name to Anton Paar in 2004. These three companies are the major interactional manufacturers of rheometers as of the time of publication of this book.

2 Traditional Rheological Tests

Both important terms and concepts used in the food industry and example configurations of some rheology tests are explained in the section. The rheological concepts and tests presented here are all widely used in industry or research applications. This section provides an overview of three major rheological tests: rotational tests, oscillatory tests, and creep relaxation tests. More detailed information on these tests and their use is provided in Chapter "Rheological Testing for Semisolid Foods: Traditional Rheometry".

2.1 Rheology Basics

Rheological behaviors are the deformation response to an applied torque or vice versa. In fundamental rheological testing, deformation may be converted to strain and torque may be converted to stress to account for the geometry used for testing. Still, all rheological tests involve measurements of torque and deformation, making these two parameters of critical importance in rheological testing. Understanding a material's response to an applied torque or deformation is the foundation for a complete analysis of its rheological behavior.

Foods are typically classified as fluid, semisolid, and solid. These classifications do not necessarily line up with their rheological classification, which typically is Newtonian (ideal) fluid, viscoelastic fluid, viscoelastic solid, or Hookean (ideal) solid. Hookean solids have a linear relationship between applied torque and subsequent deformation or vice versa. Likewise, Newtonian fluids have a linear relationship between the rate of applied deformation and subsequent deformation. In other words, they have constant viscosity regardless of applied torque. When a torque or deformation is applied to a Hookean solid, all applied energy is stored in the material and released when the torque or deformation is released, returning the material to its original shape. Newtonian fluids, on the other hand, dissipate all energy imparted to them as heat. Thus, they flow readily under an applied torque or deformation and do not return to their original shape once the torque or deformation is removed.

Few fluid foods display Newtonian behavior; notable examples of such foods include water, honey, and simple sugar syrups. Likewise, even fewer solid foods display Hookean behavior. Typically, only protein gels prepared at high protein concentration (e.g. >10% w/w gelatin gels or >20% w/w whey protein isolate gels) exhibit behavior that can be considered Hookean when tested below strains that induce structural failure. Most foods display viscoelastic behavior. Viscoelastic materials both store energy through their elastic component and dissipate energy through their viscous component. Viscoelastic solids store more energy than they dissipate, while viscoelastic fluids dissipate more energy than they store. Most solid foods are viscoelastic solids with a relatively high proportion of elastic to viscous behavior; most fluid foods are viscoelastic fluids with a relatively high proportion of viscous to elastic behavior. Semisolid foods can be either viscoelastic solids or viscoelastic fluids, depending on their structural features.

One of the main drivers behind rheological testing of foods is to determine their flow behaviors and viscoelastic profiles. Determining these behaviors and how they change under different conditions aids in understanding how foods will behave under industrial processing, storage, and oral processing conditions. For example, a viscoelastic fluid will sag under its own weight and must be stored in rigid packaging, while a viscoelastic solid with little viscous behavior can support its own weight and be stored in more flexible packaging. A more elastic food many be springy or chewy during consumption; a fluid with viscosity that depends on applied torque or deformation may feel different in the mouth when consumed at different rates or while using different oral motions.

In rheological testing of semisolid foods, the food is often placed between two parallel plates (Fig. 1). The upper plate is typically moved while the lower plate is held stationary. During the test, the upper plate receives a shear force over its area. This force results in a subsequent moving velocity of upper plate, causing the edge of the plate to travel a corresponding distance in a given amount of time. Accordingly, shear stress τ (Pa), shear strain γ (unitless), and shear rate $\dot{\gamma}$ (s^{-1}) are defined from the force, deformation, and rate of deformation placed on the sample.

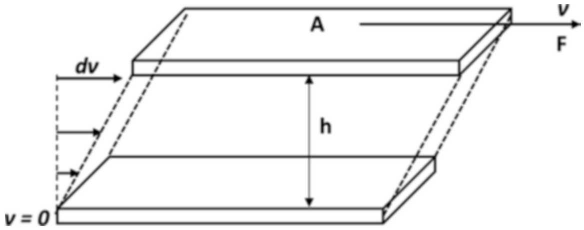

Fig. 1 Two-plate model demonstrating shear associated parameters. (Redrawn and adapted from Mezger (2014))

Rheological testing of semisolid foods can be classified into two main categories: rotational and transient. Both categories of tests provide valuable information on food rheological behaviors under industrial or oral processing conditions. Because the rheological behaviors of foods are often complex, multiple types of tests may be needed to fully characterize the rheological behaviors of food products. Typically, the more ingredients a food product contains, the greater the challenge to properly characterize its rheological behaviors.

2.2 *Rotational Tests*

Rotational tests are often used for plotting flow (viscosity) curves as a function of shear rate or shear stress; thus, these tests are applicable to both fluid and semisolid foods. Rotational tests may be run in two different modes. In controlled strain mode, the correspondent shear stresses are measured at different preset shear rates. In controlled stress mode, shear rate is measured at different preset shear stresses. In both modes, the viscosities (η, Pa.s) are calculated values using Eq. 1:

$$\eta = \frac{\tau}{\dot{\gamma}} \tag{1}$$

Both concentric cylinder and cone-plate geometries can be used in rotational testing. Controlled strain mode is generally used for characterizing flow behavior of materials without a yield point, and it is useful in pipeline flow behavior simulation, as the controlled shear rates may be converted to volumetric flow rate using the pipe radius. This allows the viscosity of material in the pipeline to be calculated at any given flow rate based on the flow curve function. Controlled stress mode is typically used for determining yield point (yield stress) for gelled semisolid foods.

2.2.1 Shear-Dependent Materials

The presence of viscoelastic behavior in a fluid or semisolid material generally manifests as shear-dependent behavior. This means that the relationship between shear rate and the resulting stress is not linear, as it is for a Newtonian fluid. The nonlinearity can manifest as a yield stress, shear thinning, shear thickening, or viscosity plateaus at very low or very high shear rates. Figures 2 and 3 illustrate potential viscosity curves of shear-dependent materials (Levinson et al. 2016; Rao et al. 1997). Most foods with shear-dependent behavior are shear thinning: their viscosity decreases with shear rate. Thus, it is important to know what shear rates are encompassed by the process of interest. For instance, 1–100 s^{-1} mimics mixing and kneading processes, 10–100 s^{-1} represents oral processing (chewing and swallowing), and 10–10^4 s^{-1} represents pipeline flow (Mezger 2014).

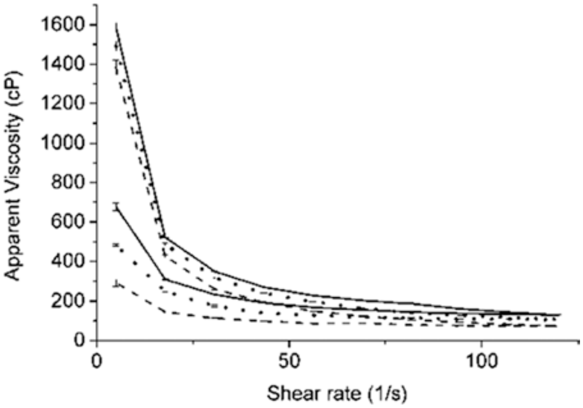

Fig. 2 Flow behavior (viscosity curve) of different fat-free yogurts. The decreasing trends of viscosity as responses of increase of shear rate indicate shear-thinning flow behavior. (Levinson et al. 2016)

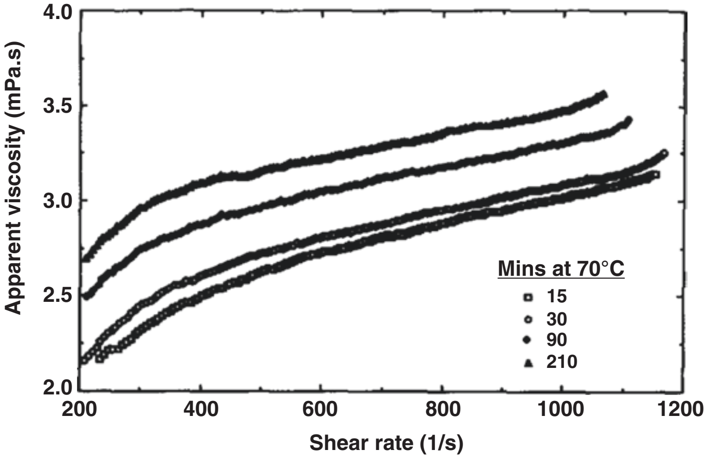

Fig. 3 Shear-thickening flow behavior of a heat-treated (70 °C) starch dispersion system (2.6% starch, w/w). (Rao et al. 1997)

It is important to point out that flow behavior for many semisolid food materials is temperature-dependent. One needs to fix the measuring temperature according to the specific application need. For example, if the viscosity curve is developed for simulating pipeline flow at low temperature (e.g. 4 °C), then testing should be conducted at the same temperature. If the viscosity curve is developed for sensory prediction, then the test temperature is better set to mouth temperature (37 °C).

2.2.2 Flow Behavior Assessment

As previously mentioned in Sect. 1, multiple flow behavior models have been developed to account for a wide variety of flow behaviors, including shear-dependent behaviors, yield stress, zero shear viscosity, and infinite shear viscosity. Shear-

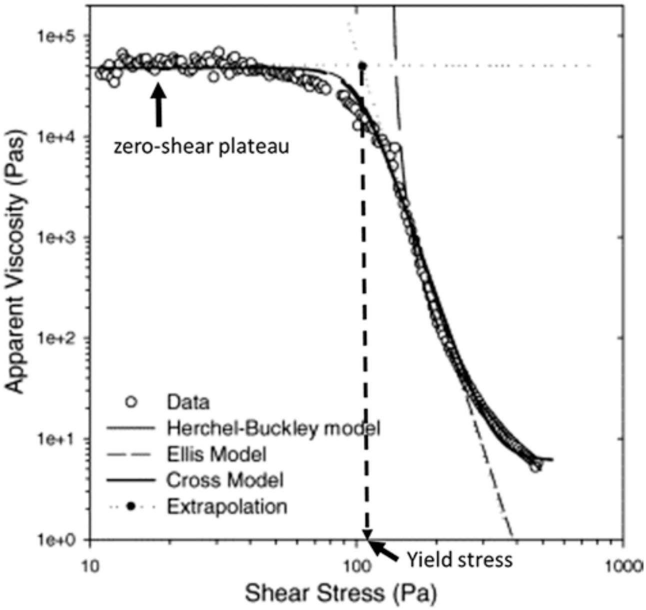

Fig. 4 Viscosity curve of mayonnaise as an example for showing zero-shear viscosity and identified yield stress. The curve is plotted from controlled shear stress sweep method. (Adapted from Stokes and Telford (2004))

dependent behaviors are typically measured by subjecting a material to a series of increasing shear rates and recording the resulting stress. Zero-shear viscosity and yield stress may be measured using a controlled stress sweep method (Fig. 4). Other techniques used for measuring yield behaviors of structured food materials may be found in (Stokes and Telford 2004).

The power law model is one of the most widely used models for food materials and has been used to model the viscosity of stirred yogurt as function of shear rate (Keogh and O'Kennedy 1998). However, the disadvantage of this model is that it does not fit many materials well in the low-shear and high-shear ranges. Because viscosity at low shear rates is important for characterizing the stability of many foods, models that account for zero-shear viscosity are needed for proper modeling of these food systems. Moreover, for a relatively highly viscoelastic gelled food material, e.g. Greek yogurt, a certain amount of force or stress (yield stress) is needed before it starts to flow. Thus, more comprehensive models that express both yield point and flow behavior is needed for better describing a food material. Examples of these models are shown in Chapter "Overview: Semisolid Foods". For additional models and a more detailed explanation of the models presented in Chapter "Overview: Semisolid Foods", the reader is encouraged to review Metzger's The Rheology Handbook (2014).

Certain materials show thixotropic behavior, or thinning due to shearing over time. Thixotropy can be measured instrumentally by conducting a shear rate

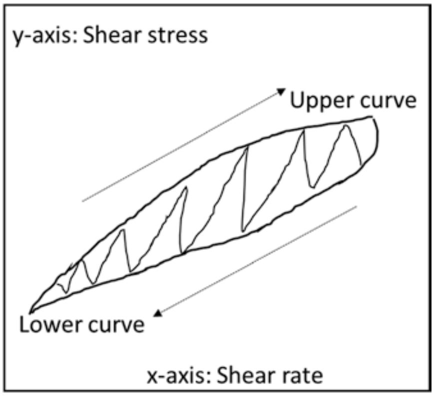

Fig. 5 Schematic illustration of thixotropic loop and thixotropic area (shaded)

ramp from low to high shear, then high to low shear on the same sample. If desired, the material can be sheared continuously at the highest shear rate for a set period of time between the two ramps. Thixotropy manifests as hysteresis between the two viscosity curves obtained from the shear rate ramps. The thixotropic area may be obtained by subtracting the difference between the areas under the lower curve from the area under the upper curve (Fig. 5) (Dolz et al. 1995, 2007; Roussel 2006). Thixotropic behavior indicates a structural feature of food material (Basim 2003). It may govern foaming in some foamed foods (Rajeev et al. 2008). The impact of thixotropic behavior of foods on the motor aspect of oropharyngeal swallowing and sensory was also pointed out (Atsuko et al. 2010; Štern et al. 2008).

2.3 Oscillatory Tests

2.3.1 Basic Concepts of Oscillatory Testing

Oscillatory tests are used to measure the viscoelastic and deformation behavior of materials. Such methods also known as dynamic mechanical analysis (DMA) are applicable to liquid, semisolid and solid materials. Parallel plate, cone-plate, and concentric cylinder geometries may be used to conduct oscillatory tests (Anema 2010; Coviello and Burchard 1992) by oscillating the upper tool at a given frequency (ω) and holding the lower plate or cup stationary. Parallel plate and cone and plate devices are preferred over concentric cylinder devices, as concentric cylinders have high inertia and can be difficult to oscillate precisely, particularly at high frequencies.

Oscillatory tests either import a sinusoidal deformation on a sample and measure the resulting torque, or impart a sinusoidal torque on a sample and measure the resulting deformation. Regardless of the input variable, the combination of the stress and strain waves can be used to determine material viscoelastic behaviors.

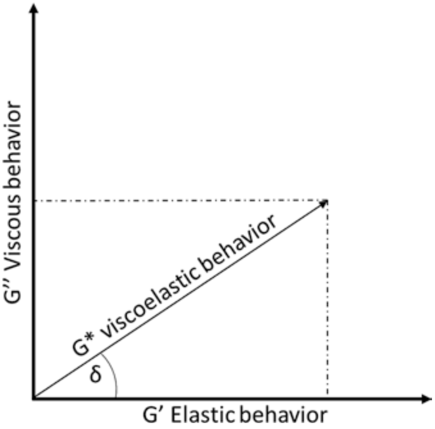

Fig. 6 Schematic vector diagram showing G^*, an indicator of viscoelastic behavior (including magnitude and phase angle δ), is a result of integration of G' (magnitude) and G'' (magnitude). (Redrawn based on Mezger (2014))

Viscoelastic moduli, including the storage modulus (G', Pa), loss modulus (G'', Pa), and complex modulus (G^*, Pa) can be calculated from stress-strain data; their relationship to each other is shown in Fig. 6 (Mezger 2014). The complex modulus is calculated by dividing the amplitude of the stress wave by the amplitude of the strain wave. Storage and loss moduli are calculated using the phase angle (δ, rad). Storage modulus is an indication of the amount of energy stored in each cycle, while loss modulus is an indication of the energy dissipated in each cycle. In other words, storage modulus represents elastic (solid-like) behavior and loss modulus represents viscous (fluid-like) behavior. The phase angle describes the extent of elastic to viscous behavior; it is usually reported as the tangent of the phase angle (tan δ). When the extent of elastic and viscous behaviors are equal, tan $\delta = 1$. Elastic-dominant materials (viscoelastic solids) have tan $\delta < 1$, while viscous-dominant materials (viscoelastic fluids) have tan $\delta > 1$.

tan δ is an important rheological parameter for characterizing gelled semisolid foods, e.g. dairy gels (Lucey 2001, 2002; Lucey and Singh 1997). For instance, in rennet induced dairy gels, higher tan δ values were associated with higher syneresis (van Vliet et al. 1991). However, while tan δ and G^* values of many foods have been measured (Piska and Štětina 2004; Ring and Stainsby 1985; Svegmark and Hermansson 1991), their statistical correlations with other meaningful characteristics related to their processability, quality, and sensory attributes are poorly understood. Typically, G^* is considered to be an indicator of the overall rigidity of semisolid food materials (Bowland and Foegeding 2001). However, additional work is needed to further understand the significance of G^* and tan δ in terms of food processing ability and sensory characteristics.

Complex viscosity (η^*) is an additional parameter derived from oscillatory tests. η^* is an alternative concept used for describing viscoelastic behavior. Similar to complex modulus, complex viscosity is calculated from a viscous (η') and an elastic (η'') component (Fig. 7) (Mezger 2014). In characterization or quality control of semisolid foods, dairy foods with higher complex viscosity values showed more elastic behavior (solid-like) behavior (Pralle et al. 2000).

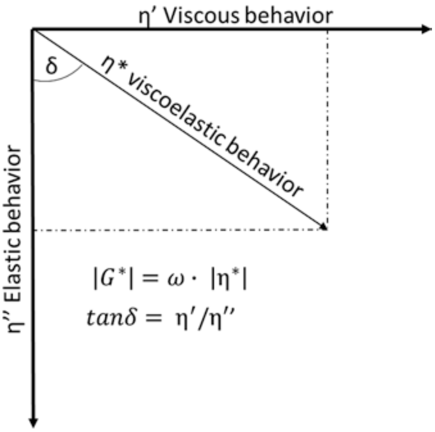

Fig. 7 Schematic vector diagram showing η^* as an indicator of viscoelastic behavior is a result of integration of η' (magnitude) and η'' (magnitude). The upper equation is used for calculating η^* if G^* has been already determined from strain sweep data at a given frequency, ω. The lower equation shows how to compute tan δ using η' and η''. (Redrawn from Mezger (2014))

A few notes on oscillatory testing are needed:

All moduli and phase angle values should be determined within the reversible-elastic deformation range, also called the linear viscoelastic region (LVR). This is because the equations for calculating these values, as well as their relationship shown in Fig. 6, only hold in this region. Beyond this region, the material is likely to undergo significant permanent deformation and structural breakdown, which violates the assumption of linear viscoelastic behavior. Furthermore, in standard rheometry, only the amplitude of the input and output waves are used. More recently, mathematical approaches to allow analysis of oscillatory data at high strains and frequencies have allowed rheologists to explore the region of nonlinear viscoelastic behavior. These approaches use the entire output wave to determine additional rheological information about the material of interest. These topics are covered in Chapter "LAOS (Large Amplitude Oscillatory Shear) Applications for Semisolid Foods".

Complex modulus differs from shear modulus (*G*), as complex modulus is determined from an oscillatory test in which both shear stress and shear strain continuously vary. Therefore, complex modulus is always written with an asterisk to indicate time-dependence. However, both complex modulus and shear modulus can be used to indicate the degree of rigidity of a material and can be used to compare the structural strength of different solid and semisolid foods. Similarly, complex viscosity is measured under transient conditions and is differentiated from viscosity measured using rotational tests with an asterisk.

2.3.2 Amplitude Sweeps

Amplitude sweeps are often used for characterizing the structural nature of food materials. They may be conducted in strain- or stress-controlled mode and are typically conducted at moderate frequencies (0.1–10 rad s^{-1}). Strain (amplitude) sweeps impart an oscillatory strain ramp on the sample and measure the resulting stress response wave; stress (amplitude) sweeps impart an oscillatory stress ramp and

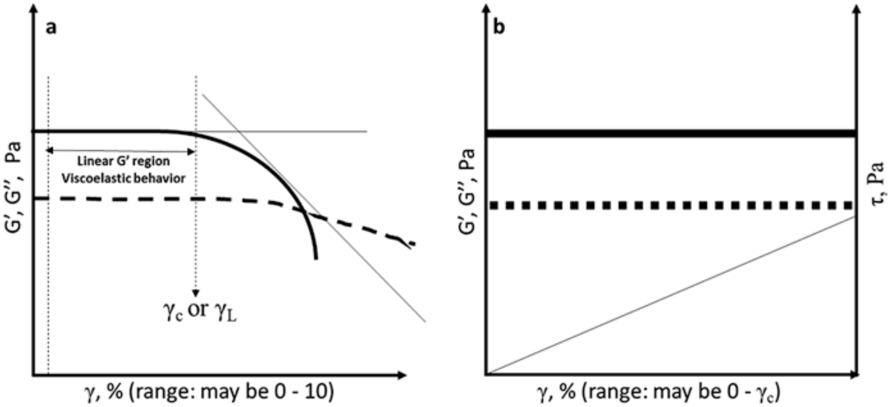

Fig. 8 Schematic illustration of a strain (γ) sweep for a gelled or semisolid food in which elastic behavior dominates viscous behavior. For a, solid line: G'; dashed line: G''; linear viscoelastic region (LVR) is highlighted using a double-headed arrow, critical strain or LVR strain (γ_L) is indicated with a vertical arrow. For b, magnified view of the LVR; bold solid line: linear viscoelastic region of G', dashed line: linear viscoelastic region of G'', diagonal solid line: measured stress (τ) as a function of γ. (illustration is based on example result from Rok et al. (2017))

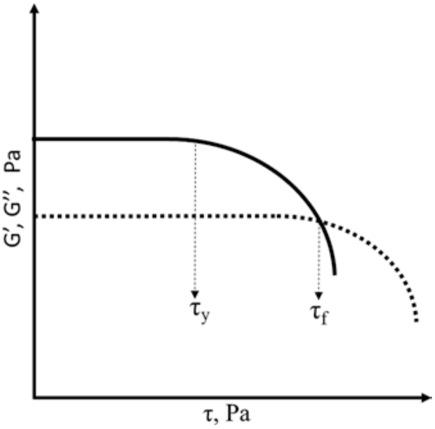

Fig. 9 Schematic illustration of a stress (τ) sweep for a gelled or semisolid food material. For a, solid line: G'; dashed line: G'', both yield stress (τ_y) and flow stress (τ_f) are indicated with single-headed arrows. (Adapted from Mezger (2014))

measure the resulting strain response wave. Both tests are performed at constant temperature and frequency. They can be used to measure viscoelastic moduli and phase angle, and thus rigidity of internal structure.

Amplitude sweeps are generally conducted to determine the LVR. To do this, adjacent complex moduli values are compared and the end of the LVR is considered to be when two adjacent values differ by more than 2–10%; the analysis software in most commercial rheometers defaults to 3%. The strain at which the LVR ends is called the critical strain (γ_c or γ_L, Fig. 8a); the stress at which the LVR ends is called the yield point (τ_y, Fig. 9) (Patel et al. 2014). The end of the LVR indicates the greatest stress or strain that can be applied to the material and still maintain the internal structure before it is disrupted (at the end of the LVR). In the LVR, moduli values are generally assumed to be constant (Fig. 8b), although this is not always true for semisolid foods that do not have a clear yield point. Outside of the LVR, structural disruption results in a decrease in moduli values, and a crossover of storage and loss modulus is possible of the structure is disrupted enough for the material to flow.

2.3.3 Frequency Sweeps

Frequency sweeps impart an oscillating frequency ramp to a sample at constant strain and temperature. This technique evaluates material viscoelastic behaviors at different time scale and can also be used to reveal in-depth insights of structural features of gelled food systems (Tunick 2011). Frequency sweeps can be used to make qualitative comparisons of gel structural type (Fig. 10a) (Tunick 2011) and direct comparisons of gel viscoelastic behaviors as a function of temperature or other treatment variables (Fig. 10b) (Egelandsdal et al. 1986). Soft gels show viscoelastic moduli with a strong dependence on frequency: they may have fluid-like behavior at low frequencies then shift to solid-like behavior at higher frequencies (Stading and Hermansson 1990; Tunick 2011). These gels comprise entangled networks of biopolymer materials, and gelation is a result of polymer–solvent interaction and non-specific conformational entanglement of disordered polymer chains. Food hydrocolloids such as non-gelling starch, locust bean gum, and carboxymethylcellulose can form soft gels (Morris 1986; Stading and Hermansson 1990). Physical gels may show some dependency of frequency, however, a viscoelastic modulus crossover is normally absent and the gels shown viscoelastic solid behavior (Stading and Hermansson 1990). These gels are considered semi-hard gels, and it is believed that non-covalent interactions are involved in their gelation process. Casein micelles can form a physical gel when prepared at acidic pH (pH 4.5–4.6). Hard or strong gels have moduli values that are independent of frequency and show viscoelastic solid behavior (Stading and Hermansson 1990). Covalent crosslinking (e.g. disulfide bonding) is involved in gel structure construction. For example, transglutaminase induces protein gelation networks via disulfide bonding; disulfide bond bridging may also be involved in whey protein gel networks induced by both heat treatment and acidification (Alting et al. 2000; Shimada and Cheftel 1989).

2.4 Creep-Relaxation Test

Creep-relaxation tests are two-part tests that involve stress application and removal (Fig. 11). While a creep test is a transient test rather than a rotational test, it also differs from oscillatory testing in that a constant stress is used. Creep testing may be viewed as a very low-frequency oscillatory test, as it given an indication of the material's tendency to flow over long time periods. In the creep portion of the test, a

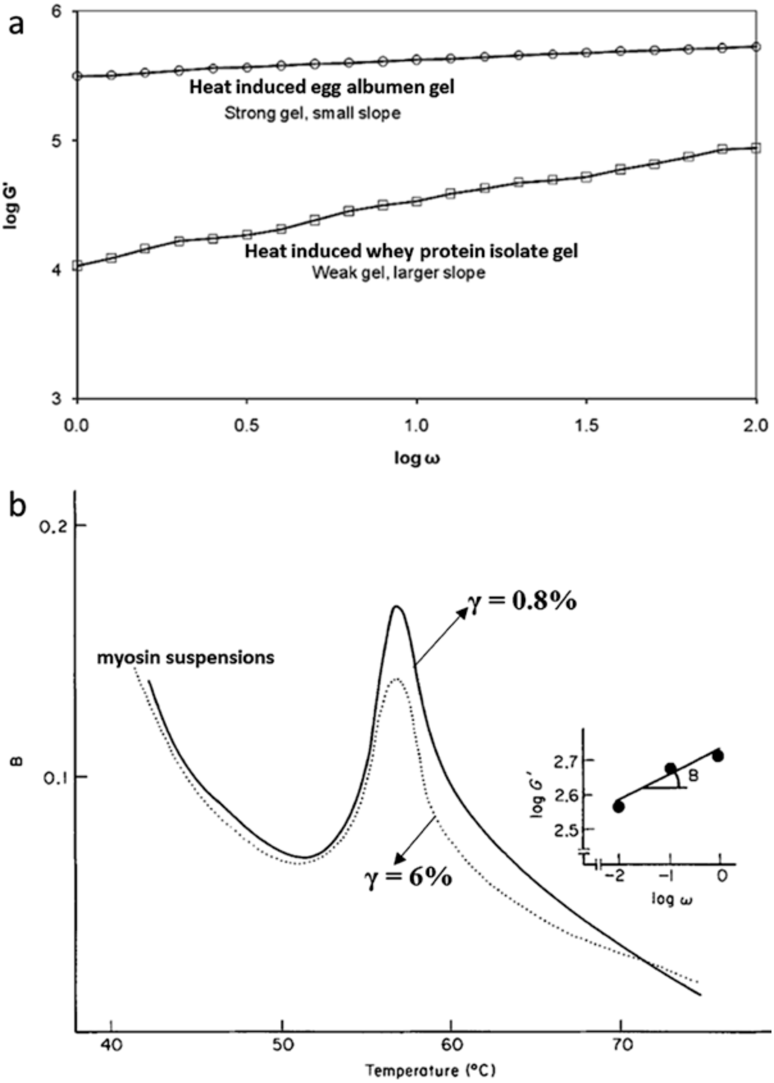

Fig. 10 Application of frequency sweeps for characterizing structure features and structure changes as response of treatments. In (**a**), the upper line shows a relatively small increase in $log(G')$ for an egg albumen gel (20% w/w, induced gelation at 80 °C) with increasing $log(\omega)$; the lower line shows a relatively larger increase of $log(G')$ for a whey protein isolate gel (20% w/w, induced gelation at 80 °C) with increasing $log(\omega)$. The smaller slope of $log(G')$ indicates stronger gel structure (data from Tunick 2011). In (**b**), two different strain amplitudes were used to monitor heat-induced gelation of a myosin suspension (10 mg/mL). The frequency range used was 0.01–1 Hz, B is defined in the inset as the slope of log G′ and log ω. (Data from Egelandsdal et al. 1986)

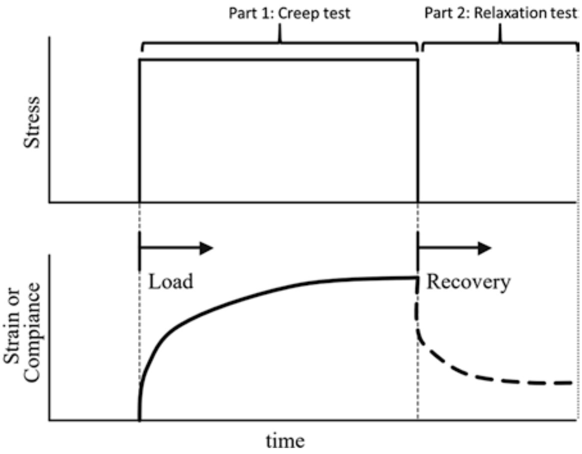

Fig. 11 Schematic illustration of a creep and relaxation test. The upper graph shows the step application of constant stress, holding the stress for a period of time (creep), sudden removal of the stress, and holding for a period of time without stress (recovery). The lower graph shows the measured strain or compliance over the measurement duration. (Redrawn and adapted from Foegeding et al. (2003))

constant shear stress is applied to sample as quickly as possible and the sample is held at that stress for a certain time period. During the relaxation portion, the stress is completely removed and the sample is held at rest for a second time period. Sample deformation (strain) is monitored for the duration of the test. Because creep-recovery testing should be conducted in the LVR, a strain sweep needs to be carried out first to identify the LVR (Foegeding et al. 2003; Foegeding and Drake 2007; Pereira et al. 2001; Tunick 2000). More rigid foods will show a lower strain change during creep testing due to their stronger structure; more elastic foods will show larger recovery during the relaxation portion of the test due to their higher amounts of stored energy. Therefore, creep-relaxation tests can be used to compare structural strength and viscoelastic behaviors of food materials (Tunick 2000). Additionally, creep compliance, or the ratio of strain to stress during creep testing, indicates a material's elastic recoil. This may be important in sensory texture: cheese creep compliance has been significantly correlated with several sensory attributes including hand and chewing firmness, springiness, and adhesiveness (Foegeding et al. 2003).

3 Significance of Rheology in the Food Industry

Some rheological properties of raw food materials and manufactured food products are measured in the food industry as routine quality control parameters. Additional rheological behaviors are profiled or modeled in research and development projects via various rheological techniques. Although the key fundamental knowledge of rheoloigcal concepts is available in the public domain, it is still a challenge for novice rheologists to properly interpret the significance of individual rheological attributes and rheological measurements in a given application or research publication. A comprehensive review of rheological testing is provided in Chapter "Rheological Testing for Semisolid Foods: Traditional Rheometry". In the following sections, a brief overview of how rheology is used in the food industry is provided, with examples used for illustration of the applications.

3.1 Process Engineering

Many semisolid foods, especially dairy products (e.g. yogurts), show both shear- and time-dependent flow behaviors: their viscosity decreases or increases with flow velocity and over time. Therefore, understanding flow behavior changes in industrial flow systems under different processing conditions is essential for designing manufacturing processes. Factors such as pipeline geometry, pump selection, volumetric flow rate, and heat transfer rate are major processing concerns relevant to rheological parameters including wall shear rate, viscosity and time-dependent flow behavior or pressure-dependent flow behavior. Therefore, modeling of flow behavior is critical to good performance of flow systems. Modeling is one of the engineering approaches for solving industry problems. It has shown advantages over the trial and error approach in food process engineering, as reliable models can eliminate unnecessary trials and predict product flow behaviors in pipelines, therefore reducing research and development costs and processing risks (e.g. improperly sized pumps). Although shear- and time-dependent flow behaviors of semisolid food material in pipelines may be complex, researchers have used multiple approaches for modeling the flow-related parameters of such material. Empirical models (power law-based models) developed via experimental data fitting are widely used for predicting flow behaviors of foods (Butler and O'Donnell 1999; Doublier and Durand 2008). However, these models do not necessarily consider structural or fracture-related factors. A structural approach was applied in investigation of stirred yogurt as a thixotropic fluid; the authors constructed a prediction model which was able to predict friction coefficient in a horizontal rectilinear cylindrical pipe. The model described relationships between pressure drop, an important processing parameter that indicates the suitability of the process for transporting the given fluid, Reynolds number, fracture properties, and shear stress (Schmitt et al. 1998). It should be noted that flow behavior models are much more commonly applied to food process design than structural models, as flow behavior models tend to be simpler to work with and food flow behaviors are relatively easy to measure. Another modeling technique in use for food products is finite element analysis, a diverse and useful numerical tool used to find approximate solutions for complex problems (Hughes 2012; Puri and Anantheswaran 1993; Szabó et al. 1991). For example, it was employed to predict the pressure drop of cultured dairy foods at certain flow rates (Butler and O'Donnell 1999).

Often, it is necessary to predict food rheological behaviors under specialized conditions. Extrusion stretching is normally involved in industrial manufacture of mozzarella cheese, among other products. Accordingly, capillary extrusion analytical techniques have been used to determine flow curves in which different length-to-diameter ratios of the tube were considered (Muliawan and Hatzikiriakos 2008). The modeled flow curves reflected indications of processability of the cheese in realistic situations. Additionally, filament stretching rheometery has provided an opportunity for quantitatively expressing how foods react when stretched under different conditions. For example, the batch filling processability of non-Newtonian foodstuff was found to be a combination of heat transfer and visco-elasto-capillary necking (Tripathi et al. 2000).

In yogurt manufacturing, yogurt milk often blends with hydrocolloids, or thickeners and texturizers, such as starch and other polysaccharides (e.g. pectin). During the pasteurization step of yogurt production, the hydrocolloids completely hydrate, which alters the rheological properties of the yogurt milk. In addition, the non-Newtonian stirred yogurt gel needs to be cooled to storage temperature using a plate heat exchanger after fermentation and smoothing of the yogurt curds. The heat transfer during this cooling process is conducted by both conductive and convective heat transfer. It has been found that the convective heat transfer coefficient during yogurt cooling via plate heat exchanger is related to the Prandtl number, or the ratio of viscous diffusivity to thermal diffusivity, and the design of the plate heat exchanger. The Prandtl number is highly dependent on the dynamic viscosity. Thus, flow behavior does not only govern pipeline flow processes but also influences the efficiency of heat transfer processes for semisolid dairy foods (Afonso et al. 2003).

3.2 Product Stability

Many semisolid foods are oil-in-water (o/w) emulsion or suspension-based systems that are governed by Stokes' Law:

$$v = \frac{2\mathrm{gr}^2\left(\rho_2 - \rho_1\right)}{9\eta_1} \tag{2}$$

Here, v is the creaming or sedimentation velocity (m/s), g is the gravitational acceleration (m/s^2), r is the radius of the particle or emulsion droplet (m), ρ_2 is the density of the oil droplet or particle (kg/m^3), ρ_1 is the density of the continuous phase (kg/m^3), and η_1 is the viscosity of the continuous phase (Pa.s). Therefore, a relatively high continuous phase viscosity may result in a lower creaming or sedimentation rate, yielding a relatively more stable emulsion or suspension system. Moreover, viscosity is one of the essential measurable factors for the prediction of phase separation rate of emulsion or suspension systems when Stokes' Law is used. The stability of an emulsion system is a kinetic concept and dependent on multiple factors, including the physicochemical nature of the emulsifier and oil, droplet size distribution, and the pH and ionic strength of the continuous phase. As we are focusing on the discussion of rheology in this chapter, only the impact of rheological aspects on emulsion and suspension stability is highlighted in this section. More comprehensive reviews of emulsion and suspension stability are available in the literature; interested readers may refer to (Boyd et al. 1972; Dickinson 1993, 2001; McClements 2007; Rousseau 2000; Tadros 2012).

Emulsion droplets can be stabilized with an emulsifier that forms an interfacial film layer on the surfaces of droplets. Stable emulsion-based semisolid foods contain individual droplets that do not coalesce. Rigid interfaces result in robust emulsion droplets and therefore hinder the coalescence phenomenon, making the emulsion system more stable (Edwards and Wasan 1991). Droplet interfaces may present different physical features such as varying degrees of viscoelasticity, and may be quantitatively described by interfacial rheology, the study of flow or deformation behaviors of thin films at interfacial phases (Elmanan et al. 2008; Rousseau 2000). Food emulsions are complexed systems, as they often contain a mixture of different types emulsifiers, e.g. protein and water- or oil-soluble low-molecular weight surfactants. Competitive adsorption of different emulsifiers may occur, resulting in different interfacial compositions with varying interfacial rheological behaviors, which impact stability (Maldonado-Valderrama and Patino 2010). For example, addition of low-molecular weight surfactants to protein-stabilized emulsion system results in protein depletion from the interfacial layer but increased surfactant concentration on the droplet surface (Mackie et al. 2007). Furthermore, increased concentration of surfactant in a stable emulsion system can result in decreased bulk elasticity of the system (Derkatch et al. 2007). This information implies that bulk rheological properties are impacted by alteration of interfacial rheology (Murray 2002). Therefore, by studying the interfacial rheological properties of emulsion droplets, one can better characterize, predict, or even control the phase stability or physical shelf life of emulsion-based food products (Dickinson 2001; Elmanan et al. 2008; Langevin 2000).

The flocculation of food emulsion droplets over time destabilizes the emulsion system. Emulsion flocculation can be induced when van der Waals attraction is prevalent over other repulsive forces, or when Stokes' Law indicates creaming or settling is likely. Droplet flocculation is often characterized by laser diffraction techniques in which the particle size distribution of the population is revealed or by microscopy (Dickinson and Golding 1997; Dickinson et al. 1992). However, these techniques can only show the flocculation phenomenon or the degree of flocculation after it has occurred. Rheological techniques offer an alternative and sensitive means to understand even weak flocculation effects and may be used to indicate flocculation in real time. Shear rheology has been suggested as an effective experimental method for indicating droplet flocculation in moderately concentrated emulsion systems (Dickinson 1998). Rheological flow behavior models and the factors associated with these models have been found to be relevant to flocculation; therefore, rheological techniques and flow behavior models may be used for characterizing emulsion flocculation (Tadros 2004). For instance, a higher yield point and plastic viscosity in the Bingham model indicates a more flocculated emulsion; however, this is only qualitative characterization (Tadros 2004). Zero shear viscosity and critical shear stress are also able to quantitatively express the degree of flocculation of an emulsion system; an increase of these parameters over storage time may indicate flocculation. These parameters may be gained from a plot of viscosity as a function of shear stress, as well as from a series of constant stress (creep) tests (Tadros 1993, 2004). The method for measuring zero shear viscosity is introduced in this chapter in Sect. 2.2.2 and further discussed in Chapter "Rheological Testing for Semisolid Foods: Traditional Rheometry".

3.3 Food Structure Design & Sensory Prediction

The sensory attributes of semisolid foods are texture-dependent. The specific texture is a result of dedicated arrangements among different food components; such arrangements are expressed as micro- and macrostructural features. Textural attributes and food quality-related properties are structure-dependent (Chung and McClements 2014; Kilcast and Clegg 2002; Pascua et al. 2013; Wilkinson et al. 2000). Therefore, engineering structures is one of the primary tasks in a food product development project to improve product textural attributes. Because these structural features also control food rheological behaviors, semisolid food rheological properties can be related to their textural attributes. In general, both descriptive sensory evaluation and rheological testing are both analytical means for understanding food textural attributes (Joyner 2018), but rheological data collected from instruments is relatively more reproducible and objective. However, sensory evaluation methods are still essential during product development or quality assurance because only sensory data can determine food liking and preference. Nevertheless, rheological measurements can be useful: rheological tests are less time-consuming compared to sensory tests, so using characteristic rheological parameters as benchmarks is a strategy for shortening the research and development process when large number of ingredients or processing parameters need to be screened.

In non-Newtonian food systems, structure, rheological behaviors, and stability are interrelated: a critical stress is able to trigger a coalescence effect among emulsion droplets, and such critical stress is determined by the volume fraction of added thickening/gelling polysaccharide; non-linear creep test, a rheology method, may be used as a fast tool to assess shear induced structural and stability changes (Santos et al. 2015). At the end of the 1960s, Sherman described a concept of texture profile of solid, semisolid, and liquid food materials using a mathematical perspective (Sherman 1969). The theory consists of three categories of food properties. The primary category consists of composition, particle size, and particle size distribution. Rheological properties such as elasticity, viscosity, and adhesion comprise the secondary category, while the tertiary category contains sensory textural attributes. The theory suggested that the tertiary category attributes may be explained by a number of rheological parameters from the secondary category. Many different sensory prediction models have been developed since that time. The model development is based on three major steps: (1) developing a fundamental understanding of the mechanisms of perception of a textural attribute during mastication; (2) generating data on a broad spectrum of mechanical and physicochemical properties using proper empirical methodology or mathematical models, and (3) determining significant correlations among instrumental and sensory data.

Creaminess is one of the key sensory attributes that determine consumers' acceptability of dairy products (Richardson-Harman et al. 2000; Soukoulis et al. 2010). However, understanding creaminess is challenging due to the lack of a standard definition for creaminess or creaminess measurements (Frøst and Janhøj 2007). Creaminess is a complex sensory attribute, it may be even considered as a combination of other textural sensory attributes, e.g. thickness and smoothness (Kokini 1987; Kokini and Cussler 1983). In fact, creaminess is considered a consumer term by a number of sensory scientists because it is so difficult to describe and quantitatively measure. Based on these considerations, it is not surprising that more than just rheological parameters are needed for constructing reliable prediction models of creaminess perception. Indeed, rheological properties of both the initial undisrupted food and the food after mechanical and enzymatic structural breakdown are necessary for constructing reliable partial least square (PLS) models of creaminess prediction for semisolid foods (Janssen et al. 2007). In the aforementioned study, the authors basically followed Sherman's three-step method for developing sensory prediction models. First, both the initial structural and rheological features and subsequent enzymatic and structural breakdown during oral processing were hypothesized to relate to creaminess perception. Next, rotational and dynamic oscillatory tests were used to characterize the rheological properties of the food at the beginning of structural breakdown caused by mastication, then principal component analysis was applied to consolidate significant correlations. Finally, partial least squares models containing significant factors were constructed for predicting different sensory attributes.

Aside from rheology, soft or "oral" tribology has been highlighted in recent research due to the significance of friction behaviors in food textural perception (Pradal and Stokes 2016; van Aken 2010). Although food rheology and tribology contribute complementary information for understanding food textures, the two sciences are characterized as two different aspects of food behavior (Chen and Stokes 2012); therefore, the detailed application of tribology in food structure design and sensory evaluation will not be discussed here. Additional information on tribology as performed on semisolid foods is presented in Chapter "Semisolid Food Tribology".

3.4 Food Digestion

Rheological behaviors and digestion kinetics are interrelated (A. Mackie et al. 2016; Morell et al. 2014; Prakash et al. 2014). Recently, investigation of the role of food structure in regulating digestion processes in the gastrointestinal tract has become a topic of interest in both the scientific community and industry. As previously mentioned, interfacial rheology is related to stability of food emulsions; changes to interfacial rheology and interfacial composition among emulsion droplets during and after consumption may promote macrostructural changes of the emulsion system and may have impact on adsorption of digestive enzymes on the surface of emulsion droplets (McClements et al. 2008). Additionally, not only the composition of food but also the microstructure of food system determine its digestion process during and after consumption (Bornhorst and Singh 2014; Singh et al. 2009). Studies have shown that such changes of bulk rheological behaviors can influence protein digestion and amino acid absorption kinetics of the GI tract. For example, a study on dairy protein foods suggested that gelation of a dairy matrix increase stomach retention time, ingestion of liquid matrices is more favorable for muscle protein synthesis (i.e. better protein absorption), and gelled dairy matrices are a more satiating food (Barbé et al. 2013).

Although (bio-)chemistry approaches are often used for understanding food digestion kinetics, modeling stomach geometry and motility of gastric content are complementary means for revealing a comprehensive understanding of food digestion mechanism in the gastrointestinal tract. Computational fluid dynamics is a mathematical means of numerically solving the governing partial differential equations of fluid flow; it is used for expressing sophisticated fluid flow and deformation behaviors as a function of multiple variables, including mass, acceleration, energy, space, and time (Wendt 2008). For example, Ferrua and Singh used computational fluid dynamics to describe digestion in the gastrointestinal tract and revealed that there was an inhomogeneous mixture of gastric contents in digesting high viscous foods rather than a homogenous mixture (Ferrua and Singh 2010). Additionally, modeling of β-glucan digestion showed that rheological attributes such as viscosity indirectly indicated digestion and absorption processes of β-glucan in the small intestine. It was also found that the change of diffusion coefficient of β-glucan was related to digestion processes and that diffusion coefficients decreased somewhat with increased viscosity (Shelat et al. 2011).

4 Summary

Rheology is a useful tool for characterizing the flow and deformation behaviors of food products. Over its long history, rheologists have developed multiple methods of characterizing material rheological behaviors. Rotational tests are typically used to determine flow behaviors, while oscillatory and other transient tests are used to determine viscoelastic behaviors. Rheological behaviors can be modeled through a variety of equations and play a key role in understanding material processing and sensory behaviors. While rheologists have made great strides in understanding how materials react to imparted torque and deformation, much work remains to be completed before a full understanding of material flow, deformation behaviors is achieved. This is especially true for food products, whose complex structures and inhomogeneities make rheological characterization difficult. Nevertheless, rheology remains a valuable tool for product and process development in the food industry.

References

Afonso, I. M., Hes, L., Maia, J. M., & Melo, L. F. (2003). Heat transfer and rheology of stirred yoghurt during cooling in plate heat exchangers. *Journal of Food Engineering, 57*(2), 179–187.

Atsuko Igarashi, Maiko Kawasaki, Shu-ichi Nomura, Yuji Sakai, Mayumi Ueno, Ichiro Ashida, Yozo Miyaoka, (2010) Sensory and Motor Responses of Normal Young Adults During Swallowing of Foods with Different Properties and Volumes. Dysphagia 25 (3):198-206

Alting, A. C., Hamer, R. J., de Kruif, C. G., & Visschers, R. W. (2000). Formation of disulfide bonds in acid-induced gels of preheated whey protein isolate. *Journal of Agricultural and Food Chemistry, 48*(10), 5001–5007.

Anema, S. G. (2010). Effect of pH at pressure treatment on the acid gelation of skim milk. *Innovative Food Science & Emerging Technologies, 11*(2), 265–273.

Barbé, F., Ménard, O., Le Gouar, Y., Buffière, C., Famelart, M.-H., Laroche, B., Le Feunteun, S., Dupont, D., & Rémond, D. (2013). The heat treatment and the gelation are strong determinants of the kinetics of milk proteins digestion and of the peripheral availability of amino acids. *Food Chemistry, 136*(3), 1203–1212.

Basim Abu-Jdayil. (2003). Modelling the time-dependent rheological behavior of semisolid foodstuffs. *Journal of Food Engineering, 57*(1):97–102.

Belmar-Beiny, M. T., Gotham, S. M., Paterson, W. R., Fryer, P. J., & Pritchard, A. M. (1993). The effect of Reynolds number and fluid temperature in whey protein fouling. *Journal of Food Engineering, 19*(2), 119–139.

Bornhorst, G. M., & Singh, R. P. (2014). Gastric digestion in vivo and in vitro: How the structural aspects of food influence the digestion process. *Annual Review of Food Science and Technology, 5*(1), 111–132.

Bowland, E. L., & Foegeding, E. A. (2001). Small strain oscillatory shear and microstructural analyses of a model processed cheese. *Journal of Dairy Science, 84*(11), 2372–2380.

Boyd, J., Parkinson, C., & Sherman, P. (1972). Factors affecting emulsion stability, and the HLB concept. *Journal of Colloid and Interface Science, 41*(2), 359–370.

Butler, F., & O'Donnell, H. J. (1999). Modelling the flow of a time-dependent viscous product (cultured buttermilk) in a tube viscometer at 5°C. *Journal of Food Engineering, 42*(4), 199–206.

Chakrabandhu, K., & Singh, R. K. (2005). Rheological properties of coarse food suspensions in tube flow at high temperatures. *Journal of Food Engineering, 66*(1), 117–128.

Chen, J., & Stokes, J. R. (2012). Rheology and tribology: Two distinctive regimes of food texture sensation. *Trends in Food Science & Technology, 25*(1), 4–12.

Chiang, B. H., & Cheryan, M. (1986). Ultrafiltration of skimmilk in hollow fibers. *Journal of Food Science, 51*(2), 340–344.

Chung, C., Degner, B., & McClements, D. J. (2013). Designing reduced-fat food emulsions: Locust bean gum–fat droplet interactions. *Food Hydrocolloids, 32*(2), 263–270.

Chung, C., & McClements, D. J. (2014). Structure–function relationships in food emulsions: Improving food quality and sensory perception. *Food Structure, 1*(2), 106–126.

Coviello, T., & Burchard, W. (1992). Criteria for the point of gelation in reversibly gelling systems according to dynamic light scattering and oscillatory rheology. *Macromolecules, 25*(2), 1011–1012.

Derkatch, S. R., Levachov, S. M., Kuhkushkina, A. N., Novosyolova, N. V., Kharlov, A. E., & Matveenko, V. N. (2007). Rheological properties of concentrated emulsions stabilized by globular protein in the presence of nonionic surfactant. *Colloids and Surfaces A: Physicochemical and Engineering Aspects, 298*(3), 225–234.

Dervisoglu, M., & Kokini, J. L. (1986). Steady shear rheology and fluid mechanics of four semi-solid foods. *Journal of Food Science, 51*(3), 541–546.

Dickinson, E. (1993). Emulsion stability. In K. Nishinari & E. Doi (Eds.), *Food hydrocolloids: Structures, properties, and functions* (pp. 387–398). Boston, MA: Springer US.

Dickinson, E. (1998). Structure, stability and rheology of flocculated emulsions. *Current Opinion in Colloid & Interface Science, 3*(6), 633–638.

Dickinson, E. (2001). Milk protein interfacial layers and the relationship to emulsion stability and rheology. *Colloids and Surfaces B: Biointerfaces, 20*(3), 197–210.

Dickinson, E., & Golding, M. (1997). Depletion flocculation of emulsions containing unadsorbed sodium caseinate. *Food Hydrocolloids, 11*(1), 13–18.

Dickinson, E., Hunt, J. A., & Horne, D. S. (1992). Calcium induced flocculation of emulsions containing adsorbed β-casein or phosvitin. *Food Hydrocolloids, 6*(4), 359–370.

Dolz, M., Hernández, M. J., Delegido, J., Alfaro, M. C., & Muñoz, J. (2007). Influence of xanthan gum and locust bean gum upon flow and thixotropic behaviour of food emulsions containing modified starch. *Journal of Food Engineering, 81*(1), 179–186.

Dolz, M., Hernández, M. J., Pellicer, J., & Delegido, J. (1995). Shear stress synergism index and relative thixotropic area. *Journal of Pharmaceutical Sciences, 84*(6), 728–732.

Doublier, J.-L., & Durand, S. (2008). A rheological characterization of semi-solid dairy systems. *Food Chemistry, 108*(4), 1169–1175.

Edwards, D. A., & Wasan, D. T. (1991). A micromechanical model of linear surface rheological behavior. *Chemical Engineering Science, 46*(5), 1247–1257.

Egelandsdal, B., Fretheim, K., & Harbitz, O. (1986). Dynamic rheological measurements on heat-induced myosin gels: An evaluation of the method's suitability for the filamentous gels. *Journal of the Science of Food and Agriculture, 37*(9), 944–954.

Elmanan, M., Al-Assaf, S., Phillips, G. O., & Williams, P. A. (2008). Studies on Acacia exudate gums: Part VI. Interfacial rheology of Acacia senegal and Acacia seyal. *Food Hydrocolloids, 22*(4), 682–689.

Ferrua, M. J., & Singh, R. P. (2010). Modeling the fluid dynamics in a human stomach to gain insight of food digestion. *Journal of Food Science, 75*(7), R151–R162.

Foegeding, A., Brown, J., Drake, M., & Daubert, C. R. (2003). Sensory and mechanical aspects of cheese texture. *International Dairy Journal, 13*(8), 585–591.

Foegeding, A., & Drake, M. A. (2007). Invited review: Sensory and mechanical properties of cheese texture. *Journal of Dairy Science, 90*(4), 1611–1624.

Frøst, M. B., & Janhøj, T. (2007). Understanding creaminess. *International Dairy Journal, 17*(11), 1298–1311.

Gajo, A. A., de Resende, J. V., Costa, F. F., Pereira, C. G., de Lima, R. R., Antonialli, F., & de Abreu, L. R. (2017). Effect of hydrocolloids blends on frozen dessert "popsicles" made with whey concentrated. *LWT - Food Science and Technology, 75*, 473–480.

Gogate, P. R. (2011). Hydrodynamic cavitation for food and water processing. *Food and Bioprocess Technology, 4*(6), 996–1011.

Gonçalves, B. J., Pereira, C. G., Lago, A. M. T., Gonçalves, C. S., Giarola, T. M. O., Abreu, L. R., & Resende, J. V. (2017). Thermal conductivity as influenced by the temperature and apparent viscosity of dairy products. *Journal of Dairy Science, 100*(5), 3513–3525.

Hemar, Y., & Horne, D. S. (2000). Dynamic rheological properties of highly concentrated protein-stabilized emulsions. *Langmuir, 16*(7), 3050–3057.

Hughes, T. J. R. (2012). *The finite element method: Linear static and dynamic finite element analysis*. Dover Publications, INC. Mineola, New York.

Janssen, A. M., Terpstra, M. E. J., De Wijk, R. A., & Prinz, J. F. (2007). Relations between rheological properties, saliva-induced structure breakdown and sensory texture attributes of custards. *Journal of Texture Studies, 38*(1), 42–69.

Javanmard, M., Wong, E., Howes, T., & Stokes, J. R. (2018). Application of the thixotropic elasto-viscoplastic model as a structure probing technique for acid milk gel suspensions. *Journal of Food Engineering, 222*, 250–257.

Joyner, H. S. (2018). Explaining food texture through rheology. *Current Opinion in Food Science, 21*, 7–14.

Karaman, S., Yilmaz, M. T., Toker, O. S., & Dogan, M. (2016). Stress relaxation/creep compliance behaviour of kashar cheese: Scanning electron microscopy observations. *International Journal of Dairy Technology, 69*(2), 254–261.

Kealy, T. (2006). Application of liquid and solid rheological technologies to the textural characterisation of semi-solid foods. *Food Research International, 39*(3), 265–276.

Keogh, M. K., & O'Kennedy, B. T. (1998). Rheology of stirred yogurt as affected by added milk fat, protein and hydrocolloids. *Journal of Food Science, 63*(1), 108–112.

Kilcast, D., & Clegg, S. (2002). Sensory perception of creaminess and its relationship with food structure. *Food Quality and Preference, 13*(7), 609–623.

Kokini, J. L. (1987). The physical basis of liquid food texture and texture-taste interactions. *Journal of Food Engineering, 6*(1), 51–81.

Kokini, J. L., & Cussler, E. L. (1983). Predicting the texture of liquid and melting semi-solid foods. *Journal of Food Science, 48*(4), 1221–1225.

Langevin, D. (2000). Influence of interfacial rheology on foam and emulsion properties. *Advances in Colloid and Interface Science, 88*(1), 209–222.

Levinson, Y., Ish-Shalom, S., Segal, E., & Livney, Y. D. (2016). Bioavailability, rheology and sensory evaluation of fat-free yogurt enriched with VD3 encapsulated in re-assembled casein micelles. *Food & Function, 7*(3), 1477–1482.

Lobato-Calleros, C., Ramírez-Santiago, C., Vernon-Carter, E. J., & Alvarez-Ramirez, J. (2014). Impact of native and chemically modified starches addition as fat replacers in the viscoelasticity of reduced-fat stirred yogurt. *Journal of Food Engineering, 131*, 110–115.

Lucey, J. A. (2001). The relationship between rheological parameters and whey separation in milk gels. *Food Hydrocolloids, 15*(4), 603–608.

Lucey, J. A. (2002). Formation and physical properties of milk protein gels. *Journal of Dairy Science, 85*(2), 281–294.

Lucey, J. A., & Singh, H. (1997). Formation and physical properties of acid milk gels: A review. *Food Research International, 30*(7), 529–542.

Mackie, A., Bajka, B., & Rigby, N. (2016). Roles for dietary fibre in the upper GI tract: The importance of viscosity. *Food Research International, 88*, 234–238.

Mackie, A. R., Ridout, M. J., Moates, G., Husband, F. A., & Wilde, P. J. (2007). Effect of the interfacial layer composition on the properties of emulsion creams. *Journal of Agricultural and Food Chemistry, 55*(14), 5611–5619.

Maher, P. G., Fenelon, M. A., Zhou, Y., Kamrul Haque, M., & Roos, Y. H. (2011). Optimization of β-casein stabilized nanoemulsions using experimental mixture design. *Journal of Food Science, 76*(8), C1108–C1117.

Maldonado-Valderrama, J., & Patino, J. M. R. (2010). Interfacial rheology of protein–surfactant mixtures. *Current Opinion in Colloid & Interface Science, 15*(4), 271–282.

McClements, D. J. (2007). Critical review of techniques and methodologies for characterization of emulsion stability. *Critical Reviews in Food Science and Nutrition, 47*(7), 611–649.

McClements, D. J., Decker, E. A., Park, Y., & Weiss, J. (2008). Designing food structure to control stability, digestion, release and absorption of lipophilic food components. *Food Biophysics, 3*(2), 219–228.

Mezger, T. G. (2014). *The rheology handbook: For users of rotational and oscillatory rheometers*. Vincentz Network, Hanover, Germany.

Morell, P., Fiszman, S. M., Varela, P., & Hernando, I. (2014). Hydrocolloids for enhancing satiety: Relating oral digestion to rheology, structure and sensory perception. *Food Hydrocolloids, 41*, 343–353.

Morris, E. (1986). Molecular origin of hydrocolloid functionality. In G. O. Phillips, D. J. Wedlock, & P. A. Williams (Eds.), *Gums and stabilisers for the food industry*. London: Elsevier Applied Science.

Muliawan, E. B., & Hatzikiriakos, S. G. (2008). Rheology of mozzarella cheese: Extrusion and rolling. *International Dairy Journal, 18*(6), 615–623.

Murray, B. S. (2002). Interfacial rheology of food emulsifiers and proteins. *Current Opinion in Colloid & Interface Science, 7*(5), 426–431.

Nakauma, M., Ishihara, S., Funami, T., & Nishinari, K. (2011). Swallowing profiles of food polysaccharide solutions with different flow behaviors. *Food Hydrocolloids, 25*(5), 1165–1173.

Nindo, C. I., Tang, J., Powers, J. R., & Takhar, P. S. (2007). Rheological properties of blueberry puree for processing applications. *LWT - Food Science and Technology, 40*(2), 292–299.

Pascua, Y., Koç, H., & Foegeding, E. A. (2013). Food structure: Roles of mechanical properties and oral processing in determining sensory texture of soft materials. *Current Opinion in Colloid & Interface Science, 18*(4), 324–333.

Patel, A. R., Cludts, N., Sintang, M. D. B., Lesaffer, A., & Dewettinck, K. (2014). Edible oleogels based on water soluble food polymers: Preparation, characterization and potential application. *Food & Function, 5*(11), 2833–2841.

Pereira, R. B., Bennett, R. J., Hemar, Y., & Campanella, O. H. (2001). Rheological and microstructural characteristics of model processed cheese analogues. *Journal of Texture Studies, 32*(5–6), 349–373.

Piska, I., & Štětina, J. (2004). Influence of cheese ripening and rate of cooling of the processed cheese mixture on rheological properties of processed cheese. *Journal of Food Engineering, 61*(4), 551–555.

Pradal, C., & Stokes, J. R. (2016). Oral tribology: Bridging the gap between physical measurements and sensory experience. *Current Opinion in Food Science, 9*, 34–41.

Prakash, S., Ma, Q., & Bhandari, B. (2014). Rheological behaviour of selected commercially available baby formulas in simulated human digestive system. *Food Research International, 64*, 889–895.

Pralle, A., Keller, P., Florin, E. L., Simons, K., & Horber, J. K. (2000). Sphingolipid-cholesterol rafts diffuse as small entities in the plasma membrane of mammalian cells. *The Journal of Cell Biology, 148*, 997–1008.

Ptaszek, A. (2010). Rheological equation of state for shear-thickening food systems. *Journal of Food Engineering, 100*(2), 322–328.

Puri, V. M., & Anantheswaran, R. C. (1993). The finite-element method in food processing: A review. *Journal of Food Engineering, 19*(3), 247–274.

Ramaswamy, H. S., & Basak, S. (1991). Rheology of stirred yogurts. *Journal of Texture Studies, 22*(2), 231–241.

Rao, M. A. (1977). Measurement of flow properties of fluid foods - developments, limitations, and interpretation of phenomena. *Journal of Texture Studies, 8*(3), 257–282.

Rao, M. A., Okechukwu, P. E., Da Silva, P. M. S., & Oliveira, J. C. (1997). Rheological behavior of heated starch dispersions in excess water: Role of starch granule. *Carbohydrate Polymers, 33*(4), 273–283.

Rok, K., Michael, G., Ana, G., & Saša, N. (2017). Viscoelastic behaviour of hydrogel-based composites for tissue engineering under mechanical load. Biomedical Materials, 12(2), 025004

Richardson-Harman, N. J., Stevens, R., Walker, S., Gamble, J., Miller, M., Wong, M., & McPherson, A. (2000). Mapping consumer perceptions of creaminess and liking for liquid dairy products. *Food Quality and Preference, 11*(3), 239–246.

Ring, S. G., & Stainsby, G. (1985). A simple method for determining the shear modulus of food dispersions and gels. *Journal of the Science of Food and Agriculture, 36*(7), 607–613.

Rousseau, D. (2000). Fat crystals and emulsion stability — A review. *Food Research International, 33*(1), 3–14.

Roussel, N. (2006). A thixotropy model for fresh fluid concretes: Theory, validation and applications. *Cement and Concrete Research, 36*(10), 1797–1806.

Rozzi, S., Massini, R., Paciello, G., Pagliarini, G., Rainieri, S., & Trifirò, A. (2007). Heat treatment of fluid foods in a shell and tube heat exchanger: Comparison between smooth and helically corrugated wall tubes. *Journal of Food Engineering, 79*(1), 249–254.

Sablani, S. S., & Shayya, W. H. (2003). Neural network based non-iterative calculation of the friction factor for power law fluids. *Journal of Food Engineering, 57*(4), 327–335.

Santos, J., Calero, N., Guerrero, A., & Muñoz, J. (2015). Relationship of rheological and microstructural properties with physical stability of potato protein-based emulsions stabilized by guar gum. *Food Hydrocolloids, 44*, 109–114.

Schmitt, L., Ghnassia, G., Bimbenet, J. J., & Cuvelier, G. (1998). Flow properties of stirred yogurt: Calculation of the pressure drop for a thixotropic fluid. *Journal of Food Engineering, 37*(4), 367–388.

Selway, N., & Stokes, J. R. (2013). Insights into the dynamics of oral lubrication and mouthfeel using soft tribology: Differentiating semi-fluid foods with similar rheology. *Food Research International, 54*(1), 423–431.

Shaker, R. R., Jumah, R. Y., & Abu-Jdayil, B. (2000). Rheological properties of plain yogurt during coagulation process: Impact of fat content and preheat treatment of milk. *Journal of Food Engineering, 44*(3), 175–180.

Sharma, P., Munro, P. A., Gillies, G., Wiles, P. G., & Dessev, T. T. (2017). Changes in creep behavior and microstructure of model Mozzarella cheese during working. *LWT - Food Science and Technology, 83*, 184–192.

Shelat, K. J., Vilaplana, F., Nicholson, T. M., Gidley, M. J., & Gilbert, R. G. (2011). Diffusion and rheology characteristics of barley mixed linkage β-glucan and possible implications for digestion. *Carbohydrate Polymers, 86*(4), 1732–1738.

Sherman, P. (1969). A texture profile of foodstuffs based upon well-defined rheological properties. *Journal of Food Science, 34*(5), 458–462.

Shimada, K., & Cheftel, J. C. (1989). Sulfhydryl group/disulfide bond interchange reactions during heat-induced gelation of whey protein isolate. *Journal of Agricultural and Food Chemistry, 37*(1), 161–168.

Singh, H., Ye, A., & Horne, D. (2009). Structuring food emulsions in the gastrointestinal tract to modify lipid digestion. *Progress in Lipid Research, 48*(2), 92–100.

Soukoulis, C., Lyroni, E., & Tzia, C. (2010). Sensory profiling and hedonic judgement of probiotic ice cream as a function of hydrocolloids, yogurt and milk fat content. *LWT - Food Science and Technology, 43*(9), 1351–1358.

Stading, M., & Hermansson, A.-M. (1990). Viscoelastic behaviour of β-lactoglobulin gel structures. *Food Hydrocolloids, 4*(2), 121–135.

Štern P., Pokorný J., Šedivá A., Z. Panovská Z. (2008). Rheological and sensory characteristics of yoghurt-modified mayonnaise. Czech Journal of Food Sciences 26 (No. 3):190–198.

Stokes, J. R., & Telford, J. H. (2004). Measuring the yield behaviour of structured fluids. *Journal of Non-Newtonian Fluid Mechanics, 124*(1), 137–146.

Svegmark, K., & Hermansson, A.-M. (1991). Changes induced by shear and gel formation in the viscoelastic behaviour of potato, wheat and maize starch dispersions. *Carbohydrate Polymers, 15*(2), 151–169.

Szabó, B., Szabo, B. A., & Babuška, I. (1991). *Finite element analysis*. New York: Wiley.

Tadros, T. F. (1993). Industrial applications of dispersions. *Advances in Colloid and Interface Science, 46*, 1–47.

Tadros, T. F. (2004). Application of rheology for assessment and prediction of the long-term physical stability of emulsions. *Advances in Colloid and Interface Science, 108-109*, 227–258.

Tadros, T. F. (2012). *Dispersion of powders in liquids and stabilization of suspensions*. Weinheim: Wiley.

Taherian, A. R., Fustier, P., Britten, M., & Ramaswamy, H. S. (2008). Rheology and stability of beverage emulsions in the presence and absence of weighting agents: A review. *Food Biophysics, 3*(3), 279–286.

Tárrega, A., Durán, L., & Costell, E. (2004). Flow behaviour of semi-solid dairy desserts. Effect of temperature. *International Dairy Journal, 14*(4), 345–353.

Thakur, R. K., Vial, Ch., Djelveh, G. (2008). Effect of composition and process parameters on elasticity and solidity of foamed food. Chemical Engineering and Processing: *Process Intensification, 47*(3):474–483.

Tripathi, A., Whittingstall, P., & McKinley, G. H. (2000). Using filament stretching rheometry to predict strand formation and "processability" in adhesives and other non-Newtonian fluids. *Rheologica Acta, 39*(4), 321–337.

Tunick, M. H. (2000). Rheology of dairy foods that gel, stretch, and fracture. *Journal of Dairy Science, 83*(8), 1892–1898.

Tunick, M. H. (2011). Small-strain dynamic rheology of food protein networks. *Journal of Agricultural and Food Chemistry, 59*(5), 1481–1486.

van Aken, G. A. (2010). Modelling texture perception by soft epithelial surfaces. *Soft Matter, 6*(5), 826–834.

van Vliet, T., van Dijk, H. J. M., Zoon, P., & Walstra, P. (1991). Relation between syneresis and rheological properties of particle gels. *Colloid and Polymer Science, 269*(6), 620–627.

Vélez-Ruiz, J. F., & Barbosa-Cánovas, G. V. (1998). Rheological properties of concentrated milk as a function of concentration, temperature and storage time. *Journal of Food Engineering, 35*(2), 177–190.

Verheul, M., Roefs, S. P. F. M., Mellema, J., & de Kruif, K. G. (1998). Power law behavior of structural properties of protein gels. *Langmuir, 14*(9), 2263–2268.

Wendt, J. F. (2008). *Computational fluid dynamics: An introduction*. Berlin Heidelberg: Springer.

Wilkinson, C., Dijksterhuis, G. B., & Minekus, M. (2000). From food structure to texture. *Trends in Food Science & Technology, 11*(12), 442–450.

Wium, H., Qvist, K. B., & Gross, M. (1997). Uniaxial compression of uf-feta cheese related to sensory texture analysis. *Journal of Texture Studies, 28*(4), 455–476.

Wu, B.-C., Degner, B., & McClements, D. J. (2013). Creation of reduced fat foods: Influence of calcium-induced droplet aggregation on microstructure and rheology of mixed food dispersions. *Food Chemistry, 141*(4), 3393–3401.

Zhao, Q., Kuang, W., Fang, M., Sun-Waterhouse, D., Liu, T., Long, Z., & Zhao, M. (2015). Frozen, chilled and spray dried emulsions for whipped cream: Influence of emulsion preservation approaches on product functionality. *LWT - Food Science and Technology, 62*(1, Part 1), 287–293.

Overview: Semisolid Foods

Juzhong Tan

1 Overview: Semisolid Foods

Foods can be classified into fluids, semisolids, and solids by their physical properties, such as rheological behavior and texture (Rao 2013). Fluid foods do not have the ability to support their own weight and retain their shape, but flow readily under an applied force, including gravitational forces. Solid foods, other the other hand, have the ability to retain their shape and do not flow under applied force. Rather, they tend to deform and fracture under sufficiently high forces. Semisolid foods share some properties with both fluid and solid foods, having the ability to retain their shape but flowing under pressure or force. Although semisolid foods can be recognized by determining whether they can hold their shape under an applied force, there is no specific measurable parameter (e.g. elasticity, viscosity, or yield stress) that can be used to quantitatively determine whether a material is semisolid. Typically, semisolid food materials exhibit both elastic and viscous behaviors, having higher viscosity than fluid materials and lower elasticity than solid materials. At the microscopic scale, semisolid food materials typically are amorphous solids, with disordered structure and randomly distributed molecules. Unlike many solid materials which have ionic bonding, semisolid materials are covalent substances, which have weaker bonds compared to ionic bonds. The microstructure of semisolid foods determines their flow behaviors and texture. Table 1 shows the wide variety of flow behaviors, textural attributes, and structuring components that can be present in semisolid foods.

J. Tan (✉)
Department of Food Science, Rutgers, The State University of New Jersey, New Brunswick, NJ, USA
e-mail: jt928@sebs.rutgers.edu

H. S. Joyner (ed.), *Rheology of Semisolid Foods*, Food Engineering Series,
https://doi.org/10.1007/978-3-030-27134-3_2

Table 1 Semisolid food examples and their flow behavior models, texture, and structuring components

Food	Viscosity range (Pa.s)	Flow behavior model	Important textural attributes	Structuring components	References
Mayonnaise	1.5–13.8	Herschel-Bulkley, Power law	Creaminess, cohesiveness, firmness, consistency, viscosity	Egg yolk lectin, fat droplet amount and size distribution	Maruyama et al. (2007); Ma and Barbosa-Cánovas (1995); Liu et al. (2007)
Yogurt	0.045–4.39	Power law, Casson, Herschel-Bulkley	Thickness, ropiness, smoothness, graininess	Casein network, fat globule amount and size distribution, gum	Karagül-Yüceer and Drake (2013); Benezech and Maingonnat (1994)
Butter spread	0.01–350	Herschel-Bulkley, Casson, Bingham	Creaminess, spreadability, firmness	Stabilizers, emulsifiers, fat crystal amount and size distribution	Taghizadeh and Razavi (2009); Singh et al. (2000); Totlani and Chinnan (2007)
Sauce	0.1–20.0	Power law, Casson, Herschel-Bulkley, Mizrahi-Berk	Smoothness, creaminess, thickness, viscosity	Stabilizers, emulsifiers, vegetable tissues	Rao et al. (1986); Sikora et al. (2007); Gamonpilas et al. (2011)
Ice cream	~1.0	Power law	Firmness, creaminess, coldness, coarseness	Ice and fat crystal size distribution, air bubble size distribution, overrun, stabilizers, emulsifiers	Bahramparvar et al. (2010)
Ice cream mix	0.01–0.1	Power law	Creaminess, firmness	Stabilizers and emulsifiers, fat crystals	Cottrell et al. (1980); Kuş et al. (2005)
Whipped cream	0.1–1.0	Cross model	Creaminess	Stabilizers and emulsifiers, fat crystals, air bubble size distribution, overrun, milk proteins	Camacho et al. (2005); Noda and Shiinoki (1986)
Salad dressing	0.5–2.5	Power law	Thickness, firmness, grittiness	Stabilizers, oil droplets	Ma et al. (2013); Lai and Lin (2004)

1.1 Typical Semisolid Food Behaviors

Although semisolid foods vary widely in their structural features, rheological behaviors, and texture attributes, they generally exhibit at least some degree of the behaviors described below. These behaviors can be used to qualitatively separate foods that are soft solids or high-viscosity fluids from foods that are semisolids.

1.1.1 Slumping

Semisolid foods can temporarily hold their shape. However, under external forces such as gravity, their shape may collapse. This phenomenon is called 'slumping' (Fig. 1). Slumping may be induced by phase transition. For example, at room temperature (20–25 °C), ice cream slumps when fat and water crystals partially or totally melt. Some semisolid foods, such as yogurt, salad dressing, and mayonnaise, may slump due to their supporting structure collapsing under its own weight.

Torsion, shear, and uniaxial compression can also make semisolid foods slump. Food gels, such as tofu, can dictate the failure mode of slumping and serum expulsion under compression force (Truong and Daubert 2000). Gellan gels (~1% w/w gellan gum) (Lelievre et al. 1992) and casein gels (Konstance et al. 1995) also slump under uniaxial compression and shear forces.

1.1.2 Spreading

Some semisolid foods, such as peanut butter and margarine, need to be spreadable at room temperature. Those foods require a certain amount of stress (yield stress) for adequate spreading and deformation (Daubert et al. 1998). Spreadability indicates how easily a food can be spread evenly over a surface and is one of the most essential features perceived by consumers (Glibowski et al. 2008). The spreadability of semisolid foods is the net result of a combination of rheological behaviors, of which viscosity is the most important. Increased viscosity typically decreases spreadability due to the increased resistance to flow. Additionally, increasing solid fat content in some lipid-based semisolid foods, such as spreads, margarine, cream cheese, and butter, can cause an increase in hardness and decrease spreadability.

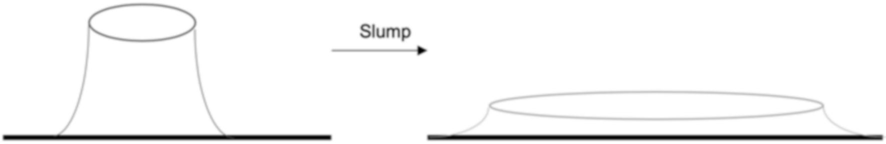

Fig. 1 Schematic of slumping

Typically, the consumer assesses the spreadability of semisolid foods using a knife. In a study by Kokini and Dickie (1982), the inverse of the torque needed to generate a given deformation was assessed as spreadability. The spreading action was then modeled by relating spreadability to the torque on a knife during application, which was used to estimate a transient, maximum shear stress.

1.1.3 Separation

Under some conditions, such as temperature variation, stirring or agitating, and pH change, semisolid foods can sperate into two or more phases. For example, peanut butter can show a visible oil layer on top and yogurt syneresis causes a layer of fluid whey to appear on the surface of the yogurt gel; neither of these separated products is appealing to consumers. These semisolid foods typically contain emulsions structures (see Sect. 2.1), and the separation is caused by the destabilization of the emulsion structure. The separation of an emulsion into its component phases is a two-step process. The first step is flocculation (aggregation, agglomeration, or coagulation), where the droplets clump together, forming aggregates or "flocs". The second step is coalescence, in which water/oil droplets coalesce together to form a continuous phase. This is an irreversible process that leads to a decrease in the number of water droplets and eventually to complete separation of the emulsion phases (Schramm 1992; Bobra 1990) (Fig. 2).

Syneresis is a phenomena during which liquid is expressed from a hydrogel. This phenomena can happen during yogurt storage and is considered as a defect. Syneresis can be induced by heat, external force, and pH, which can cause removal or break down of hydrophilic sites (Mizrahi 2010). Yogurt syneresis can be reduced by increasing the milk solids to ~15%, using stablizers (e.g. polysaccharides), or using exopolysaccharide (EPS)-producing starter cultures (Amatayakul et al. 2006).

Application of heat promotes the separation process of emulsions in semisolid food. Increased temperature can reduce the viscosity of the oil and the mobility of the water/oil droplets, promoting droplet collisions and favoring coalescence. Heat also weakens or ruptures the film on water/oil droplets because of water expansion and enhances film drainage and coalescence (Chen and Tao 2005).

In some cases, agitating or stirring increase the stability of emulsions. High speed agitating or stirring can causes violent mixing of oil and water and leads to smaller

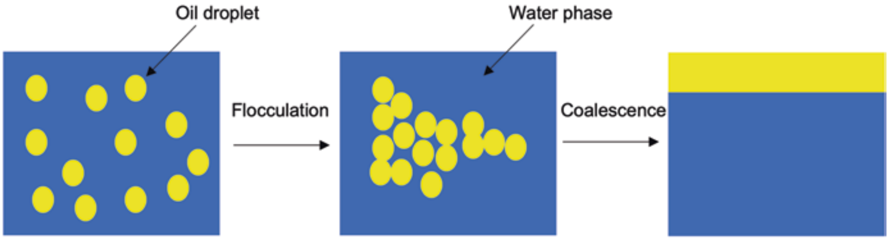

Fig. 2 Destabilization of an o/w emulsion

droplet sizes, which are relatively more stable than larger droplets (Floury et al. 2003). In some cases, such as butter churning, the stability of emulsions is affected adversely by agitation due to high speed collisions between droplets (Buldo et al. 2013).

2 Structural Variety in Semisolid Foods

Semisolids foods typically consist of two or more immiscible components such as water, oil, and fibers. The stabilization of their structure is achieved by processing methods such as homogenization, thermal treatment, and acidification to form stable structures. Emulsions and protein–polysaccharide networks are two common structures of semisolid foods. Both of these structures play an important role in sustaining stability (Dickinson 2009), delivering desirable sensory attributes (Chen 2014), and maintaining flavors (Mao et al. 2017). Several comprehensive reviews on food emulsions (Muschiolik 2007; Dalgleish 2010) and protein–polysaccharide networks (Lam and Nickerson 2013) have been published; these topics are covered in more detail in these reviews.

2.1 Emulsions

Emulsions are colloidal systems containing either water dispersed in oil (w/o) or oil dispersed in water (o/w). Water and oil are mixed in a way that droplets of one fluid are dispersed within another (Fig. 3) (Dickinson 2010). These droplets may vary in size from the micro-to the nanometer scale. Therefore, while there are still two different phases in the material, properly stabilized emulsions look homogeneous on a macroscopic scale. Emulsions may be stabilized by emulsifiers, which have a polar, hydrophilic section and a nonpolar, hydrophobic section. Due to these amphiphilic properties, emulsifiers are able to coat the emulsion droplets, aligning their polar and nonpolar regions with the water and oil phases, respectively. This reduced the

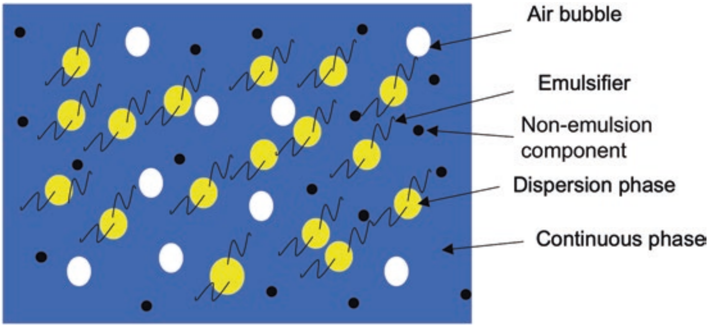

Fig. 3 Schematic of a stabilized emulsion

likelihood of the emulsion droplets to flocculate or coalesce (Dickinson 1987). Many semisolid foods, including salad dressing, yogurt, whipped cream, frozen desserts, and margarine, are stabilized emulsions.

2.1.1 Oil-in-Water Emulsions

Oil-in-water (o/w) emulsions are common in semisolid foods. For example, the crema in espresso is an unstable oil-in-water emulsion, in which the milkfat is the oil phase and the coffee is the water phase. Mayonnaise is an o/w emulsion with a high oil volume fraction (70–80%), which provides its high viscosity (Nikzade et al. 2012). Because the oil volume fraction is so high, mayonnaise must be stabilized with egg yolk lecithin or other stabilizers or it will separate during storage. Salad dressing is vegetable oil droplets dispersed in water (vinegar); other ingredients, such as vegetable pices and spices, may be suspsended in the water phase as well. Ice cream mix is a stabilized o/w emulsion that is converted into a foam when air is incorporated during production. The stability of the ice cream emulsion controls its texture: poorly stabilized ice cream may have a coarse texture due to formation of large fat crystals and improper incorporation of air.

2.1.2 Water-in-Oil Emulsions

Water-in-oil (w/o) emulsions are less common in foods, but still exist. For example, butter is an emulsion of water droplets dispersed in milkfat. Solid margarines are also a w/o emulsion with tiny water droplets disperse in a fat phase that is in a stable crystalline form. Margarine and butter have similar fat content (≥80% fat). However, margarine consists not only of a relatively wide range of triacylglycerols but also contains different ingredients in the aqueous phase, such as emulsifiers and preservatives. Conversely, the composition of butter is relatively consistent: in the US, butter is not legally permitted to contain any ingredients but Grade A milk, salt, and colorants. The only compositional changes result from milk composition variation due to the breed of cow, the type of feed provided to the cow, and stage of lactation (Juriaanse and Heertje 1988).

2.1.3 Emulsion Destabilization

Destabilization of emulsions happens when the driving force for coalescence promotes flocculation of small droplets, which subsequently form large droplets, and eventually form a continuous phase of the formerly dispersed fluid. Destabilization typically is not desirable for semisolid foods (Syrbe et al. 1998). For example, oil separation in peanut butter and salad dressing is not palatable to consumers. To prevent emulsion destabilization, hydrocolloids (emulsifiers) can be used to provide physical barriers to prevent droplets from coming together. Reducing the driving force between droplets by reducing the thermodynamic energy level of the system through changing pH or ionic strength can also help prevent destabilization (Dalgleish 2006). Furhtermore, reducing oil droplet size can help stabilize emulsions, as this increases the time needed for coaleascence based on Stokes' Law (see Chapter "Introduction: Measuring Rheological Properties of Foods").

2.2 Protein and Polysaccharide Networks

Some semisolids foods are structured by aggregated proteins with trapped or attached polysaccharide molecules. For example, yogurts have protein networks formed by aggregated casein micelle chains or clusters when the pH of heat-treated milk drop to the isoelectric point of casein (pH 4.6) (Lee and Lucey 2010). Polysaccharides, including gums, starches, pectin, and dietary fibers, are often used to modify the structure by attaching and embedding to the protein networks (Fig. 4). Adding functional ingredients to yogurt or using different processing strategies or treatments can change the microstructure of yogurts, influencing their physicochemical properties and texture.

2.3 Crystallization of Triacylglycerols

Solid or partially solid lipds can also serve as structuring materials. The specific structure of the lipid depends on its origin. For example, shortening is composed of fluid oil and fat crystals; it is structured by a network of fat crystals (Heertje et al. 1987). Margarine has a fat crystal network that similar to shortening. The main difference in structure is the presence of water droplets in margarine, which disrupts the continuous fat phase (Juriaanse and Heertje 1988). Ice cream has a complex microstructure consisting of ice crystals, air bubbles, and partially coalesced and aggregated fat globules, all of which are surrounded by a continuous matrix of sugars, proteins, salts, polysaccharides, and water (Clarke 2015).

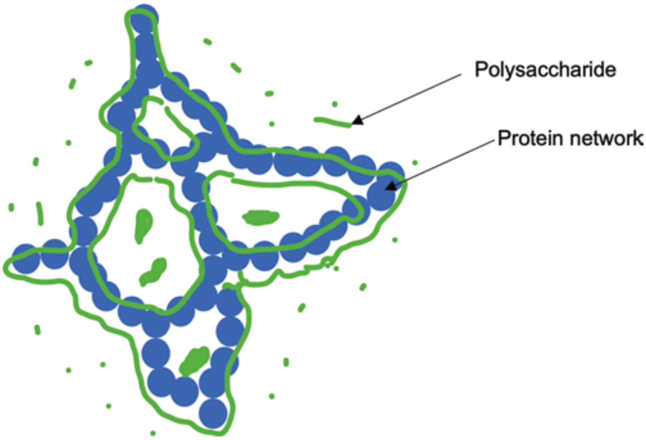

Fig. 4 Typical yogurt microstructure

Fat droplets in food may coalesce or aggregate upon whipping or freezing, which results in large particle sizes and a more heterogeneous particle size distribution. In ice cream, decreased fat cystal size can reduce the storage modulus and increase metling time (Granger et al. 2005). Particle size of fat crystals also contributes to the sensory attributes of ice cream. For example, particle sizes between 0.1 and 2 um provide a creamy sensation; however, particles >3 um can result in a gritty or powdery mouthfeel (Ohmes et al. 2010).

3 Rheological Behaviors of Semisolid Food

3.1 Viscosity

Viscosity measures the ability of a materials to resist flow and gradual deformation by shear stress or tensile stress (Vocaldo 2007). For semisolid foods, viscosity typically refers to dynamic viscosity or apparent viscosity, which is calculated by:

$$\eta = \frac{\sigma}{\left(\frac{\Delta u}{\Delta x}\right)} \tag{1}$$

where η is apparent viscosity (Pa.s), σ is shear stress (Pa), and $\frac{\Delta u}{\Delta x}$ is the velocity gradient (1/s). Depending on the geometry used for viscosity measurement, the velocity gradient can be represented by shear rate ($\dot{\gamma}$), e.g. when parallel plates are used. A demonstration of a setup used to measure dynamic viscosity is shown in Fig. 5. In viscosity measurements, a shear rate or shear rate sample is applied to a material and the resulting shear stress measured. Viscosity is then calculated using Eq. 1. Measuring viscosity over a range of shear rates allows a flow profile of the material to be generated. This flow profile can be used to predict the material's viscosity and flow behaviors under a range of industrial and oral processing conditions.

There are several types of viscosity aside from apparent viscosity. Kinematic viscosity can be obtained by dividing apparent (dynamic) viscosity by density. Bulk viscosity (volume viscosity) measures the internal friction resistance to flow when a compressible fluid or semisolid is compressed or expanded evenly by sound or shock waves. It can be used to explain the loss of energy in sound and shock waves

Fig. 5 Diagram of dynamic viscosity

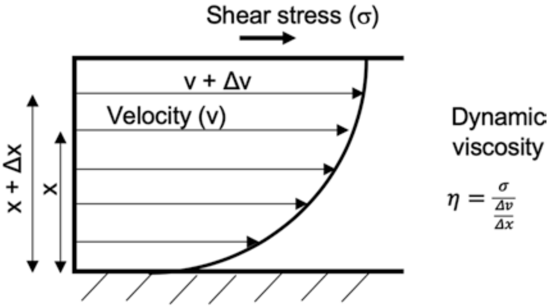

Table 2 Apparent viscosity of liquid and semisolid materials

Food	Temperature (°C)	Viscosity range (Pa.s)	Physical state	Reference
Water	25	0.001	Liquid	Kestin et al. (1978)
Honey	25	3–24	Liquid	Yanniotis et al. (2006)
Corn syrup	25	1.3806	Liquid	Lide (2003)
Milk	25	0.002–0.06	Liquid	Bakshi and Smith (1984)
Seed oil	26	0.032–0.057	Liquid	Diamante and Lan (2014)
Mayonnaise	25	13.8–1.5	Semisolid	Maruyama et al. (2007)
Stirred yogurt	25	0.045–0.057	Semisolid	Ramaswamy and Basak (1991)
Set yogurt	20	2.28–4.39	Semisolid	Paseephol et al. (2008)
Goat milk yogurt	5	0.5–2	Semisolid	Li and Guo (2006)
Nonfat yogurt	10	5.38–120	Semisolid	Teles and Flôres (2007)

described by Stokes' law of sound attenuation (Hirai and Eyring 1958). Note that this is not the same Stokes' Law used for determining the rate of suspension creaming or settling, although G. G. Stokes did publish both laws.

The viscosity ranges of selected typical fluids and semisolids at certain temperatures are listed in Table 2. Fluid foods typically have low viscosity; for example, seed oil has viscosity of 2–60 mPa.s. Semisolid materials, however, have much higher viscosity than fluid materials; for example, mayonnaise has a viscosity of 1.5–13.8 Pa.s, a threefold increase in order of magnitude compared to many fluids. Viscosity of many semisolid and fluid foods are temperature-dependent. Generally, higher temperatures promote lower viscosities because the increased thermal energy allows the molecules in the material to more more freely. However, the viscosity changes in some foods due to temperature fluctuations can change the physical state of the food or food components, significantly increasing or decreasing the viscosity. These changes may be reversible or irreversible. For example, fluid egg becomes solid at temperatures >60 °C due to protein denaturation and gelation (Icier and Bozkurt 2011); hard candies become semisolid below their glass transition temperature (Tan and Kerr 2017); food polymer solutions (whey protein, carrageenan, and casein) transform from fluid to a solid gel at temperatures >80 °C due to increased entanglements, structural rearrangement, and gelation (Tan and Joyner 2018); and milk (fluid) turns into to yogurt (semisolid) due to the heat and acidification during yogurt production, which causes whey proteins to denature and casein proteins to aggregate, forming a gel (Lee and Lucey 2010). An example of how tomato salad dressing viscosity changes as a function of temperature and shear rate is shown in Fig. 6. These changes may cause noticeable differences in processing ability and texture perception.

3.1.1 Newtonian Behavior

Newtonian behavior is a flow behavior with a simple linear relation between shear stress and shear rate (Fig. 7). This relation is known as Newton's law of viscosity, in which shear stress is equal to the product of of viscosity and shear rate. Because shear

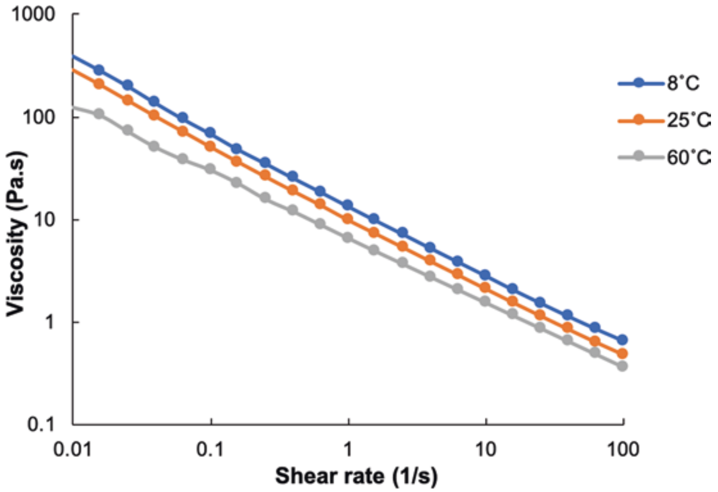

Fig. 6 Viscosity of tomato salad dressing as a function of shear rate at different temperatures

Fig. 7 Shear stress of Newtonian and Bingham plastic fluids as a function of shear rate

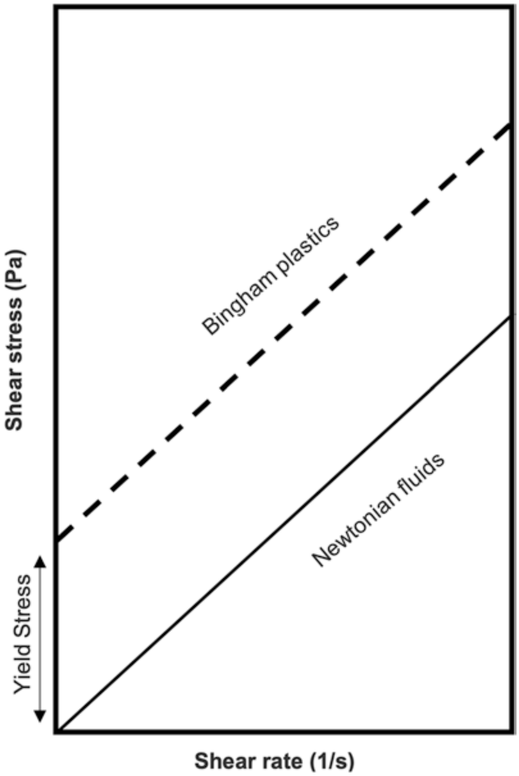

stress scales linearly with shear rate, the viscosity of Newtonian fluids is constant over all shear rates. Newtonian fluids typically comprise small isotropic molecules, which can easily orient to the direction of flow (Walters 1962). Some example of Newtonian fluids are water, honey, milk, mineral oil, and organic solvents. Some large anisotropic molecules in dilute solutions, such as protein or polysaccharides, can also exhibit Newtonian behavior (Hemar et al. 2001). However, higher concentrations of these polymers result in non-Newtonian behaviors, which can manifest in a variety of ways.

3.1.2 Non-Newtonian Behavior: Yield Stress

Fluids and semisolids may require an external force to initiate flow. This force is called yield stress. Materials that require a yield stress to flow but show Newtonian behavior upon the initiation of flow are called Bingham plastics (Bingham 1916). It is also possible for these materials to show non-Newtonian flow behaviors; these behaviors are discussed further in subsequent sections. Typical Bingham plastic foods include mayonnaise and tomato paste. The following equation, known as the Bingham model, describes the relationship between the shear stress and shear rate of a Bingham plastic material. Figure 7 shows the viscosity of Bingham plastics as a function of shear rate compares to Newtonian fluids.

$$\sigma = \sigma_o + \mu_{pl}\dot{\gamma} \tag{2}$$

Here, σ_o is the yield stress (Pa.s) and μ_{pl} is the plastic viscosity (Pa.s).

Materials that exhibit a yield stress are considered to have a structural network extending throughout the entire volume of the system. The strength of this network is dependent on the strength and type of interactions between the molecules comprising the network as well as the structure of the dispersed phase and the strength and type of its interactions with the network. Typically, after the yield stress is reached, the viscosity is relatively low; however, before the applied force reaches the yield stress, the strong interactions among the structural components can cause the material to behave like a solid, deforming instrad of flowing (Larson 1999).

3.1.3 Non-Newtonian Behavior: Shear-Dependency

Most semisolid foods are non-Newtonian, which means their viscosity is dependent on shear rate. Unlike Newtonian fluids, non-Newtonian materials do not have a linear relationship between shear stress and shear rate. The ratio of the two parameters, which is viscosity, increases (dilatant fluids) or decreases (pseudoplastic fluids) as shear rate increases (Fig. 8).

The viscosity of pseudoplastic fluids decreases with the rate of shear; therefore, another term for this behavior is shear-thinning. A dilatant or shear-thickening material is one in which viscosity increases with shear rate. This behavior is typically observed in suspensions or colloids instead of homogeneous materials. While

Fig. 8 Shear rate dependency of Herschel-Bulkley, pseudoplastic, Newtonian, and dilatant fluids

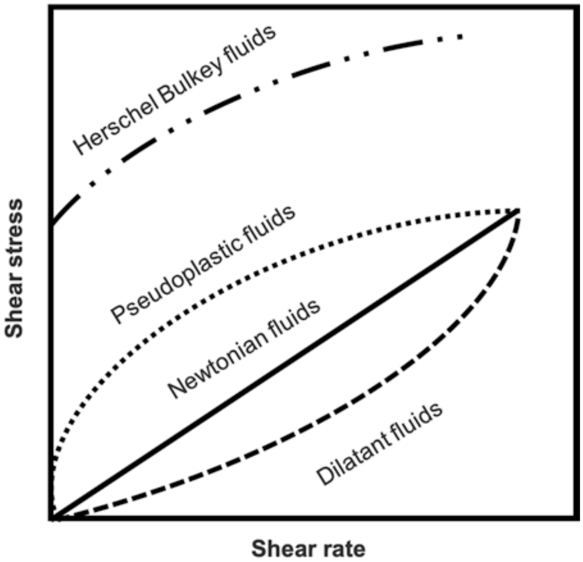

there are not many shear-thickening food materials, a classic example is a suspension of cornstarch and water. Many semisolid foods, such as yogurt, hydrocolloid solutions, cheese sauces, and chocolate milk show shear-thinning behavior. It is hypothesized that shear-thinning behaviors are due to large molecular chains that tumble at random, and the large hydrodynamic radius can significantly affect the resistance to flow of fluids under low shear. Under increasing shear rates, these large molecular chains gradually align themselves in the direction of the shear force, which allows them to slip past each other and decreases the resistance of flow (Saramito 2016). In the case of case of full fat yogurt, the large molecules that align with applied force incldue caseins, fat globules, and whey proteins.

The power law equation is often sufficient for describing shear-dependent behaviors:

$$\sigma = K\left(\dot{\gamma}\right)^{n} \tag{3}$$

where K is the flow consistency index (Pa.s^n) and n is the flow behavior index (unitless). n typically falls between 0 and 1 for pseudoplastic materials. If n is >1, the flow behavior is dilatant, and if n is equal to 1, the flow behavior is Newtonian, and the equation collapses to the equation for Newtonian fluids.

Many shear-dependent materials also have a yield stress. A general model for these materials, the Herschel-Bulkley model, is established by adding a yield stress term to the power law model:

$$\sigma = \sigma_0 + K\left(\dot{\gamma}\right)^{n} \tag{4}$$

Herschel-Bulkley flow behavior is shown in Fig. 8. Note that the example of Herschel-Bulkley flow in this figure is of a material that shows pseudoplastic behavior after intiation of flow. It is possible for the material to exhibit dilatant behavior after flow initiation, but this is not common in food products.

One disadvantage of the power law and Herschel-Bulkley models is that they do not fit many materials well in the low-shear and high-shear ranges. Because zero-shear viscosity is important for characterizing the stability of many foods, models that account for zero-shear viscosity are needed for proper modeling of these food systems. Moreover, for a relatively highly viscoelastic gelled food material, e.g. Greek yogurt, a certain amount of force or stress (yield stress) is needed before it starts to flow. Thus, more comprehensive models that include zero-shear viscosty, infinite-shear viscosity, or both are needed for better describing certain semisolid food materials. Examples of these models are shown in the equations below. For additional models and a more detailed explanation of the models presented here, the reader is encouraged to review Metzger's The Rheology Handbook (Mezger 2014).

Casson model:

$$\sigma^{\frac{1}{2}} = \sigma_C^{\frac{1}{2}} + \left(\eta_C \dot{\gamma}\right)^{\frac{1}{2}} \tag{5}$$

Cross model (simplified version):

$$\frac{\eta(\dot{\gamma})}{\eta_0} = \frac{1}{1 + \left(C\dot{\gamma}\right)^p} \tag{6}$$

Carreau model (simplified version):

$$\frac{\eta(\dot{\gamma})}{\eta_0} = \frac{1}{\left(1 + \left(C_1\dot{\gamma}\right)^2\right)^{P_c}} \tag{7}$$

In the equations above, σ_C is the Casson yield stress; η_C is Casson viscosity (Pa), C is the Cross constant (s), P is the Cross exponent, η_0 is zero-shear viscosity (Pa.s), C_1 (s) is the Carreau constant (s), and P_c is the Carreau exponent.

Like other semisolid foods, the viscosity and shear-dependent behavior of yogurt can be modified. Many factors including fat and whey protein content, heating temperature and time, and microbial cultures used for fermentation can impact the rheological properties of yogurts. Temperature and duration influence yogurt viscosity by changing the aggregate size of whey proteins, which in turn is influenced by covalent (disulfide) interactions arising from denaturation of globular whey proteins (Shaker et al. 2000). Formulation can have a dramatic impact on yogurt flow behaviors. Decreased fat content in yogurt can also result in low viscosity due to the decrease in total milk solids. Fat content also has a significant influence on the firmness of yogurt gels (Shaker et al. 2000). Higher whey protein concentration can result in higher yield stress and viscosity in yogurt by forming more dense and intense network (Damin et al. 2009). Adding dietary fibers to yogurt can either increase or decrease the apparent viscosity of yogurt depending on the source of fiber and its interaction with the other yogurt ingredients. Previous work has indicated that adding apple fiber can significantly increase yogurt apparent viscosity; however, addition of bamboo, wheat, and inulin fibers slightly decreased its apparent viscosity (Dello Staffolo et al. 2004). Addition of other food polymers such as pectin also contributes to an increase of apparent viscosity and flow behavior index (reduced shear shinning) (Basak and Ramaswamy 1994). Calcium-fortified fruit yogurt has less shear-thinning behavior and higher apparent viscosity than non-fortified yogurt due to the increased number of colloidal calcium phosphate (CCP) linkages between casein micelles and hence, a stronger yogurt gel network (Singh and Muthukumarappan 2008). Figure 9 shows the mechanism of how CCP strengthens the casein network in yogurt.

Figure 10 shows diagrams of the mechanism of shear-thickening behaviors in a colloidal system. Here, repulsion forces (van der Waals forces) keep the suspended particles from aggregating with other particles. When shear force become dominant, the particles begin to flocculate, forming bigger particles. This disrupts the suspension system, resulting in a viscosity increase (Morrison and Ross 2002).

3.1.4 Non-Newtonian Behavior: Time Dependency

The viscosity of some semisolid food materials changes over time due to continually applied shear. Thixotropic materials show a decrease in viscosity over time, while rheopectic materials show an increase in viscosity over time (Fig. 11). After the applied shear is removed or at least lowered to minimal shear, the material may return to its original viscosity over time. Thixotropy is observed when shear forces disrupt the microstructure of materials; this structure may partially or totally recover when the material is quiescent. The driving force for thixotropic behavior is the

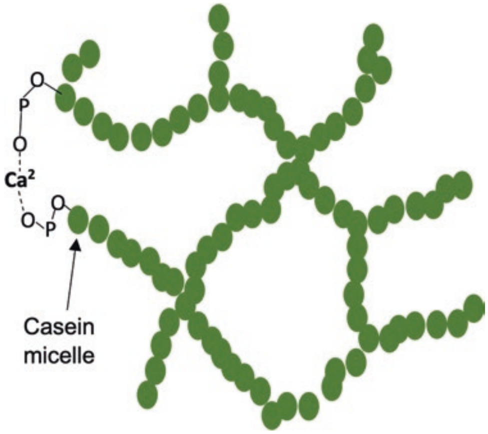

Fig. 9 Colloidal calcium phosphate (CCP) in a casein network

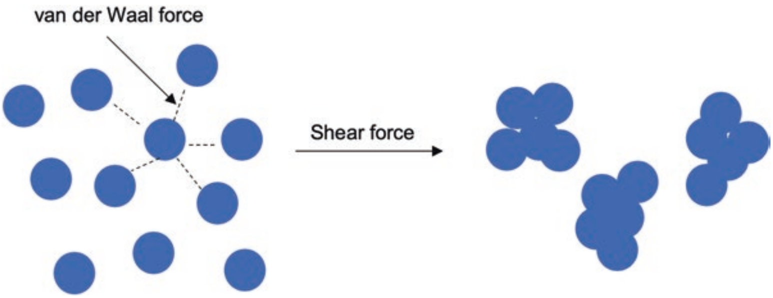

Fig. 10 Microstructural changes in a shearing-thinning material under shear

Fig. 11 Thixotropic and rheopectic fluid behaviors

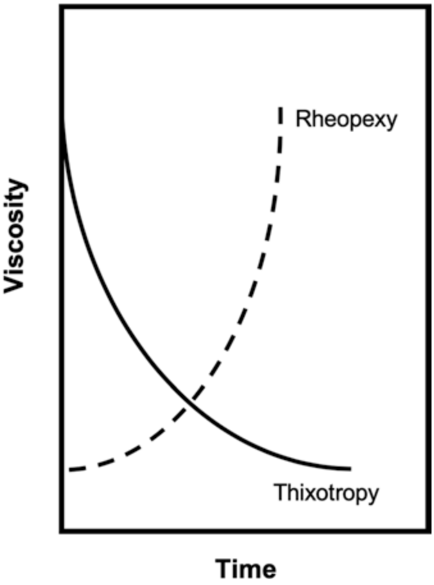

competition between structural breakdown due to applied force and structural buildup due to in-flow collisions and Brownian motion (Barnes 1997). Foods with time-dependent behavior typically show thixotropy. While some foods appear to be rheopectic, the increase in viscosity is actually due to a change in their composition or a fundamental, permanent change in the configuration of individual molecules, not a shear-induced arrangement of molecules over time, as is the case in true rheopexy. For example, whipped cream is not rheopectic even though it can be sheared until it forms a relatively stiff material. This increase in viscosity and rigidity is due to the incorporation of air and the subsequent unfolding of proteins at the air–water interface. Thus, this is a compositional and microstructural change. Similarly, the churning of cream into butter is not rheopexy because buttermilk is removed from the final butter mass (compositional change) and there is a fundamental shift in structure that is more than just simple molecular jamming: the o/w emulsion in cream shifts to a w/o emulsion in butter.

Exponential models are typically used to characterize thixotropic behavior:

$$\sigma\left(t\right)=\sigma_0 e^{-kt} \tag{8}$$

$$\sigma\left(t\right)=\sigma_\infty+\left(\sigma_0-\sigma_\infty\right)e^{-kt} \tag{9}$$

where σ_0 is the stress at the onset of shearing (yield stress, Pa), σ_∞ is the equilibrium stress after shearing for infinite time (Pa), and k is the consistency coefficient (1/s). $\sigma_0 > \sigma_\infty$ due to the fact that the microstructure of a material is intact at the beginning stage of shearing and thus has more resistance to shearing than after the original microstructure begins to collapse.

As previously mentioned, the sturcutre of thixotropic semisolid foods such as yogurt can partially or totally rebuild after the removal of shear, resulting in an increase in viscosity up to the orginal viscosity if the material is left at rest. The exponential model for characterizing this rebuilding behavior is:

$$\sigma\left(t\right)=\sigma_0-\left(\sigma_0-\sigma_\infty\right)e^{-kt} \tag{10}$$

The thixotropic behaviors of many food materials can be modified by altering their formulations. For example, calcium-fortified yogurt sheared at a constant rate had significantly less decrease in apparent viscosity over time as compared to non-fortified yogurt. In addition, after long-time quiescence, less reduction in initial apparent viscosity was observed in calcium-fortified yogurt than non-fortified yogurt (Singh and Muthukumarappan 2008). This was due to an increased number of CCP linkages between casein micelles in calcium-fortified yogurt, so an increased force was required to break those bonds, and formation of more CCP linkages was promoted after shearing ended. Similarly, addition of hydrocolloids to yogurt, such as pectin and fiber, also decreased viscosity reduction from shearing and increased viscosity recovery after the shear force was removed (Basak and Ramaswamy 1994). This result may have been due to greater heterogeneity among large particles (pectin, fiber, and caseins), requiring higher shear force to align all particles to the direction of flow (Fig. 12).

Yogurt fermented by different cultures may also influence thixotropic behavior. For example, dairy lactic acid bacteria, such as *Lactobacillus delbrueckii ssp. bulgaricus* is able to produce exopolysaccharides, which are long polymer chains that can attach to casein micelles and decrease viscosity reduction during shearing (Rawson and Marshall 1997). This is in agreement with studies on the effects of added hydrocolloids on yogurt viscosity (Basak and Ramaswamy 1994).

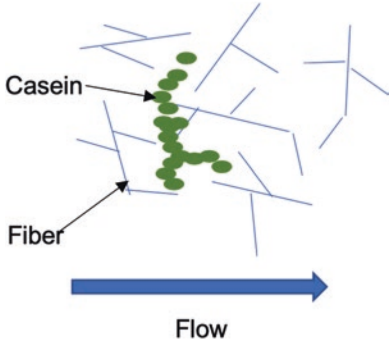

Fig. 12 Microstructure of fiber-enriched yogurt under shear

3.2 *Viscoelastic Behaviors*

3.2.1 Viscoelasticity

Viscoelastic materials exhibit both elastic and viscous behaviors. Viscous behaviors manifest as the dissipation of imparted energy by flow and viscous heating (Stachurski 2009). Models for flow behaviors are discussed in Sect. 3.1. Elastic behavior is the ability to store deformational energy when an external force is applied (Stachurski 2009), then return to its initial shape and size after the force is removed (Timoshenko and Goodier 1986). Multiple parameters can be used to quantify elastic behavior, including Young's modulus, shear modulus, and bulk modulus. The principal differences among these moduli are the direction of applied force (Fig. 13). For Young's modulus, the applied force is perpendicular to the surface of a material. Shear modulus measures elastic behavior when the direction of force is parallel to the interacting surface. Bulk modulus is measured when pressure is applied to all surfaces of a material, resulting in a change in volume.

Many semisolid foods, such as cheeses, butters, yogurts, doughs, gels, and ketchup show viscoelastic behaviors. The viscoelastic properties of semisolid materials are typically determined by geometries that provide an oscillating torque (stress) to a material at a given amplitude and frequency, and measure the resulting deformation (strain), or vice versa (Zhong and Daubert 2013). Viscoelastic moduli and phase angle can be derived from the oscillatory shear data. For a detailed description of viscoelastic parameters and the measurements used for evaluating viscoelastic behaviors, please refer to Chapters "Introduction: Measuring Rheological Properties of Foods" and "Rheological Testing for Semisolid Foods: Traditional Rheometry".

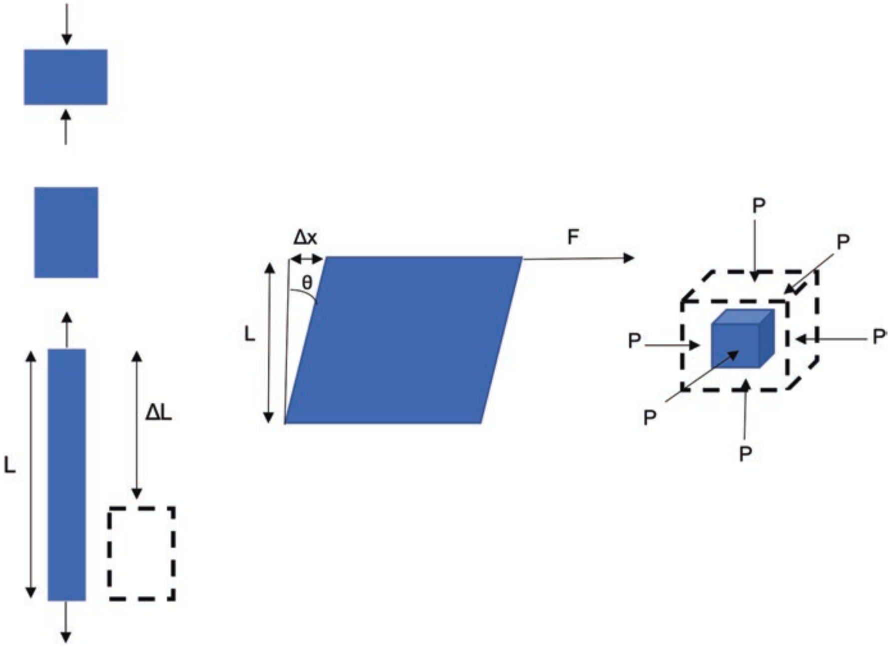

Fig. 13 Diagram of mechanical moduli: Young's modulus, shear modulus, and bulk modulus (left to right)

3.3 *Modification of Viscoelastic Properties*

The viscoelastic properties of semisolid foods can be modified by either formula or physical treatments. For example, studies have reported that adding dietary fibers, such as orange fiber with a particle size range from 0.4 to 1.0 mm, resulted in increased yogurt viscoelastic moduli with increased fiber addition (0.2–1.0% w/w), while maintaining a relatively constant phase angle(~0.3 rad) (Sendra et al. 2010). These results indicated that addition of orange fibers promoted a more rigid yogurt gel but did not alter its ratio of elastic to viscous behavior. Similarly, addition of gelatin to yogurts can also increase viscoelastic moduli values (Supavititpatana et al. 2008). However, adding inulin, a dietary fiber containing fructans, decreased storage modulus values while loss modulus values remained relatively unchanged. Thus, addition of inulin promoted a weaker, more fluid yogurt gel (Paseephol et al. 2008).

Viscoelastic properties of yogurt can be starter culture-dependent. 'Ropy' and 'non-ropy' starter cultures are used for the manufacture of stirred and set types of yogurt, respectively (Hassan et al. 2002). Ropy cultures include *Streptococcus salivarius ssp. thermophilus* and *Lactobacillus delbrueckii ssp. bulgaricus,* which can produce extracellular polysaccharides during fermentation (Vlahopoulou and Bell 1993). These polysaccharides provide a long, stringy texture to the yogurt and can increase both the yogurt viscosity and its extent of fluid-like behavior. Yogurts fermented by ropy cultures were found to have increased viscous and decreased elastic behavior than yogurt fermented with non-ropy cultures. The extracellular polysaccharides added to the yogurt gels did not help to build the yogurt structural network; however, they did increase yogurt viscosity (Vlahopoulou and Bell 1993).

Homogenization of skim milk or whey protein concentrate solutions during yogurt manufacture can also significantly increase yogurt storage modulus values. Homogenization at 10–20 MPa reduces the size of milk fat globules to 0.1–1 um; smaller milk fat globules more readily facilitate the incorporation of fat into the protein network during yogurt manufacture due to their increased surface area to volume ratio (Chandan 2007). The increased surface area favors interactions among fat and milk proteins, casein, and denatured whey during acidification, promoting gel formation (Cano-Ruiz and Richter 1997).

3.4 Creep-Recovery Behavior

Creep-recovery tests are conducted by applying a constant force (uniaxial stress or shear stress) to a material and recording the strain as a function of time during the time of force application and after the force is removed (Fig. 14). For semisolid foods, recovery is usually incomplete and requires a significant amount of time. Creep-recovery testing can provide important parameters, such as zero shear viscosity (η_0) and creep compliance (J), or the ratio of strain to stress during creep or recovery, for characterizing rheological behaviors of food. For example, cookie doughs which had nearly the same viscosities showed significant differences in compliance and elastic recoil, which are important for predicting the shape of the dough after extruding to avoid variations in product size (Franck 2005).

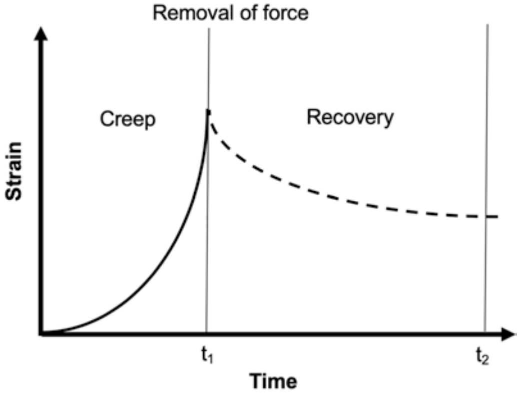

Fig. 14 Creep-recovery behaviors after applying and removing force

3.4.1 Creep-Recovery Model

Due to the complexity of creep-recovery behaviors of semisolid materials, it is common to characterize them by combining damper and spring elements, which represent pure viscous and elastic behavior, respectively. These models usually contain some arrangement of a certain number of Maxwell and Kelvin models (Fig. 15). Maxwell and Kelvin models are used to represent different types of viscoelastic behavior. In the Maxwell model, the material is represented by a purely viscous damper element and a purely elastic spring element connected in series (Eu 1985). Whena Maxwell materials are subjected to a stress, the spring compresses first, followed by the damper depressing. In other words, the material stores energy from the imparted stress over short time periods, but dissipates the energy (relaxes) over long time periods. Conversely, the Kelvin model consists of a damper element and a spring element is in parallel. If a sudden constant stress is applied to a Kelvin material, the spring and the damper act simulatenously, meaning that the material both stores energy and relaxes (dissipates energy) at the same time.

One common model for creep compliance of semisolid materials as a function of time is the Burgers model, which consisits a Kelvin model acting in series with a Maxwell model (Fig. 16, Eqn. 11):

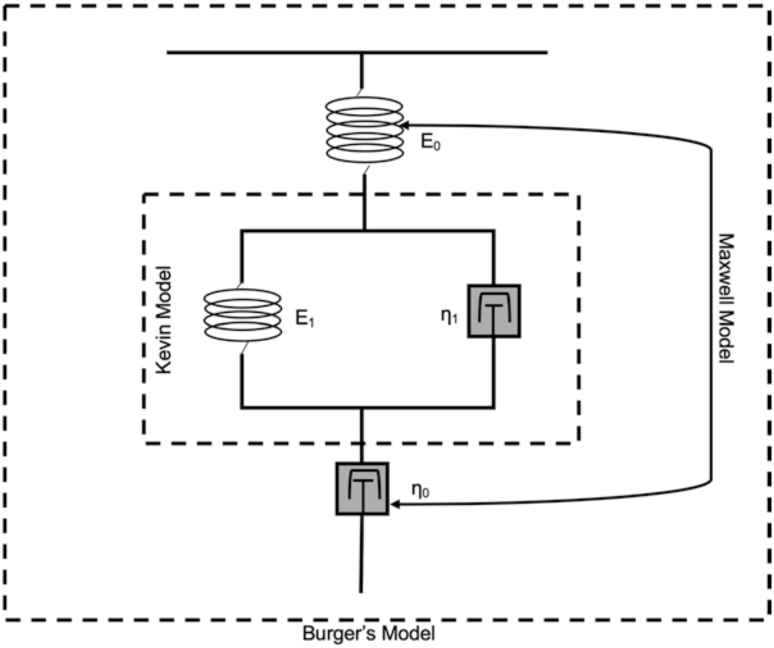

Fig. 15 Diagram of Maxwell, Kelvin, and Burgers models

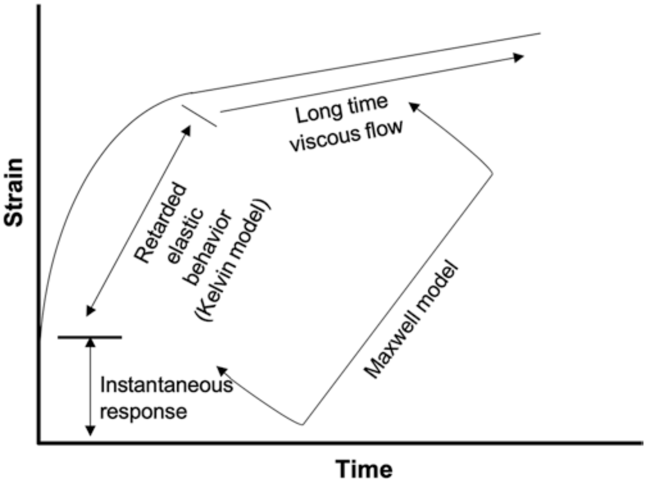

Fig. 16 Creep behavior characterized by the Burgers model

$$J(t) = J_0 + J_1\left(1 - e^{\frac{t}{\lambda_{\text{ret}}}}\right) + \frac{t}{\eta_0} \tag{11}$$

where J_0 is the instantaneous compliance, which is the reciprocal of elastic modulus, E (1/Pa), or strain over stress; J_1 is the retarded compliance defined as $1/E_1$, or the reciprocal of the elastic modulus of the compound spring (1/Pa); t is time (s), λ_{ret} is the retardation time (s), or the time needed for the compliance needed to reach 63.2% of its final value; and η_0 is the Newtonian viscosity of the free dashpot (Pa.s).

3.4.2 Modification of Creep-Recovery Behaviors

Because creep and recovery are linked to visoelastic behaviors, creep-recovery behaviors of semisolid foods can be modified by both formula and physical treatments in the same manner as viscoelastic behaviors. In full-fat yogurt, casein is the main milk protein used to form an uninterrupted network composed of protein chains and clusters (Kalab 1979). Fat globules can interact with the gel casein matrix as binders, providing a strong elastic structure (Lucey et al. 1988). Previous studies indicated that whey protein isolate incorporated into skim milk (10.5 g whey protein/L) combined with heat treatment at 80 °C for 10 min can make non-fat yogurt, in which whey protein provides structure, had smaller values of J_0 and λ_{ret} than full-fat yogurt, which implied that the elasticity of whey protein-fortified yogurt was higher than that of full-fat yogurt, so less time was needed to recover from sudden stress application. Other studies showed that incorporation of whey protein in reduced-fat yogurt tended to form chains of casein micelles (protein particles linked in chains) rather than clusters (large protein aggregates), with whey proteins occupying the spaces between the casein chains and increasing the yogurt gel strength (Puvanenthiran et al. 2002; Lobato-Calleros et al. 2004). However, adding microparticulated whey protein to yogurt (particle size 1–2 um) can significantly increase J_0 and J_1, indicating a greater degree of deformation, lower recovery ability, and a predominatly viscous nature of the protein network. It was hypothesized that addition of microparticulated whey protein to yogurt gels reinforced the gel microstructure by forming a secondary network in the interstices between casein chains, interrupting the casein micelles clusters and chains (Sandoval-Castilla et al. 2004), which was in agreement with the other aforementioned studies.

4 Texture and Oral Processing Features of Semisolid Foods

Consumer acceptability is key to success of a food product. For semisolid foods, in addition to price, consumer acceptability is determined by food sensory attributes including flavor, texture/mouthfeel, and food and packaging appearance. Although rheological properties cannot be used to completely replace food texture measurements conducted by sensory panels, many studies have related semisolid food rheological behaviors to texture attributes such firmness, creaminess, smoothness, graininess, thickness, stickiness, and coarseness (Nishinari 2004). Additionally, changes in rheological behaviors may be reflected in modification of multiple texture attributes.

4.1 Sensory Attributes of Semisolid Foods

The texture characteristics of semisolid foods can be grouped into six categories: (1) viscosity-related attributes, e.g. non-oral and oral viscosity; (2) surface texture attributes, e.g. smoothness; (3) attributes related to bulk homogeneity or heterogeneity, e.g. smooth; (4) attributes related to adhesion or cohesion, e.g. stickiness; (5) attributes related to sensations of wetness and dryness; and (6) attributes associated with fat sensations, e.g. creaminess (Weenen et al. 2003). Six important sensory attributes of semisolid foods will be introduced in the next six subsections.

4.1.1 Firmness

Firmness, or the resistance of the food to deformation under an applied force, is one of the most researched texture attributes for a wide variety of foods. It can be determined either by human senses using touch or sight or instrumentally measured by rheometers (Faber et al. 2017). Firmness of yogurt and ice cream were reported positively correlated to complex modulus; however, firmness was negatively correlated to syneresis (Folkenberg et al. 2006; Akalin and Erişir 2008). The magnitude of expected and preferred firmness is product-specific; for example, Greek yogurt is expected to be significantly firmer than stirred yogurt.

4.1.2 Ropiness

Ropiness is an important sensory attribute for semisolid foods, especially yogurts. It describes the degree to which a strand (rope) will form when a spoon is dipped into the product and slowly pulled out (Drake et al. 2000). Determination of ropiness can be achieved by evaluating the amount of threads or drops that form when introducing the spoon vertically into the sample and raising it vertically from the sample (Ares et al. 2007). Viscosity hysteresis loop area has been found to have a power law relationship with yogurt ropiness (Folkenberg et al. 2006):

4.1.3 Creaminess

Creaminess is a descriptor that is often used to describe the sensory properties of lipid-based foods. Altough it is difficult to define—some sensory scientists consider it to be a consumer term and do not use it in descriptive sensory analysis—it is an important indicator of consumper perception of product richness and high quality (Kilcast and Clegg 2002). Previous study indicated that granularity or grittiness decreases creaminess sensation, and creamy-textured soups should have a very smooth mouthfeel, with complete absence of a powdery sensation when consumed (Wood 1974). Thickness, smoothness, and in some cases, slipperiness have been empiricaly found to relate to creaminess through a power law replationship (Kokini et al. 1977). While the sensations of thickness, smoothness, and slipperiness contribute to the sensation of creaminess, they do not completely describe it.

Some previous studies (Daget et al. 1987; Daget and Joerg 1991) found correlations between creaminess and instrumentally measured viscosity and flow behavior index in caramel creams and soups. Creaminess has also been determined by measuring the time needed to dissolve or mix a sample with saliva. Using this measurement method, creaminess was positively correlated to instrumentally measured yield stress, consistency coefficient, and hysteresis in the viscosity curve; it was negatively correlated to syneresis and flow behavior index (Ares et al. 2007). These results indicated that creamier samples were thicker, more pseudoplastic, and broke down more easily under shear, but were more stable during storage.

4.1.4 Viscosity

Both spoon viscosity and oral viscosity are frequently used to evaluate and differentiate semisolid foods. Spoon viscosity refers to the resistance of the sample to be stirred with a spoon (Ares et al. 2007). Oral viscosity refer to the perceived thickness of the food in the mouth during consumption (Skriver et al. 1999). Previous studies have shown that yogurt spoon viscosity was corrected to both complex modulus measured by dynamic oscillatory measurements and viscosity obtained from a viscometer operating at 5 rpm (Skriver et al. 1999). Oral viscosity was reported to be correlated with dynamic viscosity (Richardson et al. 1989; Houska et al. 1998). However, non-oral viscosity (obtained by stirring with a spoon) did not correlate well with oral viscosity (Stanley and Taylor 1993; Rohm and Kovac 1994).

4.1.5 Thickness

Thickness is a key textural attribute of semisolid foods, including yogurt, ice cream, mayonnaise, and salad dressing. It can be perceived by visual observation of flow behavior during spreading or pouring and by oral mouthfeel. It can also be determined instrumentally by measuring dynamic viscosity (Borwankar 1992). Evaluation of yogurt thickness has been performed by evaluating the residual mouthcoat, or the perception of the layer of residual food that covers the palate and tongue after swallowing the sample. These thickness measurements were positively correlated to viscosity measured at high shear rates (Skriver et al. 1999). Additionally, thickness has been correlated to the shear stress on the tongue during oral processing (Dickie and Kokini 1983):

4.1.6 Smoothness

Smoothness has been described as the sensation a material produces on soft tissues (Szczesniak 1979). To assess smoothness, the tongue is moved lightly across the food product, and the perception of the sensations between the food, the tongue, and the roof of the mouth are recorded. Smoothness has been inversely related to the friction force required to have skin slip across skin or food (Kokini 1987). Typically, smoothness is a desirable trait in semisolid foods, including yogurt, pudding, custard, sour cream, and dairy spreads.

4.2 Texture Modification

Similar to modification of semisolid food rheological behaviors, modification of semisolid food textural attributes can be achieved by altering its formulation or processing parameters. This is because semisolid food microstructural features can influence both rheological and texture characteristics. This topic is discussed in further detail in Chapters "Structuring Semisolid Foods" and "Relationships Among Semisolid Food Microstructures, Rheological Behaviors, and Sensory Attributes"; a brief overview of methods for texture modification are described in the following sections.

4.2.1 Storage Time

The influence of storage time on semisolid food texture is mainly due to time-dependent destabilization of emulsions in the foods or syneresis. For example, oil droplets in peanut butter can coalesce to form a continuous oil phase that forms a surface layer, resulting in a decrease in sensory quality (Gills and Resurreccion 2000). Yogurt after 14 days of storage had lower thickness and graininess compared to yogurt after 1 day of storage time. These textural differences were reflected by significantly increased viscosity and storage modulus (Biliaderis et al. 1992). In a different study, chewiness and iciness of ice cream increased with increased storage time (Schaller-Povolny and Smith 1999).

4.2.2 Solid Content

The impact of altering solid content on semisolid food sensory quality varies based on both the total solids contant and the solids used in the product. For example, stirred yogurt with small amounts of added whey protein (<4.2%) showed a lower score in smoothness compared to yogurt with a larger amount of whey protein (6.0%) (Janhøj et al. 2006). Both creaminess and smoothness have shown dependency on viscosity and dynamic moduli, so increasing viscosoity and viscoelastic moduli by increasing the solids content of the product would increase creaminess and therefore increase sensory quality. On the other hand, changing solids content may not have any relationship to the measured sensory attributes. For example, while stirred yogurt yield stresses varied with different fat content and whey protein addition, their yield streses were not correlated to any sensory attributes (Janhøj et al. 2006).

4.2.3 Fat Content

The fat content of semisolid foods has significant influence on their texture, namely on creaminess and smoothness. It was reported that the creaminess and smoothness of a group of semisolid foods composed of mayonnaises, low-fat yogurt (fat content <1%), custards, and white sauces, which had a broad range of fat content (0–80%), were positively correlated to fat content (Kilcast and Clegg 2002; de Wijk et al. 2006). In general, foods that are higher in fat tend to be perceived as thicker, smoother, and creamier, with a higher degree of mouthcoat.

4.2.4 Polysaccharide and Calcium

Polysaccharides are commonly used in semisolid foods as texture modifiers. Similarly, calcium can be used as a texture modifier in dairy products because it has a notable influence on casein–casein interactions. For example, addition of xanthan gum and guar gum to salad dressing (Tanaka and Fukuda 1976), mayonnaise (Su et al. 2010), and cream (Cottrell et al. 1979), can significantly increase the thickness by increasing the viscosity of the foods. In dairy products, addition of dietary fiber from wheat, bamboo, and inulin improved yogurt texture scores and slightly decreased their viscosity (Dello Staffolo et al. 2004). Calcium-fortified yogurt with up to 40% more calcium than a traditional yogurt had slightly decreased appearance and texture scores; however, its viscosity was significantly increased (Singh and Muthukumarappan 2008).

5 Conclusion

The physiochemical properties and texutre of semisolid foods are a result of the intra- and intermolecular connections among the polymers, e.g. lipids, polysaccharide, and proteins; and small molecules, e.g. water and ions, that comprise their formulation. These structures, including emulsions protein-polysaccharide networks, and fat or ice crystal networks, give semisolids unique rheological behaviors, product stability, texture, flavor, and appearance. Thus, the use of appropriate stablizers, processing methods, and formula is critical to control the quality of semisolid foods.

References

Akalin, A. S., & Erişir, D. (2008). Effects of inulin and oligofructose on the rheological characteristics and probiotic culture survival in low-fat probiotic ice cream. *Journal of Food Science, 73*, M184–M188. https://doi.org/10.1111/j.1750-3841.2008.00728.x.

Amatayakul, T., Sherkat, F., & Shah, N. P. (2006). Syneresis in set yogurt as affected by EPS starter cultures and levels of solids. *International Journal of Dairy Technology, 59*, 216–221. https://doi.org/10.1111/j.1471-0307.2006.00264.x.

Ares, G., Gonçalvez, D., PÉrez, C., Reolón, G., Segura, N., Lema, P., et al. (2007). Influence of gelatin and starch on the instrumental and sensory texture of stirred yogurt. *International Journal of Dairy Technology, 60*, 263–269. https://doi.org/10.1111/j.1471-0307.2007.00346.x.

Bahramparvar, M., Razavi, S. M. A., & Khodaparast, M. H. H. (2010). Rheological characterization and sensory evaluation of a typical soft ice cream made with selected food hydrocolloids. *Food Science and Technology International, 16*, 79–88. https://doi.org/10.1177/1082013209353244.

Bakshi, A. S., & Smith, D. E. (1984). Effect of fat content and temperature on viscosity in relation to pumping requirements of fluid milk products. *Journal of Dairy Science, 67*, 1157–1160. https://doi.org/10.3168/jds.S0022-0302(84)81417-4.

Barnes, H. A. (1997). Thixotropy - A review. *Journal of Non-Newtonian Fluid Mechanics, 70*, 1–33. https://doi.org/10.1016/S0377-0257(97)00004-9.

Basak, S., & Ramaswamy, H. S. (1994). Simultaneous evaluation of shear rate and time dependency of stirred yogurt rheology as influenced by added pectin and strawberry concentrate. *Journal of Food Engineering, 21*, 385–393. https://doi.org/10.1016/0260-8774(94)90081-7.

Benezech, T., & Maingonnat, J. F. (1994). Characterization of the rheological properties of yoghurt-A review. *Journal of Food Engineering, 21*, 447–472. https://doi.org/10.1016/0260-8774(94)90066-3.

Biliaderis, C. G., Khan, M. M., & Blank, G. (1992). Rheological and sensory properties of yogurt from skim milk and ultrafiltered retentates. *International Dairy Journal, 2*, 311–323. https://doi.org/10.1016/0958-6946(92)90035-K.

Bingham, E. C. (1916). An investigation of the laws of plastic flow. *Bulletin of the Bureau of Standards, 13*, 309. https://doi.org/10.6028/bulletin.304.

Bobra, M. A study of the formation of water-in-oil Proceedings of Thirteenth Arctic Marine Oil Spill Program Technical Seminar. Environment Canada, Ottawa, Ontario, 1990, p. 87–117.

Borwankar, R. P. (1992). Food texture and rheology: A tutorial review. *Journal of Food Engineering, 16*, 1–16. https://doi.org/10.1016/0260-8774(92)90016-Y.

Buldo, P., Kirkensgaard, J. J. K., & Wiking, L. (2013). Crystallization mechanisms in cream during ripening and initial butter churning. *Journal of Dairy Science, 96*, 6782–6791. https://doi.org/10.3168/jds.2012-6066.

Camacho, M. M., Martínez-Navarrete, N., & Chiralt, A. (2005). Rheological characterization of experimental dairy creams formulated with locust bean gum (LBG) and λ-carrageenan combinations. *International Dairy Journal, 15*, 243–248. https://doi.org/10.1016/j.idairyj.2004.07.008.

Cano-Ruiz, M. E., & Richter, R. L. (1997). Effect of homogenization pressure on the milk fat globule membrane proteins. *Journal of Dairy Science, 80*, 2732–2739. https://doi.org/10.3168/jds.S0022-0302(97)76235-0.

Chandan, R. C. (2007). *Manufacturing yogurt and fermented milks*. Ames: Blackwell Publishing. https://doi.org/10.1002/9780470277812.

Chen, J. (2014). Food oral processing: Some important underpinning principles of eating and sensory perception. *Food Structure, 1*, 91–105. https://doi.org/10.1016/j.foostr.2014.03.001.

Chen, G., & Tao, D. (2005). An experimental study of stability of oil-water emulsion. *Fuel Processing Technology, 86*, 499–508. https://doi.org/10.1016/j.fuproc.2004.03.010.

Cottrell, J. I. L., Pass, G., & Phillips, G. O. (1979). Assessment of polysaccharides as ice cream stabilisers. *Journal of the Science of Food and Agriculture, 30*, 1085–1088. https://doi.org/10.1002/jsfa.2740301111.

Cottrell, J. I. L., Pass, G., & Phillips, G. O. (1980). The effect of stabilisers on the viscosity of an ice cream mix. *Journal of the Science of Food and Agriculture, 31*, 1066–1070.

Clarke, C. (2015). The science of ice cream. Cambridge, Royal Society of Chemistry.

de Wijk, R. A., Terpstra, M. E. J., Janssen, A. M., & Prinz, J. F. (2006). Perceived creaminess of semi-solid foods. *Trends in Food Science and Technology, 17*, 412–422. https://doi.org/10.1016/j.tifs.2006.02.005.

Daget, N., & Joerg, M. (1991). Creamy perception ii: In model soups. *Journal of Texture Studies, 22*, 169–189. https://doi.org/10.1111/j.1745-4603.1991.tb00012.x.

Daget, N., Joerg, M., & Bourne, M. (1987). Creamy perception I: In model dessert creams. *Journal of Texture Studies, 18*, 367–388. https://doi.org/10.1111/j.1745-4603.1987.tb00913.x.

Dalgleish, D. G. (2006). Food emulsions - Their structures and structure-forming properties. *Food Hydrocolloids, 20*, 415–422. https://doi.org/10.1016/j.foodhyd.2005.10.009.

Dalgleish, D.(2010). Food emulsions. Encyclopedic handbook of emulsion technology. doi:https://doi.org/10.1201/9781420029581.ch9.

Damin, M. R., Alcântara, M. R., Nunes, A. P., & Oliveira, M. N. (2009). Effects of milk supplementation with skim milk powder, whey protein concentrate and sodium caseinate on acidification kinetics, rheological properties and structure of nonfat stirred yogurt. *LWT - Food Science and Technology, 42*, 1744–1750. https://doi.org/10.1016/j.lwt.2009.03.019.

Daubert, C. R., Tkachuk, J. A., & Truong, V. D. (1998). Quantitative measurement of food spreadability using the vane method. *Journal of Texture Studies, 29*, 427–435. https://doi.org/10.1111/j.1745-4603.1998.tb00814.x.

Dello Staffolo, M., Bertola, N., Martino, M., & Bevilacqua, A. (2004). Influence of dietary fiber addition on sensory and rheological properties of yogurt. *International Dairy Journal, 14*, 263–268. https://doi.org/10.1016/j.idairyj.2003.08.004.

Diamante, L. M., & Lan, T. (2014). Absolute viscosities of vegetable oils at different temperatures and shear rate range of 64. 5 to 4835 s − 1. *Journal of Food Process, 2014*, 1–6. https://doi.org/10.1155/2014/234583.

Dickie, A. M., & Kokini, J. L. (1983). An improved model for food thickness from non-Newtonian fluid mechanics in the mouth. *Journal of Food Science, 48*, 57–61.

Dickinson, E. (1987). *Food emulsions and foams*. London: Elsevier.

Dickinson, E. (2009). Hydrocolloids as emulsifiers and emulsion stabilizers. *Food Hydrocolloids, 23*, 1473–1482. https://doi.org/10.1016/j.foodhyd.2008.08.005.

Dickinson, E. (2010). Food emulsions and foams: Stabilization by particles. *Current Opinion in Colloid & Interface Science, 48*, 307–309. https://doi.org/10.1111/j.1536-7150.1989.tb03180.x.

Drake, M. A., Chen, X. Q., Tamarapu, S., & Leenanon, B. (2000). Soy protein fortification affects sensory, chemical, and microbiological properties of dairy yogurts. *Journal of Food Science, 65*, 1244–1247. https://doi.org/10.1111/j.1365-2621.2000.tb10272.x.

Eu, B. C. (1985). Theory of viscoelasticity of fluids. *The Journal of Chemical Physics, 82*, 4683–4689. https://doi.org/10.1063/1.448677.

Faber, T. J., Jaishankar, A., & McKinley, G. H. (2017). Describing the firmness, springiness and rubberiness of food gels using fractional calculus. Part I: Theoretical framework. *Food Hydrocolloids, 62*, 311–324. https://doi.org/10.1016/j.foodhyd.2016.05.041.

Floury, J., Desrumaux, A., Axelos, M. A. V., & Legrand, J. (2003). Effect of high pressure homogenisation on methylcellulose as food emulsifier. *Journal of Food Engineering, 58*, 227–238. https://doi.org/10.1016/S0260-8774(02)00372-2.

Folkenberg, D. M., Dejmek, P., Skriver, A., Skov Guldager, H., & Ipsen, R. (2006). Sensory and rheological screening of exopolysaccharide producing strains of bacterial yoghurt cultures. *International Dairy Journal, 16*, 111–118. https://doi.org/10.1016/j.idairyj.2004.10.013.

Franck, A. (2005). AAN022 creep recovery,1–7.

Gamonpilas, C., Pongjaruvat, W., Fuongfuchat, A., Methacanon, P., Seetapan, N., & Thamjedsada, N. (2011). Physicochemical and rheological characteristics of commercial chili sauces as thickened by modified starch or modified starch/xanthan mixture. *Journal of Food Engineering, 105*, 233–240.

Gills, L. A., & Resurreccion, A. V. A. (2000). Sensory and physical properties of peanut butter treated with palm oil and hydrogenated vegetable oil to prevent oil separation. *Journal of Food Science, 65*, 173–180. https://doi.org/10.1111/j.1365-2621.2000.tb15975.x.

Glibowski, P., Zarzycki, P., & Krzepkowska, M. (2008). The rheological and instrumental textural properties of selected table fats. *International Journal of Food Properties, 11*, 678–686. https://doi.org/10.1080/10942910701622599.

Granger, C., Leger, A., Barey, P., Langendorff, V., & Cansell, M. (2005). Influence of formulation on the structural networks in ice cream. *International Dairy Journal, 15*, 255–262. https://doi.org/10.1016/j.idairyj.2004.07.009.

Hassan, A. N., Corredig, M., & Frank, J. F. (2002). Capsule formation by nonropy starter cultures affects the viscoelastic properties of yogurt during structure formation. *Journal of Dairy Science, 85*, 716–720. https://doi.org/10.3168/jds.S0022-0302(02)74128-3.

Heertje, I., Leunis, M., WJM, V. Z., & Berends, E. (1987). Product morphology of fatty products. *Food Struct, 6*, 1–8.

Hemar, Y., Tamehana, M., Munro, P. A., & Singh, H. (2001). Viscosity, microstructure and phase behavior of aqueous mixtures of commercial milk protein products and xanthan gum. *Food Hydrocolloids, 15*, 565–574. https://doi.org/10.1016/S0268-005X(01)00077-7.

Hirai, N., & Eyring, H. (1958). Bulk viscosity of liquids. *Journal of Applied Physics, 29*, 810–816. https://doi.org/10.1063/1.1723290.

Houska, M., Valentova, H., Novotna, P., Strohalm, J., Sestak, J., & Pokorny, J. (1998). Shear rates during oral and nonoral perception of viscosity of fluid foods. *Journal of Texture Studies, 29*, 603–615. https://doi.org/10.1111/j.1745-4603.1998.tb00188.x.

Icier, F., & Bozkurt, H. (2011). Ohmic heating of liquid whole egg: Rheological behaviour and fluid dynamics. *Food and Bioprocess Technology, 4*, 1253–1263. https://doi.org/10.1007/s11947-009-0229-4.

Janhøj, T., Petersen, C. B., Frøst, M. B., & Ipsen, R. (2006). Sensory and rheological characterization of low-fat stirred yogurt. *Journal of Texture Studies, 37*, 276–299. https://doi.org/10.1111/j.1745-4603.2006.00052.x.

Juriaanse, A. C., & Heertje, I. (1988). Microstructure of shortenings, margarine and butter - A review. *Food Microstructure, 7*, 181–188.

Kalab, M. (1979). Microstructure of dairy foods. 1. Milk products based on protein. *Journal of Dairy Science, 62*, 1352–1364. https://doi.org/10.3168/jds.S0022-0302(79)83424-4.

Karagül-Yüceer, Y., & Drake, M. (2013). Sensory analysis of yogurt. In *Manufacturing yogurt fermented milks* (2nd ed.). Wiley-Blackwell. https://doi.org/10.1002/9781118481301.ch16.

Kestin, J., Sokolov, M., & Wakeham, W. A. (1978). Viscosity of liquid water in the range −8 °C to 150 °C. *Journal of Physical and Chemical Reference Data, 7*, 941–948. https://doi.org/10.1063/1.555581.

Kilcast, D., & Clegg, S. (2002). Sensory perception of creaminess and its relationship with food structure. *Food Quality and Preference, 13*, 609–623. https://doi.org/10.1016/S0950-3293(02)00074-5.

Kokini, J. L. (1987). The physical basis of liquid food texture and texture-taste interactions. *Journal of Food Engineering, 6*, 51–81. https://doi.org/10.1016/0260-8774(87)90021-5.

Kokini, J. L., & Dickie, A. N. N. (1982). A model of food spreadability from fluid mechanics. *Journal of Texture Studies, 13*, 211–227.

Kokini, J. L., Kadane, J. B., & Cussler, E. L. (1977). Liquid texture perceived in the mouth. *Journal of Texture Studies, 8*, 195–218. https://doi.org/10.1111/j.1745-4603.1977.tb01175.x.

Konstance, R. P., Holsinger, V. H., & Thompson, M. P. (1995). Instrumental texture parameters and solvation characteristics of mixed casein gels. *Journal of Dairy Science, 78*, 784–793.

Kuş, S., Altan, A., & Kaya, A. (2005). Rheological behavior and time-dependent characterization of ice cream mix with different salep content. *Journal of Texture Studies, 36*, 273–288. https://doi.org/10.1111/j.1745-4603.2005.00016.x.

Lai, L. S., & Lin, P. H. (2004). Application of decolourised hsian-tsao leaf gum to low-fat salad dressing model emulsions: A rheological study. *Journal of the Science of Food and Agriculture, 84*, 1307–1314. https://doi.org/10.1002/jsfa.1757.

Lam, R. S. H., & Nickerson, M. T. (2013). Food proteins: A review on their emulsifying properties using a structure-function approach. *Food Chemistry, 141*, 975–984. https://doi.org/10.1016/j.foodchem.2013.04.038.

Larson, R. G. (1999). *The structure and rheology of complex fluids*. New York: Oxford University Press. https://doi.org/10.1029/2006EO230009.

Lee, W. J., & Lucey, J. A. (2010). Formation and physical properties of yogurt. *Asian-Australasian Journal of Animal Sciences, 23*, 1127–1136. https://doi.org/10.5713/ajas.2010.r.05.

Lelievre, J., Mirza, I. A., & Tung, M. A. (1992). Failure testing of gellan gels. *Journal of Food Engineering, 16*, 25–37. https://doi.org/10.1016/0260-8774(92)90018-2.

Li, J., & Guo, M. (2006). Effects of polymerized whey proteins on consistency and water-holding properties of goat ' s milk yogurt. *Food and Chemical Toxicology, 71*, C34–C38. https://doi.org/10.1111/j.1365-2621.2006.tb12385.x.

Lide, D. R. (2003). CRC handbook of chemistry and physics, 84th Edition, 2003-2004. Handb Chem Phys. doi:https://doi.org/10.1136/oem.53.7.504.

Liu, H., Xu, X. M., & Guo, S. D. (2007). Rheological, texture and sensory properties of low-fat mayonnaise with different fat mimetics. *LWT - Food Science and Technology, 40*, 946–954. https://doi.org/10.1016/j.lwt.2006.11.007.

Lobato-Calleros, C., Martínez-Torrijos, O., Sandoval-Castilla, O., Pérez-Orozco, J. P., & Vernon-Carter, E. J. (2004). Flow and creep compliance properties of reduced-fat yoghurts containing protein-based fat replacers. *International Dairy Journal, 14*, 777–782. https://doi.org/10.1016/j.idairyj.2004.02.012.

Lucey, J. A., MP, A., & Singh, H. (1988). Rheological properties and microstructure of acid milk gels as affected by fat content and heat treatment. *Journal of Food Science, 63*, 660–664. https://doi.org/10.1111/j.1365-2621.1998.tb15807.x.

Ma, L., & Barbosa-Cánovas, G. V. (1995). Rheological characterization of mayonnaise. Part II: Flow and viscoelastic properties at different oil and xanthan gum concentrations. *Journal of Food Engineering, 25*, 409–425. https://doi.org/10.1016/0260-8774(94)00010-7.

Ma, Z., Boye, J. I., Fortin, J., Simpson, B. K., & Prasher, S. O. (2013). Rheological, physical stability, microstructural and sensory properties of salad dressings supplemented with raw and thermally treated lentil flours. *Journal of Food Engineering, 116*, 862–872. https://doi.org/10.1016/j.jfoodeng.2013.01.024.

Mao, L., Roos, Y. H., Biliaderis, C. G., & Miao, S. (2017). Food emulsions as delivery systems for flavor compounds: A review. *Critical Reviews in Food Science and Nutrition, 57*, 3173–3187. https://doi.org/10.1080/10408398.2015.1098586.

Maruyama, K., Sakashita, T., Hagura, Y., & Suzuki, K. (2007). Relationship between rheology, particle size and texture of mayonnaise. *Food Science and Technology Research, 13*, 1–6. https://doi.org/10.3136/fstr.13.1.

Mezger, T. G. (2014). *The Rheology Handbook, for users of rotational and oscillatory rheometers*. Hanover: Vincentz Network.

Mizrahi, S. (2010). Syneresis in food gels and its implications for food quality. In *Chemical deterioration and physical instability of food and beverages*. Cambridge: Woodhead Publishing Limited. https://doi.org/10.1533/9781845699260.2.324.

Morrison, I. D., & Ross, S. (2002). Colloidal dispersions: Suspensions, Emulsions and Foams. Colloid Dispersions Suspens Emuls Foam. Hoboken, Wiley-Interscience.

Muschiolik, G. (2007). Multiple emulsions for food use. *Current Opinion in Colloid & Interface Science, 12*, 213–220. https://doi.org/10.1016/j.cocis.2007.07.006.

Nikzade, V., Tehrani, M. M., & Saadatmand-Tarzjan, M. (2012). Optimization of low-cholesterol-low-fat mayonnaise formulation: Effect of using soy milk and some stabilizer by a mixture design approach. *Food Hydrocolloids, 28*, 344–352. https://doi.org/10.1016/j.foodhyd.2011.12.023.

Nishinari, K. (2004). Rheology, food texture and mastication. *Journal of Texture Studies, 35*, 113–124. https://doi.org/10.1111/j.1745-4603.2004.tb00828.x.

Noda, M., & Shiinoki, Y. (1986). Microstructure and rheological behavior of whipping cream. *Journal of Texture Studies, 17*, 189–204. https://doi.org/10.1111/j.1745-4603.1986.tb00404.x.

Ohmes, R. L., Marshall, R. T., & Sensory, H. H. (2010). Physical properties of ice creams containing milk fat or fat replacers. *Journal of Dairy Science, 81*, 1222–1228. https://doi.org/10.3168/jds.s0022-0302(98)75682-6.

Paseephol, T., Small, D. M., & Sherkat, F. (2008). Rheology and texture of set yogurt as affected by inulin addition. *Journal of Texture Studies, 39*, 617–634. https://doi.org/10.1111/j.1745-4603.2008.00161.x.

Puvanenthiran, A., Williams, R. P. W., & Augustin, M. A. (2002). Structure and visco-elastic properties of set yoghurt with altered casein to whey protein ratios. *International Dairy Journal, 12*, 383–391. https://doi.org/10.1016/S0958-6946(02)00033-X.

Ramaswamy, H. S., & Basak, S. (1991). Rheology of stirred yogurts. *Journal of Texture Studies, 22*, 231–241. https://doi.org/10.1111/j.1745-4603.1991.tb00016.x.

Rao, A. (2013). Rheology of fluid, semisolid, and solid foods: Principles and applications. Rheol fluid, semisolid, solid food. https://doi.org/10.1007/978-1-4614-9230-6.

Rao, M. A., Cooley, H. J., Nogueira, J. N., & McLellan, M. R. (1986). Rheology of apple sauce: Effect of apple cultivar, firmness, and processing parameters. *Journal of Food Science, 51*, 176–179. https://doi.org/10.1111/j.1365-2621.1986.tb10864.x.

Rawson, H. L., & Marshall, V. M. (1997). Effect of "ropy" strains of *Lactobacillus delbrueckii* ssp. *bulgaricus* and *Streptococcus salivarius* ssp. *thermophilus* on rheology of stirred yogurt. *International Journal of Food Science and Technology, 32*, 213–220. https://doi.org/10.1046/j.1365-2621.1997.00395.x.

Richardson, R. K., Morris, E. R., Ross-Murphy, S. B., Taylor, L. J., & Dea, I. C. M. (1989). Characterization of the perceived texture of thickened systems by dynamic viscosity measurements. *Topics in Catalysis, 3*, 175–191. https://doi.org/10.1016/S0268-005X(89)80002-5.

Rohm, H., & Kovac, A. (1994). Effects of starter cultures on linear viscoelastic and physical properties of yogurt gels. *Journal of Texture Studies, 25*, 311–329. https://doi.org/10.1111/j.1745-4603.1994.tb00763.x.

Sandoval-Castilla, O., Lobato-Calleros, C., Aguirre-Mandujano, E., & Vernon-Carter, E. J. (2004). Microstructure and texture of yogurt as influenced by fat replacers. *International Dairy Journal, 14*, 151–159. https://doi.org/10.1016/S0958-6946(03)00166-3.

Saramito, P. (2016). Complex fluids*, 79*:63–91. doi:https://doi.org/10.1007/978-3-319-44362-1.

Schaller-Povolny, L. A., & Smith, D. E. (1999). Sensory attributes and storage life of reduced fat ice cream as related to inulin content. *Journal of Food Science, 64*, 555–559. https://doi.org/10.1111/j.1365-2621.1999.tb15084.x.

Schramm, L. L. (1992). Fundamentals and applications in the petroleum Industry. *Advanced Chemistry, 231*, 3–24.

Sendra, E., Kuri, V., Fernández-López, J., Sayas-Barberá, E., Navarro, C., & Pérez-Alvarez, J. A. (2010). Viscoelastic properties of orange fiber enriched yogurt as a function of fiber dose, size and thermal treatment. *LWT - Food Science and Technology, 43*, 708–714. https://doi.org/10.1016/j.lwt.2009.12.005.

Shaker, R. R., Jumah, R. Y., & Abu-Jdayil, B. (2000). Rheological properties of plain yogurt during coagulation process: Impact of fat content and preheat treatment of milk. *Journal of Food Engineering, 44*, 175–180. https://doi.org/10.1016/S0260-8774(00)00022-4.

Sikora, M., Kowalski, S., Tomasik, P., & Sady, M. (2007). Rheological and sensory properties of dessert sauces thickened by starch-xanthan gum combinations. *Journal of Food Engineering, 79*, 1144–1151. https://doi.org/10.1016/j.jfoodeng.2006.04.003.

Singh, G., & Muthukumarappan, K. (2008). Influence of calcium fortification on sensory, physical and rheological characteristics of fruit yogurt. *LWT - Food Science and Technology, 41*, 1145–1152. https://doi.org/10.1016/j.lwt.2007.08.027.

Singh, S. K., Castell-Perez, M. E., & Moreira, R. G. (2000). Viscosity and textural attributes of reduced-fat peanut pastes. *Journal of Food Science, 65*, 849–853. https://doi.org/10.1111/j.1365-2621.2000.tb13599.x.

Skriver, A., Holstborg, J., & Qvist, K. B. (1999). Relation between sensory texture analysis and rheological properties of stirred yogurt. *The Journal of Dairy Research, 66*, 609–618. https://doi.org/10.1017/S0022029999003763.

Stachurski, Z. H. (2009). Mechanical behavior of materials. *Materials Today, 12*, 44. https://doi.org/10.1016/S1369-7021(09)70086-0.

Stanley, N. L., & Taylor, L. J. (1993). Rheological basis of oral characteristics of fluid and semi-solid foods: A review. *Acta Psychologica, 84*, 79–92. https://doi.org/10.1016/0001-6918(93)90074-2.

Su, H. P., Lien, C. P., Lee, T. A., & Ho, J. H. (2010). Development of low-fat mayonnaise containing polysaccharide gums as functional ingredients. *Journal of the Science of Food and Agriculture, 90*(5), 806–812. https://doi.org/10.1002/jsfa.3888.

Supavititpatana, P., Wirjantoro, T. I., Apichartsrangkoon, A., & Raviyan, P. (2008). Addition of gelatin enhanced gelation of corn-milk yogurt. *Food Chemistry, 106*, 211–216. https://doi.org/10.1016/j.foodchem.2007.05.058.

Syrbe, A., Bauer, W. J., & Klostermeyer, H. (1998). Polymer science concepts in dairy systems - An overview of milk protein and food hydrocolloid interaction. *International Dairy Journal, 8*, 179–193. https://doi.org/10.1016/S0958-6946(98)00041-7.

Szczesniak, A. S. (1979). Classification of mouthfeel characteristics of beverages. *Food Texture and Rheology*, 1–20.

Taghizadeh, M., & Razavi, S. M. A. (2009). Modeling time-independent rheological behavior of pistachio butter. *International Journal of Food Properties, 12*, 331–340. https://doi.org/10.1080/10942910701772048.

Tan, J., & Joyner, H. S. (2018). Characterizing wear behaviors of κ-carrageenan and whey protein gels by numerical modeling. *Journal of Food Engineering, 235*, 98–105. https://doi.org/10.1016/j.jfoodeng.2018.05.002.

Tan, J., & Kerr, W. L. (2017). Determination of glass transitions in boiled candies by capacitance based thermal analysis (CTA) and genetic algorithm (GA). *Journal of Food Engineering, 193*, 68–75. https://doi.org/10.1016/j.jfoodeng.2016.08.010.

Tanaka, M., & Fukuda, H. (1976). Studies on the texture of salad dressings containing xanthan gum. *Canadian Institute of Food Science and Technology Journal, 9*, 130–134.

Teles, C. D., & Flôres, S. H. (2007). The influence of additives on the rheological and sensory properties of nonfat yogurt. *International Journal of Dairy Technology, 60*, 270–276. https://doi.org/10.1111/j.1471-0307.2007.00354.x.

Timoshenko, S., & Goodier, J. N. (1986). Theory of elasticity. *Journal of Elasticity, 1*, 125–143. https://doi.org/10.1007/BF00046464.

Totlani, V. M., & Chinnan, M. S. (2007). Effect of stabilizer levels and storage conditions on texture and viscosity of peanut butter. *Peanut Science, 34*, 1–9. https://doi.org/10.3146/0095-3679(2007)34[1:eoslas]2.0.co;2.

Truong, V. D., & Daubert, C. R. (2000). Comparative study of large strain methods for assessing failure characteristics of selected food gels. *Journal of Texture Studies, 31*, 335–353. https://doi.org/10.1111/j.1745-4603.2000.tb00294.x.

Vlahopoulou, I., & Bell, A. E. (1993). Effect of various starter cultures on the viscoelastic properties of bovine and caprine yogurt gels. *International Journal of Dairy Technology, 46*, 61–63. https://doi.org/10.1111/j.1471-0307.1993.tb00862.x.

Vocaldo. (2007). Definition of viscosity. Encyclopedia. doi:2016-11-02.

Walters, K. (1962). Non-newtonian effects in some elastico-viscous liquids whose behaviour at small rates of shear is characterized by a general linear equation of state. *Quarterly Journal of Mechanics and Applied Mathematics, 15*, 63–76. https://doi.org/10.1093/qjmam/15.1.63.

Weenen, H., Van Gemert, L. J., Van Doorn, J. M., Dijksterhuis, G. B., & De Wijk, R. A. (2003). Texture and mouthfeel of semisolid foods: Commercial mayonnaises, dressings, custard desserts and warm sauces. *Journal of Texture Studies, 34*, 159–179. https://doi.org/10.1111/j.1745-4603.2003.tb01373.x.

Wood, F. W. (1974). An approach to understanding creaminess. *Starch-Stärke, 26*, 127–130.

Yanniotis, S., Skaltsi, S., & Karaburnioti, S. (2006). Effect of moisture content on the viscosity of honey at different temperatures. *Journal of Food Engineering, 72*, 372–377. https://doi.org/10.1016/j.jfoodeng.2004.12.017.

Zhong, Q., & Daubert, C. R. (2013). Food rheology. In *Handbook of farm, dairy and food machinery engineering* (2nd ed.). Norwich, NY: William Andrew Publishing. https://doi.org/10.1016/B978-0-12-385881-8.00015-X.

Rheological Testing for Semisolid Foods: Traditional Rheometry

Judith K. Whaley, Catherine Templeton, and Mohammad Anvari

1 Introduction

A wide range of foods can be classified as semisolid foods, including soft candies, thickened soups and sauces, dressings, spreads, spreadable cheeses, puddings, ice cream, yogurt, sour cream, and most cultured dairy products. These foods are characterized by a complex microstructure and rheology which in turn lead to complex processing behavior and textural attributes. As a result, food formulators seek to better understand and predict the behavior of semisolid foods to more quickly and effectively design foods that exhibit desirable processing behavior and eating qualities.

Rheological studies can be used to gain insight on the structure and flow behavior of semisolid foods. In this chapter, we review key rheology definitions (Sect. 2), describe the pros and cons of selected rheology measurements (Sect. 3), present a framework for understanding semisolid foods (Sect. 4), and illustrate how this framework can be applied to understand yogurt behavior and to develop predictive design tools (Sect. 5). We conclude the chapter with a look at the future of research in this area (Sect. 6), highlighting exciting prospects for additional research to unlock fully the potential of predictive modeling of the rheology and texture of semisolid foods.

J. K. Whaley (✉) · C. Templeton · M. Anvari
Tate & Lyle, PLC, Hoffman Estates, IL, USA
e-mail: judith.whaley@tateandlyle.com; catherine.templeton@tateandlyle.com; mohammad.anvari@tateandlyle.com

H. S. Joyner (ed.), *Rheology of Semisolid Foods*, Food Engineering Series,
https://doi.org/10.1007/978-3-030-27134-3_3

2 Common Rheological Terms

In this section, key rheological terms are defined. These terms are then used in Sect. 3 to describe the rheological tests that are commonly performed on semisolid materials. The terms which are defined in this section describe different types of materials (Sect. 2.1), different types of flow fields (Sect. 2.2), different types of tests and geometries (Sect. 2.3), rheological variables (Sect. 2.4), and classifications of viscous (Sect. 2.5) and viscoelastic behavior (Sect. 2.6).

2.1 Types of Materials

The rheological behavior of specific materials depends on their state of matter, as liquids can flow when force is applied, while solids will deform by a fixed amount and then regain their original shape when the force is removed (or alternately fracture above a critical force). Semisolids are unique in that they typically flow over long time scales of deformation but retain their shape over short time scales. Alternately, some semisolids may exhibit solid-like behavior at low stresses and liquid-like behavior at high stresses. In this chapter, we will examine in detail the implications of this time-scale dependent behavior.

2.2 Types of Flow Fields

There are two types of flow field that can be generated within fluid materials: shear and extensional flow. In shear flow, molecules move past each other in planar sheets, while in extensional flow, molecules move towards or away from each other. An illustration of shear versus extensional flow is shown in Fig. 1.

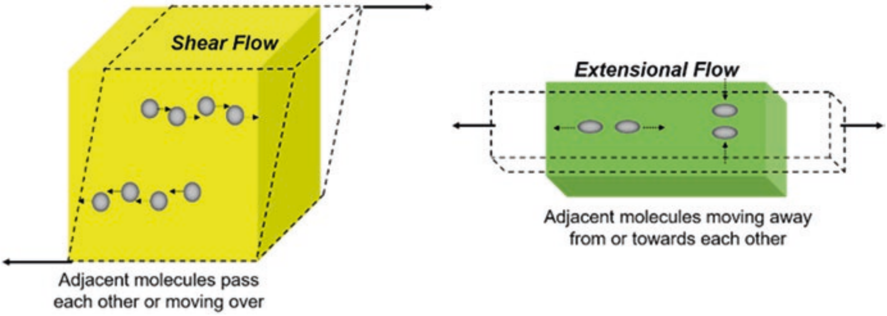

Fig. 1 Typical molecular motions in shear and extensional flows

In Fig. 1, the illustration of extensional flow shows uniaxial extensional flow: the material is extended in one dimension while contracting in the other two dimensions. In addition to uniaxial extension, it is also possible to generate biaxial extension, where the material is compressed in one dimension and extended in the other two dimensions, and planar extensional flows, where the material is extended in one dimension while it is compressed in another dimension with the third dimension held fixed. These types of flow are described in detail in rheology textbooks (Barnes 2000).

In this chapter, we will focus primarily on shear flow measurements, which are widely used to characterize semisolid foods.

2.3 Types of Test and Geometries

For the purpose of this chapter, rheological tests are classified as either empirical tests or as fundamental tests.

2.3.1 Empirical Tests

Empirical tests that are commonly used on semisolid foods such as yogurt include:

- *Flow on inclines* (with different cone and plane geometries),
- *Penetrometry* or *"punch" tests* (with a range of probes), and
- *Spindle-viscometry* (with an array of spindles)

These tests are described as "empirical" as the flow fields generated during testing are not well-enough defined to report rheological information as a function of specific rheological parameters. As a result, the differences measured on samples will reflect partially the material's mechanical properties and partially the equipment on which the material was measured. In addition, the test results will not be able to be duplicated on other equipment with different geometric configurations. Empirical tests may be performed using a variety of equipment.

Flow on Inclines

The measurement of flow on inclines is widespread due to the simplicity of the associated tests and equipment. Equipment includes cones as well as fixed and adjustable wedges (Figs. 2 and 3). The cone incline and plane incline geometries do not allow for controlled flow fields because the flowing material sticks at the surface of the device but flows more rapidly at the top of the material layer. As a result, the shear rate varies across the sample in an undefined manner, and it is not possible to report rheological data under controlled conditions. These tests are suitable for semisolids which flow under gravity over short time scales such as stirred yogurts.

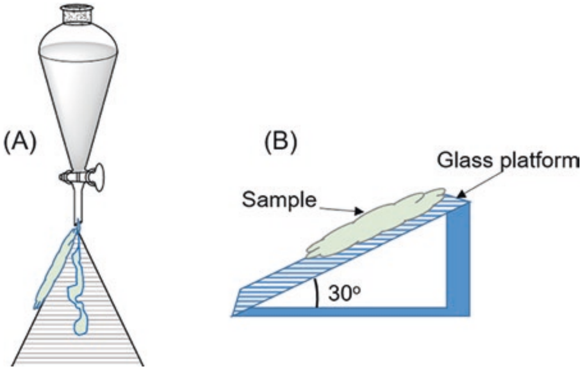

Fig. 2 Illustration of inclined plane geometry, including (**a**) cone with liquid applied at the apex through a stopcock, and (**b**) wedge with fluid applied at top of wedge

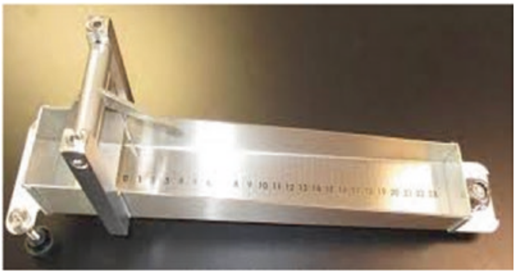

Fig. 3 An inclined plane with adjustable angle and gate for releasing fluid to flow down the slope

Penetrometry

A range of penetrometry techniques are used to look at semisolids that exhibit some degree of shape retention. These techniques include more sophisticated "punch" tests where probes that can vary in shape are forced into a material and simpler "penetration" tests where probes of specified weights are placed on a surface and allowed to indent the surface. Probes include cones of various sizes and weights as well as needles or ball indenters; a cone-with-needle geometry is illustrated in Fig. 4. Penetrometry tests have the advantage of being simple to execute and can be applied to samples without disrupting the structure prior to testing as no sample transfer is required.

Spindle Viscometry

It is common to measure apparent viscosity of semisolids using viscometers (Fig. 5). A synchronous induction type motor gives a series of speeds of rotation that are constant. Various spindles that take the form of cylinders, disks, and T bars are attached to a small chuck. When the spindle is immersed in the liquid and the motor switched on, the viscous drag of the fluid on the spindle is registered as torque on a dial which is converted to viscosity. Brookfield viscometers are a classic example of a spindle viscometer.

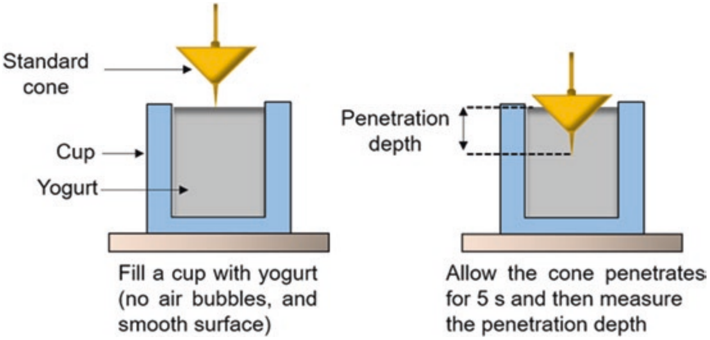

Fig. 4 Illustration of a cone-with-needle-tip geometry

Fig. 5 Schematic of a typical viscometer with a spindle attached

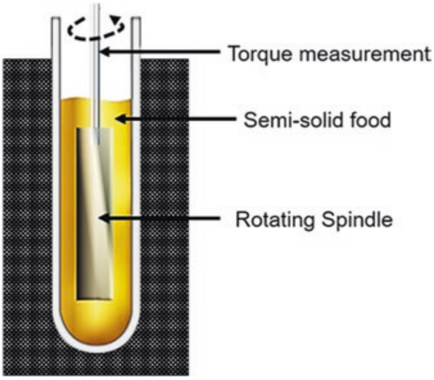

This type of system has the advantage of being simple to operate and portable, and can be used to evaluate materials with a range of viscosities by adjusting the choice of spindle or disk. A disadvantage of this type of equipment is that torque measurement ranges are limited, forcing a change in geometry if samples span a wide range of viscosity, making it impossible to compare the data across the range where the spindles have been changed.

2.3.2 Fundamental Tests

Fundamental rheological properties are independent of the instruments on which they are measured, so different instruments should give identical results on the same material. These fundamental rheological tests are possible when the geometry of the test device is designed to allow controlled flow fields to be generated. The cone-and-plate geometry, parallel-plate geometry, and concentric-cylinder geometry are the most common configurations used for fundamental testing (Fig. 6).

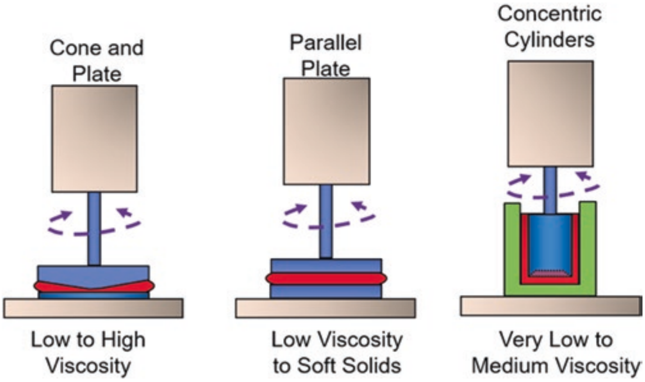

Fig. 6 Schematic of cross sections of common measuring geometries

Parallel Plate Geometry

This geometry allows for creation of well-defined flow fields. The main advantage of this geometry is that the user can define the gap between the plates. The gap should be set to values larger than those of typical particles in the material to be tested. It can also be changed to probe wall slip effects (Barnes and Walters 1985). This geometry also needs only a small volume of sample and is easy to clean. While the flow field is well-defined in the parallel plate geometry, it does changes with radial position. Because of this, the measurement is taken at the edge of the plate, which can be problematic for samples that are prone to edge drying during testing. Another disadvantage of this geometry is that low-viscosity materials can be ejected from between the plates at high rotational speeds.

Cone-and-Plate Geometry

The main advantage of the cone-and-plate geometry is that the flow field is uniform across the sample. As with the parallel-plate geometry, the volume of sample used is small and the fixtures are easy to clean. When using the cone-and-plate geometry, the size of particles in the sample should be less than 10–20% of the gap between the tip of the cone and the plate, which ranges typically from 5 to 20 microns. This prevents jamming of particles in the gap. As with the parallel-plate geometry, low-viscosity materials can be ejected from the gap when the rotation speed is high, although this event will occur at a higher shear rate for cone-and-plate geometries compared to parallel plate geometries because the gap in the cone-and-plate geometry is smaller.

Concentric Cylinder Geometry

This geometry, which also has well-defined flow fields, is preferred for products with lower viscosity because they can be tested at high rotational rates without being ejected from the geometry. Furthermore, the concentric cylinder geometry has a larger surface area that provides a greater torque signal during rotation than the cone-and-plate and parallel plate geometries. Thus, the torque signal obtained from using a concentric cylinder geometry to measure lower-viscosity fluids is more likely to be in the detection range of the instrument. However, the narrow gaps (<1 mm) in the concentric cylinder system are not suitable for materials containing larger solid particles, as they may jam the instrument; settling and slippage of solids may also occur during measurements, resulting in inaccurate data (Bongenaar et al. 1973).

2.4 *Rheological Variables*

Different rheological variables are associated with each type of deformation that is applied to materials and with each type of test setup. Below, we define a short list of terms which is associated with shear deformations. The terms described in this section are all described in more detail by Ferry (1980) in his book on viscoelasticity, in addition to a broader set of rheology parameters.

The stress, σ (Pa), is defined as the force, F (N), per unit area, A (m^2), applied to a material. Shear stress is commonly measured by placing a sample between two surfaces, then applying a force to move one surface while holding the second surface fixed. A transducer is used to measure the force exerted on the fixed surface due to the motion of the other surface; stress is calculated as the ratio of the force to the area:

$$\sigma = \frac{F}{A} \tag{1}$$

The strain, γ (unitless), on a material is a measure of how much the material is deformed. For example, when a material is placed between parallel plates of radius, R (m), and sheared by holding one surface fixed while rotating the other surface a specified angle, θ (rad), the shear strain is defined as the distance traveled by the rotating circular surface at its outer edge, θR, divided by the gap between the surfaces, H_o (m):

$$\gamma = \frac{\theta R}{H_o} \tag{2}$$

The definition of strain is closely linked to the specific geometry used for a rheological test, with different equations to describe strain in different test geometries.

Strain rate, $\dot{\gamma}$ (1/s), is a measure of the speed at which a material is deformed. It is defined as the velocity gradient established in a fluid as a result of an applied stress, and can be defined in terms of the strain as:

$$\dot{\gamma} = \frac{d\gamma}{dt} \tag{3}$$

Here, t is time (s). The term "strain rate" can be used interchangeably with the more common term "shear rate" when a shear strain is applied.

The viscosity, $\eta(\dot{\gamma})$ (Pa.s), is the internal friction of a fluid or its tendency to resist flow. Viscosity is most typically measured by applying a constant strain rate to material while measuring the resulting stress. Viscosity is defined as the ratio of the stress to the strain rate:

$$\eta(\dot{\gamma}) = \frac{\sigma(\dot{\gamma})}{\dot{\gamma}} \tag{4}$$

The shear modulus, G (Pa), is a measure of the stiffness or rigidity of a material. Modulus is defined generically as the ratio of stress to strain, but different types of moduli can be measured, depending upon the type of deformation applied to the material. If the deformation is applied by instantaneously deforming a material to a fixed strain, γ_o, the modulus is referred to as the relaxation modulus:

$$G(t) = \frac{\sigma(t)}{\gamma_o} \tag{5}$$

If an oscillatory strain, $\gamma(t) = \gamma_o \sin(\omega t)$, is applied to a material at a frequency ω (rad/s), resulting in a sinusoidal stress response $\sigma(t) = \sigma_o \sin(\omega t + \delta)$, with a phase lag (also called phase angle) δ (rad), two new modulus terms are defined. The sinusoidal stress response is decoupled into an in-phase and out-of-phase stress response. The storage modulus, $G'(\omega)$ (Pa), is defined as the ratio of the in-phase stress to strain:

$$G'(\omega) = \left(\frac{\sigma_o}{\gamma_o}\right)\cos(\delta) \tag{6}$$

The loss modulus, $G''(\omega)$ (Pa), is defined as the ratio of the out-of-phase stress response to strain:

$$G''(\omega) = \left(\frac{\sigma_o}{\gamma_o}\right)\sin(\delta) \tag{7}$$

The complex modulus, $G^*(\omega)$ (Pa), is defined as

$$G^* = \sqrt{G' + G''} \tag{8}$$

Chapter "Introduction: Measuring Rheological Properties of Foods" includes a schematic of how these moduli and the phase angle are related in a Pythagorean relationship.

The phase angle, δ, is a measure of the elasticity of the material and varies from 0 to 90°, with 0° representing a purely elastic material and 90° representing a purely viscous (inelastic) material. The tangent of the phase angle, *tan* δ, is often reported instead of the phase angle itself and is defined simply as: $\tan\delta = \frac{G''}{G'}$.

The shear compliance, J (1/Pa), is a measure of how easily a material flows under stress. Compliance is defined generically as the ratio of strain to stress, but different types of compliance can be measured depending upon the stress profile applied. If the applied stress, σ_o, is applied instantaneously as a constant stress, the compliance is referred to as the creep compliance:

$$J(t) = \frac{\gamma(t)}{\sigma_o} \tag{9}$$

Creep compliance testing is often used to assess how materials flow over very long time periods. For example, creep tests can be configured where a sample which is solid at short time scales is cut into a rectangular film and hung from a clamp with a weight attached to the bottom end of the clamped strip to apply a constant stress. Creep tests can also be conducted in shear mode using parallel plate geometries. Such creep tests have been done over periods spanning years to evaluate very slow-flowing materials.

2.5 Viscous Behavior

All foods have unique viscous behavior, which impacts their performance in a large number of industrial applications. Viscous materials can be classified based on their stress versus shear rate profiles under shear. An illustration of different types of viscous behavior is provided in Fig. 7. Viscosity data can also be displayed as a viscosity versus strain rate curve instead of a stress-versus-strain-rate curve. The information is the same in both curves, though the visualization is different. The viscosity versus strain rate curve (the flow curve) is widely used by engineers to predict behavior of liquid and semisolid foods under a range of processing conditions. Flow behavior models can be constructed from either stress versus shear rate or viscosity versus strain rate curves. Examples of these flow behavior models are discussed in Chapter "Overview: Semisolid Foods".

Newtonian materials, whose viscosity is not dependent on shear rate, exhibit a straight line passing through the origin on a plot of stress versus shear rate. Non-Newtonian materials, whose viscosities are shear-rate dependent, exhibit nonlinear curves on a stress versus shear rate plot (Fig. 7) or alternately may exhibit a linear profile that does not pass through the origin of the plot. Flow behavior may depend only on shear rate and not on the duration of shear (time-independent) or may depend also on the duration of shear (time-dependent). Non-Newtonian fluids and semisolids can be further classified, based on the shape of the nonlinear stress versus shear rate profile, into shear-dependent materials and materials with a yield stresses.

2.5.1 Shear-Dependent Materials

Shear dependency can manifest as shear-thinning or shear-thickening behaviors. In materials with shear-thinning behavior, the curve starts at the origin of the shear stress-shear rate plot but an increasing shear rate gives a less than proportional

Fig. 7 Typical flow curves for different type of flow behaviors

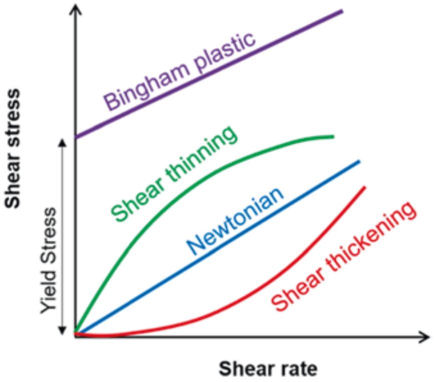

increase in shear stress (Fig. 7). Shear-thinning materials are generally called pseudoplastic. The term "shear-thinning" is preferred to "pseudoplastic" as it is a more accurate definition of the shear rate-shear stress curve. In shear-thickening behavior, the curve also starts from the origin of the shear stress-shear rate plot and is concave downwards (Fig. 7), which means an increasing shear stress is not proportional with increasing the shear rate.

2.5.2 Yield Stress Materials

For materials with yield stresses, the applied stress must be above the yield stress before the material can flow (Fig. 7). If the material shows Newtonian flow behavior after the initiation of flow, it is called a Bingham plastic fluid. However, if the material shows non-Newtonian behavior, another flow behavior model is needed (examples provided in Chapter "Overview: Semisolid Foods"). Barnes and Walters (1985) posited that yield stress is a myth: if a material can flow at high stress it will also be able to flow at low stress, albeit slowly. Nevertheless, the viscosity in many dispersed systems is so high that the material will need years before flow is measurable. Accordingly, yield stress is an engineering reality (Spaans and Williams 1995), and this parameter can be useful in material characterization, in relationship to the range of shear rates and time scales encountered in commercial processes (Papanastasiou 1987).

2.6 Viscoelastic Behavior

Although viscous flow behaviors can adequately describe the flow behaviors of relatively simple fluid systems, many flow phenomena cannot be explained by viscous behavior alone because elastic behavior also influences these phenomena (Steffe 1996). In this section, a brief list of terms relevant to viscoelastic behavior are defined, including linear viscoelasticity and nonlinear viscoelasticity. For a complete description of viscoelasticity, the work of Ferry (1980) provides a comprehensive overview.

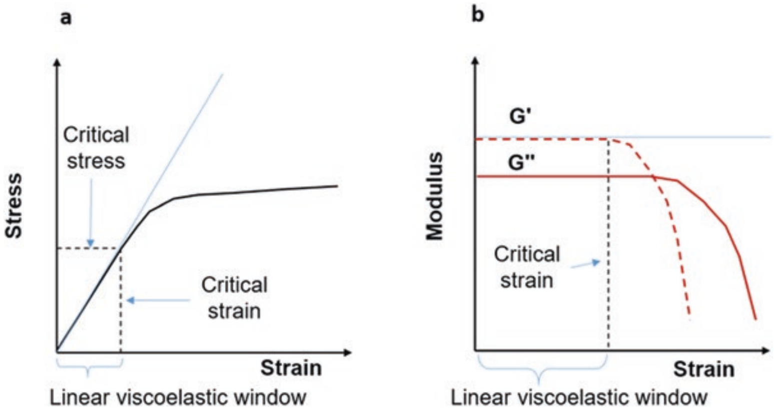

Fig. 8 The linear viscoelastic region for a material defined by looking at (**a**) a stress-strain plot generated from a step-strain-rate test or (**b**) storage-modulus-strain plot generated from an oscillatory shear strain sweep test

Deformations which are very small can be applied to materials such that no change in the underlying structure of the material occurs as a result of the deformation. These small perturbations allow the experimenter to probe the structure of the material itself, as the mechanical stress response to applied strain (or vice versa) is indicative of the underlying structure. Deformations performed in this window of small stresses and strains are referred to as linear viscoelastic. Many different types of linear viscoelastic deformations can be applied, including application of an instantaneous constant stress to the material (creep), application of an instantaneous constant strain to the material (stress relaxation), or application of an oscillatory stress or strain to a material. Oscillatory shear tests are also commonly referred to as small amplitude oscillatory shear (SAOS). For the deformation to be considered linear viscoelastic, the stress and strain should be related linearly; this is typically true up to a critical stress (or strain). Above the critical stress or strain, the material deforms enough to change the underlying structure of the material; this is termed nonlinear viscoelastic behavior. The linearity of the response can be tested in multiple ways, but two of the most common techniques are illustrated in Fig. 8.

Large deformations can be applied to materials which do cause changes in the underlying material structure. Such deformations are referred to as nonlinear and can be applied using the same types of deformation as used for linear viscoelastic tests, including application of an instantaneous constant stress to the material (creep), application of an instantaneous constant strain to the material (stress relaxation), or application of an oscillatory stress or strain to a material. The key difference between nonlinear viscoelastic tests and linear viscoelastic tests is that in the former the stress or strain applied to the material exceeds the critical limit, while in the latter the stress or strain applied to the material is less than the critical limit.

3 Rheological Tests

Rheological tests can be classified based on the rheological parameter which is controlled during the tests and include five types of test: (1) tests with uncontrolled rheological parameters (Sect. 3.1), (2) tests which have controlled shear rate (Sect. 3.2), (3) tests which have controlled stress (Sect. 3.3), (4) tests which have controlled strain (Sect. 3.4), and (5) tests which have oscillatory shear stress and strain (Sect. 3.5).

3.1 Tests with Uncontrolled Parameters

A wide variety of empirical rheological tests can be performed using the geometries described in Sect. 2.3.1:

3.1.1 Time to Flow a Fixed Distance Down an Incline

This type of test includes the sliding index test, which is conducted by placing a fixed volume of the material to be tested in a funnel supported on a ring over the tip of the cone, then allowing the material to flow over the cone; the elapsed time for flow from the vertex to the end of the cone is recorded (Yoo et al. 1995). This empirical data is used to infer relative viscosities, with longer time indicating high viscosity. While this method is simple to execute and inexpensive, significant variation in results can occur due to changes in product temperature, differences in funnel loading techniques, and differences between analysts in determining the conclusion of the slide. Alternatively, this type of test can be conducted by pouring a fixed volume of the material to be tested onto a wedge tilted at 30°; the elapsed time for the material to flow from the top to the bottom of the wedge is recorded (Yoo et al. 1995). This method has similar advantages and disadvantages as flow down a cone. Whether a cone or a wedge incline is used, the collected data cannot be directly converted to well-defined rheological parameters, such as viscosity, due to the uncontrolled flow field as well as the influence of surface tension and wetting power on the flow.

3.1.2 Distance Traveled Down an Incline over a Fixed Time Period

This test is conducted by pouring the test material at the top of an incline, set at a specified angle, and measuring the distance traveled along a horizontal trough over a set time period. This empirical data is also used to infer relative viscosities, with shorter distance indicating high viscosity. Barringer et al. (1998) confirmed that these readings are directly proportional to kinematic viscosity for selected materials, though it is evident that this test generates uncontrolled flow fields which prevent the experimenter from converting the data to viscosity at a specific shear rate. As with the flow down an incline tests, these tests are also impacted by surface tension and wetting effects.

3.1.3 Penetration Force as a Function of Distance and Time at a Fixed Penetration Speed

This test is conducted by driving a probe at a constant speed into the surface of the test material while measuring the force as a function of time and distance. It requires no sample loading and therefore has the advantage of not disrupting the test sample prior to measurement. This measurement cannot be converted to a modulus or viscosity because the uncontrolled flow field does not allow calculation of fundamental rheological properties.

3.1.4 Penetration Distance of a Fixed Weight

This test is conducted by placing a weighted probe on the surface of the test material and measuring the penetration distance after a fixed time. Although this test has the advantage of not disrupting the test material prior to testing, the resulting data cannot be converted to modulus or viscosity because the uncontrolled flow field does not allow reporting in terms of strain or shear rate.

3.1.5 Viscosity as a Function of Rotation Speed at Constant Temperature

Commonly performed via spindle rotation, this test is conducted by inserting the selected spindle for the viscometer into the test material held at constant temperature, then rotating the spindle at a fixed speed for a period of time until equilibrium torque is obtained before stepping up to the next speed. The step up in speed is repeated until the upper limit of speed for the experiment is reached. This type of test is easy to complete on samples in their original containers, as the spindle can be easily inserted and the vessel size is not constrained. By eliminating the loading procedures required for more controlled geometries, the tests can be performed on undisturbed materials and significant experimental time is saved. The resulting torque data is typically converted to viscosity based on the spindle calibration with Newtonian fluids. The shear rate of the test, however, is indeterminate as there is no control of the flow field in a constrained geometry, particularly with spindles with complex geometry.

3.1.6 Viscosity as a Function of Time Constant Rotation Speed

Similar to the previous test, this test is conducted by inserting a selected viscometer spindle into the test material, then rotating the spindle at a fixed speed over the experimental duration. This test has the same advantages and disadvantages of the previous test.

3.1.7 Viscosity as a Function of Temperature at Constant Rotation Speed

Again similar to the previous test, this test is conducted by inserting a selected viscometer spindle into the test material, then rotating at a fixed speed while the temperature is ramped at a predefined rate, with a hold at each selected temperature to allow equilibrium to be reached. This test has the same advantages and disadvantages as the previous two tests.

3.2 Controlled Shear Rate Tests

Fundamental rheology tests with controlled shear rate can be conducted while varying time, temperature, and/or shear rate. If the material to be tested can recover from the disruption during loading and is relatively low viscosity, then the concentric cylinder geometry described in Sect. 2.3.2 is preferred for large deformations as the material is contained within the cup. If the test material is easily disrupted during loading, then careful placement between parallel plates is preferred to minimize disruption of the structure. When using parallel plates, higher shear rates may have to be avoided to ensure sample is not ejected during the test. In these tests, viscosity can be measured as a function of time, temperature, or shear rate.

3.2.1 Viscosity at a Series of Shear Rates

A shear rate sweep test is conducted by applying a series of instantaneous shear rate steps to a sample, starting from a low shear rate and increasing with each step until final high shear rate is achieved. Since the viscosity at each shear rate is time-dependent for non-Newtonian materials, it is critical in this test that the length of time in each shear rate zone be sufficiently long to allow the viscosity to reach equilibrium at that shear rate. The viscosity number reported is then the equilibrium viscosity at each rate. For materials with Newtonian behavior, a constant viscosity value will be obtained as function of shear rate, while for materials with shear-thinning (pseudoplastic) behavior, the viscosity decreases as shear rate increases. In contrast, shear-thickening (dilatant) behavior can be observed when viscosity rises as the shear rate increases (Fig. 9).

3.2.2 Viscosity as Function of Time

Step shear rate tests are conducted by applying an instantaneous change in shear rate to a sample initially at rest while measuring the stress induced in the material. The measured stress is divided by the applied constant shear rate to obtain viscosity as a function of time (Fig. 10). Materials which exhibit non-Newtonian rheology are often classified based on their viscosity-time profiles as either being thixotropic

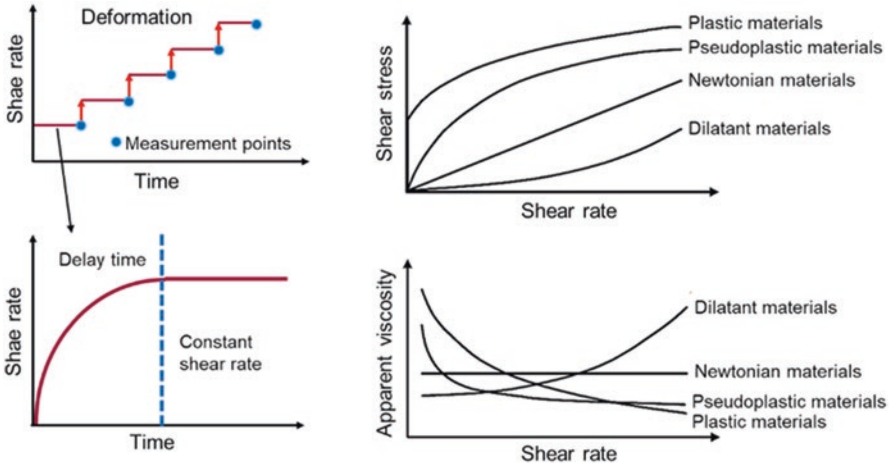

Fig. 9 Illustration of the input (shear rate) and output (stress, viscosity) curves seen for different types of materials for a shear rate sweep test

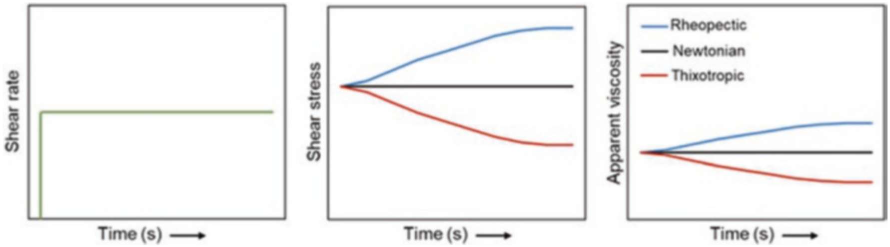

Fig. 10 Illustration of the inputs and outputs for a step shear rate test including shear rate, stress, and viscosity

(decrease in viscosity over time a specific shear rate) or rheopectic (increase in viscosity over time as a fixed shear rate). Newtonian materials, by contrast, exhibit constant viscosity over time.

3.2.3 Viscosity as Function of Temperature

Viscous temperature ramp tests are conducted by applying a constant shear rate to a sample while simultaneously ramping the temperature at a predefined fixed ramp rate. The stress is measured as a function of the changing temperature. The measured stress is divided by the applied constant shear rate to obtain viscosity as a function of temperature. Temperature ramp tests can be difficult to interpret if materials are non-Newtonian and show either thixotropic or rheopectic behavior, as such materials will change over time under shear at the same time they are changing with temperature. This can make interpretation of temperature ramps conducted in rotational mode ambiguous. Therefore, it is often preferable to use temperature ramps performed under oscillation at small strains and moderate frequencies to understand the temperature-dependent changes in thixotropic and rheopectic materials, as these oscillatory tests do not cause changes in the material over time that overlap with the changes due to temperature.

3.3 Controlled Stress Tests

Fundamental controlled-stress rheology tests include creep tests, which track changes in strain or compliance over time, and stress sweep tests, which track changes in shear rate or viscosity with stress. When testing at high stresses where the shear rate is likely to become high, it is preferred to use the concentric cylinder geometry described in Sect. 2.3.2, as long as the sample can recover from loading into the cylinder. If the sample is likely to be disrupted during loading, then the parallel plate geometry is preferred for tests at high stress so that the sample can be placed in the device with minimal disruption. For linear viscoelastic controlled-stress testing, the cone-and-plate geometry is preferred as long as there are no particles in the sample; if particles are present, then the parallel plate geometry is preferred.

3.3.1 Strain as a Function of Time (Creep and Recovery)

In a creep test, an instantaneous constant stress is applied to the sample and the change in strain (called the creep) is recorded over time. The compliance, $J(t)$ (Pa^{-1}), is calculated by dividing the measured strain by the applied constant stress. When the stress is released, some recovery can be observed as the sample attempts a return to its initial shape. Creep tests can be done in either the linear viscoelastic domain (small stresses that do not cause permanent microstructural damage) or in the nonlinear viscoelastic domain (large stresses that disrupt sample microstructures). They are useful for examining long-time relaxation behaviors (Fig. 11), as these behaviors are not easily measurable with an oscillatory test.

3.3.2 Viscosity at a Series of Stresses

Stress sweep tests are conducted by applying a series of instantaneous stress steps to a sample, starting from a low stress and increasing to a final high stress. The hold time at each stress level must be sufficiently long for the material to achieve a constant shear rate, thereby allowing the calculation of the viscosity as the applied stress divided by the equilibrium shear rate achieve at that stress. Stress sweep tests are typically performed in the nonlinear viscoelastic domain and may be considered to be a series of sequential creep tests. Data from this type of test may be visualized

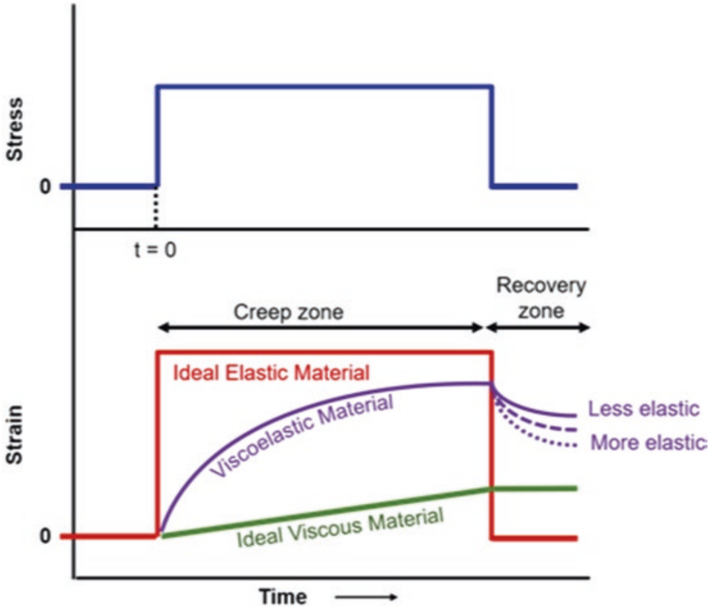

Fig. 11 Illustration of inputs (stress) and outputs (strain) for a creep and recovery test

as viscosity versus stress or as viscosity versus shear rate curve and gives an indication of the material's behavior under repeated loading and unloading.

3.4 *Controlled Strain Tests*

The primary fundamental rheology test with controlled strain is the stress relaxation test, which can be performed at small strains in the linear viscoelastic region or at large strains in the nonlinear viscoelastic region. As discussed in Sections 3.2 and 3.3, the choice of geometry depends upon whether the test is performed at large or small strains and whether the sample is easily disrupted during loading on the testing device with the selected test geometry.

The most common controlled strain test is a stress relaxation test. In this test, the material is exposed to an instantaneous change in strain, and the stress is measured over time. The relaxation modulus, $G(t)$ (Pa), is calculated by dividing the measured stress by the applied constant strain. The stress versus time curve is used to identify the relaxation time, defined as the time required for stress to decay to about 37% of the original level (Gunasekaran and Ak 2003. Elastic solids exhibit a perfect memory of their original state and have a constant stress and relaxation modulus over time, while the stress of ideal viscous liquids declines to zero immediately when strain is applied. Viscoelastic materials exhibit and intermediate behavior and relax gradually with the end point depending on the molecular structure of the tested material (Fig. 12).

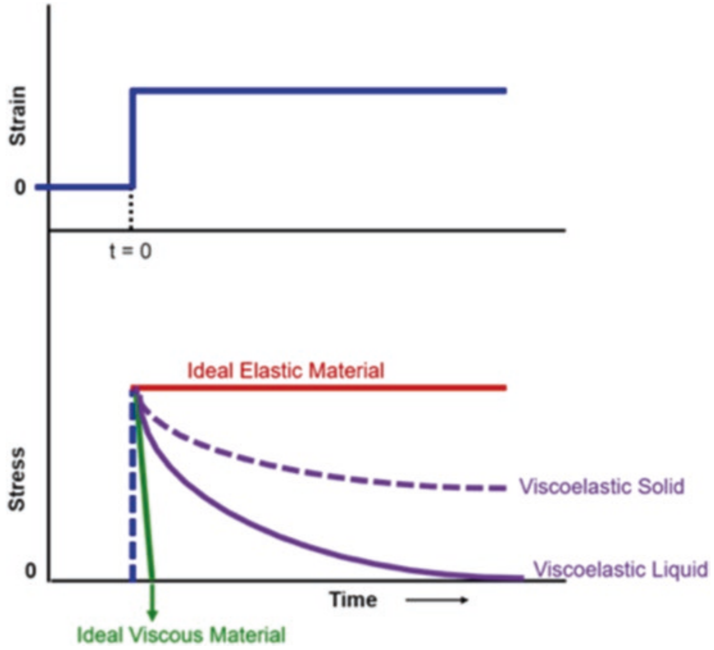

Fig. 12 Illustration of inputs (strain) and outputs (stress) for a stress relaxation test

3.5 *Oscillatory Shear Tests*

Fundamental rheology tests using oscillatory shear are a useful tool for characterizing rheologically complex materials such as semisolids and food pastes (Tsardaka 1990; Rao and Steffe 1992; Steffe 1996; Reilly 1997). Small-strain oscillatory shear testing is the preferred technique for evaluating time-dependent changes in materials such as gelling due to the non-destructive nature of the test. A number of tests are commonly done, including shear stress or strain sweeps, frequency sweeps, time sweeps, and temperature sweeps (Fig. 13).

In an oscillatory shear stress or strain sweep test, the frequency of the oscillation is held constant while the stress or strain amplitude is gradually increased. As described in Sect. 2.6, the linear viscoelastic region can be found by locating the plateau in which storage modulus does not depart significantly from a constant value (Fig. 8); above the critical strain, the modulus decreases. These tests are primarily used to locate the linear viscoelastic region for additional oscillatory testing in the linear viscoelastic region.

When the frequency, strain, and temperature are held constant, the resulting plot is a time sweep. Time sweeps are often used for monitoring reactions, structural assembly, and degradation in food systems. Furthermore, this test, often called a "gel cure" experiment, is well suited for characterizing structural develop-

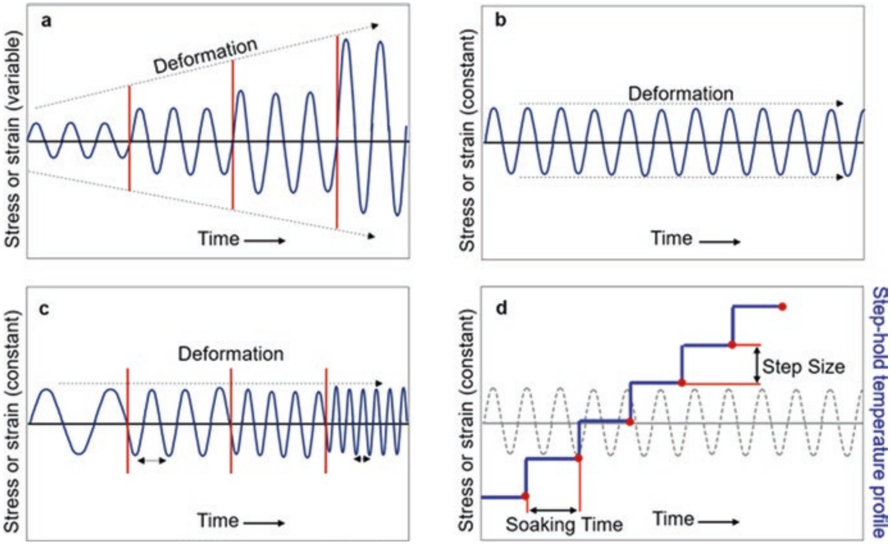

Fig. 13 Strain and stress inputs and output for selected oscillatory shear tests including (**a**) strain or stress sweep, (**b**) time sweep, (**c**) frequency sweep, and (**d**) temperature sweep

ment in physical gels. Importantly, time sweeps should only be conducted when the timescale over which significant change is happening in the sample is longer than $t = 1/\omega$ because the modulus and phase angle measurements are valid only if the sample is not changing over the time scale of sinusoidal perturbation applied. The importance of working at an appropriate frequency is described in the work of Winter and Mours (1997), in which they assessed the reliability of oscillatory shear data collected at different frequencies over time for polymer samples undergoing a liquid-to-solid transition in comparison to data collected on samples which had been quenched at specific times during the treating process and measured independently.

The frequency sweep is a commonly used oscillatory test because it displays how the viscous and elastic behavior of the material vary with the frequency of the applied strain or stress. In this test, the frequency is increased while the amplitude of the input signal (stress or strain) is held constant. It is used to fingerprint material viscoelastic behaviors, which are typically classified as fluid-like, solid-like, or semisolid.

Temperature sweeps ramp temperature at fixed frequency and strain and have been used widely to track phase and state transitions that depend upon temperature. It is important to ensure that no other time-dependent changes are occurring (such as time-dependent gelation) over the time period of the temperature sweep because the time-dependent and temperature-dependent changes become conflated.

4 Semisolid Food Rheology

Semisolid foods have complex microstructures and rheology, which can make it challenging for formulators to design specific textural and processing properties. For targeted formulation of food products with specific textures, the desired structural features of foods need to be identified, and their ingredient functional behavior needs to be classified. When developing semisolid foods, their structure (to some extent) and functional behaviors can be examined with rheological testing. However, there are often measurement challenges that need to be addressed. Proper testing of semisolid foods provides an understanding of the links between semisolid food structure–function relationships and viscous and viscoelastic behavior.

4.1 Semisolid Food Microstructures

The compounds present in foods are organized into microstructures, including foams, emulsions, suspensions, entangled solutions, and gels. Many semisolid foods have more than one microstructure present. Rheological tests probe the macroscopic behavior of the food, which is a function of the microstructure of the system (Rao 2006). Therefore, to predict processing behavior and textural properties, it is necessary to understand the microstructures in the food.

Food emulsions are typically oil-in-water systems which include some puddings, high-oil sauces, dressings, low-fat spreads, most dairy products, and beverage flavor systems. Texturizers in these foods may directly texturize the water phase through thickening or gelling, or they may migrate to the interface between the phases and stabilize the emulsion as a result of their surface-active properties. The link between structure and function for simple emulsions (with no texturizer in the water phase) has been well-documented in books on the topic (e.g. Tadros 2013). In these reviews, maps have been shared which illustrate how to predict the rheology of the final emulsion as a function of the emulsion internal phase droplet size and how to predict which phase will be internal and its droplet size as a function of processing equipment and parameters. For more complex emulsions which include texturizers in a continuous water phase, it is possible to use simple composite model predictions such as those described in fluid mechanics texts where the internal oil phase is modeled on the basis of the previously discussed simple emulsion approaches (Tadros 2013), and the aqueous phase is modeled separately with the composite model weighting the contribution to the rheology of each phase using a simple linear weighting based on the volume fraction of the phase.

Food suspensions can be based on hard or soft particles. Hard particle suspensions include cocoa particles in chocolate drinks and casein in milk beverages. Soft particle suspensions include starch-thickened soups, sauces, dressings, and fillings as well as legume, vegetable, and fruit suspensions with swollen polysaccharide gums and cellulosic components such as tomato sauces, fruit smoothies, salsas, guacamole, and hummus and similar spreads. Literature shows that hard particle suspensions are well described by models (Krieger and Doughherty 1959) which depend upon knowing the concentration of the particle and its density so that the volume fraction in the suspending phase can be calculated. Soft particle suspensions are also readily modeled using approaches described for a swollen starch particle suspension (Steeneken 1989). These models can be used to predict the rheology of the soft particle systems with only the concentration and swelling behavior of the particle as inputs to calculate the volume fraction of the soft particle in the system.

Food foams incorporate air in a liquid matrix. Foamed semisolid foods would include whipped cream, whipped yogurt, and mousses. Prediction of foam properties remains a challenge, largely due to the high levels of instability exhibited by most foamed semisolid foods. This is an area where further research is needed to develop predictive texture models.

Food gels are based on physical interactions between particles or macromolecules to form a sample-spanning, three-dimensional network with persistent interactions. Macromolecular gels are formed due to local associations between chains, typically triggered through helix formation and association, sometimes mediated with ions (Harris 1990). Examples of foods texturized with macromolecular gels include gelled desserts, some puddings, and jellies. Examples of foods texturized with particle gels include cup-set yogurt and melted high-fat ice cream which retains its shape after melting due to a network of fat particles, protein particles, and air bubbles. The gelling behavior of macromolecular food gels is well-studied and empirical data are available that comprehensively describe the viscoelastic properties of the most common systems as a function of concentration, ion content, and molecular weight of the gelling agent; these data are readily used to create fitted models.

Soluble proteins and carbohydrates form viscoelastic solutions with time-dependent relaxation mechanisms. Semisolid texture is observed when the molecular sizes are large enough to allow entanglements between chains, though long-time observations typically reveal liquid-like flow. Some starches, guar, xanthan, and some alginates thicken via this mechanism. This behavior is readily modeled as a function of concentration, entanglement density, and molecular weight.

4.2 Structure and Function of Texturants

Foods are primarily comprised of texturizing agents based on protein, carbohydrate, lipid and/or water. To predict the texture of complex microstructures in food, it is necessary to know how each lipid, carbohydrate, and protein component is distributed within the microstructure and to classify their functional behavior. Most food texturizers can be classified based on their ability to provide thickening, gelling, or interface stabilizing functionality.

4.2.1 Thickeners

Thickeners include both macromolecule thickeners and particulate thickeners. Food ingredients classified as thickeners increase the viscosity of the aqueous phase in foods without exhibiting permanent shape-retention (i.e. they do not increase the extent of elastic behavior). Particulate thickeners, which raise viscosity through particle-to-particle interactions, include some starches (Steeneken 1989), modified whey proteins (Gunasekaran et al. 2007), and vegetable and fruit pulps. Macromolecular thickeners, which thicken through entanglements, include some starches, guar, xanthan, some cellulosics, and some alginates.

4.2.2 Gelling Agents

Gelling agents include macromolecular compounds such as gelatin, pectin carrageenan, some starches, some alginates, agar, and an array of additional polysaccharides described in texts on the subject (Harris 1990). Macromolecular gelling agents form gels through interchain associations. Compounds that form hard particle gels include casein, sugar crystals, and fat crystals; these gelling agents form networks through particle-to-particle association. Food ingredients classified as gelling agents form sample-spanning, three-dimensional networks with effectively permanent interactions. Common gelling agents include gelatin, whey protein, soy protein, pectin, alginate, agar, and some modified celluloses.

4.2.3 Interfacial Stabilizers

Compounds which stabilize air-water or oil-water interfaces contribute to the rheology of these systems because they impact the particle size distribution of the discrete phase and influence the elasticity associated with it. These materials include small-molecule stabilizers such as lecithin, mono- and di-glycerides, and polysorbates (Norn 2015). Large molecules, such as gelatin and gum arabic, also act as interfacial stabilizers, particularly those that can absorb as films at the targeted interface. In addition to the small-molecule surfactants and the film-forming surfactants, there are a number of food-compatible materials that stabilize semisolid foods through particle absorption on the interface to form Pickering emulsions or foams (Lam et al. 2014).

4.3 Measurement Challenges

Semisolid food rheological properties can be difficult to measure for several reasons. First. it is relatively easy to disrupt their structure during loading onto test equipment. Additionally, semisolid foods tend to exhibit macroscopic phase separation and other instabilities over time. While these challenges can be partially addressed through careful sample preparation, test selection, and geometry selection, care must be taken when analyzing rheological data so that artifacts are not interpreted as rheological behaviors. For example, sedimentation during a shear rate sweep may result in an artificially low viscosity.

4.3.1 Disruption of Structure During Test Loading

Sample loading onto rheological equipment can disrupt shear- or compression-sensitive food structures. The approaches for resolving this issue depends upon how soft the sample is and whether it is necessary to obtain fundamental rheological data.

For samples with more rigid structures, this issue can be addressed by carefully cutting a thin layer from the sample, transferring it with minimal disruption to a parallel plate geometry, then setting the gap in manner that only gently squeezes the food (i.e. using normal force rather than height to control gap setting). This technique allows for collection of fundamental rheological data. A second technique used for evaluation of properties for stiffer products is the vane and cup geometry, which has been shown to give equivalent results to other fundamental methods for small-strain experiments on more rigid samples such as set-style yogurt and softer cheeses.

For samples that have more fluid structures, it may be necessary to design molds which can be affixed to a customized rheometer plate. These molds have a rigid baseplate which can be screwed into the rheometer plate and a flexible layer of plastic 1–2 mm in thickness that is adhered to the baseplate with grease. The flexible plastic layer has a circular hole in the middle cut to a dimension slightly larger than the top fixture for the rheology test. With this customized geometry, it is possible to pour foods into the mold after processing and allow them to gel in place. Prior to testing, the flexible plastic is removed and the baseplate is screwed to the bottom rheology fixture. The top fixture is lowered until it fully contacts the molded sample, the sample is trimmed, and the test is executed. The advantage of this approach is that it allows collection of fundamental rheological parameters using a standard geometry. However, given that this approach requires customized tools, it is more common to use non-standard geometries, penetration tests and/or spindle viscometry to collect empirical data. While these techniques can allow collection of information without disruption of the sample, they do not provide data that can be easily compared to other materials using fundamental material parameters such as viscosity at a defined shear rate, modulus, phase angle, or compliance.

4.3.2 Instability of Foods

For some semisolid foods, the texture destabilizes rapidly over time, limiting the types of rheological testing that can be conducted. Examples include foams that are susceptible to coalescence, emulsions that are susceptible to coalescence or creaming, and suspensions that are susceptible to settling. For these foods, rheological testing is not recommended to track the instability. Instead, tracking via optical techniques or direct visual observation is more commonly used.

4.3.3 Phase Separation of Foods

Some semisolid foods are prone to macroscopic phase separation. Examples include yogurt susceptible to syneresis, dressings that separate into oil and water phases, and juices with precipitated pulp. For these systems, the experimenter can mix the phases and test the rheology before re-separation occurs or separate the phases and test each phase independently. Preliminary testing is needed to determine the time at which the phase separation causes significant changes to the rheological behavior of the material, and subsequent testing should be kept within this timeframe. Shearing at a constant rate over time is a good test to determine this time period, since phase separation can cause noticeable changes in viscosity.

4.4 Viscous Properties of Semisolid Foods

The viscous behaviors of foods are directly related to their functional properties, the components present, and how those components are incorporated into the food microstructure. Foods exhibit different viscosity behaviors do so because they have different microstructures which include components with different functional behavior. Specific flow behaviors are discussing in Sect. 2.5; this section discusses how semisolid food structures and components impact these flow behaviors.

Foods that exhibit Newtonian flow behavior typically contain low-molecular weight components (e.g., sugars) and do not contain large concentrations of dissolved or suspended high-molecular weight molecules, such as starch, pectin, or proteins. Examples of Newtonian foods include water, sugar syrups, honeys, edible oils, and milk (Steffe 1996). These foods are typically single-phase, without microstructure, and are thickened due to soluble solids. While these foods are fluids, not semisolids, they are used as components in some semisolid foods that have microstructures which cause the complete food to be a semisolid.

Shear-thinning flow behavior is observed due to temporary or permanent disruption of structure in a food system. Foods that exhibit shear-thinning behavior may contain thickeners, gelling agents, or emulsifiers, all of which form structures that can be disrupted during flow. Gelled foods, foods with high volume fraction emulsions (Tadros 2013), foods with soft-particle suspensions approaching close-packing

(Doublier and Durand 2008), and food foams all show shear-thinning (Steffe 1996). Example food products include salad dressings, thickened sauces and soups, creams, yogurt, and some concentrated juices.

Shear-thickening behavior is observed when suspensions of hard particles, such as slightly gelatinized starch dispersions, are sheared. In general, shear-thickening behavior can be seen when structure is created as a result of flow, such as when hard particle thickeners align to form chains under shear flow. Corn starch in water suspensions are a classic example of a shear-thickening food.

Yield stresses are common in foods with significant three-dimensional structure, which causes the food to act as a solid under low stresses and strains. Foods with yield stresses and subsequent Newtonian behavior upon flow include tomato pastes (Steffe 1996). Foods that have a yield stress and exhibit shear-thinning behavior upon flow include tomato concentrates, tomato ketchup, mustard, mayonnaise, and most semisolid dairy products, such as yogurt, sour cream, cream cheese, and dairy spreads.

4.5 Viscoelastic Properties of Semisolid Foods

In general, semisolid foods that exhibit non-Newtonian viscous behavior also exhibit viscoelastic behavior. A wide array of tests can be conducted on semisolid foods to assess viscoelastic properties, including all of those described in Sects. 3.3, 3.4, and 3.5. A few illustrative examples from the literature are described below.

Information obtained from creep tests can be used to assign the retardation time of foods, which is a characteristic time beyond which the material flows at a particular applied stress (Foegeding et al. 2003). This can be used to predict the "creep" which happens when cheese is gently compressed under its own weight during storage and distribution. This information can be used to determine whether the cheese will slump under its own weight, which is important for packaging and sensory texture considerations.

Oscillatory shear tests are commonly used to probe the structural changes in the materials tested. Strain sweeps have been applied to distinguish weak and strong gels: strong gels will remain in the linear viscoelastic region over higher strains than weak gels (Song et al. 2006). Frequency sweeps are useful for comparing various food systems or comparing the effects of different ingredients and processing conditions on food rheology. Frequency sweep data can exhibit characteristic patterns that are different for dilute solutions, concentrated solutions, and gels (Steffe 1996). In dilute solutions, $G'' > G'$ throughout the frequency range tested, but the values may become similar at higher frequencies. For a concentrated solution, $G'' > G'$ at lower frequencies, displaying more liquid-like features, but $G'' < G'$ at higher frequencies, indicating greater solid-like behaviors. For gels, $G' > G''$ throughout the examined frequency range.

Temperature sweeps are useful to investigate temperature-induced structural changes, including gel formation when a heated dispersion is cooled (Rao and

Cooley 1993), gelatinization of starch solutions through heating (Tattiyakul 1997), and protein gelation (Owen et al. 1992).

5 Yogurt Rheology

Yogurt has a complex structure and rheology. There are three main types of spoonable yogurts on the market: set yogurt, stirred yogurt (Ramaswamy and Basak 1991), and Greek yogurt, which is a strained stirred yogurt. Set yogurt has a firm gel structure that exhibits a clean break pattern when scooped with a spoon. Stirred yogurt is sheared after fermentation, which produces a semisolid consistency. Greek yogurt is stirred yogurt that undergoes a straining step after fermentation to remove additional whey, resulting in a firmer body and thick texture. Stabilizers, fruit pieces and flavors are commonly added to all three types of yogurts. Drinking yogurt, a more fluid product, can be produced by diluting a stirred yogurt with water or fruit juice concentrates.

5.1 Structural Features of Yogurt

Rheological and textural features of yogurt impact the overall quality and consumer acceptability, and are closely linked to the structure, which is influenced by the formulation and processing conditions (Bourne 2002). The primary structuring component of yogurt is casein, which aggregates to form a particle-gel when acidified through culturing (Lucey 2004) or direct acidification (Lucey et al. 1997). The organization of casein particles within the gel influence the properties of the yogurt (Lee and Lucey 2010). Other milk proteins can influence yogurt microstructure. Through denaturation, β-lactoglobulin interacts with the κ-casein on the casein micelle surface, creating disulfide bonds, which are responsible for the increase of gel strength and viscosity of yogurt (Dannenberg and Kessler 1988; Lucey et al. 1997). Furthermore, yogurt fat content directly influences the rheology and final strength of the gel network structure (Bourne 2002; Briggs et al. 1996). By tuning yogurt formulation, yogurt gels can be formed with more or less porosity structures, producing different sensory textures.

Processing variables influence the structure of yogurt, including milk heat treatment conditions, incubation temperature, pH at breaking, cooling conditions, and handling of product post-manufacture (Ozcan 2013; Bourne 2002; Briggs et al. 1996). Stirring of yogurt can also change gel structure from more chain-like clusters to more ball-like clusters. Therefore, it is necessarily to tightly control processing variables to avoid undesirable changes in yogurt microstructure, and therefore its rheology and texture attributes.

5.2 Measurement Challenges

Viscometers are widely used in the food industry to characterize yogurt. Since stirred yogurt exhibits non-Newtonian behavior, its viscosity is dependent on shear rate (Ozcan 2013). However, as a viscometer with a spindle only measures an "apparent" viscosity at one spindle speed that is empirically selected as "consistent" reading after some shearing period, using this measurement method results in an inability to convert the empirical data into more fundamental measurements of stress and shear rate (Ozcan 2013). Moreover, because these tests are typically conducted at one or two rotational speeds, the results can cause a lack or misunderstanding of yogurt flow behaviors, leading to incorrect assumptions about its processing and sensory behaviors. Yogurt flow behaviors can be quite complex and need to be measured over a range of shear rates for proper understanding of the full flow behavior profile.

Similarly, penetration tests involving a probe are commonly conducted on yogurt. These tests are able to capture information on yogurt without disrupting the structure prior to testing. However, they suffer from similar limitations as simple viscometry tests in that the tests provides only limited information on yogurt flow behaviors and the force–distance curves cannot be converted to fundamental material functions such as modulus, stress, and strain.

Fundamental rheological measurements, such as steady shear and oscillatory shear tests, have the potential to provide more complete information on the rheology of concentrated yogurts than traditional empirical viscometry techniques, but to conduct these experiments, it is necessary to prepare and load samples in a manner that preserves the structure of the yogurt. This can be difficult for set-style yogurts because removing them from their containers usually results in gel breakage. Transferring stirred and Greek yogurts may also result in structural damage if the yogurt contains shear-sensitive structures. In general, disruption of the gel matrix during sample preparation and loading will result in rheological data that is not representative of the undisturbed yogurt (Karagül-Yüceer and Drake 2013). For example, structural disruption can result in artificially low viscosity and moduli values; it can also give the sample artificially high fluid-like viscoelastic behavior.

Once the yogurt gel structure is disturbed, it cannot be fully reformed because yogurt gels are metastable. To preserve the gel structure and texture of the yogurt samples, portions need to be scooped gently, minimizing stirring of yogurt which will cause the gel structure to break and whey to separate, leading to further changes in viscosity and viscoelasticity. For yogurts with soft-gel structures, customized molds (see Sect. 4.3) may be used to minimize sample disruption.

Rheological data is gathered, in part, to gain insight on the textural attributes of yogurt, as texture is a critical element of overall consumer acceptance (Brown 2010). Yogurt has been described using a range of terms such as gel-like, graininess, ropiness, over-firmness, body weakness, free whey, and lumpiness (Brown 2010) as well as firmness, creamy, viscosity, curdy, and chalky (Brown 2010; Muir and Hunter 1992). Traditionally, yogurt textural properties have been evaluated with descriptive sensory methodology (Ozcan 2013). Additional techniques included visual evaluation of mounding on a spoon, cutting characteristics, spreadability, and pourability. Instrumental analyses, such as viscosity tests, also have been performed (Ozcan 2013) on yogurt evaluated for sensory attributes, and the viscosity data has most often been correlated with perceived thickness (watery, too thick) of the product.

5.3 Viscous Properties of Yogurt

A large number of studies have been reported on the viscous behavior of set and stirred yogurt (Skriver et al. 1993; Skriver 1995; van Marle et al. 1999; Afonso and Maia 2000; Haque et al. 2001; Lee and Lucey 2006). Since set and stirred yogurt have solid-like behaviors owing to the formation of a weak gel structure, they exhibit non-Newtonian characteristics, such as time-dependency and yield stress (Tárrega et al. 2004). These studies reveal the flow behaviors of yogurt to be dependent on shear rate, time, and applied stress.

All yogurts can be recognized as shear-thinning materials which exhibit reduction in viscosity with increasing shear rate. Yogurt products also show thixotropy that is not fully reversible once the shear is removed. In several studies, stirred yogurt viscosity was measured after the original set gels were empirically agitated using a spoon or a high-speed mixer (Skriver et al. 1993; van Marle et al. 1999). The preparation and loading of the yogurt into the measurement device disrupted the structure of the yogurt, leading to a reduction in measured viscosity. This reduction in viscosity due to disruption of the gel structure during loading was only partially restored after the shearing was stopped. Recovery of structure, or “rebodying”, was shown to be time-dependent phenomenon (Skriver et al. 1993; van Marle et al. 1999).

Time-dependency of yogurt flow behaviors can be analyzed under a shear rate cycle or hysteresis loop. A hysteresis in the shear stress versus shear rate flow curve indicates that shearing at high shear rate changes the material structure (Doublier and Durand 2008). The area of the hysteresis loop correlated with extent of structural breakdown through the shearing cycle (Halmos and Tiu 1981).

Ramaswamy and Basak (1991) considered the flow properties of stirred yoghurts under three consecutive shear rate cycles (Fig. 14). The hysteresis loop area related to the first cycle is greater than those associated with the following cycles, indicating that the first shearing cycle induced the main degradation of the sample structure. The hysteresis loop areas correlated with the second and third shearing cycles were comparable to each other, suggesting similar structure changes. The overlapping of the ascending shear curve of the second or third cycle with its preceding descending shear curves suggested that the structural loss in the ascending shearing process can be partially recovering through the descending shearing process (Ramaswamy and Basak 1991). To characterize the recovery of the thixotropic structural breakdown, Ramaswamy and Basak (1991) rested the yogurt samples for an hour after three con-

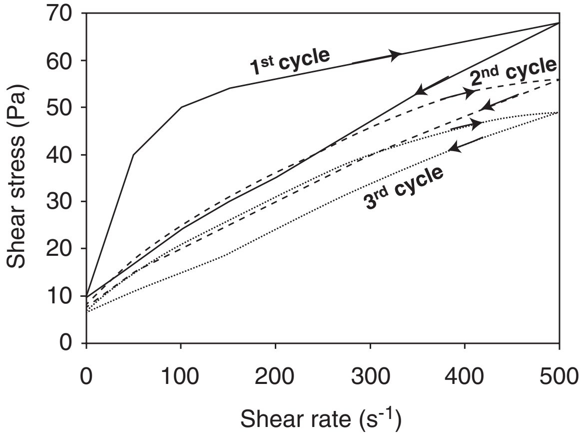

Fig. 14 The typical hysteresis loops in the flow curves (shear stress vs. shear rate) of a stirred yogurt during three consecutive shear cycles. Data obtained from Ramaswamy and Basak (1991)

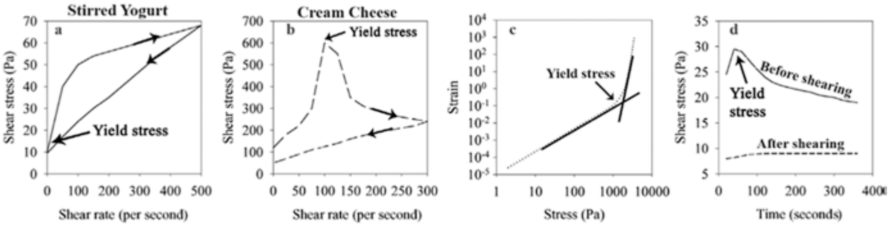

Fig. 15 Determination of yield stress from flow curves of shear-stress-versus-shear-rate of (**a**) stirred yoghurt and (**b**) cream cheese; (**c**) from the stress-strain profile (dotted line) for cream cheese; and (**d**) from a stress versus time profile measured using a vane geometry at a constant rotation rate for a custard model. Assigned yield stresses are marked. (Data obtained from Ramaswamy and Basak (1991), Sanchez et al. (1994), Kealy (2006), and Doublier and Durand (2008))

secutive shearing cycles. The shear stress of yogurt in the repeating test did not reach the same magnitude measured during the first test, indicating that the thixotropic structural breakdown during shearing was not completely reversible within 1 hr.

Semisolid dairy products, including yogurt, exhibit yield stresses which can be identified using shear rate sweep or step-shear rate data (Fig. 15). The yield stress can be determined as the initial stress value in a shear stress versus shear rate curve, which is the minimum stress required to initiate flow (Fig. 15a) (Ramaswamy and Basak 1991). Alternately, yield stress can be assessed by finding the maximum value from the shear stress versus shear rate curve (Fig. 15b) (Sanchez et al. 1994). In a separate study, Kealy (2006) measured yield stress of cream cheese samples using a controlled-stress rheometer to perform a continuous shear stress ramp. Yield stress was determined as the intersection of the two linear regions in the displacement profile (Fig. 15c). Yield stress can also be determined as the maximum stress value in a shear stress versus time curve (Fig. 15d) (Doublier and Durand 2008).

5.4 Viscoelastic Properties of Yogurt

Oscillatory (sinusoidal) stress or strain tests can be applied to yogurt within the linear viscoelastic region (Ramaswamy and Basak 1991; Steffe 1996; Rao 1999; Lee and Lucey 2010). As reviewed in Sect. 2.4, several rheological parameters can be measured, including viscoelastic moduli and phase angle, that provide useful information about the structure of yogurt gels. These methods have been used to characterize the final texture of the yogurt as well as the time-dependent gelling process.

Oscillatory measurements performed at constant strain or stress, frequency, and temperature over time have been widely used to determine different rheological properties of yogurts during and after the gel formation process (or fermentation) without inducing damage to the weak gel network structure. An example of a typical gelation profile during the fermentation of yogurt as determined by this type of test is shown in Fig. 16. During fermentation, a protein gel forms and G'values increase due to the associations between protein particles. At intermediate times, there is an increase in the tan δ value, which may result from a partial loosening of gel network as the calcium phosphate in the casein micelles became soluble. The tan δ value then subsequently decreases as the attractive interactions between casein particles begin to dominate, the casein approaches its isoelectric point ($pI = 4.6$), and further gelation occurs (Lucey 2004). Lankes et al. (1998) and Lucey et al. (1999) found that the viscoelastic moduli for set and stirred yogurts increased with incubation temperature and protein concentration. They concluded that the higher G' values resulted from stronger protein bonds contributing to the elastic characteristics and the higher G'' values were due to weaker bonds.

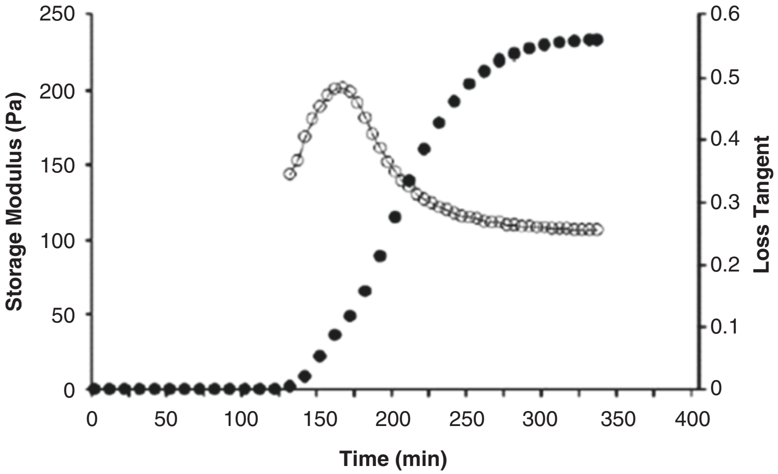

Fig. 16 Typical gelation profile of yogurts. Yogurt gels were produced from milk preheated at 90 °C for 30 min and incubated at 40 °C. Solid (●) and open (○) symbols are storage modulus and loss tangent, respectively. (Data obtained from Lee and Lucey (2010))

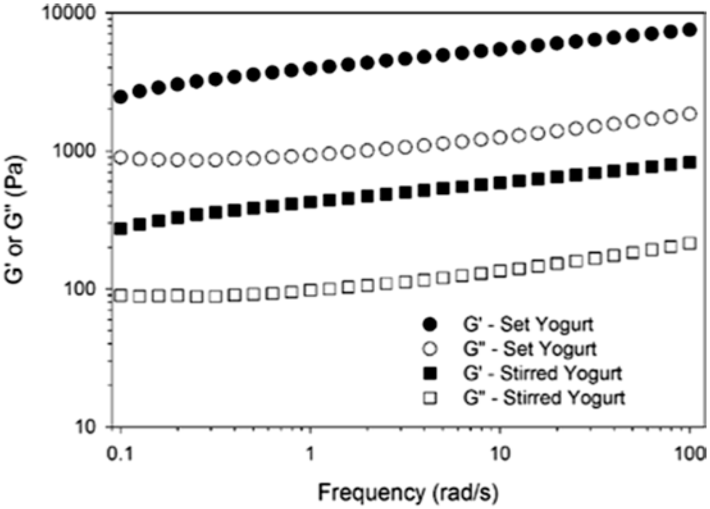

Fig. 17 Typical dynamic mechanical behavior of set and stirred and set yogurts at 5 °C

Another oscillatory shear test that has been extensively used to characterize structural properties of yogurts is the frequency sweep. The test reveals the response of the structure to different experimental times: a relatively low frequency such as 0.01 Hz could be considered a long time (100 s), as opposed to a relatively high frequency such as 100 Hz, which would be a short time (0.01 s). Bonds between particles in a sample may deform, break, and reform through the observation time, either spontaneously or from applied strain or stress. Bond-breaking and bond-making lead to structural changes that affect rheological properties (Renard et al. 2006).

Frequency sweeps over at least three decades of frequency can be used to determine the type of the gel formed in the sample. Protein gels in yogurt can be classified as cross-linked (via β-lactoglobulin disulfide interactions) and/or physical gels (via hydrophobic associations between casein particles) (Tunick 2011). Yogurt can be classified as a physical gel since the dynamic moduli increase with the frequency and $G' > G''$ throughout of the test (i.e. there is no moduli crossover) (Fig. 17). Similar behavior has been reported for yogurt prepared with different fat contents, various fat replacers, or treated under varied processing conditions. Higher G' and G'' values were seen for set yogurts in comparison with those of stirred yogurts, indicating a stronger, more developed gel structure that resulted from greater protein–protein connectivity.

6 Looking Forward

While it is clear that rheological data provides insight on the structural and functional properties of semisolid foods such as yogurt, there are significant opportunities to enhance the knowledge derived from such data through research and collaborative development on several fronts, including:

- Research on improved standardized sample preparation techniques using molds and related fixtures that can be affixed to rheometers and to compression testing equipment such that fundamental shear and extensional rheology data can be collected without disrupting the structure of the food; ideally these fixtures would be widely available through equipment vendors,
- Alignment and standardization of the specific rheological tests that should be conducted for each class of semisolid food with recommended tabular data collection at specific measurement conditions to allow creation of databases that can be widely shared,
- Creation of shared databases by food type, capturing data from standardized methods, with peer-reviewed experimental designs and data collection, and
- Development of predictive models based on large datasets in shared databases that capture the impact of composition and processing on the rheological properties of the foods studied.

This review of the wide-ranging research conducted on the physics, structure, and rheology of semisolid foods shows the promise of using such data to more reliably predict processing behavior and textural attributes, and accordingly shorten the product design process. However, greater collaboration amongst researchers and alignment of research studies to deliver sharable knowledge is required to fulfill that promise.

References

Afonso, I. M., & Maia, J. M. (2000). Rheological monitoring of structure development and rebodying of set-style yoghurt. *Applied Rheology, 10*, 73–79.

Barnes, H. A. (2000). *A handbook of elementary rheology*. Dyfed, Wales: University of Wales.

Barnes, H. A., & Walters, K. (1985). The yield stress myth. *Rheologica Acta, 24*, 324–326.

Barringer, S. A., et al. (1998). On-line prediction of Bostwick consistency from pressure differential in pipe flow for ketchup and related tomato products. *Journal of Food Processing & Preservation, 22*, 211–220.

Bongenaar, J. J. T., Kossen, N. W. F., Metz, B., & Meijboom, F. (1973). A method for characterizing the rheological properties of viscous fermentation broths. *Biotechnology and Bioengineering, 15*, 201–206.

Bourne, M. (2002). *Food texture and viscosity: Concept and measurement*. San Diego: Academicn Press.

Briggs, J. L., Steffe, J. F., & Ustunol, Z. (1996). Vane method to evaluate the yield stress of frozen ice cream. *Journal of Dairy Science, 79*, 527–553.

Brown, M. (2010). *Sensory characteristics and classification of commercial and experimental plain yogurts.* M. S. thesis.:University of Delware.

Dannenberg, F., & Kessler, H. G. (1988). Effect of denaturation of β-lactoglobulin on texture properties of set-style nonfat yoghurt. 1. Syneresis. *Milchwissenschaft, 43*, 632–635.

Doublier, J. L., & Durand, S. (2008). A rheological characterization of semi-solid dairy systems. *Food Chemistry, 108*(4), 1169–1175.

Ferry, J. D. (1980). *Viscoelastic properties of polymers*. Canada: Wiley.

Foegeding, E. A. B. J., Drake, M. A., & Daubert, C. R. (2003). Sensory and mechanical aspects of cheese texture. *International Dairy Journal, 13*(8), 585–591.

Gunasekaran, S., & Ak, M. M. (2003). *Cheese rheology and texture*. Boca Raton: CRC Press.

Gunasekaran, S., Ko, S., & Xiao, L. (2007). Use of whey protein for encapsulation and controlled delivery applications. *Journal of Food Engineering, 83*, 31–40.

Halmos, A. L., & Tiu, C. (1981). Liquid foodstuffs exhibiting yield stress and shear degradability. *Journal of Texture Studies, 12*, 39–46.

Haque, A., Richardson, R. K., & Morris, E. R. (2001). Effect of fermentation temperature on the rheology of set and stirred yogurt. *Food Hydrocolloids, 15*, 593–602.

Harris, P. (1990). *Food gels*. London: Elsevier Applied Science.

Karagül-Yüceer, Y., & Drake, M. A. (2013). Sensory analysis of yogurt. In *Manufacturing yogurt and fermented milks* (pp. 353–367). UK: Blackwell Publishing.

Kealy, T. (2006). Application of liquid and solid rheological technologies to the textural characterization of semi-solid foods. *Food Research International, 39*(3), 265–276.

Krieger, I. M., & Doughherty, T. J. (1959). A mechanism for non-Newtonian flow in suspensions of rigid spheres. *Transactions. Society of Rheology, 3*, 137–152.

Lam, S., Velikov, K., & Veliv, O. (2014). Pickering stabilization of foams and emulsions with particles of biological origin. *Current Opinion in Colloid and Interface Science, 19*, 490–500.

Lankes, H., Ozer, B. H., & Robinson, R. K. (1998). The effect of elevated milk solids and incubation temperature on the physical properties of natural yoghurt. *Milchwissenschaft, 53*(9), 510–513.

Lee, W. J., & Lucey, J. A. (2006). Impact of gelation conditions and structural breakdown on the physical and sensory properties of stirred yogurts. *Journal of Dairy Science, 89*, 2374–2385.

Lee, W. J., & Lucey, J. A. (2010). Formation and physical properties of yogurt. *Asian-Australasian Journal of Animal Sciences, 23*(9), 1127–1136.

Lucey, J. A. (2004). Cultured dairy products: An overview of their gelation and texture properties. *International Journal of Dairy Technology, 57*, 77–84.

Lucey, J. A., Munro, P. A., & Singh, H. (1999). Effects of heat treatment and whey protein addition on the rheological properties and structure of acid skim milk gels. *International Dairy Journal, 9*, 275–279.

Lucey, J. A., Teo, C. T., Munro, P. A., & Singh, H. (1997). Rheological properties at small (dynamic) and large (yield) deformations of acid gels made from heated milk. *The Journal of Dairy Research, 64*, 591–600.

Muir, D., & Hunter, W. A. (1992). Sensory evaluation of fermented milks: Vocabulary development and the relations between sensory properties and composition and between acceptability and sensory properties. *International Journal of Dairy Technology, 45*, 73–80.

Norn, V. (2015). *Emulsifiers in food technology* (2nd ed.). Chichester: Wiley.

Owen, S. R., Tung, M. A., & Paulson, A. T. (1992). Thermorheological studies of food polymer dispersions. *Journal of Food Engineering, 16*, 39–53.

Ozcan, T. (2013). *Determination of yogurt quality by using rheological and textural parameters* (pp. 118–122). Singapore: IACSIT Press.

Papanastasiou, T. C. (1987). Flows of materials with yield. *Journal of Rheology, 31*, 385–404.

Ramaswamy, H. S., & Basak, S. (1991). Rheology of stirred yogurts. *Journal of Texture Studies, 22*(2), 231–241.

Rao, M. A. (1999). Rheological behavior of processed fluid and semisolid foods. In *Rheology of fluid and semisolid foods: Principles and applications* (pp. 223–338). New York: Springer.

Rao, M. A. (2006). Influence of food microstructure on food rheology. In *Understanding and controlling the microstructure of complex foods* (pp. 411–422). Cambridge: Woodhead Publishing Ltd.

Rao, M. A., & Cooley, H. J. (1993). Dynamic rheological measurement of structure development in high-methoxyl pectin/fructose gels. *Journal of Food Science, 58*, 876–879.

Rao, M. A., & Steffe, J. F. (1992). *Viscoelastic properties of foods*. London: Elsevier Applied Science.

Reilly, D. L. (1997). Food rheology. In *Chemical engineering in the food industry* (pp. 195–232). London: Springer Science + Business Media.

Renard, D., van deVelde, F., & Visschers, R. W. (2006). The gap between food gel structure, texture and perception. *Food Hydrocolloids, 20*, 423–431.

Sanchez, C., et al. (1994). Rheological and textural behavior of double cream cheese. II: Effect of curd cooling rate. *Journal of Food Engineering, 23*(4), 595–608.

Skriver, A. (1995). *Characterization of stirred yoghurt by rheology, microscopy and sensory analysis. Dissertation.* s.l.:The Royal Veterinary and Agricultural University.

Skriver, A., Roemer, H., & Qvist, K. B. (1993). Rheological characterization of stirred yoghurt viscometry. *Journal of Texture Studies, 24*, 185–198.

Song, K. W., Kuk, H. A., & Chang, S. G. (2006). Rheology of concentrated xanthan gum solutions: Oscillatory shear flow behavior. *Korea-Australia Rheology Journal, 18*(2), 67–81.

Spaans, R. D., & Williams, M. C. (1995). Letter to the editor: At last, a true liquid-phase yield stress. *Journal of Rheology, 39*, 241–246.

Steeneken, P. A. (1989). Rheological properties of aqueous suspensions of swollen starch granules. *Carbohydrate Polymers, 11*, 23–42.

Steffe, J. F. (1996). *Rheological methods in food process engineering*. East Lansing: Freeman Press.

Tadros, T. F. (2013). *Emulsion formation and stability* (1st ed.). Weinheim: Wiley-VCH Verlag GmbH & Co. KGaA.

Tárrega, A., Durán, L., & Costell, E. (2004). Flow behavior of semi-solid dairy desserts. Effect of temperature. *International Dairy Journal, 14*(4), 345–353.

Tattiyakul, J. (1997). *Studies on granule growth kinetics and characteristics of tapioca starch dispersion during gelatinization using particle size analysis and rheological methods.* S.l.:Cornell University.

Tsardaka, E. D. (1990). *Viscoelastic properties and compaction behavior of pharmaceutical particulate materials.* s.l.:University of Bath.

Tunick, M. H. (2011). Small-strain dynamic rheology of food protein networks. *Journal of Agricultural and Food Chemistry, 59*, 1481–1486.

van Marle, M. E., van den Ende, D., de Kruif, C. G., & Mellema, J. (1999). Steady-shear viscosity of stirred yogurts with varying ropiness. *Journal of Rheology, 43*, 1643–1662.

Winter, H. H., & Mours, M. (1997). Rheology of polymers near liquid-solid transitions. *Advances in Polymer Science, 134*, 165–234.

Yoo, B., Rao, M. A., & Steffe, J. F. (1995). Yield stress of food dispersions with the vane method at controlled shear rate and shear stress. *Journal of Texture Studies, 26*, 1–10.

LAOS (Large Amplitude Oscillatory Shear) Applications for Semisolid Foods

Gamze Yazar, Ozlem Caglar Duvarci, Merve Yildirim Erturk, and Jozef L. Kokini

1 Nonlinear Rheology

1.1 LAOS (Large Amplitude Oscillatory Shear)

1.1.1 Theory

Small amplitude oscillatory shear (SAOS) tests have been one of the most commonly used rheological testing methods to study the linear viscoelastic properties of a wide range of soft materials and complex fluids (Bird et al. 1987; Hyun et al. 2011). SAOS measurements investigate the material's response by observing the strain and frequency dependence of the storage modulus (G', Pa) and loss modulus (G'', Pa) in the linear viscoelastic region (LVR) at small strains and provides information without significantly disturbing the three-dimensional structure of the materials (Duvarci et al. 2017b). However, most food materials are subjected to large, rapid deformations in most uses, including sensory evaluation during consumption, processing operations, transportation, and storage. Thus, nonlinear rheological properties may offer a more detailed understanding of food rheological behaviors under these real application conditions, which may not be obtainable through SAOS measurements. This fuller understanding of the system requires the evaluation of

---

G. Yazar
Food Science Department, Purdue University, West Lafayette, IN, USA

School of Food Science, University of Idaho, Moscow, ID, USA

O. Caglar Duvarci
Food Science Department, Purdue University, West Lafayette, IN, USA

Department of Chemical Engineering, Izmir Institute of Technology, Izmir, Turkey

M. Yildirim Erturk · J. L. Kokini (✉)
Food Science Department, Purdue University, West Lafayette, IN, USA
e-mail: jkokini@purdue.edu

H. S. Joyner (ed.), *Rheology of Semisolid Foods*, Food Engineering Series,
https://doi.org/10.1007/978-3-030-27134-3_4

material nonlinearities through nonlinear test protocols that can provide full material characterization (Hyun et al. 2011).

A new fundamental theory of nonlinear viscoelastic behavior was developed by Ewoldt, McKinley, and their group (2007), which unraveled the progressive transition from linear to nonlinear viscoelastic rheological responses of complex fluids and soft solids. They developed sound rheological parameters to characterize viscoelastic behavior in the nonlinear viscoelastic region through the elegant use of Fourier transforms coupled with Chebyshev polynomials (Ewoldt et al. 2007; Hyun et al. 2011; Ewoldt 2013; Liu et al. 2014). A brief overview of this theory is presented below; for full details, the reader is encouraged to review the seminal paper by Ewoldt et al. (2008).

The linear viscoelastic properties of a material are traditionally measured at very low strain amplitudes (SAOS region) where G' and G'' are constant as strain increases at a constant frequency. SAOS is a non-destructive test, and the stress response is a perfect sinusoidal wave when a small sinusoidal strain is applied (Fig. 1). After a critical strain value, G' and G'' are no longer constant, and the material displays nonlinear viscoelastic behavior. The region where the nonlinear material response is probed by conducting oscillatory shear tests beyond the LVR is defined as the large amplitude oscillatory shear (LAOS) region. LAOS tests involve the systematic increase of the amplitude of the applied strain or stress at fixed frequencies (Hyun et al. 2011) and measuring the stress or strain response. The resulting material response is represented by Lissajous-Bowditch curves (see Sect. 1.1.2),

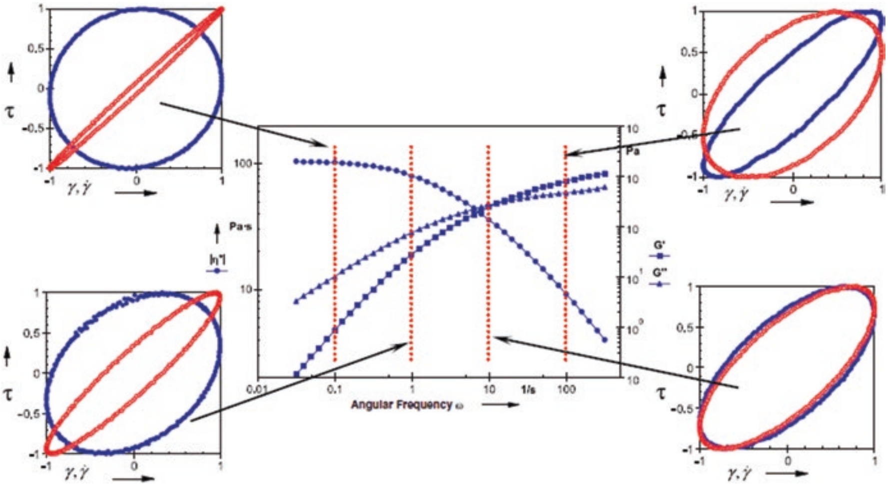

Fig. 1 Lissajous-Bowditch curves for a frequency sweep measurement (at 0.1, 1, 10, and 100 rad/s) and at a constant strain of 1%. Blue lines in Lissajous-Bowditch plots are elastic planes of stress ($\tau(\gamma)$); red lines are viscous planes of stress ($\tau(\dot{\gamma})$) (Läuger and Stettin 2010)

which are intracycle stress versus strain plots typically normalized using the amplitude of stress and strain. The intracycle stress-strain plots can also be deconvoluted into viscous and elastic contributions. A rheological fingerprint of a material may be constructed by plotting Lissajous-Bowditch curves (or their elastic and viscous components) in the form of Pipkin diagrams, or an arrangement of the curves over a variety of frequencies and strains (Ewoldt et al. 2007).

In the nonlinear viscoelastic region, the stress response is not sinusoidal and thus cannot be defined by a sinusoidal wave function. This non-sinusoidal stress response needs to be described by a different mathematical method, such as a Fourier series, which consists of an infinite sum of sine and cosine functions with progressively increasing frequencies (higher harmonics) where the transient data is transformed from the time domain to the frequency domain. The Fourier series can be decoupled into two different series that represent elastic (stress–strain behavior, Eq. 1) and viscous (stress–strain rate behavior, Eq. 2) behavior:

$$\sigma\left(t;\omega,\gamma_0\right)=\gamma_0\sum_{n\,\mathrm{odd}}\left[G_n'\left(\omega,\gamma_0\right)\sin n\omega t+G_n''\left(\omega,\gamma_0\right)\cos n\omega t\right] \tag{1}$$

$$\sigma\left(t;\omega,\dot{\gamma}_0\right)=\dot{\gamma}_0\sum_{n\,\mathrm{odd}}\left[\eta_n''\left(\omega,\gamma_0\right)\sin n\omega t+\eta_n'\left(\omega,\gamma_0\right)\cos n\omega t\right] \tag{2}$$

where t represents time (s), ω is the imposed oscillation frequency (rad s^{-1}), γ_0 is the strain amplitude (unitless), n is number of odd harmonics, G_n' is elastic modulus of nth harmonic (Pa), G_n'' is viscous modulus of nth harmonic (Pa), $\dot{\gamma}_0$ is the resulting strain rate (s^{-1}), and η_n' and η_n'' are dynamic viscosities of the nth harmonic (Pa.s) (Ewoldt et al. 2008).

In the LAOS region, as the stress response is non-sinusoidal, the storage modulus (G', Pa) and the loss modulus (G'', Pa) lose their physical meanings and become a function of the strain amplitude as well as the applied frequency ($G'(\gamma_0, \omega)$) and $G''(\gamma_0, \omega)$) (Nam et al. 2010; Hyun et al. 2011). Ewoldt et al. (2008) deconvoluted the generic nonlinear, non-sinusoidal stress response into a superposition of an elastic stress $\sigma'(x)$ (Pa), where $x = \gamma/\gamma_0 = \sin \omega t$, and viscous stress $\sigma''(y)$ (Pa), where $y=\dot{\gamma}/\dot{\gamma}_0=\cos\omega t$. The sum of elastic and viscous contributions is expressed as the total periodic stress, $\sigma(t) = \sigma'(t) + \sigma''(t)$, and they are linked to the Fourier decomposition as indicated below:

$$\sigma' \equiv \frac{\sigma\left(\gamma,\dot{\gamma}\right)-\sigma\left(-\gamma,\dot{\gamma}\right)}{2}=\gamma_0\sum_{n\,\mathrm{odd}}G_n'\left(\omega,\gamma_0\right)\sin n\omega t \tag{3}$$

$$\sigma'' \equiv \frac{\sigma\left(\gamma,\dot{\gamma}\right)-\sigma\left(\gamma,-\dot{\gamma}\right)}{2}=\gamma_0\sum_{n\,\mathrm{odd}}G_n''\left(\omega,\gamma_0\right)\cos n\omega t \tag{4}$$

Note that only odd harmonics are used to describe the rheological response of the sample (Läuger and Stettin 2010). Higher-order harmonics usually occur at larger amplitudes of strain; however, only odd harmonics are considered because they are caused by the rheological response of the fluid as a result of odd symmetry with respect to the directionality of shear strain or strain rate (Fig. 1). The presence of even harmonics might be due to wall slip, secondary flows, and fluid inertia and are less relevant (Graham 1995; Reimers and Dealy 1998; Yosick et al. 1998; Atalik and Keunings 2002).

The strain dependence of material properties is uniquely described using Chebyshev polynomials as follows:

$$\sigma'(x) = \gamma_0 \sum_{n:\text{odd}} e_n(\omega,\gamma_0) T_n(x) \tag{5}$$

$$\sigma''(y) = \dot{\gamma}_0 \sum_{n:\text{odd}} v_n(\omega,\gamma_0) T_n(y) \tag{6}$$

where e_n and v_n are the nth-order Chebyshev coefficients and $T_n(x)$ and $T_n(y)$ are the nth-order Chebyshev polynomials for variables x and y, respectively. The first ($T_1(x) = x$), third ($T_3 = 4x^3 - 3x$), and fifth ($T_5 = 16x^5 - 20x^3 + 5x$) Chebyshev polynomials are independent from each other due to their orthogonality. This is a key feature of the work: previous models used non-independent coefficients, meaning that their values changed if a different number of harmonics was used in the calculation. If a material showed a different number of harmonics above the noise level when run on multiple instruments, the coefficient values for each harmonic would change based on the number of harmonics used and the results would not be fundamental. Thus, Ewoldt et al. selected Chebyshev polynomials to remove this dependence, allowing different numbers of harmonics to be used in the calculation of the coefficients without impacting their values (Ewoldt et al. 2008).

Ewoldt et al. (2008) astutely recognized that $e_n(\omega, \gamma_0)$ represented the elastic Chebyshev coefficients and $v_n(\omega, \gamma_0)$ the viscous Chebyshev coefficients, and that these coefficients were related to the Fourier coefficients as follows:

$$e_n = G_n'(-1)^{(n-1)/2} \qquad n:\text{odd} \tag{7}$$

$$v_n = \frac{G_n''}{\omega} = \eta_n' \qquad n:\text{odd} \tag{8}$$

The first-order Chebyshev and Fourier coefficients (e_1 and G_1', v_1 and G_1'') are a measure of the average elasticity and dissipated energy in a full sinusoidal strain cycle that includes both the contribution of deformation in the linear viscoelastic region and nonlinear viscoelastic region. When, $e_3/e_1 \ll 1$ and $v_3/v_1 \ll 1$, there is no contribution of nonlinearity and the material is in the linear viscoelastic region. Since the contribution of the fifth Chebyshev polynomial is very small, the third Chebyshev polynomial is used as a measure of nonlinearity. Therefore, the third-order Chebyshev coefficients (e_3 and v_3) may be used to interpret the deviations from linearity and evaluate the local nonlinear viscoelastic behavior of the material.

The total stress calculated by Ewoldt et al. (2008) is an improvement on the equation provided by Reimers and Dealy (1996), which is an expression of Fourier transform rheology in terms of amplitude and phase:

$$\sigma = \gamma_0 \sum_{n:\text{odd}} \left|G_n^*\right| \sin\left(n\omega t + \delta_n\right) \tag{9}$$

where $\left|G_n^*\right| = \sqrt{G'^2_n + G''^2_n}$ (Pa), γ_0 is strain amplitude (unitless), G_n^* is complex modulus (Pa), G_n' is the nth harmonic elastic modulus (Pa), G_n'' is viscous modulus of nth harmonic (Pa), n is the number of odd harmonics (unitless), ω is the imposed oscillation frequency (rad/s), t is time (s), and δ_n is phase angle of the imperfect wave with respect to the input strain signal $\gamma(t) = \gamma_0 \sin \omega t$ (rad). At $\omega t = 0$, the third harmonic contribution is $\left|G_n^*\right| \sin\left(\delta_3\right)$, and oscillates with a frequency of $3\omega_1$ for $\omega t > 0$. The parameter δ_3 determines the initial value of the viscous and elastic third harmonic contributions and must range from $0 \le \delta_3 \le 2\pi$. Using these equations, Ewoldt et al. (2008) related the $n = 3$ Chebyshev coefficients and the third-order phase angle with the intracycle stiffening/softening and thickening/thinning behaviors as follows:

$$e_3 = -\left|G_3^*\right| \cos\delta_3 \quad \begin{matrix} 0 \text{ for } 0 < \delta_3 < \pi/2 \text{ and } 3\pi/2 < \delta_3 < 2\pi, \quad \text{strain stiffening} \\ = 0 \text{ for } \delta_3 = \pi/2, 3\pi/2, \quad \text{linear elastic} \\ \pi/2 < \delta_3 < 3\pi/2, \quad \text{strain softening} \end{matrix} \tag{10}$$

$$v_3 = \frac{\left|G_3^*\right|}{\omega} \sin\delta_3 \quad \begin{matrix} > 0 \text{ for} 0 < \delta_3 < \pi, \quad \text{shear thickening} \\ = 0 \text{ for} \delta_3 = 0, \pi, \quad \text{linear viscous} \\ < 0 \text{ for} \pi < \delta_3 < 2\pi, \quad \text{shear thinning} \end{matrix} \tag{11}$$

It is important to point out that the linear material functions G' and G'' (equivalent to G_1' and G_1'') represent the average stress responses equivalent to the first-order Chebyshev coefficients e_1 and v_1, respectively. These moduli are commonly used to quantify the transition from SAOS to LAOS: the onset of nonlinear viscoelastic behavior is generally considered to occur when the deviation of G' is higher than 3% of its previous value. However, the magnitude of the third-order order elastic and viscous Chebyshev coefficients e_3 and v_3 can be used to indicate SAOS to LAOS transitions. Moreover, e_3 and v_3 can reveal the underlying cause(s) driving the nonlinear elastic and viscous intracycle stress response.

Note that these descriptions of strain- and shear-related behavior are derived from the decoupled elastic and viscous stress–strain curves, not the total stress–strain curve. Furthermore, these coefficients do not indicate the absolute or relative magnitude of elastic versus viscous behavior in a given sample; For example, it is possible for a viscoelastic solid with a low phase angle to exhibit shear-thinning or shear-thickening behavior according to its Chebyshev coefficients. A result like this would not indicate that the material is flowing during stress, merely that its viscous component is displaying shear-thinning behavior. Therefore, care must be taken when interpreting LAOS data, and a variety of parameters should be examined to provide an accurate description of material behaviors under LAOS.

1.1.2 Lissajous-Bowditch Curves

Lissajous-Bowditch curves consist of plots of the intracycle periodic stress normalized for stress amplitude, $\sigma/\sigma_0(t;\, \omega, \gamma_0)$, plotted against the strain data normalized for strain amplitude, γ/γ_0 (Ewoldt et al. 2008). These curves provide visual depictions of the characteristic transitions from the linear to the nonlinear viscoelastic region and the dramatic changes in the shape of the curve in the nonlinear viscoelastic region. Lissajous curves can also be decomposed into elastic and viscous components following the definitions in Equations 5 and 6.

To obtain the necessary data for these curves, strain sweep tests are conducted to obtain the linear viscoelastic region (SAOS region) followed by the transition from linear to the onset of nonlinear viscoelastic behavior (MAOS region) and finally the region of full nonlinear viscoelastic behavior (LAOS region). In the SAOS region, the Lissajous-Bowditch curves are elliptical regardless of frequency (Fig. 1). However, applied frequency can have a significant effect on the response of fluids and semisolids. A transition from more fluid-like to more solid-like flow behavior can be seen by a decrease in the enclosed area of $\tau(\gamma)$ and an increase in the enclosed area of $\tau\left(\dot{\gamma}\right)$ in Lissajous-Bowditch curves as frequency increases (Fig. 2).

LAOS measurements can be conducted using both strain-controlled and stress-controlled rheometers. Strain-controlled rheometers give inertia-free strain–frequency data. Stress-controlled rheometers can also be used for LAOS

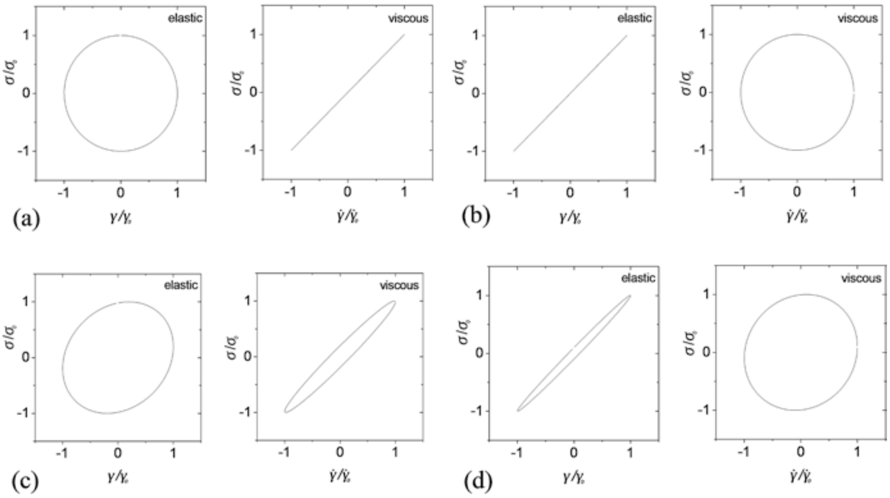

Fig. 2 Elastic and viscous Lissajous-Bowditch curves of (**a**) a purely viscous liquid, (**b**) a purely elastic solid, (**c**) a viscoelastic liquid, and (**d**) a viscoelastic solid

measurements if the torque inertia does not affect the sinusoidal shape of the applied strain (Bae et al. 2013). There is a third control mode known as direct strain oscillation (DSO) that uses a real-time position control and an electronically-commutated motor (EC motor). The desired sinusoidal strain input can be applied by direct control of the position (displacement) of the measuring system in each oscillation cycle as the motor applies torque. Thus, this control method is a hybrid of stress- and strain-controlled modes. It is important to note that differences in response can be observed between three different measurement modes. For example, the intracycle behavior of xanthan gum is shear-thickening for a sinusoidal strain input, but shear thinning for a sinusoidal stress input (Läuger and Stettin 2010). Because of these differences, caution is needed when comparing data collected using two different control modes.

Normalized intracycle stress data can be plotted versus both strain and strain rate. Stress versus strain plots provide elastic Lissajous-Bowditch curves; stress versus strain rate plots give viscous Lissajous-Bowditch curves. This pair of plots offers insights related to microstructural changes for a given imposed strain at a fixed frequency and temperature. A purely viscous fluid shows a perfect circle in the elastic plane and a straight line in the viscous plane (Fig. 2a) because purely viscous fluids dissipate all energy during deformation. A purely elastic solid stores all energy input, resulting in a straight line in the elastic plane and a perfect circle in the viscous plane (Fig. 2b). Hence, it can be said that the area of Lissajous-Bowditch curves in the stress–strain plane gives the energy lost during intracycle deformation and the area of the curves in the stress–strain rate plane is related to the stored energy during intracycle deformation. Because viscoelastic materials have elements of both viscous and elastic behavior, the Lissajous-Bowditch curves of these materials have elliptical shapes. Viscoelastic fluids show elliptically shaped Lissajous-Bowditch curves with a longer minor axis in the elastic plane and a shorter minor axis in the viscous plane (Fig. 2c). However, if the material is a viscoelastic solid, it shows a shorter minor axis and a longer minor axis in Lissajous-Bowditch curves in the elastic and viscous planes, respectively (Fig. 2d).

The new parameters defined by Ewoldt et al. (2008) lead to new and previously untapped insightful information on the nonlinear viscoelastic behavior of complex structured food materials. For example, the viscoelastic behaviors of tomato paste vary widely with the amplitude of an applied strain. At 0.01% strain, tomato paste is in the linear viscoelastic region and the elastic Lissajous-Bowditch curve has a narrow elliptical shape (Fig. 3a). As strain increases to 180%, the elliptical Lissajous-Bowditch curves become wider because the viscous forces rapidly increase in the nonlinear viscoelastic region and tomato paste starts to show highly fluid-like behavior. Furthermore, the elastic component of stress (σ') is no longer a pure sine wave due to the extent of nonlinear viscoelastic behavior, so the stress–strain curve becomes an odd orthogonal polynomial function (Fig. 3b).

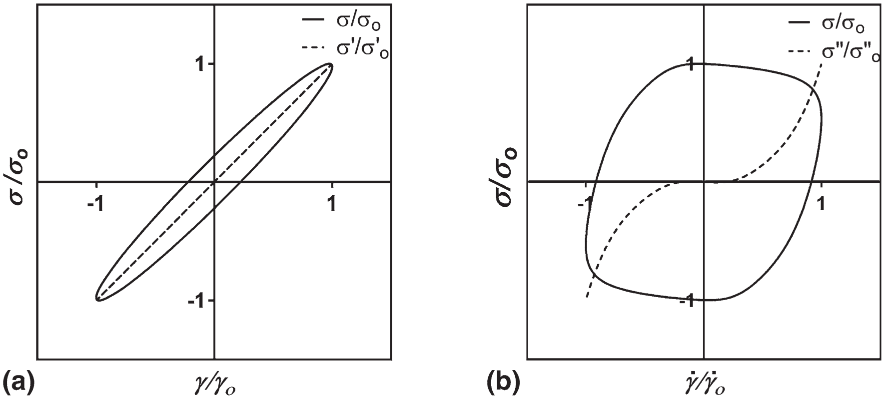

Fig. 3 Lissajous-Bowditch curves of tomato paste at (**a**) 0.01% strain and (**b**) 180% strain at 1 rad/s and 25 °C

1.1.3 New Parameters for LAOS Testing

For further understanding and quantification of nonlinear elastic behavior, intracycle moduli at $\gamma = 0$ and $\gamma = \gamma_o$, defined as the minimum strain modulus (G'_M) and large strain modulus (G'_L), respectively, are used. In the linear viscoelastic region where $e_3/e_1 \ll 1$, $G'_M = G'_L = G'_1 = G'(\omega)$. Note that when commercial rheometers report G', they are effectively reporting G'_1.

$$G'_M \equiv \left.\frac{d\sigma}{d\gamma}\right|_{\gamma=0} = \sum_{n\,\mathrm{odd}} nG'_n = e_1 - 3e_3 + \ldots \tag{12}$$

$$G'_L \equiv \left.\frac{\sigma}{\gamma}\right|_{\gamma=\pm\gamma_0} = \sum_{n\,\mathrm{odd}} G'_n \left(-1\right)^{\frac{n-1}{2}} = e_1 + e_3 + \ldots \tag{13}$$

Similarly, for the interpretation of viscous nonlinearities, intracyle instantaneous viscosities, the minimum rate instantaneous viscosity (η'_M) and large rate instantaneous viscosity (η'_L) are obtained at strain rates of $\dot{\gamma} = 0$ and $\dot{\gamma} = \dot{\gamma}_o$, respectively. Like G', in the linear viscoelastic region where $\nu_3/\nu_1 \ll 1$, the following equations reduce to $\eta'_L = \eta'_M = \eta'_1 = \eta'(\omega)$. Also as for G', when commercial rheometers report η', they are effectively reporting η'_1.

$$\eta'_M \equiv \left.\frac{d\sigma}{d\dot{\gamma}}\right|_{\dot{\gamma}=0} = \frac{1}{\omega}\sum_{n\,\mathrm{odd}} nG''_n \left(-1\right)^{(n-1)/2} = v_1 - 3v_3 + \ldots \tag{14}$$

$$\eta'_L \equiv \left.\frac{\sigma}{\dot{\gamma}}\right|_{\dot{\gamma}=\pm\dot{\gamma}_0} = \frac{1}{\omega}\sum_{n\,\mathrm{odd}} G''_n = v_1 + v_3 + \ldots \tag{15}$$

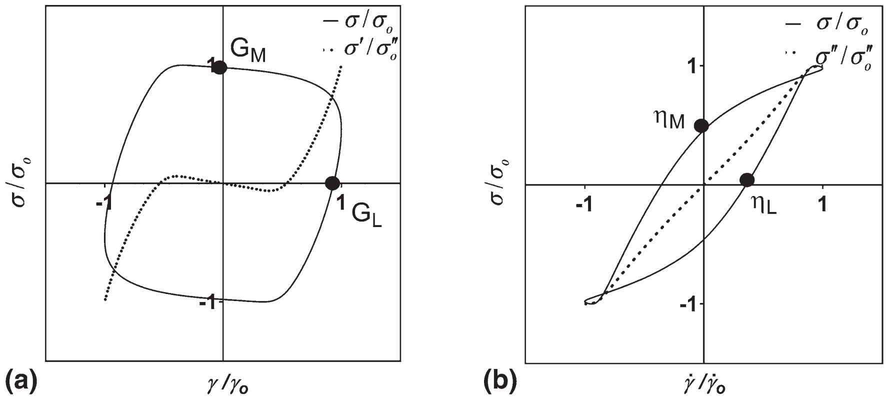

Fig. 4 Graphical descriptions and definitions of G'_M, G'_L, η'_M, and η'_L determined from Lissajous-Bowditch curves in the nonlinear viscoelastic region. Data were collected for tomato paste at 200% strain and 0.5 rad/s

These parameters are determined by plotting the stress response against strain (Fig. 4a) and strain rate (Fig. 4b), drawing tangent lines at zero strain or strain rate and secant lines at maximum strain or strain rate, and calculating the slope of each tangent line to determine the moduli and viscosity values (Ewoldt et al. 2008).

1.1.4 Dimensionless Characterization of Nonlinear Viscoelastic Behaviors

An alternative interpretation of G'_M, G'_L, η'_M, and η'_L involves defining relations between them. If $G'_L > G'_M$ the response of the material is strain-stiffening. Hence, the strain-stiffening ratio S is defined as:

$$S = \frac{G'_L - G'_M}{G'_L} = \frac{4e_3 + \ldots}{e_1 + e_3 + \ldots} \tag{16}$$

In the linear viscoelastic region, $S = 0$. It is positive when the material shows strain-stiffening behavior and negative when the material shows strain-softening behavior.

Similarly, the shear thickening ratio (T) is defined by Eq. 17. This ratio is greater than zero for intracycle shear-thickening, equal to zero in the linear viscoelastic region and less than zero for intracycle shear-thinning behavior.

$$T = \frac{\eta'_L - \eta'_M}{\eta'_L} = \frac{4v_3 + \ldots}{v_1 + v_3 + \ldots} \tag{17}$$

Nonlinear viscoelastic responses for both the elastic and viscous components of stress may also be extracted using the Chebyshev coefficients. Negative and positive values for e_3/e_1 reflect strain-softening and strain-stiffening behavior, respectively, whereas negative values for v_3/v_1 correspond to shear-thinning and positive-values indicate shear thickening behavior (Ewoldt et al. 2008).

In summary, detailed structural information can be obtained from LAOS data by using three sets of parameters: (1) the Chebyshev coefficients (e_3 and v_3), (2) the derivatives of stress response with respect to strain and strain rate at zero and maximum intracycle strain values ($G_M^{'}$, $G_L^{'}$, $\eta_M^{'}$, and $\eta_L^{'}$), and (3) the ratios of strain stiffening and shear thickening (S and T). These parameters ($G_M^{'}$, $G_L^{'}$, $\eta_M^{'}$, $\eta_L^{'}$, e_3/e_1, v_3/v_1, S, and T) are referred to as LAOS parameters for the remainder of this chapter and can be used to interpret the intracycle behavior, providing insight into nonlinear viscoelastic behavior that cannot be obtained through SAOS measurements.

1.1.5 Frequency Considerations for LAOS Testing

The imposed frequency has an important impact on nonlinear viscoelastic rheological behavior. Since the energy delivered to the complex structure of food materials is carried out at different time periods, it may be advantageous to probe the material at different frequencies. The Lissajous-Bowditch curves enable the systematic evaluation of the evolution of intracycle rheological behavior at different strains and frequencies. Secondary loops have been observed in the stress–strain rate plane at progressively increasing frequency for many materials, such as molten polymers (Stadler et al. 2008), polystyrene solutions (Hoyle et al. 2014), polymer-clay suspensions (Hyun et al. 2012), tomato paste (Duvarci et al. 2017a), guar gum solutions (Szopinski and Luinstra 2016), egg white foams (Ptaszek et al. 2016), mashed potato paste (Joyner (Melito) and Meldrum 2016), and gluten-free dough samples (Yazar et al. 2017a). The mathematical interpretation of these loops has been offered by Ewoldt and McKinley (2010). Loops are formed in the viscous plot when the stress response has repeated values at a given strain rate (Fig. 5b). However, the

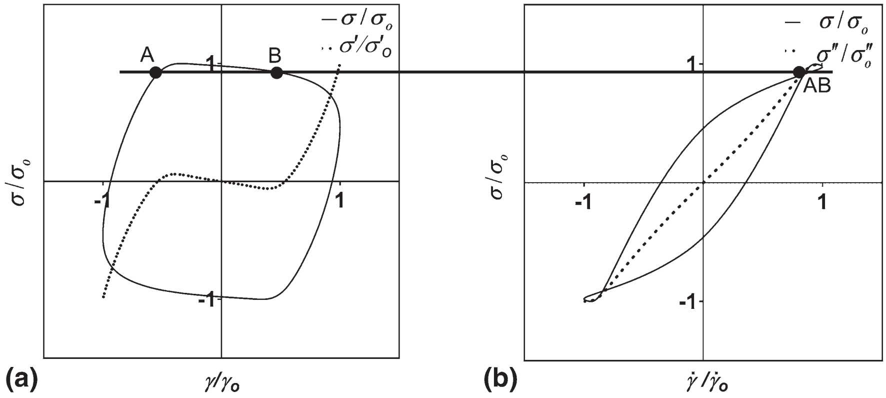

Fig. 5 Secondary loops of tomato paste at a strain of 200%, a frequency of 0.5 rad/s, and 25 °C: (**a**) elastic plane, (**b**) viscous plane

elastic plot may not show these loops because the stress values at each strain value are unique (Fig. 5a). This behavior is related to a strong nonlinearity in elasticity and there should be a partial reversible structural change depending on the time scale of deformation which reoccur periodically. The origin of this distinctive behavior is aging and thixotropy and can be used to differentiate between structures of materials. Similarly, loops appearing in elastic stress versus strain plots but not viscous stress versus strain rate indicate strong nonlinear viscous behavior (Ewoldt and McKinley 2010).

2 Experimental Challenges during LAOS Measurements

2.1 Inertia Corrections

LAOS tests are prone to artifacts at high frequencies for low-viscosity samples due to large instrumental inertia contribution. The cyclic change in the motor shaft influences total torque at high frequencies. When the torque required to overcome the instrument inertia exceeds the torque required to deform the sample, the stress results become questionable and need correction (Franck 2006). Two types of inertia have been reported to be related to oscillatory shear tests. One type is instrumental inertia, which is related to the moving parts of the instrument, while the second type is sample inertia that occurs due to secondary flows, viscoelastic waves, and momentum diffusion. To obtain reliable data in oscillatory shear tests, test parameters should be set to minimize instrumental inertia or, if this is not possible, necessary corrections should be performed. To correct data for inertia, the first step is to identify whether the measurement is governed by instrument inertia. There are two parameters that need to be examined: raw phase and ratio of inertial torque to sample torque. Total torque applied by the rheometer leads to both acceleration of the moving parts of the rheometer and deformation of the sample (Läuger and Stettin 2016). The ratio of these two is given by:

$$\frac{M_a}{M_s} = \frac{I\omega k}{\left|\eta^*\right|} \tag{18}$$

where M_a is acceleration torque (N.m), M_s is the torque delivered to the sample for deformation (N.m), I is the moment of inertia of the rheometer (kg.m^2), ω is frequency of oscillation (rad/s), k is a geometry constant unique to the instrument geometry (1/m^3 for parallel-plate geometries), and $|\eta^*|$ is magnitude of complex viscosity (Pa.s). When this ratio exceeds 0.2, instrumental inertia distorts the data (Merger and Wilhelm 2014), which then needs to either be discarded or corrected to eliminate inertia effects.

The second parameter to monitor instrumental inertia is the raw phase angle. It is defined as the angle between the total torque and the elastic component of torque during sample deformation (Fig. 6). If the raw phase angle exceeds 100 degrees,

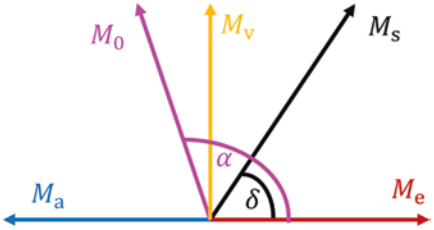

Fig. 6 Vector representation of the raw phase angle (δ); M_o: total torque, M_e: elastic component of sample torque, M_v: viscous component of sample torque, M_a: acceleration torque, M_s: sample torque

instrumental torque exceeds the torque required to deform the sample, and the data should be discarded or corrected.

The type of rheometer used can impact what inertial corrections are necessary. If the rheometer is a separate motor transducer type, the measurements are not affected by instrumental inertia friction (Franck 2006) because the torque-receiving elements in the rheometer remain immobile during the measurement, and the torque of the drive is not used for deforming the sample (Läuger and Stettin 2016). The measured torque at the transducer is controlled to a fixed position and its movements are very small. These small movements lead to small instrumental inertial effects. However, in combined motor-transducer design rheometers, the torque is not completely available for deforming the sample being tested; part of the total torque is needed for accelerating the moving parts of the instruments. This difference creates instrumental inertia effects. Hudson et al. (2017) provided an enhanced rheometer inertia correction procedure (ERIC) for combined motor-transducer rheometers, which builds on the procedure proposed by Franck (2006). Post-acquisition corrections on the data is carried out according to:

$$G'_m = G'_s - I\omega^2 k_g \tag{19}$$

$$G''_m = G''_s \tag{20}$$

where G'_m and G''_m are material properties (Pa) and G'_s is a measured value (Pa). The measured value (G'_s, Pa) is proportional to the moment of the rheometer inertia (I, kg.m^2), the square of the applied frequency (ω^2, rad^2/s^2), and the geometry constant (k_g if a parallel plate geometry is used, 1/m^3). The measured loss modulus (G''_s Pa) does not need any correction since it is associated with the imaginary part of the measured sample.

2.2 Wall Slip

The presence of wall slip in LAOS tests results in nonlinear, non-sinusoidal stress waveforms. Because material responses under high oscillatory strains can also cause nonlinear, non-sinusoidal stress responses, wall slip can easily be conflated with true nonlinear viscoelastic material behaviors. In particular, application of high-frequency–strain combinations using smoth parallel plate geometries can cause significant slip. It is therefore important to determine if the distorted stress waveforms are due to nonlinearity or slip. The presence of even Chebyshev harmonics (e.g. $n = 2, 4, 6\ldots$) and their corresponding coefficients are associated with slip since they are caused by broken shear symmetry (i.e. with responses that have not yet reached the time periodic state), similar to wall slip that inhibits steady-state. However, even harmonics are not always related to wall slip (Yoshimura and Prud'homme 1988; Macias-Rodriguez et al. 2018). The presence of slip can be evaluated by testing the same material using parallel plates at multiple gap heights but the same frequency and strain. If stress waveforms from both gaps are identical, this is an indication that slip does not occur and the nonlinearities and phase shifts are due to bulk fluid properties (Yoshimura and Prud'homme 1988). This approach was used to determine if observed nonlinearities in LAOS tests were caused by wall slip (Macias-Rodriguez et al. 2018). The lack of overlap of first harmonic viscoelastic moduli ($G_1^{'}$ and $G_1^{''}$) at different sample thicknesses (gap heights) was reported to be an indication of slip, internal fracture planes, or other non-ideal kinematics that derivate from homogeneous simple shear. To mitigate slip issues in oscillatory shear rheology, geometry modifications are commonly applied; for example, filter paper or sand paper can be attached to the surfaces of the plates to improve sample adhesion and minimize wall slip during measurements (Duvarci et al. 2017a, b; Yazar et al. 2016a, b, 2017a, b; Macias-Rodriguez et al. 2018).

3 LAOS Measurements and Interpretation for Different Food Systems

3.1 Applications of LAOS Principles to Characterize Food and Food Components

LAOS tests are able to offer more detailed understanding about the structural changes occurring in food systems during processing and consumption since food products are subjected to large deformations in these situations (Duvarci et al. 2017a). Many food materials have been studies using LAOS, including tomato paste (Duvarci et al. 2017a), mashed potato (Joyner (Melito) and Meldrum 2016), native starch in water (Klein et al. 2008), soy protein isolate-flax seed gum dispersions (Bi et al. 2013), gum extracted from Alyssum homolocarpum seed (Anvari et al. 2018), carragenan gels (Klein et al. 2008; Melito et al. 2013a), gelatin-alginate mixtures (Goudoulas and Germann 2017), whey protein-agar complexes (Rocha et al. 2014), agar with locust bean gum (Sousa and Goncalves 2015), crosslinked tapioca starch-polysaccharide systems (Fuongfuchat et al. 2012), tuna myofibrillar protein gels (Liu et al. 2014), waxy maize starch paste (Wang et al. 2012), waxy rice starch (Precha-Atsawanan et al. 2018), chewing gum (Martinetti et al. 2014), mayonnaise (Duvarci et al. 2017a), dark chocolate (van der Vaart et al. 2013), fish gelatin-gum arabic mixture in oil (Anvari and Joyner (Melito) 2018), water-in-oil emulsions (Shu et al. 2013); wheat dough (Lefebvre 2006; Yazar et al. 2016a, b), gluten-free doughs (Yazar et al. 2017a), cheddar, Mozarella, and American cheese (Melito et al. 2013b), fat crystal networks (Macias-Rodriguez et al. 2018), gluten (Ng et al. 2011), crude fractions of gliadin and glutenin (Yazar et al. 2017b), yeast biofilms (Brugnoni et al. 2014), and egg white protein foam with added apple pectin and xanthan gum (Ptaszek et al. 2016). Through these studies, much has been learned about the rheological behaviors of foods in the nonlinear viscoelastic region to supplement studies using SAOS measurements, and LAOS application and in-depth interpretation is rapidly progressing. These studies show that rich nonlinear viscoelastic behavior can be captured by LAOS analysis. Additionally, it is possible to determine the nonlinear viscoelastic behaviors of different food structures such as concentrated or dilute suspensions, emulsions, foams, gels, and soft elastic networks. It is also possible to distinguish structural changes in foods that arise due to different preparation methods, applied process parameters, and formulations. As examples of how LAOS can be used to interpret food behaviors, Sects. 3.2, 3.3, 3.4, and 3.5 discuss the current understanding of LAOS behaviors of common food systems and how those behaviors are related to the structure and texture of the food.

3.2 LAOS Behavior of Wheat Flour Dough

Dough rheology has been the focus of a large number of studies due to its unique viscoelastic behaviors. Wheat flour dough is reported to be in the linear viscoelastic region below strains of approximately 0.2% depending on the type of wheat (i.e. hard red winter or soft red winter) and becomes highly nonlinear beyond this strain level. Nonlinearity is related to the breakdown of the elastic gluten protein network. The gluten network is known to be held together by covalent disulfide bonds and secondary bonding interactions. The breakdown in the network occurs as a result of increasing mechanical energy as the amplitude of strain increases, overcoming the strength of both secondary bonding interactions and covalent bonds (Dus and Kokini 1990; Amemiya and Menjivar 1992). Nonlinearity of wheat flour dough has been studied by multiple groups (Hibberd and Parker 1979; Khatkar and Schofield 2002; Lefebvre 2006; Lefebvre 2009; Ng et al. 2006; Yazar et al. 2016a, b; Duvarci et al. 2017a). The presence and magnitude of higher-order harmonics in Fourier transformations of oscillatory stress response curves of dough leads to distinct nonlinear behavior on Lissajous-Bowditch curves (Lefebvre 2006). The nonlinear behavior of dough was attributed to the viscous component of dough, and the presence of starch and free water are responsible for the low linearity limit. A study on the LAOS behavior of dough at different stages of farinograph mixing showed that gluten network formation has a major effect on nonlinear viscoelastic behavior, especially on elastic modulus. These effects are related to the changes occurring in the protein fibrils in gluten network during farinograph mixing (Yazar et al. 2016a, b).

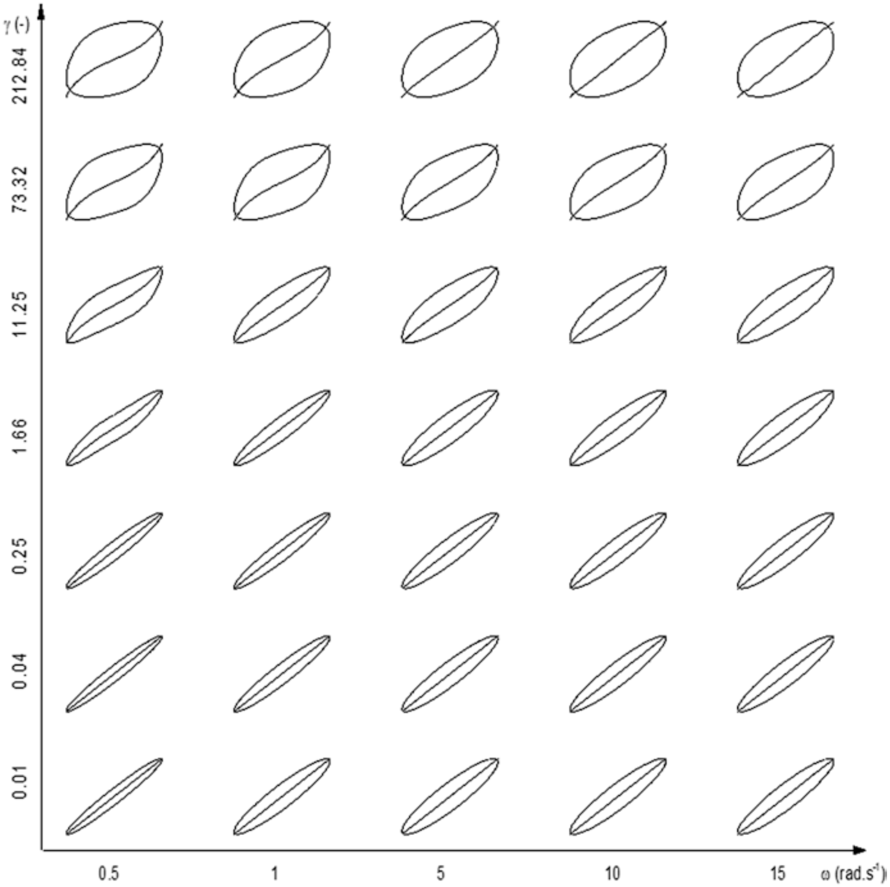

Fig. 7 Elastic Lissajous-Bowditch curves of soft dough at 25 °C. All curves are plotted ($\sigma(t)/\sigma_{\max}$) and ($\sigma'(t)/\sigma_{\max}$) vs. $\gamma(t)/\gamma_o$

Plots of Lissajous-Bowditch curves at different strains and frequencies provide a comprehensive understanding of the structural evolution of dough with increasing strain and frequency. The elastic and viscous planes of normalized Lissajous-Bowditch curves of soft flour dough in the SAOS and LAOS region are given in Figs. 7 and 8. The curves are narrow ellipses in the elastic plane and circular in the viscous plane at low strains and frequencies, which indicate elastic-dominant rheological behavior.

Because energy delivery from applied strain at higher frequencies is quite rapid, there is limited time for gluten filaments to recreate network junctions in the flow direction that are lost during stretching. An incomplete arrangement of chain orientation and alignment, and higher rate of network junction loss than the rate of creation results in less elastic and more viscous behavior. However, increased frequency does not necessarily promote increased nonlinear behavior of soft flour dough

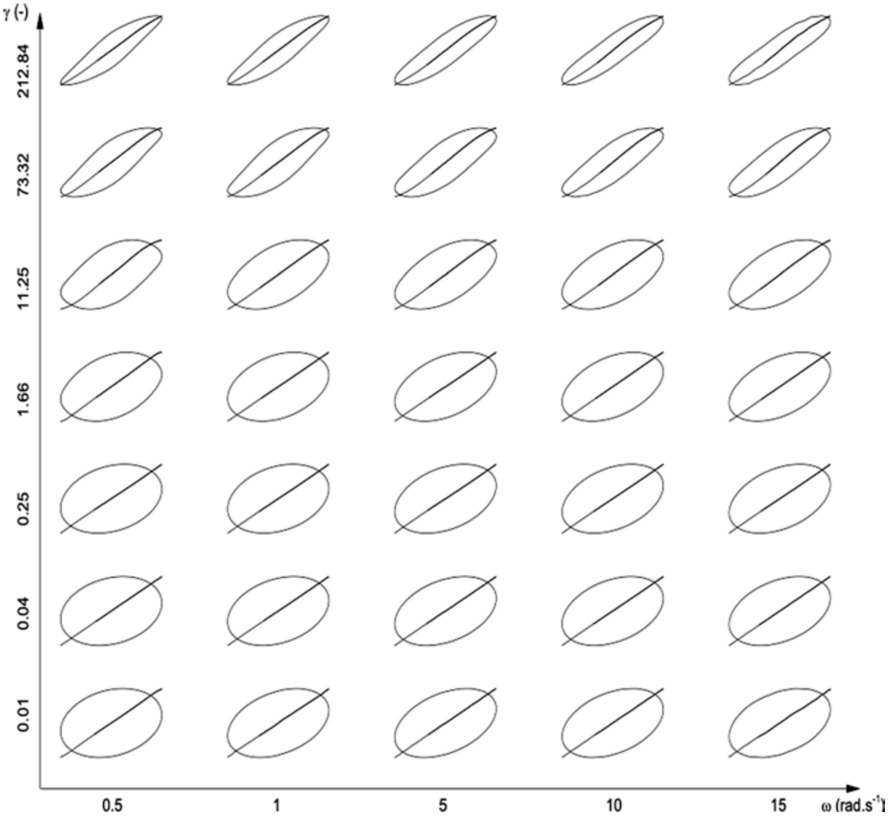

Fig. 8 Viscous Lissajous-Bowditch curves of soft wheat flour dough at 25 °C. All curves are plotted ($\sigma(t)/\sigma_{\max}$) and ($\sigma''(t)/\sigma_{\max}$) vs. $\dot{\gamma}(t)/\dot{\gamma}_{\max}$

(Figs. 7 and 8). On the other hand, the emergence of higher-order harmonics at higher strains, denoting nonlinear behavior, profoundly affects the shape of the normalized Lissajous-Bowditch curves. There is greater area encompassed by the elastic plane curves, and their shape becomes distorted from that of an ellipse. Additionally, the major axis of the ellipses rotates either clockwise (strain-stiffening behavior) or counterclockwise (strain-softening behavior) at maximum strain. Similarly, clockwise and counterclockwise rotations of the major axes at maximum strain rate can be seen in the viscous plane for shear-thinning and shear-thickening behavior, respectively.

The third-order harmonic is the most significant of the higher-order harmonics, and can be used to calculate multiple nonlinear viscoelastic and LAOS parameters. The variation of G_M', G_L', and G' with respect to strain is given in Fig. 9a for soft dough. $G_M' = G_L' = G_1'$ in the linear viscoelastic region; all three of these values decreased at strains beyond the critical strain. At >10% strain, G_M', G_L', and G' could be differentiated, indicating nonlinear viscoelastic behavior. G'', η_M', and η_L'

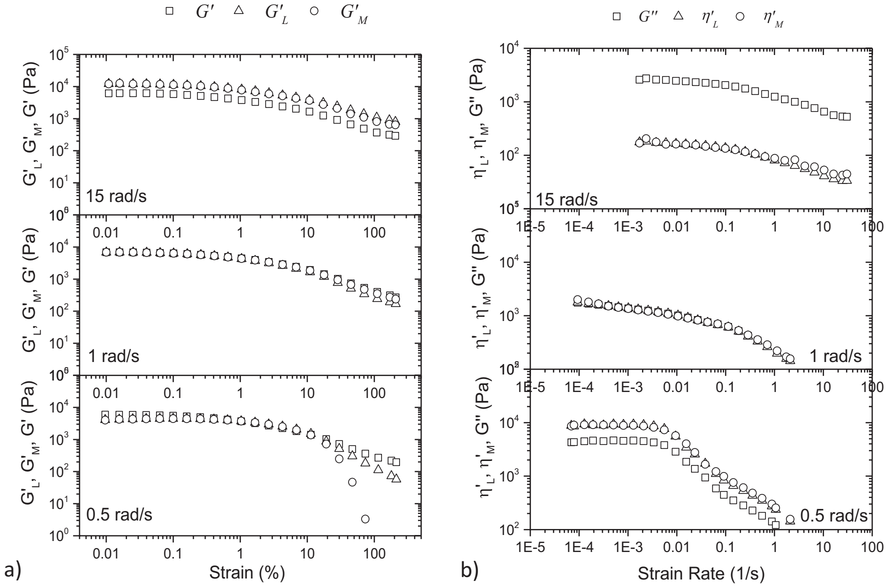

Fig. 9 Variation of (**a**) $G_M^{'}$, $G_L^{'}$, and $G^{'}$ with respect to strain, (**b**) $\eta_M^{'}$, $\eta_L^{'}$ and $G^{''}$ with respect to strain rate. All data are for soft dough with measurement conducted at 0.5, 1, and 15 rad/s

showed a decreasing trend with strain rate, corresponding to shear-thinning behavior (Fig. 9b). The maximum strain rate was 2.07, 2.47 and 32 s^{-1} when the frequency was 0.5, 1, and 15 rad/s, respectively. $\eta^{'}$, $\eta_M^{'}$, and $\eta_L^{'}$ had a decreasing trend, indicating shear-thinning behavior.

The values of e_3, e_3/e_1, and S were approximately zero in the linear viscoelastic region, as expected. When the wheat flour dough samples were subjected to strains beyond the linear viscoelastic region, both soft and hard dough showed strain stiffening ($e_3/e_1 > 0$, $S > 0$), which may be associated with the stretching of the gluten network in the direction of flow. The presence of starch granules and free water also contribute to the reorganization of the dough structure. Although-shear-thinning behavior was indicated from the decrease in $\eta_M^{'}$, $\eta_L^{'}$ and G'' values (Fig. 9b), the ratio of viscous coefficients (ν_3/ν_1) showed intracycle shear-thickening behavior. Soft dough showed positive ν_3 values in the linear viscoelastic region followed by a decrease in ν_3 in the nonlinear viscoelastic region. Strain values had a shoulder at 6.9% strain for soft dough and 11% for hard dough, and a minimum value at about 113% for soft dough (Fig. 9a). These two peaks may be related with the two stages of dough structural reorganization reflected in the viscous component. Both doughs showed positive T values, an indication of intracycle shear thickening.

The LAOS behavior of gluten protein over a wide range of strain and frequencies in the nonlinear viscoelastic region offers additional interesting insights and shows major changes in both the elastic and viscous components' stress responses. The

Lissajous-Bowditch curves were much more elliptical, indicating a very strong elastic structure of gluten dough in nonlinear viscoelastic region. The clockwise rotation of the major axis of the stress–strain loop indicated a gradual intracycle softening of gluten dough, followed by an increase in stress that indicated intracycle strain stiffening (Fig. 7). Gluten dough maintained a considerable amount of its elasticity after experiencing larger deformations. LAOS behavior of gluten was further investigated by fractionating gluten into its main two fractions, gliadin and glutenin (Yazar et al. 2017b). Lissajous curves in the elastic analysis of both fractions showed that gliadin had broad ellipses with a rapid clockwise rotation in their major axes axis as strain increased, suggesting more fluid-like behavior and strain softening. Conversely, glutenin showed more elastic-dominant behavior: its Lissajous curves were narrower and the rate of clockwise rotation of the ellipse axes was considerably slower compared to gliadin, indicating a stiffer, more elastic structure that was more resistant to strain softening compared to gliadin. Glutenin also showed strain-softening behavior; however, the decay in elasticity with increasing strain and frequency for glutenin was notably slower than that of gliadin because the elliptic loops widen more slowly, and the rate of clockwise rotation of the elliptical axes is also slower compared to that for gliadin. These results ere due to the intermolecular disulfide bonds in glutenin that create a strong network compared to gliadin, in which there are no intermolecular disulfide covalent bonds to form a three-dimensional network.

3.3 LAOS Behavior of Yogurt Samples with Different Fat Levels

The effect of different levels of fat in yogurt samples obtained from the two commercial brands national brand and store brand were explored using LAOS tests at strain amplitudes of 0.01–1000% at a frequency of 1 rad/s. At the lowest applied strain (0.01%), all yogurt samples showed linear viscoelastic behavior that was not a function of applied strain. Deviation from linearity began as the strain amplitude reached 3–4%, and both G' and G'' values started to decrease as the strain amplitude continued to increase up to 1000% (Fig. 10). A crossover point was observed for the national brand yogurt samples at ~20% strain, whereas a crossover in viscoelastic moduli occurred at ~30% strain for the store brand samples, suggesting a relatively stronger structure for the store brand yogurts. The crossover point was attributed to the breakdown of a gel-like structure and formation of aggregate spheres; the further decrease in the viscoelastic moduli can be attributed to further disruption of aggregate spheres. As strain increased, microstructural elements found in the yogurt, such as lipid droplets, whey protein-coated casein micelles, and microbial constituents in the serum, aligned themselves in the direction of flow and caused shear-thinning behavior (Van Marle et al. 1999).

The crossover of G' and G'' occurred at almost the same strain for all national brand yogurts with different fat levels. Since fat globules act as a filler in yogurt

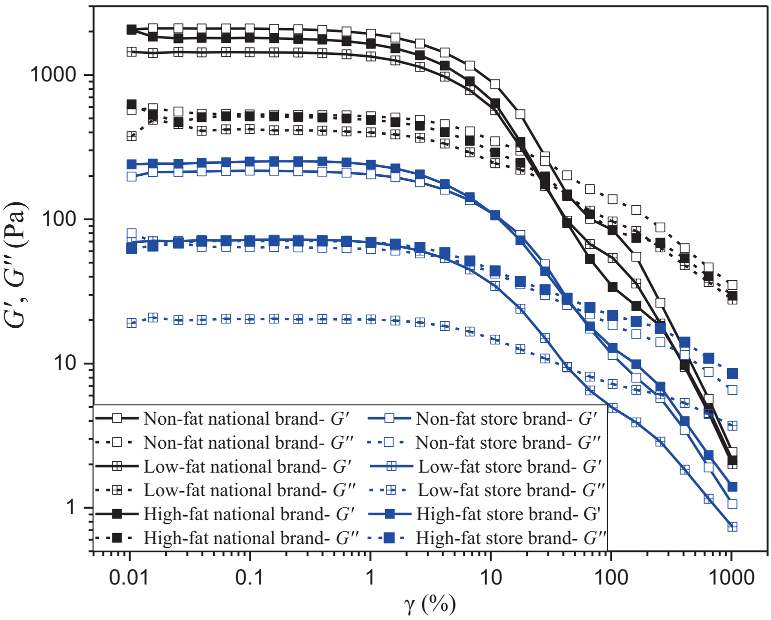

Fig. 10 G' and G'' values for yogurt samples with different fat levels

structure (Lucey et al. 1998), low-fat store brand yogurt (2% fat) showed significantly lower G' and G'' values compared to high-fat store brand yogurt (5% fat). However, the non-fat and high-fat store brand yogurts presented similar G' and G'' values. These results suggested that fat replacers, such as hydrocolloids, gums, and starches, were added to the non-fat store brand yogurt to enhance the structure. On the other hand, the national brand yogurts with different fat levels all showed similar G' and G'' values, suggesting a more precise adjustment in formulating the low-fat and non-fat yogurts to mimic the rheological behavior of the high-fat yogurt. Hydrocolloids and stabilizers are often used in the yogurt industry to increase consumer acceptance of yogurts by altering their rheological and textural characteristics (Mudgil et al. 2018).

An overall comparison of the strain sweep data for the two commercial yogurt brands revealed that national brand yogurts had higher G' and G'' values than store brand yogurts. In the linear viscoelastic region, the national brand yogurts showed G' values between 1500 and 2100 Pa, whereas G' values of store brand yogurts ranged from 40 to 200 Pa. This result could be due to the differences in the raw material composition, homogenization (which impacts the size of fat globules), shear used to break the gel after fermentation, fermentation conditions, the pH reached during fermentation, the culture or other ingredients used, or some combination of these (Lee and Lucey 2010; Sfakianakis and Tzia 2014; Pascual et al. 2016). Although the G' and G'' values of the national brand yogurts were found to be almost an order of magnitude higher compared to those of the store brand yogurts in the linear viscoelastic region, the structural network of the national brand yogurts deformed more quickly than those of the store brand yogurts. This difference in structural strength is likely due to the addition of pectin to the store brand yogurts but not the national brand yogurts. The addition of a high molecular weight polysaccharide with gel-forming ability appeared to delay significant deformation of the gel structure of the store brand yogurts, but was not able to enhance the elasticity of the structure and provide G' and G'' values similar to those of the national brand yogurts.

SAOS tests showed perfect sinusoidal oscillatory stress responses as evidenced by the absence of higher harmonics (Fig. 11). At small strains (0.04%), the stress response was also small and was difficult to differentiate from equipment noise. As the strain amplitude increased above 0.4%, the equipment noise became insignificant compared to the stress response of the sample, and smooth, sinusoidal stress response curves appeared. As the strain amplitude further increased (>4%) deviation from a perfect sinusoidal response was observed, indicating the presence of higher-order harmonics and that the yogurt samples had entered the nonlinear viscoelastic region. The distortion of the stress response wave continued to increase with increasing strain, indicating increased nonlinear viscoelastic behavior.

Comparison of the raw stress waves for the yogurt samples with different fat levels (Fig. 11) revealed that the characteristic stress waveforms for all yogurt types correlated with the information obtained through the strain sweep data. Increasing amplitude of strain resulted in a strong stress response for the non-fat yogurt compared to other samples and a lower response for the low-fat yogurt compared to high-fat yogurt. At the highest strain amplitude applied (1000%), the raw stress waves for the non-fat samples represented triangular-shaped sharper-edged trajectories at large strains, which is indicative of strain hardening according to the characteristic functions defined by Hyun et al. (2011). The waveforms obtained for low-fat store brand yogurt at high strains were more like the saw-tooth function which arises due to shear bands or wall slip.

The structural changes of materials can be observed by plotting stress data with respect to both strain and strain rate in three-dimensional plots. Because these plots can be used to visualize the stress response projections against the strain and strain rate simultaneously, the elastic and viscous components of a material's intracycle nonlinear behavior can be analyzed synchronously. The stress–strain projection provides information about the elastic perspective of the material, while the stress–strain rate projection gives a viscous perspective. For all yogurt samples, as the amplitude of strain gradually increased, the elastic Lissajous curves showed wider elliptical trajectories (Fig. 12), indicating viscous-dominated intracycle nonlinear viscoelastic behavior. The magnitude of the stress amplitude was found to be higher for the national brand yogurts (250–320 Pa, Fig. 12a–c) compared to store brand yogurts (<80 Pa, Fig. 12d–f), which concurs with the strain sweep data (Fig. 10). In particular, the low-fat store brand yogurt had the lowest magnitude of elastic stress among all other yogurt samples over the entire strain range, indicating increased viscous-dominant behavior. Examining the stress–strain rate (viscous) projection, the ellipses for the national brand yogurts showed clockwise rotation with increased

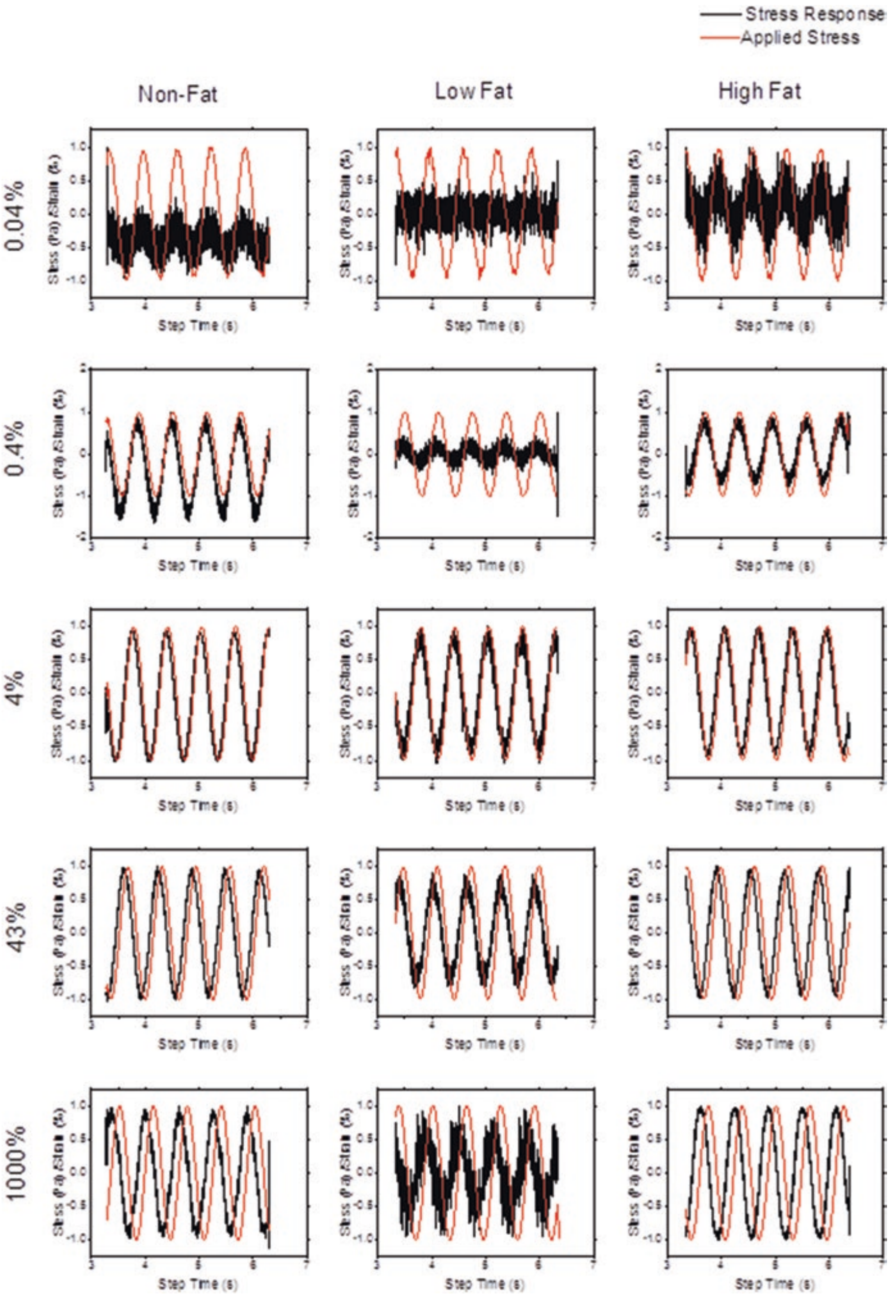

Fig. 11 Raw stress responses of store brand yogurts with different fat levels at 1 rad/s in SAOS, MAOS, and LAOS regions

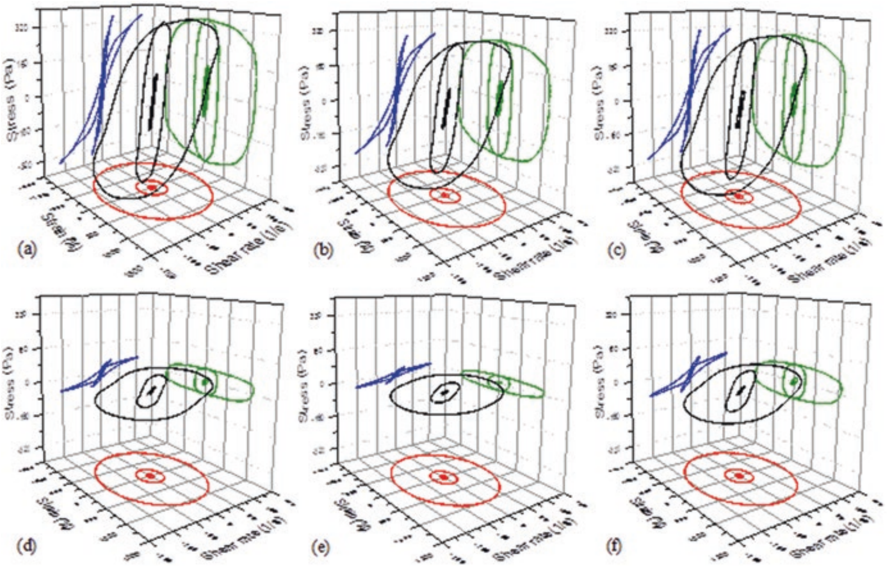

Fig. 12 Three-dimensional un-normalized Lissajous-Bowditch curves of stress response (black), elastic component (green), and viscous component (blue) versus strain and strain rate for yogurt with different fat content and brand: (**a**) non-fat, (**b**) low-fat, and (**c**) high-fat national brand yogurt; (**d**) non-fat, (**e**) low-fat, and (**f**) high-fat store brand yogurt. Data were collected at 0.063%, 0.25%, 1.01%, 4.21%, 18%, 69%, 266%, and 1051% strain

strain, which suggested intracycle shear-thinning behavior (Ewoldt et al. 2008). The viscous projections of store brand yogurts displayed clockwise rotation at lower strain values, indicating an onset of shear-thinning behavior at smaller strains for store brand yogurts compared to national brand yogurts.

Upon review of the normalized Lissajous curves, both viscous and elastic Lissajous curves for the store brand yogurts were found to be impacted by experimental noise at small strains, resulting in wavy structures (Fig. 13). The elastic Lissajous curves showed narrow elliptical trajectories at low strain amplitudes, an indication of linear viscoelastic behavior. As strain amplitude gradually increased, the ellipses widened, suggesting fluid-like viscoelastic nonlinear behavior for all yogurts. Distortion in the elliptical trajectories appeared at strain >4.21% for both the elastic and the viscous contributions. At the highest strain, the elastic Lissajous curves of the national brand yogurts, regardless of fat content, displayed rectangular trajectories, indicating both gel-like and reversible stick-slip flow-induced microstructure (Hyun et al. 2011). On the other hand, the ellipses in the viscous projection for all yogurt samples narrowed with increased strain, indicating more fluid-like behavior in the nonlinear viscoelastic region; this results was consistent with the elastic projections. The ellipses of the national brand yogurts in the viscous projection were narrower than those for the store brand yogurts at large strains, indicating that national brand yogurts had more fluid-like behavior. The stronger clockwise

Fig. 13 Elastic and viscous Lissajous-Bowditch curves for the store brand yogurts with different levels of fat at 1 rad/s; — σ/σ_o, — σ'/σ_o, — σ''/σ_o

rotation observed for the national brand yogurts at the highest strain suggested a higher degree of intracycle shear thinning (Fig. 14). The viscous Lissajous curves of the national brand yogurts at the highest strain showed narrow ends and a slight thickening in the center. This is similar to loop behavior: the stress response has repeated values as the oscillation reaches the highest intracycle strain value and decreases. It indicated reversible structural change under these strain conditions. Additionally, elastic Lissajous curves for both store and national brand non-fat yogurts displayed narrower trajectories, while viscous Lissajous curves displayed

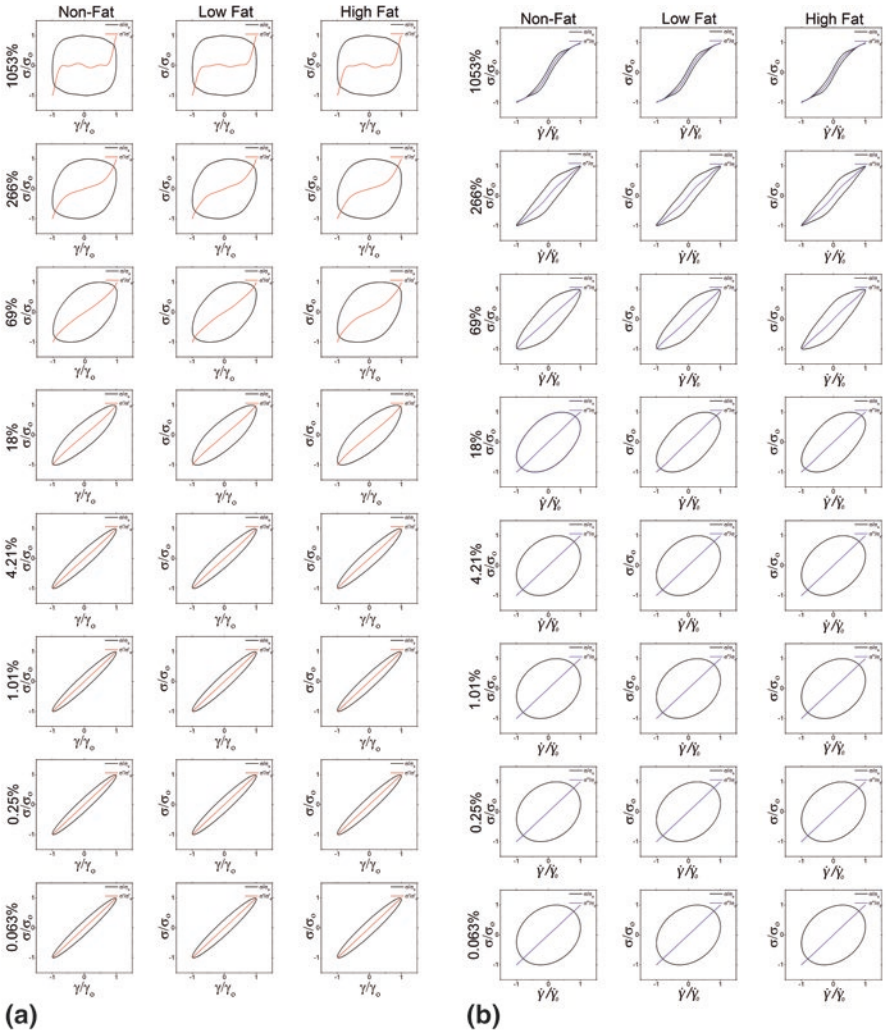

Fig. 14 (**a**) Elastic and (**b**) viscous Lissajous-Bowditch curves for national-brand yogurts with different levels of fat at 1 rad/s; —σ/σ_o, —σ'/σ_o, —σ''/σ_o

wider ellipses at large strains compared those of to low-fat and high-fat samples, suggesting less viscous-dominant viscoelastic nonlinear behavior for non-fat yogurts.

The nonlinearities of the yogurt samples can also be observed via LAOS parameters. Figure 15 shows $G_L^{'}$, $G_M^{'}$, $\eta_L^{'}$, and $\eta_M^{'}$ of each sample in terms of oscillatory strain and strain rate, respectively. In the linear viscoelastic region, between 0.01% and 2% strain, $G_L^{'}$ and $G_M^{'}$ values of yogurt samples with different fat levels were similar for each brand, except for the low-fat store brand yogurt, which showed

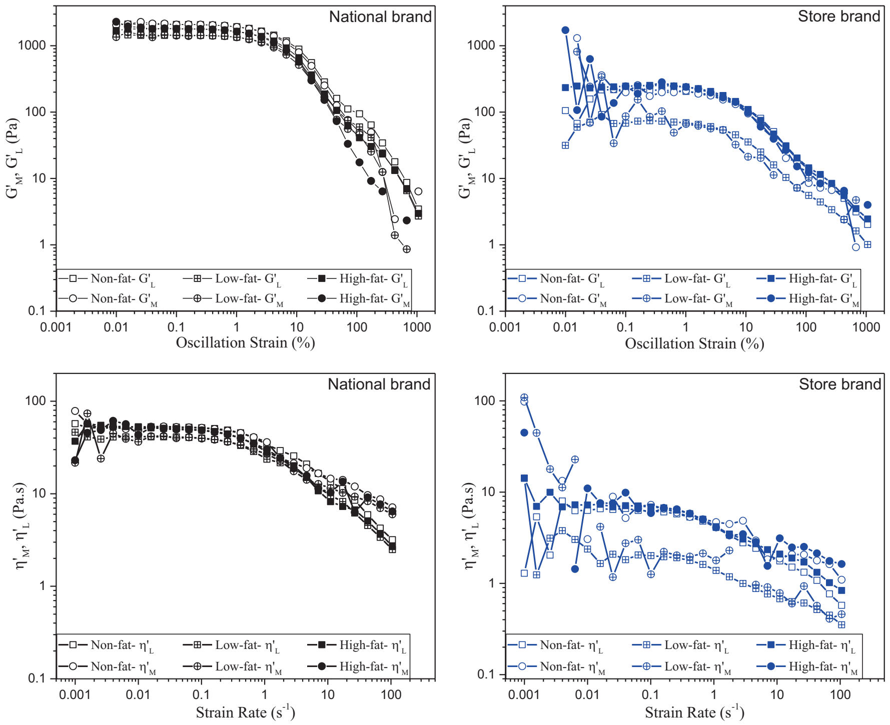

Fig. 15 G'_L, G'_M and η'_L, η'_M values for yogurts with different fat levels at 1 rad/s

lower intracycle moduli values throughout the entire applied strain range. National brand yogurts had higher moduli values compared to store brand yogurts. As strain amplitude increased, G'_L values became higher than G'_M values for all yogurt samples from both brands, indicating intracycle strain-stiffening behavior. The deviations of G'_L and G'_M from G' at small strains were attributed to unsteady and irregular flows due to low applied strain at the beginning of the experiment. Additionally, all yogurt samples showed higher minimum strain viscosities than large strain viscosities in the nonlinear viscoelastic region ($\eta'_M > \eta'_L$), which was in agreement with the information obtained through the viscous Lissajous curves that indicated intracycle shear thinning for the yogurt samples analyzed.

All of these outcomes were found to be consistent with the ratios of the third order Chebyshev coefficients to the first order Chebyshev coefficients (e_3/e_1, ν_3/ν_1) extracted from the LAOS data obtained both in the linear and nonlinear viscoelastic regions (Fig. 16). All yogurt samples showed strain-stiffening behavior ($e_3/e_1 > 0$) in the nonlinear viscoelastic region. Furthermore, all national brand yogurts and the non-fat store brand yogurt showed continuously increasing strain-stiffening behavior up to the highest applied strain (1000%), whereas low-fat and high-fat store brand yogurts showed increasing strain-stiffening followed by a plateau at 1000%

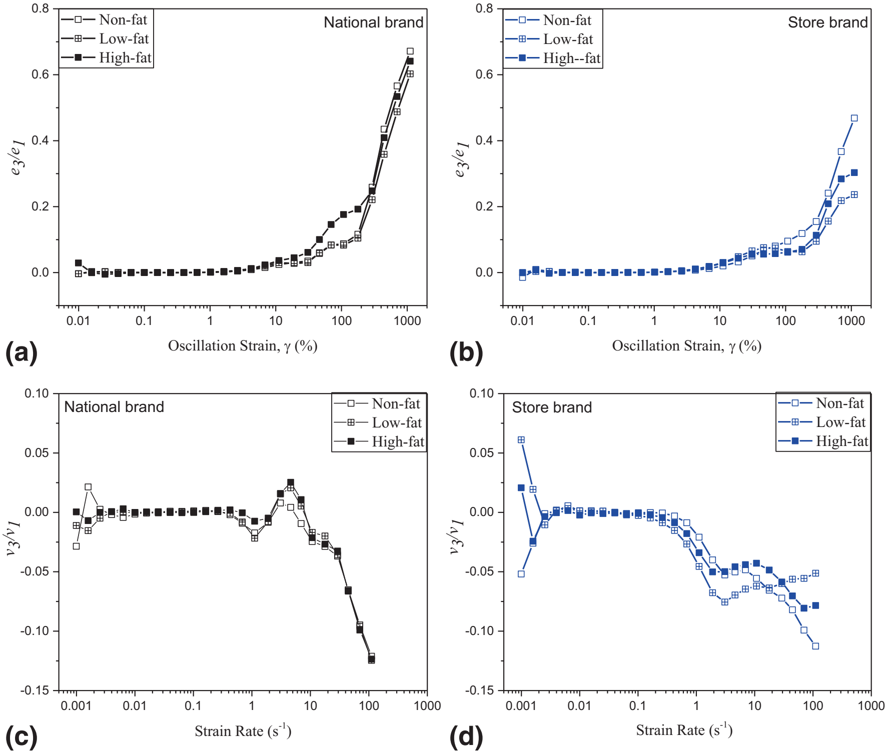

Fig. 16 e_3/e_1 and ν_3/ν_1 values for yogurts with different fat levels at 1 rad/s

strain, indicating a decrease in the intensity of strain stiffening at high strain compared to the other samples. The intensity of strain-stiffening behavior was found to be higher for the national brand yogurts (Fig. 16a) compared to the store brand yogurts (Fig. 16b). For store brand yogurts, intracycle strain stiffening behavior and its intensity were dependent on the fat level, which was consistent with the information obtained through the raw stress responses (Fig. 11).

Store brand yogurts all showed shear-thinning behavior ($v_3/v_1 < 0$) in the nonlinear viscoelastic region (Fig. 16d). The intensity of the intracycle shear-thinning behavior for the low-fat store brand yogurt was found to be the lowest. All national brand yogurts showed slight shear-thickening behavior between 2% and 10% strain followed by shear-thinning behavior in the nonlinear viscoelastic region (Fig. 16c). The shear-thickening behavior observed for the national brand yogurts right after the onset of the nonlinear viscoelastic region was attributed to the formation of aggregate proteins spheres in the microstructures as a result of the disruption of the yogurt gel structure by the increasing strain. As strain increased further, the transition from shear-thickening to shear-thinning behavior may have been due to further breakdown of the aggregate spheres into their constituents, such as caseins, micelles, and bacterial cells. Store brand yogurts showed an onset of intracycle shear-thinning

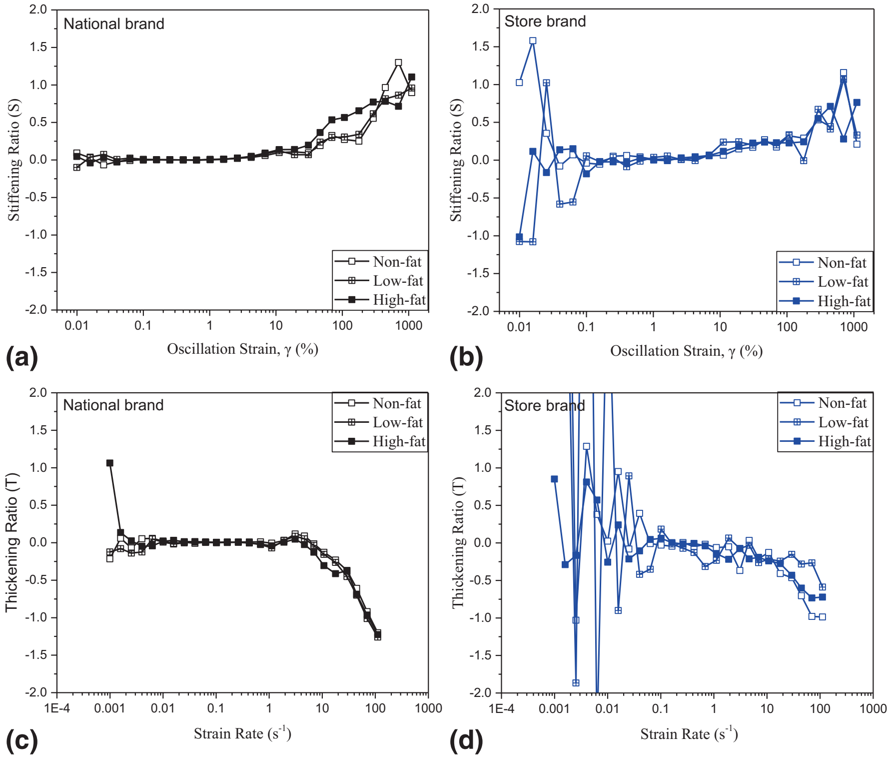

Fig. 17 Strain stiffening ratio (S) and shear thickening ratio (T) values for the yogurt samples with different fat levels at 1 rad/s

behavior at smaller strains, which concurred with the information obtained through the three-dimensional Lissajous plots (Fig. 12).

The transition from the linear viscoelastic response to the nonlinear viscoelastic response was further analyzed using the dimensionless LAOS parameters S (strain-stiffening ratio) and T (shear-thickening ratio). Positive S values ($S > 0$) were obtained for both national brand and store brand yogurts at 1 rad/s (Fig. 17a, b). The store brand yogurts showed T values that were slightly below zero ($T \leq 0$), whereas the national brand yogurts all showed negative values ($T < 0$) of a significantly higher magnitude than those of the store brand yogurts, indicating that they had a higher level of shear-thinning behavior (Fig. 17c, d). This information concurred with the information obtained by the viscous Lissajous curves (Figs. 13 and 14). The irregularities observed for the S and T values of the store brand yogurts at initial strains (0.01–0.1%) were attributed to wall slip and the unsteady local velocities occurring within the sample. In general, the information obtained from the S and T values solidified the evaluations of the nonlinear viscoelastic rheological behavior yogurt samples through the analyses of the SAOS and LAOS parameters, along with the elastic and viscous Lissajous curves.

3.4 LAOS Behavior of Tomato Paste and Mayonnaise

LAOS tests conducted within the strain range of 0.01–200% at 1 rad/s frequency showed that tomato paste and mayonnaise samples displayed nonlinearity at strain values of 1.24% and 4.3%, respectively (Duvarci et al. 2017a). Although a longer viscoelastic region was found for mayonnaise, tomato paste had higher G' and G'' values. An overshoot was observed for mayonnaise G'' values at the onset of the nonlinear viscoelastic region with the maximum occurring at 12% strain, while both moduli values for tomato paste decreased with increasing strain. The information obtained through the strain sweep data revealed that tomato paste showed Type I nonlinearity and mayonnaise showed Type III nonlinearity based on the classification proposed by Hyun et al. (2002). Both tomato paste and mayonnaise displayed intracycle strain stiffening captured through the upward turn of the elastic stress versus strain curves at large strains. The counterclockwise rotation of the ellipses suggested a gradual softening for both mayonnaise and tomato paste as the strain increased. Secondary loops were observed at the lowest frequency (0.5 rad/s) for tomato paste Lissajous-Bowditch curves, indicating reversible structural deformation and thixotropic behavior (Duvarci et al. 2017b). Both tomato paste and mayonnaise showed slight strain-stiffening ($e_3/e_1 > 0$, $S > 0$) and shear-thickening ($v_3/v_1 > 0$, $T > 0$) behaviors in the nonlinear viscoelastic region at 1 and 15 rad/s, which decreased at larger strains. At 0.5 rad/s, negative and decreasing v_3/v_1 and T values over strain rate were observed for tomato paste, while these values showed a maximum followed by a decrease for mayonnaise in the nonlinear viscoelastic region, similar to the trend observed for the G'' values (Duvarci et al. 2017a). These findings indicated that large strain rates were the driving force behind the gradual softening observed for tomato paste and mayonnaise, while unraveling the differences in the nonlinearities of these two concentrated dispersions.

3.5 Additional Selected LAOS Studies

LAOS analysis has also been used to evaluate the effects of food formulation changes and chemical composition on their rheological behaviors. For example, the effect of formulating mashed potato with different potato starch preparations (Joyner (Melito) and Meldrum 2016), the impact of particle size and addition of soy lecithin to dark chocolate (van der Vaart et al. 2013), the addition of xanthan gum and pectin to egg white foams (Ptaszek et al. 2016), and the effect of debranching on waxy rice starch gels (Precha-Atsawanan et al. 2018) have been studied. Increased starch damage in mashed potato composition was reported to cause an increase in viscous-dominant rheological behavior and a decrease in nonlinear viscoelastic behavior at large strains, which may have been due to granule shape and size enabling damaged granules to more easily flow past each other. All samples, except for the sample prepared directly from potato starch, displayed shifts from elastic- to viscous-dominated behavior at large strains, which was captured by Lissajous-Bowditch curves and phase angle values (Joyner (Melito) and Meldrum 2016). In dark chocolate, a larger particle size of solids, such as sugar and cocoa, resulted in higher strain-stiffening intensity, while added lecithin did not significantly impact the strain-stiffening behavior. On the other hand, dark chocolate shear-thinning behavior was found to increase as the particle size increased, and the onset of shear thickening occurred at lower strains. Low levels of added lecithin decreased shear-thinning behavior, which could be attributed to its lubricating effect (van der Vaart et al. 2013). The addition of pectin, which is capable of gelling, and xanthan gum, which behaves like a soft gel but does not form a three-dimensional network structure on its own, eliminated the secondary loops associated with thixotropic behavior in egg white foams. Addition of xanthan gum and pectin to egg white foams also caused a shift to strain-hardening behavior in the nonlinear viscoelastic region, compared to the strain-softening behavior observed in egg white foams without these stabilizers (Ptaszek et al. 2016). Debranching increased the strain-stiffening and shear-thinning intensities in waxy rice gels. S values were positive above 1% strain for debranched gels, while positive values did not appear until 100% strain for waxy gels. At high strains, elastic Lissajous curves for debranched gels displayed an almost square shape, indicating abrupt yielding; their viscous curves exhibited an S-shape, showing a high degree of shear-thinning. Elastic and viscous Lissajous-Bowditch curves for waxy starch gels changed from an elliptical to a rhomboidal shape, indicating less pronounced strain-stiffening and lower shear-thinning behavior along with gradual yielding (Precha-Atsawanan et al. 2018).

As discussed in Sect. 1.1.4, e_3/e_1 and v_3/v_1 can be used to determine nonlinear viscoelastic behaviors (Ewoldt et al. 2008). Specifically, the profile of these ratios over the applied strain range can provide an in-depth understanding about how nonlinear viscoelastic material behavior changes with strain. The difference between hard and soft red winter wheat flour doughs in terms of gluten quantity and quality was probed by the decay observed on the intensities of e_3/e_1 within the applied strain range (Yazar et al. 2016a, b). Dough samples from both flours showed intracycle strain stiffening. However, as the strain amplitude increased from 44% to 70%, strain-stiffening behavior decreased for the soft wheat flour dough as observed by the decrease in the intensity of e_3/e_1. Hard wheat flour doughs showed a similar decrease at ~100% strain. These results revealed that the hard wheat flour dough had higher stability against large deformations due to its stronger gluten network.

These Chebyshev coefficients have been used to analyze the nonlinear viscoelastic behavior of other foods. For example, LAOS analysis of brittle and ductile fats showed that fat crystals had increasing v_3/v_1 values as strain increased towards the onset of nonlinearity; after the onset of nonlinear viscoelastic behavior, these values decreased, indicating a shift from intracycle shear-thickening to shear-thinning behavior. Positive e_3/e_1 values (intracycle strain stiffening) were recorded in the nonlinear viscoelastic region, showing that the elastic softening in fat crystals was driven by large strain rates. Additionally, brittle fats were reported to exhibit stronger nonlinearities as evidenced by higher positive elastic Chebyshev coefficients and lower negative viscous Chebyshev coefficients (Macias-Rodriguez et al. 2018).

Chebyshev coefficients have also been used to show that tomato paste and mayonnaise at 1 rad/s (Duvarci et al. 2017a) and agarose gels (Melito et al. 2012) exhibited strain-softening and shear-thinning behavior at the beginning of their nonlinear viscoelastic regions; they displayed strain stiffening and shear-thickening behaviors at higher strains. In contrast to the rheological behavior of these systems, dark chocolate (van der Vaart et al. 2013), egg white protein foams (Ptaszek et al. 2016), and fat crystals (Macias-Rodriguez et al. 2018) showed strain-stiffening and shear-thickening behavior in the linear viscoelastic region and strain-stiffening and shear-thinning behavior in the nonlinear viscoelastic region.

Another example of the complex rheological behavior captured through e_3/e_1 values was observed for buckwheat flour dough (Yazar et al. 2017a). Strain stiffening behavior was observed at the beginning of the nonlinear viscoelastic region ($e_3/e_1 > 0$). As strain increased gradually at a constant frequency of 10 rad/s, strain softening behavior occurred ($e_3/e_1 < 0$) due to the lack of a network formation such as that formed by gluten in wheat flour doughs, followed by strain stiffening behavior at >100% strain. At lower frequencies, this strain softening behavior was not observed. Furthermore, shear thinning dominated the rheological behavior in the nonlinear viscoelastic region at all applied frequencies. This shows frequency mainly affected the nonlinearity for the elastic component in the buckwheat flour dough. Evaluation of the stored and dissipated energy mechanisms simultaneously in the nonlinear viscoelastic region is not possible by the application of a rheological test other than LAOS. It is possible in the linear viscoelastic region through SAOS applications. However, linking nonlinear viscoelasticity to macroscopic performance is more relevant, since materials are exposed to large deformations under processing conditions.

The emergence of third order and higher harmonics due to significant nonlinear viscoelastic behaviors during the transition from SAOS to LAOS was also reported to be important to capturing microstructural differences (Ewoldt and Bharadwaj 2013). This transition region, termed the intrinsic regime, comprises relatively low strains covering a range from linear viscoelastic behavior to the onset of nonlinearity. This region is idea for physical interpretation of higher-order harmonics because the experimental errors associated with the magnitude of the third harmonic observed at large strains (e.g. wall slip, secondary flows) are minimized. Ewoldt and Bharadwaj (2013) defined the material functions in the intrinsic region using a single-mode Giesekus model; they obtained a slope of 2 when $\log(e_3/e_1)$ and $\log(v_3/v_1)$ are plotted against $\log(\gamma)$. Yazar et al. (2017b) evaluated the intrinsic behavior of crude gluten fractions at 0.6–10% strain. They scaled the first harmonic moduli ($G_1^{'}$ and $G_1^{''}$) using the value of the complex modulus G^* obtained in the intrinsic region. Third-order harmonic Chebyshev coefficients (e_3 and ν_3) were scaled using the corresponding linear viscoelastic material function ($G' = e_1$ and $G'' = \nu_1$) at the same frequency within the intrinsic region. Slope values ranging between 0.45 and 2 were obtained for both gluten fractions. Higher slope values were obtained for gliadin, suggesting that the model to characterize intrinsic LAOS function (Ewoldt and Bharadwaj 2013) was a better fit for gliadin than glutenin.

As discussed in Sect. 1.1.1, the first-order viscoelastic moduli, G_1' and G_1'', can also be used to provide useful material characterization when plotted as a function of stress amplitude (τ_1). For example, ductile fat crystals exhibited a steady decrease in G_1' and G_1'' at around 1000 Pa, whereas brittle fat crystals showed a gradual decrease at 1500 Pa followed by a sudden drop and a backward bending at 4000 Pa. These significantly different responses were also captured through plotting the stress amplitude (τ_1) versus strain amplitude. Ductile fat showed a maximum stress of 4000 Pa, whereas brittle fat crystals had a maximum stress of 4900 Pa. After reaching the maximum stress, ductile fat crystals displayed a plateau in stress values. However, an instantaneous drop in stress was observed for brittle fats. These data were reported to be consistent with the qualitative behavior provided by third-order harmonic Fourier data (Macias-Rodriguez et al. 2018).

Another LAOS analysis method uses the profile of G_1' and G_1'' as a function of input strain amplitude to provide information related to the microstructure of complex fluids. Four different types of nonlinear viscoelastic behavior are defined as Type I, or strain thinning; Type II, or strain hardening; Type III, or weak strain overshoot; and Type IV, or strong strain overshoot (Hyun et al. 2002). Studies conducted on food materials showed that fresh gels of gelatin-alginate (1:1 concentration ratio) exhibited Type IV behavior, in which both G' and G'' increased to a maximum and then decreased in the nonlinear viscoelastic region. Layer gels, however, showed Type III behavior, with steadily decreasing G' values and increasing and then decreasing (overshoot) G'' values (Goudoulas and Germann 2017). Crosslinked tapioca starch with added guar gum and xanthan gum showed Type III behavior, while gels made with crosslinked tapioca starch and either guar gum or xanthan gum showed Type I behavior, with both G' and G'' values decreasing continuously in the nonlinear viscoelastic region (Fuongfuchat et al. 2012). Fat crystals have also been shown to exhibit Type III behavior (Macias-Rodriguez et al. 2018).

Several studies on food products have linked LAOS data to applications that impose large deformations on materials. Dough development throughout farinograph mixing was monitored for wheat dough samples through LAOS tests (Yazar et al. 2016a, b). G_L' and G_M' values for gluten-free dough samples were correlated to loaf volume of the resulting bread samples (Yazar et al. 2017a). This correlation generated a better understanding of how final product quality was impacted by both the deformations dough samples undergo during fermentation and baking and the capacity of the dough to endure these deformations. LAOS behavior has also been linked to tribological parameters of concentrated emulsions with added fish gelatin–gum Arabic mixture (Anvari and Joyner (Melito) 2018) and *Alyssum homolocarpum* seed gum (Anvari et al. 2018). The results of both LAOS and tribological tests were attributed to the different molecular structure features of the samples, as well as how those molecular structures were disturbed during testing. Determining relationships between food microstructure and LAOS and other rheological data is important, as it can provide information about food mechanical and friction properties that may contribute to their sensory behaviors.

4 Conclusions

LAOS parameters can be utilized to capture the unique nonlinear behaviors of semisolid foods such as yogurt, wheat flour dough, gluten, mayonnaise, and tomato paste. The emergence of nonlinearities are observed by the change in the shape of the periodic stress response to a sinusoidal strain input, typically displayed as a Lissajous-Bowditch plot. These plots can display the total stress versus strain, the elastic stress versus strain, or the viscous stress versus strain rate. In addition, nonlinear viscoelastic information can be determined from the intracycle strain moduli ($G_L^{'}$, $G_M^{'}$) and instantaneous viscosities ($\eta_L^{'}$, $\eta_M^{'}$) (Ewoldt et al. 2008). Moreover, G' and G'' for the whole strain range help determine the overall type of nonlinear viscoelastic behavior exhibited by a given semisolid food (Hyun et al. 2002), while Chebyshev coefficients (particularly e_3/e_1 and v_3/v_1, since the signs of the third-order harmonics indicate the driving cause of the deviation from linearity) provide insights regarding the dominating intracycle strain-stiffening or -softening and shear-thickening or -thinning behavior (Ewoldt and Bharadwaj 2013). This information can be coupled with the information obtained through the Lissaous-Bowditch curves and S and T parameters. The LAOS technique is therefore a useful tool that can mimic the large deformations these food products are exposed to during manufacturing and oral processing. A wide range of examples for utilizing LAOS parameters on different semisolid foods revealed that the LAOS technique is able to probe the differences occurring in material nonlinearities due to production process parameters, oral processing, and formulation variation that cannot be fully probed by empirical rheological testing methods or fundamental SAOS tests.

References

Amemiya, J. I., & Menjivar, J. A. (1992). Comparison of small and large deformation measurements to characterize the rheology of wheat flour doughs. *Journal of Food Engineering, 16*, 91–108.

Anvari, M., & Joyner (Melito), H. S. (2018). Effect of fish gelatin and gum arabic interactions on concentrated emulsion large amplitude oscillatory shear behavior and tribological properties. *Food Hydrocolloids, 79*, 518–525.

Anvari, M., Tabarsa, M., & Joyner (Melito), H. S. (2018). Large amplitude oscillatory shear behavior and tribological properties of gum extracted from Alyssum homolocarpum seed. *Food Hydrocolloids, 77*, 669–676.

Atalik, K., & Keunings, R. (2002). Non-linear temporal stability analysis of viscoelastic plane channel flows using a fully-spectral method. *The Journal of Non-Newtonian Fluid Mechanics, 102*, 299–319.

Bae, J.-E., Lee, M., Cho, K. S., Seo, K. H., & Kang, D.-G. (2013). Comparison of stress-controlled and strain-controlled rheometers for large amplitude oscillatory shear. *Rheologica Acta, 52*, 841–857.

Bi, C.-H., Li, D., Wang, L.-J., Wang, Y., & Adhikari, B. (2013). Characterization of non-linear rheological behavior of SPI–FG dispersions using LAOS tests and FT rheology. *Carbohydrate Polymers, 92*, 1151–1158.

Bird, R. B., Armstrong, R. C., & Hassager, O. (1987). *Dynamics of polymeric liquids*. New York: Wiley.

Brugnoni, L. I., Tarifa, M. C., Lozzano, J. E., & Genovese, D. (2014). In situ rheology of yeast biofilms. *Biofouling, 30*(10), 1269–1279.

Dus, S. J., & Kokini, J. L. (1990). Prediction of the nonlinear viscoelastic properties of a hard wheat flour dough using the Bird-Carreau constitutive model. *Journal of Rheology, 34*(7), 1069–1084.

Duvarci, O. C., Yazar, G., & Kokini, J. L. (2017a). The comparison of LAOS behavior of structured food materials (suspensions, emulsions and elastic networks). *Trends in Food Science & Technology, 60*, 2–11.

Duvarci, O. C., Yazar, G., & Kokini, J. L. (2017b). The SAOS, MAOS and LAOS behavior of a concentrated suspension of tomato paste and its prediction using the Bird-Carreau (SAOS) and Giesekus models (MAOS-LAOS). *Journal of Food Engineering, 208*, 77–88.

Ewoldt, R. H., Hosoi, A. E., & McKinley, G. H. (2007). Rheological fingerprinting of complex fluids using large amplitude oscillatory shear (LAOS) flow. *Annual Transactions of the Nordic Rheology Society, 15*, 3–8.

Ewoldt, R. H., Hosoi, E., & McKinley, G. H. (2008). New measures for characterizing nonlinear viscoelasticity in large amplitude oscillatory shear. *Journal of Rheology, 5*, 1427–1458.

Ewoldt, R. H., & McKinley, G. H. (2010). On secondary loops in LAOS via self-intersection of Lissajous-Bowditch curves. *Rheologica Acta, 49*(2), 213–219.

Ewoldt, R. H. (2013). Defining nonlinear rheological material functions for oscillatory shear. *Journal of Rheology, 57*(1), 177–195.

Ewoldt, R. H., & Bharadwaj, N. A. (2013). Low-dimensional intrinsic material functions for nonlinear viscoelasticity. *Rheologica Acta, 52*, 201–219.

Franck, A. J. (2006). *Understanding instrument compliance correction in oscillation*. TA Instruments Product Note APN, 13. New Castle, DE. (http://www.tainstruments.com/pdf/literature/APN013_V1_Understanding_Instrument_Compliance.pdf).

Fuongfuchat, A., Seetapan, N., Makmoon, T., Pongjaruwat, W., Methacanon, P., & Gamonpilas, C. (2012). Linear and non-linear viscoelastic behaviors of crosslinked tapioca starch/polysaccharide systems. *Journal of Food Engineering, 109*, 571–578.

Goudoulas, T. B., & Germann, N. (2017). Phase transition kinetics and rheology of gelatin-alginate mixtures. *Food Hydrocolloids, 66*, 49–60.

Graham, M. (1995). Wall slip and the nonlinear dynamics of large amplitude oscillatory shear flows. *Journal of Rheology, 39*, 697–712.

Hibberd, G. E., & Parker, N. S. (1979). Dynamic viscoelastic behavior of wheat flour doughs, Part 4: Non-linear behavior. *Rheologica Acta, 14*, 151–157.

Hoyle, D. M., Auhl, D., Harlen, O. G., Barroso, V. C., Wilhelm, M., & McLeish, T. C. B. (2014). Large amplitude oscillatory shear and Fourier transform rheology analysis of branched polymer melts. *Journal of Rheology, 58*, 969–997.

Hudson, R. E., Holder, A. J., Hawkins, K. M., Williams, P. R., & Curtis, D. J. (2017). An enhanced rheometer inertia correction procedure (ERIC) for the study of gelling systems using combined motor-transducer rheometers. *Physics of Fluids, 29*, 121–602.

Hyun, K., Kim, S. H., Ahn, K. H., & Lee, S. J. (2002). Large amplitude oscillatory shear as a way to classify the complex. *Journal of Non-Newtonian Fluid Mechanics, 107*, 51–65.

Hyun, K., Lim, H. T., & Ahn, K. H. (2012). Nonlinear response of polypropylene (PP)/Clay nanocomposites under dynamic oscillatory shear. *Korea-Australia Rheology Journal, 24*, 113–120.

Hyun, K., Wilhelm, M., Klein, C. O., Cho, K. S., Nam, J. G., Ahn, K. H., Lee, S. J., Ewoldt, R. H., & McKinley, G. H. (2011). A review of nonlinear oscillatory shear tests: Analysis and application of large amplitude oscillatory shear (LAOS). *Progress in Polymer Science, 36*, 1697–1753.

Joyner (Melito), H. S., & Meldrum, A. (2016). Rheological study of different mashed potato preparations using large amplitude oscillatory shear and confocal microscopy. *Journal of Food Engineering, 169*, 326–337.

Khatkar, S. B., & Schofield, J. D. (2002). Dynamic rheology of wheat flour dough. I. Non-linear viscoelastic behavior. *Journal of the Science of Food and Agriculture, 82*, 827–829.

Klein, C., Venema, P., Sagis, L., & van der Linden, E. (2008). Rheological discrimination and characterization of carrageenans and starches by Fourier transform rheology in the non-linear viscous regime. *Journal of Non-Newtonian Fluid Mechanics, 151*, 145–150.

Läuger, J., & Stettin, H. (2010). Differences between stress and strain control in the non-linear behavior of complex fluids. *Rheologica Acta, 49*, 909–930.

Läuger, J., & Stettin, H. (2016). Effects of instrument and fluid inertia in oscillatory shear in rotational rheometers. *Journal of Rheology, 60*(3), 393–406.

Lee, W. J., & Lucey, J. A. (2010). Formation and physical properties of yogurt. *Asian Australasian Journal of Animal Sciences, 23*(9), 1127–1136.

Lefebvre, J. (2006). An outline of the non-linear viscoelastic behavior of wheat flour dough in shear. *Rheologica Acta, 45*, 525–538.

Lefebvre, J. (2009). Nonlinear, time-dependent shear flow behavior, and shear-induced effects in wheat flour dough rheology. *Journal of Cereal Science, 49*, 262–271.

Liu, Q., Bao, H., Xi, C., & Miao, H. (2014). Rheological characterization of tuna myofibrillar protein in linear and nonlinear viscoelastic regions. *Journal of Food Engineering, 121*, 58–63.

Lucey, J. A., Munro, P. A., & Singh, H. (1998). Rheological properties and microstructure of acid milk gels as affected by fat content and heat treatment. *Journal of Food Science, 63*(4), 660–664.

Macias-Rodriguez, B. A., Ewoldt, R. H., & Marangoni, A. G. (2018). Nonlinear viscoelasticity of fat crystal networks. *Rheologica Acta, 57*, 251–266.

Martinetti, L., Mannion, A. M., Voje, W. E., Jr., Xie, R., Ewoldt, R. H., Morgret, L. D., Bates, F. S., & Macosco, C. W. (2014). A critical gel fluid with high extensibility: The rheology of chewing gum. *Journal of Rheology, 58*(4), 821–838.

Merger, D., & Wilhelm, M. (2014). Intrinsic nonlinearity from LAOStrain experiments on various strain- and stress-controlled rheometers: A quantitative comparison. *Rheologica Acta, 53*(8), 621–634.

Melito, H. S., Daubert, C. R., & Foegeding, E. A. (2012). Creep and large amplitude oscillatory shear behavior of whey protein isolate/-carrageenan gels. *Applied Rheology, 22*(6), 521–534.

Melito, H. S., Daubert, C. R., & Foeeding, E. A. (2013a). Relating large amplitude oscillatory shear and food behavior: Correlation of nonlinear viscoelastic, rheological, sensory and oral processing behavior of whey protein isolate/−carrageenan gels. *Journal of Food Process Engineering, 36*, 521–534.

Melito, H. S., Daubert, C. R., & Foeeding, E. A. (2013b). Relationships between nonlinear viscoelastic behavior and rheological, sensory and oral processing behavior of commercial cheese. *Journal of Texture Studies, 44*, 253–288.

Mudgil, P., Jumah, B., Ahmad, M., Hamed, F., & Maqsood, S. (2018). Rheological, microstructural and sensorial properties of camel milk yogurt as influenced by gelatin. *LWT- Food Science and Technology, 98*, 646–653.

Nam, J. G., Ahn, K. H., Lee, S. J., & Hyun, K. (2010). First normal stress difference of entangled polymer solutions in large amplitude oscillatory shear flow. *Journal of Rheology, 54*(6), 1243–1266.

Ng, T. S. K., McKinley, G. H., & Padmanabhan, M. (2006). Linear to non-linear rheology of wheat flour dough. *Applied Rheology, 16*(5), 265–274.

Ng, T. S. K., McKinley, G. H., & Ewoldt, R. H. (2011). Large amplitude oscillatory shear flow of gluten dough: A model power-law gel. *Journal of Rheology, 55*(3), 627–654.

Pascual, P. A. L., Le, T. T., & Dewettinck, K. (2016). Rheological characteristics of yoghurt with varying levels of milk fat globule membrane. *Journal of Science, Engineering and Technology, 4*, 35–43.

Precha-Atsawanan, S., Uttapap, D., & Sagis, L. M. C. (2018). Linear and nonlinear rheological behavior of native and debranched waxy rice starch gels. *Food Hydrocolloids, 85*, 1–9.

Ptaszek, P., Meciej, K., Ptaszek, A., Kaczmarczyk, K., Krik, J., & Bieńczak, A. (2016). The analysis of the influence of xanthan gum and apple pectins on egg white protein foams using the large amplitude oscillatory shear. *Food Hydrocolloids, 54*, 293–301.

Reimers, M. J., & Dealy, J. M. (1996). Sliding plate rheometer studies of concentrated polystyrene solutions: Large amplitude oscillatory shear of a very high molecular weight polymer in diethyl phthalate. *Journal of Rheology, 40*, 167–186.

Reimers, M. J., & Dealy, J. M. (1998). Sliding plate rheometer studies of concentrated polystyrene solutions: Nonlinear viscoelasticity and wall slip of two high molecular weight polymers in tricresyl phosphate. *Journal of Rheology, 42*, 527–548.

Rocha, C. M. R., Souza, H. K. S., Magalhães, N. F., Andrade, C. T., & Gonçalvez, M. P. (2014). Rheological and structural characterization of agar/whey proteins insoluble complexes. *Carbohydrate Polymers, 110*, 345–353.

Sfakianakis, P., & Tzia, C. (2014). Conventional and innovative processing of milk for yogurt manufacture; development of texture and flavor: A review. *Food, 3*(1), 176–193.

Shu, R., Sun, W., Wang, T., Wang, C., Liu, X., & Tong, Z. (2013). Linear and nonlinear viscoelasticity of water-in-oil emulsions: Effect of droplet elasticity. *Colloids and Surfaces A: Physicochemical and Engineering Aspects, 434*, 220–228.

Sousa, A. M. M., & Goncalves, M. P. (2015). The influence of locust bean gum on native and alkali-modified agar gels. *Food Hydrocolloids, 44*, 461–470.

Stadler, F. J., Leygue, A., Burhin, H., & Baily, C. (2008). The potential of large amplitude oscillatory shear to gain an insight into the long-chain branching structure of polymers. *Polymer Preprints, 49*, 121–122.

Szopinski, D., & Luinstra, G. A. (2016). Viscoelastic properties of aqueous guar gum derivative solutionsunder large amplitude oscillatory shear (LAOS). *Carbohydrate Polymers, 153*, 312–319.

van der Vaart, K., Depypere, F., De Graef, V., Schall, P., Fall, A., Bonn, D., & Dewettinck, K. (2013). Dark chocolate's compositional effects revealed by oscillatory rheology. *European Food Research and Technology, 236*, 931–942.

Van Marle, M. E., Dirk, E., De Kruif, C. G., & Mellema, J. (1999). Steady-shear viscosity of stirred yogurts with varying ropiness. *Journal of Rheology, 43*, 1643–1662.

Wang, B., Wang, L.-J., Li, D., Wei, Q., & Adhikari, B. (2012). The rheological behavior of native and high-pressure homogenized waxy maize starch pastes. *Carbohydrate Polymers, 88*, 481–489.

Yazar, G., Duvarci, O., Tavman, S., & Kokini, J. L. (2016a). Effect of mixing on LAOS properties of hard wheat flour dough. *Journal of Food Engineering, 190*, 195–204.

Yazar, G., Duvarci, O., Tavman, S., & Kokini, J. L. (2016b). Non-linear rheological properties of soft wheat flour dough at different stages of farinograph mixing. *Applied Rheology, 26*, 1–11.

Yazar, G., Duvarci, O., Tavman, S., & Kokini, J. L. (2017a). Non-linear rheological behavior of gluten-free flour dough samples and their correlation with bread properties. *Journal of Cereal Science, 74*, 28–36.

Yazar, G., Duvarci, O., Tavman, S., & Kokini, J. L. (2017b). LAOS behavior of the two major gluten fractions: Gliadin and glutenin. *Journal of Cereal Science, 77*, 201–210.

Yoshimura, A. S., & Prud'homme, R. K. (1988). Wall slip effects on dynamic oscillatory measurements. *Journal of Rheology, 32*, 575–584.

Yosick, J. A., Giacomin, J. A., Stewart, W. E., & Ding, F. (1998). Fluid inertia in large amplitude oscillatory shear. *Rheologica Acta, 37*, 365–373.

Semisolid Food Tribology

Helen S. Joyner

1 Tribology Basics

Tribology comprises the study of friction, lubrication, and wear behaviors between two sliding surfaces. In the engineering, material science, and medical fields, tribometry has been used since the middle of the twentieth century to evaluate performance and lifetime of bearing surfaces, coatings, and lubricants. However, tribological analysis of semisolid and fluid food products has only recently been shown significant attention, gaining traction in the first decade of the twenty-first century and becoming increasingly popular since. The current goal of food tribological measurements is to uncover key factors impacting food texture that cannot be measured by traditional rheometry. This can allow better prediction of food texture through instrumental analysis. Unfortunately, tribological behaviors are sensitive to many parameters and tribological testing adopted from other fields for use with foods may hinge on assumptions that are violated in a food tribological system. A sound understanding of basic tribological principles and careful control of the tribological system is needed for accurate, repeatable food friction measurements.

H. S. Joyner (✉)
School of Food Science, University of Idaho, Moscow, ID, USA
e-mail: hjoyner@uidaho.edu

H. S. Joyner (ed.), *Rheology of Semisolid Foods*, Food Engineering Series,
https://doi.org/10.1007/978-3-030-27134-3_5

1.1 Lubricated Sliding

1.1.1 Friction Coefficient

The primary focus of tribological studies of semisolid foods is their friction and lubrication behaviors. When two hard surfaces slide against each other in relative motion, friction is the force that opposes sliding motion (Fig. 1). The amount of friction force between the two surfaces can be described by Eq. 1:

$$\mu = \frac{F_F}{F_N} \tag{1}$$

Here, μ is friction coefficient (unitless), F_F is friction force (N), and F_N is applied normal load (N). While friction force is typically measured directly by the testing apparatus, it is a function of the sliding surface material and physicochemical properties, as well as any lubricant used between the sliding surfaces and the environmental conditions during the test (e.g. temperature, humidity). In semisolid food tribological testing, the food product acts as a lubricant between the two sliding surfaces. Under these conditions, Eq. 1 can be used to calculate the friction coefficient of the food under the testing conditions.

Because friction is a system property, food friction coefficients are highly dependent on the testing apparatus and environment. This will be further discussed in later sections.

1.1.2 Stribeck Curve

The Stribeck curve, which is a plot of friction coefficient versus sliding speed, was developed primarily for measuring performance of Newtonian lubricants on hard sliding surfaces (Joyner (Melito) et al. 2014a, b). Under these conditions, friction between the two sliding surfaces is classified in one of three regimes: boundary, mixed, and hydrodynamic (Fig. 2) (Prakash et al. 2013; Stokes 2012; Greene et al. 2013). In the boundary regime, which occurs at low sliding speeds, the asperities in the sliding surface have significant contact and bear most of the applied normal

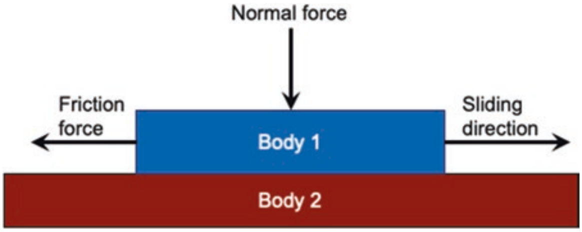

Fig. 1 Schematic of sliding countersurfaces

Fig. 2 Stribeck curve

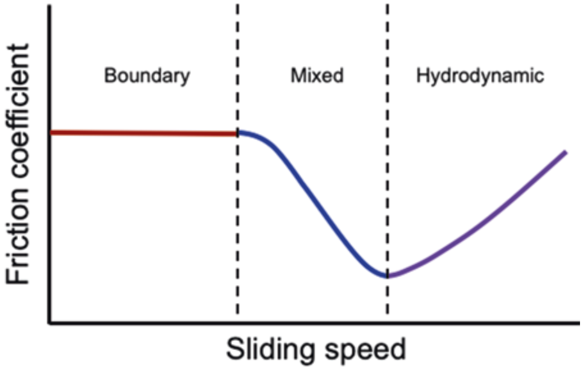

load, resulting in incomplete separation of the sliding surfaces and a relatively high, constant friction coefficient. Here, the properties of the sliding surfaces have a dominant effect on friction behavior.

As sliding speed increases, fluid pressure builds in the contact zone between the surfaces. The increase in pressure pushes the sliding surfaces farther apart, although they still have some contact between their asperities. This increasing surface separation results in more of the normal load being carried by the lubricant, causing the friction coefficient to decrease with increasing sliding speed. At the end of the mixed regime, the friction coefficient reaches a minimum and the sliding surfaces have minimal contact.

Increasing sliding speed further causes a transition to the hydrodynamic regime. In this regime, the fluid pressure in the contact zone is sufficient to fully separate the sliding surfaces and all load is carried by the fluid. Friction increases with sliding speed because of viscous drag; highly viscous lubricants can produce friction coefficients greater than those in the boundary regime. Thus, lubricant viscosity plays a key role in friction behaviors of systems exhibiting hydrodynamic sliding (Chen and Engelen 2012).

1.1.3 Using the Stribeck Curve in Food Tribology

Studies of lubricated sliding in many engineering fields focus on Newtonian lubricant performance in hydrodynamic sliding on hard surfaces, such as performance of lubricants on engine pistons and ball bearings. However, food tribology studies use soft surfaces, defined as deformable materials with Young's modulus in the kPa to low MPa range, similar to the modulus of soft oral surfaces (Dresselhuis et al. 2008a; Payan and Perrier 1997), and most food products exhibit non-Newtonian behavior. Additionally, it is not always possible to evaluate food products over a range of sliding speeds sufficient to generate all three regimes of sliding behavior (Joyner (Melito) et al. 2014c). Therefore, friction behaviors of foods do not always follow the Stribeck curve shape; example friction profiles for food products are

Fig. 3 Potential shapes of friction coefficient versus sliding speed curves for food friction behavior

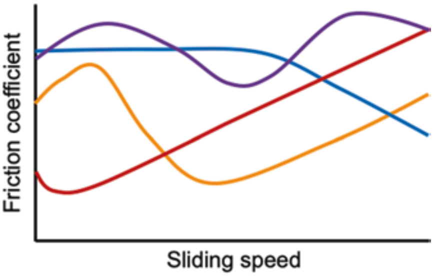

shown in Fig. 3. This complexity in friction behavior can make the friction profiles both difficult to interpret and difficult to relate to fundamental food properties or textural attributes.

However, there are several steps that can be taken to simplify data analysis, including correction for dissimilar and non-Newtonian viscosities. Viscosity corrections are important because viscosity can have a profound effect on friction results (Stokes et al. 2013). Because higher-viscosity fluids are more able to support applied normal loads in the contact zone, these fluids display hydrodynamic behavior at lower sliding speeds compared to lower-viscosity fluids (Chen and Stokes 2012). This effect has been observed for multiple food products (Joyner (Melito) et al. 2014a; de Vicente et al. 2005a; Li et al. 2018). It is possible to account for the effect of viscosity on friction coefficient by plotting friction coefficient versus sliding speed multiplied by viscosity (Fig. 4a, b) (de Vicente et al. 2005a). For Newtonian materials, the viscosity correction is straightforward. However, most foods have non-Newtonian viscosity profiles, and the shear rate in the gap changes with both sliding speed and gap height. This makes the viscosity correction more complex, as the shear rate and thus apparent viscosity of the lubricant in the contact zone will change over the duration of the test. One approach to simplify the viscosity correction is to assume that the food has a viscosity plateau at shear rates >100,000 s^{-1}; these high shear rates are typical of those experienced during tribological measurements. This viscosity can be measured using a parallel plate setup with a narrow gap (50–100 μm) (Davies and Stokes 2008). Correcting data for viscosity differences allows more accurate comparison of samples with significantly different viscosities (Fig. 4b). It also allows superpositioning of similar samples at different concentrations to create an entire Stribeck curve when testing apparatus do not allow for creation of a full Stribeck curve for any one sample (Fig. 4c) (de Vicente et al. 2005a).

When analyzing food tribological data, one must keep in mind the assumptions underpinning the Stribeck curve. Most food tribological tests violate both the assumption that the hard surfaces are used for testing and the assumption that the lubricant is Newtonian. Therefore, food tribological data should be interpreted with care. Potential pitfalls of interpretation of food tribological data are further discussed in Sects. 2.4, 3.2, 3.3, and 3.4.

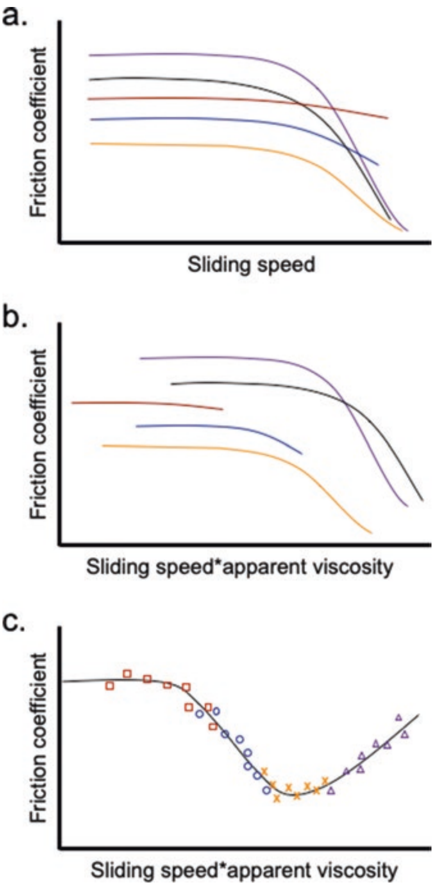

Fig. 4 Stribeck curve showing correction for differences in lubricant viscosity for sample foods ((**a**) before correction, (**b**) after). This correction can be used to (**c**) superposition curves of materials with similar components but different concentrations. Note that different data are used for (**a**) and (**b**) than for (**c**)

1.2 *Factors Impacting Friction*

Perhaps the most important fact to know about friction is that *friction is a system property, not a material property* (Schipper et al. 2007). This also holds true for other tribological behaviors, i.e. lubrication and wear. Any changes to the system will change the friction behavior. Thus, there are numerous factors that impact friction, including countersurface hardness, roughness, and surface chemistry; amount of lubricant; lubricant viscosity profile, composition, particle size, particle shape, and physicochemical properties; applied normal load; sliding speed; and environmental conditions during the test. While the precise effects on friction are system-dependent, several general statements about system parameters on friction behavior can be made:

- Attractive interactions between countersurfaces or between the countersurface and lubricant increase friction (de Vicente et al. 2005b; Crockett 2014; Gong and Osada 1998)

- When soft surfaces are used, contact area is load-dependent (Bongaerts et al. 2007a; Prinz et al. 2007; Myant et al. 2010a), and the load selected for testing can significantly impact friction coefficients
- Very rough and very smooth surfaces tend to produce higher friction coefficients than surfaces with moderate roughness (Chojnicka-Paszun and De Jongh 2014; Pettersson and Jacobson 2003; Derler et al. 2007)
- Lubricants with higher viscosity exhibit hydrodynamic behavior at lower sliding speeds compared to lower-viscosity lubricants (Bongaerts et al. 2007a; Campbell et al. 2017; De Vicente et al. 2006)
- Larger and rougher particles increase friction coefficient (Yakubov et al. 2015a; de Wijk and Prinz 2005; Liu et al. 2016a), provided they are not too large to be excluded from the gap (Yakubov et al. 2015b; Garrec and Norton 2012; Malone et al. 2003b)

2 Semisolid Food Tribological Measurements

A wide variety of instruments have been used to measure the tribological behaviors of foods. Commonly used instruments include the Mini-Traction Machine (MTM; specifically designed for friction measurements), rheometers with specialized attachments, and uniaxial compression equipment with specialized attachments (Prakash et al. 2013). The specific setup of the friction test is dependent on the individual instrument and attachment, and each setup has different capabilities, advantages, and disadvantages.

2.1 Testing Geometry

Tribological testing geometries have three main movement types, linear sliding, rotational sliding, and rolling. Of these movement types, rotational sliding and rolling are most commonly used in tribological studies as of 2019, but there has been some study of food friction behaviors under linear sliding, including how acceleration and deceleration in reciprocating linear sliding impacts friction coefficients (Campbell et al. 2017).

In semisolid food tribology, the most common geometry used is a ball(s)-on-plate setup (Fig. 5). The food is spread on the plate in a thin layer and the ball(s) is(are) rotated on the plate. In the MTM setup, the plate is rotated and the ball is held stationary; the ball may also be set to rotate in place as the sliding occurs. The ball(s) is(are) generally considered to be a point contact on the plate, although this is not necessarily the case if the plate and balls are made of soft materials. Still, the ball(s) do(es) provide a relatively small, elliptical contact area, which is important for the assumptions underpinning friction coefficient calculations using Hertzian theory (Adams and Nosonovsky 2000).

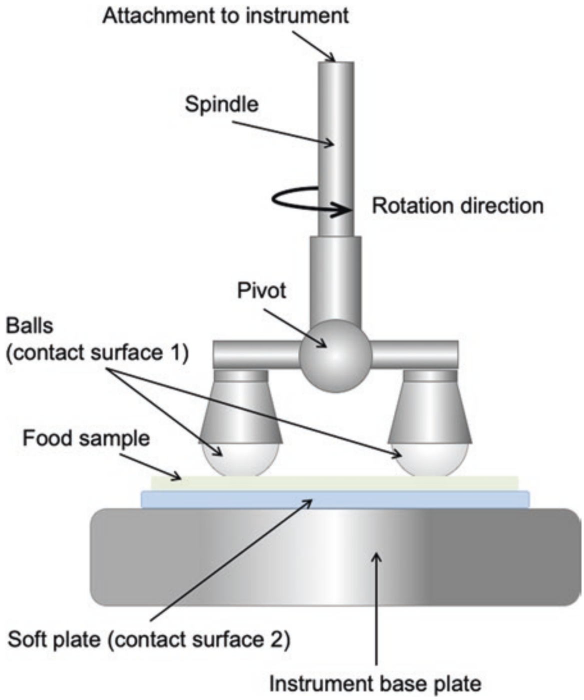

Fig. 5 Example of a ball-on-plate testing setup for food tribology

2.2 *Testing Surfaces*

Food tribological studies typically use soft surfaces in an effort to mimic oral surfaces (Nguyen et al. 2015). It is desirable to mimic oral surfaces because food tribological data are mainly used to better understand influences on food textural attributes that do not relate well to rheological properties, such as grittiness, mouthcoating, and smoothness (Prakash et al. 2013; Chen and Stokes 2012). Soft surfaces that have been used for food products include elastomers (e.g. neoprene) (Nguyen et al. 2015; Chojnicka et al. 2008a, 2009; Zinoviadou et al. 2008), whey protein isolate gels (Joyner (Melito) et al. 2014a, c), polydimethylsiloxane (PDMS) (Li et al. 2018; Selway and Stokes 2013; Dresselhuis et al. 2007; Yakubov et al. 2015c; Joyner (Melito) and Damiano 2015; Liu et al. 2016b), Transpore tape (Nguyen et al. 2015, 2016; Godoi et al. 2017), and porcine oral tissue (Dresselhuis et al. 2008a; De Hoog et al. 2006). Of these surfaces, PDMS is the most commonly used because it can be modified in terms of surface chemistry (Dresselhuis et al. 2007; Ranc et al. 2006), roughness (Bongaerts et al. 2007a), and elastic modulus (Dresselhuis et al. 2008a), allowing it to more easily mimic properties of the tongue and soft palate. PDMS is naturally hydrophobic but can be made hydrophilic with plasma treatments if desired (Bongaerts et al. 2007a). The roughness of the PDMS surface can be controlled by adjusting the surfaces roughness of the mold into which PDMS is cast. Typically, PDMS plates used in food tribological studies have a ratio of 10:1 base:crosslinker and smooth surfaces.

PDMS is a relatively inert material, so does not readily interact with food materials. However, it is still possible for foods with a greater affinity for the PDMS surface than the other food components to adhere to PDMS, resulting in the formation of a layer of that component on the PDMS surface. This surface layer can have a dramatic impact on friction behaviors (Tsui et al. 2016). For example, foods containing liquid fat can deposit a layer of fat onto the PDMS plate over time, which can noticeably decrease friction profiles. Cleaning the plates with an effective solvent, such as petroleum or ethyl ether, to remove fat buildup, minimizes the impact of surface layer buildup. However, it is still recommended that the sliding surfaces be changed after approximately 5 runs to limit the impact of surface wear and fouling on food tribological measurements.

2.3 Measurement Parameters

When performing tribological testing of food products, sliding speed and normal load are the two variables of primary interest. Temperature and test duration can also be controlled. Typically, tribological testing is performed at 25 or 37 °C; these temperatures correspond to shelf storage and oral temperatures, respectively. Tests at 25 °C can also be used to evaluate friction behaviors that are served cold and have a short residence time in the mouth. This short residence time does not allow the food to warm to body temperature before swallowing. For example, yogurt, which has a serving temperature of about 8 °C, is at approximately 25 °C when swallowed because it has an oral residence time of <10 s.

Matching the temperature of the food at serving or during consumption allows more accurate determination of relationships between tribological and sensory data. While it would also be helpful to measure tribological behaviors over similar timescales as those observed for oral processing (<10s for fluid and semisolid foods (de Wijk et al. 2006a)), it is impractical to do so because of the limitations of current instrumentation. To generate a Stribeck curve with a reasonable degree of data precision and accuracy, one must collect at least 5 points per decade of sliding speed and allow sufficient time at each sliding speed for the instrument to reach steady-state before data collection. As a result, these tribological tests can have a duration of 15–60 minutes. This timescale difference should be taken into consideration during testing and data analysis, particularly for time-sensitive samples that can change significantly during the duration of the test. Using a single sliding speed rather than a sliding speed range does allow one to examine food tribological behaviors on similar timescales to those of oral processing. However, this type of test is comparable to single-point viscosity testing; the test should be run at several sliding speeds to generate a more complete picture of the material's tribological behaviors at short timescales.

Sliding speed is typically varied between 0.01 to 100 mm s^{-1} to generate data for the Stribeck curve. However, if changes to friction behaviors over time are to be evaluated, the sliding speed can be held constant and friction coefficient recorded over time. This setup is especially of interest when evaluating changes to food friction behaviors upon addition of saliva (Selway and Stokes 2013; Vardhanabhuti et al. 2011). The applied load of the ball(s) against the plate is typically set to a given value and the sliding speed of the ball(s) relative to the plate is typically varied to generate Stribeck-type data. Sliding speeds of 10–100 mm s^{-1} are often of interest in food tribological studies; this sliding speed range is typically considered to be representative of oral sliding speeds (Malone et al. 2003a; Prinz et al. 2007; Campbell et al. 2017; Steele and Van Lieshout 2009; de WIjk and Prinz 2006). Additional considerations for selection of sliding speeds include the capabilities of the instrument and the quality of the data. Data collected at high sliding speeds (>100 mm s^{-1}) may be inaccurate if the sample is ejected from the testing geometry or the instrument is not capable of generating high sliding speeds. Data collected at very low sliding speeds (<0.01 mm s^{-1}) may be inaccurate due to lack of instrument precision and stick-slip or startup phenomena. This is particularly true when testing on soft surfaces such as elastomer plates. In ball-on-plate stick-slip with rotating balls, the balls stick to the plate at low rotational speeds (Tsui et al. 2016). However, because the plate deforms as the ball attachment rotates, the balls appear as if they are moving even though the surfaces are not moving relative to each other. After the elastic limit of the soft plate is reached, the plate stops stretching and the balls slide on the plate, often with a higher velocity than desired for the measurement. The instrument will correct the sliding speed, slowing the balls and causing the process to repeat until the sliding speed increases to the point at which there is insufficient time for the plate and balls to adhere, and the balls will slide smoothly over the plate. Stick-slip behavior often manifests as either a gradual increase in friction coefficient at the beginning of the test or noisy data (Fig. 6).

In the great majority of food tribological testing, the normal force is held constant. Typical values of normal force are 1–3 N, which is based on the reported values of contact pressures during oral processing (3–27 kPa) (Bongaerts et al. 2007a; De Vicente et al. 2006; Hayashi et al. 2002). The normal force should be great enough to generate friction but not so great that it causes rapid wear of the sliding surfaces. Wear of the sliding surfaces during the test or over multiple replicates can cause artifacts in the data. However, the soft surfaces used in food tribological testing are relatively resistant to wear under typical testing conditions. Regular replacement of the testing surfaces (e.g. after every 4–6 runs) minimizes surface wear and data artifacts related to surface wear.

2.4 Data Analysis

Current studies of food tribological behaviors have two primary goals: better understanding of what factors contribute to friction behaviors and determination of how friction behaviors relate to sensory attributes. Analyzing tribological data can include mean comparison of friction coefficients at selected sliding speeds,

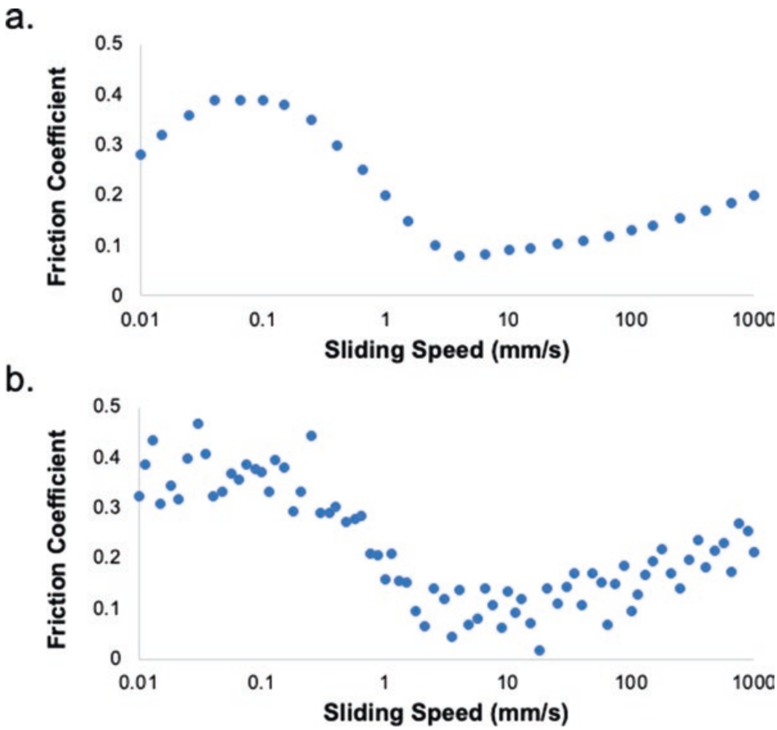

Fig. 6 Potential manifestation of sample stick-slip behaviors in food friction profiles: (**a**) startup phenomena, (**b**) noisy data

correlation of tribology data to rheological, sensorial, or microstructural data, and qualitative comparisons. Qualitative comparison of tribological data is relatively common in food tribology studies and generally involves comparing the relative shapes of food friction profiles and relative magnitudes of friction coefficients at different sliding speeds. While qualitative comparison generally considers the entire friction profile, it is not possible to determine if the entire profile of each sample is statistically different from that of a second sample or just visually different. This is particularly problematic for samples with large standard errors. Comparing means of friction coefficients determines if the samples are statistically similar for each data point. This method adds statistical rigor to the analysis but does require each point to be compared individually, making the analysis cumbersome. Correlation of tribological data to other data has similar issues. Although correlation analyses can determine whether two parameters are related (e.g. friction coefficient and grittiness score), only one friction coefficient value is used in the correlation analysis. This is typically friction coefficient at oral sliding speed, approximately 30 mm s^{-1} (Steele and Van Lieshout 2009). However, this sliding speed may not be relevant to the parameter to which the tribological data are being correlated. Certain oral movements may be performed at faster or slower speeds, or over a range of speeds.

Furthermore, sliding speeds during industrial processing may be much higher or lower than oral sliding speeds, depending on processing parameters. Therefore, care must be taken in both selecting appropriate tribological data for correlation analysis and interpretation of the analysis results.

One method of incorporating more of a large data set into a mean separation or correlation analysis is to model the data set with an equation or set of equations and use the equation parameters (e.g. coefficient values) for the analysis. This is analogous to modeling flow profile data with an equation for viscosity and comparing the constants in the equation. However, there are no standard models for either the entire Stribeck curve or parts of the Stribeck curve that are applicable to non-Newtonian lubricants on soft surfaces. Additionally, these models tend to be highly complex and require property data that are not readily available for the materials used in food studies. On the other hand, it is possible to empirically model tribological data and use model parameters for correlation or mean separation analyses. Ultimately, the choice of whether or not to use a model for tribological data analysis is dependent on the goals of the study and the resources available to the research group.

Tribological data for foods can be noisy because of the soft testing surfaces that deform and relax under an applied load. This changes the actual load on the surface, requiring the testing apparatus to continually adjust the applied normal load to maintain the target value. Unfortunately, the limitations of adjustment speed and precision of most testing apparatuses used in food tribology result in potentially large fluctuations in normal force. Although the formula for friction coefficient accounts for normal load (Eq. 1), these fluctuations can affect data validity because changes in applied load can change the contact area of soft surfaces (Joyner (Melito) et al. 2014c, d; De Hoog et al. 2006). While the data can be corrected to account for actual contact area assuming elastic (Hertzian) contact (De Vicente et al. 2006) and Johnson-Kendall-Roberts (JKR) contact theory (Greene et al. 2013), this is often difficult because the instantaneous contact area is not known. To reduce the noise, the data should be screened for normal force and all data outside of a set range around the set normal force should be removed (Fig. 7). A range of ±5–10% around the set normal force is generally sufficient to reduce noise from large normal force fluctuations (Joyner (Melito) et al. 2014c, d). This screening procedure allows for more accurate comparison among samples. However, a relatively high data density (>20 points per individual sliding speed tested) is recommended to perform this screening procedure (Joyner (Melito) et al. 2014d) so that there is still sufficient data density after screening to support statistical analyses.

3 Semisolid Food Tribological Behaviors

There has been significant interest in semisolid food tribological behaviors over the last decade. This interest is primarily driven by the desire to better understand drivers behind semisolid food textures. Although viscosity behaviors can explain certain semisolid food sensory attributes related to viscosity, such as thickness

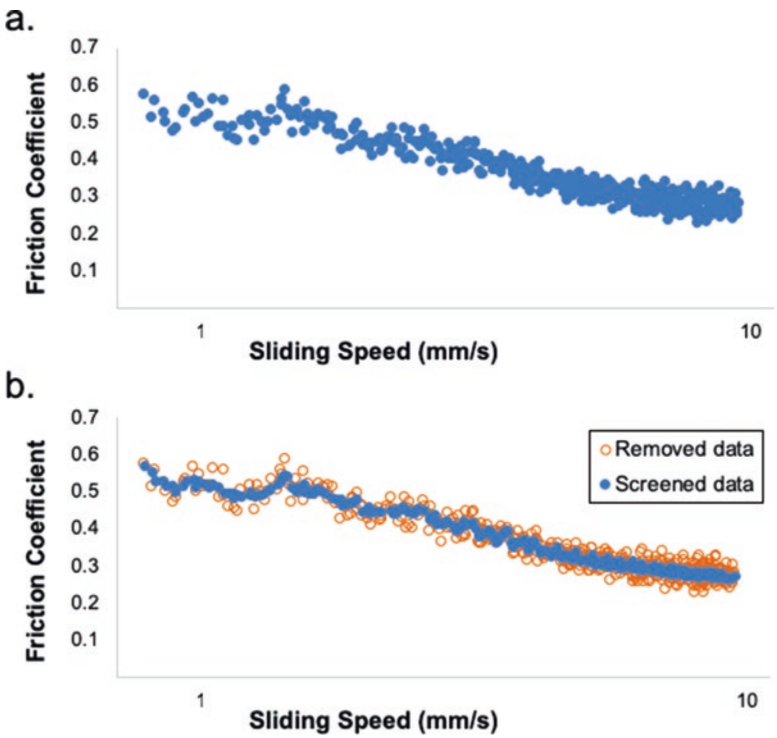

Fig. 7 Screening procedure for data (**a**) before screening procedure is applied and (**b**) after screening

(Van Aken et al. 2007; Akhtar et al. 2005; Kokini 1987; Dickie and Kokini 1983), they cannot fully explain many sensory attributes that are key to consumer liking. These attributes, such as smoothness (Malone et al. 2003a; Chen and Stokes 2012; Kokini 1987; Laiho et al. 2017), chalkiness (Joyner (Melito) et al. 2014a), astringency (Chen and Stokes 2012; Vardhanabhuti et al. 2011), mouthcoat (Laiho et al. 2017; Nguyen et al. 2017), slipperiness (Chen and Stokes 2012), grittiness/roughness (Prakash et al. 2013), and the somewhat controversial creaminess (Chen and Stokes 2012; Laiho et al. 2017; Sonne et al. 2014; Kokini and Cussler 1983; de Wijk and Prinz 2007), have been found to relate to tribological behaviors. Because many of these terms are friction-related, it is generally hypothesized that they are related to semisolid food friction behaviors. Accordingly, the friction behaviors of custards (Godoi et al. 2017; de Wijk and Prinz 2007; De Wijk et al. 2004, 2006b), mayonnaise (de Wijk and Prinz 2007; Giasson et al. 1997), yogurts (Selway and Stokes 2013; Laiho et al. 2017; Nguyen et al. 2017; Sonne et al. 2014; Morell et al. 2017; Laguna et al. 2017), white sauce (de Wijk and Prinz 2007), ice cream (Kokini and Cussler 1983), and cream cheese (Nguyen et al. 2016; Kokini and Cussler 1983) have been studied; these studies have focused on relating semisolid food friction behaviors to rheological behaviors (Joyner (Melito) et al. 2014a; Selway and Stokes 2013;

Liu et al. 2016b; Nguyen et al. 2016, 2017; Laguna et al. 2017), microstructural features (Liu et al. 2015, 2016b; Laiho et al. 2017; Sonne et al. 2014), particle size (Nguyen et al. 2016; Laiho et al. 2017; Laguna et al. 2017), and sensory attributes (Laiho et al. 2017; Kokini and Cussler 1983; de Wijk and Prinz 2007; Laguna et al. 2017). But because friction is a system property and semisolid food friction is dependent on a multitude of parameters, the relationships between food friction and other properties and behaviors are not always straightforward and there are few relationships that are truly universal.

3.1 Key Factors Impacting Semisolid Food Friction Behaviors

3.1.1 Formulation

Fat plays a major role in food friction behaviors. An excellent lubricant, fat significantly decreases food friction coefficient values (Chojnicka et al. 2009; Selway and Stokes 2013; Sonne et al. 2014; Chojnicka-Paszun et al. 2012). In fact, tribological testing can differentiate among foods with different fat content but similar rheology (Joyner (Melito) et al. 2014a; Selway and Stokes 2013; Nguyen et al. 2016). These behaviors have been found to relate to sensory attributes such as fattiness/fatty mouthfeel (Liu et al. 2015; Dresselhuis et al. 2008b), creaminess (de Wijk and Prinz 2005; Chojnicka-Paszun et al. 2012), and oral viscosity (Sonne et al. 2014). However, it has been observed that above a certain fat content, the specific fat content being dependent on sliding speed, increased fat content caused no changes in friction behavior (de Wijk and Prinz 2005). It was hypothesized that the contact area became completely filled with fat at a certain fat contentration, so there was no effect of further increasing fat content (Malone et al. 2003a). Additionally, care must be taken when relating fat-related friction behaviors to fat-related sensory behaviors, as the ability to differentiate samples with different fat content is dependent on surface selection and human sensitivity for differentiating fat content does not necessarily align with instrumental sensitivity (Chojnicka-Paszun et al. 2012).

The lubricating properties of fat are thought to strongly impact food texture attributes; formulating lower-fat foods can be challenging because fat replacers often do not mimic the lubrication properties of fat, even if they can replicate fat functional behaviors. For example, polysaccharide-based fat replacers tend to promote hydrodynamic behavior over the range of sliding speeds tested in food tribology (Joyner (Melito) et al. 2014a), while fat shows boundary and mixed behavior (Sonne et al. 2014). It has been found that fat replacers with smaller particle size that provide higher viscosity and lower friction coefficients are more successful in mimicking both friction and sensory behaviors of full-fat semisolid foods (Sonne et al. 2014). Additionally, the level of fat replacer is key to frictional properties, and the level of fat replacer needed to replicate friction behaviors of fat is dependent on the specific fat replacer (Brennan and Tudorica 2008).

In addition to total fat content, solid fat content, type, binding to the food matrix, and deposition on sliding surfaces is also important to friction behavior. In food gels, high solid fat content, lower binding to other ingredients and higher fat content reduced friction and increased fatty mouthfeel; however, only binding and total fat content related to sensory attributes (Liu et al. 2015). Bound fat droplets in emulsions had higher friction coefficients and less fatty mouthfeel than emulsions made with unbound fat droplets (Camacho et al. 2015). Fat deposition on sliding surfaces can be due to shear-induced coalescence of fat droplets in the contact zone, with the resulting coalesced droplets remaining in the valleys between asperities after the sliding contact passes (Chojnicka-Paszun et al. 2012). To date, there is little information in the literature about how fat impacts food friction beyond the amount of fat added. Further work is needed in this area to determine the precise role that fat plays in food lubrication.

Proteins provide structure to semisolid foods, typically through formation of a network that traps water, fat, and small molecular weight solids. Protein concentration, type, and content has been found to impact the friction behaviors of yogurts; friction increases with increased total protein, particularly at higher sliding speeds (Sonne et al. 2014). A higher casein to whey ratio generally decreased friction coefficient in yogurts (Laiho et al. 2017; Sonne et al. 2014), with a significant interaction with total protein content (Sonne et al. 2014). These effects are likely due to changes in food microstructures: higher whey protein content tends to produce a coarse, particulate network made of whey protein aggregates (Laiho et al. 2017). Whey protein aggregates in solution have been shown to increase friction coefficients, particularly at lower sliding speeds. In contrast, fibrillar proteins such as egg ovalbumin can align with the shear field in the contact zone, allowing them to interact with the contact surafces and reduce friction on rougher surfaces (Chojnicka et al. 2008a). Small protein aggregates can also decrease friction coefficients: microparticulated whey protein particles reduced friction in solutions and emulsion-filled gels. These results were attributed to the ball-bearing effect of microparticulated whey protein particles (Liu et al. 2016c), which is further discussed in Sect. 3.2. To date, much of the tribological literature concerning food product ingredients and their influence on food friction behaviors has focused on the effects of fat content, and type and concentration of hydrocolloids, especially starch. More work is needed to improve the understanding of the influence of protein type, concentration, and conformation on fluid and semisolid food friction behaviors.

Polysaccharides, which are typically evaluated in solution, generally exhibit both high adhesion to the sliding surfaces and low friction coefficients (Crockett 2014). While this may seem contradictory, it is the manner in which polysaccharides adhere to the sliding surfaces that can cause this effect. Polysaccharides interact with each other and sliding surfaces through hydrogen bonding. If the affinity of the polysaccharide for the sliding surface is higher than for itself or the solvent, it will adhere to the surface. However, the presence of water can dissolve polysaccharide-polysaccharide hydrogen bonds, allowing the chains to easily slide past each other and reducing friction.

The charge on polysaccharides has a significant impact on friction behavior. Charged polysaccharides can interact with surfaces through electrostatic interactions, whereas neutral polysaccharides mainly interact with surfaces through hydrophobic interactions and hydrogen bonding (Crockett 2014). Hydrogen bonds are weaker electrostatic interactions and hydrophobic interactions; for good lubrication, these forces need to be balanced. The polysaccharide–surface interactions need to be strong enough to prevent the polysaccharide chains from being excluded from the gap at low sliding speeds. On the other hand, attractions that are too strong prevent water from properly solvating the polysaccharide chains, increasing their interactions and thus increasing friction (Crockett 2014).

Polysaccharide conformation and concentration are additional factors that impact their friction behaviors. Polymers that cannot physically fit into the contact area do not contribute to friction behaviors; this was observed for guar gum solutions at lower sliding speeds (Malone et al. 2003b). Extended coil and rigid rod and conformations were more likely to influence friction behaviors of hydrocolloid solutions, as they can fit into the contact area (Garrec and Norton 2012). Starch–locust bean gum solutions showed lower friction coefficients than solutions of locust bean gum alone, particularly in the boundary region. These results were likely due to the ability of the starch granules to fit into the contact area even at low sliding speeds; guar gum did not fit into the contact area at low sliding speeds (Zinoviadou et al. 2008). Increased concentration generally decreased friction coefficient of polysaccharide solutions at moderate sliding speeds (Yakubov et al. 2015b; Garrec and Norton 2012), although friction coefficients may increase at low sliding speeds due to exclusion of polymers from the contact area (Garrec and Norton 2012). The effects of conformation and concentration can combine, such as the effects seen in a study on native and gelatinized rice starch (Liu et al. 2016a). Friction coefficients were higher for native rice starch versus gelatinized rice starch, likely due to the more irregular shape and increased hardness of the starch granules. Friction coefficients also increased with increased concentration of both native and gelatinized rice starch. For the native rice starch, the concentration effects were due to an increased amount of rough particles. For the gelatinized rice starch, the effects were attributed to the “stickiness” of leached amylose that caused surface–surface adhesion and increased friction (Liu et al. 2016a).

Interactions of polysaccharides with food components can alter friction behaviors as well. For example, addition of starch reduced friction coefficients in high-protein yogurts, which was related to the smoother mouthfeel reported in sensory analysis (Morell et al. 2017). These effects were attributed to the deposition of starch onto the sliding surfaces (Morell et al. 2017). Yogurts made with different hydrocolloids (carrageenan, gelatin, starch, and/or xanthan gum) showed significantly different friction behaviors, which were attributed to different interactions of the hydrocolloids with the protein network in the yogurt microstructures (Nguyen et al. 2017). It should be noted that most of the work on polysaccharide tribology focuses on solutions of individual polysaccharides, and there is only a small amount of information in the literature on the effects of polysaccharide interactions with other food components and the subsequent impact on semisolid friction behaviors.

Further study of this area is needed for a better understanding of the impact of starch on more complex foods.

The importance of food–saliva and food component–saliva interactions should not be understated; these interactions will be discussed in Sect. 3.1.4. In general, breakdown of starch through interaction of saliva can have a dramatic impact on friction behaviors of semisolid foods, significantly changing friction coefficients and potentially changing the shape of the entire friction curve (Joyner (Melito) et al. 2014a; De Wijk et al. 2006b).

3.1.2 Measurement Protocol

As previously discussed, friction behaviors are highly dependent on system conditions. This includes the shape of the sliding surfaces (e.g. sphere, ring, cylinder, flat plate), contact area, sliding speed, constant versus changing velocity of the sliding surfaces, pressure in the contact area, amount of rotation of one or both of the sliding contacts, surface roughness and chemistry of the contacts, temperature, and humidity (Stokes 2012; Greene et al. 2013; Prinz et al. 2007; De Hoog et al. 2006; Ranc et al. 2006; Lu et al. 2006). All of these parameters can affect the specific composition of the material in the contact area, material rheology during the test, and interactions between the material and sliding surfaces.

The composition of the material in the contact is not necessarily the composition of the bulk semisolid food. Surface separation in the contact area is typically <1 um (de Vicente et al. 2005a), which can be smaller than particles in semisolid foods. If the particles are easy to deform, they may be able to fit into small gaps. On the other hand, more rigid particles may not be able to enter the gap, reducing their overall contribution to friction behavior at lower sliding speeds.

While it is difficult to directly measure the composition of the food in the gap, it may be estimated by determining particle diameters of the different particles present in the food and comparing those to the gap in the contact area. This method requires some knowledge about the ability of the particles to deform under the conditions as well as the gap between the sliding surfaces at different sliding speeds. Unfortunately, it is not always possible to determine particle deformability, nor are the calculations for determining gap height simple because deformation of soft surfaces changes the actual contact area. Another, simpler way to estimate composition of the food in the gap is to by testing different formulations of the food, each made with one or more components omitted. If the friction behavior of the original food is the same as that of the food formulated with one or more components omitted, one can assume that either the omitted components are not present in the gap or do not significantly contribute to friction behaviors (see Fig. 8 for an example of this). This method can also be used to estimate the gap between the sliding surfaces at different sliding speeds, provided the particle sizes of the food components are known.

Similar to composition, the rheological behaviors of semisolid foods in the contact are can be significantly different than bulk rheological behaviors. Because the

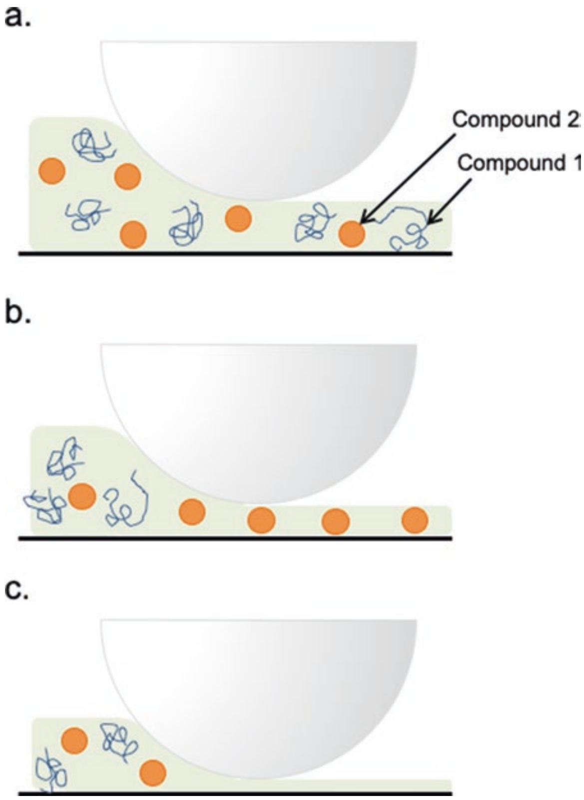

Fig. 8 Schematic of a polymer solution where (**a**) all components are able to fit into the contact area, (**b**) Component 1 is excluded from the contact area due to size, and (**c**) Components 1 and 2 are excluded from the contact area due to size

fluid film in the contact area is typically 0.5–2 um (de Vicente et al. 2005a; Yakubov et al. 2015b; Myant et al. 2010b) and contact pressures are 60–350 kPa (Myant et al. 2010b; Chojnicka et al. 2008b), the semisolid food is exposed to much higher shear rates (>10,000 s^{-1}) than are measured in a standard measurement of viscosity profile (Selway and Stokes 2013). Thus, it is necessary to measure viscosity at very high shear rates to properly understand the rheological behaviors of semisolid foods under tribological testing conditions. These high shear measurements can be performed with either a capillary rheometer or by using parallel plates with a narrow gap (<100 um) (Davies and Stokes 2008). Parallel plates with a 100 um gap can be used to reach shear rates of >10,000 s^{-1} (Davies and Stokes 2008), similar to shear rates experienced in the contact area in a tribological test. The gap is also large enough to minimize the effects of plate misalignment and inertia, provided the appropriate calculations are used to correct for these factors. Corrections for misalignment (Eq. 2) and normal stress changes due to inertia (Eq. 3) are as follows (Davies and Stokes 2008):

$$\eta = \eta_M \frac{\delta + \varepsilon}{\delta} \tag{2}$$

$$\Delta F_{N,inertia} = \frac{3\pi\rho\Omega^2 R^4}{40} \tag{3}$$

Here, η is corrected apparent viscosity (Pa.s), η_M is measured apparent viscosity (Pa.s), δ is gap height (mm), ε is gap height error (mm), $\Delta F_{N,\ inertia}$ is the change in normal force due to inertial effects from high shear rates (N), ρ is the density of the fluid (kg m^{-3}), Ω is angular velocity (s^{-1}), and R is radius of the parallel plate (m). It should be noted that a 100 um gap is sufficient for measurement of semisolid foods with particles with 10 um diameter. If the food has larger particles, they may stick in the gap, resulting in inaccurate measurement (Davies and Stokes 2008). In this case, a larger gap needs to be used. Accordingly, the rule of thumb for parallel plate gap height is a 10:1 gap height:largest particle diameter. However, using larger gaps means that the maximum achievable shear rate is decreased. This issue can be addressed by using a rheometer capable of geometry counterrotation, such as those manufactured by Anton Paar (MCR7XX series), which doubles the maximum achievable shear rate, or by modeling the available viscosity data and using the model value for viscosity in the contact zone. Sometimes, it is appropriate to assume that the viscosity in the gap is an infinite shear viscosity, particularly at low sliding speeds where the gap between the sliding surfaces is small. If this assumption is made, the data for generating the model should be generated from as wide a shear rate range as possible, the appropriate corrections applied for inertia and plate misalignment, and the viscosity data critically examined to ensure that the infinite shear plateau is not due to a high-shear measurement artifact or selection of an inappropriate viscosity model.

Contact surface–food interactions can have significant impact on tribological behaviors. Testing hydrophobic (e.g. high-fat) foods on hydrophobic surfaces results in low friction coefficients in the boundary and mixed regimes, while testing those same foods on hydrophilic surfaces results in higher friction coefficients, or vice versa (Bongaerts et al. 2007a). This is because of the ability of foods to spread well on surfaces with similar hydrophobicity, which gives them good lubricating ability. This phenomenon can be predicted somewhat with the contact angle of a quiescent drop of the food on the surface. Low contact angles correspond to high spread of the droplet, leading to good lubrication (Ranc et al. 2006). However, this effect becomes negligible in hydrodynamic sliding, as the bulk fluid behavior dominates the friction response in the contact zone (Bongaerts et al. 2007a).

In addition to overall hydrophobicity similarity, affinity of food components for the contact surfaces can influence friction behaviors. If a particular food component has a higher affinity for the contact surface than the bulk food, it will deposit onto the contact surface, eventually forming a surface layer (Malone et al. 2003b). If this surface layer causes the sliding surfaces to adhere, friction will increase. If the surface layer causes the sliding surfaces to repel each other or allows the surfaces to slide past each other more easily, friction will decrease (Gong and Osada 1998). For example, deposition of fat onto PDMS plates can create a slippery fatty layer that can decrease friction coefficient. The rate at which this layer forms is dependent on the testing conditions and the specific affinity of the compound for the contact surface rather than the bulk food. Interferometry techniques can be used to estimate the rate of layer formation (Myant et al. 2010b). Other potential contact surface–food interactions include entrainment of small particles in asperities, absorption of food components onto the contact surface, repulsion of food components from the contact surface, and chemical reactions between the food and the contact surface. The latter two issues can be minimized by selection of nonabsorptive, nonreactive contact surfaces, such as PDMS. The first issue can be minimized by reducing asperity height of the contact surfaces. Normally, particle entrapment in large asperities is not an issue in food tribology because the plates used are prepared in smooth molds. However, if one wishes to mimic the rougher surface of the tongue, it is important to keep in mind how the asperities may trap food particles and impact food friction behaviors.

3.1.3 Viscosity Profile

Semisolid foods have widely varying viscosities, ranging from ~100 mPa.s to over 10 Pa.s. A large variation in viscosity among samples necessitates the sliding speed corrections discussed in Sect. 1.1.3 for proper comparison of different semisolid food samples.

In addition to the variation in viscosity, semisolid foods generally exhibit non-Newtonian behavior, including shear-dependency and yield stress. They may also have zero shear and infinite shear viscosity plateaus. All of these behaviors can affect their friction behaviors, and the effects will change depending on the shear rate in the gap between the sliding surfaces. While the shear rate in the gap does decrease with increased sliding speed due to increased pressure that forces the sliding surfaces apart, shear rates in the contact zone are still quite high compared to the shear rates used in a traditional shear rate sweep. Understanding the viscosity behaviors of semisolid foods under these high shear rates is important for understanding how their particular non-Newtonian behaviors impact tribological data. Flow behaviors that characterize semisolid foods at lower shear rates may be significantly different than those that appear at the high shear rates experienced during tribological testing. In addition, phenomena that occur only in narrow gaps under high shear, such as slip and depletion of material at the sliding surfaces, can significantly impact rheological behavior (Davies and Stokes 2008). Therefore, it is important to not only account for different viscosity values, but also to measure viscosity profiles under high shear rates as discussed in Sect. 3.1.2.

Viscosity profiles may also impact selection of geometry for measuring friction coefficients. Thinner samples may flow to the bottom of pitched or vertical plates, resulting in sample starvation in the gap and incorrectly large friction coefficients. Samples with a relatively high yield stress may be pushed out of the sliding path of ball geometries and be unable to flow back into the contact zone due to their yield stress. High-viscosity samples may have significantly higher viscous drag than lower-viscosity samples, which could result in artificially higher friction coefficients because of the higher torque required to move the sliding surface(s). Preliminary trials are often needed to ensure accurate, repeatable measurements on a specific geometry with a specific food.

3.1.4 Saliva

The use of saliva in testing of food rheological and tribological behaviors has gained increasing attention in the literature over the last decade. Because saliva can cause significant changes to food structures during oral processing, including emulsion and starch breakdown (Van Aken et al. 2007), food properties during chewdown and bolus formation are often quite different from those of the original food (Stokes et al. 2013; Chen 2009; Pascua et al. 2013). Additionally, saliva forms a lubricating layer on the oral surfaces, which comprises a bound layer directly on the oral surfaces and a surface layer that mixes with food during oral processing (Chen and Engelen 2012). Both saliva itself and food–saliva interactions can play a major role in food tribological behaviors during oral processing, which can have significant impact on oral textures.

Secreted by the parotid, sublingual, and submandibular glands, human saliva is composed of approximately 98–99% water; the remainder comprises alpha-amylase and other digestive enzymes, ions, and proteins such as alpha-amylase, immunoglobulins, mucins, and other glycoproteins (Kupirovič et al. 2017; Carpenter 2013). Saliva flowrate and composition changes dramatically from rest to consumption of food, from an average of about 0.3 mL/min to up to 7 mL/min, respectively (Humphrey and Williamson 2001). The flowrate and composition of saliva can also change based on many factors, including hunger, stimulus in the oral cavity, nature of the stimulus, health status, medication, and time of day (Humphrey and Williamson 2001; Dawes 1975; Dawes 1996). Regardless of these factors, it is the non-water components that give saliva its notable viscoelastic behavior, although they are only a small fraction of saliva's composition (Bongaerts et al. 2007b). However, although the bulk viscosity has some contribution to the lubricating abilities of saliva (Gibbins and Carpenter 2013), viscoelasticity was found to have little impact on saliva friction behaviors, particularly at lower sliding speeds (Bongaerts et al. 2007b). It is the amphiphilic nature of these proteins that allows saliva to form films on oral surfaces (Bongaerts et al. 2007b; Lindh et al. 2001, 2002a, b; Christersson et al. 2000; Shi and Caldwell 2000).

Saliva friction and lubrication behaviors on oral surfaces are impacted by both its interaction with oral surfaces and the presence of certain food components. As previously stated, saliva forms two layers on oral surfaces: a bound layer and a surface layer. In the bound layer, called the pellicle, small molecular weight proteins and non-proline sections of larger proteins adhere to the contact surface primarily through hydrophobic interactions (Stokes 2012; Lindh et al. 2002a; Gibbins et al. 2014). This layer is difficult to remove and serves as an anchor for the surface layer. The surface layer is composed of the hydrophilic portions of glycosolated proteins such as mucins (Macakova et al. 2010; Cárdenas et al. 2007a; Cárdenas et al. 2007b). Because of its viscoelastic behavior and low viscosity (~2 mPa.s) (Chen and Engelen 2012; Stokes and Davies 2007), this surface layer provides good lubrication (Chen and Engelen 2012), keeping the oral surfaces from sticking to each other when one is not eating or drinking. It also helps food to move along the oral surfaces during oral processing (Chen and Engelen 2012).

Addition of saliva can cause multiple physicochemical changes to semisolid foods, and these changes can significantly alter friction profiles (see Sect. 3.1.4). Therefore, many studies on food friction–texture relationships have elected to add either human saliva (Joyner (Melito) et al. 2014a; Selway and Stokes 2013; De Wijk et al. 2006b; Morell et al. 2017) or an artificial saliva containing mucins and amylase in a buffer solution (Morell et al. 2017; Laguna et al. 2017) to foods and testing the friction behaviors of the resulting mixture. Addition of saliva decreases friction coefficients of yogurt (Morell et al. 2017) and starch-based custards (De Wijk et al. 2006b), and can dramatically alter friction profiles of acid milk gels (Joyner (Melito) et al. 2014a).

Food-saliva interactions have been related to multiple oral texture sensations. In particular, astringency, defined as a dry, puckering feeling in the mouth after consumption of food, (Vardhanabhuti et al. 2011; Gibbins and Carpenter 2013) and creaminess have generated interest over the past decade because they are thought to be more closely tied to thin film and friction behaviors rather than bulk rheology. However, neither of these attributes have simple relationships to friction behavior. Astringency–friction relationships appear to be dependent on the specific mechanism for the astringent sensation. As of 2019, there have been four different mechanisms proposed for astringency: (1) aggregation of salivary proteins due to complexation with food components that form particles that cause a rough or gritty sensation, (2) disruption of the pellicle and exposure of the oral surfaces, (3) disruption of the mobile saliva layer and subsequent loss of lubrication provided by that layer, and (4) exposure of receptors on the oral surface that produce an astringent sensation when bound to food components (Gibbins and Carpenter 2013). Activation of these mechanisms appears to be dependent on the specific compounds in the food, and multiple mechanisms can occur simultaneously. For example, polyphenols complex with proline-rich proteins to form aggregates, resulting in an astringent mouthfeel (Prinz and Lucas 2000). Whey proteins have similar astringency mechanisms (Beecher et al. 2008; Andrewes et al. 2011; Ye et al. 2011). However, mixtures of saliva and epicatechin showed no difference in friction behavior from saliva alone, indicating that epicatechin, which is perceived as astringent, does not complex with saliva in the same way as polyphenols or whey proteins.

Astringency is not always related to tribological behaviors, even with addition of saliva (Vardhanabhuti et al. 2011). Several studies on relatively simple fluid systems (e.g. solutions of β-lactoglobulin (Vardhanabhuti et al. 2011), red wine (Brossard et al. 2016), epigallocatechin gallate (Rossetti et al. 2009), and alum (Vardhanabhuti et al. 2011)) have found relationships between food friction profiles and strength of astringent sensation. However, in studies on more complex systems, such as yogurt, relationships between instrumental friction and astringent sensations were not straightforward, and no direct correlation between the two were found (Morell et al. 2017). Additionally, mixing astringency-mediating substances, such as milk or maltodextrin, with astringent compounds does not necessarily result in reduced friction coefficients when the mixtures are evaluated in the presence of saliva (Rossetti et al. 2009). There is still much to be discovered about astringency mechanisms, particularly those in complex foods, and their role in food friction behaviors.

Temporal changes of food products upon addition of saliva can be observed through friction measurements. During the measurement, food can either be added to an adsorbed saliva film on one of the sliding surfaces (generally the plate) (Selway and Stokes 2013) or saliva can be added to the food. In these tests, sliding speed is held constant and changes to the friction coefficient are observed over time. The changes to friction coefficient and duration of the changes are specific to the interactions between the saliva and food product components. Addition of saliva to yogurt caused a nearly instantaneous increase to a plateau value in friction coefficient, but addition of saliva to custards showed a slow increase in friction coefficient over about 10 min to a plateau value (Selway and Stokes 2013). Fat content impacted the degree of friction coefficient increase: higher-fat yogurt and custard samples showed notably less increase in friction coefficient (Selway and Stokes 2013). Beta-lactoglobulin showed increased friction coefficient upon addition of saliva, with a much more rapid increase in friction at $\mathrm{pH} = 3.5$ compared to $\mathrm{pH} = 7.0$ (Vardhanabhuti et al. 2011). This result was in agreement with astringency perceptions of whey protein solutions (Beecher et al. 2008; Andrewes et al. 2011; Ye et al. 2011), as previously discussed. Temporal investigations of food–saliva mixtures are not yet commonplace in the literature but can reveal valuable information of how foods change in the presence of saliva. Indeed, the information from this method of tribological testing can be used to better understand temporal sensory attributes and the mechanisms behind these attributes.

3.2 Relationships to Structural Features

Dispersed particles in foods can have significant influence on food tribological behaviors, with particle size and shape being the most influencing factors on friction coefficient. Unsurprisingly, rougher, larger particles can increase friction coefficients (de Wijk and Prinz 2005, 2006; Krzeminski et al. 2014), provided they are not excluded from the gap. For example, exclusion of protein particles from the gap resulted in fat content influencing friction coefficients at lower speeds and protein content influencing friction coefficient at higher speeds (Sonne et al. 2014). Furthermore, whey protein particle size has been directly correlated with friction coefficient (Laiho et al. 2017).

Smaller, rounder particles can lower fiction coefficients (de WIjk and Prinz 2006). In fact, particles that are round, smooth, and relatively hard, such as soluble starch granules, can exhibit rolling behavior in narrow gaps, such as the contact zone in tribological measurements. This rolling behavior, termed the ball bearing effect, can significantly reduce friction due to the combination of sliding and rolling that promotes surface slip (Yakubov et al. 2015b). The ball bearing effect has been found in starch solutions (Zhang et al. 2017), liquid and semisolid foods containing microparticulated whey protein (Liu et al. 2016b), and yogurts containing starch (Morell et al. 2017). Even without this ball bearing effect, smoother particles have been shown to reduce friction coefficients in mayonnaise and custards (de Wijk and Prinz 2005).

Structural features and changes to those features under testing conditions can have a major impact on friction behaviors. Decreased microstructure homogeneity and larger void volumes were shown to increase friction coefficients in yogurts with increased whey protein content (Laiho et al. 2017). On the other hand, cream cheese with lower fat content had lower spreadability and higher rigidity and friction coefficients, which was attributed to fewer fat globules dispersed in a more compact protein matrix. The lower-fat samples also showed large, gelled aggregates compared to the higher-fat samples (Ningtyas et al. 2017). Charged food polymers, such as anionic polysaccharides, can reduce friction by binding to testing surfaces and forming a lubricating layer (Macakova et al. 2010). This effect is similar to the lubrication mechanism of saliva. Rapid breakup of starch granules under tribological testing can also reduce friction coefficient due to the ball bearing effect (Zhang et al. 2017). Similarly, breakdown of the gel matrix in emulsion filled gels was hypothesized to be the cause of differences in friction behaviors of these gels; different breakdown pathways would release different components, which would have varied effects on friction behaviors (Liu et al. 2016a). Aside from breakdown due to shear forces, disruption of semisolid food microstructures due to the addition of saliva may be responsible for differences in the rate of change of friction coefficient (Selway and Stokes 2013), as discussed in Sect. 3.1.4.

Phase separation that is local to the contact area, or dynamic phase separation, may result in significantly different friction behaviors among samples with similar bulk rheological behavior. For example, a high-fat sample may undergo dynamic phase separation, resulting in the contact area being filled with fat and a subsequent decrease in friction coefficient (Selway and Stokes 2013). This has been observed in emulsions with varying sensitivity to coalescence: coalesced emulsions had lower friction coefficients than more stable emulsions (Dresselhuis et al. 2008b).

3.3 Relationships to Rheological Behaviors

The primary focus on rheology–tribology behaviors in semisolid foods to date has been on the relationship between viscosity and friction regime. As discussed in Sects. 1.1.3 and 3.1.3, increased viscosity promotes transition into mixed and hydrodynamic sliding at lower sliding speeds, and a viscosity correction can assist in more accurate comparisons among samples.

Although viscosity can be important in terms of specific behaviors at a given sliding speed, it does not necessarily relate to all tribological differences observed in foods. For example, acid milk gels (Joyner (Melito) et al. 2014a), yogurts (Selway and Stokes 2013), and custards (Selway and Stokes 2013) with similar viscosities showed significantly different friction profiles, potentially due to differences in composition and surface-related interactions (Selway and Stokes 2013). Furthermore, rheological and tribological behaviors may not be related because they evaluate different mechanical behaviors. No correlation was found between rheological and tribological behaviors of commercial yogurts (Selway and Stokes 2013; Huc et al. 2016) or custards (Selway and Stokes 2013); the analyses were proposed to be complimentary for assessing instrumental indicators of textural attributes (Huc et al. 2016). In general, rheological and tribological analyses are generally performed in an effort to better understand drivers of sensory texture rather than determine rheology–tribology relationships; there is little focus on food rheology–tribology relationships in the literature as of 2019.

Relationships between rheological behaviors and tribological behaviors may be due to structural features that impact both behaviors. For example, gelatinized starch solutions that break down under shear show reduced friction coefficient and lower viscoelastic moduli values (Zhang et al. 2017). Emulsion breakdown can result in higher viscosity due to droplet flocculation and reduced friction coefficients due to accumulation of the oil phase in the contact zone (Van Aken et al. 2007). Structural evaluation, especially under high-shear conditions, should be incorporated into any food tribological evaluation for a better understanding of the drivers of friction behaviors.

3.4 Relationships to Texture Attributes

One of the key drivers of food tribological studies is the desire to use tribology to more fully understand food textural attributes. This is particularly true of semisolid foods, which have textures that can be difficult to relate to traditional rheometry data. Accordingly, studies published on semisolid food tribology–sensory relationships have examined what specific texture attributes relate to friction (de Wijk and Prinz 2005; Nguyen et al. 2017; Sonne et al. 2014; De Wijk et al. 2006b; Morell et al. 2017; Laguna et al. 2017; Huc et al. 2016), what measurement protocols provide friction data that either better differentiates samples that can be differentiated by sensory analysis but not rheological analysis (Chojnicka-Paszun and De Jongh 2014; Nguyen et al. 2015; Selway and Stokes 2013) or provide closer approximation to oral processing (Tsui et al. 2016; Huc et al. 2016), and how addition of saliva during tribological measurements impacts friction–texture relationships (Joyner (Melito) et al. 2014a; Selway and Stokes 2013; Morell et al. 2017).

As friction is a system property, it is not surprising that the relationships between semisolid food friction behaviors are highly dependent on semisolid food composition and testing conditions. Addition of starch to high-protein yogurts reduced friction coefficients and increased smoothness and creaminess perception (Chapter 12).

These relationships are likely related to the structural features that control friction behaviors (discussed in Sect. 3.2): structural features can control both friction and sensory behaviors. Addition of saliva to acid milk gels made with different hydrocolloids resulted in better alignment of friction profiles with friction-related sensory attributes, such as smoothness and astringency, compared to friction profiles of acid milk gels tested without saliva (Joyner (Melito) et al. 2014a). Emulsions that were more sensitive to coalescence had higher creamy and fatty mouthfeel and lower friction coefficients (Dresselhuis et al. 2008b). Creaminess has also been found to be related to yogurt particle size and friction coefficient (Laiho et al. 2017; Sonne et al. 2014), as has graininess (Krzeminski et al. 2014). Similarly, reduced roughness and increased creaminess is related to lower friction coefficients in custards (de Wijk and Prinz 2005). However, friction and texture measurements do not always align. Yogurts with added whey protein concentrate were perceived as astringent, but friction coefficients were not impacted by whey protein concentrate (Morell et al. 2017). In addition, friction behaviors were not in line with yogurt and cream cheese mouthfeel and afterfeel as evaluated by an untrained panel (Laguna et al. 2017).

It can be difficult to relate semisolid food friction behaviors and texture attributes due to the complex nature of the foods in question. While a few general relationships can be made, such as lower friction coefficient, decreased roughness, and increased smoothness, friction–sensory relationships in semisolid foods are not usually straightforward. Because structural features can control both friction behaviors and sensory attributes, evaluating semisolid food microstructure, friction behaviors, and textural attributes can elucidate relationships among these data groups—or at least reasons why there are no relationships. Unfortunately, there are not many studies that consider the fuller picture of semisolid food structure, rheological and friction behaviors, and texture. Most studies focus on two of these three categories. More work is needed to better establish the relationships among semisolid food structure, function, and texture.

4 Yogurt Tribology

As of 2019, major consumer trends for yogurt include clean label, high protein, presence of probiotics or prebiotics, lower sugar, drinkable products, and non-traditional (e.g. savory) flavors (Prepared Foods 2018; Loria 2017; Mordor Intelligence 2018). While consumers demand greater health benefits and formulations with fewer, simpler ingredients, they do not want to sacrifice flavor or texture. These demands present a major challenge for yogurt manufacturers because many of these formulation changes result in less desirable textures. Removal of polysaccharide stabilizers, which provide viscosity and texture, can cause a watery, low-viscosity yogurt with little body in the mouth (Tribby 2008; Ares et al. 2007; Sandoval-Castilla et al. 2004). Adding protein or fiber to yogurt can result in a chalky, powdery, or astringent mouthfeel (Morell et al. 2017; Saint-Eve et al. 2006; Isleten and Karagul-Yuceer 2006; Drake et al. 2000). This is particularly true of casein (Isleten and Karagul-Yuceer 2006; Drake et al. 2000) and milk protein concentrates, which are difficult to disperse at room temperature (Meena et al. 2017; Crowley et al. 2014). Although rheometry can be used to detect changes in yogurt viscosity, yield stress, and viscoelastic behaviors, it is often difficult to fully understand drivers of yogurt texture with only rheological measurements. Tribometry has shown some success in determining additional factors that impact yogurt texture; however, additional study is needed to fully understand yogurt structure–function–texture relationships.

Yogurt comprises milk and two bacterial cultures (*Lactobacillus delbrueckii* ssp. *bulgaricus* and *Streptococcus thermophilus*); it also commonly contains sugars, stabilizers and texturing agents, flavor, and fruit pieces. All of these ingredients can impact yogurt friction behaviors, with the specific effects dependent on the level of addition and the interaction of the ingredient with the other components in the yogurt system, as well as the interaction of the ingredient on sliding surfaces. Many of the effects of these ingredients are covered in Sect. 3. Because of the complexity of the effects of ingredients on yogurt systems (Selway and Stokes 2013), may studies use model systems, such as acid milk gels (Joyner (Melito) et al. 2014a) or highly simplified plain yogurts (e.g. milk, cultures, and 1–2 other ingredients) in an effort to isolate the specific effects of individual ingredients on overall yogurt behavior. While these model systems can be useful for this purpose, it may be difficult to translate the results to a full yogurt system: friction is a system property and can be impacted not only by ingredients, but also by interactions among the ingredients or between the ingredients and the sliding surfaces.

Addition of saliva can have a major impact on yogurt friction behaviors, particularly yogurts containing starch. Understanding how saliva affects yogurt friction profiles can aid in understanding differences in yogurt texture profiles. Friction profiles of yogurt–saliva mixtures can have notably different shapes than friction profiles of yogurt alone, including shifting from one sliding regime to another. An example of this is shown in Fig. 9: acid milk gels, a yogurt analog, that contained starch showed hydrodynamic behavior without saliva and a complex friction profile that did not exhibit a classical Stribeck shape.

While great progress has been made in the last few decades on understanding how yogurt friction behaviors impact their textural properties, much more work remains to fully map how yogurt tribological behaviors relate to their structure, rheological behaviors, and texture attributes. Future work on yogurt friction should include determination of appropriate sliding speeds for evaluating yogurt friction properties, the specific composition of material in the contact area during different sliding speeds, and the precise effects of saliva on yogurt structure during oral processing and how those effects impact friction behavior. All of this information will allow a more fundamental understanding of why yogurts have specific mouthfeels and how to formulate healthier yogurts with enjoyable textures.

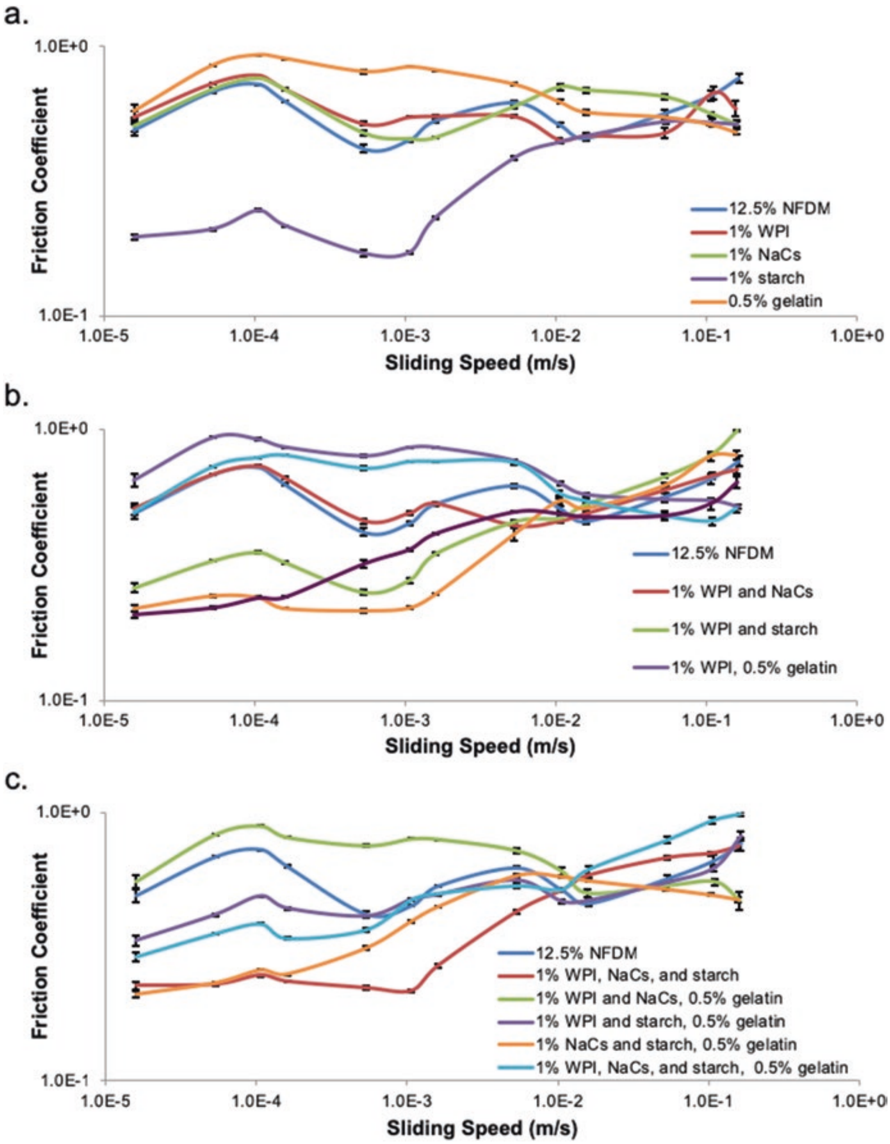

Fig. 9 Different formulations of acid milk gels tested (**a**) without saliva and (**b**) with saliva. (Joyner (Melito) et al. 2014a)

References

Adams, G. G., & Nosonovsky, M. (2000). Contact modeling — forces. *Tribology International, 33*, 431–442.

Akhtar, M., Stenzel, J., Murray, B. S., & Dickinson, E. (2005). Factors affecting the perception of creaminess of oil-in-water emulsions. *Food Hydrocolloids, 19*, 521–526.

Andrewes, P., Kelly, M., Vardhanabhuti, B., & Foegeding, E. A. (2011). Dynamic modelling of whey protein–saliva interactions in the mouth and relation to astringency in acidic beverages. *International Dairy Journal, 21*, 523–530.

Ares, G., et al. (2007). Influence of gelatin and starch on the instrumental and sensory texture of stirred yogurt. *International Journal of Dairy Technology, 60*, 263–269.

Beecher, J. W., Drake, M. A., Luck, P. J., & Foegeding, E. A. (2008). Factors regulating astringency of whey protein beverages. *Journal of Dairy Science, 91*, 2553–2560.

Bongaerts, J. H. H., Fourtouni, K., & Stokes, J. R. (2007a). Soft-tribology: Lubrication in a compliant PDMS-PDMS contact. *Tribology International, 40*, 1531–1542.

Bongaerts, J. H. H., Rossetti, D., & Stokes, J. R. (2007b). The lubricating properties of human whole saliva. *Tribology Letters, 27*, 277–287.

Brennan, C. S., & Tudorica, C. M. (2008). Carbohydrate-based fat replacers in the modification of the rheological, textural and sensory quality of yoghurt: Comparative study of the utilisation of barley beta-glucan, guar gum and inulin. *International Journal of Food Science and Technology, 43*, 824–833.

Brossard, N., Cai, H., Osorio, F., Bordeu, E., & Chen, J. (2016). "Oral" tribological study on the astringency sensation of red wines. *Journal of Texture Studies, 47*, 392–402.

Camacho, S., Liu, K., van der Linden, A., Stieger, M., & van de Velde, F. (2015). Formation, clearance and mouthfeel perception of oral coatings formed by emulsion-filled gels. *Journal of Texture Studies, 46*, 399–410.

Campbell, C. L., Foegeding, E. A., & van de Velde, F. (2017). A comparison of the lubrication behavior of whey protein model foods using tribology in linear and elliptical movement. *Journal of Texture Studies, 48*, 335–341.

Cárdenas, M., et al. (2007a). Human saliva forms a complex film structure on alumina surfaces. *Biomacromolecules, 8*, 65–69.

Cárdenas, M., Elofsson, U., & Lindh, L. (2007b). Salivary Mucin MUC5B could be an important component of in vitro pellicles of human saliva: An in situ ellipsometry and atomic force microscopy study. *Biomacromolecules, 8*, 1149–1156.

Carpenter, G. H. (2013). The secretion, components, and properties of saliva. *Annual Review of Food Science and Technology, 4*, 267–276.

Chen, J. (2009). Food oral processing- a review. *Food Hydrocolloids, 23*, 1–25.

Chen, J., & Engelen, L. (2012). *Food oral processing: Fundamentals of eating and sensory perception*. (p. 320). West Sussex, UK: John Wiley & Sons.

Chen, J., & Stokes, J. R. (2012). Rheology and tribology: Two distinctive regimes of food texture sensation. *Trends in Food Science and Technology, 25*, 4–12.

Chojnicka, A., De Jong, S., De Kruif, C. G., & Visschers, R. W. (2008a). Lubrication properties of protein aggregate dispersions in a soft contact. *Journal of Agricultural and Food Chemistry, 56*, 1274–1282.

Chojnicka, A., de Jong, S., de Kruif, C. G., & Visschers, R. W. (2008b). Lubrication properties of protein aggregate dispersions in a soft contact. *Journal of Agricultural and Food Chemistry, 56*, 1274–1282.

Chojnicka, A., Sala, G., DeKruif, C., & van de Velde, F. (2009). The interactions between oil droplets and gel matrix affect the lubrication properties of sheared emulsion-filled gels. *Food Hydrocolloids, 23*, 1038–1046.

Chojnicka-Paszun, A., & De Jongh, H. H. J. (2014). Friction properties of oral surface analogs and their interaction with polysaccharide/MCC particle dispersions. *Food Research International, 62*, 1020–1028.

Chojnicka-Paszun, A., de Jongh, H. H. J., & de Kruif, C. G. (2012). Sensory perception and lubrication properties of milk: Influence of fat content. *International Dairy Journal, 26*, 15–22.

Christersson, C. E., Lindh, L., & Arnebrant, T. (2000). Film-forming properties and viscosities of saliva substitutes and human whole saliva. *European Journal of Oral Sciences, 108*, 418–425.

Crockett, R. (2014). Friction and adhesion of polysaccharides. *Tribology Online, 9*, 154–163.

Crowley, S. V., et al. (2014). Heat stability of reconstituted milk protein concentrate powders. *International Dairy Journal, 37*, 104–110.

Davies, G. A., & Stokes, J. R. (2008). Thin film and high shear rheology of multiphase complex fluids. *Journal of Non-Newtonian Fluid Mechanics, 148*, 73–87.

Dawes, C. (1975). Circadian rhythms in the flow rate and composition of unstimulated and stimulated human submandibular saliva. *The Journal of Physiology, 244*, 535–548.

Dawes, C. (1996). Factors influencing salivary flow rate and composition. *Saliva Oral Health, 2*, 27.

De Hoog, E. H. A., Prinz, J. F., Huntjens, L., Dresselhuis, D. M., & Van Aken, G. A. (2006). Lubrication of oral surfaces by food emulsions: The importance of surface characteristics. *Journal of Food Science, 71*, E337–E341.

de Vicente, J., Stokes, J. R., & Spikes, H. A. (2005a). The frictional properties of Newtonian fluids in rolling-sliding soft-EHL contact. *Tribology Letters, 20*, 273–286.

de Vicente, J., Stokes, J. R., & Spikes, H. A. (2005b). Lubrication properties of non-adsorbing polymer solutions in soft elastohydrodynamic (EHD) contacts. *Tribology International, 38*, 515–526.

De Vicente, J., Stokes, J. R., & Spikes, H. A. (2006). Soft lubrication of model hydrocolloids. *Food Hydrocolloids, 20*, 483–491.

de Wijk, R. A., & Prinz, J. F. (2005). The role of friction in perceived oral texture. *Food Quality and Preference, 16*, 121–129.

de WIjk, R. A., & Prinz, J. F. (2006). Mechanisms underlying the role of friction in oral texture. *Journal of Texture Studies, 37*, 413–427.

de Wijk, R. A., & Prinz, J. F. (2007). Fatty versus creamy sensations for custard desserts, white sauces, and mayonnaises. *Food Quality and Preference, 18*, 641–650.

De Wijk, R. A., Prinz, J. F., Engelen, L., & Weenen, H. (2004). The role of alpha-amylase in the perception of oral texture and flavour in custards. *Physiology & Behavior, 83*, 81–91.

de Wijk, R. A., Wulfert, F., & Prinz, J. F. (2006a). Oral processing assessed by M-mode ultrasound imaging varies with food attribute. *Physiology & Behavior, 89*, 15–21.

De Wijk, R. A., Prinz, J. F., & Janssen, A. M. (2006b). Explaining perceived oral texture of starch-based custard desserts from standard and novel instrumental tests. *Food Hydrocolloids, 20*, 24–34.

Derler, S., Schrade, U., & Gerhardt, L.-C. (2007). Tribology of human skin and mechanical skin equivalents in contact with textiles. *Wear, 263*, 1112–1116.

Dickie, A. M., & Kokini, J. L. (1983). An improved model for food thickness from non-Newtonian fluid mechanics in the mouth. *Journal of Food Science, 48*, 57–61.

Drake, M. A., Chen, X. Q., Tamarapu, S., & Leenanon, B. (2000). Soy protein fortification affects sensory, chemical, and microbiological properties of dairy yogurts. *Journal of Food Science, 65*, 1244–1247.

Dresselhuis, D. M., et al. (2007). Tribology of o/w emulsions under mouth-like conditions: Determinants of friction. *Food Biophysics, 2*, 158–171.

Dresselhuis, D. M., de Hoog, E. H. A., Cohen Stuart, M. A., & van Aken, G. A. (2008a). Application of oral tissue in tribological measurements in an emulsion perception context. *Food Hydrocolloids, 22*, 323–335.

Dresselhuis, D. M., de Hoog, E. H. A., Cohen Stuart, M. A., Vingerhoeds, M. H., & van Aken, G. A. (2008b). The occurrence of in-mouth coalescence of emulsion droplets in relation to perception of fat. *Food Hydrocolloids, 22*, 1170–1183.

Garrec, D., & Norton, I. T. (2012). The influence of hydrocolloid hydrodynamics on lubrication. *Food Hydrocolloids, 26*, 389–397.

Giasson, S., Israelachvili, J., & Yoshizawa, H. (1997). Thin film morphology and tribology study of mayonnaise. *Journal of Food Science, 62*, 640–652.

Gibbins, H. L., & Carpenter, G. H. (2013). Alternative mechanisms of astringency - what is the role of saliva? *Journal of Texture Studies, 44*, 364–375.

Gibbins, H. L., Yakubov, G. E., Proctor, G. B., Wilson, S., & Carpenter, G. H. (2014). What interactions drive the salivary mucosal pellicle formation? *Colloids and Surfaces. B, Biointerfaces, 120*, 184–192.

Godoi, F. C., Bhandari, B. R., & Prakash, S. (2017). Tribo-rheology and sensory analysis of a dairy semi-solid. *Food Hydrocolloids, 70*, 240–250.

Gong, J., & Osada, Y. (1998). Gel friction: A model based on surface repulsion and adsorption. *The Journal of Chemical Physics, 109*, 8062–8068.

Greene, G. W., et al. (2013). Lubrication and wear protection of natural (bio)systems. *Polymer Adhesion, Friction, and Lubrication*, 83–133. https://doi.org/10.1002/9781118505175.ch3.

Hayashi, R., et al. (2002). A novel handy probe for tongue pressure measurement. *The International Journal of Prosthodontics, 15*, 385.

Huc, D., Michon, C., Bedoussac, C., & Bosc, V. (2016). Design of a multi-scale texture study of yoghurts using rheology, and tribology mimicking the eating process and microstructure characterisation. *International Dairy Journal, 61*, 126–134.

Humphrey, S. P., & Williamson, R. T. (2001). A review of saliva: Normal composition, flow, and function. *The Journal of Prosthetic Dentistry, 85*, 162–169.

Isleten, M., & Karagul-Yuceer, Y. (2006). Effects of dried dairy ingredients on physical and sensory properties of nonfat yogurt. *Journal of Dairy Science, 89*, 2865–2872.

Joyner (Melito), H. S., & Damiano, H. (2015). Influence of various hydrocolloids on cottage cheese cream dressing stability. *International Dairy Journal, 51*, 24–33.

Joyner (Melito), H. S., Pernell, C. W., & Daubert, C. R. (2014a). Impact of formulation and saliva on acid milk gel friction behavior. *Journal of Food Science, 79*, E867.

Joyner (Melito), H. S., Pernell, C. W., & Daubert, C. R. (2014b). Impact of oil-in-water emulsion composition and preparation method on emulsion physical properties and friction behaviors. *Tribology Letters, 56*, 143–160.

Joyner (Melito), H. S., Pernell, C. W., & Daubert, C. R. (2014c). Beyond surface selection: The impact of different methodologies on tribological measurements. *Journal of Food Engineering, 134*, 45–58.

Joyner (Melito), H. S., Pernell, C. W., & Daubert, C. R. (2014d). Impact of parameter settings on normal force and gap height during tribological measurements. *Journal of Food Engineering, 137*, 51–63.

Kokini, J. L. (1987). The physical basis of liquid food texture and texture-taste interactions. *Journal of Food Engineering, 6*, 51–81.

Kokini, J. L., & Cussler, E. L. (1983). Predicting the texture of liquid and melting semi-solid foods. *Journal of Food Science, 48*, 1221–1225.

Krzeminski, A., Prell, K. A., Busch-Stockfisch, M., Weiss, J., & Hinrichs, J. (2014). Whey protein–pectin complexes as new texturising elements in fat-reduced yoghurt systems. *International Dairy Journal, 36*, 118–127.

Kupirovič, U. P., Elmadfa, I., Juillerat, M.-A., & Raspor, P. (2017). Effect of saliva on physical food properties in fat texture perception. *Critical Reviews in Food Science and Nutrition, 57*, 1061–1077.

Laguna, L., Farrell, G., Bryant, M., Morina, A., & Sarkar, A. (2017). Relating rheology and tribology of commercial dairy colloids to sensory perception. *Food & Function, 8*, 563–573.

Laiho, S., Williams, R. P. W., Poelman, A., Appelqvist, I., & Logan, A. (2017). Effect of whey protein phase volume on the tribology, rheology and sensory properties of fat-free stirred yoghurts. *Food Hydrocolloids, 67*, 166–177.

Li, Y., Joyner, H. S., Carter, B. G., & Drake, M. A. (2018). Effects of fat content, pasteurization method, homogenization pressure, and storage time on the mechanical and sensory properties of bovine milk. *Journal of Dairy Science, 101*, 2941.

Lindh, L., Glantz, P.-O., Isberg, P.-E., & Arnebrant, T. (2001). An in vitro study of initial adsorption from human parotid and submandibular/sublingual resting saliva at solid/liquid interfaces. *Biofouling, 17*, 227–239.

Lindh, L., Glantz, P.-O., Carlstedt, I., Wickström, C., & Arnebrant, T. (2002a). Adsorption of MUC5B and the role of mucins in early salivary film formation. *Colloids and Surfaces. B, Biointerfaces, 25*, 139–146.

Lindh, L., Glantz, P.-O., Strömberg, N., & Arnebrant, T. (2002b). On the adsorption of human acidic proline-rich proteins (PRP-1 and PRP-3) and Statherin at solid/liquid interfaces. *Biofouling, 18*, 87–94.

Liu, K., Stieger, M., Van Der Linden, E., & Van De Velde, F. (2015). Fat droplet characteristics affect rheological, tribological and sensory properties of food gels. *Food Hydrocolloids, 44*, 244–259.

Liu, K., Stieger, M., van der Linden, E., & van de Velde, F. (2016a). Tribological properties of rice starch in liquid and semi-solid food model systems. *Food Hydrocolloids, 58*, 184–193.

Liu, K., Tian, Y., Stieger, M., Van der Linden, E., & Van de Velde, F. (2016b). Evidence for ball-bearing mechanism of microparticulated whey protein as fat replacer in liquid and semi-solid multi-component model foods. *Food Hydrocolloids, 52*, 403–414.

Liu, K., Stieger, M., van der Linden, E., & van de Velde, F. (2016c). Effect of microparticulated whey protein on sensory properties of liquid and semi-solid model foods. *Food Hydrocolloids, 60*, 186–198.

Loria, K. (2017). New trends are stirring up the yogurt segment. *Food Dive*. Available at: https://www.fooddive.com/news/new-trends-are-stirring-up-the-yogurt-segment/443758/. Accessed 8 Oct 2018.

Lu, X., Khonsari, M. M., & Gelinck, E. R. M. (2006). The stribeck curve: Experimental results and theoretical prediction. *Journal of Tribology, 128*, 789–794.

Macakova, L., Yakubov, G. E., Plunkett, M. A., & Stokes, J. R. (2010). Influence of ionic strength changes on the structure of pre-adsorbed salivary films. A response of a natural multi-component layer. *Colloids and Surfaces. B, Biointerfaces, 77*, 31–39.

Malone, M. E., Appelqvist, I. A. M., & Norton, I. T. (2003a). Oral behaviour of food hydrocolloids and emulsions. Part 1. Lubrication and deposition considerations. *Food Hydrocolloids, 17*, 763–773.

Malone, M., Appelqvist, I. A., & Norton, I. (2003b). Oral behaviour of food hydrocolloids and emulsions. Part 1. Lubrication and deposition considerations. *Food Hydrocolloids, 17*, 763–773.

Meena, G. S., Singh, A. K., Panjagari, N. R., & Arora, S. (2017). Milk protein concentrates: Opportunities and challenges. *Journal of Food Science and Technology*. https://doi.org/10.1007/s13197-017-2796-0.

Mordor Intelligence. Yogurt market - segmented by application and geography – growth, trends, and forecast (2018–2023). (2018). Available at: https://www.mordorintelligence.com/industry-reports/yogurt-market. Accessed 8 Oct 2018.

Morell, P., Chen, J., & Fiszman, S. (2017). The role of starch and saliva in tribology studies and the sensory perception of protein-added yogurts. *Food & Function, 8*, 545–553.

Myant, C., Spikes, H. A., & Stokes, J. R. (2010a). Influence of load and elastic properties on the rolling and sliding friction of lubricated compliant contacts. *Tribology International, 43*, 55–63.

Myant, C., Fowell, M., Spikes, H. A., Stokes, J. R., & Chang, L. (2010b). An investigation of lubricant film thickness in sliding compliant contacts. *Tribology Transactions, 53*, 684–694.

Nguyen, P. T. M., Nguyen, T. A. H., Bhandari, B., & Prakash, S. (2015). Comparison of solid substrates to differentiate the lubrication property of dairy fluids by tribological measurement. *Journal of Food Engineering, 185*, 1–8.

Nguyen, P. T. M., Bhandari, B., & Prakash, S. (2016). Tribological method to measure lubricating properties of dairy products. *Journal of Food Engineering, 168*, 27–34.

Nguyen, P. T. M., Kravchuk, O., Bhandari, B., & Prakash, S. (2017). Effect of different hydrocolloids on texture, rheology, tribology and sensory perception of texture and mouthfeel of low-fat pot-set yoghurt. *Food Hydrocolloids, 72*, 90–104.

Ningtyas, D. W., Bhandari, B., Bansal, N., & Prakash, S. (2017). A tribological analysis of cream cheeses manufactured with different fat content. *International Dairy Journal, 73*, 155–165.

Pascua, Y., Koç, H., & Foegeding, E. A. (2013). Food structure: Roles of mechanical properties and oral processing in determining sensory texture of soft materials. *Current Opinion in Colloid & Interface Science, 18*, 324–333.

Payan, Y., & Perrier, P. (1997). Synthesis of V-V sequences with a 2D biomechanical tongue model controlled by the equilibrium point hypothesis. *Speech Communication, 22*, 185–205.

Pettersson, U., & Jacobson, S. (2003). Influence of surface texture on boundary lubricated sliding contacts. *Tribology International, 36*, 857–864.

Prakash, S., Tan, D. D. Y., & Chen, J. (2013). Applications of tribology in studying food oral processing and texture perception. *Food Research International, 54*, 1627–1635.

Prepared Foods. Comax: Yogurt trends, preferences. (2018). Available at: https://www.preparedfoods.com/articles/120856-comax-yogurt-trends-preferences. Accessed 8 Oct 2018.

Prinz, J. F., & Lucas, P. W. (2000). Saliva tannin interactions. *Journal of Oral Rehabilitation, 27*, 991–994.

Prinz, J. F., de Wijk, R. A., & Huntjens, L. (2007). Load dependency of the coefficient of friction of oral mucosa. *Food Hydrocolloids, 21*, 402–408.

Ranc, H., et al. (2006). Friction coefficient and wettability of oral mucosal tissue: Changes induced by a salivary layer. *Colloids and Surfaces A: Physicochemical and Engineering Aspects, 276*, 155–161.

Rossetti, D., Bongaerts, J. H. H., Wantling, E., Stokes, J. R., & Williamson, A. M. (2009). Astringency of tea catechins: More than an oral lubrication tactile percept. *Food Hydrocolloids, 23*, 1984–1992.

Saint-Eve, A., Lévy, C., Martin, N., & Souchon, I. (2006). Influence of proteins on the perception of flavored stirred yogurts. *Journal of Dairy Science, 89*, 922–933.

Sandoval-Castilla, O., Lobato-Calleros, C., Aguirre-Mandujano, E., & Vernon-Carter, E. J. (2004). Microstructure and texture of yogurt as influenced by fat replacers. *International Dairy Journal, 14*, 151–159.

Schipper, R. G., Silletti, E., & Vingerhoeds, M. H. (2007). Saliva as research material: Biochemical, physicochemical and practical aspects. *Archives of Oral Biology, 52*, 1114–1135.

Selway, N., & Stokes, J. R. (2013). Insights into the dynamics of oral lubrication and mouthfeel using soft tribology: Differentiating semi-fluid foods with similar rheology. *Food Research International*. https://doi.org/10.1016/j.foodres.2013.07.044.

Shi, L., & Caldwell, K. D. (2000). Mucin adsorption to hydrophobic surfaces. *Journal of Colloid and Interface Science, 224*, 372–381.

Sonne, A., Busch-Stockfisch, M., Weiss, J., & Org Hinrichs, J. (2014). Improved mapping of in-mouth creaminess of semi-solid dairy products by combining rheology, particle size, and tribology data. *LWT - Food Science and Technology*. https://doi.org/10.1016/j.lwt.2014.05.047.

Steele, C. M., & Van Lieshout, P. (2009). Tongue movements during water swallowing in healthy young and older adults. *Journal of Speech, Language, and Hearing Research, 52*, 1255–1267.

Stokes, J. R. (2012). 'Oral'Tribology. In *Food oral processing: Fundamentals of eating and sensory perception* (p. 265). West Sussex, UK: Blackwell Publishing Ltd.

Stokes, J. R., & Davies, G. A. (2007). Viscoelasticity of human whole saliva collected after acid and mechanical stimulation. *Biorheology, 44*, 141–160.

Stokes, J. R., Boehm, M. W., & Baier, S. K. (2013). Oral processing, texture and mouthfeel: From rheology to tribology and beyond. *Current Opinion in Colloid & Interface Science*. https://doi.org/10.1016/j.cocis.2013.04.010.

Tribby, D. (2008). Yogurt. In *The sensory evaluation of dairy products* (pp. 191–223). New York, NY: Springer.

Tsui, S., Tandy, J., Myant, C., Masen, M., & Cann, P. M. (2016). Friction measurements with yoghurt in a simulated tongue-palate contact. *Biotribology, 8*, 1–11.

Van Aken, G. A., Vingerhoeds, M. H., & De Hoog, E. H. A. (2007). Food colloids under oral conditions. *Current Opinion in Colloid and Interface Science*. https://doi.org/10.1016/j.cocis.2007.07.011.

Vardhanabhuti, B., Cox, P. W., Norton, I. T., & Foegeding, E. A. (2011). Lubricating properties of human whole saliva as affected by β-lactoglobulin. *Food Hydrocolloids, 25*, 1499–1506.

Yakubov, G. E., Branfield, T. E., Bongaerts, J. H. H., & Stokes, J. R. (2015a). Tribology of particle suspensions in rolling-sliding soft contacts. *Biotribology, 3*, 1–10.

Yakubov, G. E., et al. (2015b). Lubrication of starch in ionic liquid-water mixtures: Soluble carbohydrate polymers form a boundary film on hydrophobic surfaces. *Carbohydrate Polymers, 133*, 507–516.

Yakubov, G. E., Macakova, L., Wilson, S., Windust, J. H. C., & Stokes, J. R. (2015c). Aqueous lubrication by fractionated salivary proteins: Synergistic interaction of mucin polymer brush with low molecular weight macromolecules. *Tribology International, 89*, 34–45.

Ye, A., Streicher, C., & Singh, H. (2011). Interactions between whey proteins and salivary proteins as related to astringency of whey protein beverages at low pH. *Journal of Dairy Science, 94*, 5842–5850.

Zhang, B., et al. (2017). Tribology of swollen starch granule suspensions from maize and potato. *Carbohydrate Polymers, 155*, 128–135.

Zinoviadou, K. G., Janssen, A. M., & De Jongh, H. H. J. (2008). Tribological properties of neutral polysaccharide solutions under simulated oral conditions. *Journal of Food Science, 73*, E88.

Structuring Semisolid Foods

Juzhong Tan

1 Overview of Semisolid Food Microstructures

Food microstructure, or how the molecules in materials are orientated, distributed, arranged, and associated with themselves and each other to form different networks, plays a critical role in determining food mechanical properties and texture attributes. A single difference in microstructural features can result in significant differences in functional properties. For example, cocoa butter, which comprises mainly triglycerides derived from palmitic acid, oleic acid, and stearic acid (Fig. 1), has different melting temperatures (16–37 °C) as well as different textures (Lopes et al. 2015) depending on how the triglycerides are oriented and packed (Fig. 2). Microstructure also determines whether a food material is fluid, semisolid, or solid. At the microscopic scale, semisolid food materials are typically amorphous solids with a disordered structure and randomly distributed molecules, similar to molecules in a fluid. Unlike many solid materials that have ionic bonding, semisolid materials are covalently or electrostatically bonded, which are weaker bonds compared to ionic bonds.

Many semisolid foods are emulsion-based, including salad dressing, sour cream, ice cream, full-fat yogurt, and mayonnaise. The structure of emulsion-based foods is affected by multiple factors, including the lipid to water ratio, type of lipid used, and presence of emulsifiers (e.g. lecithin and glycerides) and stabilizers (e.g. proteins and polysaccharides). In particular, different combinations of stabilizers and emulsifiers can have a great influence on semisolid food microstructures, rheological properties, and textures. In addition, increasing ion strength, e.g. by adding calcium ions, can induce aggregation and flocculation among droplets, thus modifying the microstructure and rheological properties of the semisolid food. Moreover,

J. Tan (✉)
Department of Food Science, Rutgers, The State University of New Jersey,
New Brunswick, NJ, USA
e-mail: jt928@sebs.rutgers.edu

H. S. Joyner (ed.), *Rheology of Semisolid Foods*, Food Engineering Series,
https://doi.org/10.1007/978-3-030-27134-3_6

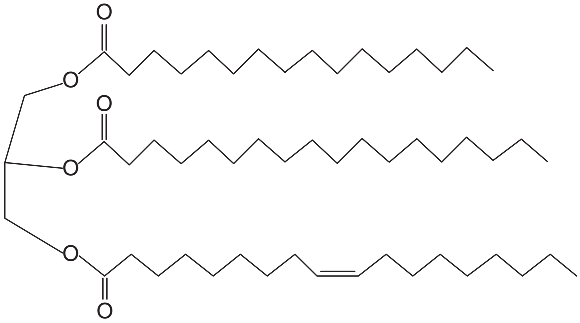

Fig. 1 Structure of cocoa butter

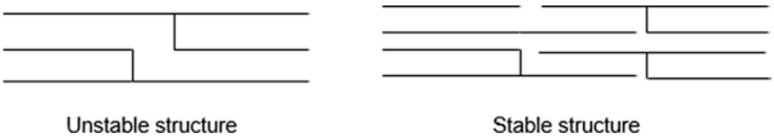

Fig. 2 Two steric structure of cocoa butter triglycerides

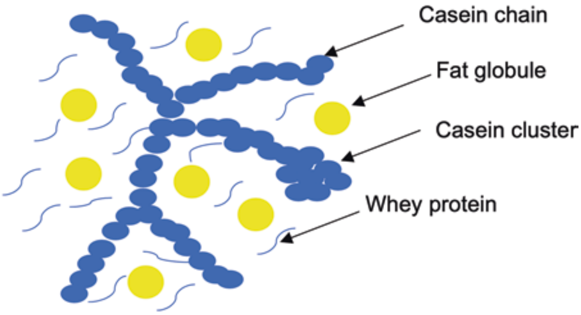

Fig. 3 Typical microstructure of yogurt

semisolid food structural properties are also influenced by processing parameters, such as shear, temperature, and pressure.

Yogurt is a semisolid food that has rheological properties and sensory texture attributes that are strongly depend on its microstructure. There are two major types of yogurt: set yogurt and stirred yogurt. Set yogurt has a continuous gel structure; however, the stirred yogurt gel is purposely disrupted during processing (hence the name), resulting in a structure that is a dispersion of protein aggregates (Karam et al. 2013). The microstructure of both set and stirred yogurt (Fig. 3) is created by aggregated casein micelle chains or clusters that form when the pH of heat-treated milk drops to the isoelectric point of casein (pH = 4.6) (Lee and Lucey 2010). Acidification can be either induced by acidulant, such as glucono delta-lactone, or culture, such as *Streptococcus* ssp. *thermophilus* and *Lactobacillus delbrueckii* ssp.

bulgaricus, which generate lactic acid to decrease pH (Karam et al. 2013). Adding functional ingredients to yogurt and/or using different processing parameters can change yogurt microstructures, influencing their mechanical properties and texture attributes.

2 Structuring Materials for Semisolid Foods

Proteins and polysaccharides are two important structuring materials for semisolid foods. Using appropriate structing materials can not only give desirable texture and physiochemical properties, but can also be used to make heathier food products with similar textures to those of their full-fat or full-calorie counterparts.

Yogurts typically have fat contents between 0.5% and 3.5% (Lucey and Singh 1997). In the past few decades, the demand for reduced-calorie foods, including dairy products, has been grown steadily due to concerns of the current rates of obesity and obesity-related diseases (Tamime et al. 1996). Therefore, products such as non-fat or low-fat yogurt (fat content <1.5% w/w) have become more popular. In yogurt, the solids content of and type of solids used in the base milk determines the physical and textural properties of the final yogurt. Reduction of fat results in reduction of the total solids content, resulting in poor texture, weak body, and whey separation during storage (Aziznia et al. 2008). In addition, fat globules can form links between proteins in yogurt, which contributes to the overall strength of the protein network. To avoid a quality reduction in lower-fat yogurts, fat replacers, including whey protein concentrate, waxy maize starch, gelatin, xanthan gum, locust bean gum, low methoxy pectin, guar gum, and λ-carrageenan, have been used to fortify yogurt microstructures (Zhang et al. 2015).

2.1 Proteins

Proteins are important structural ingredient for the food industry. Many animal proteins, such as whey protein, casein, and gelatin, are good structuring materials for semisolid foods. In a semisolid food system, proteins can either aggregate to form protein network or interact with other food ingredients, such as polysaccharides, to build a heterogeneous network structure. The rheological properties of the final food products are heavily dependent on the structure built by the protein and its interaction with other ingredients in the food.

2.1.1 Casein

Casein is the major proteinaceous component of mammalian milk, comprising 80% of milk protein by weight, and it consists of many phosphorylated proteins (Dahbi et al. 2010). Casein monomers are amphiphilic molecules with a strong tendency for self-assembly. There are four main classes of casein: α_{s1}, α_{s2}, β, and κ. These caseins will assemble into a micelle with the α_{s1}-, α_{s2}-, and β-casein in the center of the micelle and κ-caseins on the outside of the micelle forming a "hairy" layer. This structure is held together primarily by casein interactions with calcium phosphate (Dickinson 2006). This layer prevents aggregation, keeping the micelles suspended in the milk. Casein proteins have a relatively disordered secondary structure. Their molecular structures in solution are determined by the local environment, such as pH and temperature; their structures are flexible enough to allow flow (Akhtar et al. 2006; Dickinson 2006). While they are fairly sensitive to pH, they are relatively stable even at high temperatures. Overall, these properties make casein proteins good structuring materials for foods, including cheese, milk, cream, and yogurt.

In cheese and yogurt, the lower pH, and chymosin cleavage of the glycomacropeptide from κ-casein in cheese allow casein micelles (mean size ~300 nm) to aggregate and form a network that provides the characteristic texture and rheological properties of these products (Keogh and O'Kennedy 1998). To destabilize or strengthen the casein micelle network and therefore adjust product texture, the relative proportions of the different monomeric caseins, processing temperature and pH, ionic strength, and/or calcium ion concentration can all be manipulated (Huppertz and de Kruif 2008).

2.1.2 Whey Proteins

Whey protein comprises multiple serum-soluble milk proteins, including α-lactalbumin, β-lactoglobulin, bovine serum albumin (BSA), and immunoglobulins (Ercelebi and Ibanoğlu 2007). Whey protein, whey protein concentrate (typically 40–70% w/w protein), and whey protein isolate (>80% w/w protein) are widely used as structuring materials for semisolid food, such as yogurt, ice cream, and chocolate milk. Because whey protein isolate contains both hydrophobic and hydrophilic regions, it can be rapidly adsorbed at the oil–water interface in the form of a protective film, providing structural support for oil droplets through a combination of electrostatic and steric interactions (Sun and Gunasekaran 2009) (Fig. 4). However, using whey protein isolates as fat replacer in yogurt can result in a compact structure consisting of fused casein particles and large whey protein aggregates that form a relatively uniform protein network (Fig. 5) (Sandoval-Castilla

Fig. 4 Microstructure of full-fat yogurt stabilized by whey protein

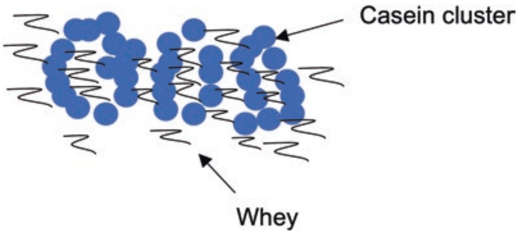

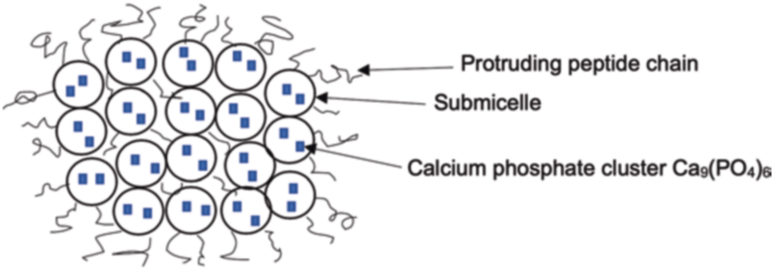

Fig. 5 Microstructure of lower-fat yogurt with whey protein as a fat replacer

et al. 2004; Zhang et al. 2015). Individual protein chains were not visible in these yogurts (Aziznia et al. 2008). Whey proteins will self-aggregate when they are present in excess proportions, resulting in the formation of larger clusters and fewer individual strands.

2.1.3 Gelatin

Gelatin comprises proteins derived from animal collagen, which is obtained from bones, skin, hooves, and other animal body parts. Porcine and bovine collagen are the most common sources of gelatin in the food industry. Gelatin is widely used as a structuring material, gelling agent, and emulsifier in food products (Djagny et al. 2001), although it has been removed from many food products due to concerns of meeting kosher and halal requirements. Gelatin has a strong emulsifying ability when used alone, but it is often combined with other polysaccharides, such as gums, starch, and pectin to stabilize emulsions (Dickinson 2009). Covalent linkage (amide bond) of gelatin protein to polysaccharide can be achieved by mixing gelatin under alkaline conditions (Diftis et al. 2005). A schematic of gelatin–polysaccharide stabilized emulsion is shown in Fig. 6. Gelatin is relatively unique compared to other food structural proteins in that gelatin gels melt upon heating and reform upon cooling; most other food proteins will gel irreversibly when heated. While this melting ability can provide highly palatable textures, such as high meltaway, it also results in destabilization of products that are stabilized by gelatin when the product is heated or stored above room temperature (Michon et al. 1997).

2.1.4 Egg Protein

Both egg yolk protein (mainly vitellogenin) (Byrne et al. 1989) and egg white protein (mainly ovalbumin) (Stevens 1991) are good emulsifiers and foam agents. They are often used to stabilize semisolid foods, such as mayonnaise, which is an oil-in-water emulsion stabilized by egg yolk lecithin. Because mayonnaise contains a high

Fig. 6 Microstructure of mayonnaise, displaying potential distortions in oil droplet shape due to close-packing

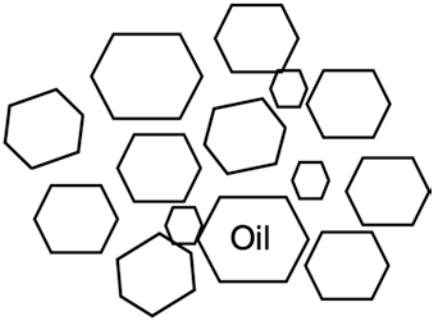

Fig. 7 Microstructure of yogurt stabilized by gelatin

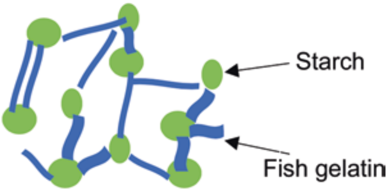

percentage of oil (78.5% or more) (Worrasinchai et al. 2006) (Fig. 7), the droplets are close-packed and distorted from a spherical shape, which is not a stable state because the surface energy is high. Therefore, mayonnaise requires stabilization to reduce the surface energy and prevent oil droplet coalescence, creaming, and phase separation during storage (Depree and Savage 2001).

Egg proteins are also used to stabilize whipped cream emulsions, a emulsion-based foam with a fat content of 35–40% (Mine 1998). With addition of stabilizers to prevent the emulsion from breaking due to shear during the whipping process for incorporation of air to create a foam, 'stiff' (rigid) foams with around 100–120% overrun can be formed. The stabilizers also promote more uniform bubble size and a transition of the foam from a viscous fluid to a viscoelastic solid (Murray 2007).

2.1.5 Fish Protein

Fish protein, primarily myofibrillar proteins, is an important byproduct from fish tissues that are considered processing waste and not generally used as food (Mackie 1982). The use of fish protein as food ingredient has gained traction in the late twentieth and early twenty-first century due to the increasing world-wide demand for new protein-rich foods. In addition, fish gelatin has good functional properties, such as structuration and water holding (Kristinsson and Rasco 2000). Fish protein has strong gelling capability due to the large quantities of myofibrillar proteins present. During gelation, fish proteins form a three-dimensional network that stabilizes water physically and chemically within the gel structure. This structure, in many

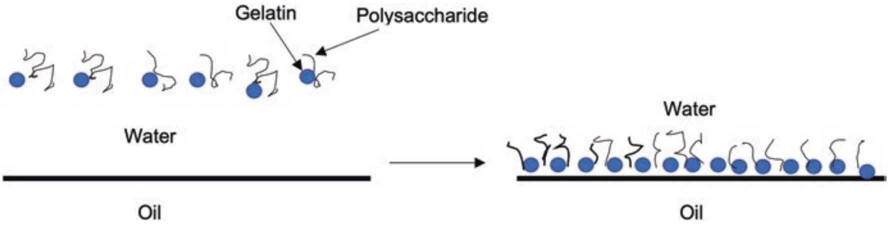

Fig. 8 Microstructure of an emulsion stabilized by both polysaccharide and gelatin

cases, helps to connect or hold other constituent particles in food, such as starch granules (Fig. 8). In general, fish gelatin is similar in functionality to porcine or bovine gelatin, although it does have a notably lower melting point (Karim and Bhat 2009). Previous studies have indicated that using fish protein as structural materials can significantly increase the structural strength of crackers (Kyaw et al. 2001), egg protein gels (Badii and Howell 2006), and food packaging materials (Cuq et al. 1995).

2.2 *Polysaccharides*

Polysaccharides are commonly used in food products to increase viscosity, promote gelation, or strengthen the protein network. They are also used as fat replacers and texture enhancers (Su et al. 2010). There are multiple sources for food polysaccharides, including plants, seaweed, and microbial byproducts. Given the variety of sources for polysaccharides, it is not surprising that they have a broad array of structures and functional properties.

2.2.1 Gums

Gums are plant-derived polysaccharides that are composed of long chains of monosaccharide units linked by glycosidic linkages. These chains can be broken into monosaccharides or oligosaccharides by enzymes and severe processing conditions, but are generally stable under typical food product processing and storage conditions as well as during oral processing (i.e. they are not sensitive to salivary enzymes). Gums are excellent stabilizing and thickening agents for many foods, including semisolid foods (Kaur et al. 2008) such as pudding, ice cream, custard, and yogurt. Gums with charged regions can also be good emulsifiers: their hydrophobic regions can bind to oil droplets to form a stabilizing surface layer. Furthermore, gums can interact with proteins to provide steric stabilization (Dickinson 2009). The most widely used gums in food applications are gum arabic, xanthan gum, gellan gum, guar gum, locust bean gum, and cellulose gum (Dickinson 2009).

The functionality provided by each gum is dependent on its structure, including chain length, overall charge, and size and charge of side groups (Dawkins and Nnanna 1995). The amount of xanthan gum used in whipped cream was positively correlated to the firmness, cohesiveness, and viscosity of the final product. However, increased xanthan gum also resulted in partial coalescence of fat in the whipped cream, increasing the average size of the foam bubbles (Zhao et al. 2009). Similarly, addition of locust bean gum to heavy cream increased its viscosity but also increased the time to form the whipped cream foam (Camacho et al. 1998). Using xanthan gum as a stabilizer for mayonnaise was reported to increase the droplet size; however, the rheological properties, such as yield stress, viscosity and flow behavior index were not significantly modified (Su et al. 2010). These studies highlight the need for careful consideration of how addition of a given hydrocolloid will impact not only food rheological behaviors but also their stability.

Gums have been widely used as fat replacers in yogurts. However, it is not always possible for certain gums to completely mimic the behavior of fat in food systems or provide structures that lead to desirable textures. For example, yogurt enriched with gum tragacanth had a coarser and notably more open structure than non-fat yogurt (Aziznia et al. 2008). During yogurt fermentation, the decrease in pH solubilizes colloidal calcium phosphate, which binds to the polysaccharide gum instead of casein, resulting in formation of larger pores and coarser structure (Lee and Lucey 2004). On the other hand, using locust bean gum and xanthan gum as fat replacers for yogurt did not change the size of openings in that casein protein network compared to non-fat yogurt. Instead, structures for yogurts with xanthan and locust bean gums contained filaments and small aggregates located at the surface of casein particles (Fig. 9). The filaments provided connections between casein particles without casein aggregation (Sanchez et al. 2000).

2.2.2 Carrageenans

Carrageenans are a family of sulfated, linear polysaccharides of D-galactose and 3,6- anhydro-D-galactose monomers that are extracted from red seaweed (genus *Rhodophyceae*). The interaction between carrageenan and proteins, especially casein, is important for structuring semisolid dairy foods, such as yogurt and milk. Figure 10 show a schematic drawing of the interactions between κ-carrageenan and either κ-casein or casein micelles. While calcium ions can be used to induce α-casein–carrageenan and β-casein–carrageenan electrostatic interactions, calcium is not needed for these interactions to occur (Snoeren et al. 1976). However, it is important to keep in mind that calcium promotes these interactions when working with products during which calcium release or addition is involved in the manufacturing process, such as when colloidal calcium phosphate is released during the fermentation step in cheese or yogurt production. Depending on the concentration of carrageenan used, these interactions can either promote stronger structures (low concentration) or cause phase inversion and potential precipitation (high concentrations) (Çakir and Foegeding 2011). Carrageenans are widely used as stabilizers for

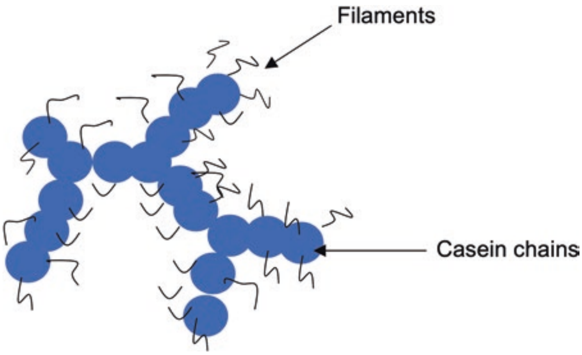

Fig. 9 Microstructure of yogurt stabilized with xanthan or locust bean gum

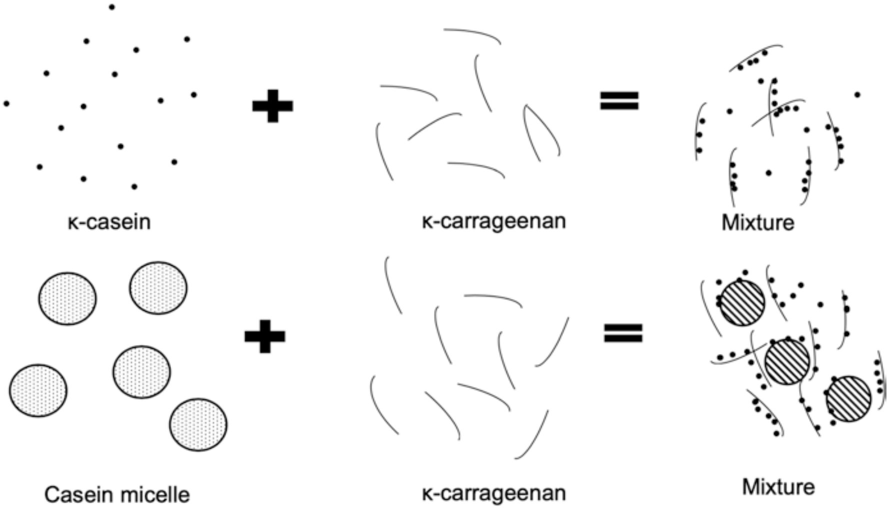

Fig. 10 Microstructure of yogurt stabilized with κ-carrageenan

food emulsions, particularly in dairy products such as cocoa milk, creams, ice-creams and mousses due to their ability to modify texture and stability. Stabilizing ice cream, mousses, and cream results in greater stability, increased creaminess, and better consumer acceptance (Gu et al. 2005; Heertje 2014).

2.2.3 Starch

Starch is a polymeric carbohydrate comprising long glucose chains; it can be obtained from many food materials such as potatoes, wheat, maize, rice, and cassava. Unmodified starches from different sources exhibit wide variations in granule appearance and structure (Fitt and Snyder 1984). For example, large, lenticular granules and small, spherical granules have been observed in native wheat starches.

Potato starch has large, round granules (Gallant et al. 1997). Mucuna beans have oval and round granule shapes with a heterogeneous size dispersion (Adebowale and Lawal 2003). However, in most starch-stabilized semisolid food products, such as instant pudding and low-fat sour cream and yogurt, starch is not present in its native form, but gelatinized by heating in the presence of water. When held at their gelatinization temperature in water, starch granules undergo irreversible swelling as they absorb free water (Ratnayake and Jackson 2008). Gelatinized starch granules can be cooled and dried into a powder to create pre-gelatinized starch, which readily absorbs cold or room temperature water and is thus used to make many ready-to-mix products (Liu et al. 2017).

Aside from pre-gelatinization, starches can undergo other modifications to alter their functional properties. Heat-modified starch solutions consist of a continuous phase enriched in amylose and a dispersed phase enriched mainly in amylopectin (Mandala et al. 2004a, b). Starches can be modified by enzymatical, physical, or chemical treatment, for example, oxidizing starch with sodium hypochlorite, treating starch with sodium hydroxide or potassium hydroxide, and treating starch with enzymes to make maltodextrin and cyclodextrin (Commission 2008). The functionality of the modified starch is usually dependent on the type and extent of modification used. Starches are usually modified to increase their solubility, alter their swelling and gelation properties, or increase their stability at lower pH (Roach and Hoseney 1995).

Modified starches have been extensively used to stabilize fluid and semisolid foods, particularly emulsified foods. Starches generally promote emulsion stabilization by binding free water to increase product viscosity and reduce flocculation and creaming rates, forming an interfacial layer on lipid droplets, or both (Charoen et al. 2011). The mechanism of stabilization is dependent on the type of starch used and the modifications made to that starch. Salad dressings stabilized by modified starch had greater storage modulus values and higher viscosity compared to unstabilized dressings (Dolz et al. 2006). Additionally, using enzyme-treated starch to stabilize mayonnaise increased both droplet size and yield stress (Mun et al. 2009). Emulsions stabilized with hydrophobic starch particulates were reported to have smaller particle size and greater stability (Yusoff and Murray 2011).

Yogurts that are stabilized by starch have structures that comprise casein micelles linked in chains. While non-fat yogurt has a relatively open, loose structure, starch-enriched yogurt has a large number of interspaced voids of varying dimensions. The interspaced voids can significantly increase firmness and adhesiveness, and reduce cohesiveness (Sandoval-Castilla et al. 2004). During the pasteurization step in yogurt processing, starch granules absorb water and gelatinize. The swelling process often results in leakage of amylose molecules into the surrounding serum phase. Continued heating, especially under shear, can lead to starch granule rupture and release of more amylose molecules and amylopectin. Some of the solubilized amylose can penetrate into the casein micelle network and generate open spaces in the protein network, disrupting the continuous casein micelle network. On the other hand, if sufficient free amylose is present, it can form an interpenetrating gel structure with the protein network, increasing yogurt gel strength (Fig. 11) (Sandoval-Castilla et al. 2004).

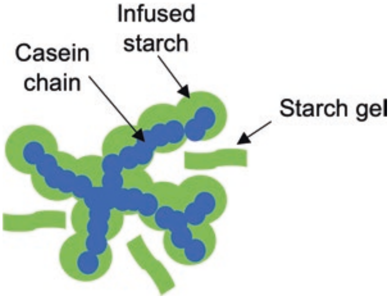

Fig. 11 Microstructure of yogurt with an interpenetrating starch and protein network

2.2.4 Dietary Fiber

Dietary fiber is a mixture of non-digestible plant carbohydrate polymers, both oligosaccharides and polysaccharides, that includes cellulose, hemicelluloses, pectic substances, gums, resistant starch, and inulin. It cannot be digested by enzymes found in the human body because human enzymes do not have the correct activation sites to cleave the bonds connecting the monomers in fiber (Slavin 2005). For example, human α-amylase can leave the α-1-4 bonds in starch, but not the β-1-4 bonds in cellulose. Therefore, cellulose is not digested in the body and considered dietary fiber (Van Soest et al. 2010).

Dietary fibers can be found primarily in edible plant foods such as cereals, fruits, vegetables, dried peas, nuts, lentils, and grains (Elleuch et al. 2011). Some dietary fibers are water soluble, including oat bran, barley bran, and psyllium. Soluble fibers can lower blood lipid levels and slow food digestion by attracting water to increase the viscosity of the food or form a weak gel with the stomach and intestinal contents, delaying stomach emptying and making the digesta less accessible to enzymes. Insoluble fibers, such as cellulose and wheat bran, are typically linked to laxative properties because they increase the bulk of the mass moving through the intestines and absorb water, which softens the mass and makes it easier to transport (Slavin 2008). Because dietary fiber has multiple health benefits, increased fiber in the diet is encouraged. But although the recommended intake for total fiber is 38 g for men and 25 g/d for women, the median intake of dietary fiber is only 16.5–17.9 g/d for men and 12.1–13.8 g/day for women (Slavin 2005). Accordingly, there is a push to increase the amount of fiber added to food products, and many food manufacturers are seeking to create palatable high-fiber foods, including energy bars, yogurt, and beverages.

Unfortunately, adding fiber to foods can create challenges in terms of palatability and functionality. Added fiber tends to product a rough, gritty, particulate texture, which is especially unpalatable in foods that generally have a smooth texture, such as yogurt (Iriondo-Dehond et al. 2018). Fiber can also modify the food's microstructure, which may significantly change the rheological properties and thus the sensory texture (Dello Staffolo et al. 2004). Both soluble and insoluble fiber can have these effects. For example, adding soluble fiber from the Mexican yam bean to yogurt resulted in the formation of a cotton candy-like structure that covered the

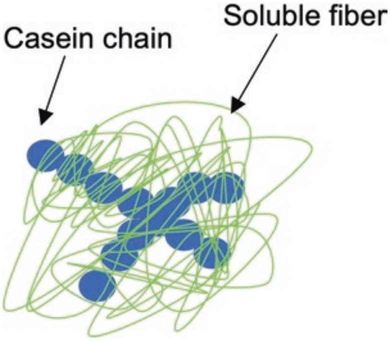

Fig. 12 Influence of stirring on yogurt stabilized with Mexican yam bean soluble fiber

protein network (Fig. 12). It also promoted a more open and relaxed protein network than the one observed in a non-fat yogurt control (Ramirez-Santiago et al. 2010). It was also reported that adding up to 4% inulin, a starchy substance found in many fruits, vegetables, and herbs, resulting in a less compact protein network in both non-fat and full fat yogurts (Guggisberg et al. 2009). Inulin can form gel structures in yogurt, breaking the continuous phase of protein network and promoting a more open microstructure (Crispín-Isidro et al. 2015). However, addition of soluble fibers to yogurt does not necessarily result in a less compact protein network. Yogurt with added pectin derived from passion fruit and bacterial exopolysaccharides had a protein network with a more compact structure. The pectin was present in the casein gel as a needle-shaped blade (Fig. 13); this shape allowed it to penetrate the protein network without disrupting it (Espírito-Santo et al. 2013). In addition to pectin, agave fructans, a soluble fiber derived from the agave plant, can act as a sort of "cement" for casein-based microstructures by covering the casein micelles and promoting particle flocculation to form a gel (Fig. 14). Increased agave fructan concentration resulted in thicker branches of the protein network and more compact structure comparing to that found in full fat yogurt (Crispín-Isidro et al. 2015).

Unlike soluble fibers, insoluble fibers derived from soy, rice, oat, corn, apple, wheat, bamboo, and sugar beet do not bind with or penetrate into the casein protein network. Rather, they act as a bulking agent in yogurt and tend to disrupt the continuity of the protein chains and clusters, producing a looser protein network (Fig. 15) (Dello Staffolo et al. 2004; Fernández García and McGregor 1997).

2.3 *Lipids and Water*

Both water and lipid, in different forms, play a major role in food structure, physicochemical properties, mechanical properties, and textural characteristic. For semi-solid foods such as yogurt, milk, and ice cream, lipids and water help build structure through formation of droplets or crystals of different sizes and shapes and interaction with other food components (Heertje 2014).

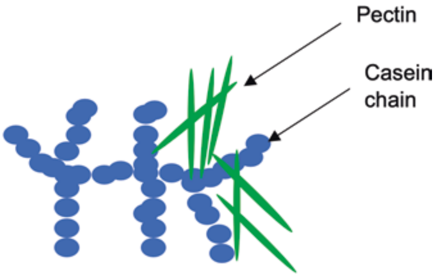

Fig. 13 Microstructure of yogurt stabilized with pectin

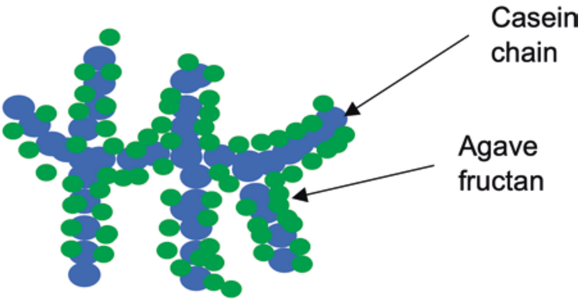

Fig. 14 Microstructure of yogurt stabilized with agave fiber

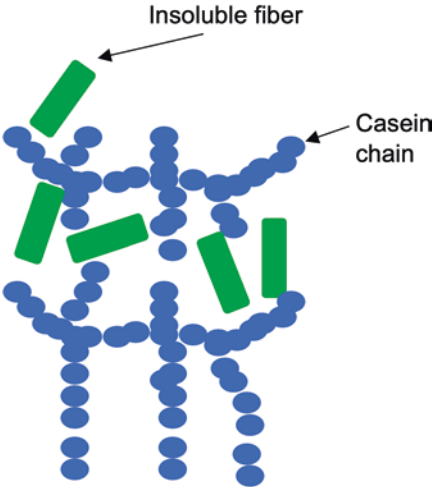

Fig. 15 Microstructure of yogurt with added insoluble fiber

2.3.1 Lipids

Lipids are hydrophobic or amphiphilic small molecules that do not or do not easily dissolve in water. These molecules include fatty acids, waxes, sterols, fat-soluble vitamins, monoglycerides, diglycerides, triglycerides, and phospholipids. In semisolid dairy products such as sour cream, dairy spreads, yogurt, and whipped cream, the major lipid composition is milk fat, which consists of >400 individual fatty acids. About 15–20 fatty acids comprise 90% w/w of milk fat: straight chain, saturated fatty acids that have 4 to 18 carbons (4:0, 6:0, 8:0, 10:0, 12:0, 14:0, 16:0, 18:0); monounsaturated fatty acids (16:1, 18:1); and polyunsaturated fatty acids (18:2, 18:3) (Fox and Mcsweeney 2015). Due to the high saturated fat content, milkfat is a soft solid at room temperature.

In milk, milkfat droplets are dispersed during processing by homogenization, which breaks the fat phase into small droplets, preventing it from separating into a cream layer during storage (Fig. 16). Milkfat droplet or crystal particle size not only influences the microstructure, but also plays a major role in the microstructures of products made from the milk, such as cheese (Michalski et al. 2004), yogurt (Ciron et al. 2010), and milk gels (Xiong et al. 1991). Small oil droplets can fill the voids in protein networks, but big oil droplets may disrupt the continuous phase of the protein network. For fat crystals, butter with larger fat crystals has a higher melting point and is easier to spread (Narine and Marangoni 1999).

Plant oils or vegetable oils such as canola oil, cocoa butter, avocado oil, coconut oil, and olive oils, are triacylglycerol-based lipids that are generally liquid at room temperature (Gunstone 2011). They are often used for structuring salad dressings (e.g. Fig. 17) and providing textural features such as fatty mouthcoat, reduced firmness, and creaminess. Smaller oil droplets have been shown to increase salad dressing viscosity (Carrillo and Kokini 1988; Lai and Lin 2004). Similar rheological behavior was also reported in mayonnaises; however, sensory evaluation indicated that mayonnaises with larger oil droplets were more acceptable (Liu et al. 2007).

2.3.2 Water

Water is a key component of both semisolid and fluid foods; it often makes up the bulk of the food's weight. Water in foods can be present as a continuous phase, such as in oil-in-water emulsions (Fig. 17); in droplet form, such as in water-in-oil emulsions; or in crystal form (ice crystals), such as in ice cream (Fig. 18). The particle size distribution of water droplets, and therefore the subsequent ice crystals upon freezing, can be controlled by using different processing strategies, such as

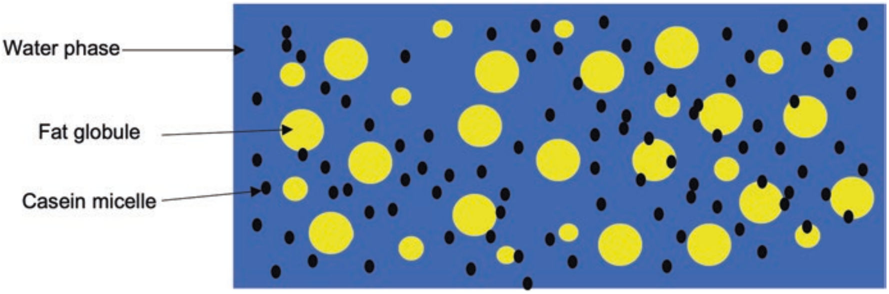

Fig. 16 Schematic of milk microstructure after homogenization

Fig. 17 Microstructure of tomato salad dressing, an oil-in-water emulsion made with vegetable oil

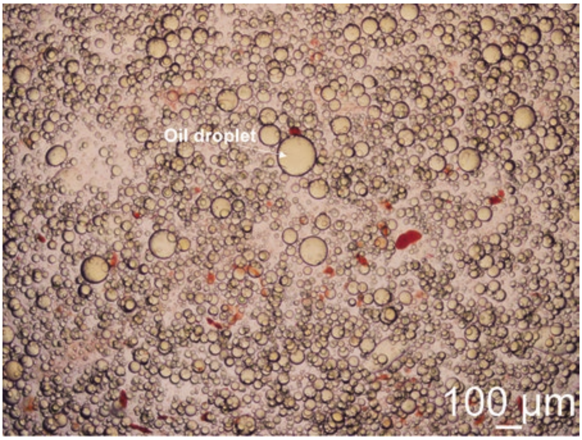

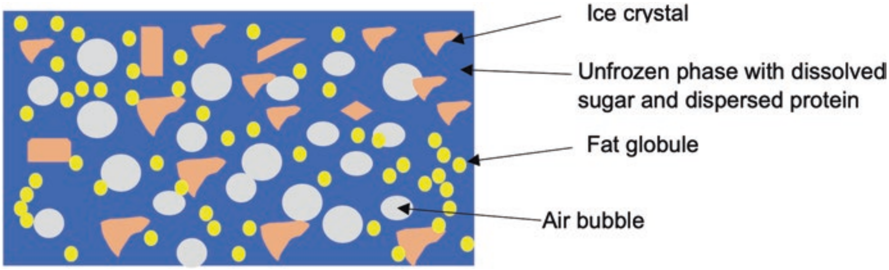

Fig. 18 Microstructure of ice cream

homogenization (Innocente et al. 2009), shear force during mixing (Lian et al. 2006), and rapid freezing (Goff 1997). The size of ice crystals can significantly influence the texture and rheological properties of ice cream: large ice crystals promote a coarse, icy texture, while smaller crystals provide a smoother, more palatable texture (Trgo et al. 1999; Wildmoser et al. 2004).

3 Ingredient Strategies for Adjusting Semisolid Food Structures

It is often necessary to adjust semisolid food textures to yield products that are easier to process, have better storage stability, and possess palatable textures. This is especially true for emulsions and foams, which can separate or collapse rapidly if not properly stabilized. One way to provide stabilization while also adjusting rheological and sensory behaviors is to incorporate various functional ingredients into the food formulation. Because the specific functionality of a given ingredient is often system-dependent, a proper understanding of the food system and ingredient functionality over a broad range of environments is needed to select appropriate stabilizing and texturizing ingredients for a given food emulsion or foam.

3.1 Emulsions

Many semisolid foods are emulsion-based, e.g. frozen desserts, margarine, full-fat yogurt, sour cream, and custard. Emulsions are colloidal systems containing either water droplets dispersed in a continuous oil phase (w/o emulsions) or oil droplets dispersed in a continuous water phase (o/w emulsions). (Dickinson 2010). Most food emulsions are o/w; butter, being a w/o emulsion, is a notable exception.

Emulsions are thermodynamically unstable and will separate into two phases if not stabilized. Phase separation can be slowed by decreasing droplet size and the density difference between the two phases. Additionally, emulsions can stabilized by surfactants and emulsifiers. Both of these are molecules with a hydrophilic (polar) section and a hydrophobic (non-polar) section. As the molecules reach the interface between the oil and aqueous phase, they align so that the hydrophilic portion is in the aqueous phase and the hydrophobic end is in the oil phase (Fig. 19). Sufficient concentration of emulsifiers or surfactants allow complete coating of all droplets in the system, preventing the droplets from flocculating or coalescing (Dickinson 1987). The primary difference between an emulsifier and a surfactant is that surfactants is their size and stabilization mechanism. Surfactants, such as mono- and diglycerides, have relatively low molecular weight and promote emulsion stability by lowering the interfacial surface tension, making the conditions to form an emulsion more favorable (Kralova and Sjöblom 2009). Emulsifiers, such as proteins and polysaccharides, have higher molecular weights and stabilize emulsions by forming a continuous interfacial layer that provides steric stabilization, electrostatic repulsion, or both. Both emulsifiers and surfactants can be used in the same food system; however, care must be taken when selecting the particular emulsifier(s) and surfactant(s) and their respective concentrations (Hasenhuettl and Hartel 2008).

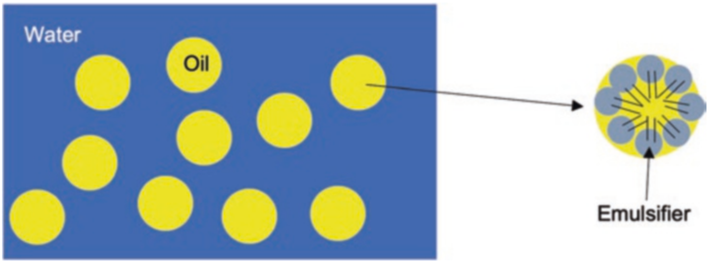

Fig. 19 Schematic of an oil-in-water emulsion system

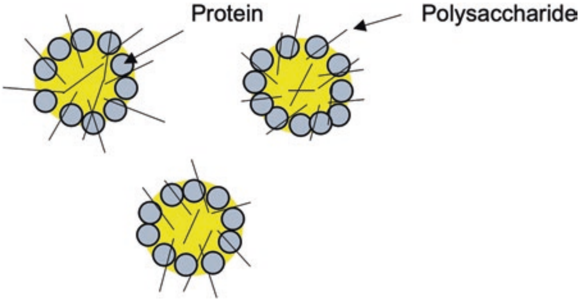

Fig. 20 Schematic of protein/polysaccharide emulsion

Certain combinations of surfactants and emulsifiers can result in emulsifier–surfactant competition for the interface, which can destabilize the emulsion and promote phase separation (Kralova and Sjöblom 2009).

Amphiphilic proteins and polysaccharides are often used as emulsifiers for semisolid foods (Fig. 20). While surfactants can also be used to stabilize emulsions, the push for clean-label foods has encouraged food manufacturers to remove these ingredients from their formulations and replace them with proteins and polysaccharides, providing a more consumer-friendly label. Potato protein and chitosan have been used as emulsifiers for stabilizing high-oleic sunflower o/w emulsions. Higher concentrations of chitosan resulted in smaller oil droplets and greater emulsion stability during storage. The viscosity and complex modulus of these emulsions also increased with higher chitosan concentration, generating a thicker and more elastic texture (Calero et al. 2013). Similar observations were reported for o/w emulsion systems stabilized with soy protein (Roesch and Corredig 2003), whey protein and gum arabic (Chanamai and McClements 2002), whey protein and xanthan gum (Sun and Gunasekaran 2009), pectin and guar gum (Erçelebi and Ibanoğlu 2009) and milk protein and locust gum (Mandala et al. 2004a, b).

3.2 Foams

Many semisolid foods are foams, including ice cream, beaten egg whites, and whipped cream. Foams have similar structure to emulsions, but foams comprise a gas, usually air or carbon dioxide, dispersed within a fluid. They can be formed by applying high shear and agitation to a fluid over a certain period of time. The combination of shear and agitation entrains small air bubbles into the fluid (Fig. 21). The factors affecting stability of emulsions also apply to foams (Brooker 1993). In general, foams with smaller air bubbles are more stable.

Foam characteristics of primary importance include foaming ability, foam volume, and stability (Kralova and Sjöblom 2009). Foaming ability refers to the amount of energy required to form the foam, while foam volume refers to how much air can be incorporated into the foam. Foam stability refers to the time elapsed before significant foam drainage and collapse (Ansbacher et al. 2010; Panyam

Fig. 21 Arrangement of food components around an air bubble in ice cream

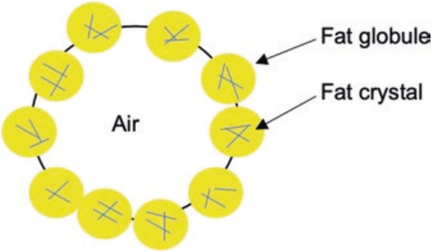

1996). In general, foams with good foaming ability, volume, and stability are desired by the food industry. Unfortunately, fluids that foam easily and with high volume typically do not have good stability, and vice versa. Two classic examples of this phenomena are milk and egg white foams. As can be seen by giving a young child a glass of milk and a straw, milk protein foams with high volume are quite easy to form. However, these foams also collapse quickly due to the high drainage rate of the fluid phase (Ansbacher et al. 2010). Egg white foams, on the other hand, are much more stable, but as anyone who has tried to whip egg whites by hand has noticed, they require large amounts of energy to form and do not have nearly the volume of a foam formed by an equivalent amount of milk protein solution (Pernell et al. 2002).

Foam stability is a major concern in the food industry, as the time needed for an unstabilized foam to collapse (minutes to hours) is notably shorter than the desired shelf life of foamed products (days to weeks). For example, the milk foams on many coffee beverages will quickly collapse, requiring these products to be made right before they are given to the consumer rather than prepared ahead of time. To stabilize a foam, the gas bubbles must be protected by a stable interfacial film that mitigates fluid drainage and bubble coalescence. In general, a good emulsifier, such as proteins and polysaccharides, is also a good foaming agent. However, the main differences between an emulsion and a foam are that the size of foam bubbles are generally much bigger than emulsions droplets and the continuous phase surrounding the gas bubbles is very thin because the volume fraction of air in a foam is much higher than the volume fraction of oil in an emulsion (Green et al. 2013; Heertje 1993; Patino et al. 1999). Therefore, foams have poor stability compared to emulsions.

Among the many food foaming agents, egg white has been reported be the best foaming agent for food (McClements 2015). When egg white is whipped, the proteins denature and interact with each other to form a stable, viscoelastic, interfacial film. Moreover, egg white proteins include glycoproteins, which contain carbohydrate. When these proteins adsorb at the fluid–air interface, the carbohydrate sections orient toward the aqueous phase. The proteins bind water due to their hydrophilicity and increase the viscosity of the fluid. This helps to reduce drainage, increasing foam stability (McClements 2015).

Food foams are often made from combination of proteins and polysaccharides. Foams made with a combination of whey protein and xanthan gum showed that increased whey protein content resulted in more homogeneous and smaller bubbles.

Foam stability and density also increased with higher whey protein and xanthan gum content, while foam viscosity increased with higher xanthan gum concentration (Martínez-Padilla et al. 2015). A mixture of guar gum, carrageenan, locust bean gum, and soy lecithin significantly decreased bubble size in whipped cream, resulting in increased foam stability (Smith et al. 2000). A combination of egg proteins and a potato maltodextrin stabilizer showed higher moduli values and greater elastic-type behavior with increased maltodextrin concentration, indicating that maltodextrin was an effective stabilizer for this system (Pycia et al. 2016).

4 Processing Strategies for Altering Semisolid Food Structures

4.1 Manipulating Ionic Strength

Ionic strength can influence emulsion stability. In an emulsion system, stability is influenced by electrostatic repulsion and steric stabilization (Fig. 22). Reducing electrostatic repulsion by adding ions to neutralize charges can destabilize an emulsion. For example, adding small amounts of calcium ions to caseinate-stabilized emulsions can improve emulsion stability, but higher amounts of calcium result in flocculation (Dickinson and Golding 1998). The mechanism for stability is primarily electrostatic repulsion. When no calcium is added, the adsorbed caseinates at the oil–water interface are attracted to each other, and depletion flocculation occurs. Adding small amounts of calcium ions promotes casein aggregation, which actually inhibits depletion flocculation because the binding sites on the free casein molecules become occupied by calcium and cannot interact with the absorbed casein. However, addition of greater amounts of calcium ions results in a flattening of the emulsifier layer around the droplets due to increased charge screening and casein–casein interactions, reducing the effectiveness of steric stabilization (Dickinson et al. 2003; Radford et al. 2004).

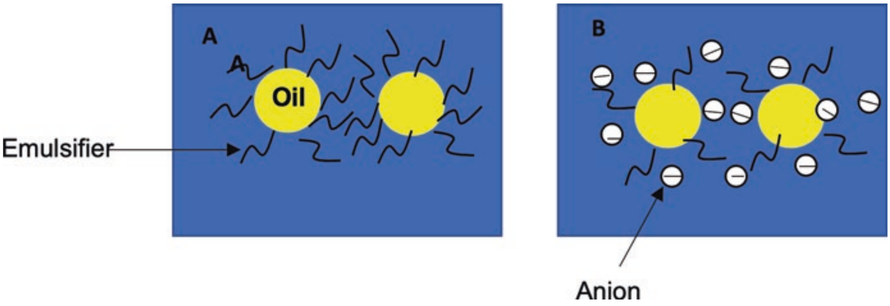

Fig. 22 Emulsions stabilized by (**a**) steric stabilization and (**b**) electrostatic repulsion

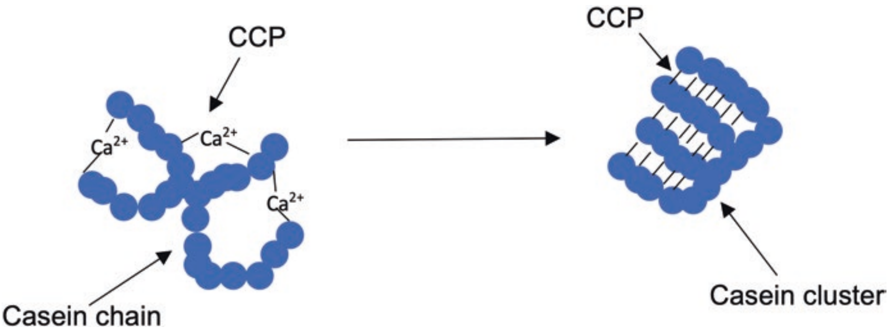

Fig. 23 Microstructure of calcium enriched yogurt; addition of calcium results in a structural shift from loose chains to larger, tighter clusters

Calcium is commonly used to manipulate the ionic strength of food systems, especially dairy systems. A diavalent cation, the double charge on calcium compared to sodium or potassium makes calcium highly effective for adjusting ionic strength at low concentrations, reducing the impact on food flavor. Moreover, calcium is an importance micronutrient and is widely used in food manufacturing as a nutritional additive. However, it is far from an inert substance in foods. Calcium can form ionic bonds and serves as a bonding agent in many food materials such as yogurt, improving their texture (Singh and Muthukumarappan 2008). In yogurt, casein micelles are held together primarily by hydrophobic interactions and colloidal calcium phosphate crosslinks (Fig. 23). Calcium enrichment is often used to improve both yogurt texture and nutritional quality. Increasing the number of casein–calcium crosslinks typically increases the attractive forces between and within casein chains, forming large protein clusters and agglomerates (Fig. 23) (Lee and Lucey 2010). Yogurts made from milk containing 23% more calcium than a standard yogurt formula formed protein clusters with an average diameter > 50 um. Large pores with diameters that were >20 um could also be observed in this network. Yogurts made from milk containing 28% more colloidal calcium phosphate showed larger protein agglomerates than a non-fat control yogurt (Karam et al. 2013). These additional crosslinks and larger agglomerates promote a firmer yogurt gel.

4.2 *Including Exopolysaccharides*

In yogurt fermentation, 'ropy' starter cultures, such as certain strains of *Lactobacillus delbrueckii* ssp. *bulgaricus* and *Streptococcus salivarius* ssp. *thermophilus*, can produce exopolysaccharides (EPS) (Gentès et al. 2011). A portion of the secreted EPS connect the surface of the bacteria to the casein network; other EPS are neither attached to the protein network nor the surface of bacteria cells, but are present as free molecules (Fig. 24) (Espírito-Santo et al. 2013). EPS in yogurt contribute to

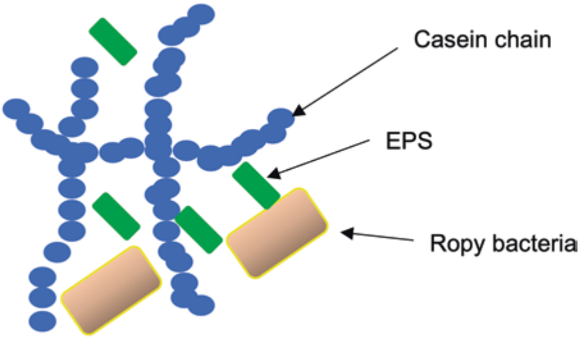

Fig. 24 Microstructure of yogurt fermented by ropy bacteria, which includes the exopolysaccharides (EPS) produced by the bacteria

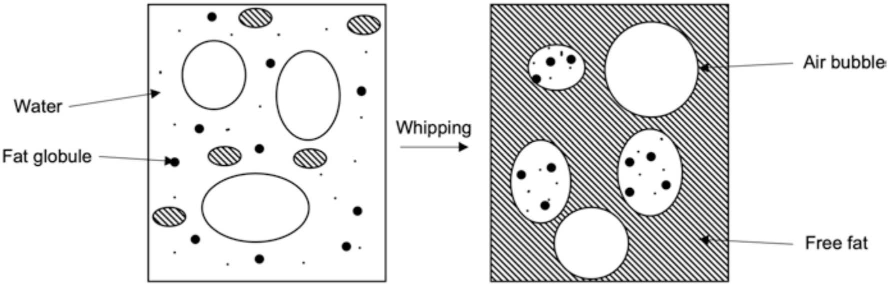

Fig. 25 Microstructure of cream before and after whipping

desirable rheological properties and texture characteristics. They typically create a long, stringy texture in yogurts. Depending on the concentration and type of EPS in the yogurt, this texture can be smooth or slimy (Martin et al. 1999). The texture produced by a particular EPS is often a function of its structure; the structure of EPS produced by different bacterial strains can vary significantly. Factors that affect the structural characteristic of EPS in fermented milk include monosaccharide composition, charge, linkage types, branching, molecular weight, and the ability to interact with milk protein (Espírito-Santo et al. 2013). Thus, it is important to select the appropriate ropy bacterial strain for generating a particular textural profile in the finished product.

4.3 Applying External Force

External shear forces, such as agitating, whipping, and stirring, are critical for forming desirable semisolid food structures. For example, during whipping of cream, the size of air bubbles decreases, proteins unfold, and the lipid phase breaks into free fat and aggregated fat globules. Therefore, the o/w emulsion in the original cream breaks down and a three-dimensional protein–lipid framework structure forms in the continuous phase. This structure becomes increasingly rigid as whipping (shear-

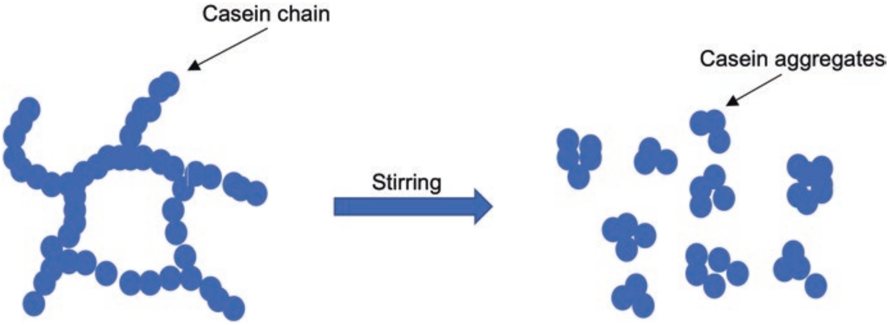

Fig. 26 Influence of stirring on yogurt microstructure

ing) continues, more proteins unfold, and fat interacts with the newly unfolded proteins (Noda and Shiinoki 1986). The structure traps the air bubbles incorporated into the fluid, forming a foam (Fig. 25). During ice cream production, agitating or stirring can break down large ice crystals into smaller ones and make cooling more efficient (Hartel 1996).

External force can also influence the texture and microstructure of yogurts. Stirring modifies the microstructure of yogurt gels by breaking down the protein network into small gel pieces (Fig. 26). Stirred yogurt is a concentrated dispersion of aggregates consisting of 30 um-diameter protein particles (van Marle 1998). For yogurt fermented by ropy culture, EPS detaches from the surface of the bacteria at high shear rate (>200 s^{-1}) (Teggatz and Morris 1990). It should be noted that because yogurt is thixotropic, excessive shearing of yogurt gels, by using too high shear rates, overly long shearing times, or both, can result in a thin, runny yogurt body. This texture is not desirable in most yogurt products, and the original thickness is usually not recoverable even after prolonged storage. Various stabilizers can be used to decrease the shear sensitivity of yogurt, such as modified starches and xanthan gum, but care is still needed during processing to prevent overshearing yogurt. In general, the gel of stirred yogurt should be broken using low shear rates and the resulting semisolid should be pumped at low velocities to the packaging unit to prevent an unwanted drop in viscosity.

4.4 Adjusting Thermal Treatment

Thermal treatments are commonly used to modify the texture, microstructure, and rheological properties of yogurt. The intensity and duration of heat treatment can significantly modify yogurt structures. Yogurt thermal treatments during processing typically range from 75 °C for 1–5 min to 95 °C for 5–10 min. In some cases, different combination of temperature and time are employed, such as high temperature short time (HTST) or ultra-high temperature (UHT) (Sodini et al. 2004;

Fig. 27 Influence of heat treatment on yogurt microstructure

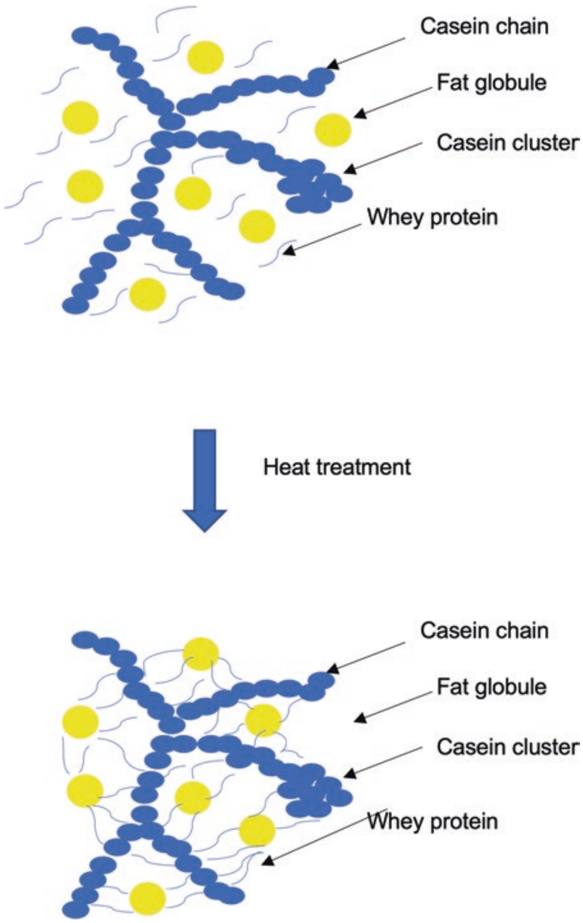

Supavititpatana et al. 2008) . The major impact of heat treatments on yogurt microstructure is the extent of whey protein denaturation and aggregation of whey proteins with caseins and fat globules (Fig. 27). Heat-denatured whey proteins become a cross-linking agent due to heat-induced exposure of previously inaccessible hydrophobic groups (Lucey et al. 1997). Under temperatures >90 °C and time >60 min, two main types of whey protein–casein micelles interactions occur: (1) a direct interaction between β-lactoglobulin and casein micelles via κ-casein binding and (2) an interaction between α-lactalbumin and β-lactoglobulin within the casein micelles (Mottar et al. 2010). Although heat treatment alters the interactions between casein and whey, the solubilization of calcium, inorganic phosphate, and magnesium from the micelles are not significantly influenced during heat treatment (Singh et al. 1996). Therefore, the overall casein micelle structure is not significantly affected.

Scanning electron microscopy has shown that yogurt produced with no heat treatment has a tortuous, clustered network composed of large casein particles joined together in large clusters or aggregates. The size of the void spaces in these particles range from 5 um to 20 um. However, after heat treatment, yogurt exhibited a finer and more continuous branched kind of network, and the size of void spaces decreased to 3–10 um (Kalab 1990; Parnell-Clunies 1987). The finer microstructure of yogurt formed by heat treatment was ascribed to the increase of bridging capacity of denatured whey proteins which decreased the size of micelle (Kalab et al. 1976). Overall, heat treatment is an easy way to adjust yogurt microstructure and therefore its texture attributes.

4.5 High Pressure Processing

High (hydrostatic) pressure processing (HPP) has received increasing attention in the early twenty-first century as a non-thermal processing technique that can improve both the quality and safety of food products. In HPP, the food is sealed in a flexible package and placed in a hydrostatic chamber. The chamber is pressurized to up to 900 MPa with water, held at this pressure for a certain amount of time, then depressurized. The extreme pressure can denature proteins and burst microbial cells, making HPP a potential tool for enhancing the microbial safety of food products. The protein denaturation can have significant impact on the structure, rheological behaviors, and sensory texture of the HPP-treated food. For example, HPP treatment of milk induces a partial and irreversible dissociation of casein–casein bonding (hydrogen bonds, hydrophobic bonds and ionic bonds) and whey protein unfolding. These changes give rise to the formation of disulfide bonds between the denatured whey proteins and the caseins, which leads to the formation of a number of interaction products. In addition, more compact casein micelle structures can be formed after pressure release (Harte et al. 2003; Needs et al. 2000; Walsh-O'Grady et al. 2001). Figure 28 shows a diagram of how HPP influences the formation of casein-whey network compared to heat treatment.

HPP (100–800 MPa) has been used to treat yogurt milk base to change the microstructure of the final yogurt, leading to modifications in rheological properties and texture, such as increased firmness and smoothness (Penna et al. 2007). High-pressure treatments (676 MPa for 5 min) were also reported to significantly reduce the particle size and the appearance of casein micelles compared to those in heat-treated milks. Casein micelles in HPP-treated milk have more uniform particle size and more spherical shape compared to casein micelles in heat-treated milks (Penna et al. 2007). In addition, HPP-treated yogurt exhibited more interconnected clusters of densely aggregated proteins (Sanchez et al. 2000). Furthermore, HPP-treated ice cream mix had higher viscosity and produced a final ice cream with significantly higher overrun compared to a conventionally processed ice cream. The acceptance and stability of the ice cream was also improved by high pressure (Lim et al. 2008). While HPP shows promise as a tool to modify food structure and tex-

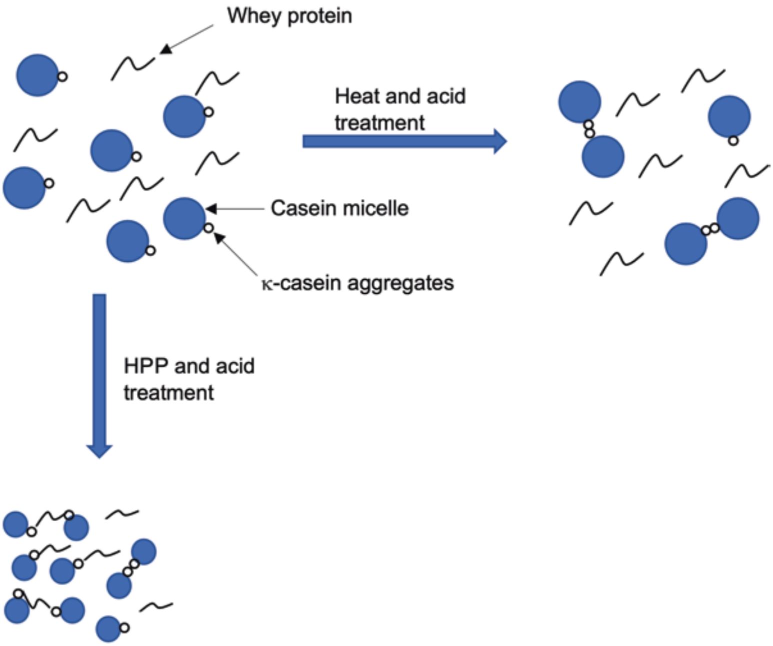

Fig. 28 Influence of HPP on yogurt microstructure compared to heat treatment

ture, it is a relatively new and expensive technology that is difficult to scale to full commercial production quantities. Additional research and technological breakthroughs are needed before HPP becomes commonly used in the food industry (Naik et al. 2013).

4.6 *Adjusting pH*

Electrostatic interactions and steric stabilization are two major contributors to emulsion stability in semisolid foods. However, electrostatic interactions can be attenuated by adjusting pH close to the isoelectric point of the protein emulsifiers, causing aggregation and flocculation. Previous studies reported that emulsions stabilized with κ- and ι-carrageenan were very unstable at pH 6 (Gu et al. 2005), emulsions stabilized by gum arabic and whey protein were easy to flocculate at pH 7 (Chanamai and McClements 2002), and emulsions stabilized by sodium caseinate and guar gum were unstable at pH 5.5 (Neirynck et al. 2007). During product development, the final food pH should be considered when selecting emulsifiers, as their performance can be notably different at different pH.

Yogurt pH is adjusted by either acid-producing bacterial cultures or a chemical acidulant, such as glucono-delta-lactone. Typically, yogurt fermentation is stopped at pH 4.6, although both microbial and chemical acidulants can reduce the pH further. The final pH and the rate at which pH decreases affects yogurt microstructure by influencing intermicellar interactions. At pH below their isoelectric point (pH = 4.6), casein micelles are positively charged; therefore, the repulsion force between micelles below the isoelectric point is greater than that at the isoelectric point, where there is no net charge. The increased repulsion results in larger pores in the protein network and more whey separation (serum expulsion) during storage (Harwalkar and Kalab 1986). In addition, some studies indicated that pH <4.6 also promoted the production of EPS by ropy bacteria (Beal et al. 1999; Martin et al. 1999), which would promote a stronger network structure and a longer, smoother texture.

4.7 Adjusting Storage Time

Storage time can significantly change the microstructure of stirred yogurt. Longer storage times allow stirred yogurt to form more bonds between the protein molecules, which can reinforce stirred yogurt structure and promote a firmer texture. In addition, longer storage time results in more EPS production by ropy bacteria and more protein hydration (Beal et al. 1999), also promoting a firmer texture. However, increased storage time can also result in increased serum expulsion from the gel, resulting in a more compact gel structure with a layer of free serum on the surface of the yogurt. While the exact mechanism of this serum expulsion is unknown, it can be exacerbated by improper formulation, processing, and storage conditions, such as lack of stabilizer or improper stabilization, pasteurization at too high a temperature, overagitation of the gel during gel breaking, and vibration or temperature cycling during storage (Beal et al. 1999).

Typically, for all semisolid foods containing emulsions, the emulsion droplet size increases with longer storage time due to flocculation and coalescence of small particles into bigger droplets. Previous studies have reported such phenomena in milk (Chen and Dickinson 1993), cream (Korhonen et al. 2001), whipped cream (Long et al. 2012), and mayonnaise (Karas et al. 2002). Time-dependent emulsion destabilization also resulted in more shear-thinning behavior, lower apparent viscosity, and lower storage modulus in semisolid foods (Korhonen et al. 2001; Long et al. 2012). In ice cream, longer storage time, especially under temperature cycling, can result in melting and recrystallization of ice crystals, generating larger ice crystals and altering sensory attributes, such as hardness, firmness, and creaminess (Dolan et al. 1985).

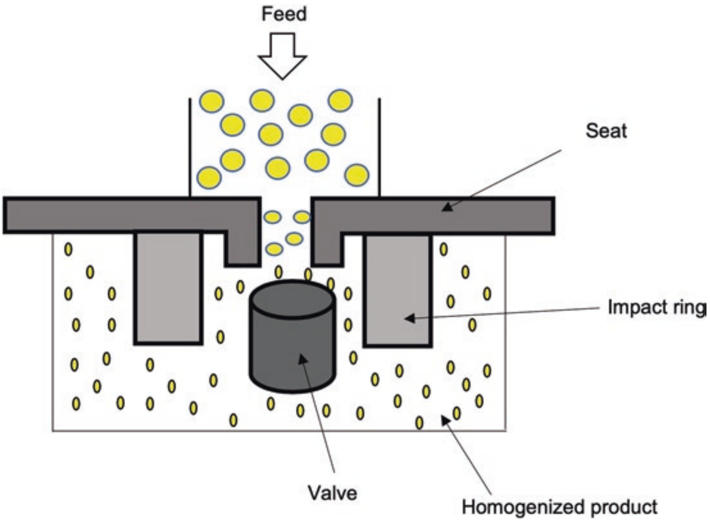

Fig. 29 Homogenization of a food product. Here, the valve provides the high pressure needed to disrupt the droplets

4.8 Adjusting Homogenization Parameters

Homogenization is used to create an emulsion of two or more immiscible fluids. This is achieved by breaking down one continuous phase into extremely small droplets distributed uniformly throughout the other fluid. Homogenization can also be used to evenly disperse particulates through a fluid. In the food industry, this is typically achieved by a homogenizer, which applies high shear and pressure to the fluids, providing the energy required to break up the dispersed phase into tiny droplets (Fig. 29). Through homogenization, the particle size of food materials can be reduced significantly, which usually results in textural changes such as increased smoothness and reduced grittiness and graininess (Amador-Espejo et al. 2014).

During milk processing, the milk is usually homogenized at pressures between 10 and 20 MPa before heat treatment. Homogenization of milk can prevent fat separation during subsequent processing and storage, improve final product consistency, increase milk whiteness, and reduce whey separation in fermented products (Lucey and Singh 1997). The major effect of homogenization of the milk base for yogurt on yogurt microstructure is fat particle size reduction, which increases the overall fat surface area. It was reported that homogenization reduced the average fat globule diameter to 1.43 um, with 99.9% of globules smaller than 3 um (Aguilera and Kessler 1989). Smaller fat globules can more easily fill the void spaces in the porous structure of the gel matrix, making the system more stable (Fig. 30). These particle size changes can impact emulsion rheological properties. Increased homogenization pressure resulted in particle size reduction and increased the viscosity of o/w emul-

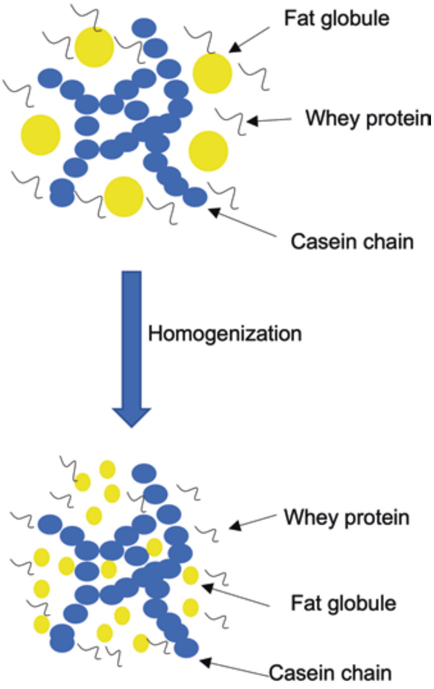

Fig. 30 Influence of homogenization on yogurt microstructure

sions stabilized by locust bean gum (Perrechil and Cunha 2010). In ice cream, homogenization can significantly reduce the size of fat globules, producing increased melting resistance (Koxholt et al. 2001). These changes can promote more palatable sensory textures, such as smoothness and creaminess (Schmidt and Smith 2010).

5 Summary

Semisolid food microstructures have great influence on their functionality, physiochemical properties, and sensory attributes. The most influential factor that determines structural features is how the molecules, including proteins, polysaccharides, lipids, water, and ions, are arranged and interact with each other. Therefore, effective approaches for manipulating food structures include adjusting the overall composition of semisolid food, pH, ionic strength, and processing temperatures, shear forces, and pressures. Using those approaches, the original inter- and intramolecular interactions can be changed, and new structures formed through aggregation, flocculation, and dispersion. A fundamental understanding of how to alter food structure allows food manufacturers to design food products with desirable processing behaviors and palatable sensory attributes.

References

Adebowale, K. O., & Lawal, O. S. (2003). Microstructure, physicochemical properties and retrogradation behaviour of mucuna bean (Mucuna pruriens) starch on heat moisture treatments. *Food Hydrocolloids*. https://doi.org/10.1016/S0268-005X(02)00076-0.

Aguilera, J. M., & Kessler, H. -G. (1989). Properties of mixed and filled-type dairy gels. *Journal of Food Science*. https://doi.org/10.1111/j.1365-2621.1989.tb05957.x.

Akhtar, M., Murray, B. S., & Dickinson, E. (2006). Perception of creaminess of model oil-in-water dairy emulsions: Influence of the shear-thinning nature of a viscosity-controlling hydrocolloid. *Food Hydrocolloids*. https://doi.org/10.1016/j.foodhyd.2005.08.006.

Amador-Espejo, G. G., Suàrez-Berencia, A., Juan, B., Bárcenas, M. E., & Trujillo, A. J. (2014). Effect of moderate inlet temperatures in ultra-high-pressure homogenization treatments on physicochemical and sensory characteristics of milk. *Journal of Dairy Science*. https://doi.org/10.3168/jds.2013-7245.

Ansbacher, S., Flanigan, G. E., & Suplee, G. C. (2010). Certain foam producing substances of milk. *Journal of Dairy Science*. https://doi.org/10.3168/jds.s0022-0302(34)93294-x.

Aziznia, S., Khosrowshahi, A., Madadlou, A., & Rahimi, J. (2008). Whey protein concentrate and gum tragacanth as fat replacers in nonfat yogurt: Chemical, physical, and microstructural properties. *Journal of Dairy Science*. https://doi.org/10.3168/jds.2007-0875.

Badii, F., & Howell, N. K. (2006). Fish gelatin: Structure, gelling properties and interaction with egg albumen proteins. *Food Hydrocolloids*. https://doi.org/10.1016/j.foodhyd.2005.06.006.

Beal, C., Skokanova, J., Latrille, E., Martin, N., & Corrieu, G. (1999). Combined effects of culture conditions and storage time on acidification and viscosity of stirred yogurt. *Journal of Dairy Science*. https://doi.org/10.3168/jds.S0022-0302(99)75283-5.

Brooker, B. E. (1993). The stabilization of air in foods containing fat -- a review. *Food Structure, 12*, 12.

Byrne, B. M., Gruber, M., & Ab, G. (1989). The evolution of egg yolk proteins. *Progress in Biophysics and Molecular Biology*. https://doi.org/10.1016/0079-6107(89)90005-9.

Çakir, E., & Foegeding, E. A. (2011). Combining protein micro-phase separation and protein-polysaccharide segregative phase separation to produce gel structures. *Food Hydrocolloids, 25*, 1538–1546. https://doi.org/10.1016/j.foodhyd.2011.02.002.

Calero, N., Muñoz, J., Cox, P. W., Heuer, A., & Guerrero, A. (2013). Influence of chitosan concentration on the stability, microstructure and rheological properties of O/W emulsions formulated with high-oleic sunflower oil and potato protein. *Food Hydrocolloids, 30*, 152–162.

Camacho, M. M., Martínez-Navarrete, N., & Chiralt, A. (1998). Influence of locust bean gum/λ--carrageenan mixtures on whipping and mechanical properties and stability of dairy creams. *Food Research International, 31*, 653–658.

Carrillo, A. R., & Kokini, J. L. (1988). Effect of egg yolk and egg yolk + salt on rheological properties and particle size distribution of model oil-in- water salad dressing emulsions. *Journal of Food Science*. https://doi.org/10.1111/j.1365-2621.1988.tb09275.x.

Chanamai, R., & McClements, D. J. (2002). Comparison of gum arabic, modified starch, and whey protein isolate as emulsifiers: Influence of pH, CaCl2 and temperature. *Journal of Food Science*. https://doi.org/10.1111/j.1365-2621.2002.tb11370.x.

Charoen, R., Jangchud, A., Jangchud, K., Harnsilawat, T., Naivikul, O., & McClements, D. J. (2011). Influence of biopolymer emulsifier type on formation and stability of rice bran oil-in-water emulsions: Whey protein, gum arabic, and modified starch. *Journal of Food Science*. https://doi.org/10.1111/j.1750-3841.2010.01959.x.

Chen, J., & Dickinson, E. (1993). Time-dependent competitive adsorption of milk proteins and surfactants in oil-in-water emulsions. *Journal of the Science of Food and Agriculture*. https://doi.org/10.1002/jsfa.2740620312.

Ciron, C. I. E., Gee, V. L., Kelly, A. L., & Auty, M. A. E. (2010). Comparison of the effects of high-pressure microfluidization and conventional homogenization of milk on particle size, water retention and texture of non-fat and low-fat yoghurts. *International Dairy Journal*. https://doi.org/10.1016/j.idairyj.2009.11.018.

Commission, C. A. (2008). Codex General Standard for Food Additives (GSFA) online database. *Codex Stand*. 118–1979.

Crispín-Isidro, G., Lobato-Calleros, C., Espinosa-Andrews, H., Alvarez-Ramirez, J., & Vernon-Carter, E. J. (2015). Effect of inulin and agave fructans addition on the rheological, microstructural and sensory properties of reduced-fat stirred yogurt. *LWT- Food Science and Technology*. https://doi.org/10.1016/j.lwt.2014.06.042.

Cuq, B., Aymard, C., Cuq, J. -L., & Guilbert, S. (1995). Edible packaging films based on fish myofibrillar proteins: Formulation and functional properties. *Journal of Food Science*. https://doi.org/10.1111/j.1365-2621.1995.tb04593.x.

Dahbi, L., Alexander, M., Trappe, V., Dhont, J. K. G., & Schurtenberger, P. (2010). Rheology and structural arrest of casein suspensions. *Journal of Colloid and Interface Science*. https://doi.org/10.1016/j.jcis.2009.10.042.

Dawkins, N. L., & Nnanna, I. A. (1995). Studies on oat gum [(1→ 3, 1→ 4)-β-D-glucan]: Composition, molecular weight estimation and rheological properties. *Food Hydrocolloids, 9*, 1–7.

Dello Staffolo, M., Bertola, N., Martino, M., & Bevilacqua, A. (2004). Influence of dietary fiber addition on sensory and rheological properties of yogurt. *International Dairy Journal*. https://doi.org/10.1016/j.idairyj.2003.08.004.

Depree, J. A., & Savage, G. P. (2001). Physical and flavour stability of mayonnaise. *Trends in Food Science and Technology*. https://doi.org/10.1016/S0924-2244(01)00079-6.

Dickinson, E. (1987). *Food emulsions and foams*. New York: Elsevier.

Dickinson, E. (2006). Structure formation in casein-based gels, foams, and emulsions. *Colloids and Surfaces A: Physicochemical and Engineering Aspects*. https://doi.org/10.1016/j.colsurfa.2006.01.012.

Dickinson, E. (2009). Hydrocolloids as emulsifiers and emulsion stabilizers. *Food Hydrocolloids*. https://doi.org/10.1016/j.foodhyd.2008.08.005.

Dickinson, E. (2010). Food emulsions and foams: Stabilization by particles. *Current Opinion in Colloid & Interface Science*. https://doi.org/10.1111/j.1536-7150.1989.tb03180.x.

Dickinson, E., & Golding, M. (1998). Influence of calcium ions on creaming and rheology of emulsions containing sodium caseinate. *Colloids and Surfaces A: Physicochemical and Engineering Aspects*. https://doi.org/10.1016/S0927-7757(98)00573-1.

Dickinson, E., Radford, S. J., & Golding, M. (2003). Stability and rheology of emulsions containing sodium caseinate: Combined effects of ionic calcium and non-ionic surfactant. *Food Hydrocolloids*. https://doi.org/10.1016/S0268-005X(02)00055-3.

Diftis, N. G., Pirzas, T. A., & Kiosseoglou, V. D. (2005). Emulsifying properties of gelatin conjugated to pectin under alkaline conditions. *Journal of the Science of Food and Agriculture*. https://doi.org/10.1002/jsfa.2029.

Djagny, K. B., Wang, Z., & Xu, S. (2001). Gelatin: A valuable protein for food and pharmaceutical industries: Review. *Critical Reviews in Food Science and Nutrition*. https://doi.org/10.1080/20014091091904.

Dolan, K. D., Singh, R. P., & Wells, J. H. (1985). Evaluation of time-temperature related quality changes in ice cream during storage. *Journal of Food Processing & Preservation*. https://doi.org/10.1111/j.1745-4549.1985.tb00725.x.

Dolz, M., Hernández, M. J., & Delegido, J. (2006). Oscillatory measurements for salad dressings stabilized with modified starch, xanthan gum, and locust bean gum. *Journal of Applied Polymer Science*. https://doi.org/10.1002/app.24125.

Elleuch, M., Bedigian, D., Roiseux, O., Besbes, S., Blecker, C., & Attia, H. (2011). Dietary fibre and fibre-rich by-products of food processing: Characterisation, technological functionality and commercial applications: A review. *Food Chemistry*. https://doi.org/10.1016/j.foodchem.2010.06.077.

Ercelebi, E. A., & Ibanoğlu, E. (2007). Influence of hydrocolloids on phase separation and emulsion properties of whey protein isolate. *Journal of Food Engineering*. https://doi.org/10.1016/j.jfoodeng.2006.05.027.

Erçelebi, E. A., & Ibanoğlu, E. (2009). Rheological properties of whey protein isolate stabilized emulsions with pectin and guar gum. *European Food Research and Technology*. https://doi.org/10.1007/s00217-009-1056-6.

Espírito-Santo, A. P., Lagazzo, A., Sousa, A. L. O. P., Perego, P., Converti, A., & Oliveira, M. N. (2013). Rheology, spontaneous whey separation, microstructure and sensorial characteristics of probiotic yoghurts enriched with passion fruit fiber. *Food Research International*. https://doi.org/10.1016/j.foodres.2012.09.012.

Fernández García, E., & McGregor, J. U. (1997). Fortification of sweetened plain yogurt with insoluble dietary fiber. *Zeitschrift für Lebensmittel-Untersuchung und -Forschung*. https://doi.org/10.1007/s002170050108.

Fitt, L. E., & Snyder, E. M. (1984). Photomicrographs of starches. In *Starch: Chemistry and technology*. https://doi.org/10.1016/B978-0-12-746270-7.50029-X.

Fox, P., & Mcsweeney, P. (2015). *Dairy chemistry and biochemistry*. https://doi.org/10.1007/978-3-319-14892-2.

Gallant, D. J., Bouchet, B., & Baldwin, P. M. (1997). Microscopy of starch: Evidence of a new level of granule organization. *Carbohydrate Polymers*. https://doi.org/10.1016/S0144-8617(97)00008-8.

Gentès, M.-C., St-Gelais, D., Turgeon, S. L., Gentès, M.-C., St-Gelais, D., & Turgeon, S. L. (2011). Gel formation and rheological properties of fermented milk with in situ exopolysaccharide production by lactic acid bacteria. *Dairy Science & Technology, 91*, 645–661. https://doi.org/10.1007/s13594-011-0039-0.

Goff, H. D. (1997). Colloidal aspects of ice cream - A review. *International Dairy Journal*. https://doi.org/10.1016/S0958-6946(97)00040-X.

Green, A. J., Littlejohn, K. A., Hooley, P., & Cox, P. W. (2013). Formation and stability of food foams and aerated emulsions: Hydrophobins as novel functional ingredients. *Current Opinion in Colloid & Interface Science, 18*, 292–301.

Gu, Y. S., Decker, E. A., & McClements, D. J. (2005). Influence of pH and carrageenan type on properties of β-lactoglobulin stabilized oil-in-water emulsions. *Food Hydrocolloids*. https://doi.org/10.1016/j.foodhyd.2004.04.016.

Guggisberg, D., Cuthbert-Steven, J., Piccinali, P., Bütikofer, U., & Eberhard, P. (2009). Rheological, microstructural and sensory characterization of low-fat and whole milk set yoghurt as influenced by inulin addition. *International Dairy Journal*. https://doi.org/10.1016/j.idairyj.2008.07.009.

Gunstone, F. (2011). *Vegetable oils in food technology: Composition, properties and uses*. Hoboken: John Wiley & Sons.

Harte, F., Luedecke, L., Swanson, B., & Barbosa-Cánovas, G. V. (2003). Low-fat set yogurt made from milk subjected to combinations of high hydrostatic pressure and thermal processing. *Journal of Dairy Science*. https://doi.org/10.3168/jds.S0022-0302(03)73690-X.

Hartel, R. W. (1996). Ice crystallization during the manufacture of ice cream. *Trends in Food Science and Technology*. https://doi.org/10.1016/0924-2244(96)10033-9.

Harwalkar, V. R., & Kalab, M. (1986). Relationship between microstructure and susceptibility to syneresis in yoghurt made from reconstituted nonfat dry milk. *Food Structure, 5*, 13.

Hasenhuettl, G. L., & Hartel, R. W. (2008). *Food emulsifiers and their applications*. New York: Springer.

Heertje, I. (1993). Structure and function of food products: A review. *Food Structure, 12*, 7.

Heertje, I. (2014). Structure and function of food products: A review. *Food Structure*. https://doi.org/10.1016/j.foostr.2013.06.001.

Huppertz, T., & de Kruif, C. G. (2008). Structure and stability of nanogel particles prepared by internal cross-linking of casein micelles. *International Dairy Journal*. https://doi.org/10.1016/j.idairyj.2007.10.009.

Innocente, N., Biasutti, M., Venir, E., Spaziani, M., & Marchesini, G. (2009). Effect of high-pressure homogenization on droplet size distribution and rheological properties of ice cream mixes. *Journal of Dairy Science*. https://doi.org/10.3168/jds.2008-1797.

Iriondo-Dehond, M., Miguel, E., & Del Castillo, M. D. (2018). Food byproducts as sustainable ingredients for innovative and healthy dairy foods. *Nutrients*. https://doi.org/10.3390/nu10101358.

Kalab, M. (1990). Microparticulate protein in foods. *Journal of the American College of Nutrition*. https://doi.org/10.1080/07315724.1990.10720396.

Kalab, M., Emmons, D. B., & Sargant, A. G. (1976). Milk gel structure. V. Microstructure of yoghurt as related to the heating of milk. *Milchwissenschaft, 31*, 402–408.

Karam, M. C., Gaiani, C., Hosri, C., Burgain, J., & Scher, J. (2013). Effect of dairy powders fortification on yogurt textural and sensorial properties: A review. *The Journal of Dairy Research*. https://doi.org/10.1017/S0022029913000514.

Karas, R., Skvarča, M., & Žlender, B. (2002). Sensory quality of standard and light mayonnaise during storage. *Food Technology and Biotechnology*.

Karim, A. A., & Bhat, R. (2009). Fish gelatin: Properties, challenges, and prospects as an alternative to mammalian gelatins. *Food Hydrocolloids*. https://doi.org/10.1016/j.foodhyd.2008.07.002.

Kaur, L., Singh, J., Singh, H., & McCarthy, O. J. (2008). Starch-cassia gum interactions: A microstructure - Rheology study. *Food Chemistry*. https://doi.org/10.1016/j.foodchem.2008.03.027.

Keogh, M. K., & O'Kennedy, B. T. (1998). Rheology of stirred yogurt as affected by added milk fat, protein and hydrocolloids. *Journal of Food Science*. https://doi.org/10.1111/j.1365-2621.1998.tb15687.x.

Korhonen, M., Hellen, L., Hirvonen, J., & Yliruusi, J. (2001). Rheological properties of creams with four different surfactant combinations - effect of storage time and conditions. *International Journal of Pharmaceutics*. https://doi.org/10.1016/S0378-5173(01)00675-5.

Koxholt, M. M. R., Eisenmann, B., & Hinrichs, J. (2001). Effect of the fat globule sizes on the meltdown of ice cream. *Journal of Dairy Science*. https://doi.org/10.3168/jds.S0022-0302(01)74448-7.

Kralova, I., & Sjöblom, J. (2009). Surfactants used in food industry: A review. *Journal of Dispersion Science and Technology*. https://doi.org/10.1080/01932690902735561.

Kristinsson, H. G., & Rasco, B. A. (2000). Fish protein hydrolysates: Production, biochemical, and functional properties. *Critical Reviews in Food Science and Nutrition*. https://doi.org/10.1080/10408690091189266.

Kyaw, Z. Y., Yu, S. Y., Cheow, C. S., Dzulkifly, M. H., & Howell, N. K. (2001). Effect of fish to starch ratio on viscoelastic properties and microstructure of fish cracker ('keropok') dough. *International Journal of Food Science and Technology*. https://doi.org/10.1046/j.1365-2621.2001.00481.x.

Lai, L. S., & Lin, P. H. (2004). Application of decolourised hsian-tsao leaf gum to low-fat salad dressing model emulsions: A rheological study. *Journal of the Science of Food and Agriculture*. https://doi.org/10.1002/jsfa.1757.

Lee, W. J., & Lucey, J. A. (2004). Structure and physical properties of yogurt gels: Effect of inoculation rate and incubation temperature. *Journal of Dairy Science*. https://doi.org/10.3168/jds.S0022-0302(04)73450-5.

Lee, W. J., & Lucey, J. A. (2010). Formation and physical properties of yogurt. *Asian-Australasian Journal of Animal Sciences*. https://doi.org/10.5713/ajas.2010.r.05.

Lian, G., Moore, S., & Heeney, L. (2006). Population balance and computational fluid dynamics modelling of ice crystallisation in a scraped surface freezer. *Chemical Engineering Science*. https://doi.org/10.1016/j.ces.2006.08.075.

Lim, S.-Y., Swanson, B. G., Ross, C. F., & Clark, S. (2008). High hydrostatic pressure modification of whey protein concentrate for improved body and texture of lowfat ice cream. *Journal of Dairy Science*. https://doi.org/10.3168/jds.2007-0391.

Liu, H., Xu, X. M., & Guo, S. D. (2007). Rheological, texture and sensory properties of low-fat mayonnaise with different fat mimetics. *LWT- Food Science and Technology*. https://doi.org/10.1016/j.lwt.2006.11.007.

Liu, Y., Chen, J., Luo, S., Li, C., Ye, J., Liu, C., & Gilbert, R. G. (2017). Physicochemical and structural properties of pregelatinized starch prepared by improved extrusion cooking technology. *Carbohydrate Polymers*. https://doi.org/10.1016/j.carbpol.2017.07.084.

Long, Z., Zhao, M., Zhao, Q., Yang, B., & Liu, L. (2012). Effect of homogenisation and storage time on surface and rheology properties of whipping cream. *Food Chemistry*. https://doi.org/10.1016/j.foodchem.2011.09.028.

Lopes, D. G., Becker, K., Stehr, M., Lochmann, D., Haack, D., Zimmer, A., & Salar-Behzadi, S. (2015). Role of lipid blooming and crystallite size in the performance of highly soluble drug-loaded microcapsules. *Journal of Pharmaceutical Sciences*. https://doi.org/10.1002/jps.24660.

Lucey, J. A., & Singh, H. (1997). Formation and physical properties of acid milk gels: A review. *Food Research International*. https://doi.org/10.1016/S0963-9969(98)00015-5.

Lucey, J. A., Teo, C. T., Munro, P. A., & Singh, H. (1997). Rheological properties at small (dynamic) and large (yield) deformations of acid gels made from heated milk. *The Journal of Dairy Research*. https://doi.org/10.1017/S0022029997002380.

Mackie, I. M. (1982). Fish protein hydrolysates. *Process Biochemistry, 17*, 26–27.

Mandala, I., Michon, C., & Launay, B. (2004a). Phase and rheological behaviors of xanthan/amylose and xanthan/starch mixed systems. *Carbohydrate Polymers*. https://doi.org/10.1016/j.carbpol.2004.07.003.

Mandala, I. G., Savvas, T. P., & Kostaropoulos, A. E. (2004b). Xanthan and locust bean gum influence on the rheology and structure of a white model-sauce. *Journal of Food Engineering*. https://doi.org/10.1016/j.jfoodeng.2003.10.018.

Martin, N. C., Skokanova, J., Latrille, E., Beal, C., & Corrieu, G. (1999). Influence of fermentation and storage conditions on the sensory properties of plain low fat stirred yogurts. *Journal of Sensory Studies*. https://doi.org/10.1111/j.1745-459X.1999.tb00109.x.

Martínez-Padilla, L. P., García-Rivera, J. L., Romero-Arreola, V., & Casas-Alencáster, N. B. (2015). Effects of xanthan gum rheology on the foaming properties of whey protein concentrate. *Journal of Food Engineering*. https://doi.org/10.1016/j.jfoodeng.2015.01.018.

McClements, D. J. (2015). *Food emulsions: principles, practices, and techniques*. Boca Raton: CRC press.

Michalski, M.-C., Camier, B., Briard, V., Leconte, N., Gassi, J.-Y., Goudédranche, H., Michel, F., & Fauquant, J. (2004). The size of native milk fat globules affects physico-chemical and functional properties of Emmental cheese. *Le Lait*. https://doi.org/10.1051/lait:2004012.

Michon, C., Cuvelier, G., Relkin, P., & Launay, B. (1997). Influence of thermal history on the stability of gelatin gels. *International Journal of Biological Macromolecules*. https://doi.org/10.1016/S0141-8130(97)00024-X.

Mine, Y. (1998). Emulsifying characterization of hens egg yolk proteins in oil-in-water emulsions. *Food Hydrocolloids*. https://doi.org/10.1016/S0268-005X(98)00054-X.

Mottar, J., Bassier, A., Joniau, M., & Baert, J. (2010). Effect of heat-induced association of whey proteins and casein micelles on yogurt texture. *Journal of Dairy Science*. https://doi.org/10.3168/jds.s0022-0302(89)79355-3.

Mun, S., Kim, Y. L., Kang, C. G., Park, K. H., Shim, J. Y., & Kim, Y. R. (2009). Development of reduced-fat mayonnaise using 4αGTase-modified rice starch and xanthan gum. *International Journal of Biological Macromolecules*. https://doi.org/10.1016/j.ijbiomac.2009.02.008.

Murray, B. S. (2007). Stabilization of bubbles and foams. *Current Opinion in Colloid & Interface Science*. https://doi.org/10.1016/j.cocis.2007.07.009.

Naik, L., Sharma, R., Rajput, Y. S., & Manju, G. (2013). Application of high pressure processing technology for dairy food preservation-future perspective: A review. *Journal of Animal Production Advances, 3*, 232–241.

Narine, S. S., & Marangoni, A. G. (1999). Relating structure of fat crystal networks to mechanical properties: A review. *Food Research International*. https://doi.org/10.1016/S0963-9969(99)00078-2.

Needs, E. C., Capellas, M., Bland, A. P., Manoj, P., Macdougal, D., & Paul, G. (2000). Comparison of heat and pressure treatments of skim milk, fortified with whey protein concentrate, for set yogurt preparation: Effects on milk proteins and gel structure. *The Journal of Dairy Research*. https://doi.org/10.1017/S0022029900004301.

Neirynck, N., Dewettinck, K., & Van Der Meeren, P. (2007). Influence of pH and biopolymer ratio on sodium caseinate—guar gum interactions in aqueous solutions and in O/W emulsions. *Food Hydrocolloids, 21*, 862–869.

Noda, M., & Shiinoki, Y. (1986). Microstructure and rheological behavior of whipping cream. *Journal of Texture Studies*. https://doi.org/10.1111/j.1745-4603.1986.tb00404.x.

Panyam, D. (1996). Enhancing the functionality of food proteins by enzymatic modification. *Trends in Food Science and Technology*. https://doi.org/10.1016/0924-2244(96)10012-1.

Parnell-Clunies, E. (1987). Microstructure of yogurt as affected by heat treatment of milk. *Milchwissenschaft, 42*, 413–417.

Patino, J. M. R., Nino, M. R. R., Dickinson, E., & Patino, J. M. R. (1999). *Food emulsions and foams: Interfaces, interactions and stability*. Cambridge: Royal Society of Chemistry.

Penna, A. L. B., Subbarao, G., & Barbosa-Canovas, G. V. (2007). High hydrostatic pressure processing on microstructure of probiotic low-fat yogurt. *Food Research International*. https://doi.org/10.1016/j.foodres.2007.01.001.

Pernell, C. W., Foegeding, E. A., Luck, P. J., & Davis, J. P. (2002). Properties of whey and egg white protein foams. *Colloids and Surfaces A: Physicochemical and Engineering Aspects*. https://doi.org/10.1016/S0927-7757(01)01061-5.

Perrechil, F. A., & Cunha, R. L. (2010). Oil-in-water emulsions stabilized by sodium caseinate: Influence of pH, high-pressure homogenization and locust bean gum addition. *Journal of Food Engineering*. https://doi.org/10.1016/j.jfoodeng.2009.10.041.

Pycia, K., Juszczak, L., & Gałkowska, D. (2016). Effect of native potato starch maltodextrins on stability and rheological properties of albumin foams. *Starch-Stärke, 68*, 611–620.

Radford, S. J., Dickinson, E., & Golding, M. (2004). Stability and rheology of emulsions containing sodium caseinate: Combined effects of ionic calcium and alcohol. *Journal of Colloid and Interface Science*. https://doi.org/10.1016/j.jcis.2003.12.045.

Ramirez-Santiago, C., Ramos-Solis, L., Lobato-Calleros, C., Peña-Valdivia, C., Vernon-Carter, E. J., & Alvarez-Ramírez, J. (2010). Enrichment of stirred yogurt with soluble dietary fiber from Pachyrhizus erosus L. Urban: Effect on syneresis, microstructure and rheological properties. *Journal of Food Engineering*. https://doi.org/10.1016/j.jfoodeng.2010.06.023.

Ratnayake, W. S., & Jackson, D. S. (2008). Starch gelatinization. *Advances in Food and Nutrition Research, 55*, 221.

Roach, R. R., & Hoseney, R. C. (1995). Effect of certain surfactants on the swelling, solubility and amylograph consistency of starch. *Cereal Chemistry, 72*, 571.

Roesch, R. R., & Corredig, M. (2003). Texture and microstructure of emulsions prepared with soy protein concentrate by high-pressure homogenization. *LWT- Food Science and Technology*. https://doi.org/10.1016/S0023-6438(02)00208-6.

Sanchez, C., Zuniga-Lopez, R., Schmitt, C., Despond, S., & Hardy, J. (2000). Microstructure of acid-induced skim milk-locust bean gum-xanthan gels. *International Dairy Journal*. https://doi.org/10.1016/S0958-6946(00)00030-3.

Sandoval-Castilla, O., Lobato-Calleros, C., Aguirre-Mandujano, E., & Vernon-Carter, E. J. (2004). Microstructure and texture of yogurt as influenced by fat replacers. *International Dairy Journal*. https://doi.org/10.1016/S0958-6946(03)00166-3.

Schmidt, K. A., & Smith, D. E. (2010). Effects of homogenization on sensory characteristics of vanilla ice cream. *Journal of Dairy Science*. https://doi.org/10.3168/jds.s0022-0302(88)79523-5.

Singh, G., & Muthukumarappan, K. (2008). Influence of calcium fortification on sensory, physical and rheological characteristics of fruit yogurt. *LWT- Food Science and Technology*. https://doi.org/10.1016/j.lwt.2007.08.027.

Singh, H., Roberts, M. S., Munro, P. A., & Teo, C. T. (1996). Acid-induced dissociation of casein micelles in milk: Effects of heat treatment. *Journal of Dairy Science*. https://doi.org/10.3168/jds.S0022-0302(96)76490-1.

Slavin, J. L. (2005). Dietary fiber and body weight. *Nutrition*. https://doi.org/10.1016/j.nut.2004.08.018.

Slavin, J. L. (2008). Position of the American Dietetic Association: Health implications of dietary fiber. *Journal of the American Dietetic Association*. https://doi.org/10.1016/j.jada.2008.08.007.

Smith, A. K., Goff, H. D., & Kakuda, Y. (2000). Microstructure and rheological properties of whipped cream as affected by heat treatment and addition of stabilizer. *International Dairy Journal*. https://doi.org/10.1016/S0958-6946(00)00043-1.

Snoeren, T. H. M., Both, P., & Schmidt, D. G. (1976). An electron-microscopic study of carrageenan and its interaction with kappa-casein. *Netherlands Milk and Dairy Journal, 30*, 132.

Sodini, I., Remeuf, F., Haddad, C., & Corrieu, G. (2004). The relative effect of milk base, starter, and process on yogurt texture: A review. *Critical Reviews in Food Science and Nutrition*. https://doi.org/10.1080/10408690490424793.

Stevens, L. (1991). Egg white proteins. *Comparative Biochemistry and Physiology - Part B: Biochemistry*. https://doi.org/10.1016/0305-0491(91)90076-P.

Su, H. P., Lien, C. P., Lee, T. A., & Ho, J. H. (2010). Development of low-fat mayonnaise containing polysaccharide gums as functional ingredients. *Journal of the Science of Food and Agriculture*. https://doi.org/10.1002/jsfa.3888.

Sun, C., & Gunasekaran, S. (2009). Effects of protein concentration and oil-phase volume fraction on the stability and rheology of menhaden oil-in-water emulsions stabilized by whey protein isolate with xanthan gum. *Food Hydrocolloids*. https://doi.org/10.1016/j.foodhyd.2007.12.006.

Supavititpatana, P., Wirjantoro, T. I., Apichartsrangkoon, A., & Raviyan, P. (2008). Addition of gelatin enhanced gelation of corn-milk yogurt. *Food Chemistry*. https://doi.org/10.1016/j.foodchem.2007.05.058.

Tamime, A. Y., Barrantes, E., & Sword, A. M. (1996). The effect of starch based fat substitutes on the microstructure of set-style yogurt made from reconstituted skimmed milk powder. *International Journal of Dairy Technology*. https://doi.org/10.1111/j.1471-0307.1996.tb02612.x.

Teggatz, J. A., & Morris, H. A. (1990). Food structure changes in the rheology and microstructure of ropy yogurt during shearing. *Food Structure, 9*, 133.

Trgo, C., Koxholt, M., & Kessler, H. G. (1999). Effect of freezing point and texture regulating parameters on the initial ice crystal growth in ice cream. *Journal of Dairy Science*. https://doi.org/10.3168/jds.S0022-0302(99)75254-9.

van Marle, M. E. (1998). *Structure and rheological properties of yoghurt gels and stirred yoghurts*.

Van Soest, P. J., Robertson, J. B., & Lewis, B. A. (2010). Methods for dietary fiber, neutral detergent fiber, and nonstarch polysaccharides in relation to animal nutrition. *Journal of Dairy Science*. https://doi.org/10.3168/jds.s0022-0302(91)78551-2.

Walsh-O'Grady, C. D., O'Kennedy, B. T., Fitzgerald, R. J., & Lane, C. N. (2001). A rheological study of acid-set "simulated yogurt milk" gels prepared from heat-or pressure-treated milk proteins. *Le Lait, 81*, 637–650.

Wildmoser, H., Scheiwiller, J., & Windhab, E. J. (2004). Impact of disperse microstructure on rheology and quality aspects of ice cream. *LWT - Food Science and Technology*. https://doi.org/10.1016/j.lwt.2004.04.006.

Worrasinchai, S., Suphantharika, M., Pinjai, S., & Jamnong, P. (2006). β-Glucan prepared from spent brewer's yeast as a fat replacer in mayonnaise. *Food Hydrocolloids*. https://doi.org/10.1016/j.foodhyd.2005.03.005.

Xiong, Y. L., Aguilera, J. M., & Kinsella, J. E. (1991). Emulsified milkfat effects on rheology of acid-induced milk gels. *Journal of Food Science*. https://doi.org/10.1111/j.1365-2621.1991.tb14606.x.

Yusoff, A., & Murray, B. S. (2011). Modified starch granules as particle-stabilizers of oil-in-water emulsions. *Food Hydrocolloids*. https://doi.org/10.1016/j.foodhyd.2010.05.004.

Zhang, T., Mccarthy, J., Wang, G., Liu, Y., & Guo, M. (2015). Physiochemical properties, microstructure, and probiotic survivability of nonfat goats' milk yogurt using heat-treated whey protein concentrate as fat replacer. *Journal of Food Science*. https://doi.org/10.1111/1750-3841.12834.

Zhao, Q., Zhao, M., Yang, B., & Cui, C. (2009). Effect of xanthan gum on the physical properties and textural characteristics of whipped cream. *Food Chemistry*. https://doi.org/10.1016/j.foodchem.2009.02.079.

Rheological Properties of Yogurt: Effects of Ingredients, Processing and Handling

Stephanie Clark, Minto Michael, and Karen A. Schmidt

1 Introduction

Yogurt is one of the oldest and most popular fermented milk products consumed throughout the world. By definition, yogurt is a dairy product prepared by fermenting milk with the starter culture combination of *Lactobacillus delbrueckii* ssp. *bulgaricus* (*L. bulgaricus*) and *Streptococcus salivarius* ssp *thermophilus* (*S. thermophilus*). In the U.S., standards of identity specified in the U.S. Food and Drug Administration Code of Federal Regulations (CFR Title 21 part 131.200; USFDA 2018) dictate the optional base dairy ingredients to which the cultures are added: cream, milk, partially skimmed milk, or skim milk, used alone or in combination. This standard of identity also specifies other optional ingredients, nutritive carbohydrate sweeteners, and the minimum milk solids nonfat content (8.25%), minimum fat content (3.25%) and minimum titratable acidity (0.90%, expressed as lactic acid) required for the finished yogurt. The CFR provides flexibility in the use of flavoring ingredients, color additives, and stabilizers in yogurt. While yogurt by definition is made from whole milk, in today's U.S. market, "whole milk yogurt" is sold at a premium price. For decades, the predominant yogurt products available in the U.S. market were low-fat yogurt (required to contain not less 0.5% and not more than 2% fat) or nonfat yogurt (required to contain <0.5% fat) because of the perception that fat of all forms should be minimized in the human diet. Lite or light yogurts contain 1/3 fewer calories or 50% reduc-

S. Clark
Department of Food Science and Human Nutrition, Iowa State University, Ames, IA, USA

M. Michael (✉)
School of Food Science, Washington State University, Pullman, WA, USA
e-mail: minto.michael@wsu.edu

K. A. Schmidt
Food Science Institute, Kansas State University, Manhattan, KS, USA

H. S. Joyner (ed.), *Rheology of Semisolid Foods*, Food Engineering Series,
https://doi.org/10.1007/978-3-030-27134-3_7

tion of fat compared to the regular yogurt. Additionally, they are typically sugar-free, and contain non-nutritive, high-intensity sweeteners.

The popularity of yogurt has increased in recent decades predominantly because of the health benefits associated with yogurt consumption. In the U.S., per capita consumption of yogurt increased from 6.5 lbs in 2000 to 13.7 lbs in 2017 (USDA-ERS 2018). The health benefits of yogurt are mainly attributed to the active starter and probiotic cultures used in the fermentation, along with the bioavailability of nine essential nutrients naturally present in yogurt (Chandan et al. 2017; Hill et al. 2017). The popularity of yogurt is maintained by the diversity of the yogurt products available in the market, ranging from plain to fruit-flavored and from drinkable to thick, spoonable Greek styles (Hill et al. 2017).

Along with health benefits, good sensory attributes are vital for the popularity of any yogurt product among consumers. Choices of culture type, ingredients in the formulation (such as addition of hydrocolloids, prebiotics, or high-intensity sweeteners), heat treatment of the yogurt mix, and fermentation temperatures used in manufacturing can significantly affect yogurt sensory attributes. Therefore, yogurt manufacturers and food scientists have conducted numerous scientific studies to understand the effects of the aforementioned parameters on the textural, rheological and other sensory attributes of yogurt. However, many publications in the food science literature highlight ingredients that “improve” yogurt texture, but do not set the context for what the “improvement” is. There is no single ideal yogurt body or texture: preferences for yogurt body and texture vary throughout the world. For instance, in China, yogurt is commonly consumed with a straw, but in the Middle East, a spoon is essential for yogurt consumption. Yogurt products from countries outside of the U.S. vary considerably in name, formulation, processing, and body and texture. For this reason, it is misleading when manuscripts include the word “better” or “improved” when describing the impact of particular ingredients or processing conditions on yogurt body or texture. It is essential, for this reason, for authors to describe changes in texture more explicitly and define “improvement” within the specific context of the expectations of the intended audience.

Although the market for non- and low-fat yogurt has been strong for many years, reducing or eliminating milkfat from the yogurt mix, which changes the rheological and textural properties of yogurt, continues to be of interest to consumers and processors. One negative outcome of removing milkfat from yogurt is an increase in syneresis, or free whey on the surface of yogurt. Research-based recommendations are available to counteract negative impacts of reduced milk fat in yogurt, including increased total solids in the yogurt mix by adding nonfat dry milk (NDM), skim milk powder (SMP), whey protein concentrates (WPCs) and isolates (WPIs), and caseinates; incorporation of stabilizers (such as gelatin, xanthan gum, guar gum, modified starch, etc.) into the formulation; and alterations of fermentation temperature and/or time (Nguyen et al. 2017; Teles and Flores 2007; Damin et al. 2009). Nevertheless, many challenges remain in developing stable lower-fat yogurt formulations with palatability similar to that of full-fat yogurts.

This chapter will begin with terminology related to rheological properties of yogurt, and review the effect of ingredients, processing, storage, and handling on yogurt rheological properties.

2 Terminology Related to Yogurt Rheological Properties

Broadly speaking, the term "rheological properties" encompasses concepts such as body, texture, mouthfeel, and microstructure. Although commonly used interchangeably, the terms body and texture are actually different. The term *body* generally refers to the overall physical structure of the bulk or majority of the yogurt. Some sub-terms that relate to yogurt body include, but are not limited to, firm, gel-like, lumpy, and weak (Tribby 2008). It is worth noting that the attribute "hardness", though used commonly in literature regarding texture analysis of yogurt, is not entirely appropriate, since hardness is a measure of solid foods. Since yogurt is a semisolid food, the attribute "firmness" should be used.

The term *texture* should be used to more specifically refer to microstructure or arrangement of small constituent parts of yogurt. Szczesniak (2002) defined texture as the sensory and functional manifestation of the structural, mechanical and surface properties of foods detected through vision, hearing, touch and kinesthetics. Some sub-terms that relate to yogurt texture include, but are not limited to, chalky, grainy, mealy, grainy, and sandy.

Rheology is the study of flow and deformation of material. Hence, yogurt rheology is defined as how the yogurt gel flows and deforms under normal and/or tangential stresses. Key rheological concepts are outlined here, with more detail provided in Chapters "Introduction: Measuring Rheological Properties of Foods" and "LAOS (Large Amplitude Oscillatory Shear) Applications for Semisolid Foods".

Shear stress is the force applied parallel or tangentially to the product cross-section. *Shear rate* is the rate at which shear is applied. *Shear strain* is the resultant deformation, or change in shape, size or volume of the material. *Yield stress* is the stress at which a material begins to deform. Rheological parameters used to describe yogurt consist of *(apparent) viscosity* (η), consistency index, *storage modulus* (G'), *loss modulus* (G'') and loss tangent (δ or G''/G') (Lubbers et al. 2004; Nguyen et al. 2017). Viscosity is the resistance to flow due to the internal friction of moving particles of fluid under force. While water is Newtonian (sheer stress directly proportional to shear rate), most yogurt products are non-Newtonian. Yogurt gels typically exhibit weak viscoelastic and *shear-thinning***,** or *pseudoplastic* behavior (Damin et al. 2009; Lubbers et al. 2004; Sah et al. 2016), wherein the viscosity decreases with increased shear rate or stress. The increased shear rate changes the particle orientation of shear-thinning materials, causing a decrease of internal friction of the particles in the material. Shear stress and shear rate data of non-Newtonian fluids including yogurt can be analyzed using mathematical models. The Herschel-Bulkley model is the most commonly used model, but Ostwald, Steiger-Ory, Bingham, Ellis and Eyring models have also been used successfully (Dönmez et al. 2017; Hassan et al. 2003; Mathias et al. 2011).

On application of stress, viscoelastic materials store some deformation energy in their structure and lose some energy in the flow. The amount of energy stored versus dissipated is useful for determining various yogurt behaviors. For example, gelation in yogurt has been defined as the strain at which $G' > 1$ Pa. Yield stress (σ_{yield}) can be characterized as the point when shear stress value begins to decrease, which is observed by a decrease in the moduli values. Similarly, yield strain (τ_{yield}) can be defined as the corresponding strain value at that point (Lee and Lucey 2006). Low δ values indicate more solid-like, rubbery gels, while high δ values indicate more fluid-like, weak gels.

Numerous instrumental techniques are used to evaluate the body and texture of semisolid foods like yogurt, including but not limited to scanning electron microscopy, rheology, dynamic mechanical analysis, and tribology. With rheometry, microstructural changes that occur during gel formation or in the gel state can be revealed (Boubellouta et al. 2011). Oscillatory tests are particularly good at revealing mechanical spectra relating to G' and G'' (Chen and Stokes 2012; Stokes and Frith 2008; Conti-Silva et al. 2018). However, to ensure valid data that are comparable across multiple yogurt types and datasets, testing must be carried out under well-defined conditions and geometries. With spectroscopic methods, molecular structure changes in micelles throughout the acidification processes can be observed (Boubellouta et al. 2011). Synchronous fluorescence and infrared spectra are sensitive to changes in the micelle structure (phosphate dissolution, swelling of caseins) and interactions (casein with water, aggregation of particles), to help reveal interaction mechanisms (Boubellouta et al. 2011). Tribology, a newer technique, encompasses both rheological properties of the food and the surface properties of tongue and palate in relative motion (Nguyen et al. 2017; Conti-Silva et al. 2018). A fuller discussion of tribological testing of solid foods is presented in Chapter "Semisolid Food Tribology". Applications of techniques commonly used in the industry are discussed in Chapter "Rheological Testing for Semisolid Foods: Traditional Rheometry".

3 Styles of Yogurt

In the U.S. alone, there are over a dozen styles of yogurt commonly sold in the market, multiplied by the additional variations of each, resulting from different fat content (whole, low-fat, nonfat), sugar-free (light, lite), and flavor options. Brief explanations of several available yogurt products in the market are included in this section.

Cup-set yogurt is yogurt that is produced by blending ingredients, pasteurizing (with or without homogenizing), culturing, and filling of cups (or glass) with yogurt mix prior to incubation. When adequate fermentation has been completed (titratable acidity above 0.90%), cups are cooled. French yogurt is essentially cup-set yogurt. It may be flavored but does not contain fruit pieces.

Sundae-style yogurt is a cup-set yogurt typically called “fruit on the bottom” in supermarkets. After culturing, the yogurt mix is delivered on top of a fruit preparation that has been dropped into the bottom of cups. The sundae cups are subsequently incubated, then cooled after fermentation.

Swiss-style yogurt is also known as blended or stirred yogurt. After culturing, the yogurt mix is incubated in a large tank to the desired completion of fermentation. During cooling, flavoring, coloring, and fruits are gently blended into the curd. After blending, the yogurt cups are filled, sealed, and refrigerated. A newer option in the market, Australian yoghurt, is similar to Swiss-style yogurt, but is made with whole milk.

Custard-style yogurt is similar to Swiss-style except that it contains enough hydrocolloids to increase the firmness to create a custard-like consistency.

Cream-top yogurt is any style of yogurt that made from yogurt mix that has not been homogenized. During storage, the cream layer will rise to the top of the yogurt body, providing the cream top in the name.

In the case of drinkable yogurt, homogenization of the set curd occurs once the desired fermentation has taken place. Because the homogenization is performed at a higher shear rate, the final product has a lower viscosity than Swiss-style yogurt. Addition of flavoring and coloring may take place before or after the homogenization step. For a shelf-stable product, ultra-pasteurization and aseptic packaging are required steps. Kefir, a cousin of drinkable yogurt, is fermented by a diverse family of microorganisms, which include yeasts and lactic acid bacteria, contained in kefir grains.

Greek yogurt, also known as “strained” or Greek-style yogurt, is made by straining or centrifuging plain yogurt curd. It takes approximately 3 kg of regular yogurt to make 1 kg of Greek yogurt. Alternatively, dairy solids can be added to increase the protein content and thicken the yogurt. Greek-style yogurts contain approximately twice as much protein as conventional yogurt due to the removal of whey.

Icelandic yogurt is similar to Greek yogurt in that it is strained. However, it is typically made with nonfat yogurt mix and contains little to no sugar, making it quite sour to the American palate. Labneh, particularly popular in the Middle East, is similar to Greek yogurt in body, with a total solids content typically ranging from 23–25%, but the fat content is typically over 9% (Saleh et al. 2018). Dahi is very popular in India is similar to stirred yogurt. Varying from nonfat to full fat, dahi is prepared with multiple starter cultures, and the final product has higher acidity than stirred yogurts.

Whipped yogurt is made in a similar fashion as ice cream, wherein air is injected and entrapped in the structure. However, heat is not removed from the system so no freezing occurs. Compared to more traditional yogurts, whipped yogurts typically contain more sweeteners and hydrocolloids (typically gelatin) to maintain the foam structure.

In the U.S., frozen yogurt is a misnomer in that it is not pure yogurt that is frozen. Frozen yogurt is essentially low-fat ice cream mix that contains some (typically less than 15%) yogurt.

Incorporation of potentially probiotic bacteria during or after yogurt fermentation is common. Potentially probiotic microorganisms, sometimes listed on yogurt labels, include *Bifidobacterium bifidum*, *B. animalis*, *B. longum*, *Lactobacillus acidophilus*, *L. casei*, *L. plantarum*, *L. reuteri*, and *L. rhamnosus* (Chandan 2006; Hill et al. 2017). For a yogurt to be truly probiotic, however, rigorous testing must be conducted to determine the live cell count over the shelf life of the product and demonstrate the beneficial effects on the human gastrointestinal tract

4 Rheological Changes in Yogurt Resulting from Ingredients

In its most basic form, yogurt is composed of pasteurized milk and cultures, yet most yogurt in the U.S. contains more than those two ingredients. Each ingredient plays a critical role in the rheological properties and consumer experience with yogurt. The roles of these ingredients, in six broad categories, are summarized in the following subsections. Overall, the information in this section emphasizes the need for careful consideration of all ingredients in a yogurt formulation, including milk source, byproducts of microbial cultures, functional and flavoring ingredients, and added micronutrients.

4.1 Use of Milk from Different Species

Considering the importance of mammals other than cows around the world, yogurt made from the milk of buffalos, camels and small ruminants should not be overlooked. For example, yogurt made with goat milk forms softer curds than yogurt made from bovine milk because of the naturally lower amount of alpha$_{s1}$-casein in goat milk. Similarly, camel milk produces a weak yogurt body (Abou-Soliman et al. 2017). Sheep milk, on the other hand, has a higher solids content and produces yogurt with a more firm and resilient curd structure, especially compared to yogurt made from goat milk (Gursel et al. 2016).

Gursel et al. (2016) manufactured goat milk yogurts with fortification of 2% (w/v) skim goat milk powder (SGMP), sodium caseinate (NaCN), WPC, WPI, or yogurt texture improver and stored it 21 d at 5 °C. Compared with goat milk yogurt made by using SGMP, the other yogurts had higher protein content and lower acidity values. Yogurts fortified with either NaCN or yogurt texture improver had more compact structure and lower syneresis than yogurt fortified with WPC. Using WPI caused the firmest yogurt body and higher syneresis. Acetaldehyde and ethanol formation increased with the incorporation of WPI, WPC, or yogurt texture improver into the yogurt base. Counts of *S. thermophilus* were higher than counts of *L. bul-*

garicus, possibly due to a stimulatory effect of milk protein-based ingredients other than SGMP on the growth of *S. thermophilus*. Yogurt with NaCN received the highest body and texture scores from trained Turkish panelists.

Costa et al. (2015) investigated the impact of cupuassu (*Theobroma grandiflorum*); a fiber-rich acidic fruit similar to cacao that is cultivated in Brazil, Colombia, Bolivia, and Peru; to modify goat milk yogurt body. Cupuassu pulp, probiotic (*Lactobacillus acidophilus* LA-5), and prebiotic (inulin) ingredients were used to make yogurts called "natural", "probiotic", "prebiotic", "symbiotic" (probiotics plus inulin), and "probiotic with cupuassu". All yogurt samples underwent gradual decreases in pH until 7–14 d of refrigerated storage, but the probiotic bacteria remained viable (≥7 log cfu/mL) throughout 28 d of refrigerated storage. When used alone, addition of inulin and cupuassu increased the apparent viscosity of goat milk yogurts for up to 21 d storage compared to the viscosity of other yogurts. However, by day 28, no differences in yogurt viscosity were apparent. Additionally, at the end of storage, the consistency was higher in the yogurts with inulin (prebiotic and symbiotic), but no other meaningful differences were seen throughout storage, including no differences in firmness at any time. While the authors concluded that "cupuassu is an important technological strategy for the dairy goat industry", that appears to be an overstatement based upon closer inspection of the results.

Although camel milk is an important food source worldwide, it is not successful in yogurt production, in part explained by the large casein micelles, little to no β-lactoglobulin (β-lg), and small milk fat globules (Abou-Soliman et al. 2017). There has been some effort to improve camel milk yogurt with SMP (Salih and Hamid 2013) or the addition of hydrocolloids and stabilizers (Al-Zoreky and Al-Otaibi 2015) with little success. Abou-Soliman et al. (2017) investigated the impact of microbial transglutaminase (0.4% concentration) with and without bovine SMP, WPC, or β-lg on physicochemical, rheological, microstructural, and sensory properties of camel milk yogurt during 15 d storage. Fortification of camel milk with dairy ingredients alone, without microbial transglutaminase, did not set. Microbial transglutaminase treatment yielded yogurt, and the addition of bovine powders increased the protein matrix in the gel microstructure. The highest firmness values were obtained for samples made with SMP-fortified milk, and the lowest was for WPC-fortified milk. Microbial transglutaminase not only improved camel yogurt firmness, but increased the viscosity and water-holding capacity of the yogurts, showing promise for the ingredient for camel milk yogurt applications.

4.2 Optional Additional Dairy Ingredients

Common optional additional dairy ingredients used in yogurt base formulations include NFDM or SMP, caseinates and various WPCs. It is logical to think that increasing solids in yogurt yields an increase in yogurt firmness. However, that is not always the case: both the type of solids added and processing conditions impact yogurt body and texture. Additionally, increased solids may induce other changes to yogurt that may not be acceptable to the consumer (e.g., chalky or grainy). Careful selection of all ingredients used in yogurt, as well as processing and fermentation conditions, is essential.

It has long been known that the changes in chemical composition of a yogurt base due to protein fortification influence the rheological and physical properties of yogurt (Peng et al. 2009; Lee and Lucey 2010). Several studies have investigated the effects of fortification of milk with WPCs and caseinates on the physical properties of yogurt (Remeuf et al. 2003; Isleten and Karagul-Yuceer 2006; Peng et al. 2009; Marafon et al. 2011). Heat treatment of milk fortified with WPC induces crosslinking within the gel network, which results in a dense yogurt structure and increased yogurt viscosity and water holding capacity (Remeuf et al. 2003). Fortification with WPC has been shown to decrease syneresis and increase viscosity and firmness compared to fortification with SMP or whey powder. This was attributed to the disulfide bridges formed between denatured whey proteins in WPC with the casein micelles in milk (Bhullar et al. 2002; Marafon et al. 2011). Casein interactions play an important role in the textural properties of yogurt (Peng et al. 2009). For instance, a low casein content is believed to yield a more open gel structure, making the coagulum network more sensitive to syneresis (González-Martınez et al. 2002; Zhao et al. 2016). The non-protein nitrogen content of milk powders was shown to negatively influence the viscosity and thickness of fortified yogurt, which was highest for yogurt fortified with milk protein concentrate (MPC), followed by SMP, and lowest for casein hydrolysate (Sodini et al. 2002). The addition of increasing levels of β-lg has been reported to cause marked increases in storage modulus compared with α-lactalbumin (α-la), with some differences in behavior among different β-lg variants (Graveland-Bikker and Anema 2003). The amount of fat and distribution of fat was shown to improve the firmness and texture of yogurt fortified with either WPC, whey powder, or SMP (Bhullar et al. 2002).

Yu et al. (2016) studied the effect of adding instant NFDM on the physical properties and microstructure of yogurt. The physical properties of fat-free yogurt, fat-free yogurt with NFDM, whole-fat yogurt, and whole-fat yogurt with NFDM were analyzed using rheometry and imaging techniques. Not surprisingly, the two yogurts that incorporated NFDM had higher consistency coefficient, storage modulus, yield stress, and firmness. Nuclear magnetic resonance (NMR) and brightfield microscope images showed that NFDM contributed positively to strengthening the physical structure, thus altering the mechanical properties of the yogurts.

Marafon et al. (2011) evaluated the quality of Swiss-style probiotic nonfat yogurt fortified by partially replacing SMP with WPC and sodium caseinate (NaCN) compared with non-fortified yogurt. Yogurt rheological properties were measured using dynamic oscillation over a 28 d storage period. Higher G' and G'' values and more homogeneous microstructures were found in the fortified yogurts, and higher gel strength was maintained in these yogurts during storage. Neither the acidification profile nor viable counts of probiotic bacteria were affected by supplementation of the solids in the yogurt base. A sensory study with 120 untrained participants was conducted on the appearance, flavor, and texture of the yogurts using a 9-point hedonic scale. The results revealed that yogurt made with fortification of milk with WPC and NaCN had acceptable appearance, acidic taste and firmer consistency throughout their shelf life compared to yogurt made with no fortification (Marafon et al. 2011).

In an effort to increase the protein content and consistency, while imparting creaminess to yogurt, Morell et al. (2015) prepared yogurts with SMP and WPI, as well as a control without extra protein. Three additional samples were prepared by adding 2% of a physically modified starch to each. A controlled-stress rheometer was used to characterize the flow and viscoelastic properties of the samples before and after *in vitro* oral digestion, and their microstructure was observed with light microscopy and low-temperature scanning electron microscopy. Before *in vitro* oral digestion, samples with SMP showed denser areas than the control yogurt; in samples with WPI, two protein networks could be distinguished. In the samples with added starch, starch granules were embedded in the protein networks. After *in vitro* oral digestion, the protein tended to aggregate; the starch granules maintained their structure, indicating that they were not broken down by the saliva. All samples showed pseudoplastic behavior, as well as $G' > G''$, describing a weak gel structure with elastic characteristics. While samples with WPI exhibited the highest consistency index, yogurts made with starch showed higher viscosity than those without starch because the starch acted as fillers, strengthening the protein network (Morell et al. 2015).

Zhao et al. (2016) delved more deeply into the effect of casein to whey protein ratios (4:1, 3:1, 2:1, and 1:1) on gelation properties and microstructure of low-fat yogurt made with reconstituted skim milk with or without addition of WPC. The rheological properties of the low-fat yogurts were evaluated using a Universal Dynamic Spectrometer. The microstructure (measured by confocal scanning laser microscopy) became more compact with smaller pores as the ratio of casein to whey proteins decreased. When the ratio of casein to whey proteins was 2:1 or 1:1, the yogurt coagulum showed higher G' and greater yield stress, with more compact cross-linking and smaller pores than when casein levels were higher. In addition, when more SMP was replaced by WPC, a greater number of disulfide bonds were formed and hydrophobic interactions increased during heat treatment, tightening the microstructure of the final yogurt and increasing its firmness (Zhao et al. 2016).

In an effort to develop and optimize an alternative make procedure for Greek-style yogurt to reduce the amount of acid whey produced, Bong and Moraru (2014) incorporated micellar casein concentrate (MCC) into the base instead of using a straining step to increase yogurt solids. Two MCC preparations with 58 and 88% total protein were used to fortify yogurt base to 9.80% (w/w) protein, with strained Greek-style yogurt of similar protein content as the control. Regardless of inoculation level, the acidification rate was faster for the MCC-fortified Greek-style yogurt than for the control, which was attributed to the higher non-protein nitrogen content in the MCC-fortified milk. Steady shear rate rheological analysis indicated shear-thinning behavior for all Greek-style yogurt samples. Dynamic rheological analysis at 5 °C showed a weak frequency dependency of G' and G'' for all Greek-style yogurt samples, with $G' > G''$, indicating a weak gel structure. The lower water-holding capacity for the MCC-fortified Greek-style yogurt compared with the control was attributed to lower serum protein content in the MCC-fortified Greek-style yogurt. Despite some differences in the physicochemical characteristics compared to Greek-style yogurt manufactured by straining, the alternative process was considered a feasible alternative to the traditional Greek-style yogurt straining, with environmental and possibly financial benefits to the dairy industry (Bong and Moraru 2014).

The form of whey protein used as an ingredient also has an impact on rheological properties of fermented beverages. Dimitreli et al. (2013) studied the impact of heat treatment and whey protein addition on the fermentation time and the rheological properties of kefir using a pneumatic tube viscometer of novel design. Heat treatment of the milk was made prior to or after addition of various levels of WPC (to yield native or denatured whey protein, respectively). Increasing WPC concentration increased lactic acid concentration and reduced fermentation time. The flow curves of the samples demonstrated kefir's pseudoplastic fluid behavior. The apparent viscosity of kefir samples increased with increasing WPC concentration, but denatured whey proteins yielded higher consistency index values (higher apparent viscosity and lower flow behavior index values) compared with native whey proteins.

A novel ingredient that may be considered for yogurt applications in the future to help in the clean label movement may be CO_2-treated milk protein concentrate powder (TMPC). Meletharayil et al. (2018) mixed TMPC80 with NFDM in different ratios in the manufacture of acid gels with 4% (w/w) protein and 12% (w/w) total solids. Dispersions were adjusted to pH 6.5, followed by heat treatment at 90 °C for 10 min, then glucono-δ-lactone (GDL) was added and samples were incubated at 30 °C until pH 4.5 was reached (about 4 h). GDL levels were adjusted to compensate for the lower buffering capacity of samples with higher proportions of TMPC80 (attributable to the depletion of buffering minerals from the serum and micellar phase during preparation of TMPC80). When the proportion of protein contributed by TMPC80 was increased from 0% to 60%, gelation pH, gel porosity decreased and water-holding capacity and the G' of the gels at pH 4.5 increased. The authors concluded that because of decreased buffering and reduced need for hydrocolloids, the productive capacity of yogurt manufacturing plants may be improved by partial substitution of NFDM with TMPC80.

4.3 Addition of Hydrocolloids

It is common practice to add hydrocolloids of various forms to the yogurt base to bind water, thicken the final product, and reduce syneresis, which some consumers consider objectionable, during storage and shipping. It is impractical to provide a complete list of hydrocolloids that have been tested in yogurt applications, as dozens of hydrocolloids and hydrocolloid blends have been used, and more are being developed each day. Instead, an overview of some of the recent research with hydrocolloids in yogurt is summarized in this section. All of these studies highlight the impact of different hydrocolloids on yogurt rheology and texture, emphasizing the need for careful selection of hydrocolloids in the yogurt system.

In the U.S., one of the most traditional choices of hydrocolloids for yogurt applications is gelatin. Being a standard, and because it is an animal-based ingredient that is not desirable to some consumers, other hydrocolloids are often compared to gelatin. Pang et al. (2015) studied the effects of polysaccharides with different ionic charge on rheology, microstructure, texture and water-holding capacity of acid milk gels compared to gelatin. Similar to gelatin, starch (neutral) and xanthan gum (anionic) did not prevent milk gelation in the first 30 min of acidification, even at high concentrations. In contrast, two neutral polysaccharides, guar gum (≥0.05%) and locust bean gum (≥0.1%), inhibited milk gelation from the beginning of acidification. Carrageenan, another anionic polysaccharide, induced earlier milk gelation at low concentration (≤0.05%), but inhibited gelation entirely at high concentration (0.2%). The highest water-holding capacity was seen with gelatin inclusion. Xanthan gum and starch were more similar to gelatin in their effect on acid milk gels compared to guar gum, locust bean gum and carrageenan.

Later, Pang et al. (2016) combined gelling polysaccharides (xanthan/locust bean gum, carrageenan, and starch) and milk proteins (WPI, NaCN, and SMP) in an effort to use them to replace gelatin in acid milk gels. Gels with added xanthan/locust bean gum alone showed rheological and microstructural properties similar to gels with gelatin. Similar to the effect of adding gelatin, milk protein fortification enhanced water-holding capacity of the gels, with WPI being the most effective. Gels with combinations of polysaccharides (except carrageenan) and WPI were stronger and had higher water-holding capacity than gels with no stabilizer. In yogurt, the combination of WPI and xanthan/locust bean gum produced similar effects on consistency, pseudoplasticity and apparent viscosity as with gelatin. In ranking tests with 38 untrained panelists, yogurt with WPI and xanthan/locust bean gum had higher thickness and stickiness than with gelatin, and lower smoothness than with gelatin.

Hematyar et al. (2012) prepared yogurt by supplementing yogurt mixes with 0.01 and 0.005% xanthan or carrageenan and evaluated yogurt characteristics during storage (4 °C at 10 d). Viscosity of supplemented yogurts was greater than non-supplemented yogurt, and viscosity increased during storage in all supplemented yogurts but decreased in the yogurt without supplements. The increased viscosity of the carrageenan-supplemented yogurts was explained by the presence of electrostatic interactions of anionic carrageenan and the net positively-charged casein micelles, whereas the viscosity increase in the xanthan-supplemented yogurt was explained by the increased viscosity of the continuous phase due to the addition of xanthan gum, which is an excellent thickening agent.

In an effort to evaluate resistant starch from maize in a dairy application, Lobato-Calleros et al. (2014) prepared three reduced-fat stirred yogurts from reconstituted milk (12.5 g/L of milk fat) with added native maize starch, and chemically modified maize or tapioca starches (10 g/L). The chemical composition, syneresis, rotational and oscillatory shear rheological properties and syneresis of the reduced-fat yogurts were evaluated and compared with those of a full-fat control yogurt (25 g/L of milk fat) without starch. The control yogurt exhibited lower apparent viscosity-shear rate profiles and dynamic viscoelastic moduli, but higher syneresis than the reduced-fat yogurts and all exhibited weak gel microstructural networks. The reduced-fat yogurts showed little variation in their flow and viscoelastic properties over 15 d of storage time. Overall, the addition of native or chemically modified starches contributed to the formation of stable reduced-fat yogurts.

Saleh et al. (2018) investigated the effects of hydrocolloids when used as fat replacers on the physicochemical properties of labneh compared to a 16% fat control. Four sets of combinations of carboxymethylcellulose (CMC), gum arabic, κ-carrageenan, and xanthan gum were used in a three-factor mixture response surface methodology. The maximum contribution of each individual hydrocolloid was set at 5% for xanthan gum, CMC, and gum arabic, and 1% for κ-carrageenan. Xanthan gum and κ-carrageenan increased labneh water-holding capacity, while CMC decreased water-holding capacity. Most samples showed shear-thinning behavior; penetration force increased when more than two hydrocolloid types were used, which was attributed to the formation of a 3-dimensional network that physically retained water. Viscosity and penetration results were hypothesized to be related to water-holding capacity. The water-holding capacity was highest in labneh with xanthan gum, followed by gum arabic, κ-carrageenan, then CMC. They found that xanthan gum exhibited an antagonistic effect with CMC that led to the decrease in water-holding capacity. Consumer testing (n = 40) revealed that an acceptable reduced-fat labneh could be produced by using hydrocolloids as fat replacers, which is remarkable since labneh typically contains more than 9% fat.

In recent years, some authors have used crosslinked acetylated starch to improve freeze–thaw stability of starches. Crosslinking reinforces hydrogen bonds in starch granules; acetylation induces structural reorganization and increases swelling power of granules (Tang et al. 2018). Cui et al. (2014) evaluated the effect of crosslinked acetylated cassava starch on set yogurt by investigating yogurt flowability, viscoelasticity, zeta potential, conductivity, and microstructure. The results indicated that the stability and viscoelastic moduli values of the set yogurt system increased with increased concentrations of crosslinked acetylated starch. Set yogurt systems with added crosslinked acetylated starch also exhibited shear-thinning behavior. SEM micrographs demonstrated that the microstructures were mainly composed of a casein network that was strengthened by adding crosslinked acetylated starch. The authors hypothesized that the starch adsorbed onto the surface of the casein micelles, preventing flocculation of the casein micelles by electrostatic adhesion, steric stabilization, and osmotic effects.

4.4 Use of Exopolysaccharide-Producing Cultures

Exopolysaccharides (EPS) are large polymeric carbohydrates. Yogurt that contains EPS may be described with a variety of terms, such as slimy, sticky, thick, lubricating, mouth-coating, ropy, or even “snotty”, depending on the type of EPS produced. There are several types of EPS. Capsular EPS is synthesized inside the cell, and when released from the cell, remains attached to the exterior of the cell in the form of a capsule. In contrast, “ropy” EPS is excreted directly into the medium as a free-floating polysaccharide (Low et al. 1998; Cerning 1995; De Vuyst and Degeest

1999; Broadbent et al. 2003; Khanal and Lucey 2017). In some cases, bacteria can produce both forms of EPS.

Ropy describes how the yogurt strings up to follow a lifted spoon after the spoon is lifted 3–6 cm from the surface of stirred yogurt. EPS-producing or "ropy cultures" are often used, intentionally, to provide body to clean-label yogurt. Because capsular and ropy EPS possess high water-binding ability, the use of EPS-producing starter cultures helps decrease the level of whey separation in set yogurt (Wacher-Rodarte et al. 1993; Hassan et al. 1996; Jaros et al. 2002). Ropy cultures are influenced by pH, temperature, supplementation with WPC, and competition by other cultures in the yogurt base (Zisu and Shah 2003).

Ramchandran and Shah (2009) studied the effect of EPS- and non-EPS-producing *S. thermophilus* cultures on the rheological and textural properties of yogurt supplemented with inulin during 28 d storage at 4 °C. Results showed no significant changes in the yogurt firmness during storage. On the other hand, EPS-containing yogurts had lower firmness and G' and G'' values during storage compared to the non-EPS-containing yogurts. Ramchandran and Shah (2009) suggested that the interference of inulin between casein micelles could result in weaker yogurt gels. Moreover, the presence of void spaces around the EPS-producing bacteria could also contribute to the weaker yogurt structures. All yogurts showed $G' > G''$ throughout storage, confirming a weak gel microstructure. The lower G' values of EPS-containing yogurts indicated a less rigid gel microstructure compared to the non-EPS-containing yogurt. Overall, both EPS-containing and non-EPS-containing yogurts had similar loss tangent values during storage. However, the loss tangent did decrease in both types of yogurt during storage, indicating development of a more solid-like gel. All yogurts were showed pseudoplastic flow behavior at all timepoints and fit well to the Herschel-Bulkley model. Overall, yield stress increased significantly for both EPS-containing yogurts and non-EPS-containing yogurts, and yield stress was greater for non-EPS yogurts compared to EPS-containing yogurts. Ramchandran and Shah (2009) also reported a strong, significant correlation between firmness of EPS-containing yogurt ($r = 0.86$) and yield stress of non-EPS-containing yogurt ($r = 0.83$). The hysteresis loop area of EPS-containing yogurts and non-EPS-containing yogurts indicated thixotropic behavior of yogurt gels. The overall hysteresis loop area of both yogurts increased during storage and hysteresis area of EPS-containing yogurts was less than non-EPS-containing yogurt during storage. However, the thixotropic nature of yogurt gels was dependent on the type of EPS-producing strain (Ramchandran and Shah 2009; Amatayakul et al. 2006).

Later, Ramchandran and Shah (2010) studied the effect of addition of probiotics (*L. acidophilus*, *L. casei* and *B. longum*) with inulin on rheological properties of yogurt prepared with EPS- and non-EPS-producing *S. thermophilus*. The overall firmness of both yogurts increased over the 28 d storage time. Similar to their previous work, the firmness of non-EPS-containing yogurt was greater than EPS-containing yogurt at the end of storage. Similar trends were seen for yield stress and thixotropic behaviors.

Prasanna et al. (2013) prepared yogurts with starter cultures and EPS-producing *Bifidobacterium longum* ssp. *infantis* or *B. infantis* NCIMB 702205 and reported that G' values and firmness of yogurt increased during 28 d of storage at 4 °C. These increases over time were thought to be due to the rearrangement of proteins that formed the gel and increased interaction between the protein–protein and EPS–protein networks. On the other hand, Liu et al. (2017) prepared yogurts using EPS-producing *S. thermophilus* S3.3 with EPS-producing *L. bulgaricus* LTM or mutant EPS-producing *L. bulgaricus* LTM at three different fermentation temperatures (30, 37, and 42 °C), and evaluated these yogurts periodically throughout 21 d of storage at 4 °C. Liu et al. (2017) reported that yogurts prepared from the two EPS-producing *L. bulgaricus* strains differed in firmness, consistency, and cohesiveness. The differences in theses textural properties did not follow any specific trend. However, yogurts fermented at higher temperatures (37 and 42 °C) had greater firmness, consistency, and cohesiveness throughout storage compared with the yogurt fermented at 30 °C. In these systems, the milk proteins crosslinked with EPS, resulting in enhanced viscosity. Interestingly, Liu et al. (2017) reported that G' values increased during storage and hypothesized this result was related to the number of protein–EPS crosslinks. However, the specific effect of EPS on yogurt rheology varies with type of EPS-producing culture(s) and the type and quantity of EPS produced (Liu et al. 2017; Rawson and Marshall 1997).

Khanal and Lucey (2017) set out to understand if different strains of EPS-producing strains of *S. thermophilus* produce different yield and molar mass of EPS under the same conditions. Milk samples were analyzed for EPS concentration every 30 min during a fermentation period of 270 min (final pH 4.5) by using a modified quantification method. Both strains appeared to start producing significant amounts of EPS after ~150 min of fermentation, which corresponded to pH ~5.3, close to the gelation point. During the remainder of the fermentation process (150–270 min), the EPS concentration from the two strains significantly increased and was estimated to represent ~60% of the total EPS added to milk. In addition, distinct differences in rheological properties were seen between yogurts containing each of the two strains. At the end of fermentation, yogurts containing one strain produced weaker gels and higher maximum loss tangent values that occurred earlier during fermentation compared to yogurt made with the other strain. The differences were attributed to differences in chemical structures and molecular mass of the EPS produced by the two *S. thermophilus* strains since the fermentation conditions were identical (Khanal and Lucey 2017). These findings underline the importance of careful selection of culture strains to obtain desired results.

4.5 Addition of Fruit, Vegetables or Herbs

The addition of fruit to yogurt contributes to the abundance of options for consumers. Flavored and fruit yogurts are popular yogurts in the market. Strawberry, apple, mango, cherry, blueberry and banana are the most common fruits used in commerical yogurt in the U.S. Low-fat yogurt with fruits are particularly popular. Although addition of vegetables and herbs are being studied in yogurt preparation, these ingredients have not gained as much favor, at least in the U.S., and shelf life issues have not been fully addressed.

Lubbers et al. (2004) reported increased consistency index and apparent viscosity of stirred fruit yogurt (prepared from strawberry pulp) during 28 d of storage at 10 °C. Both consistency index and apparent viscosity increased during storage, although no significant change in flow behavior index was noticed due to fruit prep. Lubbers et al. (2004) attributed the changes in yogurt rheological behaviors during storage to the production of lactic acid and EPS from residual microbial activity, which would reinforce the protein network. On the other hand, Sengul et al. (2014) reported that yogurts supplemented with 8, 12, or 16% strawberry pulp did not exhibit an overall significant change in apparent viscosity. As viscosity depends on the yogurt acidity, the effects of fruit supplementation of yogurt depend on the preparation and physicochemical properties of the fruit supplement and its ultimate impact on yogurt acidity.

Dabija et al. (2018) studied the rheological properties of yogurt supplemented with herb extracts of thistle, hawthorn, sage, and marjoram at concentrations of 0.25–1.0% w/w. All yogurts showed thixotropic and weak gel characteristics. The overall viscosity of yogurt made without herb supplements was greater than that of the herb-supplemented yogurts on d 1; however, on d 28, the herb-supplemented yogurts had higher viscosity than the yogurt made without herb supplements. For all yogurts, $G' > G''$, and at day 28, the viscoelastic moduli values were greater in herb-supplemented yogurts compared with yogurts made without herb supplements, indicating a stronger gel network.

4.6 Yogurt with Other Functional Ingredients

A variety of functional ingredients have added to yogurt with efforts to improve nutritional properties for consumers and/or for select microorganisms. For instance, numerous dietary fibers are symbiotic because they are non-digestible and thus non-caloric to humans but promote the survival of probiotic microorganisms in the host gastrointestinal tract, and in turn benefit the host. Prebiotics are sometimes added to yogurt mix to support the growth and viability of starter and probiotic bacteria during fermentation and refrigerated storage. Functional ingredients, such as fibers, phytosterols and plant extracts, are becoming common yogurt components (Izadi et al. 2015; Sah et al. 2016). It is important that the type and quantity of additives used in the yogurt formulation not negatively impact the final sensory quality or safety attributes of the yogurt products. Yet inclusion of such ingredients can have direct impact on the body and texture of the yogurt. For instance, yogurt viscoelastic behaviors or apparent viscosity can be increased two- to three-fold by adding polysaccharides or enzymes (lactoperoxidase, protease, and transglutaminase) to the yogurt base, allowing new crosslinks to form in the gel network and enhancing gel rigidity and water-holding capacity (Zhao et al. 2016). This section elaborates on some of the recent research in the area.

Hoppert et al. (2013) analyzed the responses of a large number of young educated consumers (n = 704) on standard or 30% reduced-sugar vanilla yogurt enriched with inulin or with inulin combined with a grain mixture, a milled mixture of flakes, or a combination of grains and milled flakes (>1.5 g fiber per 100 kcal). Hedonic acceptability and Just About Right testing were conducted with 88 panelists judging each of six yogurts. Overall, sugar content was found to be the primary influence on yogurt acceptability, adapting the flavoring concentration might be an appropriate tool to mask sugar reduction, and the size of incorporated fiber should be considered in product optimization to minimize cereal flavor and appearance of fiber particles.

Sah et al. (2016) studied the effect of including 1% w/v inulin or pineapple peel powders in yogurt formulations on the physicochemical, textural, and rheological properties of set-type yogurt with or without probiotics (*L. acidophilus*, *L. casei* and *L. paracasei*) during 28 d of storage at 4 °C. All yogurts demonstrated weak gel and non-Newtonian behaviors. Sah et al. (2016) reported that the firmness of yogurts without added fiber increased during storage, which was attributed to the decrease in yogurt pH (from 4.49 on d 1 to 4.29 on d 28) during storage, resulting in the shrinkage of gel structure and elevation of gel strength. However, yogurts prepared with fiber had lower firmness throughout storage compared to yogurts without fiber. These results indicate poor compatibility between the milk proteins and inulin and pineapple peel fibers. Yogurt G' values increased during storage, which was attributed to gel shrinkage, increased gel strength, increased elastic-type behavior, or a combination of these factors. Although addition of probiotics and inulin did not affect the G' values during storage, yogurts containing pineapple peel powder did have lower G' values throughout storage, implying that pineapple peel powder fortification resulted in weaker gels with less elastic-type behavior. Further, Sah et al. (2016) reported that the loss tangent values decreased during storage, which was interpreted as a rearrangement of gel structure that improved gel elasticity. Although the apparent viscosity of the non-supplemented yogurts remained consistent during storage, the apparent viscosity of the supplemented yogurts increased. The overall yield stress, calculated using the Herschel-Bulkley model, increased during storage for the pineapple peel powder-supplemented yogurt, although this sample had the lowest yield stress throughout storage. Micrographs of yogurt structures generated by Sah et al. (2016) showed a more densely packed casein network after storage, which may explain the higher G' values at the end of the storage.

Bakirci et al. (2017) studied the effect of supplementing low-fat set-style yogurt with 0.5, 1.0, or 1.5% pumpkin fiber on the rheological properties during 14 d of storage at 4 °C. The apparent viscosity of yogurt increased with increasing pumpkin fiber concentration. Moreover, the viscosity of all pumpkin fiber-supplemented yogurts was greater than that of the non-supplemented yogurt throughout storage. As pumpkin is a good source of pectin, the increased viscosity was attributed to the pectin's contribution to the water-binding ability of the supplemented yogurts. Bakirci et al. (2017) reported that all yogurts exhibited a weak gel microstructure and elastic-dominant behavior ($G' > G''$) throughout storage. Both G' and G'' were greater in pumpkin fiber-supplemented yogurts compared to the non-supplemented yogurt. Bakirci et al. (2017) attributed the increased in viscoelastic moduli values to the increased interactions between the casein micelles and the pectin from pumpkin fibers. Scanning electron microscope images of yogurt gels showed that the pumpkin fibers filled the void spaces between the casein aggregates, creating a denser gel structure compared to non-supplemented yogurt, which showed larger voids. Bakirci et al. (2017) concluded that using pumpkin fibers as an ingredient could improve the quality and textural and nutritional properties of reduced-fat yogurts.

Knowing that interactions between polyphenols and proteins are based on weak hydrophobic, van der Waals, hydrogen bridge-binding, and ionic interactions formed between amino acid side chains and polyphenol aromatic rings, Dönmez et al. (2017) studied the effect of added green coffee powder and green tea powder on the syneresis and flow behaviors of set yogurts. Adding green coffee powder at 1 or 2% concentration decreased syneresis. However, in comparison to the control, green tea powder decreased syneresis when added at 0.02%, but increased syneresis when added at 2%. Herschel-Bulkley model parameters indicated that the consistency coefficient of the control yogurt was lower than that of green coffee powder-containing yogurts for up to 14 d, but was higher after 21 d of storage. Consistency coefficients of yogurts made with 0.01 or 0.02% green tea powder were higher than those of the controls, but consistency coefficients of yogurts made with 1 or 2% green tea powder (1 or 2%) were lower than those of the controls. Dönmez et al. (2017) hypothesized that the polyphenols in green coffee and green tea interacted with casein micelles, and differences in the polyphenol profiles of the powders played a role in the observed differences of the yogurts.

Mudgil et al. (2017) studied the effect of partially hydrolyzed guar gum (a dietary fiber) level (1–5%), culture level (1.5–3.5%), and incubation time (4–8 h) on yogurt texture profile analysis behaviors. Fortification of yogurt with partially hydrolyzed guar gum or culture beyond 2.5% decreased yogurt firmness. Partially hydrolyzed guar gum fortification also decreased gumminess and increased the adhesiveness, cohesiveness, and springiness of yogurt.

Santillan-Urquiza et al. (2017) studied the effect of fortification of set-type yogurt with iron oxide, zinc oxide, and calcium phosphate, added as inulin-coated nanoparticles or microparticles, on the physicochemical and rheological properties of yogurt during 28 d of storage at 4 °C. Yogurt flow behaviors best fit the Herschel-Bulkley model and showed pseudoplastic behavior. Flow behavior index and yield stress values of yogurt did not change significantly during storage. Furthermore, yield stress was not affected by fortification. On the other hand, yogurt firmness increased during storage, and yogurts fortified with higher levels of calcium phosphate and zinc oxide nanoparticles had greater firmness compared to unfortified yogurts. Santillan-Urquiza et al. (2017) attributed this greater firmness to binding of zinc and colloidal phosphate to the casein micelles.

5 Rheological Changes in Yogurt Resulting from Processing, Storage and Handling

Although many aspects of processing play important roles in yogurt body and texture, temperature has the greatest impact, beginning with yogurt base processing temperature and continuing through fermentation, cooling, transportation and subsequent storage, and even the mastication process. The following three subsections focus on recent research in yogurt processing, fermentation, storage, and handling conditions that impact rheological properties of yogurt.

5.1 Yogurt Base Processing

It is well known that heating milk above 70 °C causes denaturation of whey proteins and promotes interaction of those denatured proteins with caseins. When combined with acidification, either direct or from lactose fermentation by lactic acid bacteria, a gel network is formed. Compared to acid gels made from unheated milk, acid gels from heated milk have more solid-like behavior, reportedly because of increases in heat-induced interactions between caseins and whey proteins that form a stronger gel (Lucey and Singh 1997). For semisolid foods like yogurt, there is a close relationship between their rheological properties and the degree of protein denaturation during the heating process. Heating time and intensity determine the amount of α-la and β-lg bound to casein. It has been reported that under lower heat treatments, filaments of denatured β-lg on the casein micelle surface prevent micellar fusion, while at higher intensity treatments, α-lac segments precipitate onto the micelle, leading to smoother micellar surfaces and improved rheological properties (Mottar et al. 1989; Benezech and Maingonnat 1994).

It is believed that in fortified yogurts that are typically subjected to high heat treatments, coagulation happens in two stages: one at pH 5.3, the isoelectric point of β-lg, and the second at pH 4.6, the isoelectric point of casein. It is desirable that the time between these two coagulations be short, as the lower extent of interaction between the casein micelles leads to a smoother texture. Single-culture strains have longer fermentation times compared to combinations of starter cultures, and this longer time can negatively impact the smooth texture and viscosity of the fortified yogurt (Sodini et al. 2002).

Ozcan et al. (2015) prepared yogurt gels using commercial starter cultures after reconstituting skim milk and adjusting to pH 6.2, 6.7, or 7.2. After heating at 85 °C for 30 min, a portion of the heated milk samples was readjusted to pH 6.7; all samples were inoculated with 3% (w/w) yogurt starter culture and incubated at 40 °C to pH 4.6. Storage moduli values at pH 4.6 were highest in gels made from milk heated at pH 6.7 and lowest in milk heated at pH 6.2, with or without pH adjustment after heating; G' values at pH 4.6 were lower in samples after adjustment back to pH 6.7 after heating. Interestingly, microstructural differences were not observed among the treatments. The authors concluded that heating milk at its natural pH (~6.7) created an optimum balance of casein-bound and soluble denatured whey proteins, which resulted in yogurt with the highest gel firmness.

Riener et al. (2010) used thermosonication to investigate the impact of combining homogenization and pasteurization into a single unit operation on yogurt characteristics. Preheated (45 °C) milk with varying levels of fat (0.1%, 1.5% and 3.5%) was thermosonicated for 10 min at an ultrasound frequency of 24 kHz (400 W) and compared to control yogurts produced from conventionally heated milk (90 °C for 10 min). Yogurts from the thermosonicated milks had higher firmness, higher water-holding capacity, and lower syneresis. Preference tests (n = 30 consumers) revealed that panelists preferred the texture of the thermosonicated yogurts, indicating promise for the technology.

To more closely examine the impact of ultrasound on gel formation, Madadlou et al. (2010) conducted dual-frequency sonication on casein solutions (3% casein in 0.5 M phosphate buffer) to acidification. Model casein gels were prepared from solutions sonicated with 24 (low frequency or power ultrasound) and 130 kHz (medium frequency or sonochemical ultrasound) for 0, 60, or 120 min, followed by acidification with GDL (0.23 g GDL/g casein) at 30 °C. Sonication of casein solutions increased gelation time, postponing the gelation point to a lower pH, and increased the firmness and solid-like behavior of freshly-formed gels. Microstructural images revealed gels made with dual-frequency sonication had more interconnected microstructures and smaller non-distinguishable particulates, particularly for the gel made from the solution sonicated for 120 min. Madadlou et al. (2010) concluded that dual-frequency sonication may be an option for increasing the firmness of fat-free and low-fat yogurts that suffer from weak body and poor texture.

5.2 Yogurt Fermentation

Standard conditions for yogurt fermentation are meant to promote the metabolism of *S. thermophilus* and *L. bulgaricus*, which thrive at ~42 °C and 37 °C, respectively. The most vital part of yogurt production is the fermentation of lactose to lactic acid by the starter cultures. This production of acid decreases the yogurt mix pH and hence forms the gel. During fermentation, flavor compounds are produced that impart characteristic flavor to yogurt, such as acetaldehyde and lactic acid. The final characteristics of yogurt depend on the various factors during the fermentation process, which include fermentation temperature, starter culture selection (e.g. species and subspecies), and yogurt mix composition and treatment.

Lee and Lucey (2006) studied structure–function relationships between the initial yogurt gels and stirred yogurts made from these gels. Yogurt gels were made from milk preheated at 75 or 85 °C for 30 min, inoculated at 2%, and incubated at 32, 38, or 44 °C; then the gels were sheared at 5 s^{-1} for 1 min to make stirred yogurts. Gelation time decreased and pH at gelation increased when heating and incubation temperatures were increased. Set yogurt preheated at 85 °C had branched and cross-linked microstructures, while those preheated at 75 °C exhibited thinner strands and clusters in the protein network. Furthermore, the yogurts with lower heat treatment during pasteurization had higher oral viscosity and lower chalkiness in sensory tests (n = 10 trained panelists). Set yogurts incubated at 32 °C had more interconnected protein structure than the set yogurts incubated at 38 or 44 °C. Stirred yogurts exhibited much more dense protein aggregates, likely because stirring destroyed the initial network, yielding subsequent formation of weak aggregates. Tighter, interconnected structures were associated with higher firmness. Lee and Lucey (2006) concluded that the structure of the initial gel network as well as the structural breakdown process had a major impact on the physical and sensory attributes of stirred yogurts: initially weak protein networks produced weak stirred yogurts. Higher preheating temperature and lower incubation temperature resulted in higher values of apparent viscosity, G', oral viscosity, and sensory mouthcoating and smoothness for both set and stirred yogurts.

Because milk pH influences the amount of casein-bound, insoluble colloidal calcium phosphate (CCP), Peng et al. (2009) hypothesized that varying fermentation time would influence the rate and extent of solubilization of CCP during any subsequent gelation process. Yogurt base milk pH was varied to pH values ranging from 6.55 to 5.65 by pre-acidification with GDL for 4 hr at 40 °C. The fermentation time, or time to reach pH 4.6 from the initial pH, was also varied from 250 to 500 min by adding various amounts of culture at 40 °C. Pre-acidification increased the solubilization of CCP, increased the early loss of CCP crosslinks, and produced weak gels. Longer fermentation times resulted in greater loss of CCP at the pH of gelation, increased the possibility of greater casein rearrangements, and likely contributed to the increase in whey separation. Fluorescence micrographs revealed that the yogurt gels made with low pre-acidification pH values or long fermentation times had larger clusters and fewer interconnections; gels tended to be weak and had higher whey separation. On the other hand, higher pre-acidification pH values or short fermentation times yielded gels with more branching, greater interconnectivity, and a finer network structure. From these results, Peng et al. (2009) noted that pre-acidification was not recommended for the yogurt industry.

5.3 Yogurt Storage, Handling, and Sensory Evaluation

Over the years, in an effort to increase shelf-life, the viability of yogurt bacteria during storage has been studied. However, few published studies have focused on the impact of storage on the rheological and textural properties of yogurt. In yogurt, pH decreases during refrigerated storage because of the residual metabolic activity of the starter cultures (Marafon et al. 2011). This change in pH can negatively impact the structure of the yogurt gel, leading to breakdown of yogurt structure and typically an increase in syneresis.

Surprisingly, little post-acidification was noted in set-type yogurts made with whole and skim milk stored at 10 °C for 91 d (Salvador and Fiszman 2004). In addition, Salvador and Fiszman (2004) investigated the sensory, biochemical, and textural changes during accelerated (20 and 30 °C) and refrigerated (10 °C) storage of set-style yogurts compared to fresh samples. Syneresis was evident after 1 day of storage, particularly for yogurts stored at 30 °C, which exhibited the most syneresis throughout storage. Firmness increased significantly with storage at all three temperatures, and nonfat yogurt had higher firmness values. Sensory analysis on yogurts at 10 °C revealed that most changes occurred in the first week of storage; subsequent changes were less noticeable. Nonfat yogurt samples that were stored for long times had highest syneresis, and sensory firmness, maintenance of shape, chalky mouthfeel. Higher firmness, astringency, and chalky mouthfeel were associated with lower consumer acceptability scores. Salvador and Fiszman (2004) concluded that data collected at the three storage temperatures could serve as good predictors for physical characteristics of yogurt.

Instrumental analyses are more meaningful if they relate to consumer acceptability of products, so ensuring that instrumental and sensory measures align is a major area of focus in the literature. Harte et al. (2007) found that yield stress significantly correlated ($p < 0.001$) with sensory initial firmness perceived by trained panelists in both laboratory-made and retail yogurts. Apparent residual stress was significantly correlated with sensory viscosity for retail yogurts. Yogurt yield stress had more power than apparent residual stress to detect differences in initial firmness. Thus, not only were fewer samples required for evaluation, but yield stress was considered a good predictor of the sensory initial firmness perceived by panelists. Harte et al. (2007) noted that the use of yield stress as a sensory predictor could reduce the need for training panelists and conducting sensory panels and could offer the potential to manufacture yogurts with targeted yield stress and viscosity properties.

Tribology, the study of friction, lubrication, and wear, has recently emerged as an extension of rheology. It is a method that has been used to explain the lubrication behavior between oral surfaces while eating a food (Prakash et al. 2013; Sonne et al. 2014). In a typical friction test, a stainless steel ball represents the palate and a elastomer pad, such as styrene butadiene rubber, with a regularly structured surface simulates the roughness, softness, and deformability of a human tongue (Sonne et al. 2014). Sonne et al. (2014) evaluated the effects of fat, protein, and casein to whey protein ratio on the lubricating behaviors of stirred yogurt and related those behaviors to sensory properties, including graininess, viscosity, and creaminess. A decrease in friction (and sensory graininess) was associated with decreased proportion of whey protein and increased fat and protein level. These yogurts were also perceived as creamier. Sonne et al. (2014) noted that because of the complexity of the eating experience, the predictive ability of in-mouth viscosity and in-mouth creaminess was improved by combined assessments of rheological, particle size, and tribological characteristics compared to each individual instrumental measurement. Further, they suggested that greater understanding of the key drivers for creaminess would allow food manufacturers to develop reduced-fat dairy products without compromising sensory properties.

More recently, Nguyen et al. (2017) evaluated the effect of different hydrocolloids on texture, syneresis, rheology, tribology, and sensory texture and mouthfeel of set yogurts. Gelatin (0.5–1.5%), xanthan gum (0.005–0.015%), carrageenan (0.01–0.08%), and modified starch (0.5–1.5%) were incorporated into yogurts with 0.1, 1.3, and 3.8% fat. In general dispersion of fat particles within the protein network reduced gel strength. Full fat yogurt had lower viscoelastic moduli values than nonfat yogurt, and less syneresis and increased lubrication ability than reduced-fat and nonfat yogurts. Addition of gelatin to the yogurt formulations reduced syneresis and increased viscosity, gel strength and lubrication properties of the nonfat yogurt. These yogurts also had the same sensory scores for thickness, smoothness and creaminess as full-fat yogurt. Both xanthan gum and carrageenan increased the firmness and viscosity of nonfat yogurt but also significantly increased syneresis and chalkiness and lumpiness attributes. On the other hand, modified starch slightly improved the lubrication properties and sensory thickness of nonfat yogurt without significant changes in chalkiness or lumpiness.

6 Opportunities for Future Research

Yogurt is, and will likely continue to be, one of the most beloved dairy products in the world, in large part because of the multitude of styles, flavors, and rheological properties available to consumers. Moreover, as consumers are becoming more health conscious, consumption of low-fat, probiotic, and prebiotic yogurts is expected to continue and potentially expand. Although a great deal of literature is available about yogurt rheological properties and their ability to indicate sensory textures, some gaps remain and are worthy of research attention:

1. Most literature studies have investigated rheological properties during a relatively short shelf life, up to 30 d. Since commercial shelf life could be from 60 d to perhaps up to 120 d, depending on the product and temperature of storage, the impact of longer storage on rheological behavior of semisolid foods needs to be investigated. Shelf-stable yogurt, which is common in China and other populous countries, was not covered in this chapter. However, with shelf life of these prod-

ucts extending up to a year, changes in the rheological properties of shelf-stable yogurt are worthy of investigation.

2. Currently, there is a lack of robust methods to characterize the structure and rheology of semisolid foods in the primary package. The ability to characterize fundamental rheological behaviors of yogurt without disturbing its structure would be convenient in quality assurance, particularly when comparing results among different laboratories. Development of non-destructive methods will be helpful to characterize the effect of formulation, processing and storage conditions, as well as package shape and size, on the properties of the product during storage.
3. There is little information connecting the rheological behavior of semisolid foods to their micro- and nano-scale structural elements using advanced microscopic and spectroscopic techniques. Such information would be helpful in creating a fundamental understanding of rheology and building mechanistic models of rheological changes during storage.

References

Abou-Soliman, N. H. I., Sakr, S. S., & Awad, S. (2017). Physico-chemical, microstructural and rheological properties of camel-milk yogurt as enhanced by microbial transglutaminase. *Journal of Food Science and Technology, 54*(6), 1616–1627.

Al-Zoreky, N. S., & Al-Otaibi, M. M. (2015). Suitability of camel milk for making yogurt. *Food Science and Biotechnology, 24*(2), 601–606.

Amatayakul, T., Halmos, A. L., Sherkat, F., & Shah, N. P. (2006). Physical characteristics of yoghurts made using exopolysaccharide-producing starter cultures and varying casein to whey protein ratios. *International Dairy Journal, 16*, 40–51.

Bakirci, S., Dagdemir, E., Boran, O. S., & Hayaloglu, A. A. (2017). The effect of pumpkin fibre on quality and storage stability of reduced-fat set-type yogurt. *International Journal of Food Science and Technology, 52*, 180–187.

Benezech, T., & Maingonnat, J. F. (1994). Characterization of rheological properties of yoghurt – A review. *Journal of Food Engineering, 21*, 447–472.

Bhullar, Y., Uddin, M. A., & Shah, N. (2002). Effects of ingredients supplementation on textural characteristics and microstructure of yoghurt. *Milchwissenschaft, 57*(6), 328–332.

Bong, D. D., & Moraru, C. I. (2014). Use of micellar casein concentrate for Greek-style yogurt manufacturing: Effects on processing and product properties. *Journal of Dairy Science, 97*, 1259–1269.

Boubellouta, T., Galtier, V., & Dufour, E. (2011). Structural changes of milk components during acid-induced coagulation kinetics as studied by synchronous fluorescence and mid-infrared spectroscopy. *Applied Spectroscopy, 65*(3), 284–292.

Broadbent, J. R., McMathon, D. J., Welker, D. L., Oberg, C. J., & Moineau, S. (2003). Biochemistry, genetics, and applications of exopolysaccharide production in Streptococcus thermophilus: A review. *Journal of Dairy Science, 86*, 407–423.

Cerning, J. (1995). Production of exocellular polysaccharides by lactic acid bacteria and dairy propionibacteria. *Le Lait, 75*, 463–472.

Chandan, R. C. (2006). Chapter 1: History and consumption trends. In R. C. Chandan, C. H. White, A. Kilara, & Y. H. Hui (Eds.), *Manufacturing yogurt and fermented milks* (pp. 3–15). Ames: Blackwell Publishing.

Chandan, R. C., Gandhi, A., & Shah, N. P. (2017). Yogurt: Historical background, health benefits, and global trade. In N. P. Shah (Ed.), *Yogurt in health and disease prevention* (pp. 3–29). Cambridge, MA: Academic.

Chen, J. S., & Stokes, J. R. (2012). Rheology and tribology: Two distinctive regimes of food texture sensation. *Trends in Food Science and Technology, 25*(1), 4–12.

Conti-Silva, A. C., Ichiba, A. K. T., da Silveira, A. L., Albano, K. M., & Nicoletti, V. R. (2018). Viscosity of liquid and semisolid materials: Establishing correlations between instrumental analyses and sensory characteristics. *Journal of Texture Studies, 49*, 569–577.

Costa, M. P., Frasao, B. S., Silva, A. C. O., Freitas, M. Q., Franco, R. M., & Conte-Junior, C. A. (2015). Cupuassu (Theobroma grandiflorum) pulp, probiotic, and prebiotic: Influence on color, apparent viscosity, and texture of goat milk yogurts. *Journal of Dairy Science, 98*, 5995–6003.

Cui, B., Lu, Y. M., Tan, C. P., Wang, G. Q., & Li, G. H. (2014). Effect of cross-linked acetylated starch content on the structure and stability of set yoghurt. *Food Hydrocolloids, 35*, 576–582.

Dabija, A., Codina, G. G., Ropciuc, S., Gatlan, A.-M., & Rusu, L. (2018). Assessment of the antioxidant and quality attributes of yogurt enhanced with wild herbs extracts. *Journal of Food Quality*. https://doi.org/10.1155/2018/5329386.

Damin, M. R., Alcantara, M. R., Nunes, A. P., & Oliveira, M. N. (2009). Effect of milk supplementation with skim milk powder, whey protein concentrate and sodium caseinate on acidification kinetics, rheology properties and structure of nonfat stirred yogurt. *LWT- Food Science and Technology, 42*, 1744–1750.

De Vuyst, L., & Degeest, B. (1999). Heteropolysaccharides from lactic acid bacteria. *FEMS Microbiology Reviews, 23*, 153–177.

Dimitreli, G., Gregoriou, E. A., Kalantzidis, G., & Antoniou, K. D. (2013). Rheological properties of kefir as affected by heat treatment and whey protein addition. *Journal of Texture Studies, 44*, 418–423.

Dönmez, Ö., Mogol, B. A., & Gökmen, V. (2017). Syneresis and rheological behaviors of set yogurt containing green tea and green coffee powders. *Journal of Dairy Science, 100*, 901–907.

Gursel, A., Gursoy, A., Anli, E. A. K., Budak, S. O., Aydemir, S., & Durlu-Ozkaya, F. (2016). Role of milk protein–based products in some quality attributes of goat milk yogurt. *Journal of Dairy Science, 99*, 2694–2703.

Graveland-Bikker, J. F., & Anema, S. G. (2003). Effect of individual whey proteins on the rheological properties of acid gels prepared from heated skim milk. *International Dairy Journal 13*, 401–408.

González-Martınez, C., Becerra, M., Cháfer, M., Albors, A., Carot, J. M., & Chiralt, A. (2002). Influence of substituting milk powder for whey powder on yoghurt quality. *Trends in Food Science and Technology, 13*, 334–340.

Harte, F., Clark, S., & Barbosa-Canovas, G. V. (2007). Yield stress for initial firmness determination on yogurt. *Journal of Food Engineering, 80*, 990–995.

Hassan, A. N., Frank, J. F., Schmidt, K. A., & Shalabi, S. I. (1996). Textural properties of yogurt made with encapsulated nonropy lactic cultures. *Journal of Dairy Science, 79*, 2096–2103.

Hassan, A. N., Ipsen, R., Janzen, T., & Qvist, K. B. (2003). Microstructure and rheology of yogurt made with cultures differing only in their ability to produce exopolysaccharides. *Journal of Dairy Science, 86*, 1632–1638.

Hematyar, N., Samarin, A. M., Poorazarang, H., & Elhamirad, A. H. (2012). Effect of gums on yogurt characteristics. *World Applied Sciences Journal, 20*(5), 661–665.

Hill, D., Ross, R. P., Arendt, E., & Stanton, C. (2017). Microbiology of yogurt and bio-yogurts containing probiotics and prebiotics. In N. P. Shah (Ed.), *Yogurt in health and disease prevention* (pp. 69–85). Cambridge, MA: Academic.

Hoppert, K., Zahn, S., Jänecke, L., Mai, R., Hoffman, S., & Rohm, H. (2013). Consumer acceptance of regular and reduced-sugar yogurt enriched with different types of dietary fiber. *International Dairy Journal, 28*, 1–7.

Isleten, M., & Karagul-Yuceer, Y. (2006). Effects of dried dairy ingredients on physical and sensory properties of nonfat yogurt. *Journal of Dairy Science, 89*, 2865–2872.

Izadi, Z., Nasirpour, A., Garoosi, G. A., & Tamjidi, F. (2015). Rheological and physical properties of yogurt enriched with phytosterol during storage. *Journal of Science and Technology, 52*(8), 5341–5346.

Jaros, D., Rohm, H., Haque, A., Bonaparte, C., & Kneifel, W. (2002). Influence of the starter culture on the relationship between dry matter content and physical properties of set-style yogurt. *Milchwissenschaft - Milk Science International, 57*, 325–328.

Khanal, S. N., & Lucey, J. A. (2017). Evaluation of the yield, molar mass of exopolysaccharides, and rheological properties of gels formed during fermentation of milk by *Streptococcus thermophilus* strains St-143 and ST-10255y. *Journal of Dairy Science, 100*, 6906–6917.

Lee, W. J., & Lucey, J. A. (2006). Impact of gelation conditions and structural breakdown on the physical and sensory properties of stirred yogurts. *Journal of Dairy Science, 89*, 2374–2385.

Lee, W. J., & Lucey, J. A. (2010). Formation and physical properties if yogurt. *Asian-Australasian Journal of Animal Sciences, 23*(9), 1127–1136.

Liu, L., Li, C., & Liu, J. (2017). Rheological and physical characteristics of on-fate set yogurt prepared with EPS-producing *Streptococcus thermophilus* and an H^+-ATPase-defective mutant *Lactobacillus delbrueckii* subsp. b*ulgaricus*. *International Journal of Food Properties, 20*(4), 745–753.

Lobato-Calleros, C., Ramírez-Santiago, E., Vernon-Carter, J., & Alvarez-Ramirez, J. (2014). Impact of native and chemically modified starches addition as fat replacers in the viscoelasticity of reduced-fat stirred yogurt. *Journal of Food Engineering, 131*, 110–115.

Low, D., Ahlgren, J. A., Horne, D., McMahon, D. J., Oberg, C. J., & Broadbent, J. R. (1998). Role of *Streptococcus thermophilus* MR-1C capsular exopolysaccharide in cheese moisture retention. *Applied and Environmental Microbiology, 64*, 2147–2151.

Lubbers, S., Decourcelle, N., Vallet, N., & Guichard, E. (2004). Flavor release and rheology behavior of strawberry fat free stirred yogurt during storage. *Journal of Agricultural and Food Chemistry, 52*, 3077–3085.

Lucy, J. A., & Singh, H. (1997). Formation and physical properties of acid milk gels: A review. *Foodservice Research International, 30*(7), 529–542.

Madadlou, A., Emam-Djomeh, Z., Mousavi, M. E., Mohamadifar, M., & Ehsani, M. (2010). Acid-induced gelation behavior of sonicated casein solutions. *Ultrasonics Sonochemisry, 17*, 153–158.

Marafon, A. P., Sumi, A., Granato, D., Alcântara, M. R., Tamime, A. Y., & de Oliveira, M. N. (2011). Effects of partially replacing skimmed milk powder with dairy ingredients on rheology, sensory profiling, and microstructure of probiotic stirred-type yogurt during cold storage. *Journal of Dairy Science, 94*, 5330–5340.

Mathias, R. R. D. S., de Carvalho, I. C., de Carvalho, C. W. P., & Sérvulo, E. F. C. (2011). Rheological characterization of collee-flavored yogurt with different types of thickener. *Alim. Nutr. Araraquara., 22*, 521–529.

Meletharayil, G. H., Patel, H. A., Metzger, L. E., Marella, C., & Huppertz, T. (2018). Influence of partially demineralized milk proteins on rheological properties and microstructure of acid gels. *Journal of Dairy Science, 101*, 1864–1871.

Morell, P., Hernando, I., Llorca, E., & Fiszman, S. (2015). Yogurts with an increased protein content and physically modified starch: Rheological, structural, oral digestion and sensory properties related to enhanced satiating capacity. *Foodservice Research International, 70*, 64–73.

Mottar, J., Bassier, A., Joniau, M., & Baiert, J. (1989). Effect of heat induced association of whey protein and casein micelles on yoghurt texture. *Journal of Dairy Science, 72*(9), 2247–2256.

Mudgil, D., Barak, S., & Khatkar, B. S. (2017). Texture profile analysis of yogurt as influenced by partially hydrolyzed guar gum and process variables. *Journal of Food Science and Technology, 54*(12), 3810–3817.

Nguyen, P. T. M., Kravchuk, O., Bhandari, B., & Prakash, S. (2017). Effect of different hydrocolloids on texture, rheology, tribology and sensory perception of texture and mouthfeel of low-fat pot-set yoghurt. *Food Hydrocolloids, 72*, 90–104.

Ozcan, T., Horne, D. S., & Lucey, J. A. (2015). Yogurt made from milk heated at different pH values. *Journal of Dairy Science, 98*, 6749–6758.

Pang, Z., Deeth, H., & Bansal, N. (2015). Effect of polysaccharides with different ionic charge on the rheological, microstructural and textural properties of acid milk gels. *Food Research International, 72*, 62–73.

Pang, Z., Deeth, H., Prakash, S., & Bansal, N. (2016). Development of rheological and sensory properties of combinations of milk proteins and gelling polysaccharides as potential gelatin replacements in the manufacture of stirred acid milk gels and yogurt. *Journal of Food Engineering, 169*, 27–37.

Peng, Y., Horne, D. S., & Lucey, J. A. (2009). Impact of preacidification of milk and fermentation time on the properties of yogurt. *Journal of Dairy Science, 92*, 2977–2990.

Prakash, S., Tan, D. D. Y., & Chen, Y. (2013). Applications of tribology in studying food oral processing and texture perception. *Foodservice Research International, 54*, 1627–1635.

Prasanna, P. H. P., Grandison, A. S., & Charalampopoulos, D. (2013). Microbiological, chemical and rheological properties of low fat set yoghurt produced with exopolysaccharide (EPS)producing *Bifidobacterium* strains. *Food Research International, 51*, 15–22.

Ramchandran, L., & Shah, N. P. (2009). Effect of exopolysaccharides and inulin on the proteolytic, angiotensin-I-converting enzyme- and α-glucosidase-inhibitory activities as well as on textural and rheological properties of low-fat yogurt during refrigerated storage. *Dairy Science and Technology, 89*(6), 583–600.

Ramchandran, L., & Shah, N. P. (2010). Characterization of functional. Biochemical and textural properties of symbiotic low-fat yogurts during refrigerated storage. *LWT- Food Science and Technology, 43*, 819–827.

Rawson, H. L., & Marshall, V. K. (1997). Effect of 'ropy' strains of L*actobacillus delbrueckii* ssp. *bulgaricus* and *Streptococcus thermophilus* on rheology of stirred yogurt. *International Journal of Food Science and Technology, 32*, 213–220.

Remeuf, F., Mohammed, S., Sodini, I., & Tissier, J. P. (2003). Preliminary observations on the effects of milk fortification and heating on microstructure and physical properties of stirred yogurt. *International Dairy Journal, 13*, 773–782.

Riener, J., Noci, F., Cronin, D. A., Morgan, D. J., & Lyng, J. G. (2010). A comparision of selected quality characteristics of yogurts prepared from thermosonicated and conventionally heated milks. *Food Chemistry, 119*, 1108–1113.

Sah, B. N. P., Vasiljevic, T., McKechnie, S., & Donkor, O. N. (2016). Physicochemical, textural and rheological properties of probiotic yogurt fortified with fibre-rich pineapple peel powder during refrigerated storage. *LWT- Food Science and Technology, 65*, 978–986.

Saleh, M., Al-Baz, F., & Al-Ismail, K. (2018). Effects of hydrocolloids as fat replacers on the physicochemical properties of produced labneh. *Journal of Texture Studies, 49*, 113–120.

Salih, M. M., & Hamid, O. I. A. (2013). Effect of fortifying camel's milk with skim milk powder on the physicochemical, microbiological and sensory characteristics of set yoghurt. *Advance Journal of Food Science and Technology, 5*, 765–770.

Salvador, A., & Fiszman, S. M. (2004). Textural and sensory characteristics of whole and skimmed flavored set-type yogurt during long storage. *Journal of Dairy Science, 87*, 4033–4041.

Santillan-Urquiza, E., Mendez-Rojas, M. A., & Velez-Ruiz, J. F. (2017). Fortification of yogurt with nano and micro sized calcium, iron and zinc, effect on the physicochemical and rheological properties. *LWT- Food Science and Technology, 80*, 462–469.

Sengul, M., Erkaya, T., Sengul, M., & Yildiz, H. (2014). An investigation of the antioxidant activities and some physicochemical characteristics of strawberry added yogurt. *Italian Journal of Food Science, 26*, 235–242.

Sodini, I., Lucas, A., Oliveira, M. N., Remeuf, F., & Corrieu, G. (2002). Effect of milk base and starter culture on acidification, texture, and probiotic cell counts in fermented milk processing. *Journal of Dairy Science, 85*(10), 2479–2488.

Sonne, A., Gusch-Stockfisch, M., Weiss, J., & Hinrichs, J. (2014). Improved mapping of in-mouth creaminess of semi-solid dairy products by combining rheology, particle size, and tribology data. *LWT- Food Science and Technology, 59*, 342–347.

Stokes, J. R., & Frith, W. J. (2008). Rheology of gelling and yielding soft matter systems. *Soft Matter, 4*, 113–1140.

Szczesniak, A. S. (2002). Texture is a sensory property. *Food Quality and Preference, 13*, 215–225.

Tang, H. B., Qu, Y. F., Li, Y. P., & Dong, S. Q. (2018). Surface modification mechanism of cross-linking and acetylation, their influence on characteristics of high amylose corn starch. *Journal of Food Science, 83*(6), 1533–1541.

Teles, C. D., & Flores, S. H. (2007). The influence of additives on the rheological and sensory properties of nonfat yogurt. *International Journal of Dairy Technology, 60*(4), 270–276.

Tribby, D. (2008). Yogurt. In *The sensory evaluation of dairy products* (pp. 191–223). New York: Springer.

USDA-ERS (U.S. Department of Agriculture, Economic Research Service). (2018). Dairy data. Accessed on 8 Nov 2018 from https://www.ers.usda.gov/data-products/dairy-data/.

USFDA (U.S. Food & Drug Administration). (2018). Code of Federal Regulations. Title 21. Part 131. Sec. 131.200. Yogurt. Available at: https://www.accessdata.fda.gov/scripts/cdrh/cfdocs/cfcfr/cfrsearch.cfm?fr=131.200. Date Accessed 21 March 2019.

Wacher-Rodarte, C., Galvin, M. V., Farres, A., Gallardo, F., Marshall, V. M. E., & Garcia-Garibay, M. (1993). Yogurt production from reconstituted skim milk using different polymer and non-polymer forming starter cultures. *The Journal of Dairy Research, 60*, 247–254.

Yu, H.-Y., Wang, L., & McCarthy, K. L. (2016). Characterization of yogurts made with milk solids nonfat by rheological behavior and nuclear magnetic resonance spectroscopy. *Journal of Food and Drug Analysis, 24*, 804–812.

Zhao, L. L., Wang, X. L., Tian, Q., & Mao, X. Y. (2016). Effect of casein to whey protein ratios on the protein interactions and coagulation properties of low-fat yogurt. *Journal of Dairy Science, 99*, 7768–7775.

Zisu, B., & Shah, N. P. (2003). Effects of pH, temperature, supplementation with whey protein concentrate, and adjunct cultures on the production of exopolysaccharides by *Streptococcus thermophilus* 1275. *Journal of Dairy Science, 86*, 3405–3415.

Sensory and Oral Processing of Semisolid Foods

Tugba Aktar, Rituja Upadhyay, and Jianshe Chen

1 Food Texture: Solids, Semisolids and Liquids

Food texture comprises a highly complicated set of sensory attributes perceived by consumers during food consumption. It determines the way food is handled during the eating process and plays a critical role in influencing consumers' eating experience as well as their preference for a given food product. There have been many definitions of food texture, but the most-accepted definition is probably the one proposed by Szczesniak, one of the pioneers of food texture research. Szczesniak defined food texture as the "sensory manifestation of the structure of food and the manner in which this structure reacts to the forces applied during handling and, in particular, during consumption" (Szczesniak 1963). This definition includes mechanical, tactile, visual, and auditory perception of the texture perceived by the assessors. Table 1 summarizes common textural features of semisolid and solid foods and their corresponding physical parameters and sensory terminologies. While most of the sensory parameters are applicable to semisolid foods, some textural attributes such as "crumbly", "crunchy", and "brittle" are mostly used for brittle solid foods. However, some highly elastic semisolid foods (e.g. soft gelatin gels) may also show brittleness, or sharp fracture upon compression, because these foods normally fracture rather than flow under applied stress or strain.

Fluid foods tend to use notably different texture terminology largely because of their different mechanisms of oral manipulation and texture sensation compared to semisolid and solid foods. Fluid foods flow and spread readily inside the mouth.

T. Aktar
Faculty of Engineering, Food Engineering Department, Alanya Alaaddin Keykubat University, Antalya, Turkey

R. Upadhyay · J. Chen (✉)
Food Oral Processing Laboratory, School of Food Science and Biotechnology, Zhejiang Gongshang University, Hangzhou, People's Republic of China
e-mail: jschen@zjgsu.edu.cn

H. S. Joyner (ed.), *Rheology of Semisolid Foods*, Food Engineering Series,
https://doi.org/10.1007/978-3-030-27134-3_8

Table 1 Textural characterization of semisolids and solids

Sample characteristics	Primary parameters	Secondary parameters	Popular terminology
Mechanical characteristics	Firmness		Soft, hard, film
		Brittleness	Crumbly, crunchy, brittle
		Chewiness	Tender, chewy, tough
	Cohesiveness		Short, mealy, pasty
	Viscosity	Gumminess	Thin, viscous, gummy
	Springiness		Plastic, elastic
	Adhesiveness		Sticky, tacky, gooey
Geometrical characteristics	Particle size and shape		Gritty, grainy, coarse
	Particle orientation		Fibrous, cellular, crystalline
Other characteristics	Moisture content		Dry, moist, wet, watery
	Fat content	Oiliness Greasiness	Oily Greasy

Szczesniak and Kleyn (1963)

They do not require teeth for mastication; tongue compression and pushing is what normally needed for the consumption of a fluid food (Aktar et al. 2015). Table 2 summarizes sensory terminology for fluids as has been previously developed by Szczesniak (1979). From the table, flowability and spreadability are probably the two most important associated rheological and mechanical properties. These parameters are also important for semisolid foods that are manipulated using mainly the tongue and soft palate, such as yogurt, custard, pudding, sour cream, and peanut butter. In fact, many studies on semisolid food texture develop a descriptive sensory lexicon for the foods of interest that combines selected texture attributes from both solid and fluid foods, such as viscosity, smoothness, mouthcoat, firmness, grittiness, and graininess. The use of this type of lexicon is illustrated in Chapters "The Impact of Formulation on the Rheological, Tribological, and Microstructural Properties of Acid Milk Gels" and "Relationships Among Acid Milk Gel Sensory, Rheological, and Tribological Behaviors", which include the results of a descriptive sensory analysis study on stirred acid milk gels and yogurts, respectively.

In general, viscoelasticity is probably the core rheological property that impacts the majority of texture features of semisolid foods. Therefore, there had been considerable effort to link semisolid food rheological behaviors with their sensory texture attributes. Recently, the thin-layer and lubrication properties have also been recognized as highly important for the oral sensory perception of fluid foods (Chen and Stokes 2012). Accordingly, the use of oral tribology (lubrication behaviour of food) together with fluid rheology and sensory studies has become an important approach for texture interpretation of fluid as well as some semisolid foods. Chapters "Relationships Among Semisolid Food Microstructures, Rheological Behaviors, and Sensory Attributes", "The Impact of Formulation on the Rheological, Tribological, and Microstructural Properties of Acid Milk Gels" and "Relationships Among Acid Milk Gel Sensory, Rheological, and Tribological Behaviors" provide

Table 2 Classification of textural properties for liquid foods (Szczesniak 1979)

Category	Popular terminology
Viscosity-related	Thin, thick, viscous
Feeling on soft tissue surfaces	Smooth, pulpy, creamy
Carbonation-related	Bubbly, tingly, foamy
Body-related	Heavy, watery, light
Chemical effects	Astringent, sharp
Oral coating	Mouth coating, clinging, fatty, oily
Resistance to tongue movement	Slimy, syrupy, pasty
Afterfeel (mouth)	Sticky
Afterfeel (physiological)	Clean, drying, lingering, cleansing
Temperature-related	Cold, hot
Wetness-related	Wet, dry

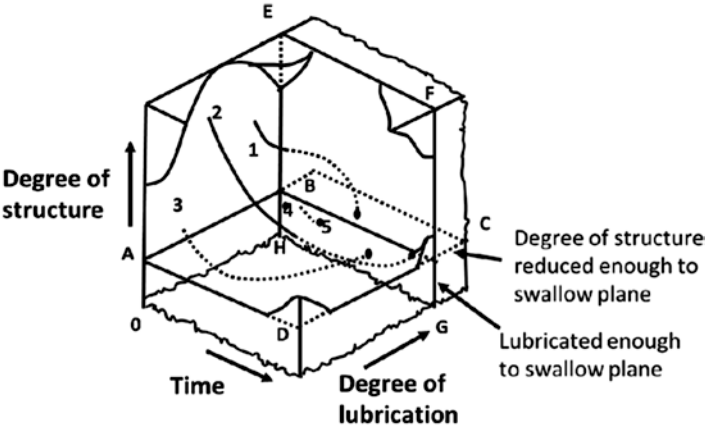

Fig. 1 Illustration of the three-degree food breakdown model for solid and semisolid food during mastication produced by Hutchings and Lillford (1988)

a series of studies on acid milk gels and yogurts that take this approach towards understand semisolid food texture behaviors in terms of their rheological and tribological properties.

As introduced by Hutchings & Lillford (1988) in the late 1980s, texture perception is a dynamic phenomenon due to the continuous processing of food and the changes in its properties during the eating process. Thus, foods with different microstructures and compositions can have notably different breakdown pathways. Furthermore, a minimum level of lubrication is essential for food bolus formation and swallowing (Fig. 1). In this model, the degree of structure, degree of lubrication, and oral processing time are considered to be the primary controlling factors of oral processing of semisolid and solid foods. This model gives a superb description of the dynamic nature of food oral breakdown in terms of particle size change and saliva secretion and incorporation. It is still widely in use to provide insight into how altering the microstructure or composition of food alters the required extent of oral movements and duration of oral processing before swallowing.

2 Oral Processing: Food Deconstruction in the Mouth

Oral processing is a relatively new area of research in food science. It quickly gained popularity in the early twenty-first century because it opened up great possibilities for manipulating food design to create controlled patterns of oral breakdown and desirable mouthfeel. The area of oral processing research includes food physics, oral physiology, sensory psychology, and neural science. While extensive studies have been conducted on food physics and oral physiological responses, research on sensory mechanisms and related neural activities is relatively limited. Work in these areas is needed because there are an enormous array of different texture sensation mechanisms at different stages of oral processing, starting at pre-mastication when the food is brought to the mouth, during mastication and bolus formation, and after bolus swallowing (Fig. 2).

Encouragingly, the growing body of research in food oral processing has led to the development of new techniques to study bolus swallowing using relevant sensory approaches in healthy and dysphagic adults. Bolus swallowing is a fast-growing research area, in particular in countries where elderly populations are steadily increasing. These populations have a higher incidence of dysphagia and other swallowing disorders that make oral processing of many foods difficult. Understanding

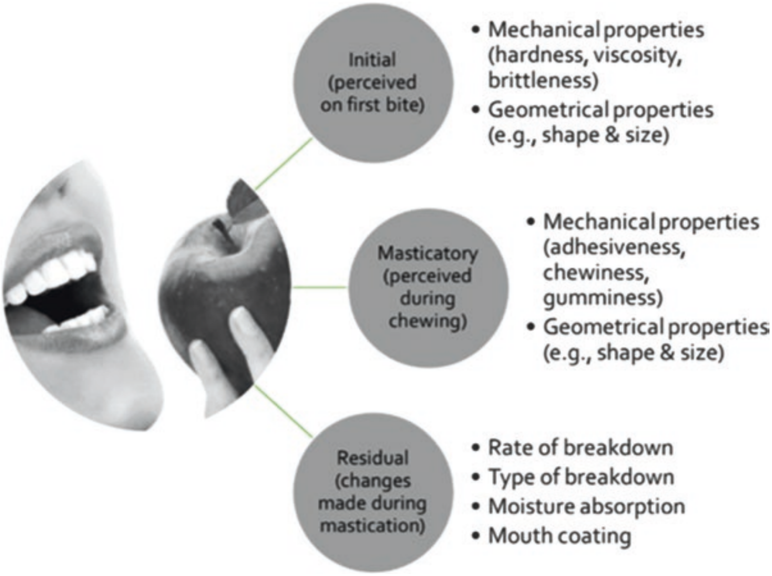

Fig. 2 Structural changes and texture sensation from original product to after bolus swallowing

the divergence from normal oral processing behavior can promote a better understanding of oral processing as a whole, as well as strategies to manipulate food textures to increase their ease of oral processing. Several studies have described the relationship between food (or food bolus) properties and oral processing behavior (Chen 2015; Foegeding et al. 2015). These studies revealed that healthy human individuals are fully capable of adapting oral movements and oral forces for food structure transformation according to the dynamic changes in food and food bolus properties during oral processing. Chewing behavior at an early stage of oral processing is influenced mainly by the composition and bulk rheological properties of the food, while the later stages of oral processing, including swallowing, are influenced mainly by the flow behaviour of the bolus and the interfacial properties (Çakır et al. 2012; Devezeaux de Lavergne et al. 2015; Koç et al. 2013, 2014; Witt and Stokes 2015).

During oral processing, however, the main challenge to food property assessment is the accessibility of the food in real time as it is chewed or palated and converted into a bolus. So far no technique is available for direct testing or imaging what happens to the food inside the mouth during an eating process. Indirect assessment by collecting bolus samples at various stages of oral processing is currently the main approach for understanding the dynamic changes to food properties and rheological behavior. The mechanical properties of the expectorated food bolus can then be determined using a texture analyzer (Devezeaux de Lavergne 2015) or a rheometer (Ishihara et al. 2011), while the particle size distribution can be determined using sieving techniques (Peyron et al. 2004), laser light diffraction (Hoebler et al. 2009), or image analysis (Hoebler et al. 2009).

Particle size distribution, saliva content, and rheological properties of the bolus at the point of swallowing have been investigated by many research groups (Engelen et al. 2005; Loret et al. 2011; Yven et al. 2010). Although these studies provide a good understanding of the final bolus properties, the evolution of bolus properties throughout mastication remains poorly understood. Peyron et al. (2011) conducted a study that analyzed the physical and sensorial properties of boluses collected at different stages of oral processing using texture profile analysis (TPA) and temporal dominance of sensations (TDS). This approach provides a way to elucidate the evolving kinetics of the food bolus as well as changes to its mechanical (textural) properties. This approach has been applied in other studies to examine food destruction during oral processing. Despite the achievements discussed above, the relationship among material properties, human texture perception, and bolus formation dynamics have yet to be thoroughly investigated and understood (Lillford 2011).

Swallowing, a simple but extraordinary task, is triggered when a food bolus reaches its “defined” state (Chen 2009). But although this view is well-supported, there is a lack of solid evidence to demonstrate what general criteria for bolus properties exist for bolus swallowing. Two very different aspects must be considered when considering bolus swallowing: human physiology and the food (bolus) properties. The crucial role of bolus physical properties has been highlighted for various foods in experiments correlating food rheological behavior to ease of swallowing (Alsanei and Chen 2014). One of the most important principles of bolus swallowing is the relationship between bolus flow properties and the swallowing capability of a given individual (Laguna and Chen 2016). There has been much effort to understand the impact of human oral physiology on differences in oral processing and bolus swallowing. This understanding will make it possible to account for inter-individual differences in swallowing and other oral processing studies.

2.1 Oral Behaviour of Semisolid Foods

Semisolid foods refer to food materials that are easily deformable and require a relatively small oral effort for oral processing and consumption (either between the teeth for size reduction and/or between the tongue and palate for compressing and deformation). During oral processing, a semisolid food absorbs the applied force until reaching its yield point, after which significant deformation and breaking will take place. For semisolid foods, the force required to reach this yield point is relatively low and can generally be achieved by palating. Therefore, most semisolid foods are palated rather than chewed. The extent and rate of semisolid food oral deformation depend primarily on its rheological properties, offering a unique textural experience to the consumers.

Semisolid foods are considered to be the most commonly consumed among all food types. An extensive range of semisolid foods are available either as processed (e.g. purees, sauces, and yogurt) or naturally available (e.g. eggs and some fruits). The texture of such foods is determined by their structure. The textural features of semisolid foods can be manipulated by controlling the size, shape, and physicochemical properties of the particle and droplets; the interfacial characteristics; and the rheological properties of the continuous phase or the gelled matrix.

Oral residence time is an important element influencing eating and sensory experience. Compared to fluid foods, such as liquid beverages, semisolid foods usually have a much longer oral residence time due to the need to form a bolus. This longer residence time offers extended sensory exposure. Even though semisolid foods usually cannot give a sharp burst of aroma and flavor release like a solid food because of the sudden increase of surface area when a solid food fractures, they offer a lasting aroma and flavor release due to its gradual mixing and kneading with saliva (e.g. cream cheese, yogurt).

Certain structural features of semisolid foods can contribute to flavor release and textural changes during oral processing. For example, the emulsion gel is a major type of semisolid food in which lipid droplets are embedded into a gel matrix either as active fillers, which interact with the matrix, or inactive fillers, which are entrapped by the matrix but do not interact with it (Chen and Dickinson 1999). The mechanical properties of gelled emulsions have been well-characterized and related to mouthfeel (Sala et al. 2007). The unique sensory feature of emulsion gel systems is the release of lipid droplets during consumption, which will not only lead to an enhanced lipid sensation on the oral surfaces but also alter the lubrication behavior in the oral cavity. In the case of droplets that are strongly associated with the gel matrix (active fillers), the release rate is determined by the melting of the gel matrix during oral processing. The release rate of unbound lipid droplets (inactive fillers) appears to depend on the size of the fragments of the shear-disrupted gel matrix.

It is important to identify the structural and physicochemical properties underlying the different sensory properties to obtain more insight into the way in which humans perceive sensory properties. Until recently, much of the research on the physicochemical properties underlying sensory perception has focused on taste and aroma (odor) characteristics. Research on the origins of texture and mouthfeel has been limited to properties such as hardness and brittleness of solid foods and perceived thickness of fluid foods. Semisolid foods, however, have a much wider possible range of texture variation; therefore, semisolid foods can be prepared with many different textures via technical manipulations of food structure design. Of all possible semisolid textural attributes, thickness, consistency, melting, smoothness, roughness, creaminess, and stickiness are probably the most relevant to semisolid food texture perception (Engelen and de Wijk 2012). The following sections will explore the underlying physical mechanisms of these textural attributes and their impacts on the oral processing and sensory perception.

2.1.1 Temporal Attribute Sensations During Oral Processing

The physical properties of semisolid foods continuously change during oral processing, which makes oral processing—and sensory perception—a dynamic process. The textural attributes that are sensed during oral processing of semisolid foods have been examined and cataloged in chronological order by de Wijk, Janssen, & Prinz (2011). Some attributes can be sensed as soon as the food is placed in the mouth, including warmness/coldness, thickness, and firmness. Sensation of other attributes may require longer oral processing time. Smoothness and creaminess are typical examples of such sensory features (de Wijk et al. 2003, 2011). van Aken et al. (2007) studied the temporal nature of certain sensory attributes in more detail and noted the chronological order of warmness/coldness, thickness, heterogeneity, creaminess, and smoothness. Thermal sensations were perceived at the first contact between the food and the outer skin of the oral cavity. Thickness sensations were sensed by the flow behavior of the food in the mouth with the help of compression forces applied by the tongue against the palate. On the other hand, heterogeneity was found to be sensed according to flow characteristics and particles after oral flow has taken place (i.e. after thickness is sensed). The sensation of creaminess normally occurred after other sensory attributes were sensed, and usually after the formation of a viscous coating on the tongue surface, more so after swallowing. Finally, smoothness sensation was perceived as the absence of small particles after the food was mixed with saliva and diluted. While this study provided insight into the order in which texture attributes may be perceived, it should be noted that the chronological order of oral sensations may vary for different food systems because of the differences in mechanical and textural characteristics of the food. Moreover, there may be individual differences in temporal oral textures due to variations in oral physiological behavior.

2.1.2 Effect of Surface and Bulk Properties on Oral Texture Sensation

The sensation of all textural attributes is directly related to oral movements. In addition, de Wijk et al. (2006) indicated that sensory attributes are linked with the surface properties of the food bolus. Therefore, the interaction capability of the food with oral tissues plays an important role in texture sensation. Furthermore, sensation of bulk attributes requires only a short amount of time but more intense oral movements, while surface attributes require longer oral processing time but less intense oral movements (de Wijk et al. 2011). This echoes the findings of van Aken et al. (2007) discussed in the previous section. For example, thickness is related to viscosity, a bulk property, and is rapidly perceived. Smoothness, on the other hand, is a surface property which takes significantly longer to perceive.

Another main factor of semisolid food texture sensation is the continuation of oral movements after bolus swallowing. This is often termed as after-feel, a sensation closely linked to mouth coating. Mouth coating is a thin layer of food–saliva mixture that covers the oral surfaces (Buettner et al. 2002). The amount and in some cases the thickness of the coating can be linked with different attributes, such as greasy, oily, creamy, and lubricating properties. The amount and thickness, as well as other properties of the oral coating, depend largely on the composition of the thin layer and the oral processing time (de Wijk et al. 2009). While it is important to understand the relationship between coating composition and sensory perception, there is not much information available in the literature at the time of publication of this book.

2.2 Tongue Movements and the Role of Saliva During Semisolid Food Oral Processing

Tongue movement plays a dominant role in the oral processing of semisolid foods. The tongue performs compression and shear by pressing the food against the hard palate while moving the food particles in lateral directions (Nicosia and Robbins 2001; van Vliet 2002). While oral deformation is predominantly shear, elements of extensional deformation have also been recognized as important, in particular during bolus swallowing (Chen and Lolivret 2011). However, the exact pattern of forces and velocities caused by oral movements is still largely unknown. In a pioneering study, Shama and Sherman (1973) showed that a wide range of shear rates could occur within the oral cavity (from below 1 s^{-1} to over 1000 s^{-1}), depending on the mechanical nature of the food. Once a bolus is swallowed, there is no longer bulk deformation but thin-layer lubrication within the oral cavity. In this case, tribology is believed to be the dominating mechanism for oral texture sensation rather than rheology. Here, oral shear and shear rates are still important, but this is because they play a role in thin-film (friction) behavior and thus friction-related sensations.

Saliva is another important factor contributing to the structural and textural alteration of semisolid foods during oral processing. The role of saliva in oral processing is multifaceted, but one of the most important roles of saliva in relation to eating and sensory perception is oral lubrication. The rate and composition of saliva secretion can be significantly influenced by food stimuli, and this may subsequently influence sensory perception, particularly the mouthfeel and afterfeel of food consumption. The tribological properties of saliva have been studied extensively, taking into consideration the various influencing factors such as the load, presence of surfactants, substrate roughness, composition, aging, and rheological behaviors (Macakova et al. 2011; Bongaerts et al. 2007; Stokes et al. 2013). These findings illustrated that the hydrophilic character of the adsorbed salivary film allows reduction of friction in the boundary regime; however, this effect is reduced at lower normal loads compared to high loads. Higher normal loads cause a gradual loss in lubrication capability (Macakova et al. 2011). In general, key factors affecting the lubrication behavior of saliva include applied load, entrainment speed, and surface roughness (Bongaerts et al. 2007). Increased surface roughness increases the friction for human saliva, where centrifugation and aging of the saliva alter the characteristic shear-thinning behavior and elasticity of the saliva, which can also impact friction behaviors (Bongaerts et al. 2007).

Surface wetting, mixing, and buffering are the main functions of saliva during food oral processing. These processes occur simultaneously with changes to the food's physicochemical properties and the formation of the food bolus. Another process occurring during food consumption is enzymatic degradation, in which salivary enzymes interact with food components and lead to the breakdown of specific molecules. For example, α-amylase exists abundantly in human saliva. This enzyme will interact with the starch-based components of the food and break them down to small sugar molecules, usually leading to a significant reduction of oral viscosity or consistency and a slightly sweet taste. The functions and impact of saliva interactions during food oral processing have been summarized by Mosca and Chen (2017) (Fig. 3).

Despite the evident role of saliva in bolus formation and its effect on bolus consistency, the incorporation of saliva in instrumental tests that measure real-time changes to food mechanical behaviors for sensory prediction has so far not been possible in any commercial device. Therefore, researchers must be careful when linking instrumental results with human sensory perception: certain sensory perceptions, such as astringency, may be highly dependent on temporal food–saliva interactions, but instrumental measurements do not capture these changes.

2.3 *Mechanoreceptors as Sensors for Textural Attributes*

All tactile sensations are perceived through various mechanoreceptors distributed under tongue surface and oral tissues. Mechanoreceptors are placed on the epidermis and dermis layers of the skin and are classified based on their functions as temporal, spatial, or frequency receptors (Klatzky et al. 2003). Temporal mechanoreceptors are activated by the continuous stimulation of the skin and have two different groups: slow-adapting and rapid-adapting. Slow-adapting receptors

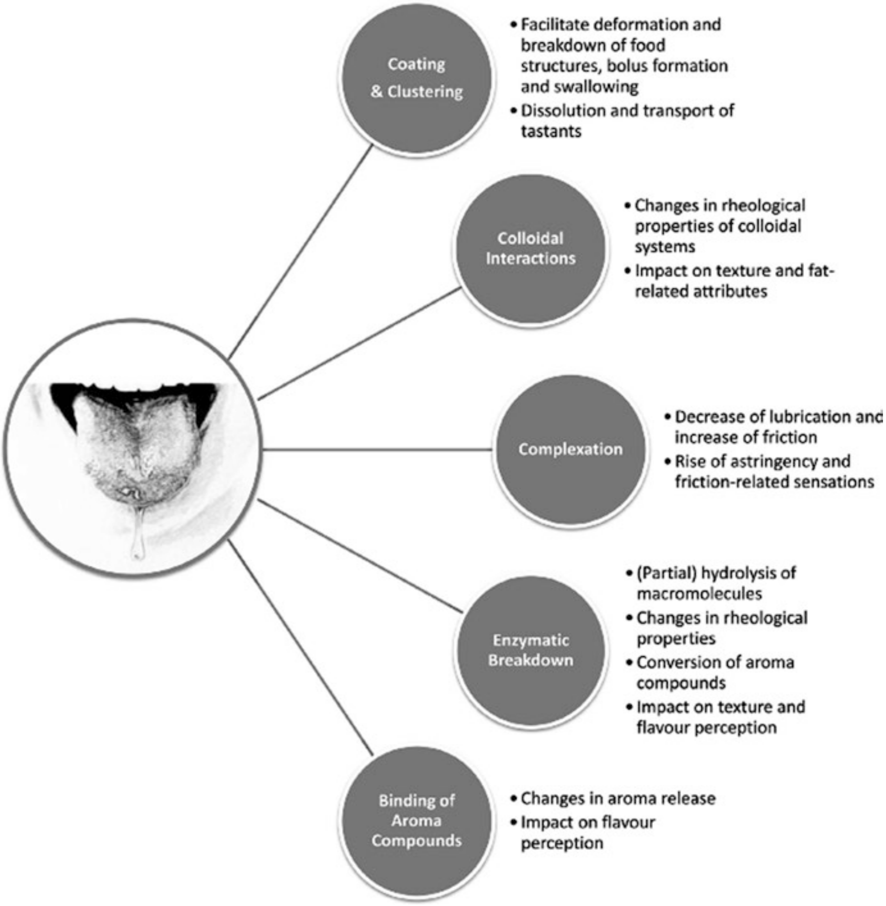

Fig. 3 Food–saliva interactions and impacts on eating and sensory perception. (Adapted from Mosca and Chen 2017)

continuously trigger the senses during stimulation. In contrast, rapid-adapting receptors fire only at the onset and offset of continuous stimulation (Tseng et al. 2009). In the oral cavity, around 35% of the mechanoreceptors have been found to be slow-adapting, which suggests that the oral cavity is more capable of detecting stimulus alteration during an eating process as compared to continuous sensing of a particular stimulus (Bukowska et al. 2010). Spatial mechanoreceptors are used to sense surface-dependent sensory attributes, such as graininess, roughness, smoothness, or lubricating effects, as well as stretching sensations or vibrations (Johnson 2001). Lastly, frequency mechanoreceptors determine the capability to sense the speed of stimulation on the skin during a particular vibration stimulus (Klatzky et al. 2003).

The mechanoreceptors located on the tongue and other oral skin surfaces show no morphological differences, but their density varies at different locations (Capra 1995; Trulsson and Johansson 2002). The hard and soft palates, tongue, and gums are considered to be the predominant locations for texture sensation through mechanoreceptors. On the other hand, mechanoreceptors under the periodontal membrane are responsible for precise detection of the force needed for fracturing both semisolid or solid foods between the opposing teeth (Boyar and Kilcast 1986). The receptors in the muscles and tendons in the jaw are responsible for regulating the speed of jaw movement (Gordon and Ghez 1991). Therefore, the dominant and active receptors for texture sensation are actually dependent on food type. For instance, texture sensation of solid foods would involve mechanoreceptors at all three locations, whereas texture sensation of semisolid foods would involve the hard and soft palates, tongue, and gums because manipulation of semisolid foods relies primarily on tongue movement (Kutter et al. 2011). However, one should keep in mind that the mechanoreceptors, regardless of their location, can work in a synergistic way for optimized sensation. Szczesniak (2002) also indicated that mechanoreceptors and tissues work together to perceive texture-related sensations. Signals from multiple receptors are instantly carried to the central nervous system by the trigeminal nerves for integrated sensory interpretation. While significant progress on understanding the role of mechanoreceptors in food texture perception has been made in the last several decades, further study is needed to more fully develop an overall picture of how mechanoreceptors.

3 Assessment of Food Texture Properties

3.1 Instrumental Assessment

The rheological behaviour of semisolid foods depends to a large extent on the constituents and microstructure of the food. As discussed in Chapters "Overview: Semisolid Foods" and "Rheological Testing for Semisolid Foods: Traditional Rheometry", viscosity is the most commonly used rheological measurement of fluid and semisolid food flow behavior. Viscosity is a measure of the resistance of a material to flow and is related to the amount of force, often expressed as stress, needed to deform the sample at a certain deformation rate. The viscosity profile of foods or viscosity at selected shear rates (e.g. 10 or 50 s^{-1}) are often related to various sensory attributes, such as thickness and mouthcoating. The viscoelastic properties of semisolid foods can also be measured for comparison to sensory behaviors. More detail on viscosity and viscoelastic measurements for semisolid foods is presented in Chapter "Rheological Testing for Semisolid Foods: Traditional Rheometry". Rheological measurements are widely used due to their consistent and objective nature, as well as the economical and time advantages compared to sensory evaluations. On the other hand, rheometry is an imperfect mimic of oral conditions;

therefore, it will not give a comprehensive image without a coordinating, well-designed sensory test.

While measuring the rheological behaviors of foods, especially when the aim is to understand oral processing mechanisms, it is crucial to include saliva in the instrumental tests. The chemical interactions of the saliva with the food causes a dramatic change in the food's texture attributes, which is reflected in alterations of the oral perception (Stokes 2012). Saliva is expected to cause structural changes to the bolus structure as well as dilution. Therefore, instrumental assessment requires mimicking the process of saliva addition to the food during oral processing. More importantly, salivary amylase will also contribute to the structural break-down of the starchy components and therefore "thickness" or "viscosity" will be the primarily affected texture attributes (de Wijk et al. 2006). However, integrating saliva into the experimental design is still considered to be too comlicated to be practival and the developed methods usually do not correspond with the natural mechanism of eating.

Tribometry has gained increased interest in recent years; these tests determine the friction behaviors of foods. Combining rheological and tribological tests can provide stronger insight into the determining mechanisms of oral sensation of food texture parameters than either alone. More details about semisolid food tribology is provided in Chapter "Semisolid Food Tribology".

3.1.1 Back Extrusion

The back extrusion test, an empirical test, uses a relatively simple testing geometry and method that allows for the generation of high forces for the characterization of the flow behavior of thick paste materials. In the back extrusion test, a cylindrical probe is pushed into a sample, then removed at a constant crosshead velocity. The force on the probe as it is moved is recorded. This test can be performed on food products in their original containers, allowing testing of the original, undisturbed food microstructures. However, care must be taken to perform the test using the same geometry, testing parameters, and amount of sample. Additionally, if the sample is transferred into a different container for testing, care must be taken to minimize the damage to the sample structure and not press-pack the sample into the container (i.e. increase the sample density). Furthermore, there may be issues with test accuracy for highly adhesive samples, as a vacuum can build up under the probe as it is extracted, causing measurement artifacts.

Steffe and Osorio (1987) and Osorio and Steffe (1991) tested particles or fibers suspensions in back extrusion. Using the methods described for power law fluids, they were able to use back extrusion to determine the flow behavior index and consistency coefficient for these materials. Similarly, appropriate testing speeds can be used to calculate the flow behavior index of boluses at different extents of mastication and at the point of a swallow. The kinetics of bolus formation can then be determined in a semi-quantitative manner.

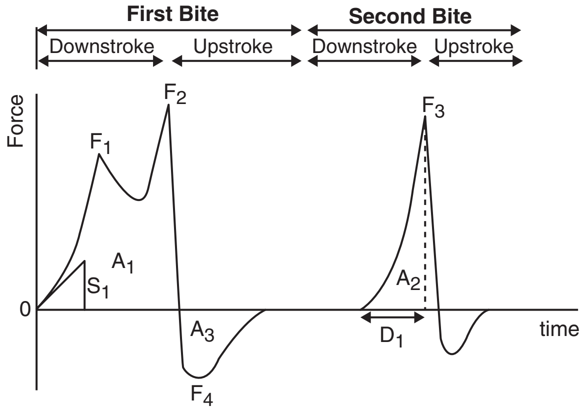

Fig. 4 Force-displacement curve from a TPA test. F_1: Fracturability, F_2: Hardness (firmness), A_2/A_1: Cohesiveness, A_3: Adhesiveness, D_1: Springiness, Gumminess: Hardness × cohesiveness, Chewiness: Hardness × cohesiveness × springiness, and S_1: Elastic modulus

3.1.2 Texture Profile Analysis (TPA)

Texture Profile Analysis (TPA) is probably the most commonly mentioned method in the literature for texture assessment of semisolid food, although it does not directly mention food texure. The method was first proposed more than a half-century ago by Friedman et al. (1963), in which the researchers used a Texturometer to perform a double compression test to obtain a set of textural features for gel-type foods. The key feature of the method is the double compression which mimics the first two bites of an eating process. The method was further promoted by Bourne some years later (Bourne 1978), who developed a systematic approach for the test conditions and texture explanation (see Fig. 4).

While the TPA method has been a landmark achievement of food texture studies and has been proved useful in many industrial applications, misuse of the method and confusion of the interpretation of its parameters are very common. Cases of TPA misuse have been discussed in detail by Bourne and Smewing (1996). Despite the fact that an expanded description of TPA analysis was later given by Bourne himself in his well-known food texture book published in 2002 (Bourne 2002), confusion of TPA analysis and data interpretation is still seen in the literature (Nishinari et al. 2013). Moreover, Corradini and Peleg (2010) have raised concerns on the scientific solidity of the defined textural parameters of TPA method. Users of TPA should carefully consider the limitations of the technique and avoid overstretching data interpretation from the method.

3.2 Sensory Evaluation

Sensory evaluation is an inseparable part of oral processing investigations. It is a crucial element for market success of the food product and consumer satisfaction. Ideally, reliable and robust instrumental assessment should correlate well to sensory evaluation, showing agreement between the two different test modalities and providing a more comprehensive explanation of food transformation during oral processing. Instrumental analyses have already been shown to be reliable, yet they are still incapable of precisely mimicking the varying oral conditions during oral processing as well as the sensory differences between individual assessors. Therefore, it is difficult for instrumental tests to induce the changes to food physicochemical properties that occur during oral processing.

Unlike instrumental assessments, sensory evaluations are still far from being economical in terms of time and expenditure. Additionally, cultural and personal differences between individuals are likely to affect the results which aim to get a description from the assessor either on numerical scales or verbal (Boyar and Kilcast 1986). Nevertheless, it is possible to overcome some of these challenges by careful design of sensory experiments, incorporation of instrumental testing to screen samples for sensory evaluation (i.e. evaluating a reduced sample set) and training panelists to minimize differences in individual sensitivity and preference.

Techniques for sensory evaluation have undergone significant development and are accepted as essesstial procedures in industry for the assessment of for taste modalities. However, we still have limited findings on textural and rheological observations in terms of sensory assessments and relation with the instrumental tests (Aktar et al. 2015, 2017). During sensory assessments, researchers generally focus on the basic 5 human senses related to the type of modality. In texture assessments of semisolid foods, the sensory experience initiates with the visual senses prior to tactile contact. After visual observation of the texture, the assessor evaluates the sample by using a tool (cutlery), picking up the food with their hands, or directly by tongue and palate depending on cultural eating habits and the type of food. It is important to note that, due to the dynamic nature of oral processing, the sample is expected to undergo catastrophic structural changes, which results in a change in the texture as well as taste and aroma (van Vliet 1999). Additionally, saliva integration into the sample initiates with the first bite, which causes modifications of the food's temperature, pH, texture, and flavor, as well as the specific perception mechanisms of these. Because food texture is dynamic and evaluated from the first sight of the food to post-swallowing, sensory evaluation of texture should measure texture at various points during consumption of the food product for a full picture of texture perception.

4 Summary

Because sensory attributes originate from the microstructure and mechanical properties of food products, texture and mouthfeel of semisolid foods exhibit a huge range of variation (Nishinari and Fang 2018). This offers food manufacturers great possibility for designing food products with desirable texture and mouthfeel that suit consumers' diverse requirements. Material properties, saliva incorporation, and human oral physiology are the three most dominant factors for the sensation and perception of food texture. Despite the usefulness of instrumental methods for food texture characterization for either quality control or prediction of consumer perception, to a certain extent, instrumental characterization only reveals the material properties of the food but not the true sensory properties. When studying food texture and relating food texture to instrumental measurements of food mechanical properties, the dynamic changes to food properties due to saliva mixing and interactions, and the variation of oral physiology among human individuals must be taken into consideration. Future food texture studies should focus more on the understanding of how the changes to food microstructure and mechanical behaviors impact texture perception during oral processing.

References

Aktar, T., et al. (2015). Evaluation of the sensory correlation between touch sensitivity and the capacity to discriminate viscosity. *Journal of Sensory Studies, 30*(2), 98–107.

Aktar, T., et al. (2017). Human roughness perception and possible factors effecting roughness sensation. *Journal of Texture Studies, 48*(3), 181–192.

Alsanei, W. A., & Chen, J. (2014). Studies of the oral capabilities in relation to bolus manipulations and the ease of initiating bolus flow. *Journal of Texture Studies, 45*(1), 1–12.

Bongaerts, J. H. H., Rossetti, D., & Stokes, J. R. (2007). The lubricating properties of human whole saliva. *Tribology Letters, 27*(3), 277–287.

Bourne, M. C. (1978). Texture profile analysis. *Food Technology, 32*, 62–66.

Bourne, M. (2002). Food texture and viscosity: concept and measurement. New York: Elsevier.

Boyar, M., & Kilcast, D. (1986). Review food texture and dental science. *Journal of Texture Studies, 17*(3), 221–252.

Buettner, A., et al. (2002). Physiological and analytical studies on flavor perception dynamics as induced by the eating and swallowing process. *Food Quality and Preference, 13*, 497–504.

Bukowska, M., Essick, G., & Trulsson, M. (2010). Functional properties of low-threshold mechanoreceptive afferents in the human labial mucosa. *Experimental Brain Research, 201*(1), 59–64.

Çakir, E., Koc, H., Vinyard, C. J., Essick, G., Daubert, C. R., Drake, M., & Foegeding, E. A. (2012). Evaluation of texture changes due to compositional differences using oral processing. *Journal of texture studies, 43*(4), 257–267.

Capra, N. (1995). Mechanisms of oral sensation. *Dysphagia, 10*(4), 235–247.

Chen, J. (2009). Food oral processing—A review. *Food Hydrocolloids, 23*(1), 1–25

Chen, J. (2015). Food oral processing: Mechanisms and implications of food oral destruction. *Trends in Food Science & Technology, 45*(2), 222–228.

Chen, J., & Dickinson, E. (1999). Effect of surface character of filler particles on rheology of heat-set whey protein emulsion gels. *Colloids and Surfaces B: Biointerfaces, 12*(3–6), 373–381.

Chen, J., & Lolivret, L. (2011). The determining role of bolus rheology in triggering a swallowing. *Food Hydrocolloids, 25*(3), 325–332.

Chen, J., & Stokes, J. R. (2012). Rheology and tribology: Two distinctive regimes of food texture sensation. *Trends in Food Science & Technology, 25*(1), 4–12.

Corradini, M. G., & Peleg, M. (2010). Comparing the effectiveness of thermal and non-thermal food preservation processes: The concept of equivalent efficacy. *In Case Studies in Novel Food Processing Technologies* (pp. 464–488). Woodhead Publishing.

de Wijk, R., Prinz, J., & Engelen, L. (2003). The role of intra-oral manipulation in the perception of sensory attributes. *Appetite, 40*, 1–7.

de Wijk, R. A., Prinz, J. F., & Janssen, A. M. (2006). Explaining perceived oral texture of starch-based custard desserts from standard and novel instrumental tests. *Food Hydrocolloids, 20*(1), 24–34.

de Wijk, R., et al. (2009). Persistence of oral coatings of CMC and starch-based custard desserts. *Food Hydrocolloids, 23*, 896–900.

de Wijk, R., Janssen, A., & Prinz, J. (2011). Oral movements and the perception of semi-solid foods. *Physiology & Behavior, 104*, 423–428.

de Lavergne, M. D. (2015). Bolus matters: Impact of food oral breakdown on dynamic texture perception. Wageningen University.

Engelen, L., Fontijn-Tekamp, A., & van der Bilt, A. (2005). The influence of product and oral characteristics on swallowing. *Archives of Oral Biology, 50*(8), 739–746.

Engelen, L., & de Wijk, R. A. (2012). Oral processing and texture perception. In J. Chen & L. Engelen (Eds.), *Food oral processing: Fundamentals of eating and sensory perception* (pp. 159–p162). Oxford, UK: Wiley-Blackwell.

Foegeding, E. A., Vinyard, C. J., Essick, G., Guest, S., & Campbell, C. (2015). Transforming structural breakdown into sensory perception of texture. *Journal of Texture Studies, 46*(3), 152–170.

Friedman, H., Whitney, J., & Szczesniak, A. (1963). The texturometer: A new instrument for objective texture measurement. *Journal of Food Science, 28*(4), 390–396.

Gordon, J., & Ghez, C. (1991). Muscle receptors and spinal reflexes: The stretch reflex. In *Principles of Neural Science* (3rd ed., pp. 565–580). New York: Elsevier.

Hoebler, C., Devaux, M.-F., Karinthi, A. (2009). Particle size of solid food after human mastication and simulation of oral breakdown. *International Journal of Food Sciences and Nutrition, 51*(5), 353–366

Hutchings, J. B., & Lillford, P. (1988). The perception of food texture — The philosophy of the breakdown path. *Journal of Texture Studies, 19*, 103–115.

Ishihara, S., Nakauma, M., Funami, T., Odake, S., & Nishinari, K. (2011). Swallowing profiles of food polysaccharide gels in relation to bolus rheology. *Food Hydrocolloids, 25*(5), 1016–1024

Johnson, K. (2001). The roles and functions of cutaneous mechanoreceptors. *Current Opinion in Neurobiology, 11*(4), 455–461.

Koç, H., Vinyard, C. J., Essick, G. K., & Foegeding, E. A. (2013). Food oral processing: Conversion of food structure to textural perception. *Annual Review of Food Science and Technology, 4*, 237–266.

Koç, H., Çakir, E., Vinyard, C. J., Essick, G., Daubert, C. R., Drake, M. A., ... & Foegeding, E. A. (2014). Adaptation of oral processing to the fracture properties of soft solids. *Journal of Texture Studies, 45*(1), 47–61.

Klatzky, R., et al. (2003). Feeling textures through a probe: Effects of probe and surface geometry and exploratory factors. *Perception & Psychophysics, 65*(4), 613–631.

Kutter, A., et al. (2011). Impact of proprioception and tactile sensations in the mouth on the perceived thickness of semi-solid foods. *Food Quality and Preference, 22*(2), 193–197.

Laguna, L., & Chen, J. (2016). The eating capability: Constituents and assessments. *Food Quality and Preference, 48*, 345–358.

Lillford, P. J. (2011). The importance of food microstructure in fracture physics and texture perception. *Journal of Texture Studies, 42*(2), 130–136.

Loret, C., Walter, M., Pineau, N., Peyron, M. A., Hartmann, C., & Martin, N. (2011). Physical and related sensory properties of a swallowable bolus. *Physiology & Behavior, 104*(5), 855–864.

Macakova, L., et al. (2011). Influence of ionic strength on the tribological properties of pre-adsorbed salivary films. *Tribology International, 44*(9), 956–962.

Mosca, A. C., & Chen, J. (2017). Food-saliva interactions: Mechanisms and implications. *Trends in Food Science & Technology, 66*, 125–134.

Nishinari, K., & Fang, Y. (2018). Perception and measurement of food texture: Solid foods. *Journal of Texture Studies, 49*(2), 160–201.

Nicosia, M. A., & Robbins, J. (2001). The fluid mechanics of bolus ejection from the oral cavity. *Journal of Biomechanics, 34*(12), 1537–1544.

Nishinari, K., Kohyama, K., Kumagai, H., Funami, T., & Bourne, M. C. (2013). Parameters of texture profile analysis. *Food Science and Technology Research, 19*(3), 519–521.

Osorio, F. A., & Steffe, J. F. (1991). Evaluating Herschel-Bulkley fluids with the back extrusion (annular pumping) technique. *Rheologica Acta, 30*(6), 549–558.

Peyron, M. A., Mishellany, A., & Woda, A. (2004). Particle size distribution of food boluses after mastication of six natural foods. *Journal of Dental Research, 83*(7), 578–582.

Peyron, M. A., Gierczynski, I., Hartmann, C., Loret, C., Dardevet, D., Martin, N., & Woda, A. (2011). Role of physical bolus properties as sensory inputs in the trigger of swallowing. *PLoS One, 6*(6), e21167.

Sala, G., Van Aken, G. A., Stuart, M. A. C., & Van De Velde, F. (2007). Effect of droplet–matrix interactions on large deformation properties of emulsion-filled gels. *Journal of Texture Studies, 38*(4), 511–535.

Shama, F., & Sherman, P. (1973). Identification of stimuli controlling the sensory evaluation of viscosity. II. Oral methods. *Journal of Texture Studies, 4*, 111–118.

Steffe, J. F., & Osorio, F. A. (1987). Back extrusion of non-Newtonian fluids. Nutrition reviews.

Stokes, J. R. (2012). 'Oral' tribology. Food oral processing: Fundamentals of eating and sensory perception, 265–287.

Stokes, J. R., Boehm, M. W., & Baier, S. K. (2013). Oral processing, texture and mouthfeel: From rheology to tribology and beyond. *Current Opinion in Colloid & Interface Science, 18*(4), 349–359.

Szczesniak, A. (1963). Classification of textural characteristics. *Journal of Food Science, 28*(4), 385–389.

Szczesniak, A. S. (1979). Recent developments in solving consumer-oriented texture problems. *Food Technology (USA), 33*, 61.

Szczesniak, A. (2002). Texture is a sensory property. *Food Quality and Preference, 13*(4), 215–225.

Szczesniak, A., & Kleyn, D. (1963). Consumer awareness of texture and other food attributes. *Journal of Food Technology, 27*, 74–77.

Tseng, K. E., Chung, C. Y., H'ng, W. S., & Wang, S. L. (2009). Early infection termination affects number of CD8+ memory T cells and protective capacities in Listeria monocytogenes-infected mice upon rechallenge. *The Journal of Immunology, 182*(8), 4590–4600.

Trulsson, M., & Johansson, R. (2002). Orofacial mechanoreceptors in humans: Encoding characteristics and responses during natural orofacial behaviors. *Behavioural Brain Research, 135*, 27–33.

van Aken, G. A., Vingerhoeds, M. H., & de Hoog, E. H. A. (2007). Food colloids under oral conditions. *Current Opinion in Colloid & Interface Science, 12*(4), 251–262.

van Vliet, T. (1999). Rheological classification of foods and instrumental techniques for their study. In A. J. Rosenthal (Ed.), *Food texture: Measurement and perception* (pp. 65–97). Gaithersburg: Aspen Publishers Inc.

van Vliet, T. (2002). On the relation between texture perception and fundamental mechanical parameters for liquids and time dependent solids. *Food Quality and Preference, 13*(4), 227–236.

Witt, T., & Stokes, J. R. (2015). Physics of food structure breakdown and bolus formation during oral processing of hard and soft solids. *Current Opinion in Food Science, 3*, 110–117.

Yven, C., Guessasma, S., Chaunier, L., Della Valle, G., & Salles, C. (2010). The role of mechanical properties of brittle airy foods on the masticatory performance. *Journal of Food Engineering, 101*(1), 85–91.

Relationships Among Semisolid Food Microstructures, Rheological Behaviors, and Sensory Attributes

Mitchell Culler

1 Understanding Rheological Measurements in Terms of Sensory Perception

Rheological measurements, particularly in recent years, have become precise measurements for distinguishing and explaining the textures of food products; however, translating these measurements into a meaningful understanding of the experience of consuming a food product can often be challenging. For example, knowing that a given beverage has an apparent viscosity of 30 mPa.s does little to characterize the experience of consuming that beverage. This difficulty is exacerbated with semisolid food or time-dependent products, which display behavior characterized by properties of both fluids and solids in response to the varied conditions in the oral cavity. Despite this difficulty, much progress has been made in this area, and new experimental techniques show promise for future studies.

1.1 Conceptualizing Oral Sensations

In the oral cavity, food is exposed to an extremely varied set of conditions. It has been reported that the tongue can move at a rate of 200 mm s^{-1} (Hiiemae and Palmer 2003) and apply loads between 0.01 to 90 N (Miller and Watkin 1996). However, oral sliding speed and thus oral shear rates will vary greatly depending on the food being consumed as well as from one oral moment to the next during oral processing of any given food product. For semisolid and other non-Newtonian food products, this will therefore result in varying apparent viscosity and produce varied sensations

M. Culler (✉)
University of Massachusetts, Amherst, MA, USA
e-mail: mculler@umass.edu

H. S. Joyner (ed.), *Rheology of Semisolid Foods*, Food Engineering Series,
https://doi.org/10.1007/978-3-030-27134-3_9

across the oral cavity in response to the differences in shear forces. In response to these forces, the food itself is changing as the structure is being broken down. Imagine how much the structure of a dry cracker must be changed during oral processing from the initial bite to the point at which the bolus it becomes can be swallowed. Still further complicating a description of oral processing is the fact that our perception of attributes such as thickness or creaminess can be influenced greatly based on our olfactory, gustatory, or visual perceptions of the food. In other words, two foods that might be identical from a standpoint of purely instrumental rheological measurements, such as full-fat and low-fat yogurts, may be perceived to have very different textural properties based on sensory cues provided by the product's smell, taste, or appearance. Defining the parameters to which a food is subjected in the oral cavity has proven to be challenging, and there is still debate about which rheological parameters and testing methodologies are the most relevant to represent perceived texture attributes and the shear rates and shear stresses that occur in the mouth, respectively, during consumption of a food product (Van Vliet 2002; Malone et al. 2003; He et al. 2016).

In an attempt to compartmentalize the major forces at work during the consumption of a food product, oral processing is typically broken into three stages: initial (first bite), masticatory (during chewing), and residual (after swallowing) (Margaret et al. 1963; Guinard and Mazzucchelli 1996; Foegeding and Drake 2007). More recently, however, it has been suggested to break oral processing into six stages so as not to inhibit the development of in vitro techniques to describe the forces the food experiences during oral processing (Stokes et al. 2013). These six stages are (1) first bite, in which the food is fractured for the first time; (2) comminution, in which the food is broken down into large pieces; (3) granulation, in which the food is broken down into small pieces and mixed with saliva; (4) bolus formation, in which the food particles plus saliva are formed into a solid, relatively homogeneous mass in preparation for swallowing; (5) swallowing; and (6) residual, in which any thin films of food or food–saliva mixture left in the mouth after swallowing are sensed. During each of these six stages, the food's structure is changed significantly, therefore the food's rheological behavior will vary greatly from one stage to the next. It should be noted that these stages form a continuum rather than marked steps, and that there is a good deal of overlap from one stage to the next. Studying these stages separately, however, has the advantage of focusing on the underlying physics governing a given stage so that insights can be obtained on the specific functionality imparted by the components of food (Stokes et al. 2013).

A range of surfaces in the mouth also affect the way in which the food is exposed to the forces exerted orally. Food can be compressed between the tongue and the palate, sheared between the teeth, or pressed along the soft surfaces of the cheeks (or numerous combinations thereof). Each of these presents a specific rheological challenge in terms of finding relevant parameters to study as well as textures and geometries to use as a model. Semisolid foods are generally palated, so shear forces in the tongue–palate and tongue–teeth contacts are likely the most important to mimic when developing instrumental tests that mimic oral processing behaviors for semisolid foods. Regardless of the test used, it is agreed at the time of publication of this book that the initial stages of oral processing are dominated by rheological properties, while at the later stages, tribological properties may be better suited to characterize the relevant forces to the oral processing experience (Pradal and Stokes 2016). Therefore, a range of instrumental tests are needed to fully capture food behaviors during all stages of oral processing.

1.2 Sensory Perception of Foods

Sensory evaluation of food is an expensive and time consuming category of analysis. Since it relies on examining individuals' perceptions, the results typically show much more variation than would be observed from taking measurements from several replicates of the same food on a rheometer or texture analyzer. Additionally, while a given rheometer or texture analyzer is manufactured to a precise set of specifications and is typically sold with a guarantee of accuracy and specific limit of detection, sensory panelists are quite the opposite. Two participants in a sensory panel may have significantly different perceptions and expectations about a product's attributes due to differences in sensitivity to tastes and flavors, methods of oral processing, and personal preference and previous history with a given food. Therefore, the experimental design of a sensory study must incorporate the variability that will be experienced between individual panelists. Typically, this means that in contrast to instrumental studies where an average of three replicates is usually sufficient to give an illustration of potential variation in the data, sensory experiments usually require a much higher number of panelists to produce data which shows meaningful correlations and trends. Since sensory evaluation is a destructive technique, this requires preparing or obtaining much larger quantities of samples and adds the logistical complications of bringing a large group of panelists together at the same time to evaluate samples. For example, the minimum number of panelists for a general (untrained) consumer sensory panel is 50 based on statistical considerations; 100 panelists is considered to be the gold standard for this type of panel. Accordingly, recruiting this many panelists can take days or weeks, and setting up and running the panel can take several days and hundreds of pounds of sample. In comparison, the five or six samples evaluated in this type of panel can be evaluated instrumentally using less than a kilogram of sample in a few hours.

Additionally, the conditions under which sensory testing is performed can also significantly impact the data. Room temperature, food temperature, airflow, lighting, and panelist comfort while sitting can all affect a panelist's perception of the food products being evaluated. Even seeing another panelist's facial expression or the visual appearance of the food before evaluation can influence panelists' perceptions of the food. To negate these effects, a set of standards have been agreed upon for the rooms in which sensory evaluation tests are typically performed (ISO 8589:2007). These standards include white lighting, positive room pressure (to avoid odors from other locations entering the room), and separate evaluation booths

Table 1 Example of sensory descriptors, their definitions, and the protocol for analysis as defined by a sensory panel

	Attribute	Definition	Protocol
Mouthfeel	Initial thickness	Pressure needed to press the sample between the tongue and the palate	Put a spoonful of sample onto the tongue, gently press the tongue against the palate 3 times
	Thickness in mouth	Pressure taken to move the sample between the tongue and the palate	Put a spoonful of sample onto the tongue, move the sample in the mouth, rub the tongue for 5 times
	Stickiness on lips	Pressure to separate the sample from the lips	Use lips to take a tip of sample (avoid touching from lips), and hold there for 5 s, then separate the lips for 3 times
	Stickiness in mouth	Elasticity of the sample between the tongue and the palate	Put a spoonful of sample onto the tongue, gently press the tongue against palate and hold there for 3 s and then separate for 5 times
	Mouth coating	Amount of residue left in the oral cavity after swallowing	Put a spoonful of sample into the mouth, move around the tongue and chew the sample for 5 times and swallow
Flavor and taste	Overall flavor	Overall intensity of flavor perceived	Put a spoonful of sample into the mouth, move around the tongue and chew the sample for 5 times and swallow
	Overall sweetness	Overall intensity of sweetness of the samples	Put a spoonful of sample into the mouth, move around the tongue and chew the sample for 5 times and swallow

Table reproduced from He et al. (2016)

for each panelist. Although they can notably improve the precision of the sensory measurements, these requirements can add an additional layer of complication to the sensory evaluation of food, as they can necessitate a specialized facility.

One way to standardize the results of sensory testing is to use descriptive sensory analysis techniques, in which the sensory panel is trained to recognize certain attributes and develops a set of standardized definitions, evaluation protocols, and reference products for these attributes. During training sessions, panelists typically first develop definitions for certain attributes of interest, such as creaminess, graininess or thickness. After this lexicon is developed and evaluation practices are agreed upon, panelists will use the reference foods as calibration standards to scale how much of a given attribute a food has. Multiple practice sessions are usually needed for proper panelist calibration; calibration can be monitored through statistical testing to evaluate intra- and inter-panelist accuracy and precision. Formal sample evaluation begins after panelist calibration is considered to be sufficient to properly evaluate the products of interest. During formal evaluations, panelists generally have access to the reference products if needed for comparison to the test samples. This practice can help standardize inter-panelist data and provide more consistent results. An example sensory lexicon for thickened carbohydrate solutions is shown in Table 1 (He et al. 2016).

Although there are numerous hurdles associated with sensory analysis, it remains the so-called “gold standard” for evaluation of many foods because it is the same method by which foods will be ultimately be judged by consumers. The numerous complications associated with sensory analysis, however, indicate that it is advantageous to food manufacturers to find relevant parameters to measure instrumentally for the purposes of quality control or for initial stages of product development when may formulations need to be rapidly screened. Therefore, finding relevant instrumental parameters that are highly correlated with food textural parameters is a timely and necessary field of study.

1.3 Instrumental Evaluation of Food Properties for Comparison to Textural Attributes

The approaches to instrumentally measuring food properties or behaviors for comparison to texture attributes have historically fallen into three categories: (1) imitative techniques designed to mimic oral movements, (2) empirical methods that seek to align a given measurement with a sensory perception, and (3) fundamental measurements of mechanical and structural properties of a food, e.g. rheometry (Stokes et al. 2013). More recently, methodologies such as direct physiological analysis and tribology have been used in an attempt to get a more holistic view of oral processing. This section discusses these categories of techniques, as well as some of the more novel techniques used for developing relationships between food sensory texture attributes and instrumentally measured parameters.

1.3.1 Imitative Techniques for Food Texture Approximation

Imitative techniques consist of using an instrument that is designed to mimic in some way the deformation of a food that occurs during oral processing. An early example is the Voldokevich bite tenderometer, which squeezed food between two rounded wedges in an attempt to simulate biting with teeth (Volodkevich 1938). Recently, texture analyzers (e.g. the TAXT manufactured by Texture Technologies) have become widely adopted. These devices have a crosshead that can be raised or lowered at a range of constant speeds to a desired distance or load force and can be fitted with a variety of probes to measure crushing, penetrating, or shearing of food. The food material to be measured is placed on a platform or in a cell at the bottom of the machine’s head; semisolid foods are typically tested in some kind of cell or container that holds them in a certain shape. These instruments interface with a computer to give rapid data collection and analysis of the force–deformation or force–time curve.

The classic example of an imitative technique is the "two-bite" test, also known as Texture Profile Analysis (TPA). During this test, which is typically run on a texture analyzer, a food is compressed and released twice, mimicking the first and second bite of a food product. TPA is useful for measuring the change in structure that occurs between the first and second "bite" of a food as this information can be useful for determining how the structure behaves in response to deformation. Consider compressing a thin wafer, which would break under an applied force, as opposed to a strong gel, where the first and second "bites" would be relatively similar (assuming the gel was not compressed to the point where the structure was completely broken). It should be noted that foods should not be fractured or ruptured when performing TPA (Friedman et al. 1963).

Analysis of the data from a two-bite test is classified into several parameters: hardness, elasticity, adhesiveness, cohesiveness, brittleness, chewiness, and gumminess. These parameters can be derived from the time-force curve produced during the two-bite test (Fig. 1). The two-bite test was first described by Friedman et al. (1963). *Hardness* is measured as the height of the first peak (or chew). Hardness values can be normalized by dividing the height of the first peak by the volts input. *Cohesiveness* is a measure of the ratio of the area of the second peak to the area of the first peak (A_2/A_1 in Fig. 1). The parameter of *elasticity* is defined as the difference between the distance B for the food product being tested and the same measurement made on a completely inelastic standardized material such as clay. *Adhesiveness* is measured as the area (A_3 in Fig. 1) of the negative peak occurring between the two compression cycles; this peak represents the work necessary to pull the plunger off of the sample. *Brittleness* (or *fracturability*) is measured as the height of the first local maximum in the first peak where the sample breaks (point C in Fig. 1). *Chewiness* is expressed as the sum of hardness, cohesiveness, and elasticity. Finally, *gumminess* is the sum of hardness and cohesiveness multiplied by 100.

As mentioned in Chapter "Sensory and Oral Processing of Semisolid Foods", TPA may not be appropriate for semisolid foods. Users of TPA should carefully consider first whether TPA is an appropriate test for the semisolid food product of

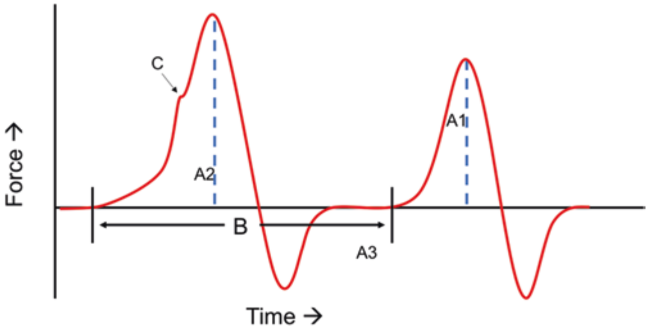

Fig. 1 A typical texturometer curve showing force vs. time. (Figure redrawn from (Martinez et al. 2004))

interest, and second, whether a given TPA parameter is appropriate for describing semisolid food behaviors. For example, firmness may be an appropriate term to describe the force needed to compress a yogurt, but yogurt can hardly be described as “chewy”. Thus, it is not appropriate to use the chewiness calculation for yogurt samples.

Early TPA measurements attempted to correlate the findings of sensory panelists with instrumental measurements and were able to do so with high correlations for food products that varied by a single attribute (Szczesniak et al. 1963). For example, the attribute of ‘chewiness’ was rated based on the time required to masticate a sample at a rate of one chew per second to the sufficient texture needed for swallowing on a seven-point scale including rye bread, gum drops, and Tootsie rolls. Later TPA testing showed good correlation among TPA parameters and first-bite sensory attributes, but fewer correlations were found among TPA parameters and chewdown or residual sensory terms (Foegeding and Drake 2007).

An advantage of imitative techniques is their adaptability, which allows them to be readily modified to be performed under certain conditions or with food products with nonhomogeneous composition or “difficult” geometries. One adaptation of this type of testing was used by Kohyama et al. (2016). They used a probe to compress a rice grain (instead of the half-inch sample height initially described by Friedman et al. (1963)) for compressive testing) to 25% of its initial height, raised the probe, recompressed the grain to 90% of its original height, and finally raised the probe again. But while the adaptability and range of imitative methods can make them extremely versatile, this feature can often hinder analysis. It is difficult to draw meaningful conclusions among experiments when different methods of analysis are used, particularly when it is not possible to convert the results to fundamental measurements (e.g. stress and strain), which is often the case. Furthermore, it can be difficult to know which parameters are relevant to sensory data. In a study examining the effect of changing the experimental parameters defined in TPA, it was found that significant differences occurred in the measured values for the same samples tested under different parameter sets (Rosenthal 2010). For example, the hardness of gels was measured to be an average 541 mN with a plunger and 880 mN with a platen. The percent deformation used in TPA is also frequently changed, ranging from 10% to 90% deformation in literature (Gupta and Sharma 2007; Birkeland and Skåra 2008), and can greatly affect the interpreted cohesiveness and hardness values (Rosenthal 2010). While variation in the percent deformation may be needed so that samples are not ruptured during the test, changes in percent deformation among studies are often due to improper use of TPA.

Another major limitation of imitative testing is that it typically only gives information about the initial sensory behaviors of the food. It is estimated that the first bite encompasses only 2–10% of the total mastication time for a food product, making it difficult to characterize the entire experience of consuming a food product using this data alone (Borne 1975). Other tests are needed to evaluate food properties and behaviors related to later mastication stages.

1.3.2 Empirical Methods

Empirical tests, by definition, measure observed characteristics of the food product. Rheological empirical tests apply a torque or deformation to a material and record the resulting changes to the material’s shape (e.g. amount of deformation or resistance to movement). A wide variety of testing geometries and sample shapes can be used in empirical tests, making them quite versatile for a variety of semisolid food products. In general, the imitative tests discussed in the previous section are empirical.

A major advantage of empirical tests is that they are often inexpensive, easy to perform, and in many cases present a good solution for measuring a given attribute of a specific product when a deeper understanding of the underlying structure is not required. One example is the Bostwick consistometer, which is frequently used for measuring the consistency of products such as tomato paste and other foods that are semisolids or thick fluids. The test apparatus consists of a trough with gradations along the bottom. The product is placed into a chamber at one end of the trough that is enclosed by a spring-loaded door. The operator starts a timer when the door is opened and records how far the product has traveled down the trough after a given amount of time has elapsed. This is useful for rapidly and easily comparing between two different samples of the same product type, e.g. between different batches as part of a manufacturing facility’s QC plan.

Another widely-used empirical instrument for measuring the consistency of semisolid food is the Adams consistometer (Adams and Birdsall 1946). Similar to the Bostwick consistometer, this device involves measuring how far a food spreads out in a given time period. Instead of placing the food in a trough, however, the Adams consistometer involves placing the food in a center, circular chamber. When the test is started, the walls of the center chamber are raised, allowing the material to flow out from the center in a circular pattern. A set of concentric rings with standardized diameters is used to measure the distance that the material has traveled in the given time. This provides an estimate of the consistency of the food.

Introduced in 1954, the Posthumus funnel is an empirical method that is commonly used to examine the texture of yogurt during production. It has been found to be an effective predictor of perceived thickness or viscosity. Skriver et al. 1999 found a strong correlation (r = 0.834) between the efflux time—the time required for the sample to drain out of the funnel—and the oral viscosity obtained by sensory evaluation. Both shear and elongational flow can occur as the funnel is drained by gravity, similar to the flow behaviors encountered in the oral cavity during processing (Van Vliet 2002; Janhøj et al. 2006). The similarities in flow behavior may contribute to the correlation between oral viscosity measurements and funnel data.

While empirical testing has several advantages, a major drawback of these tests is that it difficult to use empirical test data to determine underlying physicochemical properties such as particle size, surface tension, flow profiles, and viscoelastic moduli. For example, the consistency measured by a Bostwick consistometer cannot be converted to viscosity. In addition, due to the arbitrary test conditions used in empirical testing, it is often difficult to correlate the information obtained from empirical methods with other methodologies (Tunick 2000), convert the empirical data to fundamental data (e.g. converting force to stress or deformation to strain), or draw meaning beyond the immediate measurement given by the empirical method.

Nevertheless, empirical methods are frequently used in an industry setting to evaluate the quality of foods, and numerous methods have been developed for semisolid foods. These methods are often much more easily conducted than sensory tests, and the results can be correlated with sensory data. For instance, if the desired consistency of a product as given by a sensory panel can be correlated to a measurement on a given consistometer, it can be used as a helpful quality control tool. Indeed, these empirical methods are widely used in industry as a rapid check for quality control.

1.3.3 Fundamental Methods

Fundamental rheological methods measure well-defined mechanical properties of the food such as Young's modulus, shear modulus, flow profiles, and viscoelastic moduli. Unlike empirical methods for which measurements combine numerous physicochemical properties of the food and incorporate them into a single measurement (such as efflux time), fundamental properties are measured independently. Measurements of fundamental properties have the advantage of reproducibility when measured on different instruments because they are intrinsic to the foods themselves, as opposed to being the result of only being observed under a specific set of conditions such as those in an Adam's consistometer. However, fundamental measurements generally require more costly equipment, precisely controlled testing parameters, homogeneous samples, and standardized sample geometries. They may also require more time to perform and may need a trained operator to accurately and precisely perform measurements. Therefore, these tests are more commonly used in research laboratories to explore fundamental food properties to develop a deeper understanding of the connections among food microstructure, composition, mechanical behaviors, and sensory texture attributes. While they may also be used during the research and development process, fundamental tests are typically not used for food quality assessment during manufacturing.

Chapter "Rheological Testing for Semisolid Foods: Traditional Rheometry" discusses multiple fundamental tests in detail, including shear rate sweeps, stress and strain sweeps, and frequency sweeps. These are the most commonly used fundamental tests used for semisolid foods. While fundamental rheological properties have been correlated to multiple sensory terms, like empirical data, the correlations between food mechanical properties and sensory attributes evaluated in the later stages of mastication are generally poor (Richardson et al. 1989; Pons and Fiszman 1996; Liu et al. 2007; Foegeding et al. 2017).

1.3.4 Tribological Methods

Tribology represents a relatively new but promising avenue for the study of texture as it relates to oral processing. As with rheological measurements, a major challenge for the usage of tribology to study sensory perceptions is in correlating the data. One approach is to find an entrainment speed or speed range where the friction coefficient correlates with sensory texture attributes. However, the pitfalls of this are discussed in Chapter “Semisolid Food Tribology”, and it is not always possible to find a speed range that has meaning during oral processing and also correlates with sensory data. Additionally, the inherently complex nature of most food structures makes it difficult to separate which aspects of the food are contributing to the various sensory and friction attributes being observed (Stokes et al. 2013).

Despite these difficulties, a shift is occurring in food research from instrumentally measuring the food properties that relate to the “first bite” sensory attributes towards a more holistic examination of how the mechanical and physicochemical properties of a food change as it is transformed during oral processing (Stokes et al. 2013). This includes the lingering oral sensations after the bolus has been swallowed. As the food changes from the so-called first bite to the final bolus, there are changes that occur in the dominant behaviors which apply to the bolus (Fig. 2) (Prakash et al. 2013). As oral processing progresses, the behaviors that dominate sensory texture perception move from rheology-dominant to tribology-dominant (Stokes et al. 2013; Foegeding et al. 2017). Sensations related to thickness, firmness, melting, and breakdown are determined when bulk properties dominate the sensory profile. As the food film on the oral surfaces thins to between 0.1 to 100 μm during bolus preparation for swallowing, a person will make determinations regarding creaminess, fattiness, smoothness, and slipperiness (Stokes et al. 2013). Sensations of astringency, roughness, afterfeel, and homogeneity are determined when only residue remains, and also derived from a perception of thin-film, or tribological, characteristics (Selway and Stokes 2013).

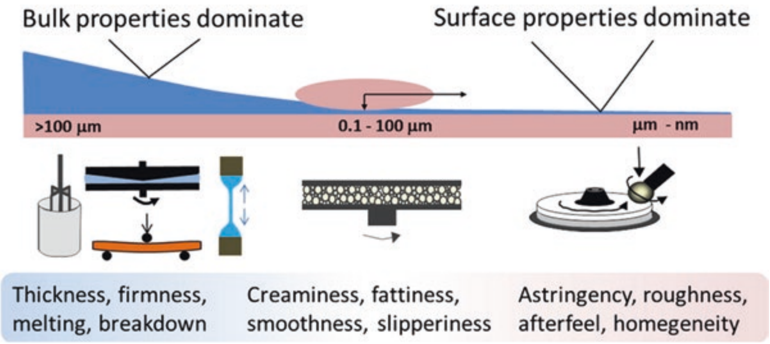

Fig. 2 Schematic diagram depicting the change in properties that are experienced as the food surface thins during oral processing. Also shown are indicators of the types of instruments that could be used to study the relevant forces during these areas of processing. (Figure reproduced from Stokes et al. 2013)

To characterize the interaction of food moving between the palate and tongue, numerous methodologies have been employed in the early twenty-first century to study friction coefficient profiles and how they can affect food sensory attributes. Reviews of these methodologies have been published by Prakash et al. 2013 and Pradal and Stokes 2016. Additional information is also presented in Chapter "Semisolid Food Tribology".

There are multiple devices that can be used to measure friction behavior of fluid and semisolid foods. One such device is the friction tester, one of the most basic tribological methods of analysis (Fig. 3). This apparatus consists of stretching a rubber band between an electric motor and a load cell. When the motor is rotating, the friction between the cylinder and the rubber band produces a force (F_1) that can be detected using the load cell. When the direction of the cylinder is reversed, the load drops to a second force, F_2. Knowing these two forces, it is possible to calculate the coefficient of friction (μ) using Eq. 1 (de Wijk and Prinz 2005):

$$\mu = \frac{1}{\pi \ln\left(\frac{F_1}{F_2}\right)} \tag{1}$$

One potential problem with this method is that it relies on the frictional forces between the food and rubber band. This is not necessarily representative of the surface interactions encountered between a tongue or palate and food (de Wijk and Prinz 2005; Prakash et al. 2013).

Several devices for studying tribology in foods have been mounted on rheometers; Chapter "Semisolid Food Tribology" provides more detail on tribological testing setups. In general, testing geometries can be made in-house or purchased from a rheometer manufacturer. These geometries include ball(s)-on-plate(s) and ring-on-plate setups (Heyer and Läuger 2009; Goh et al. 2010). The ring and plate geometry has been used to differentiate friction coefficients among cream cheeses with different fat contents (Nguyen et al. 2016), while the double-ball system has been used to study acid milk protein gels (Joyner (Melito) et al. 2014). The latter

Fig. 3 Schematic representation of a friction tester. Reproduced from de Wijk and Prinz 2004

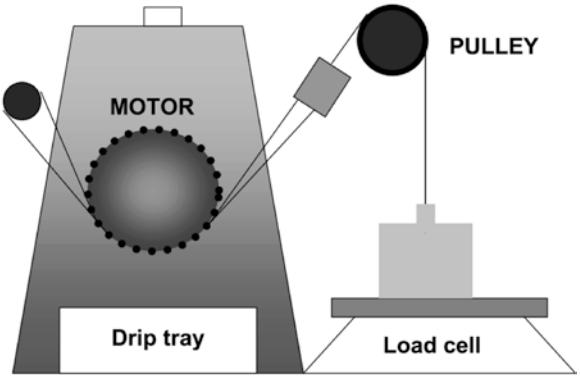

study showed promise in terms of the ability to relate instrumental friction measurements to sensory attributes. Another device that can be used for friction measurements is a texture analyzer rotated on its side so that gravity is normal to the force exerted by the texture analyzer. This device has been used to obtain friction-related information for both Newtonian and non-Newtonian fluids (Chen et al. 2014).

1.3.5 Direct Physiological Analysis

Direct physiological analysis involves the study of food texture by instrumentally measuring one or more parameters as they are occurring during oral processing. Çakir et al. (2012) investigated the effects of various textured foods on adaptation of subjects' chewing pattern by examining jaw muscle activity and kinematic measures of mastication. Self-adhering diodes were placed on subjects' chewing muscles and jaw movements were recorded using a specialized camera with 3D modeling software. In response to a reduction in the fat content of cheese, oral processing was found to adjust to consist of increased closing muscle activity, a shorter cycle duration, and an increase in the power stroke time. This unique method not only allows for data to be collected directly from oral processing (thus removing some of the difficulty between translating from instrumental to sensory analysis) but also shows different foods are subjected to different oral processing conditions based on their texture.

2 Typical Relationships Found Between Instrumental and Sensory Data

As discussed in Sect. 1, the types of data collected from sensory and instrumental evaluation of foods are quite different. Therefore it is necessary to draw correlations or develop relationships between the two data types for a proper understanding of how food rheological and sensory behaviors align. Often, it is convenient to use a simplified gel or emulsion to study how a variable can change the sensory characteristics of a food instead of a more complex food system. This has the advantage of minimizing variables as long as the model selected is still sufficiently close to the food so as to generate meaningful conclusions.

2.1 Relationships Between Rheological and Sensory Data

Semisolid food viscosity is often related to various sensory attributes such as thickness. Because many semisolid foods have shear-dependent behavior, the perceived thickness of foods determined in sensory evaluation can be used to estimate shear rates during oral processing by comparing instrumentally measured viscosity values at different shear rates to perceived thickness and determining where the data best align. This procedure was used by Wood (1968), who compared the perceived thickness of shear-thinning cream soups and Newtonian glucose syrups. When a soup and syrup were found to have similar perceived thickness, Wood theorized that the point at which the shear rates crossed on their viscosity curves would be relevant to thickness perception. This shear rate was determined to be 50 s^{-1}. The finding that complex viscosity at 50 rad s^{-1} is highly correlated with perceived thickness was corroborated by Richardson et al. (1989). Small deformation measurements of dynamic viscosity under oscillatory shear at a single frequency (50 rad s^{-1}) correlated directly with panel scores for perceived thickness of solutions without yield stress and weak gels. Panel scores for sliminess also directly correlated with instrumental values of dynamic viscosity at ~50 rad s^{-1}, irrespective of the extent of the extent of shear-thinning behavior (Richardson et al. 1989). This relationship was also found for lemon pie fillings (Hill et al. 1995).

Other studies (Shama et al. 1973) examined a range of fluid and semisolid food products including yogurt, tomato ketchup, tomato soup, and lemon curd. They found that a wide range of shear rates are involved with oral evaluation of food, extending from 10 s^{-1} to 1000 s^{-1}, with the operative shear rate depending on the flow conditions of the food. Low viscosity liquids (<0.1 Pa.s) are evaluated orally at a shear stress of approximately 10 Pa; however, for highly viscous foods, (>10 Pa.s), the viscosity is evaluated at a constant shear rate of approximately 10 s^{-1}. This finding was corroborated by Tárrega and Costell (2007), who investigated the relationship between instrumental rheological measurements and sensory measurements of seven semisolid dairy desserts and found a high correlation between their perceived oral thickness and the measured yield stress values ($r = 0.96$) and apparent viscosity values at 10 s^{-1} ($r = 0.89$). Additionally, storage modulus at 1 Hz and complex viscosity at 7.95 Hz (50 rad s^{-1}) were found to have higher correlation coefficients (0.92 for both) with the perceived oral thickness than loss modulus and complex viscosity at 1 Hz (Tárrega and Costell 2007).

More recently, tribological and rheological evaluation has been combined with microscopy to develop a better understanding of the underlying structures that lead to perceived sensory characteristics. In a study which used particle size, microstructure, rheology, tribology, and sensory evaluation to examine varying ratios of whey protein and casein in yogurt, Laiho et al. (2017) found that the gel network in yogurts with high levels of whey protein had gel microstructures comprising large whey protein–casein aggregates in addition to self-aggregated whey protein particles. In contrast, the gel network of yogurts with low levels of whey protein mostly comprised aggregates containing both whey and casein proteins. Samples with higher whey protein content had stronger protein networks due to increased crosslinking. However, under shear, both of these gel microstructures were broken down into clumps. Trained sensory panel evaluation of the yogurts showed that yogurts with high levels of whey protein had higher “lumpy in-spoon” scores for visual appearance (Laiho et al. 2017), likely because the stronger networks resisted breakdown under shear, resulting in larger lumps in the yogurt body.

In a study using custards as a model dairy semisolid food, three tribological regimes occurred in the friction profiles of the fat-containing samples: (1) fluid entrainment, characterized by a decreasing coefficient of friction; (2) gel particle entrainment, characterized by an increasing coefficient of friction; and (3) accumulation of multiple layers of material at high speeds, characterized by decreasing or constant coefficients of friction (Godoi et al. 2017). When these regimes were compared to confocal laser scanning microscopy images, it was determined that at the low speeds (0.5 mm s^{-1}) of the first regime, the ingredients were evenly dispersed. In the second regime, confocal images indicated a gel particle entrainment zone. Finally, in the third regime, an image taken at 10 mm s^{-1} showed the accumulation of multiple layers of material which favored the separation of the two rubbing surfaces (Godoi et al. 2017). This study is an excellent example of how microscopy results can be used to explain tribological phenomena. More studies like this are needed for a fuller understanding of sample behaviors during tribological testing and how those behaviors contribute to sensory textures.

2.2 Relationships Between Food Composition and Sensory Behavior

2.2.1 Fat Content

Both fat content and type of fat used in a food formulation can have a significant impact on the rheological properties and sensory attributes of the product. Fats composed of saturated fatty acids—that is, fatty acids which do not contain any double bonds between carbons in the chains—will typically have a higher melting point than fats of the same chain length which have double bonds between the carbons. This is because unsaturated fats cannot align as readily as saturated fat can due to kinks in their chains, and thus the intermolecular forces between them are weaker. This phenomenon is largely responsible for the rheological differences observed in, for example, butter (which is mostly saturated fat) and canola oil (which is predominantly unsaturated) at room temperature. Similarly, the underlying fat structure has a large effect on the texture of the finished product.

One of the most commonly examined factors of dairy products that is related to fat is creaminess. For oil-in-water emulsion systems, creaminess has been found to relate primarily to product viscosity, as well as the volume fraction of oil (Akhtar et al. 2005). Typically, creaminess is related to the amount of fat in a product; however, with the usage of fat replacers, it has been found that there are numerous factors such as viscosity, flavor, and appearance that also influence the perception of creaminess (Akhtar et al. 2005). Creaminess can also be increased by increasing the bulk viscosity of the food, using small, stable fat droplets in emulsions, adding flavors associated with creaminess such as dairy flavors, and minimizing, but not eliminating, loss of bulk viscosity during oral processing by using starches that show limited mechanical and enzymatic break-down during oral processing (De Wijk et al. 2006).

The perceived viscosity and smoothness of a sample have been found to be strong predictors of perceived creaminess (Janhøj et al. 2006; Ponne 1983):

$$creaminess = thickness^{0.54} \times smoothness^{0.84} \tag{2}$$

In emulsions, the degree of fat droplet coalescence, or the degree to which the fat droplets throughout the emulsion are able to come together to form larger droplets, has been found to relate to the level of creaminess sensation. The occurrence of coalescence in emulsions correlates with enhanced fat perception as measured by a Quantitative Descriptive Analysis panel and a lowering of the friction coefficients as measured instrumentally (Dresselhuis et al. 2008). This trend was also shown in model emulsion-filled gels. When these gels were manufactured with either bound or unbound particles, gels with bound particles were less susceptible to coalescence and had higher friction coefficients (Liu et al. 2015). Interestingly, whether the droplets were bound or unbound had a much greater impact on the sensory perception of fat than the actual solid fat content (Liu et al. 2015). This result points to the importance of free fat, not just total fat content, in sensory texture of emulsion-based foods. This importance of free versus bound fat may explain why several studies have found that fat level does not necessarily correlate with the viscosity of semisolid dairy products such as cream cheese or yogurt, but does impact friction behaviors (Selway and Stokes 2013; Nguyen et al. 2016).

2.2.2 Protein Content

Typically, when a food protein is in its native structure, the protein is folded such that the hydrophobic residues are arranged on the inside of the protein structure, with more hydrophilic moieties on the outside, allowing the protein to be soluble in water. When food proteins are denatured through heat, acid, or other means, the native structure is disrupted as the protein begins to unfold, and the hydrophobic regions of the protein may be exposed. This denaturation can result in increased aggregation and network formation due to hydrophobic association, wherein the hydrophobic regions of the proteins will associate. If the process is allowed to continue, e.g. if the food is held at a certain pH or temperature, the result is the formation of a three-dimensional gel network that is capable of entrapping fluid and small particles. At low protein concentrations (typically <1%), the gel is a semisolid and often referred to as a fluid gel.

Whey proteins are commonly used to create gels in food products; gelation can be induced by changing temperature, ionic strength, pH, or a combination of these. Changing the pH as well as the salt type and concentration of a whey protein isolate gel allows precise manipulation of the gel structure, mechanical properties, and water-holding capacity even as protein concentration remains constant (Kuhn and Foegeding 1991; Stading and Hermansson 1991; Langton and Hermansson 1992;

Mcguffey and Foegeding 2001; Gwartney et al. 2004). These properties in turn have the ability to affect the sensory perceptions of the food. In Cheddar cheese, which consists of a casein protein network entrapping water, fat, and small molecules such as salts and minerals, the strength of the casein network will change over time as the network connectivity decreases. This results in a shift from the springy texture of a fresh Cheddar (<2 mo storage) to the hardened texture more characteristic of a jammed structure in an aged Cheddar (>6 mo storage) (Rogers et al. 2009).

Furthermore, the type of protein network present has the ability to change the sensory characteristics of the food. Due to their structure, whey proteins have the ability to form either stranded or particulate gels, which can result in varied textural sensations. In a study using descriptive sensory analysis to characterize stranded and particulate whey protein gels manufactured by manipulating $CaCl_2$ content, particulate gels were described by a trained sensory panel as having high values for adhesiveness, crumbliness, cohesiveness of mass, moisture release, particle size distribution, and rate of breakdown. Stranded gels, on the other hand, were characterized as having high values of moisture, slipperiness, compressibility, springiness, surface smoothness, irregular particle shape, particle size, and smoothness (Gwartney et al. 2004). Additionally, increased particles in the mouth, such as those from precipitated proteins or flocculation of dead cells, were related to astringent sensations, reduced oral lubrication, and thus increased friction (de Wijk and Prinz 2005). These results point to the need for tribological measurements of food products for a better understanding of friction-related food texture attributes.

2.2.3 Carbohydrate Content

Certain complex carbohydrates can increase the viscosity of a food. This is particularly useful in creating low-fat versions of products where simply removing the fat would affect the structure of the product, and thus the perception of its quality if no replacement ingredient is added to maintain the structure. For example, in mayonnaise, modified starch, inulin, pectin, carrageenan, microcrystalline cellulose, and microparticulated pectin gels have been investigated for this purpose, with microparticulated pectin gels and weak pectin gels determined to be acceptable replacements for fat based on sensory analysis results (Liu et al. 2007).

In addition to their ability to increase viscosity by acting as bulking agents, many polysaccharides have the ability to form crosslinks and therefore contribute to gel structure and product firmness. Moreover, as consumers seek to add nutrients such as fiber to their diet, it is becoming more relevant for producers to add fiber to food products. Fibers such as inulin can be used as a low-calorie bulking agent or as a texturizing agent to replace fat and sugar (Tungland and Meyer 2002). In dairy products, inulin has been used to replace fat while improving taste and mouthfeel (Aryana et al. 2007; Allgeyer et al. 2010; Elleuch et al. 2011; Crispín-Isidro et al. 2015). For inulin, this functionality has been attributed to its ability to form a particulate gel network and bind water molecules (Franck 2002). Addition of inulin to model fat-free dairy desserts was shown to increase both storage modulus and complex viscosity, which was correlated with increased sensory sweetness, thickness, and creaminess (Tárrega and Costell 2006). In some low fat food products, the breakdown of starch by salivary amylase resulted in reduced oral friction, possibly due to the release and subsequent migration of fat to the surface of a starch-based matrix where it can act as a lubricant (de Wijk and Prinz 2005). This breakdown can have a notable impact on sensory texture, particularly temporal sensory attributes.

2.2.4 Flavor and Aroma Perception

Gel formation typically reduces the amount of flavor that is perceived in a food because the gel structure is essentially trapping the molecules within the network. This includes the tastant molecules as well, which are also trapped and reach the tongue in reduced quantities (Stieger and Van De Velde 2013). Similarly, when comparing high- and low-viscosity foods of the same salt concentration, the high-viscosity food will be perceived as less salty since it is more difficult for the salt molecules to diffuse to the tongue (Mills et al. 2011). On the other hand, increased flavor perception was found for brittle gels. This effect is due to the rapid rate at which brittle foods form new surfaces, and therefore have more area to interact with the tongue (Hafen et al. 2012). In another study using in vitro methods, foods such as elastic gels that break down into more and smaller particles, and thus have a larger surface area, have greater flavor release than foods such as brittle gels which break apart into fewer, larger fragments, and thus have a smaller surface area for the tastant molecules to interact with the tongue (Mills et al. 2011). Furthermore, brittle gels tend to have high syneresis; the expelled serum would carry flavor and tastant molecules to the tongue more rapidly.

3 Rheological and Sensory Evaluation of Yogurt

Yogurt provides an excellent example medium to study the rheology of semisolid foods. Although yogurt is simply fermented milk, there are numerous factors that can affect the final texture of the product. These can range from the starting ingredients (Jumah et al. 2001), such as the fat content of the milk (Sandoval-Castilla et al. 2004; Xu et al. 2007), added stabilizers (Hematyar et al. 2012; Imamoglu et al. 2017), and the type of bacteria used for fermentation (Kailasapathy 2006; Yang et al. 2016), to the pasteurization and fermentation temperature and time (Parnell-Clunies et al. 1988; Dagher and Ali 2016), shear rate experienced during processing, and whether the yogurt is set or stirred (Haque et al. 2001). Furthermore, in more complicated yogurt systems, additional ingredients such as fiber, fruit, or other ingredients may be added for fortification, flavor, and/or color that will also impact the final product gel structure and thus yogurt texture (Noisuwan et al. 2009; Considine et al. 2011; Imbachí-Narváez et al. 2018).

A large part of the structure of yogurt is due to the gelation of both casein and whey proteins (Schorsch et al. 2001; Modler and Kalab 2010). Fermentation drops the pH of the yogurt base, releasing colloidal calcium phosphate from the casein micelles and allowing the casein molecules to interact to form a gel (Pyne and McGann 1960; Dalgleish et al. 1989; Ozcan et al. 2011). During heat treatment, whey proteins denature and interact with caseins, which improves the water-holding capacity of the gel (Mottar et al. 2010). Higher heat treatments cause more denaturation, and thus more texture changes. Yogurt made with both skim milk and ultrafiltered milk was found to have higher scores for thickness and graininess than yogurt made from skim milk alone, probably due to the increased denatured whey protein available to gel the system (Biliaderis et al. 1992). Similarly, Janhøj et al. 2006 asked panelists to rate the meltdown rate, defined as “the rate by which the yogurt bolus breaks down in the mouth” and found that yogurt with a high level of added protein had the highest sensory viscosities and the slowest meltdown rate. However, further addition of microparticulated protein did not increase the viscosity, indicating that there is a limit on how much protein can alter yogurt viscosity.

The rheological properties of some yogurts are due in part to the formation of exopolysaccharides produced by bacteria, which can cause a ropy texture. The specific exopolysaccharides produced can vary depending on the strain of bacteria used to ferment the product (Tunick 2000). These hold the structure together and prevent fracture and syneresis (Cerning 1995). They also generate a long, stringy texture which can result in increased perception of smoothness or sliminess, depending on the level of exopolysaccharide present.

Stirred yogurts can be differentiated by their response to deformation in the linear (LVR) and nonlinear viscoelastic regions (Crispín-Isidro et al. 2015). The length of the LVR, as well as the food’s behavior in the LVR, is related to the structural arrangement of the food, while nonlinear viscoelastic behavior is related to the food’s response when the structure is broken or severely disrupted (Harte et al. 2007). In a study examining the effect of varying levels of fat and inulin content on yogurt rheological and sensory perception, the nonlinear viscoelastic behavior was more closely related to consumer perceptions than the behavior in the LVR (Guggisberg et al. 2009). Additionally, in a study examining the effect of different gums on yogurt texture, it was found that apparent residual stress as determined by a rheometer was significantly correlated ($r > 0.9$) with perceived sensory viscosity. Additionally, yield stress was a strong predictor of initial firmness perception (Harte et al. 2007).

For more information on how yogurt microstructures impact their rheological and sensory behaviors, Chapter “The Impact of Formulation on the Rheological, Tribological, and Microstructural Properties of Acid Milk Gels” presents rheological and tribological behaviors of acid milk gels, and Chapters “Relationships Among Acid Milk Gel Sensory, Rheological, and Tribological Behaviors”, and “Using Human Whole Saliva to Better Understand the Influences of Yogurt Rheological and Tribological Behaviors on Their Sensory Texture” present an in-depth study on microstructure–function–texture relationships of acid milk gels and yogurt, respectively.

4 Looking Forward

Due to its commercial relevance, the attempt to understand how underlying structures affect the sensory perceptions of food during oral processing has become an active area of research over the past several decades. Although new instruments and testing methodologies have greatly improved our understanding of structure–function–texture relationships, researchers are still looking to develop a reliable, low-cost and easy-to-use instrument that will generate data that can not only be used to test a wide range of food products, but will also give data that is corelated to multiple sensory attributes for those foods (Nguyen et al. 2016). Due to the complexity of most food products, it is still difficult to provide meaningful predictions about sensory characteristics from instrumental data using current approaches to understanding structure–function–texture relationships. Measurements in this area face a paradox of needing to be sophisticated enough to replicate the extremely complex conditions that occur in oral processing, yet simple enough that experimentation and data analysis can be performed as easily and quickly as possible. Combined with the need to produce fundamental data for proper replication of results, this makes developing approaches to evaluating food structure–function–texture relationships quite difficult. However, progress is being made on these approaches, particularly through multidisciplinary collaborations. As the fundamental understanding of the relationships among food microstructure, functional properties, and sensory textures continues to develop, it is highly likely that major breakthroughs in analysis protocols will emerge, further enhancing the understanding of the behaviors of complex foods.

References

Adams, M., & Birdsall, E. (1946). New consistometer measures corn consistency. *Food Industries, 18*, 844.

Akhtar, M., Stenzel, J., Murray, B. S., & Dickinson, E. (2005). Factors affecting the perception of creaminess of oil-in-water emulsions. In *Food hydrocolloids* (pp. 521–526).

Allgeyer, L. C., Miller, M. J., & Lee, S. Y. (2010). Drivers of liking for yogurt drinks with prebiotics and probiotics. *Journal of Food Science, 75*. https://doi.org/10.1111/j.1750-3841.2010.01579.x.

Aryana, K. J., Plauche, S., Rao, R. M., et al. (2007). Fat-free plain yogurt manufactured with inulins of various chain lengths and Lactobacillus acidophilus. *Journal of Food Science, 72*, 79–84. https://doi.org/10.1111/j.1750-3841.2007.00302.x.

Biliaderis, C. G., Khan, M. M., & Blank, G. (1992). Rheological and sensory properties of yogurt from skim milk and ultrafiitered retentates. *International Dairy Journal, 2*, 311.

Birkeland, S., & Skåra, T. (2008). Cold smoking of Atlantic salmon (Salmo salar) fillets with smoke condensate - an alternative processing technology for the production of smoked salmon. *Journal of Food Science, 73*. https://doi.org/10.1111/j.1750-3841.2008.00850.x.

Borne, M. (1975). Is rheology enough for food texture measurement? *Journal of Texture Studies, 6*, 259–262. https://doi.org/10.1016/j.yexmp.2014.03.001.

Çakir, E., Koç, H., Vinyard, C. J., et al. (2012). Evaluation of texture changes due to compositional differences using oral processing. *Journal of Texture Studies, 43*, 257–267. https://doi.org/10.1111/j.1745-4603.2011.00335.x.

Cerning, J. (1995). Production of exopolysaccharides by lactic acid bacteria and dairy propionibacteria. *Le Lait, 75*, 463–472. https://doi.org/10.1016/0023-7302(96)80129-1.

Chen, J., Liu, Z., & Prakash, S. (2014). Lubrication studies of fluid food using a simple experimental set up. *Food Hydrocolloids, 42*, 100–105. https://doi.org/10.1016/j.foodhyd.2014.01.003.

Considine, T., Noisuwan, A., Hemar, Y., et al. (2011). Rheological investigations of the interactions between starch and milk proteins in model dairy systems: A review. *Food Hydrocolloids, 25*, 2008–2017. https://doi.org/10.1016/J.FOODHYD.2010.09.023.

Crispín-Isidro, G., Lobato-Calleros, C., Espinosa-Andrews, H., et al. (2015). Effect of inulin and agave fructans addition on the rheological, microstructural and sensory properties of reduced-fat stirred yogurt. *LWT- Food Science and Technology, 62*, 438–444. https://doi.org/10.1016/j.lwt.2014.06.042.

Dagher, S., & Ali, A. (2016). Effect of pasteurization, centrifugation and additives on quality of concentrated yogurt (Labneh). *Journal of Food Protection, 48*, 300–302. https://doi.org/10.4315/0362-028x-48.4.300.

Dalgleish, D. G., Law, A. J. R., BAUMY, J. J., et al. (1989). pH-induced dissociation of bovine casein micelles. II. Mineral solubilization and its relation to casein release. *The Journal of Dairy Research, 56*, 727. https://doi.org/10.1017/S0022029900029290.

de Wijk, R. A., & Prinz, J. F. (2004). The role of friction in perceived oral texture. https://doi.org/10.1016/j.foodqual.2004.03.002

de Wijk, R. A., & Prinz, J. F. (2005). The role of friction in perceived oral texture. *Food Quality and Preference, 16*(2), 121–129. https://doi.org/10.1016/j.foodqual.2004.03.002.

de Wijk, R. A., Terpstra, M. E. J., Janssen, A. M., & Prinz, J. F. (2006). Perceived creaminess of semi-solid foods. *Trends Food Science Technology, 17*, 412–422. https://doi.org/10.1016/j.tifs.2006.02.005

Dresselhuis, D. M., De Hoog, E. H. A., Stuart, M. A. C., et al. (2008). The occurrence of in-mouth coalescence of emulsion droplets in relation to perception of fat. *Food Hydrocolloids, 22*, 1170–1183. https://doi.org/10.1016/j.foodhyd.2007.06.013.

Elleuch, M., Bedigian, D., Roiseux, O., et al. (2011). Dietary fibre and fibre-rich by-products of food processing: Characterisation, technological functionality and commercial applications: A review. *Food Chemistry, 124*, 411–421. https://doi.org/10.1016/j.foodchem.2010.06.077.

Foegeding, E. A., & Drake, M. A. (2007). Invited review: Sensory and mechanical properties of cheese texture. *Journal of Dairy Science, 90*, 1611–1624. https://doi.org/10.3168/jds.2006-703.

Foegeding, E. A., Stieger, M., & van de Velde, F. (2017). Moving from molecules, to structure, to texture perception. *Food Hydrocolloids, 68*, 31–42. https://doi.org/10.1016/j.foodhyd.2016.11.009.

Franck, A. (2002). Technological functionality of inulin and oligofructose. *The British Journal of Nutrition, 87*, 287–291. https://doi.org/10.1079/BJNBJN/2002550.

Friedman, H. H., Whitney, J. E., & Szczesniak, A. S. (1963). The texturometer - a new instrument for objective texture measurement. *Journal of Food Science, 28*, 390–396. https://doi.org/10.1111/j.1365-2621.1963.tb00216.x.

Godoi, F. C., Bhandari, B. R., & Prakash, S. (2017). Tribo-rheology and sensory analysis of a dairy semi-solid. *Food Hydrocolloids, 70*, 240–250. https://doi.org/10.1016/j.foodhyd.2017.04.011.

Goh, S. M., Versluis, P., Appelqvist, I. A. M., & Bialek, L. (2010). Tribological measurements of foods using a rheometer. *Food Research International, 43*, 183–186. https://doi.org/10.1016/j.foodres.2009.09.024.

Guggisberg, D., Cuthbert-Steven, J., Piccinali, P., et al. (2009). Rheological, microstructural and sensory characterization of low-fat and whole milk set yoghurt as influenced by inulin addition. *International Dairy Journal, 19*, 107–115. https://doi.org/10.1016/j.idairyj.2008.07.009.

Guinard, J.-X., & Mazzucchelli, R. (1996). The sensory perception of texture and mouthfeel. *Trends in Food Science and Technology, 7*, 213–219.

Gupta, R. K., & Sharma, A. (2007). Textural profile analysis of sunflower-sesame kernel confection (Chikki). *Journal of Texture Studies, 38*, 153–165. https://doi.org/10.1111/j.1745-4603.2007.00091.x.

Gwartney, E. A., Larick, D. K., & Foegeding, E. A. (2004). Sensory texture and mechanical properties of stranded and particulate. *Journal of Food Science volume, 69*, 333–339. https://doi.org/10.1111/j.1365-2621.2004.tb09945.x.

Hafen, C. A., Allen, J. P., Mikami, A. Y., et al. (2012). The pivotal role of adolescent autonomy in secondary school classrooms. *Journal of Youth and Adolescence, 41*, 245–255. https://doi.org/10.1016/j.foodhyd.2012.05.003.

Haque, A., Richardson, R. K., & Morris, E. R. (2001). Effect of fermentation temperature on the rheology of set and stirred yogurt. *Food Hydrocolloids, 15*, 593.

Harte, F., Clark, S., & Barbosa-Cánovas, G. V. (2007). Yield stress for initial firmness determination on yogurt. *Journal of Food Engineering, 80*, 990–995. https://doi.org/10.1016/j.jfoodeng.2006.06.027.

He, Q., Hort, J., & Wolf, B. (2016). Predicting sensory perceptions of thickened solutions based on rheological analysis. *Food Hydrocolloids, 61*, 221–232. https://doi.org/10.1016/j.foodhyd.2016.05.010.

Hematyar, N., Samarin, A. M., Poorazarang, H., & Hossein Elhamirad, A. (2012). Effect of gums on yogurt characteristics. *World Applied Sciences Journal, 20*, 661–665. https://doi.org/10.5829/idosi.wasj.2012.20.05.2353.

Heyer, P., & Läuger, J. (2009). Correlation between friction and flow of lubricating greases in a new tribometer device. *Lubrication Science, 21*, 253–268. https://doi.org/10.1002/ls.88.

Hiiemae, K. M., & Palmer, J. B. (2003). T ongue M ovements in F eeding and S peech. *Critical Reviews in Oral Biology and Medicine, 14*, 413–429. https://doi.org/10.1177/154411130301400604.

Hill, M. A., Mitchell, J. R., & Sherman, P. A. (1995). The relationship between the rheological and sensory properties of a lemon pie filling. *Journal of Texture Studies, 26*, 457–470. https://doi.org/10.1111/j.1745-4603.1995.tb00983.x.

Imamoglu, H., Coggins, P. C., & Rowe. (2017). Influence of storage time and starches on texture attributes of conventional milk yogurt using response surface methodology. *International Food Research Journal, 24*, 1721.

Imbachí-Narváez, P. C., Sepúlveda-Valencia, J. U., & Rodríguez-Sandoval, E. (2018). Effect of modified cassava starch on the rheological and quality properties of a dairy beverage prepared with sweet whey. *Food Science and Technology, 39*, 134–142. https://doi.org/10.1590/1678-457x.28017.

ISO. (2007). International Standard 8589. Sensory analysis. General guidance for the design of test rooms. Ref. No. ISO 8589:2007. International Organization for Standardization, Geneva, Switzerland.

Janhøj, T., Petersen, C. B., Frøst, M. B., & Ipsen, R. (2006). Sensory and rheological characterization of low-fat stirred yogurt. *Journal of Texture Studies, 37*, 276–299. https://doi.org/10.1111/j.1745-4603.2006.00052.x.

Joyner (Melito), H. S., Pernell, C. W., & Daubert, C. R. (2014). Impact of formulation and saliva on acid milk gel friction behavior. *Journal of Food Science, 79*, E867–E880. https://doi.org/10.1111/1750-3841.12439.

Jumah, R. Y., Shaker, R. R., & Abu-Jdayil, B. (2001). Effect of milk source on the rheological properties of yogurt during the gelation process. *International Journal of Dairy Technology, 54*, 89–93. https://doi.org/10.1046/j.1364-727x.2001.00012.x.

Kailasapathy, K. (2006). Survival of free and encapsulated probiotic bacteria and their effect on the sensory properties of yoghurt. *LWT- Food Science and Technology, 39*, 1221–1227. https://doi.org/10.1016/J.LWT.2005.07.013.

Kohyama, K., Sodhi, N. S., Suzuki, K., & Sasaki, T. (2016). Texture evaluation of cooked rice prepared from Japanese cultivars using two-bite instrumental test and electromyography. *Journal of Texture Studies, 47*, 188–198. https://doi.org/10.1111/jtxs.12172.

Kuhn, P. R., & Foegeding, E. A. (1991). Mineral salt effects on whey protein gelation∗. *Journal of Agricultural and Food Chemistry, 39*, 1013.

Laiho, S., Williams, R. P. W., Poelman, A., et al. (2017). Effect of whey protein phase volume on the tribology, rheology and sensory properties of fat-free stirred yoghurts. *Food Hydrocolloids, 67*, 166–177. https://doi.org/10.1016/j.foodhyd.2017.01.017.

Langton, M., & Hermansson, A.-M. (1992). Fine-stranded and particulate gels of β-lactoglobulin and whey protein at varying pH. *Food Hydrocolloids, 5*, 523–539. https://doi.org/10.1016/S0268-005X(09)80122-7.

Liu, H., Xu, X. M., & Guo, S. D. (2007). Rheological, texture and sensory properties of low-fat mayonnaise with different fat mimetics. *LWT- Food Science and Technology, 40*, 946–954. https://doi.org/10.1016/j.lwt.2006.11.007.

Liu, K., Stieger, M., van der Linden, E., & van de Velde, F. (2015). Fat droplet characteristics affect rheological, tribological and sensory properties of food gels. *Food Hydrocolloids, 44*, 244–259. https://doi.org/10.1016/j.foodhyd.2014.09.034.

Malone, M. E., Appelqvist, I. A. M., & Norton, I. T. (2003). Oral behaviour of food hydrocolloids and emulsions. Part 1. Lubrication and deposition considerations. In *Food hydrocolloids* (pp. 763–773).

Margaret, A. B., Elaine, Z. S., & John, A. C. (1963). Texture profile method. *Journal of Food Science, 28*, 404–409.

Martinez, O., Salmerón, J., Guillén, M. D., & Casas, C. (2004). Texture profile analysis of meat products treated with commercial liquid smoke flavourings. *Food Control, 15*, 457–461. https://doi.org/10.1016/S0956-7135(03)00130-0

Mcguffey, M. K., & Foegeding, E. A. (2001). Electrostatic effects on physical properties of particulate whey protein isolate gels. *Journal of Texture Studies, 32*, 285–305. https://doi.org/10.1111/j.1745-4603.2001.tb01049.x.

Miller, J. L., & Watkin, K. L. (1996). The influence of bolus volume and viscosity on anterior lingual force during the oral stage of swallowing. *Dysphagia, 11*, 117–124. https://doi.org/10.1007/BF00417901.

Mills, T., Spyropoulos, F., Norton, I. T., & Bakalis, S. (2011). Development of an in-vitro mouth model to quantify salt release from gels. *Food Hydrocolloids, 25*, 107–113. https://doi.org/10.1016/j.foodhyd.2010.06.001.

Modler, H. W., & Kalab, M. (2010). Microstructure of yogurt stabilized with milk proteins. *Journal of Dairy Science, 66*, 430–437. https://doi.org/10.3168/jds.s0022-0302(83)81810-4.

Mottar, J., Bassier, A., Joniau, M., & Baert, J. (2010). Effect of heat-induced association of whey proteins and casein micelles on yogurt texture. *Journal of Dairy Science, 72*, 2247–2256. https://doi.org/10.3168/jds.s0022-0302(89)79355-3.

Nguyen, P. T. M., Bhandari, B., & Prakash, S. (2016). Tribological method to measure lubricating properties of dairy products. *Journal of Food Engineering, 168*, 27–34. https://doi.org/10.1016/j.jfoodeng.2015.07.011.

Noisuwan, A., Hemar, Y., Wilkinson, B., & Bronlund, J. E. (2009). Dynamic rheological and microstructural properties of normal and waxy rice starch gels containing milk protein ingredients. *Starch/Staerke, 61*, 214–227. https://doi.org/10.1002/star.200800049.

Ozcan, T., Horne, D., & Lucey, J. A. (2011). Effect of increasing the colloidal calcium phosphate of milk on the texture and microstructure of yogurt. *Journal of Dairy Science, 94*, 5278–5288. https://doi.org/10.3168/JDS.2010-3932.

Parnell-Clunies, E., Kakuda, Y., Deman, J. M., & Cazzola, F. (1988). Gelation profiles of yogurt as affected by heat treatment of milk. *Journal of Dairy Science, 71*, 582.

Ponne, C. (1983). BibliotheekTU Delft predicting the texture of liquid and melting semi-solid foods. *Journal of Food Science, 48*, 1221–1225.

Pons, M., & Fiszman, S. M. (1996). Instrumental texture profile analysis with particular reference to gelled systems. *Journal of Texture Studies, 27*, 597–624. https://doi.org/10.1111/j.1745-4603.1996.tb00996.x.

Pradal, C., & Stokes, J. R. (2016). Oral tribology: Bridging the gap between physical measurements and sensory experience. *Current Opinion in Food Science, 9*, 34–41.

Prakash, S., Tan, D. D. Y., & Chen, J. (2013). Applications of tribology in studying food oral processing and texture perception. *Food Research International, 54*, 1627–1635.

Pyne, G. T., & McGann, T. C. A. (1960). The colloidal phosphate of milk: II. Influence of citrate. *The Journal of Dairy Research, 27*, 9–17. https://doi.org/10.1017/S0022029900010074.

Richardson, R. K., Morris, E. R., Ross-Murphy, S. B., et al. (1989). Characterization of the perceived texture of thickened systems by dynamic viscosity measurements. *Topics in Catalysis, 3*, 175–191. https://doi.org/10.1016/S0268-005X(89)80002-5.

Rogers, N. R., Drake, M. A., Daubert, C. R., et al. (2009). The effect of aging on low-fat, reduced-fat, and full-fat Cheddar cheese texture. *Journal of Dairy Science, 92*, 4756–4772. https://doi.org/10.3168/jds.2009-2156.

Rosenthal, A. J. (2010). Texture profile analysis - how important are the parameters? *Journal of Texture Studies, 41*, 672–684. https://doi.org/10.1111/j.1745-4603.2010.00248.x.

Sandoval-Castilla, O., Lobato-Calleros, C., Aguirre-Mandujano, E., & Vernon-Carter, E. J. (2004). Microstructure and texture of yogurt as influenced by fat replacers. *International Dairy Journal, 14*, 151–159. https://doi.org/10.1016/S0958-6946(03)00166-3.

Schorsch, C., Wilkins, D. K., Jones, M. G., & Norton, I. T. (2001). Gelation of casein-whey mixtures: Effects of heating whey proteins alone or in the presence of casein micelles. *The Journal of Dairy Research, 68*, 471–481. https://doi.org/10.1017/S0022029901004915.

Selway, N., & Stokes, J. R. (2013). Insights into the dynamics of oral lubrication and mouthfeel using soft tribology: Differentiating semi-fluid foods with similar rheology. *Food Research International, 54*, 423–431. https://doi.org/10.1016/j.foodres.2013.07.044.

Shama, F., Parkinson, C., & Sherman, P. (1973). Identification of stimuli controlling the sensory evaluation of viscosity I. non-oral methods. *Journal of Texture Studies, 4*, 102–110. https://doi.org/10.1111/j.1745-4603.1973.tb00656.x.

Skriver, A., Holstborg, J., & Qvist, K. B. (1999). Relation between sesnory texture analysis and rheological properties of stirred yoghurt. *The Journal of Dairy Research, 66*, 609–618.

Stading, M., & Hermansson, A.-M. (1991). Large deformation properties of β-lactoglobulin gel structures. *Food Hydrocolloids, 5*, 339–352. https://doi.org/10.1016/S0268-005X(09)80046-5.

Stieger, M., & Van De Velde, F. (2013). Microstructure, texture and oral processing: New ways to reduce sugar and salt in foods. *Current Opinion in Colloid & Interface Science*. https://doi.org/10.1016/j.cocis.2013.04.007.

Stokes, J. R., Boehm, M. W., & Baier, S. K. (2013). Oral processing, texture and mouthfeel: From rheology to tribology and beyond. *Current Opinion in Colloid & Interface Science, 18*, 349–359.

Szczesniak, A., Brandt, M., & Freidman, H. (1963). Development of standard rating scales for mechanical parameters and correlation between the objective and sensory texture measurements. *Food Technology, 22*, 50–54.

Tárrega, A., & Costell, E. (2006). Effect of inulin addition on rheological and sensory properties of fat-free starch-based dairy desserts. *International Dairy Journal, 16*, 1104–1112. https://doi.org/10.1016/j.idairyj.2005.09.002.

Tárrega, A., & Costell, E. (2007). Colour and consistency of semi-solid dairy desserts: Instrumental and sensory measurements. *Journal of Food Engineering, 78*, 655–661. https://doi.org/10.1016/j.jfoodeng.2005.11.003.

Tungland, B. C., & Meyer, D. (2002). Nondigestible oligo- and polysaccharides (dietary fiber): Their physiology and role in human health and food. *Comprehensive Reviews in Food Science and Food Safety, 1*, 90–109. https://doi.org/10.1111/j.1541-4337.2002.tb00009.x.

Tunick, M. H. (2000). Rheology of dairy foods that gel, stretch, and fracture. *Journal of Dairy Science, 83*, 1892–1898. https://doi.org/10.3168/jds.S0022-0302(00)75062-4.

Van Vliet, T. (2002). On the relation between texture perception and fundamental mechanical parameters for liquids and time dependent solids. *Food Quality and Preference, 13*, 227–236. https://doi.org/10.1016/S0950-3293(01)00044-1.

Volodkevich, N. N. (1938). Apparatus for meassurements of chewing resistance or tenderness of foodstuffs. *Journal of Food Science, 3*, 221–225. https://doi.org/10.1111/j.1365-2621.1938.tb17056.x.

Wood, F. W. (1968). Psychophysical studies on the consistency of liquid foods. *Soc Chem Ind Monogr Rheol Texture Food Stuffs*, 40–49.

Xu, Z.-M., Emmanouelidou, D. G., Raphaelides, S. N., & Antoniou, K. D. (2007). Effects of heating temperature and fat content on the structure development of set yogurt. *Journal of Food Engineering*. https://doi.org/10.1016/j.jfoodeng.2007.08.021.

Yang, Z., Yu, P., Zhang, Y., et al. (2016). Improvement of the texture of yogurt by use of exopolysaccharide producing lactic acid bacteria. *BioMed Research International, 2016*, 1–6. https://doi.org/10.1155/2016/7945675.

Part II
Case Studies

The Impact of Formulation on the Rheological, Tribological, and Microstructural Properties of Acid Milk Gels

Maryam Baniasadidehkordi and Helen S. Joyner

1 Introduction

Rheometry and tribometry are techniques that have been used to indicate food texture attributes. Rheology is the study of mechanical properties of foods, e.g. flow and deformation, which are often important to functionality and texture attributes. For example, viscosity has been correlated with several textural attributes of semisolid foods, such as mouth viscosity, sliminess, (creaminess), stickiness, and thickness (Stanley and Taylor 1993; Malone et al. 2003; Chojnicka-Paszun et al. 2014; Sonne et al. 2014). Rheological behavior of foods can be related to the manipulation of food under the shear and pressure of the oral surfaces at different sliding speeds after ingestion (Janssen et al. 2007). Nevertheless, food rheological behaviors are generally not sufficient to completely predict the perception of friction-related textural attributes such as graininess, smoothness, and chalkiness. Tribology, the science of friction, lubrication, and wear, has become popular in food texture and oral processing studies due to its ability to simulate the rubbing of two oral surfaces, producing a friction-related sensation that is important for perceiving certain textural attributes, e.g., astringency and creaminess (de Wijk and Prinz 2005; Engelen et al. 2005; Selway and Stokes 2013; Sonne et al. 2014).

Stribeck curves, which are plots of friction coefficient versus sliding speed, can be used to represent tribological behaviors of foods. These curves have three different regimes. First is the *boundary regime*, in which the contacting surfaces have a minimal gap and there is almost no space for the lubricant between surfaces. Thus, the boundary regime has high, constant friction coefficients compared to the other regimes due to significant surface–surface contact (Cassin et al. 2001). Second is the *mixed regime*. In this regime, the friction coefficient decreases to a minimum with increased sliding speed. The amount of lubricant between the contact surfaces

---

M. Baniasadidehkordi · H. S. Joyner (✉)
School of Food Science, University of Idaho, Moscow, ID, USA
e-mail: hjoyner@uidaho.edu

H. S. Joyner (ed.), *Rheology of Semisolid Foods*, Food Engineering Series,
https://doi.org/10.1007/978-3-030-27134-3_10

increases and results in increased surface separation, but the surfaces are still in contact. Third is the *hydrodynamic regime*. In this regime, the pressure from the lubricant becomes sufficient to completely separate the sliding surfaces. Creating a Stribeck curve profile with a friction coefficient vs. sliding speed can help predicting mouthfeel or after mouthfeel properties of semisolid foods during oral processing. For instance, it has been shown that astringency and slipperiness are mostly related to boundary regime (Prakash et al. 2013). Chapter 5, "Semisolid Food Tribology", provides a more detailed explanation of Stribeck curves and how they may be used for developing relationships among food behaviors.

Besides mechanical and frictional properties, microstructural imaging can help describe the textural differences in semisolid foods with different formulations. For instance, addition of starch to semisolid foods can increase the viscosity as well as the viscoelastic moduli. These results were in accordance with confocal images of acid milk gels with added potato starch that showed swollen potato starch granules embedded in the acid milk gel protein network; the density of the protein matrix increased with increased potato starch concentration (Oh et al. 2007). Indeed, viewing microstructural changes among samples can help explain why textural attributes are altered with changes in formulation or processing.

Different types (e.g. gums, proteins, starches) and concentrations of hydrocolloids can be added to reduced- or non-fat semisolid foods as texture enhancers (Ognean et al. 2006; Peng and Yao 2017). The mechanisms of hydrocolloid behaviors in a food system depend on the physicochemical properties of the hydrocolloid as well as its origin. The effect of hydrocolloids on semisolid food has received significant attention in the literature (Chojnicka-Paszun et al. (2009), Janssen et al. 2007, Oh et al. 2007, Milani and Maleki 2012, Chojnicka-Paszun et al. 2014). Whey protein powder is known to increase the viscosity of semisolid foods such as yogurt (Huc et al. 2016). However, it can have an adverse effect on sensory attributes, promoting astringency, chalkiness, and grittiness (Lucey and Singh 1997; Lee and Lucey 2010; Morell et al. 2016). Cellulose gum can mimic fat functionality but can also increase food viscosity (Cho and Prosky 1999). Starches are another category of hydrocolloids that are used as fat replacers in semisolid foods. They can improve the rheological properties of foods (Cho and Prosky 1999; Peng and Yao 2017), but they may show significantly different oral behavior compared to the original food due to amylose hydrolysis after interaction with human whole saliva (HWS) (Janssen et al. 2007). Other food ingredients can show similar sensitivity to components of HWS. Thus, considering the effect of HWS in predicting texture perception of semisolid foods is key for better interpretation of sensory data.

HWS is secreted during all the stages of oral processing. The most important role of HWS is lubrication. It softens food, helps move the formed bolus in the mouth under oral pressure and shear, and contributes to the initial breakdown of food components (Andrewes et al. 2011). In addition, HWS complexes with smaller food particles in the mouth and forms a thin lubricating layer between the palate and tongue as well as the oral surfaces and food bolus during mastication (Chen and Engelen 2012). HWS can disrupt food structure by dilution, enzymatic hydrolysis, and protein complexation. Salivary proteins, mainly mucin, can alter food structures by altering the net charge, potentially resulting in particle precipitation (Chen and Engelen 2012). Overall, α-amylase and protein concentration have been shown to have the greatest effect on texture perception of semisolid foods, particularly those that are starched-based (Engelen et al. 2007).

Temperature change is another factor that can affect texture perception of semisolid foods and needs to be considered during *in vitro* testing. Accordingly, controlling temperature, adding HWS, and using materials that mimic the oral surfaces during instrumental testing can provide a more accurate picture of how food structure changes during oral processing and contributes to texture perception of foods. Therefore, the objectives of this study were to determine how formulation and HWS impact semisolid food microstructure, rheological, and tribological behaviors of acid milk gels at 25 °C and 8 °C. This study was the first step in understanding the microstructure–rheology–texture relationships in acid milk gels with different formulations. In a followup study (Chap. 11, "Among Acid Milk Gel Sensory, Rheological, and Tribological Behaviors"), selected textural attributes of the acid milk gels used in this study were measured and correlated to their rheological and tribological behaviors to create a better understanding of these relationships. The results of these two studies can be applied to targeted development of a wide variety of reduced or non-fat semisolid foods with desirable textural properties.

2 Materials and Methods

2.1 Materials

Skim milk (WinCo Foods brand) was obtained from a local supermarket (Moscow, ID, USA). Low heat skim milk powder (SMP, Darigold brand) and Darigold brand heavy cream (40% fat) were provided by the WSU Creamery (Pullman, WA, USA). Locust bean gum (LBG) and carboxymethyl cellulose (CMC) (pre-hydrated Ticalose CMC 2500 powder) were donated by TIC Gums (TIC Gums, Inc., Belcamp, MD, USA). Corn starch (CS) and modified potato starch (PS) were donated by Ingredion (Bridgewater, NJ, USA). Whey protein isolate (WPI) (Provon 190, 89.4% protein) was donated by Glanbia Nutritionals (Fitchburg, WI, USA). Glucono-delta-lactone (GDL) was donated by Jungbunzlauer (Jungbunzlauer, Inc., MA, USA). The protein assay kit (Quick Start Bradford) used for protein measurement of HWS was purchased from Bio-Rad laboratories (Bio-Rad laboratories, Inc. CA, USA). Teflon balls (6 mm) for tribometry were purchased from McMaster-Carr (Atlanta, GA, USA). GluconoFluorescein Isothiocyanate (FITC) dye and cavity slides were purchased from Sigma (Sigma-Aldrich, St. Louis, MO., USA), and Nile red dye was purchased from TCI America (Portland, OR, USA).

2.2 Sample Preparation

Twenty-four different formulations of acid milk gels were prepared with skim milk, SMP, cream, WPI, and hydrocolloids, including LBG, corn starch, potato starch, and CMC. Specific formulations are given in Table 1. Formulations were designed to maintain a total solids content of 13% w/w in the finished acid milk gels. After adding all the hydrocolloids and cream to the skim milk at room temperature (22 ± 2 °C), the mixture was stirred with a spatula to disperse the dry powders for 3 min in a water bath (Precision, Thermo Fisher Scientific, Waltham, MA, USA) at pasteurization temperature (85 °C) for complete dissolution. The mixture was then held at 85 °C for an additional 30 min without stirring. Subsequently, the mixture was homogenized at 5000 rpm for 1 min using a stand homogenizer (Polytron, Kinematica AG, NY, USA), and cooled to 42.2 °C for addition of GDL (1.1–1.55% w/w, Table 1). The mixture was incubated at 42.2 °C for 4 hr. to reach a pH of 4.55–4.6. The gel was then broken with a metal laboratory spatula and stored in the refrigerator at 4 °C overnight. Acid milk gels were blended at 350 rpm for 10 s before testing to remove lumps; preliminary testing showed that this preshear procedure did not impact sample rheology and improved data repeatability. Each sample was made in duplicate on different days and tested within 24 hr of production.

2.3 Proximate Analysis

All proximate analysis was conducted in duplicate. Protein content was determined using a Leco FP-528 nitrogen analyzer (Leco Corp., St. Joseph, MI, USA) according to the manufacturer's instructions (Kjeldahl conversion factor = 6.38). Moisture contents were determined using a DKN 400 oven (Yamato Scientific America, Inc., Santa Clara, CA, USA), according to the method of AOAC (1999). Fat contents were determined only for samples with added cream using the Mojonnier method 989.05 (AOAC 1995a). Skim milk with negligible fat content was used for preparation of other samples. Hydrocolloids also had negligible fat content according to their specification sheets that were provided by their manufacturers. Therefore, fat content was considered zero for samples made without cream. Ash contents were determined by the method of AOAC (1995b), dry basis. Carbohydrate contents were calculated by difference.

Table 1 Experimental design of acid milk gel formulations

Formula number	SMP (w/w)	Sweet WPI (w/w)	LBG (w/w)	CMC (w/w)	Potato starch (w/w)	Corn starch (w/w)	Skim milk (w/w)	Cream (w/w)	GDL (w/w)
1	2.8	0	0	0	0	0	97.2	0	1.1–1.55
2	2.83	0	0	0	0	0	95.96	1.21	1.1–1.55
3	2.89	0	0	0	0	0	92.26	4.85	1.1–1.55
4	2.95	0	0	0	0	0	89.15	7.9	1.1–1.55
5	1.8	1	0	0	0	0	97.2	0	1.1–1.55
6	1.8	0	1	0	0	0	97.2	0	1.1–1.55
7	1.8	0	0	1	0	0	97.2	0	1.1–1.55
8	2.1	0	0	0	0.7	0	97.2	0	1.1–1.55
9	2.1	0	0	0	0	0.7	97.2	0	1.1–1.55
10	0	1.25	1.55	0	0	0	97.2	0	1.1–1.55
11	0	1.25	0	1.55	0	0	97.2	0	1.1–1.55
12	0	1.25	0	0	1.55	0	97.2	0	1.1–1.55
13	0	1.25	0	0	0	1.55	97.2	0	1.1–1.55
14	0.5	0.8	0	0.75	0.75	0	97.2	0	1.1–1.55
15	0.5	0.8	0.75	0.75	0	0	97.2	0	1.1–1.55
16	0	2.8	0	0	0	0	97.2	0	1.1–1.55
17	0	0	0	1.4	1.4	0	97.2	0	1.1–1.55
18	0	0	1.8	0	0	1	97.2	0	1.1–1.55
19	0	1.15	0.55	0.55	0.55	0	97.2	0	1.1–1.55
20	0	1.15	0	0.55	0.55	0.55	97.2	0	1.1–1.55
21	0	0	0.7	0.7	0.7	0.7	97.2	0	1.1–1.55
22	0.55	0.75	0.5	0.5	0.5	0	97.2	0	1.1–1.55
23	1	0	0.45	0.45	0.45	0.45	97.2	0	1.1–1.55
24	0.2	0.8	0.45	0.45	0.45	0.45	97.2	0	1.1–1.55

2.4 HWS Collection

Approval for collecting HWS was received from University of Idaho Institutional Review Board (protocol 17–196). HWS collection was done according to a modified method of Bongaerts et al. (2007b). HWS was collected from 5 healthy people (3 females and 2 males, ages 20–35) with normal saliva flow. Panelists were asked to refrain from eating and drinking anything except water 2 hr. prior to each collection. At the start of collection, panelists were required to rinse their mouth twice with deionized water and expectorate into a waste cup. They were given a disposable plastic pipette to chew for HWS stimulation and expectorated their saliva into a 2-oz. cup. The first two expectorations discarded were into a discard cup. Fresh HWS was collected every 2 hr to minimize aging effects during testing. HWS was used for both rheological and tribological testing within 2 hr of collection for the testing, and any excess was discarded.

For testing samples with HWS, all HWS was pooled in a single container and mixed thoroughly. 0.5 ml of the pooled HWS was pipetted and mixed with 3 g of sample and held at room temperature (22 ± 2 °C) for 5 min for complete digestion (Joyner (Melito) et al. 2014). Care was taken to minimize bubble formation in the HWS.

2.5 Rheometry

Rheological properties of acid milk gels were measured with an Anton Paar MCR 302 rheometer (Anton Paar, Graz., Austria) using a 50 mm diameter parallel plate with a measuring gap of 1 mm. All tests were carried out at 25 °C and 8 °C with and without addition of human whole saliva (HWS) collected per Sect. 2.4. Samples were equilibrated to the test temperature for 60 s prior to testing. Each sample was tested in triplicate and results were averaged for data analysis. Samples were tested with and without addition of HWS.

Shear rate sweeps (0.01–100 s^{-1}) were carried out to measure acid milk gel viscosity profiles. Oscillatory tests were performed to measure acid milk gel viscoelastic properties. Strain sweeps were performed at 0.01–100% and a frequency of 1 Hz. Frequency sweep tests were performed at 0.1–100 rad s^{-1} and 75% of the lowest critical strain calculated from strain sweeps (1.0%) so that tests would be performed in the linear viscoelastic region (LVR), using and 0.75% strain. Critical strain was calculated by determining the strain at which $G*$ deviated by >1% from the previous value within the LVR (Steffe 1996; Tunick 2010).

2.6 PDMS Plate Production

Polydimethylsiloxane (PDMS) gel plates were generated for tribometry using the method of Bongaerts et al. (2007a). Briefly, plates were made by mixing a curing agent and a base (Dow Corning Corporation, Midland, MI, USA) in a proportion of 1:10 in a beaker, then the mixture was poured into an aluminum mold (4 mm height and 60 mm diameter). Air bubbles were removed by placing them in a cabinet vacuum desiccator (Bel-Art Products, Wayne, NJ, USA) under a pressure of −90 kPag until all bubbles were removed. The PDMS plates were cured at 55 °C for 2 hr. in a DKN 400 oven (Yamato Scientific America, Inc., Santa Clara, CA, USA), then stored overnight at room temperature (22 ± 2 °C) to complete curing. The plates were removed and stored at room temperature (22 ± 2 °C) until used for testing.

2.7 Tribometry

Tribometry was performed using an Anton Paar MCR 302 (Anton Paar, Graz., Austria) with a three-ball (Teflon, 6 mm diameter) geometry on a 60-mm diameter PDMS plate. These surfaces were selected to mimic the palate–tongue contact (Johnson et al. 1993; Prakash et al. 2013). The normal force used was 1 N to mimic the in-mouth force during swallowing, which is between 0.01 and 10 N (Miller and Watkin 1996). The PDMS plate was placed on top of the original stainless plate of the rheometer and pressed firmly to adhere the two surfaces. A line was marked on both the PDMS plate and stainless steel using an indelible laboratory pen to provide visual confirmation that the PDMS plate did not move during testing. Friction coefficient was measured at sliding speeds of 0.01–1000 mm s^{-1}. Samples were tested at 25 °C. At least three replicates for each sample duplicate were performed with and without HWS. The contact surfaces were cleaned after each run with 70% ethanol and laboratory wipes for non-fat samples. 70% ethyl ether followed by a 70% ethanol rinse was used to clean the contact surfaces when testing fat-containing samples to prevent fat film buildup on the contact surfaces. Both plates and balls were changed after every 6 runs to prevent wear from affecting the results (determined by preliminary testing).

2.8 HWS Analyses

The composition of HWS can significantly affect the texture perception of semi-solid foods. Protein concentration and α-amylase activity were reported to have the greatest impact among other components of HWS (Engelen et al. 2007). Accordingly, collected HWS (Sect. 2.4) was centrifuged at 10,000 rpm (14,087 *g*) for 5 min to remove buccal cells and oral microorganisms. The clear supernatants were stored at −18 °C for further measurements and were thawed at room temperature (22 ± 2 °C) 30 min before testing (Engelen et al. 2007).

A Bradford protein kit was used to determine the protein concentration in HWS (Quick Start™ Bradford Protein Assay, Bio-Rad). Eight samples were collected from 5 healthy panelists within 2 wk. and tested in triplicate. The assay was performed according to the manufacturer's guidelines (Bio-Rad Laboratories, Inc. CA., USA). A microplate standard assay using bovine serum albumin (BSA) was used as a protein standard.

A modified Somogyi-Nelson assay was performed to determine salivary α-amylase activity (Shao and Lin 2018). Different concentrations of maltose, a source of reducing sugar, in a series of 0–0.6 mM was used to create the standard curve for the assay; maltose is one of the sugars produced by α-amylase from amylose and amylopectin from cleaving the starch chain. The curve was plotted based on absorbance as a function of sugar concentration with a linear relationship of

R^2 = 0.97. The procedure and mechanisms of this test are explained in detail by (Shao and Lin 2018).

For measuring reducing sugars in HWS, a soluble starch solution was prepared by adding 0.05 g soluble starch to 5 mL water in a Falcon tube and gelatinized in a boiling water bath for 30 min; the tube was shaken every 5 min. After heating, 50 μL of the starch solution was micropipetted into each of 15 microtubes with a 1.7 mL capacity (Sorenson, BioScience, Inc., Salt Lake City, UT, USA). A dilution of 1:250 of HWS:DI water was made due to high α-amylase activity in HWS samples. 50 μL of the diluted HWS was added to each of 15 microtubes containing the starch solution. These microtubes were incubated at 37 °C for 0, 3, 5, 7, and 9 min. Samples were further diluted with DI water at a ratio of 1:5 sample:DI water for the reaction times of 3 and 5 min, and 1:7 sample:DI water for the reaction times of 7 and 9 min. Blank samples of HWS and no soluble starch were created as a control (zero reaction time). After incubation, the mix of HWS and soluble starch was pipetted into a polypropylene 96-well microplate (Corning Company, NY, U.S.A) in triplicate, then enzymes were inactivated by boiling the microplate covered with a silicone mat and foil (Shao and Lin 2018). The covered microplate was cooled for 5 min under cold water, then 45 μL of arsenomolybdate color reagent, prepared via the method of (Nelson 1944) was added to each well. The microplate was held at room temperature (22 ± 2 °C) for 15 min, then the absorbance was read at 600 nm using a microplate reader (Spectra Max 190 Microplate Reader, Molecular Devices, CA, USA). Considering the amounts of released reducing sugar from HWS samples and their protein concentration from Bradford assay, α-amylase activity was determined as the quantity of enzyme required to produce 1 μM of maltose in 1 min per 1 mg of protein (U mg^{-1}).

2.9 *Confocal Imaging*

Microstructural properties of the acid milk gels were imaged using confocal laser scanning microscopy (CLSM). GluconoFluorescein isothiocyanate (FITC) dye and Nile red were used to stain the proteins and fat globules, respectively. 500 μL of ethanol was added to 8 mg of FITC in a 1 mL vial and was vortexed for 10 s, then another 500 μL of deionized water was transferred to the FITC solution and vortexed for another 10 s. The same procedure was repeated for making the Nile red dye, except 5 mg of Nile red was added. Both dyes were used for the samples containing fat and FITC was used for all the samples. Dyes were added to 120 g of each acid milk gel mixture before addition of GDL. Samples were then stirred with a spatula to mix the dyes evenly. Samples were incubated for 4 hr. to reach a pH of 4.55–4.6 and refrigerated overnight; microscopy analysis was performed the next day. 500 μL of each acid milk gel sample was transferred to a cavity slide and covered with a glass coverslip. Samples were imaged at 20X and 4–8 °C with an excitation wavelength of 559 nm for FITC and 488 nm for Nile red.

2.10 Data Analyses

Rheological and tribological data were plotted using Origin 8 software (OriginLab; Northampton, MA, USA). The error bars of each sample for both rheology and tribology tests were calculated using the standard deviation of the samples and their duplicates (6 data points per formulation). The average of the full viscosity profile for each formulation was calculated and the average curves were fitted to three models: Cross-Williams (Eq. 1), Cross (Eq. 2), and Herschel-Bulkley (Eq. 3) using TRIOS software (TA Instruments; New Castle, Delaware, USA).

$$\eta = \frac{\eta_o}{\left[1+\left(c\dot{\gamma}\right)^{1-n}\right]} \tag{1}$$

$$\eta = \eta_\infty + \frac{\eta_o - \eta_\infty}{1+\left(k\dot{\gamma}\right)^{n}} k\gamma^{n-1} \tag{2}$$

$$\sigma = \sigma_o + K\dot{\gamma}^{n} \tag{3}$$

In the Cross-Williams model (Eq. 1), η_o is the zero-shear rate viscosity (Pa.s). This parameter can be helpful for determining gel stability and comparing the polymer molecular weight. c is the time constant (s); $1/c$ can be indicative of a critical shear rate for the onset shear rate when shear thinning starts. n is the flow behavior index (unitless), and it is indicative of the level of viscosity dependence on shear rate. For instance, the value of n is unity for Newtonian materials. In the Cross model (Eq. 2) η_o is the zero-shear rate viscosity (Pa.s), η_∞ is the infinite viscosity plateau (Pa.s); k is the time constant (s), and n is flow behavior index (unitless). In the Herschel-Bulkley model (Eq. 3), σ_o is the yield stress (Pa), the minimum force needed to induce flow. k is the consistency coefficient (Pa.s^{1-n}) and n is the flow behavior index (unitless). In shear-thinning materials ($0 < n < 1$), pseudoplastic behavior increases as n approaches zero. These model parameters were used for statistical analysis or comparison of viscosity properties of acid milk gels.

All statistical analyses were performed with SAS version 9.1 (SAS; Cary, NC). From the rheological results, γ_c (critical strain, %), G^* (complex modulus, Pa), and tan δ (phase angle, rad) were selected for statistical analysis. Friction coefficients at 10, 15, 20, 25, and 30 mm s^{-1} sliding speeds were used for data analysis. This selection of speeds was to mimic the oral speed, reported to be 10–30 mm s^{-1} for semi-solid foods (De Wijk and Prinz 2006). Data analysis included three-way ANOVA for determining the impact of formulation, HWS, and temperature on selected rheological and tribological, as well as ANOVA (α = 0.05) followed by Tukey's HSD (Honest Significant Difference) test, which was used to determine significant differences among acid milk gel rheological, tribological, and proximate analysis results.

3 Results and Discussion

3.1 Acid Milk Gel Proximate Compositions

Acid milk gel proximate compositions showed significant differences for moisture, protein, ash, fat, and carbohydrate contents (Table 2). Total solids content was kept constant for all formulations at 13% w/w. The protein content of the formulations ranged from 3.78% to 6.78%. Sample 23 had the lowest amount of protein since it contained only non-protein hydrocolloids. Sample 16 had the highest concentration, as expected due to the higher level of WPI addition. The moisture contents of the acid milk gels prepared with LBG (sample 6, 18) or all hydrocolloids except CS (sample 19) were the greatest amount among all acid milk gels. These results were

Table 2 Acid milk gel proximate composition[a]

Samples	Protein (%)	Moisture (%)	Fat (%)	Ash (%)	Carbohydrate (%)[b]
1	4.51 ± 0.045^{de}	86.22 ± 0.043^{abcd}	0	0.63 ± 0.009^{bcde}	8.64^{efgh}
2	4.4 ± 0.054^{defgh}	85.87 ± 0.206^{abcde}	0.49 ± 0.008^{a}	0.58 ± 0.001^{cdef}	8.67^{defgh}
3	4.02 ± 0.01^{l}	82.79 ± 0.213^{i}	1.92 ± 0.142^{b}	0.59 ± 0.02^{cdef}	10.68^{b}
4	4.24 ± 0.009^{hijk}	83.88 ± 0.404^{hg}	3.36 ± 0.064^{c}	0.53 ± 0.03^{f}	8.00^{ij}
5	6.13 ± 0.02^{b}	812.17 ± 0.015^{hg}	0	0.72 ± 0.002^{a}	8.98^{defghi}
6	4.46 ± 0.04^{defg}	86.72 ± 0.29^{a}	0	0.62 ± 0.009^{cde}	8.21^{ghij}
7	4.29 ± 0.014^{ghij}	81.79 ± 0.198^{j}	0	0.69 ± 0.019^{ab}	13.23^{a}
8	4.38 ± 0.031^{efghi}	85.52 ± 0.191^{cde}	0	0.64 ± 0.006^{bc}	9.47^{cdef}
9	4.49 ± 0.014^{de}	85.52 ± 0.149^{cde}	0	0.59 ± 0.033^{cdef}	9.41^{cdef}
10	5.42 ± 0.065^{c}	85.36 ± 0.085^{fde}	0	0.56 ± 0.007^{ef}	8.66^{efghij}
11	4.51 ± 0.003^{de}	84.47 ± 0.198^{fg}	0	0.63 ± 0.013^{bcd}	10.39^{bc}
12	5.49 ± 0.119^{c}	86.3 ± 0.022^{abcd}	0	0.56 ± 0.002^{def}	7.66^{j}
13	4.26 ± 0.014^{hijk}	82.72 ± 0.043^{ij}	0	0.59 ± 0.024^{cdef}	12.43^{a}
14	4.57 ± 0.014^{d}	86.14 ± 0.12^{abcde}	0	0.64 ± 0.007^{bc}	8.66^{efghij}
15	4.3 ± 0.055^{fghij}	86.62 ± 0.177^{ab}	0	0.61 ± 0.002^{cde}	8.48^{fghij}
16	6.87 ± 0.011^{a}	83.33 ± 0.149^{hi}	0	0.58 ± 0.021^{cdef}	9.23^{defgj}
17	4.07 ± 0.092^{kl}	86.22 ± 0.001^{abcd}	0	0.72 ± 0.001^{a}	9.00^{defghj}
18	4.39 ± 0.06^{defgh}	86.82 ± 0.029^{a}	0	0.57 ± 0.014^{def}	8.22^{ghij}
19	4.49 ± 0.009^{def}	86.74 ± 0.085^{a}	0	0.62 ± 0.003^{bcde}	8.15^{hij}
20	4.46 ± 0.06^{defg}	85.47 ± 0.269^{cde}	0	0.62 ± 0.008^{cde}	9.45^{cdef}
21	12.19 ± 0.067^{ijkl}	86.4 ± 0.015^{abc}	0	0.62 ± 0.002^{cde}	8.79^{defghi}
22	4.37 ± 0.012^{efghi}	85.2 ± 0.686^{ef}	0	0.73 ± 0.001^{a}	9.71^{bcd}
23	3.78 ± 0.014^{m}	86.45 ± 0.142^{abc}	0	0.59 ± 0.047^{cdef}	9.18^{defgh}
24	12.12 ± 0.014^{jkl}	85.67 ± 0.481^{bcde}	0	0.62 ± 0.002^{bcde}	9.59^{cde}

[a] Different letters in a given column indicate significant differences in that column at $p \leq 0.05$. Fat contents of non-fat samples were considered zero based on ingredient compositions rather than fat analysis

[b] Carbohydrates were calculated by difference

attributed to the weak gel structure formed between LBG and milk proteins. The dispersion of LBG throughout the gel structure may have increased its water holding capacity and make it more difficult to escape during the moisture measurement. The sample prepared with CMC (sample 7) had the lowest moisture content. Differences in moisture content may have been due to the differences in the number of available molecules in the system for interaction with the protein network; more interactions would trap additional water and increase the retained moisture.

The fat content of acid milk gels with no added cream was considered zero since there was negligible fat in their formulations from the ingredients. Ash and carbohydrate contents of acid milk gels showed significant differences based on formulation. Moisture and carbohydrate contents appeared to have opposite trends. Sample 7 had the lowest moisture content and the most amount of carbohydrate. This effect was inversed for sample 6, which contained LBG. Full-fat acid milk gels had the lowest amount of ash and samples 5 (low level of WPI), 17 (CG and PS), and 22 (all hydrocolloids but CS) showed the highest ash content. The range of ash content in the non-fat milk powders, e.g. SMP and WPI, was higher than the ones with fat. Additionally, different gums and starches have different ash contents, which may explain the differences in ash content.

3.2 Saliva Composition

The composition analysis of 8 HWS samples showed no significant differences (p>0.05) among α-amylase activity (U mg^{-1}). However, significant differences (p≤0.05) were found for protein concentration (Appendix A). It was difficult to relate these differences to any variations in rheological, tribological, and microstructural imaging, as the time needed to test the HWS samples (over 1 hr) resulted in the samples aging past the point where they could be used for rheological and tribological testing. Thus, the samples used for compositional analysis were not the same samples used for rheological and tribological testing. On the other hand, the samples tested with added HWS were held for 5 min after mixing with saliva and before testing. This hold time would compensate for any differences in reaction rates due to HWS compositional differences, rendering any effects from compositional difference negligible.

3.3 Acid Milk Gel Microstructural Properties

Overall, all acid milk gel microstructures comprised a particulate protein network containing serum; the specific conformation of the protein network structure was dependent on acid milk gel formulation (Figs. 1, 2, and 3). The control sample (sample 1) showed a more homogenous protein network with smaller pores sizes (Fig. 1a). The branches of protein network became thicker and the size of the open-

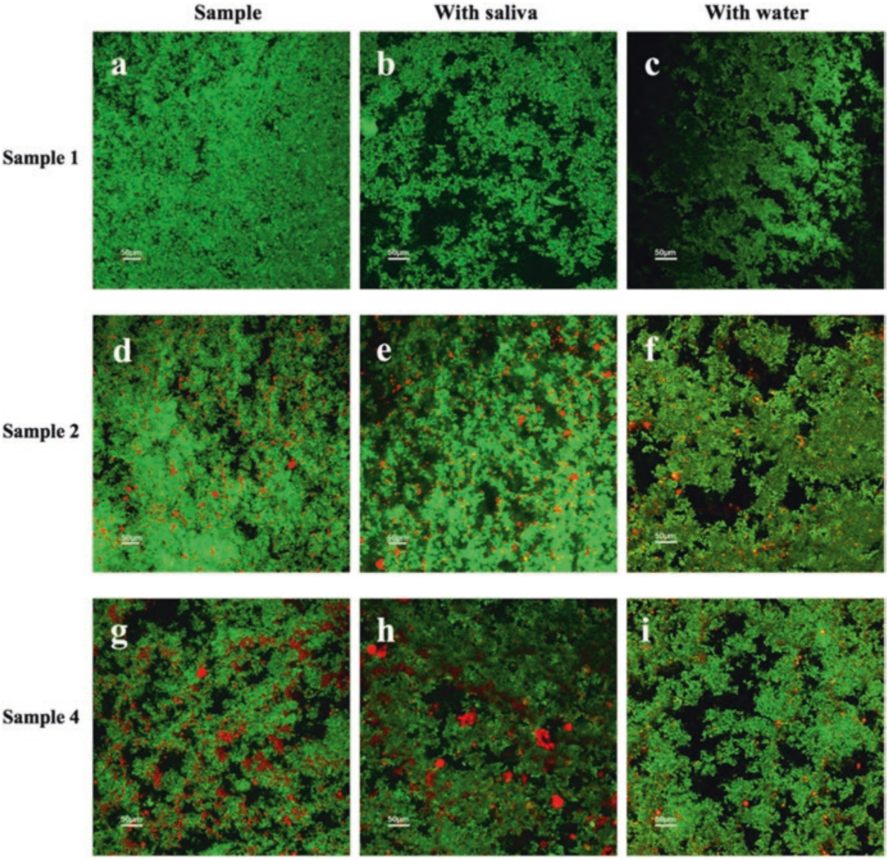

Fig. 1 CLSM results of acid milk gels; (**a**) sample 1; (**b**) sample 1: with HWS; (**c**) sample 1: with water; (**d**) sample 2; (**e**) sample 2: with HWS; (**f**) sample 2: with water; (**g**) sample 4; (**h**) sample 4: with HWS; (**i**) sample 4: with water. The protein network, fat globules, and serum pores are shown in green, red, and black, respectively

ings (aqueous phase) increased with addition of hydrocolloids. However, the microstructural features differed with the specific hydrocolloid used in the formulation. The density of the protein structure for samples with PS (sample 8, Fig. 3a) decreased and the aqueous phase increased compared to the control. However, the sample with CS (sample 9, Fig. 3d) had smaller pores and was more homogenous and similar to the control sample. Although the branches of the protein network for the sample with CMC (sample 7, Fig. 2g) were large and thick, the void area was larger than the void area for the sample with LBG (sample 6). This effect was reflected in the moisture content of these two samples (Table 2). The thickest and largest clusters in the protein network were shown in the sample with all hydrocolloids (sample 24, Fig. 3g), indicating that addition of all hydrocolloids caused the most notable differ-

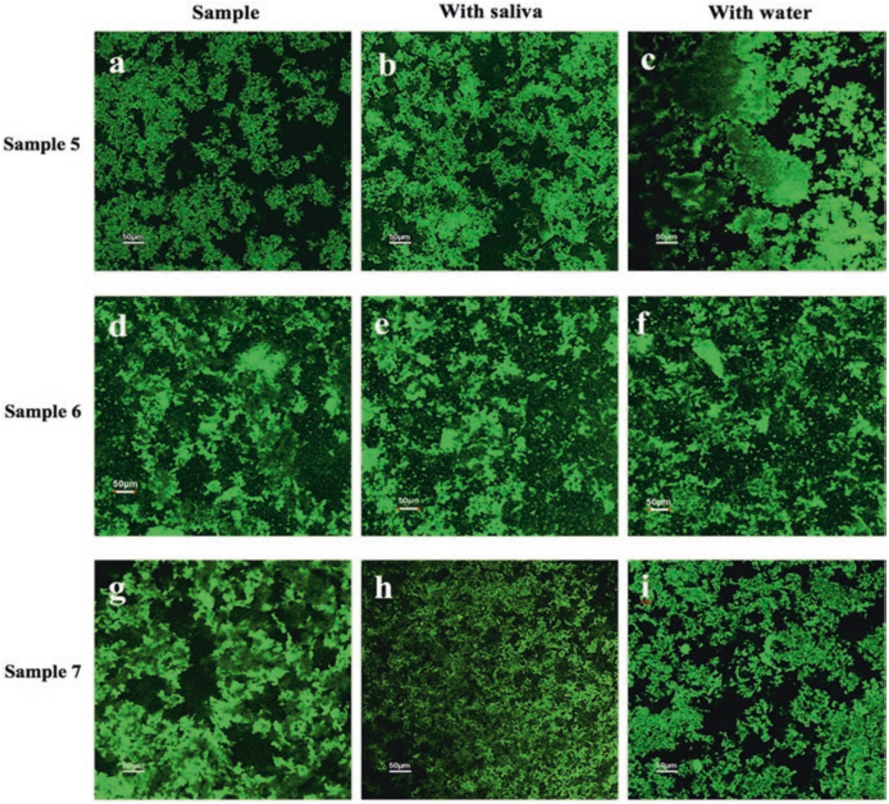

Fig. 2 CLSM results of acid milk gels; (**a**) sample 5; (**b**) sample 5: with HWS; (**c**) sample 5: with water; (**d**) sample 6; (**e**) sample 6: with HWS; (**f**) sample 6: with water; (**g**) sample 7; (**h**) sample 7: with HWS; (**i**) sample 7: with water. The protein network and serum pores are shown in green and black, respectively

ences in the protein matrix compared to the control due to different interactions of hydrocolloids with protein network.

In general, addition of water did not have as notable an effect on the microstructure as addition of HWS. More dark areas appeared for several of the samples upon addition of water, which was expected since this area corresponded to the serum phase. However, samples with added LBG (sample 6), CMC (sample 7), and PS (sample 8) did not show notable differences in the amount of serum present (Figs. 2 and 3). This result may have been due to the water-holding ability of these hydrocolloids, which would prevent larger serum pools from forming upon addition of water.

Addition of HWS generally increased protein aggregation and amount of free serum, regardless of formulation. Samples with added HWS showed more distinct protein clusters compared to samples with added water. This result was attributed to the digestive, dissolving, and coalescing effects of HWS caused by enzymes,

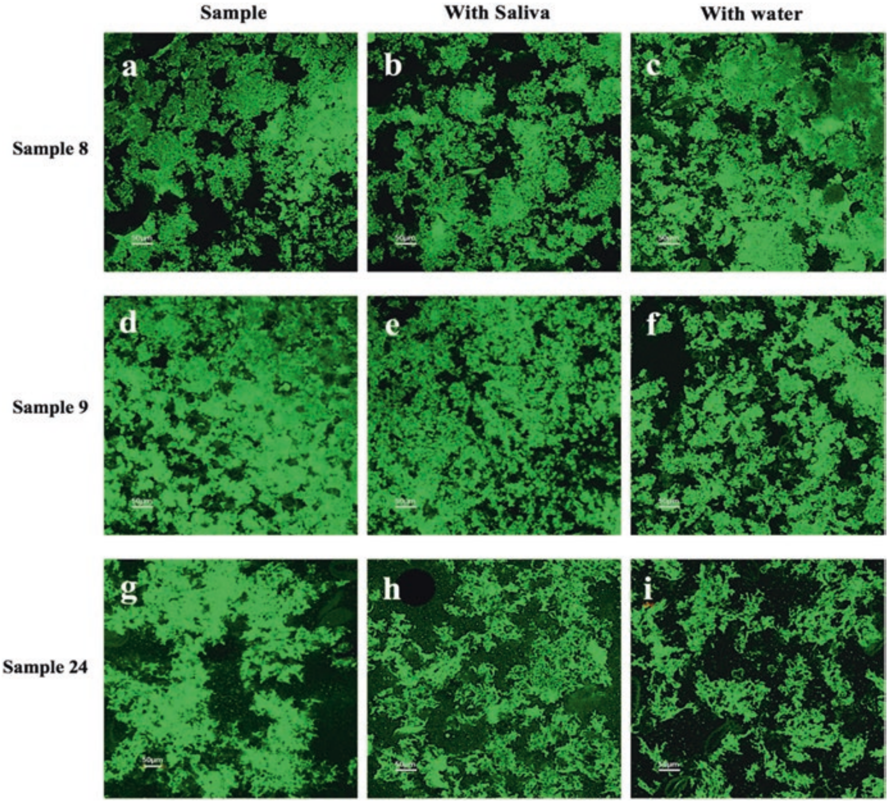

Fig. 3 CLSM results of acid milk gels; (**a**) sample 8; (**b**) sample 8: with HWS; (**c**) sample 8: with water; (**d**) sample 9; (**e**) sample 9: with HWS; (**f**) sample 9: with water; (**g**) sample 24; (**h**) sample 24: with HWS; (**i**) sample 24: with water. The protein network and serum pores are shown in green and black, respectively

salivary proteins (e.g. mucins) and electrolyte presented in HWS but not water. However, samples with added CS (sample 9, Fig. 3e) did not show many structural changes upon addition of HWS. This result was interesting considering that adding of HWS significantly impacted the structure of samples containing PS (sample 8, Fig. 3b). Amylose content can decrease the enzymatic digestion from salivary α-amylase due to its high linear amylose content and its crystalline structural conformation after gelatinization and retrogradation. This compact amylose structure can cause difficult conditions for HWS to travel throughout the system. This might be a reason for the reduced effects of HWS on samples with CS compared to those containing PS since the amylose content in CS is higher than that of PS. HWS showed the least effect on the sample with LBG (sample 6, Fig. 2e). This minimal effect can also be observed in rheological and tribological results in agreement with Zinoviadou et al. (2008).

HWS also had a significant impact on fat globule size: addition of HWS caused coalescence of fat globules. Fat coalescence was most visible in the full-fat acid milk gel with added HWS (sample 4, Fig. 1h). This result was attributed to depletion flocculation due to the osmotic pressure from salivary proteins, mainly proline-rich mucins (Chen 2015). Fat coalescence as well as protein aggregation in the protein matrix resulted in larger serum pores in the fat-containing samples (samples 2 and 4, Fig. 1). Overall, the changes to acid milk gel microstructures caused by HWS were distinctly different from those caused by addition of water, indicating that salivary changes to food products were more than simple dilution and incorporation of saliva during instrumental testing may give a better understanding of how saliva changes food rheological behaviors during oral processing.

3.4 Acid Milk Gel Flow Behaviors

All samples showed pseudoplastic behavior regardless of formulation or addition of HWS (Tables 3, 4, 5, and 6). Pseudoplastic behavior occurs when the rate of structural breakdown from external forces exceeds the rate of formation of internal entanglements, reducing the number of internal molecular interactions and resulting in decreased viscosity (Morris et al. 1981). Pseudoplastic behavior is typical in yogurt systems, particularly in yogurts prepared with hydrocolloids, which are known for their shear-thinning behavior.

The averaged viscosity profiles from 6 replicates of each formulation were individually fitted to Cross-Williams ($R^2 > 0.813$), Cross ($R^2 > 0.720$), and Herschel-Bulkley ($R^2 > 0.692$) models. The Cross model is a popular model for pseudoplastic materials that is extensively used in food dispersions and polymers. In this model, zero-shear viscosity (η_o) is the viscosity at low shear rates, which shows a Newtonian plateau. η_o can be measured at low shear rates and indicates the resistance of a material to flow at rest (Mezger 2011). Infinite viscosity (η_∞) can be used to determine food flow behaviors under high shear conditions, such as those experienced during industrial processing. This parameter is considered zero in Cross-Williams model.

For the formulations fitted to the Cross model, η_o and η_∞ decreased with increased temperature and addition of HWS. Interestingly, the decrease in η_o due to application of HWS was greater that caused by increased temperature. This may indicate that addition of HWS caused a greater reduction of protein entanglements in acid milk gels compared to the reduction promoted by greater molecular mobility at increased temperatures. Samples with WPI (samples 5, 12, and 16) had the highest $\eta_o$values. This was attributed to the greater number of casein–whey protein interactions throughout the protein network, which would result in a strong structure resistant to initial flow. The flow behavior index (*n*) and time constant (*c*) of acid milk gels decreased with addition of saliva and increasing temperature, which was expected based on the previously discussed microstructural changes. *c* has been attributed to the extent of entanglement density in a system (Bourbon et al. 2010). Acid milk gels structures were denser with more entanglements in the protein net-

Table 3 Viscosity profiles for acid milk gels (n = 24) at 8 °C without added HWS

Formula	Model	η_o (Pa.s)	η_∞ (Pa.s)	n	c (s)	k (Pa.s^{1-n})	σ_0 (Pa)	R^2
1	Cross	595	0.122	0.949	13.4	N/A	N/A	0.878
2	Herschel-Bulkley	N/A	N/A	0.992	N/A	0.096	13.9	0.709
3	Herschel-Bulkley	N/A	N/A	0.730	N/A	0.492	11.1	0.918
4	Cross	2944	0.319	0.972	47.3	N/A	N/A	0.911
5	Cross-Williamson	3251	N/A	0.923	86.7	N/A	N/A	0.888
6	Cross-Williamson	88.1	N/A	0.697	4.51	N/A	N/A	0.999
7	Cross	1238	0.135	0.893	38.5	N/A	N/A	1.000
8	Cross	385	0.214	0.910	98.7	N/A	N/A	0.832
9	Herschel-Bulkley	N/A	N/A	0.866	N/A	0.330	15.559	0.826
10	Cross-Williamson	312	N/A	0.867	2.64	N/A	N/A	0.999
11	Cross-Williamson	382	N/A	0.864	4.59	N/A	N/A	1.000
12	Cross	4180	1.15	0.922	26.5	N/A	N/A	1.000
13	Herschel-Bulkley	N/A	N/A	0.605	N/A	1.00	12.3	0.937
14	Cross-Williamson	288	N/A	0.864	3.96	N/A	N/A	1.000
15	Cross-Williamson	183	N/A	0.825	6.25	N/A	N/A	1.000
16	Cross-Williamson	4836	N/A	0.923	19.33	N/A	N/A	0.909
17	Cross-Williamson	1053	N/A	0.875	9.60	N/A	N/A	1.000
18	Cross-Williamson	275	N/A	0.812	2.44	N/A	N/A	0.999
19	Cross-Williamson	325	N/A	0.841	6.41	N/A	N/A	1.000
20	Cross-Williamson	786	N/A	0.795	78.3	N/A	N/A	1.000
21	Cross-Williamson	374	N/A	0.871	4.03	N/A	N/A	1.000
22	Cross-Williamson	159	N/A	0.827	4.35	N/A	N/A	1.000
23	Cross-Williamson	288	N/A	0.839	6.45	N/A	N/A	1.000
24	Cross-Williamson	267	N/A	0.819	8.94	N/A	N/A	1.000

work before applying HWS and/or increasing temperature (Figs. 1, 2, and 3). Because the freedom of movement for individual protein strands becomes more restricted by increasing time, the strands would require longer time to form new entanglements to replace the ones depleted by the external force (Bourbon et al. 2010). This was reflected in the higher c values for samples tested at lower temperature and without HWS.

Similar trends for the viscosity parameters were observed for the Cross-Williams results, with the exception of η_∞, which was always zero per the model assumptions. η_o values for the samples containing WPI (samples 5, 12, and 16) were significantly greater than those of the other samples. This may have been due to the heat treatment of acid milk gels at 85 °C for 30 min. During heat treatment above 70 °C, whey protein, specifically β–lactoglobulins, denature. The interaction of denatured whey proteins with κ-casein on the surface of casein micelles leads to greater protein aggregation, cross-linking throughout the gel network, and increased water-holding capacity (Lucey et al. 1997). Full-fat samples (sample 4) also had a notably high value for η_o. Fat globules interact with the protein network, resulting in a stronger gel. For samples with no added HWS, η_o increased in full-fat acid milk gels (sample 4)

Table 4 Viscosity profiles for acid milk gels (n = 24) at 8 °C with added HWS

Formula	Model	η_o (Pa.s)	η_∞ (Pa.s)	n	c (s)	k (Pa.s^{1-n})	σ_0 (Pa)	R^2
1	Herschel-Bulkley	N/A	N/A	0.572	N/A	0.956	14.4	0.901
2	Herschel-Bulkley	N/A	N/A	0.549	N/A	1.062	7.45	0.963
3	Herschel-Bulkley	N/A	N/A	0.414	N/A	0.403	3.95	0.992
4	Herschel-Bulkley	N/A	N/A	0.964	N/A	0.119	18.4	0.692
5	Cross-Williamson	1917	N/A	0.906	75.2	N/A	N/A	0.947
6	Cross-Williamson	41.2	N/A	0.648	3.37	N/A	N/A	0.998
7	Cross	521	0.145	0.857	34.3	N/A	N/A	1.000
8	Cross	92.9	0.091	0.564	48.7	N/A	N/A	0.922
9	Herschel-Bulkley	N/A	N/A	0.481	N/A	1.72	7.374	0.956
10	Cross-Williamson	204	N/A	0.831	2.55	N/A	N/A	0.999
11	Cross-Williamson	232	N/A	0.837	4.50	N/A	N/A	1.000
12	Cross	1163	0.32	0.822	13.3	N/A	N/A	1.000
13	Herschel-Bulkley	N/A	N/A	0.355	N/A	0.393	1.45	0.994
14	Cross-Williamson	146	N/A	0.832	2.97	N/A	N/A	1.000
15	Cross-Williamson	65.4	N/A	0.777	3.34	N/A	N/A	1.000
16	Cross-Williamson	2910	N/A	0.878	19.78	N/A	N/A	0.895
17	Cross-Williamson	209	N/A	0.821	5.17	N/A	N/A	0.999
18	Cross-Williamson	150	N/A	0.799	1.86	N/A	N/A	1.000
19	Cross-Williamson	103	N/A	0.791	5.01	N/A	N/A	1.000
20	Cross-Williamson	132	N/A	0.784	23.4	N/A	N/A	0.999
21	Cross-Williamson	224	N/A	0.834	3.64	N/A	N/A	1.000
22	Cross-Williamson	69.1	N/A	0.793	3.14	N/A	N/A	1.000
23	Cross-Williamson	108	N/A	0.799	5.00	N/A	N/A	1.000
24	Cross-Williamson	70.6	N/A	0.762	5.04	N/A	N/A	1.000

compared to the control acid milk gel (sample 1) in the Cross model. For samples with added HWS, σ_o in the Herschel-Bulkley models was noticeably higher in the full-fat acid milk gel compared to the control sample. The bigger size and greater number of fat globules in the full-fat sample compared to the control sample would cause increased resistance to flow (Chojnicka-Paszun et al. (2009) Chojnicka et al. 2009, Chojnicka-Paszun et al. 2012, Nguyen et al. 2017). These results are visually shown in microstructural images of acid milk gels (Figs. 1, 2, and 3).

Samples containing CMC (sample 7), PS (sample 8), and both WPI and PS (sample 12) were fitted to the Cross model and had η_∞>0; these results were attributed to greater gel strength under high shear compared to the other samples. CMC is an anionic polysaccharide (polyelectrolyte). This gum, which has a negative charge on its hydrophilic end, interacts with the positive charges on the surface of casein micelles, strengthening the protein network (Everett and McLeod 2005). Another reason for these results may be the ability of CMC to prevent casein precipitation and maintains a higher viscosity at the isoelectric point of casein (pH = 4.6) (Alakali et al. 2008; Andiç et al. 2013).

Table 5 Viscosity profiles for acid milk gels (n = 24) at 25 °C without added HWS

Formula	Model	η_o (Pa.s)	η_∞ (Pa.s)	n	c (s)	k (Pa.s^{1-n})	σ_0 (Pa)	R^2
1	Cross	380	0.080	0.908	11.1	N/A	N/A	0.720
2	Herschel-Bulkley	N/A	N/A	0.503	N/A	0.485	7.74	0.612
3	Herschel-Bulkley	N/A	N/A	0.740	N/A	0.346	4.65	0.969
4	Cross	2241	0.172	0.962	N/A	N/A	N/A	0.799
5	Cross-Williamson	1072	N/A	0.907	74.2	N/A	N/A	0.865
6	Cross-Williamson	42.6	N/A	0.604	5.32	N/A	N/A	0.998
7	Cross	517	0.106	0.823	30.7	N/A	N/A	1.000
8	Cross	105	0.114	0.833	68.6	N/A	N/A	0.737
9	Herschel-Bulkley	N/A	N/A	0.979	N/A	0.10	9.518	0.769
10	Cross-Williamson	205	N/A	0.822	2.60	N/A	N/A	0.999
11	Cross-Williamson	231	N/A	0.855	3.96	N/A	N/A	1.000
12	Cross	3447	0.50	0.860	56.5	N/A	N/A	0.999
13	Herschel-Bulkley	N/A	N/A	0.584	N/A	0.407	6.15	0.952
14	Cross-Williamson	151	N/A	0.844	2.76	N/A	N/A	1.000
15	Cross-Williamson	96.7	N/A	0.802	4.50	N/A	N/A	1.000
16	Cross-Williamson	2298	N/A	0.827	16.20	N/A	N/A	0.813
17	Cross-Williamson	467	N/A	0.873	5.96	N/A	N/A	1.000
18	Cross-Williamson	212	N/A	0.792	2.19	N/A	N/A	0.999
19	Cross-Williamson	161	N/A	0.805	4.65	N/A	N/A	1.000
20	Cross-Williamson	307	N/A	0.748	66.0	N/A	N/A	1.000
21	Cross-Williamson	190	N/A	0.843	2.98	N/A	N/A	1.000
22	Cross-Williamson	75.1	N/A	0.778	3.42	N/A	N/A	1.000
23	Cross-Williamson	143	N/A	0.794	5.18	N/A	N/A	1.000
24	Cross-Williamson	136	N/A	0.781	6.64	N/A	N/A	1.000

The greatest effect of HWS was seen in samples with PS (sample 8) and both WPI and PS (sample 12). The η_0 value in sample 12 decreased by >60% of the original value when HWS was added at both 8 and 25 °C. In sample 8 with added HWS, this decrease was >33% at 8 °C and ~50% at 25 °C. The key driver for this result was PS. α-amylase in HWS breaks down starch to smaller monosaccharides (Humphrey and Williamson 2001). The greater impact of PS on viscosity parameters compared to CS (sample 9) after addition of HWS may have been due to the larger granule size of PS and its higher swelling power, higher solubility, and lower number of amylose molecules (Bird et al. 2000; Li and Yeh 2001; Singh et al. 2003).

Acid milk gels with a yield stress (σ_o) were fitted to the Herschel-Bulkley model. As expected, k decreased with both addition of HWS and increased temperature for all samples. A smaller stress was needed to deform the acid milk gels under these conditions since the higher temperature and/or HWS addition disrupted their structure. While the values of k are related to viscosity, using this parameter alone to determine sample viscosity is not advised because it neglects shear thinning behavior. Still, it serves as a criterion for comparison when the degree of shear thinning among samples is similar.

Table 6 Viscosity profiles for acid milk gels (n = 24) at 25 °C with added HWS

Formula	Model	η_o (Pa.s)	η_∞ (Pa.s)	n	c (s)	k (Pa.s^{1-n})	σ_0 (Pa)	R^2
1	Herschel-Bulkley	N/A	N/A	0.643	N/A	0.520	6.10	0.942
2	Herschel-Bulkley	N/A	N/A	0.600	N/A	0.563	3.61	0.983
3	Herschel-Bulkley	N/A	N/A	0.407	N/A	0.936	2.71	0.992
4	Herschel-Bulkley	N/A	N/A	0.926	N/A	0.118	9.37	0.791
5	Cross-Williamson	728	N/A	0.816	68.6	N/A	N/A	0.924
6	Cross-Williamson	26.4	N/A	0.550	6.71	N/A	N/A	0.998
7	Cross	290	0.098	0.804	34.6	N/A	N/A	1.000
8	Cross	52.8	0.074	0.827	36.7	N/A	N/A	0.996
9	Herschel-Bulkley	N/A	N/A	0.622	N/A	0.642	4.285	0.961
10	Cross-Williamson	114	N/A	0.783	2.18	N/A	N/A	0.998
11	Cross-Williamson	123	N/A	0.853	2.96	N/A	N/A	1.000
12	Cross	787	0.26	0.804	51.4	N/A	N/A	1.000
13	Herschel-Bulkley	N/A	N/A	0.350	N/A	0.340	1.23	0.996
14	Cross-Williamson	73.9	N/A	0.802	2.16	N/A	N/A	0.9996
15	Cross-Williamson	34.0	N/A	0.731	2.89	N/A	N/A	1.000
16	Cross-Williamson	1773	N/A	0.721	36.55	N/A	N/A	0.821
17	Cross-Williamson	120	N/A	0.824	3.67	N/A	N/A	0.999
18	Cross-Williamson	79.2	N/A	0.782	1.18	N/A	N/A	0.999
19	Cross-Williamson	54.0	N/A	0.746	3.977	N/A	N/A	1.000
20	Cross-Williamson	45.6	N/A	0.712	18.6	N/A	N/A	1.000
21	Cross-Williamson	103	N/A	0.839	2.06	N/A	N/A	1.000
22	Cross-Williamson	30.6	N/A	0.720	2.61	N/A	N/A	1.000
23	Cross-Williamson	43.0	N/A	0.731	3.91	N/A	N/A	1.000
24	Cross-Williamson	49.3	N/A	0.705	6.85	N/A	N/A	1.000

In general, formulation (hydrocolloids used), HWS, temperature, and interaction effects of formulation and HWS and formulation and temperature showed significant differences at $p \leq 0.001$ for all viscosity parameters, with the exception of temperature not significantly affecting n values (data not shown). Interaction of HWS and temperature showed significant influence on values of c ($p < 0.05$), n ($p < 0.05$), and η_0 ($p < 0.01$). The significant effect of formulation was attributed to a combination of electrostatic bonds between oppositely charged molecules of anionic hydrocolloids with casein micelles, swollen starch granules throughout the system, and dispersion of large, neutral hydrocolloid molecules in the continuous phase, as well as depletion flocculation. These factors can significantly change the protein network structure and the overall conformation of acid milk gels (Figs. 1, 2, and 3). The significant effects from HWS can be explained by microstructural disruption and breakdown caused by salivary enzymes, proteins and electrolytes. Temperature can weaken the intermolecular bonds in a semisolid food system, decreasing resistance to flow (Berk 2018).

In summary, all acid milk gels showed non-Newtonian behavior. The mechanical forces applied during testing can resemble the shear forces during oral processing;

increasing speed and extent of oral movements would result in decreased oral viscosity of the acid milk gels. Addition of hydrocolloids and HWS significantly affected acid milk gel viscosity parameters. These parameter changes can provide useful information about how flow behaviors change under different conditions. Because these rheological properties can be related to oral processing actions as well as correlated with sensory attributes such as thickness, tuning acid milk gel flow behaviors by adjusting their structures is a feasible way to create products with desirable oral and industrial processing behaviors.

3.5 Acid Milk Gel Viscoelastic Behaviors

Formulation, HWS, temperature, and all their interactions showed significant differences ($p \leq 0.001$) for G^* (Table 7). Formulation and HWS had significant effects on tan δ ($p \leq 0.001$). Temperature and formulation significantly impacted γ_c ($p \leq 0.001$); HWS impacted γ_c ($p \leq 0.05$). These results were attributed to increased microstructural stability and rigidity when hydrocolloids were added to the samples. Gums (CMC and LBG) and starches (PS and CS) improve gel stability and rigidity by increasing the number of internal molecular interactions as well as promoting stronger bonds through different mechanisms. HWS can disrupt the structure of semisolid foods through digestion, alteration of osmotic pressure, dilution, or alteration of polymer net charges. Increasing temperature alters the thermodynamic condition of materials. Internal molecules can move faster with increased heat energy, potentially decreasing the strength of molecular bonds. As a result, microstructures become more susceptible to deformation when mechanical force is applied.

Strain sweep results showed γ_c values varied significantly with formulation, temperature, and HWS. The significance level of HWS was higher than formulation and temperature, indicating that formulation and temperature had a greater impact on γ_c values compared to HWS. In other words, HWS had less effect on disrupting the stability of the acid milk gels compared to temperature and formulation.

Addition of hydrocolloids significantly increased γ_c values (Table 8). Samples 11 (containing WPI and CMC), 21 (containing LBG, CMC, CS, and PS), and 17 (containing PS and CMC) showed the highest γ_c values, and samples 1 (control), 20 (containing WPI, CMC, PS, and CS), 13 (containing WPI and CS), and 4 (full-fat sample) had the lowest γ_c values. Oppositely charged bonds between the surface of casein micelles and hydrophilic ends of CMC (Everett and McLeod 2005) along with increased bonds between denatured–denatured, and denatured–undenatured whey proteins due to presence of additional whey proteins from WPI would result in a more stable gel in sample 11 (Lucey et al. 1998). Thus, there was a larger force required to cause permanent structural deformation. In sample 22, the strong bonds between the caseins and CMC, along with the contribution of starches and LBG that increased the viscosity of the continuous phase, resulted in a high γ_c compared to that of the control sample. The combination of PS and CMC appeared to build a

Table 7 Main sources of variation of viscosity parameters and viscoelastic properties of acid milk gels ($n = 24$)[a]

Source of variation	η_0 (Pa.s)	n	c (s)	γ_c	G^* (Pa)	tan δ (rad)
Formulations	79.2^{***}	97.5^{***}	70.6^{***}	65.4^{***}	589.9^{***}	19.4^{***}
HWS	156.7^{***}	339.1^{***}	41.9^{***}	4.7^{*}	798.5^{***}	19.8^{***}
Temperature	60.7^{***}	172.5^{***}	3.5	27^{***}	302.5^{***}	3
HWS × temperature	11.5^{**}	5.3^{*}	4.7^{*}	0.1	16.2^{***}	1.5
Formulation × HWS	18.3^{***}	18.3^{***}	7.1^{***}	1.9	100.6^{***}	1.8
Formulation × temperature	7.3^{***}	6.9^{***}	3.9^{***}	1.1	27.4^{***}	1

[a] *, **, and *** indicate significant differences at $p \leq 0.05$, $p \leq 0.01$, and $p \leq 0.001$, respectively

strong, stable gel in sample 17 whereas in sample 20, their combination with WPI and CS significantly decreased the resistance to permanent deformation.

Addition of fat had low effect on γ_c values in comparison to hydrocolloids. Increasing temperature generally increased γ_c values. This can be explained by thermodynamics occurring in acid milk gels. Heat can increase internal energy and molecular mobility, which increases fluid-like behavior. Therefore, greater instrumental stress was required to cause permanent and irreversible deformation. Addition of HWS showed different results on γ_c values depending on formulation. γ_c decreased upon addition of HWS for samples 6 (containing LBG), 8 (containing PS), 9 (containing CS), 14 (containing WPI, CMC, and PS), and 19 (containing WPI, CMC, LBG, and PS). HWS can easily disrupt the dispersion of neutral LBG molecules in the continuous phase, as there are no electrostatic bonds between LBG molecules and caseins. This disruption results in depletion flocculation and changes the osmotic pressure in the system, subsequently decreasing viscosity. The decrease in γ_c values for samples containing starches may have been due to starch digestion by amylase, which can disrupt the gel microstructure and decrease their stability and strength. This effect was stronger for PS (used in sample 8) due to its larger granules compared to CS (used in sample 9). γ_c showed no notable change after addition of HWS for several formulations. These samples were mainly those with strong bonds such as CMC and caseins, WPI, or a combination of these interactions with other gums. Saliva would not have a major impact on the number and strength of these bonds, so the structure and therefore critical strain would remain unchanged.

G^* values at critical strain for all samples decreased with addition of HWS, increased temperature, or both. $G' < G''$ for most formulations with and without added HWS for all strains tested (0.01–100%) (Table 8). Thus, these acid milk gels were viscoelastic solids in this strain range. Accordingly, tan $\delta<1$ for all samples without added HWS except for samples 6 (containing LBG) and 23 (containing all hydrocolloids but WPI). Additionally, tan $\delta>1$ for samples 6 (containing LBG) and 22 (containing all hydrocolloids but CS) when HWS was added. This viscous-dominant behavior of LBG has been also reported by (Perrechil et al. 2009). Additionally, these results were expected since these samples had relatively low G^* values even at 8 °C; the additional energy at increased temperatures would alter the network from a soft gel with an entangled matrix system to a weak physical gel with non-covalent linkages (Stading and Hermansson 1990; Tunick 2010; Tang and Liu 2013). Similarly, addition of HWS would weaken the microstructure, promoting viscous flow.

In general, increasing temperature and addition of HWS to the formulations increased tan δ values, but most acid milk gels still showed viscoelastic solid behavior. These results indicated that the mechanical forces applied at strains below γ_c were insufficient to overcome the intermolecular forces among the molecules within the acid milk gel microstructures, so samples stored more energy than they dissipated at these strains.

G^* values decreased with increasing temperature, HWS addition, or both. Applying both higher temperature and HWS resulted in the lowest G^* values. Nevertheless, samples generally maintained viscoelastic solid behavior upon addition of HWS, suggesting that the elasticity of the protein network was not strongly disrupted by HWS. The decrease in viscoelastic moduli with increased temperature was attributed to increased energy in the acid milk gel molecular structures. At higher temperatures, molecules have increased kinetic energy that can overcome the intermolecular bonding forces, allowing the samples to flow more easily. Addition of HWS can also disrupt food structures due to dilution, mucin interactions, and enzymatic breakdown of amylose by amylase (Janssen et al. 2007; Vingerhoeds et al. 2009).

Several acid milk gel samples showed a crossover between G' and G'' at >10% strain during the strain sweeps. Before the crossover point, $G'>G''$; the crossover indicated a switch from viscoelastic solid to viscoelastic fluid behavior. These results were attributed to reduced gel stability, which would result in disruption and breakdown of the protein network at higher strains. The strain range under which a formulation remained elastic-dominant (see Appendix A for data) also differed with formulation due to changes in gel stability.

Frequency sweep results were dependent on formulation (selected results shown in Fig. 4). Overall, G' and G'' decreased with increasing temperature, HWS addition, or both. Increasing temperature and application of HWS decreased G' and G''. Overall, addition of WPI (sample 16), CMC (sample 7), and fat (samples 2, 3, and 4) had the greatest impact on the moduli values compared to the control sample (sample 1) via the same mechanism explained earlier for the strain sweep results. The significant increase of viscoelastic moduli for sample 16 (high levels of WPI) was in accordance with the results of Lucey et al. (1998, 2010). Addition of WPI increases the amount of bound, denatured whey proteins due to heat treatment at 80 °C for 30 min. Furthermore, non-associated, denatured whey proteins can interact with the bound, denatured whey proteins, forming a stronger gel (Lucey et al., 1998). Viscoelastic moduli values decreased when WPI was used in combination with SMP (sample 5), likely because the protein content of WPI was higher than SMP (approximate ratio of 3:1). Because the total solids content of both formulations was equal, there would be less protein in sample 5 compared to sample 16, which was shown in the proximate results (Table 2). WPI also resulted in increased viscoelastic moduli values of samples prepared with additional hydrocol-

Table 8 Viscoelastic parameters of acid milk gels[a]

Formula number	γ_c (%) 8 °C NS	γ_c (%) 8 °C S	γ_c (%) 25 °C NS	γ_c (%) 25 °C S	G^* (Pa) 8 °C NS	G^* (Pa) 8 °C S	G^* (Pa) 25 °C NS	G^* (Pa) 25 °C S	tan δ (rad) 8 °C NS	tan δ (rad) 8 °C S	tan δ (rad) 25 °C NS	tan δ (rad) 25 °C S
1	0.411^{j}	0.417^{k}	0.411^{k}	0.555^{m}	486.62^{de}	208.64^{def}	179.2^{d}	118.9^{def}	0.300^{mn}	0.325^{h}	0.329^{nop}	0.346^{n}
2	0.976^{f}	0.73^{h}	0.975^{h}	0.975^{j}	249.6^{efgh}	101.63^{ef}	94.5^{d}	56.6^{ef}	0.307^{lm}	0.333^{h}	0.339^{mno}	0.365^{l}
3	0.730^{i}	0.411^{l}	0.975^{l}	1.30^{h}	88.8^{h}	56.0^{f}	58.12^{d}	38.12^{f}	0.311^{klm}	0.316^{h}	0.362^{m}	0.371^{l}
4	0.411^{j}	0.547^{i}	0.731^{i}	0.411^{o}	700.67^{cd}	318^{d}	284^{d}	119.45^{d}	0.319^{kl}	0.314^{h}	0.334^{mno}	0.329^{no}
5	0.731^{h}	0.731^{g}	0.731^{g}	0.731^{k}	998^{c}	782.5^{b}	697.7^{c}	503.42^{b}	0.299^{mno}	0.320^{h}	0.321^{op}	0.326^{no}
6	1.74^{e}	0.73^{h}	1.74^{h}	0.73^{l}	100^{h}	50.2^{f}	64.4^{d}	30.4^{f}	0.951^{a}	1.11^{a}	1.18^{a}	1.29^{a}
7	0.731^{h}	0.731^{g}	0.731^{g}	0.73^{l}	361^{efgh}	166.42^{def}	174.24^{d}	78.29^{def}	0.36^{lj}	0.413^{g}	0.403^{l}	0.450^{k}
8	0.731^{h}	0.547^{j}	0.975^{j}	0.975^{j}	156^{fgh}	66^{f}	118^{d}	37.66^{f}	0.316^{klm}	0.331^{h}	0.355^{mn}	0.375^{l}
9	0.731^{h}	0.411^{l}	0.975^{l}	0.73^{l}	224^{efgh}	124^{def}	130^{d}	76.61^{def}	0.326^{k}	0.314^{h}	0.355^{mn}	0.354^{lmn}
10	1.74^{e}	1.74^{e}	2.33^{e}	2.33^{f}	431^{defg}	265.5^{de}	287.6^{d}	185.8^{de}	0.618^{e}	0.71^{e}	0.745^{g}	0.815^{g}
11	10.0^{a}	10.0^{a}	10.0^{a}	13.4^{a}	172.7^{fgh}	101.4^{ef}	112^{d}	61.7^{ef}	0.518^{g}	0.606^{f}	0.561^{i}	0.692^{i}
12	0.975^{g}	0.548^{i}	0.975^{i}	0.975^{i}	1715.3^{b}	560.2^{c}	1177.7^{b}	295.1^{c}	0.248^{p}	0.293^{i}	0.250^{q}	0.301^{o}
13	0.411^{j}	0.411^{l}	0.73^{l}	0.73^{l}	145^{gh}	63.8^{ef}	73.2^{d}	42.2^{ef}	0.280^{o}	0.321^{h}	0.316^{op}	0.359^{l}
14	5.59^{b}	7.48^{b}	10.0^{a}	7.48^{c}	182.5^{fgh}	115.9^{def}	111.6^{d}	75.5^{def}	0.669^{c}	0.754^{d}	0.802^{de}	0.901^{d}
15	2.33^{d}	2.33^{d}	4.18^{d}	4.18^{d}	130^{gh}	75.5^{ef}	73.0^{d}	45.7^{ef}	0.666^{c}	0.740^{d}	0.815^{cd}	0.905^{d}
16	0.975^{f}	0.976^{f}	1.30^{f}	1.74^{g}	3600.6^{a}	1823.8^{a}	2640^{a}	879.3^{a}	0.288^{no}	0.293^{i}	0.302^{p}	0.312^{o}
17	4.18^{c}	7.48^{b}	5.59^{b}	10.0^{b}	379.2^{efgh}	100.3^{ef}	250^{d}	61^{ef}	0.386^{i}	0.606^{f}	0.436^{k}	0.677^{i}
18	1.74^{e}	2.33^{d}	3.12^{d}	4.18^{d}	450.8^{def}	224.24^{def}	315.2^{d}	140.9^{def}	0.681^{bc}	0.859^{b}	0.843^{bc}	1.08^{b}
19	2.33^{d}	1.74^{e}	3.12^{e}	4.18^{d}	219.8^{efgh}	85.64^{ef}	131.42^{d}	46^{ef}	0.621^{de}	0.713^{e}	0.758^{fg}	0.866^{f}
20	0.411^{j}	0.232^{m}	0.411^{m}	0.547^{n}	180.1^{fgh}	32^{f}	87.9^{d}	28.34^{f}	0.433^{h}	0.609^{f}	0.506^{j}	0.541^{j}
21	5.59^{b}	7.48^{b}	7.48^{b}	7.48^{c}	233.44^{efgh}	116.31^{def}	150^{d}	77.11^{def}	0.598^{f}	0.752^{d}	0.733^{g}	0.874^{f}
22	2.33^{d}	4.18^{c}	4.18^{c}	4.18^{d}	139.5^{gh}	63.64^{ef}	64.6^{d}	35.17^{ef}	0.692^{b}	0.852^{b}	0.864^{b}	1.04^{c}

(continued)

Table 8 (continued)

Formula number	γ_c (%) 8 °C NS	γ_c (%) 8 °C S	γ_c (%) 25 °C NS	γ_c (%) 25 °C S	G^* (Pa) 8 °C NS	G^* (Pa) 8 °C S	G^* (Pa) 25 °C NS	G^* (Pa) 25 °C S	tan δ (rad) 8 °C NS	tan δ (rad) 8 °C S	tan δ (rad) 25 °C NS	tan δ (rad) 25 °C S
23	1.74^{e}	2.33^{d}	2.33^{d}	3.12^{e}	201^{efgh}	78.12^{ef}	115.0^{d}	43.6^{ef}	0.635^{de}	0.775^{c}	0.779^{ef}	0.922^{d}
24	1.74^{e}	1.74^{e}	2.33^{e}	2.33^{f}	143.6^{gh}	59.5^{f}	97.9^{d}	44.21^{f}	0.638^{d}	0.750^{d}	0.692^{h}	0.759^{h}

[a] NS: no HWS added; S: HWS added

Letters that are different in each column indicate significant differences ($p<0.05$)

loids compared to when they were used individually in the formulations (samples 10, 11, 12, and 13). The presence of additional whey protein would increase the number of interactions with both other polysaccharides and caseins in the system, resulting in a stronger gel (Laneuville et al. 2000).

The effect of HWS was significant for several samples prepared with PS due to enzymatic digestion of large granules of PS with α-amylase. This effect was particularly notable when PS was used alone (sample 8) or in combination with one other hydrocolloids (samples 12 and 17). However, when PS was used with more than 2 hydrocolloids (samples 14, 19, 20, 21, 22, 23, and 24), this effect was not observed. This may have been because the quantity of PS used in these formulations

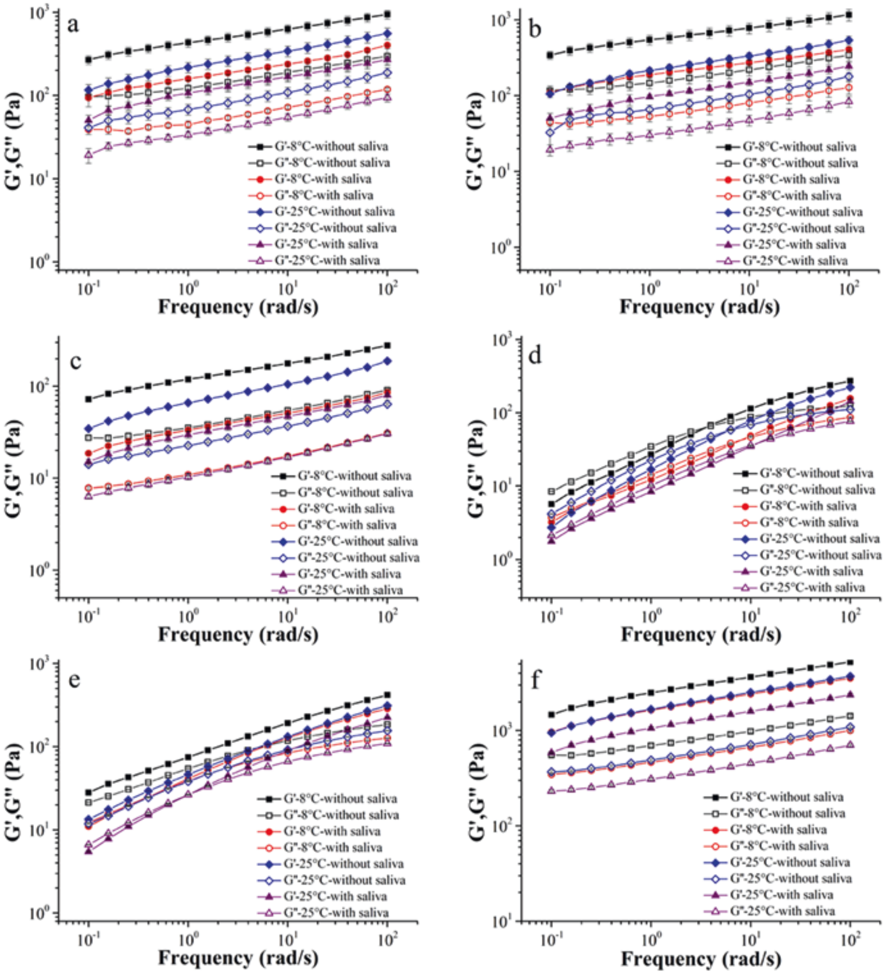

Fig. 4 Selected frequency sweep results of acid milk gels; (**a**) sample 1; (**b**) sample 4; (**c**) sample 8; (**d**) sample 6; (**e**) sample 14; (**f**) sample 16

would decrease to balance the total solids content (13% w/w in all samples), resulting in less PS available for digestion. An example of the significant impact of PS was observed for sample 14 with added HWS, for which a crossover of the moduli values occurred regardless of temperature. Digestion of the sample by HWS was sufficient to disrupt the sample and promote viscous-dominant behavior at low frequencies.

Similarly, several acid milk gel formulations showed a crossover between G' and G'' within the frequency range of 0.1–100 rad s^{-1}, and saliva was not always necessary to promote this crossover (Table 9). These samples showed viscous-dominant behavior ($G''> G'$) at low frequencies but solid-like behavior ($G'> G''$) at higher frequencies. Crossovers were attributed to the different responses of the microstructures to forces applied at different timescales. At low frequencies (long timescales), the protein molecules had time to relax and slide past each other, resulting in dissipation of energy. At higher frequencies (short timescales), the oscillation time was faster than the material's relaxation time, so the polymers tended to stretch and store energy rather than relax and dissipate energy.

Overall, HWS, formulation, and temperature had significant effects on acid milk gel viscoelastic parameters. Formulation appeared to have a greater impact than the other parameters. The rigidity, stability, and viscoelastic moduli of the samples were highly affected when WPI, fat, CMC, or a combination of more than two hydrocolloids were added to the formulations. Among the hydrocolloids used, LBG decreased viscoelastic moduli in comparison to the control, which can be explained by the neutral charge on LBG. Although LBG would not notably interfere with interactions in the protein network, it can destabilize the network by depletion flocculation due to altered osmotic pressure. The general explanation of this significant difference among formulations with added WPI and CMC was most likely the difference in strength and quantity of the electrostatic interactions as well as differences in hydrophobicity of the internal molecules. PS and CS changed the viscoelastic properties of the acid milk gels by swelling in and increasing the viscosity of the continuous phase.

Both HWS and temperature generally resulted in lower moduli values and higher phase angles HWS had the highest effects on the viscoelastic properties of formulations that included starch due to the enzymatic breakdown, especially for samples

Table 9 Crossover frequencies for acid milk gels[a]

Formula number	8 °C-S (rad s^{-1})	8 °C-NS (rad s^{-1})	25 °C-S (rad s^{-1})	25 °C-NS (rad s^{-1})
14	0.398	N/A	1	N/A
22	0.158	N/A	2.5	0.1
21	0.1	0.1	0.25	0.63
6	6.31	2.51	10	3.98
10	0.398	0.631	0.398	1
18	3.98	1	3.98	1.58

[a] NS: no HWS added; S: HWS added

with PS rather than CS due to the larger PS granule size. HWS had also a greater impact on the sample with LBG since there were no strong bonds or interaction between milk proteins and LBG molecules. The overall impact of HWS was attributed to changes in osmotic pressure and protein net charges and disruption of acid milk gel structures by digestion and dilution. Increased temperatures increased the internal mobility and weakened the internal bonds, resulting a decreased in stability, rigidity, and a resistance to permanent deformation due to the fluid-like properties of more viscous-dominant materials.

The impact of hydrocolloids, and HWS on viscoelastic properties of acid milk gels was in accordance with the notable differences in microstructural conformation in various formulations with and without addition of HWS (Figs. 1, 2, and 3). Overall, this information about viscoelastic properties of acid milk gels provides an understanding of how their formulation and testing parameters can result in different degrees of microstructural stability and a subsequent variety in viscoelastic behaviors. The information can be used to assist in proper selection of hydrocolloids during product development to generate microstructures that create desirable processing behaviors. It can also be used to indicate sensory textures, as will be discussed in Chap. 11, "Relationships Among Acid Milk Gel Sensory, Rheological, and Tribological Behaviors".

3.6 *The Effect of Different Hydrocolloids and HWS on Tribological Properties of Acid Milk Gels*

The effects of formulation, HWS, sliding speed, and the interaction of formulation with temperature and HWS on acid milk gel friction coefficients were significant ($p \leq 0.001$, Table 10). The interaction of sliding speed and HWS was significant at $p \leq 0.05$. The significant effect of formulation was attributed to the drastically different friction behaviors of the hydrocolloids used. These differences were mainly due to differences in their electrical charges and molecular size. For instance, addition of WPI may result in a larger particle size that can increase friction coefficients. The significant impact of HWS can be explained by disruption of acid milk gel structures by digestion, altered osmotic pressure, dilution, or changes to milk protein net charges, mainly caused by salivary enzymes, proteins, electrolytes, and additional water. The significant impact of sliding speed was most likely due to the thickness of the lubricant (food) between the two surfaces during tribometry, which increases with increased sliding speed and can profoundly impact the measured friction due to increased surface separation and greater dependence on the bulk rheology of the fluid at higher sliding speeds.

Stribeck curves showed that the boundary and mixed regime were the dominant regimes for all samples (Fig. 5). These regimes have been shown for semisolid food with added hydrocolloids during tribological testing (De Vicente et al. 2006; Dresselhuis et al. 2007; Chojnicka et al. 2008; Chojnicka-Paszun et al. 2012;

Table 10 Main sources of variation of frictional properties of acid milk gels (*n* = 24)[a]

Source of variation	Friction coefficient
Formulations	2612.1***
Sliding speed	92.8***
HWS	596.1***
Sliding speed*HWS	3.5*
Formulation*HWS	39.2***
Formulation * Sliding speed	3.7***

[a] *, **, and *** indicate significant differences at $p \le 0.05$, $p \le 0.01$, and $p \le 0.001$, respectively

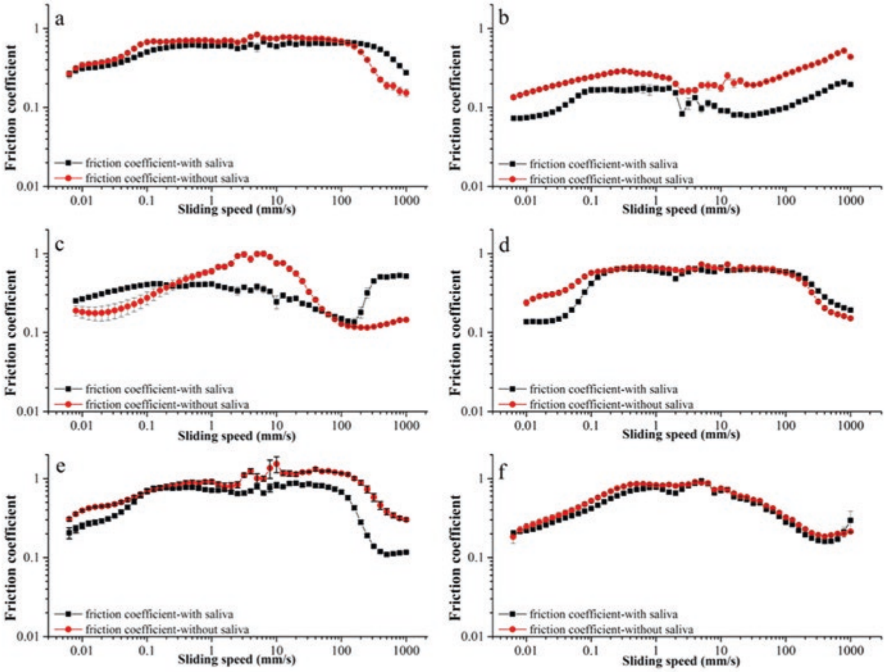

Fig. 5 Tribology results of acid milk gels; (**a**) sample 1; (**b**) sample 4; (**c**) sample 7; (**d**) sample 8; (**e**) sample 16; (**f**) sample 22

Morell et al. 2016). Most acid milk gels showed startup behaviors from 0.01 mm s^{-1} to 1 mm s^{-1} (Fig. 5). The increase in friction coefficients at these speeds was due to deformation of the PDMS plate, rather than actual sliding of the contact surfaces against each other at low sliding speeds (Zinoviadou et al. 2008).

Samples with fat (samples 2, 3, and 4) had low friction coefficients compared to the other samples; full-fat samples (sample 4) had the lowest friction coefficients among all samples. Fat globules can decrease the friction coefficient, as they can become trapped in the contact area and form a thin film of fat due to local fat coalescence or flocculation, acting as a lubricant (Huc et al. 2016). It should be noted that this behavior is typically local to the contact zone, not in the bulk material, so it is not necessary to see fat separation during or after testing for this phenomenon to occur.

Samples with formulations that included LBG or high levels of WPI (samples 6, 18, and 16) had notably increased friction coefficient within the boundary regime. Samples with high levels of WPI (sample 16) showed the highest friction coefficients. This effect of WPI may have been due to the larger particle size of protein molecules compared to the rest of the hydrocolloids (Chojnicka-Paszun et al. (2009), Huc et al. 2016). Combining WPI with CMC (sample 11) significantly reduced the friction coefficient, but the combination of WPI with LBG (sample 10) did not affect the high friction behaviors contributed by WPI. Stribeck curves for samples with high levels of LBG (sample 16) and WPI and LBG (sample 10) were similar, which was in agreement with the results for the viscoelastic properties of these two formulations. The friction results may have been due to incompatibility of the LBG with milk proteins. Although LBG can stabilize food systems, phase separation between casein micelles and LBG on the microscopic scale can occur due to depletion flocculation and thermodynamic incompatibility (Thaiudom and Goff 2003). Samples containing LBG at a lower level (sample 6) had small changes in friction coefficient within the boundary regime. This effect was also shown by (Zinoviadou et al. 2008).

Friction coefficient of all samples either decreased or was unchanged with addition of HWS. Samples with PS in combination with other hydrocolloids (samples 12, 14, 17, and 24) showed notably lower friction coefficients upon addition of HWS, but addition of HWS to samples with PS (sample 8) showed little impact on friction behaviors, which was unexpected based on the rheological results. In contrast, samples with CS (sample 9) showed a notable decrease in friction coefficient when mixed with HWS. This result was not in accordance with the viscosity and viscoelastic results for samples 8 and 9; in those results, sample 8 showed greater changes upon addition of saliva than sample 9. The differences between the rheological and tribological results for these samples support differences in sample interaction with α-amylase in HWS, as previously discussed (Sect. 3.3). These results highlight the importance of testing foods with and without HWS using a range of tests: saliva may have significantly different effects on sample behaviors under different conditions. The main reason for the decrease in friction coefficient in the remaining samples appeared to be mainly due to the lubricating effect of the proteins in HWS (mainly proline-rich mucin) and the dilution provided by saliva (Janssen et al. 2007; Vingerhoeds et al. 2009), since HWS is >99% water (Humphrey and Williamson 2001).

4 Conclusions

Addition of HWS and hydrocolloids significantly affected the microstructural, rheological, and tribological properties of acid milk gels. Samples with hydrocolloids had thicker clusters and bigger chains in their microstructures compared to the control sample, which was more homogenous with smaller pores. Samples with HWS had a distinct, more homogeneous protein network compared to the samples were imaged by water. HWS also caused visible fat coalescence for samples containing fat. The notable effects of hydrocolloids and HWS on acid milk gel microstructures as observed in confocal imaging was also observed in the differences in their viscosity and viscoelastic properties. For instance, structures comprising thicker clusters and bigger chains after addition of hydrocolloids were associated with greater mechanical viscosity. This result can be attributed to the greater resistance of those larger clusters to deformation by mechanical force, causing increased viscosity. Addition of HWS to the acid milk gels resulted in decreased viscosity, viscoelastic moduli, and frictional coefficients. A decrease in the void area after addition of saliva, observed in confocal images, was in agreement with this finding. The most notable differences were for samples with either PS individually or in combination with other hydrocolloids. However, these results were not found for CS-containing formulations, indicating that the effect may be starch-specific. WPI and LBG significantly increased friction coefficients. These results provide important information on factors that alter acid milk gel rheological and tribological behaviors, as well as how structural changes due to formulation and HWS incorporation contribute to those differences in mechanical behaviors. Illustration of the structural changes with consideration of the mechanisms during oral processing will lead to an improved ability to designing ideal textures for the human palate.

Acknowledgements Funding for this project was provided by the USDA National Institute of Food and Agriculture (grant #2015–67,018-23,069).

Appendix A: Supplemental Figures

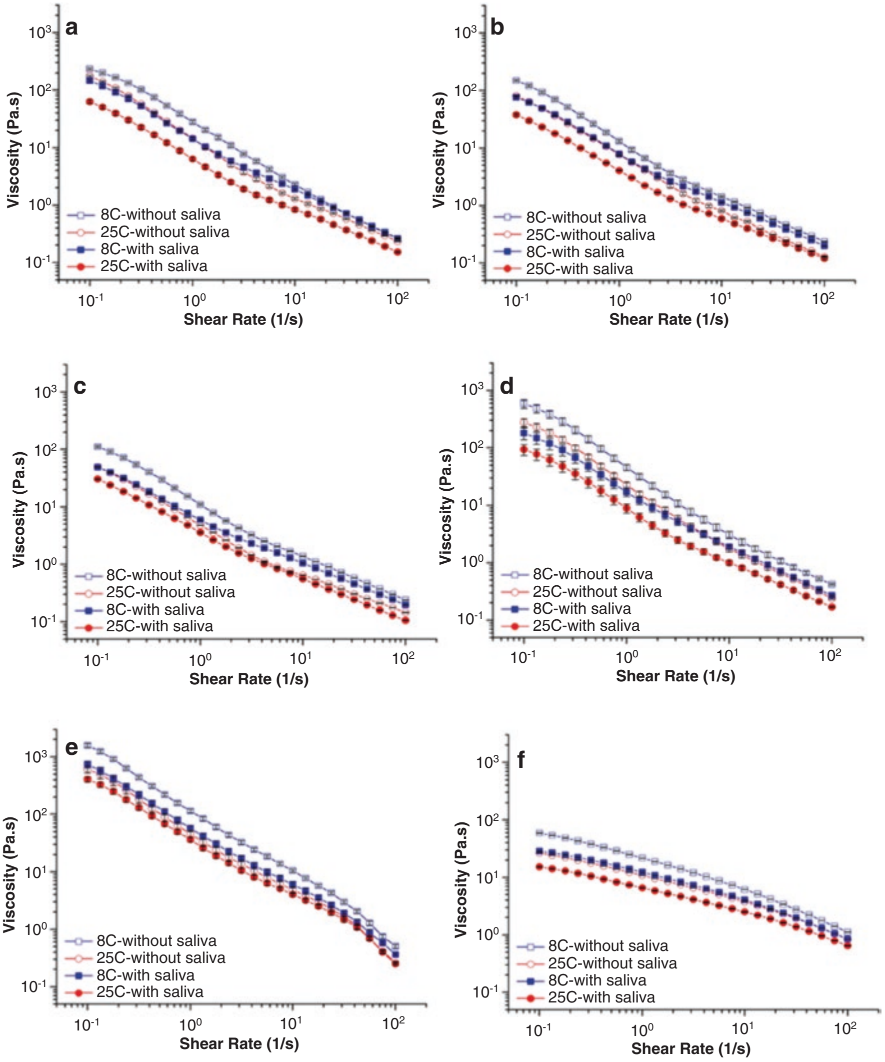

Fig. 6 Acid milk gel shear rate sweep results; (**a**) sample 1; (**b**) sample 2; (**c**) sample 3; (**d**) sample 4; (**e**) sample 5; (**f**) sample 6; (**g**) sample 7; (**h**) sample 8; (**i**) sample 9; (**j**) sample10; (**k**) sample 11; (**l**) sample 12; (**m**) sample 13; (**n**) sample 14; (**o**) sample 15; (**p**) sample 16; (**q**) sample 17; (**r**) sample 18; (**s**) sample 19; (**t**) sample 20; (**u**) sample 21; (**v**) sample 22; (**w**) sample 23; (**x**) sample 24

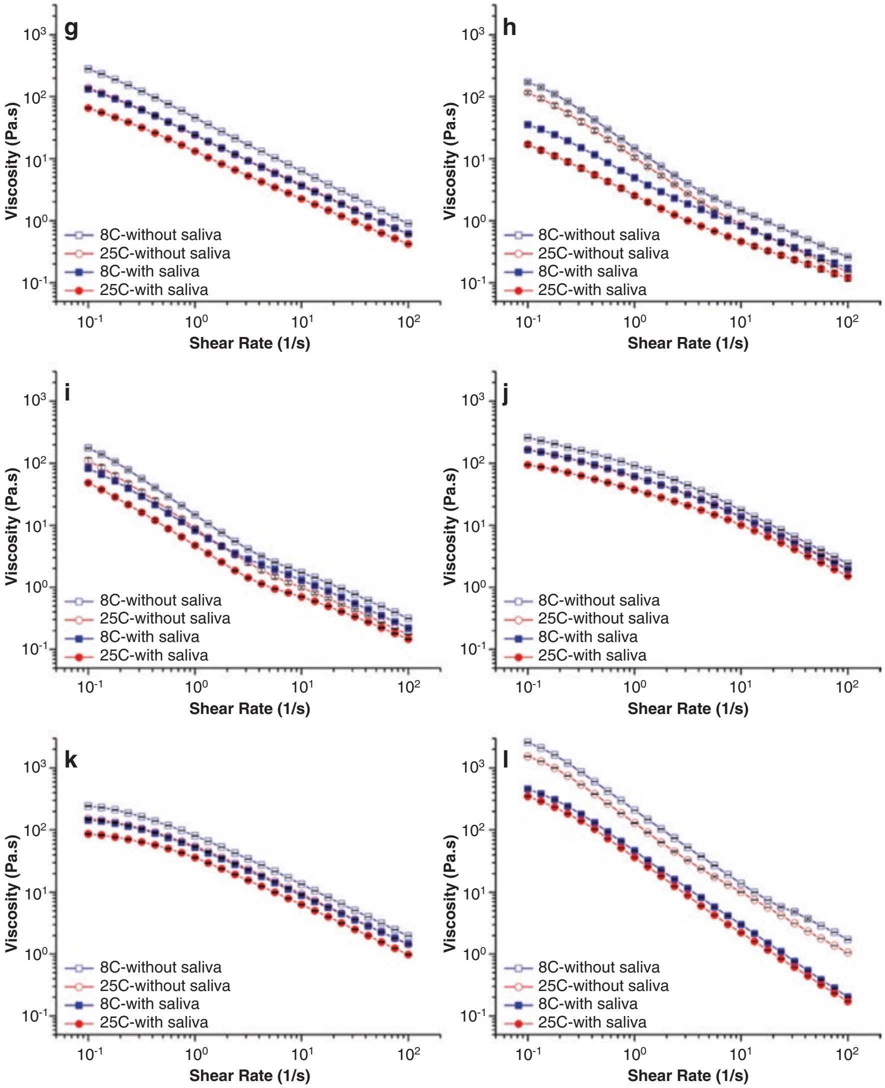

Fig. 6 (continued)

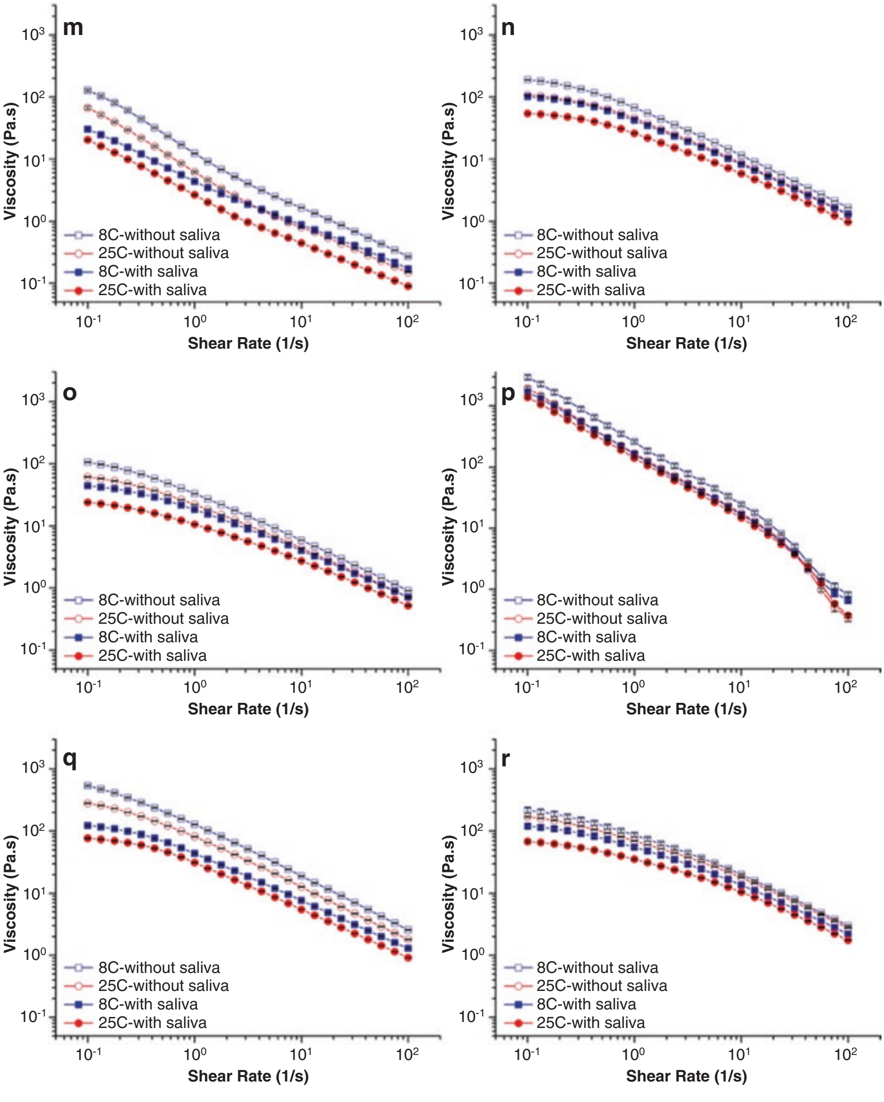

Fig. 6 (continued)

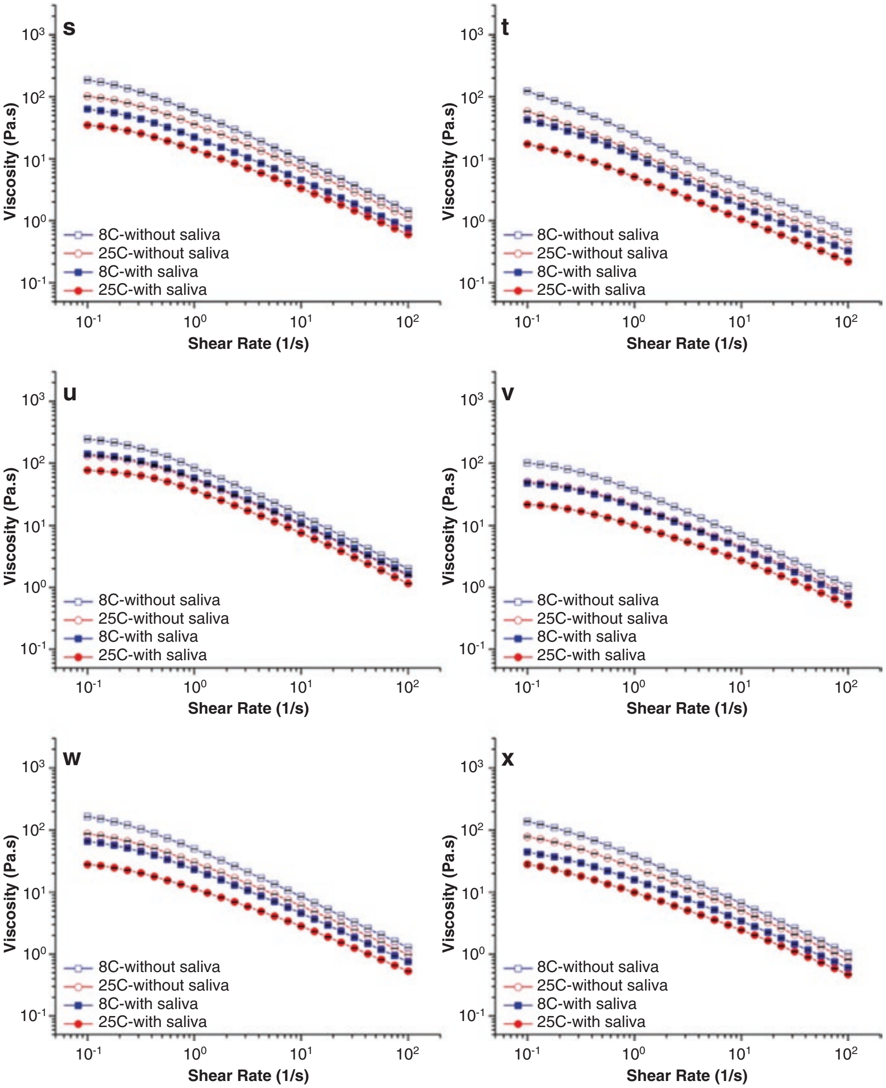

Fig. 6 (continued)

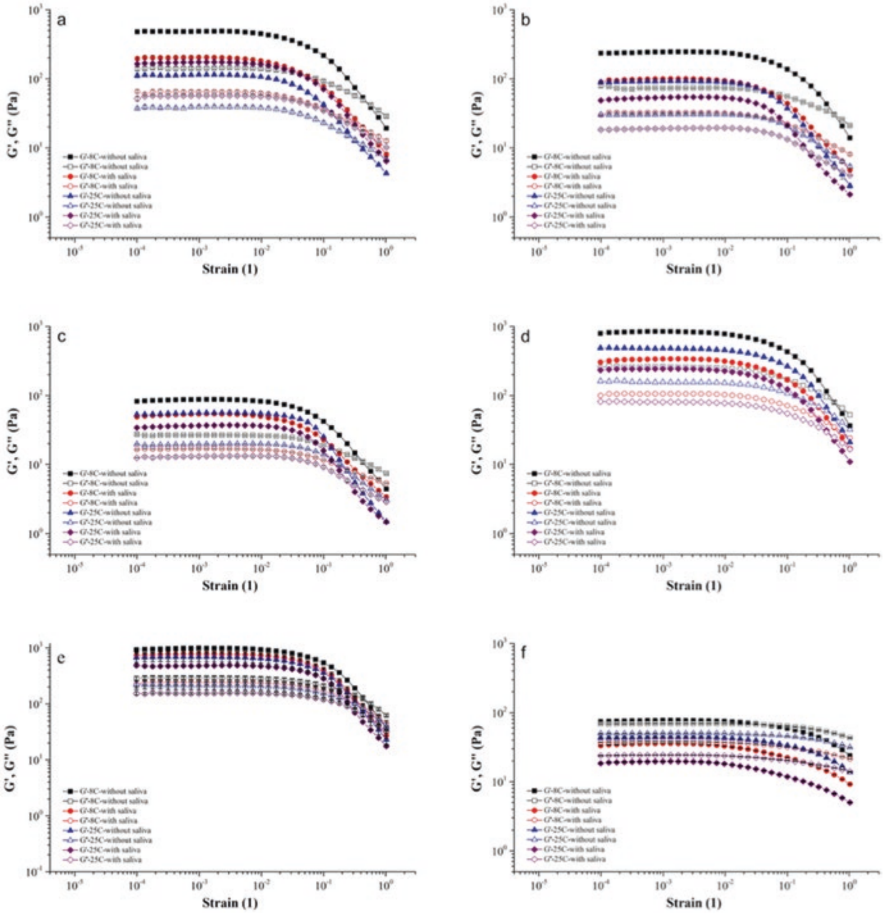

Fig. 7 Acid milk gel strain sweep results; (**a**) sample 1; (**b**) sample 2; (**c**) sample 3; (**d**) sample 4; (**e**) sample 5; (**f**) sample 6; (**g**) sample 7; (**h**) sample 8; (**i**) sample 9; (**j**) sample10; (**k**) sample 11; (**l**) sample 12; (**m**) sample 13; (**n**) sample 14; (**o**) sample 15; (**p**) sample 16; (**q**) sample 17; (**r**) sample 18; (**s**) sample 19; (**t**) sample 20; (**u**) sample 21; (**v**) sample 22; (**w**) sample 23; (**x**) sample 24

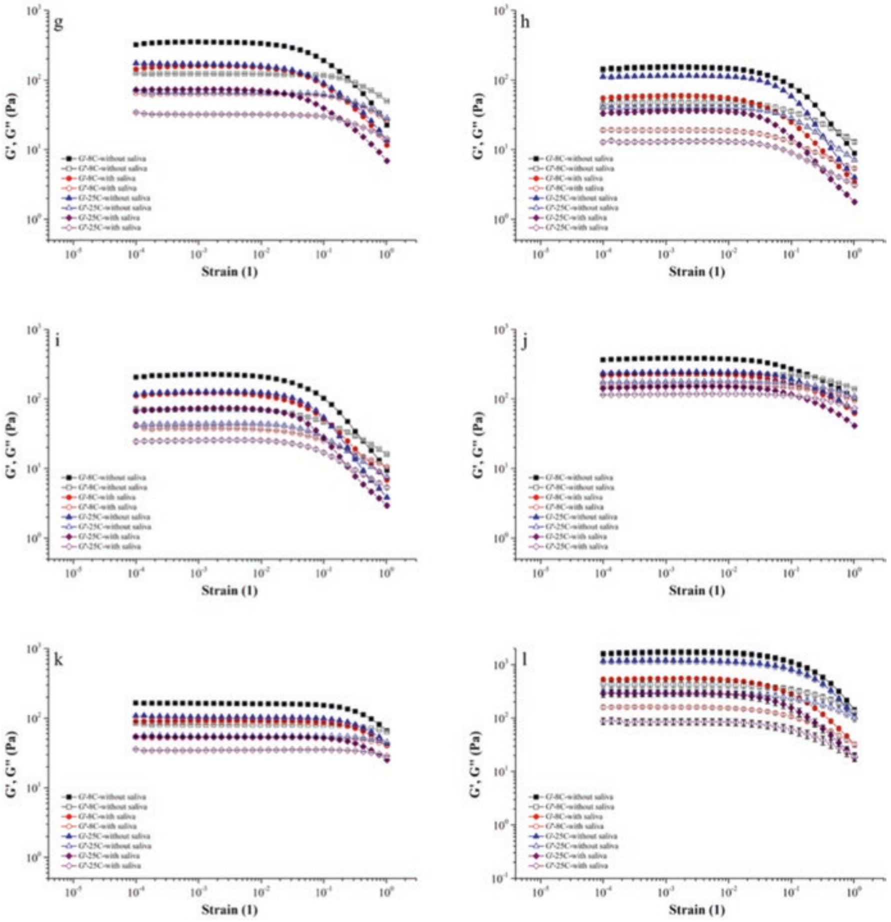

Fig. 7 (continued)

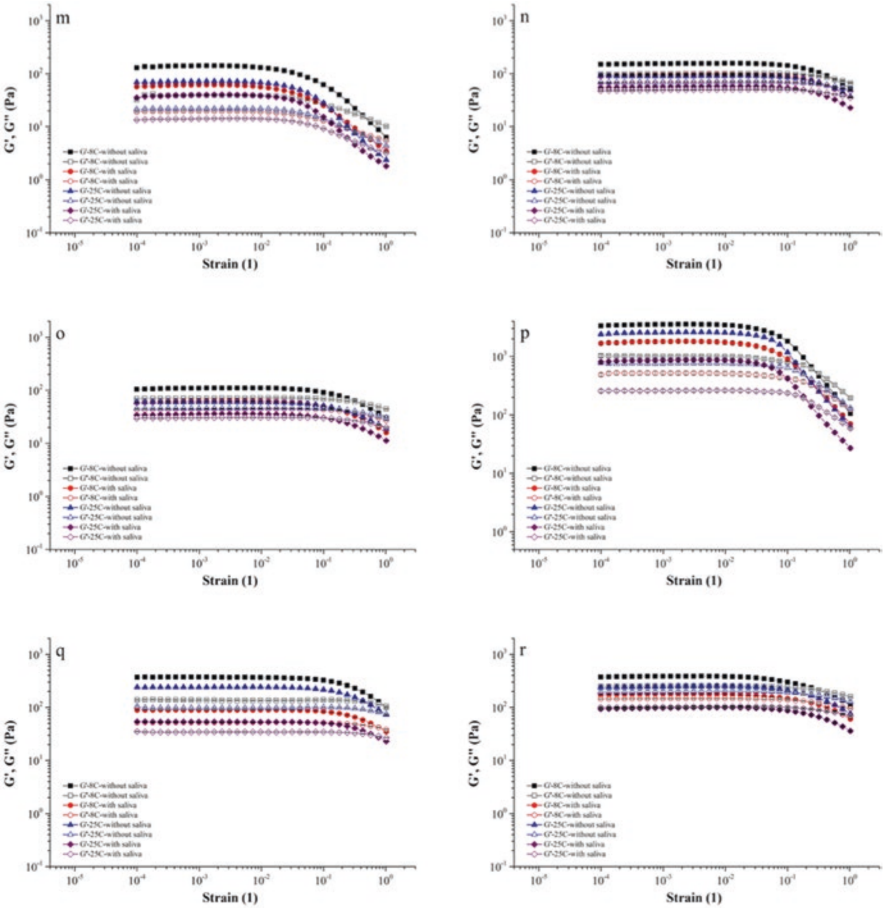

Fig. 7 (continued)

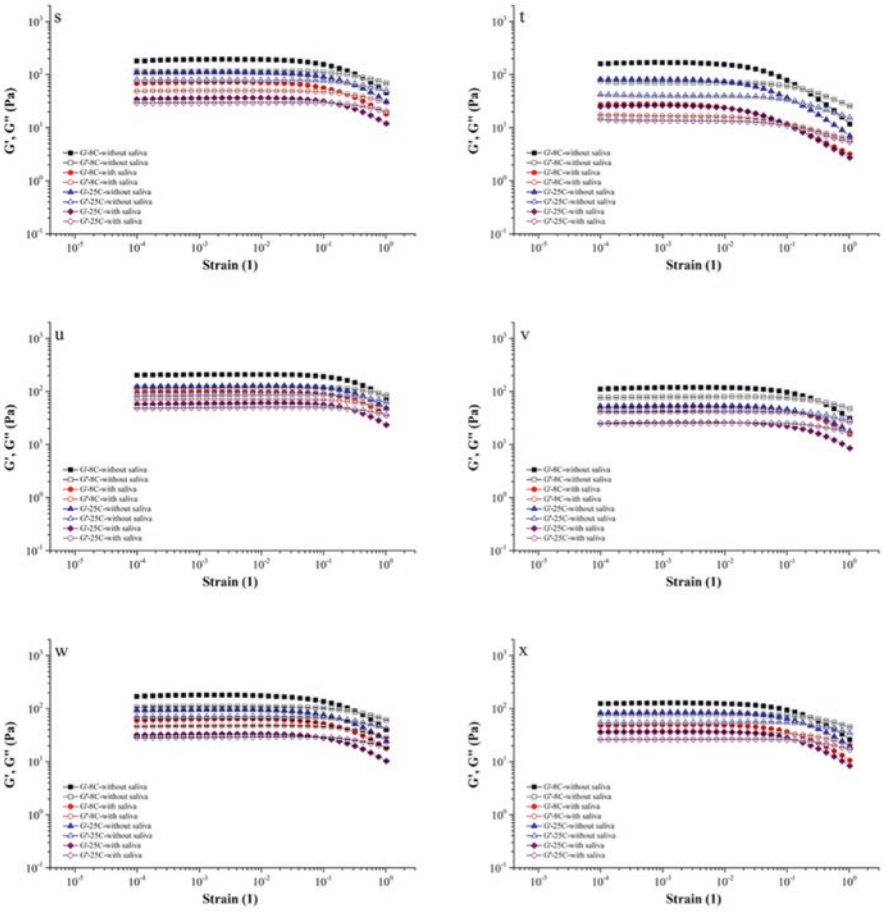

Fig. 7 (continued)

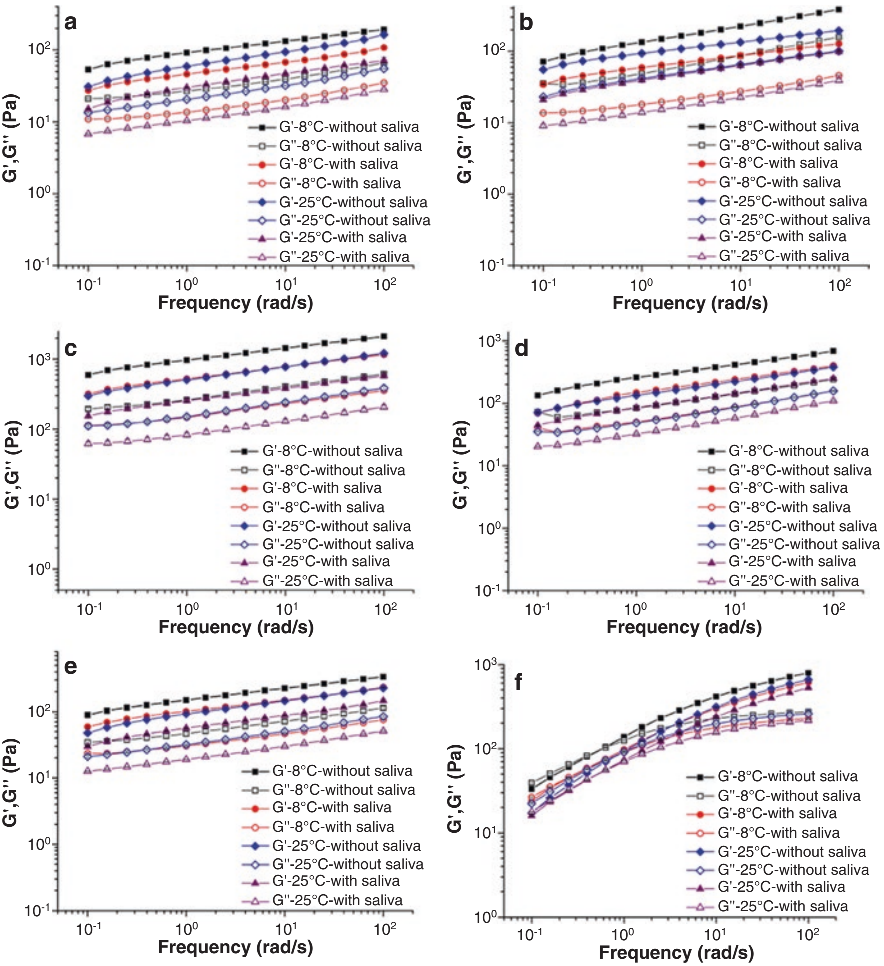

Fig. 8 Acid milk gel frequency sweep results; (**a**) sample 2; (**b**) sample 3; (**c**) sample 5; (**d**) sample 7; (**e**) sample 9; (**f**) sample 10; (**g**) sample 18; (**h**) sample 11; (**i**) sample 12; (**j**) sample13; (**k**) sample 15; (**l**) sample 17; (**m**) sample 23; (**n**) sample 19; (**o**) sample 20; (**p**) sample 21; (**q**) sample 22; (**r**) sample 24

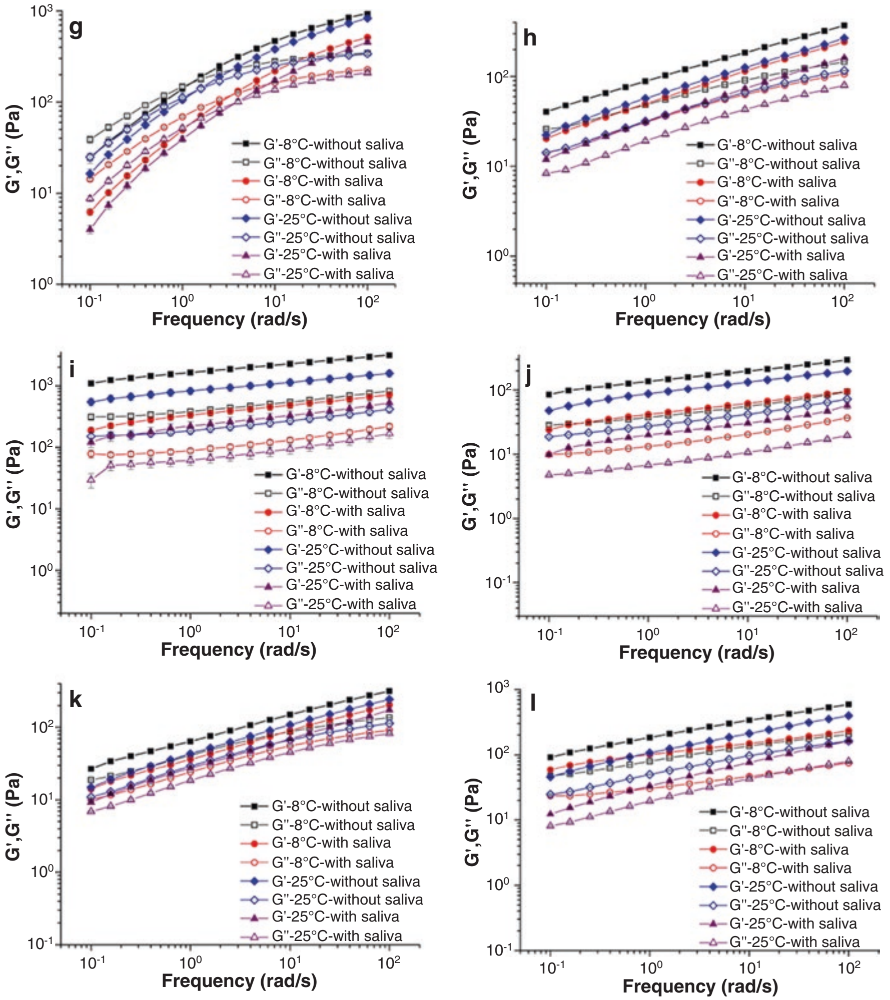

Fig. 8 (continued)

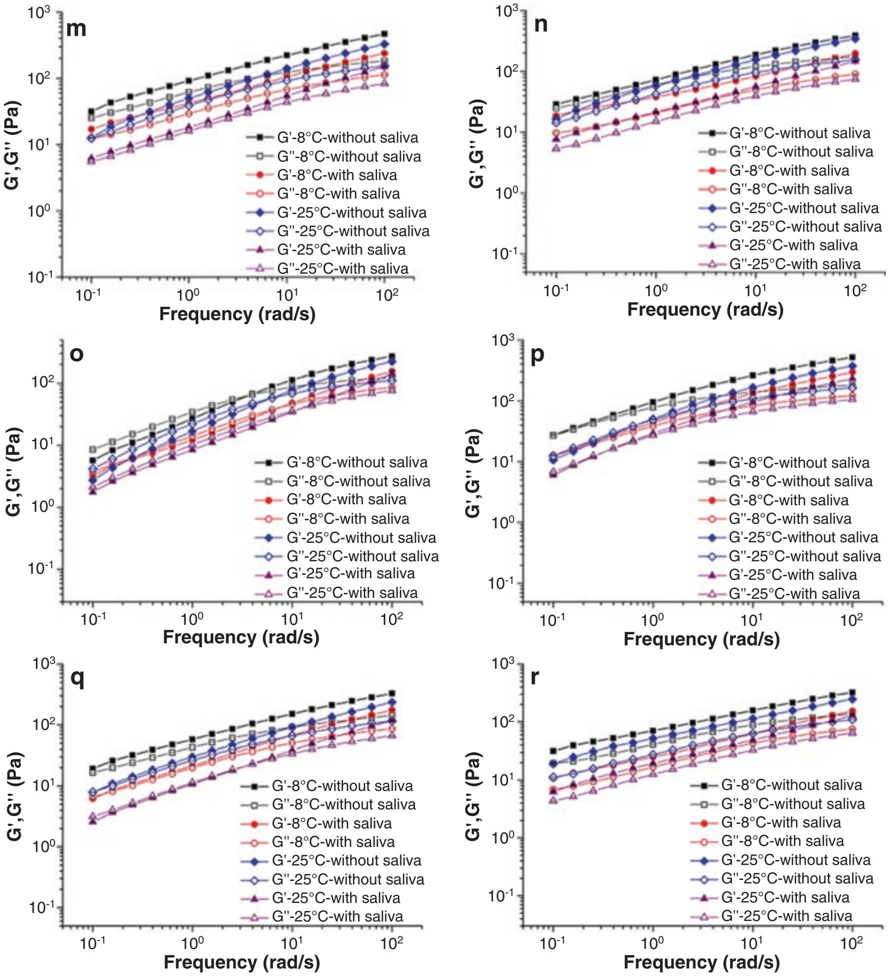

Fig. 8 (continued)

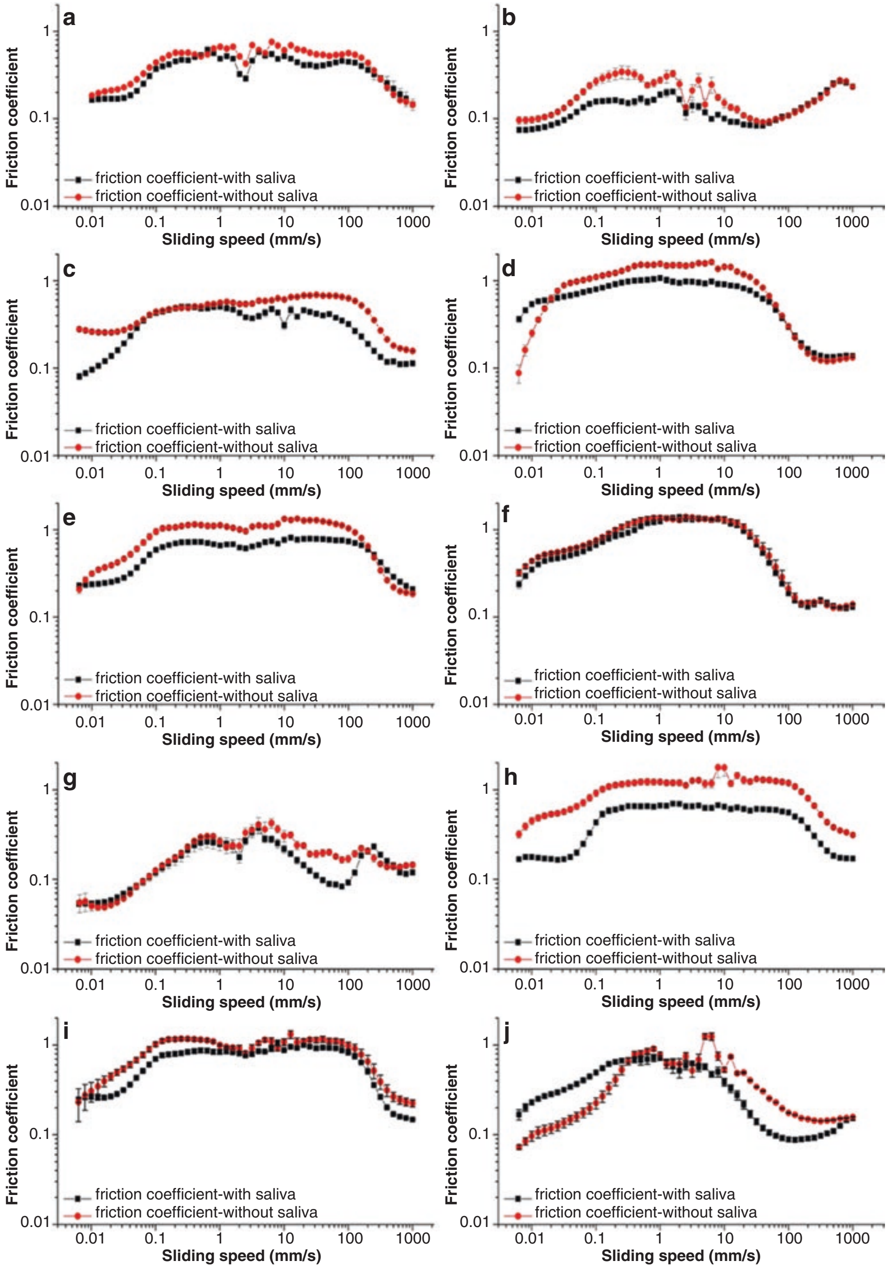

Fig. 9 Acid milk gel tribological results; (**a**) sample 2; (**b**) sample 3; (**c**) sample 5; (**d**) sample 6; (**e**) sample 9; (**f**) sample 10; (**g**) sample 11; (**h**) sample 12; (**i**) sample 13; (**j**) sample14; (**k**) sample 15; (**l**) sample 17; (**m**) sample 18; (**n**) sample 19; (**o**) sample 20; (**p**) sample 21; (**q**) sample 24; (**r**) sample 23

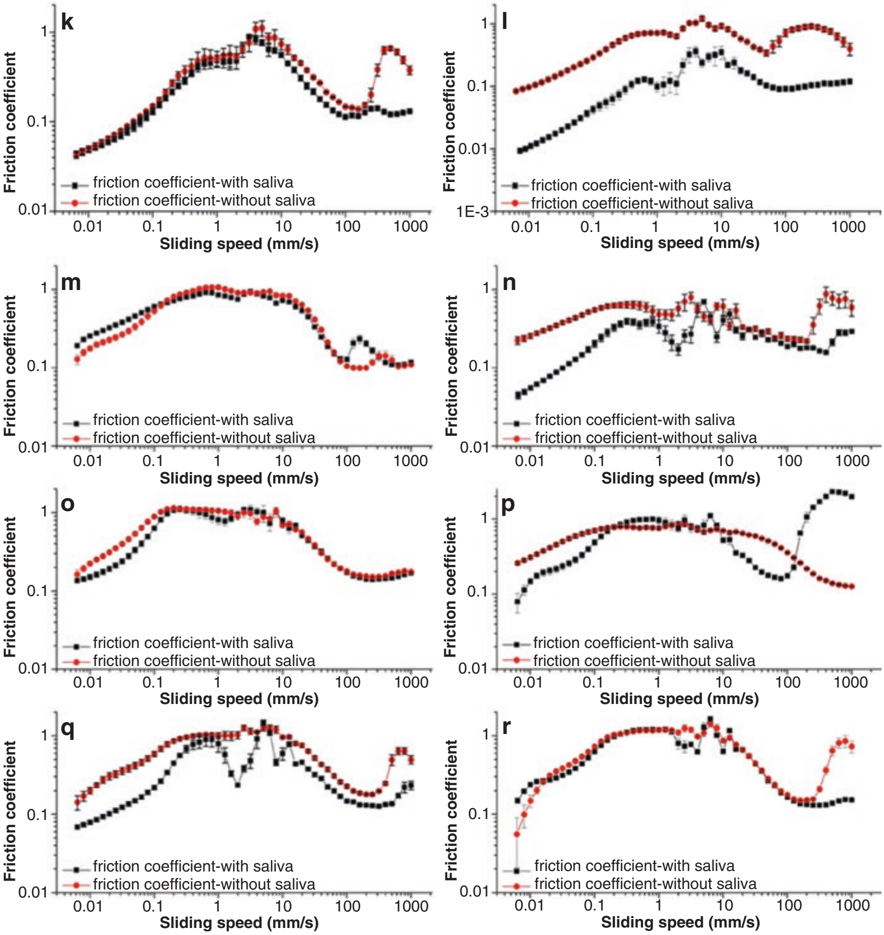

Fig. 9 (continued)

Appendix B: Supplemental Tables

Table 11 HWS composition[a]

HWS samples	α-amylase	Protein concentration
1-morning	32.1[a]	1.26[a]
2-afternoon	31.8[a]	1.24[a]
3-morning	31.7[a]	1.18[ab]
4-afternoon	31[a]	1.15[ab]
5-morning	30.8[a]	1.06[abc]
6-afternoon	30.4[a]	0.991[bcd]
7-morning	29.4[a]	0.905[dc]
8-afternoon	27.4[a]	0.816[d]

[a] Different letters in a given column indicate significant differences among HWS for protein concentration and α-amylase at $p \leq 0.05$

References

Alakali, J., Okonkwo, T., & Iordye, E. (2008). Effect of stabilizers on the physico-chemical and sensory attributes of thermized yoghurt. *African Journal of Biotechnology, 7*(2).

Andiç, S., Boran, G., & Tunçtürk, Y. (2013). Effects of carboxyl methyl cellulose and edible cow gelatin on physico-chemical, textural and sensory properties of yoghurt. *International Journal of Agriculture & Biology, 15*(2).

Andrewes, P., Kelly, M., Vardhanabhuti, B., & Foegeding, E. (2011). Dynamic modelling of whey protein–saliva interactions in the mouth and relation to astringency in acidic beverages. *International Dairy Journal, 21*(8), 523–530.

Berk, Z. (2018). *Food process engineering*. 3rd edition. Academic Press: Cambridge, MA. 742 p.

Bird, A. R., Brown, I. L., & Topping, D. L. (2000). Starches, resistant starches, the gut microflora and human health. *Current Issues in Intestinal Microbiology, 1*(1), 25–37.

Bongaerts, J., Fourtouni, K., & Stokes, J. (2007a). Soft-tribology: Lubrication in a compliant PDMS–PDMS contact. *Tribology International, 40*(10), 1531–1542.

Bongaerts, J., Rossetti, D., & Stokes, J. (2007b). The lubricating properties of human whole saliva. *Tribology Letters, 27*(3), 277–287.

Bourbon, A., Pinheiro, A., Ribeiro, C., Miranda, C., Maia, J., Teixeira, J., & Vicente, A. (2010). Characterization of galactomannans extracted from seeds of Gleditsia triacanthos and Sophora japonica through shear and extensional rheology: Comparison with guar gum and locust bean gum. *Food Hydrocolloids, 24*(2–3), 184–192.

Cassin, G., Heinrich, E., & Spikes, H. (2001). The influence of surface roughness on the lubrication properties of adsorbing and non-adsorbing biopolymers. *Tribology Letters, 11*(2), 95–102.

Chen, J. (2015). Food oral processing: Mechanisms and implications of food oral destruction. *Trends in Food Science & Technology, 45*(2), 222–228.

Chen, J., & Engelen, L. (2012). *Food oral processing: Fundamentals of eating and sensory perception*. John Wiley & Sons: Ames, IA. 320 p.

Cho, S. S., & Prosky, L. (1999). Application of complex carbohydrates to food product fat mimetics. In *Food science and technology* (pp. 411–430). New York: Marcel Dekker.

Chojnicka, A., de Jong, S., de Kruif, C. G., & Visschers, R. W. (2008). Lubrication properties of protein aggregate dispersions in a soft contact. *Journal of Agricultural and Food Chemistry, 56*(4), 1274–1282.

Chojnicka, A., Sala, G., De Kruif, C. G., & Van de Velde, F. (2009). The interactions between oil droplets and gel matrix affect the lubrication properties of sheared emulsion-filled gels. *Food Hydrocolloids, 23*(3), 1038–1046.

Chojnicka-Paszun, A., De Jongh, H., & De Kruif, C. (2012). Sensory perception and lubrication properties of milk: Influence of fat content. *International Dairy Journal, 26*(1), 15–22.

Chojnicka-Paszun, A., Doussinault, S., & De Jongh, H. (2014). Sensorial analysis of polysaccharide–gelled protein particle dispersions in relation to lubrication and viscosity properties. *Food Research International, 56*, 199–210.

Chojnicka-Paszun, A., Janssen, A. M., van de Pijpekamp, A. M., Doussinault, S., & Sala, G. (2009). Sensorial analysis of polysaccharide-protein gel particle dispersions in relation to lubrication and viscosity properties. Tribology and sensory attributes of food dispersions. Ph.D. dissertation. Wageningen University.

De Vicente, J., Stokes, J., & Spikes, H. (2006). Soft lubrication of model hydrocolloids. *Food Hydrocolloids, 20*(4), 483–491.

de Wijk, R. A., & Prinz, J. F. (2005). The role of friction in perceived oral texture. *Food Quality and Preference, 16*(2), 121–129.

De Wijk, R. A., & Prinz, J. F. (2006). Mechanisms underlying the role of friction in oral texture. *Journal of Texture Studies, 37*(4), 413–427.

Dresselhuis, D., De Hoog, E., Stuart, M. C., & Van Aken, G., (2007). Tribology as a tool to study emulsion behaviour in the mouth. E. Dickinson & M. E. Leser (Eds.), In *Food colloids* (pp. 451–461), Royal Society of Chemistry: Cambirdge, UK.

Engelen, L., de Wijk, R. A., van der Bilt, A., Prinz, J. F., Janssen, A. M., & Bosman, F. (2005). Relating particles and texture perception. *Physiology & Behavior, 86*(1), 111–117.

Engelen, L., van den Keybus, P. A., de Wijk, R. A., Veerman, E. C., Amerongen, A. V. N., Bosman, F., Prinz, J. F., & van der Bilt, A. (2007). The effect of saliva composition on texture perception of semi-solids. *Archives of Oral Biology, 52*(6), 518–525.

Everett, D. W., & McLeod, R. E. (2005). Interactions of polysaccharide stabilisers with casein aggregates in stirred skim-milk yoghurt. *International Dairy Journal, 15*(11), 1175–1183.

Huc, D., Michon, C., Bedoussac, C., & Bosc, V. (2016). Design of a multi-scale texture study of yoghurts using rheology, and tribology mimicking the eating process and microstructure characterisation. *International Dairy Journal, 61*, 126–134.

Humphrey, S. P., & Williamson, R. T. (2001). A review of saliva: Normal composition, flow, and function. *The Journal of Prosthetic Dentistry, 85*(2), 162–169.

Janssen, A. M., Terpstra, M. E., De Wijk, R. A., & Prinz, J. F. (2007). Relations between rheological properties, saliva-induced structure breakdown and sensory texture attributes of custards. *Journal of Texture Studies, 38*(1), 42–69.

Johnson, S., Gorman, D., Adams, M., & Briscoe, B. (1993). The friction and lubrication of human stratum corneum. *Tribology series, 25*, 663–672.

Laneuville, S., Paquin, P., & Turgeon, S. (2000). Effect of preparation conditions on the characteristics of whey protein—Xanthan gum complexes. *Food Hydrocolloids, 14*(4), 305–314.

Lee, W., & Lucey, J. (2010). Formation and physical properties of yogurt. *Asian-Australasian Journal of Animal Sciences, 23*(9), 1127–1136.

Li, J.-Y., & Yeh, A.-I. (2001). Relationships between thermal, rheological characteristics and swelling power for various starches. *Journal of Food Engineering, 50*(3), 141–148.

Lucey, J., & Singh, H. (1997). Formation and physical properties of acid milk gels: A review. *Food Research International, 30*(7), 529–542.

Lucey, J., Van Vliet, T., Grolle, K., Geurts, T., & Walstra, P. (1997). Properties of acid casein gels made by acidification with glucono-δ-lactone. 1. Rheological properties. *International Dairy Journal, 7*(6–7), 381–388.

Malone, M., Appelqvist, I., & Norton, I. (2003). Oral behaviour of food hydrocolloids and emulsions. Part 1. Lubrication and deposition considerations. *Food Hydrocolloids, 17*(6), 763–773.

Mezger, T. (2011). *The rheology handbook*, (p. 432, 3rd revise). Vincentz Network, Hanover.

Milani, J., & Maleki, G. (2012). Hydrocolloids in food industry. In *Food industrial processes-methods and equipment*. Rejika: InTech.

Miller, J. L., & Watkin, K. L. (1996). The influence of bolus volume and viscosity on anterior lingual force during the oral stage of swallowing. *Dysphagia, 11*(2), 117–124.

Morell, P., Chen, J., & Fiszman, S. (2016). The role of starch and saliva in tribology studies and the sensory perception of protein-added yogurts. *Food & Function, 8*, 545–553.

Morris, E. R., Cutler, A., Ross-Murphy, S., Rees, D., & Price, J. (1981). Concentration and shear rate dependence of viscosity in random coil polysaccharide solutions. *Carbohydrate Polymers, 1*(1), 5–21.

Nelson, N. (1944). A photometric adaptation of the Somogyi method for the determination of glucose. *The Journal of Biological Chemistry, 153*(2), 375–380.

Nguyen, P. T., Kravchuk, O., Bhandari, B., & Prakash, S. (2017). Effect of different hydrocolloids on texture, rheology, tribology and sensory perception of texture and mouthfeel of low-fat pot-set yoghurt. *Food Hydrocolloids, 72*, 90–104.

Official Methods of Analysis of AOAC INTERNATIONAL (1995a). AOAC INTERNATIONAL, Gaithersburg, MD, USA, Official Method 989.05

Official Methods of Analysis of AOAC INTERNATIONAL (1995b). AOAC INTERNATIONAL, Gaithersburg, MD, USA, Official Method 923.03

Official Methods of Analysis of AOAC INTERNATIONAL (1999). AOAC INTERNATIONAL, Gaithersburg, MD, USA, Official Method 934.01

Ognean, C. F., Darie, N., & Ognean, M. (2006). Fat replacers: Review. *Journal of Agroalimentary Processes and Technologies, 12*(2), 433–442.

Oh, H., Anema, S., Wong, M., Pinder, D., & Hemar, Y. (2007). Effect of potato starch addition on the acid gelation of milk. *International Dairy Journal, 17*(7), 808–815.

Peng, X., & Yao, Y. (2017). Carbohydrates as fat replacers. *Annual Review of Food Science and Technology, 8*, 331–351.

Perrechil, F., Braga, A., & Cunha, R. (2009). Interactions between sodium caseinate and LBG in acidified systems: Rheology and phase behavior. *Food Hydrocolloids, 23*(8), 2085–2093.

Prakash, S., Tan, D. D. Y., & Chen, J. (2013). Applications of tribology in studying food oral processing and texture perception. *Food Research International, 54*(2), 1627–1635.

Selway, N., & Stokes, J. R. (2013). Insights into the dynamics of oral lubrication and mouthfeel using soft tribology: Differentiating semi-fluid foods with similar rheology. *Food Research International, 54*(1), 423–431.

Shao, Y., & Lin, A. H.-M. (2018). Improvement in the quantification of reducing sugars by miniaturizing the Somogyi-Nelson assay using a microtiter plate. *Food Chemistry, 240*, 898–903.

Singh, N., Singh, J., Kaur, L., Sodhi, N. S., & Gill, B. S. (2003). Morphological, thermal and rheological properties of starches from different botanical sources. *Food Chemistry, 81*(2), 219–231.

Sonne, A., Busch-Stockfisch, M., Weiss, J., & Hinrichs, J. (2014). Improved mapping of in-mouth creaminess of semi-solid dairy products by combining rheology, particle size, and tribology data. *LWT - Food Science and Technology, 59*(1), 342–347.

Stading, M., & Hermansson, A.-M. (1990). Viscoelastic behaviour of β-lactoglobulin gel structures. *Food Hydrocolloids, 4*(2), 121–135.

Stanley, N., & Taylor, L. (1993). Rheological basis of oral characteristics of fluid and semi-solid foods: A review. *Acta Psychologica, 84*(1), 79–92.

Steffe, J. F. (1996). *Rheological methods in food process engineering*. East Lansing: Freeman Press.

Tang, C.-H., & Liu, F. (2013). Cold, gel-like soy protein emulsions by microfluidization: Emulsion characteristics, rheological and microstructural properties, and gelling mechanism. *Food Hydrocolloids, 30*(1), 61–72.

Thaiudom, S., & Goff, H. (2003). Effect of κ-carrageenan on milk protein polysaccharide mixtures. *International Dairy Journal, 13*(9), 763–771.

Tunick, M. H. (2010). Small-strain dynamic rheology of food protein networks. *Journal of Agricultural and Food Chemistry, 59*(5), 1481–1486.

Vingerhoeds, M. H., Silletti, E., De Groot, J., Schipper, R. G., & Van Aken, G. A. (2009). Relating the effect of saliva-induced emulsion flocculation on rheological properties and retention on the tongue surface with sensory perception. *Food Hydrocolloids, 23*(3), 773–785.

Zinoviadou, K., Janssen, A., & De Jongh, H. (2008). Tribological properties of neutral polysaccharide solutions under simulated oral conditions. *Journal of Food Science, 73*(2), E88–E94.

Relationships Among Acid Milk Gel Sensory, Rheological, and Tribological Behaviors

Maryam Baniasadidehkordi and Helen S. Joyner

1 Introduction

Textural optimization of reduced or non-fat semisolid foods has been an ongoing challenge to the food industry. The use of hydrocolloids is a common way to enhance the textural properties of semisolid foods, e.g. yogurt. However, hydrocolloids are often used to improve the functional properties of these products, e.g. restoring body after fat removal or maintaining emulsion stability, which can result in poor texture. Both protein and polysaccharide hydrocolloids are used in yogurts. They have different effects in a food system based on their net charge, molecular size, degree of modification, and overall structure (Thaiudom and Goff 2003; Engelen et al. 2005; Lee and Lucey 2010; Morell et al. 2015; van de Velde et al. 2015; Peng and Yao 2017). Their type and concentration need to be chosen based on the final favored texture of a food system to minimize unwanted effects such as off-flavors and chalky, gritty, or slimy textures.

Descriptive sensory analysis is a popular sensory method for evaluating food texture attributes, particularly because the results can be correlated to instrumental results. Rheological and tribological properties of semisolid foods have been reported to correlate with sensory data (Chojnicka-Paszun et al. 2012; Malone et al. 2003; Chen and Engelen 2012; Stokes et al. 2013; Sonne et al. 2014). Specifically, viscosity and viscoelastic properties of semisolid foods have been correlated to textural attributes evaluated by a trained panel, e.g. smoothness, thickness, creaminess, and sliminess (Malone et al. 2003). The shear-thinning properties of yogurt from viscosity profiles have been positively correlated with smoothness and sliminess. Additionally, semisolid food viscoelastic properties from small and large deformation have also shown correlations with sensory attributes (Malone et al. 2003; Ozcan 2013). Tribology, the study of friction, lubrication and wear, has been found to be a good

---

M. Baniasadidehkordi · H. S. Joyner (✉)
School of Food Science, University of Idaho, Moscow, ID, USA
e-mail: hjoyner@uidaho.edu

H. S. Joyner (ed.), *Rheology of Semisolid Foods*, Food Engineering Series,
https://doi.org/10.1007/978-3-030-27134-3_11

addition to rheology and sensory tests for texture perception studies, providing a greater number of textural indicators from instrumental testing. Food friction behaviors have been correlated with a different set of sensory attributes compared to those correlated to rheological behaviors (de Wijk and Prinz 2005; Stokes et al. 2013). Astringency might be the most popular sensory attribute which has been correlated with tribological properties in recent studies. The interest comes from the increased friction perceived in the mouth when salivary proteins interact with substances like tannins, polyphenols, and whey proteins in milk (de Wijk and Prinz 2005; Stokes et al. 2013). Additionally, instrumental friction measurements can be an indicator of friction-related texture attributes, such as astringency, grittiness, and graininess (de Wijk and Prinz 2005; de Wijk et al. 2006a; Krzeminski et al. 2013; Sonne et al. 2014).

Human whole saliva (HWS) can be added to foods during instrumental testing to mimic food breakdown due to HWS incorporation with food during oral processing (de Wijk and Prinz 2005; Stokes et al. 2013; Morell et al. 2016). HWS has been shown to reduce the viscosity and friction profiles of semisolid foods through multiple mechanisms, including dilution, interaction of the food with salivary proteins and α-amylase (Engelen et al. 2003; de Wijk and Prinz 2005; Janssen et al. 2007; Morell et al. 2016; Joyner (Melito) et al. 2014). Also, the components in HWS can greatly affect the perception of friction-related attributes, e.g. astringency. The cause of this has been attributed to the presence of larger particles from either precipitation of salivary proteins or interactions of saliva proteins with food components. On the other hand, salivary α-amylase breaks down food starch, which can result in a decrease in friction (Engelen et al. 2003; Janssen et al. 2007; Stokes et al. 2013; Chen 2015; Morell et al. 2016). There is a current lack of information in the literature of how addition of HWS impacts food rheological and tribological behaviors, and whether addition of HWS during instrumental testing results in stronger correlations of the resulting data with sensory texture data. In a previous study (Chapter "The Impact of Formulation on the Rheological, Tribological, and Microstructural Properties of Acid Milk Gels"), we observed that addition of HWS had a notable effect on instrumental data from acid milk gels. Therefore, the objective of this study was to determine the relationships among rheological, tribological, and sensory behaviors of semisolid foods, as well as how addition of HWS during instrumental testing impacted these relationships.

2 Materials and Methods

It should be noted that because this study was an extension of the study described in Chapter 10, "The Impact of Formulation on the Rheological, Tribological, and Microstructural Properties of Acid Milk Gels", the materials, acid milk gel preparation, saliva collection protocols, proximate analysis, rheological testing, and tribological testing were identical to those used in this study. Thus, these sections have been omitted from the Materials and Methods section in this chapter, as full details are provided in Sect. 2 of Chapter 10, "The Impact of Formulation on the Rheological, Tribological, and Microstructural Properties of Acid Milk Gels". For reference, acid milk gel formulations are provided in Table 1.

Table 1 Experimental design of acid milk gel formulations

Formula number	SMP (w/w)	WPI (w/w)	LBG (w/w)	CMC (w/w)	Potato starch (w/w)	Corn starch (w/w)	Skim milk (w/w)	Cream (w/w)	GDL (w/w)
1	2.8	0	0	0	0	0	97.2	0	1.1–1.55
2	2.83	0	0	0	0	0	95.96	1.21	1.1–1.55
3	2.89	0	0	0	0	0	92.26	4.85	1.1–1.55
4	2.95	0	0	0	0	0	89.15	7.9	1.1–1.55
5	1.8	1	0	0	0	0	97.2	0	1.1–1.55
6	1.8	0	1	0	0	0	97.2	0	1.1–1.55
7	1.8	0	0	1	0	0	97.2	0	1.1–1.55
8	2.1	0	0	0	0.7	0	97.2	0	1.1–1.55
9	2.1	0	0	0	0	0.7	97.2	0	1.1–1.55
10	0	1.25	1.55	0	0	0	97.2	0	1.1–1.55
11	0	1.25	0	1.55	0	0	97.2	0	1.1–1.55
12	0	1.25	0	0	1.55	0	97.2	0	1.1–1.55
13	0	1.25	0	0	0	1.55	97.2	0	1.1–1.55
14	0.5	0.8	0	0.75	0.75	0	97.2	0	1.1–1.55
15	0.5	0.8	0.75	0.75	0	0	97.2	0	1.1–1.55
16	0	2.8	0	0	0	0	97.2	0	1.1–1.55
17	0	0	0	1.4	1.4	0	97.2	0	1.1–1.55
18	0	0	1.8	0	0	1	97.2	0	1.1–1.55
19	0	1.15	0.55	0.55	0.55	0	97.2	0	1.1–1.55
20	0	1.15	0	0.55	0.55	0.55	97.2	0	1.1–1.55
21	0	0	0.7	0.7	0.7	0.7	97.2	0	1.1–1.55
22	0.55	0.75	0.5	0.5	0.5	0	97.2	0	1.1–1.55
23	1	0	0.45	0.45	0.45	0.45	97.2	0	1.1–1.55
24	0.2	0.8	0.45	0.45	0.45	0.45	97.2	0	1.1–1.55

2.1 Descriptive Sensory Evaluation

Sensory evaluation of acid milk gels was performed under the approval of the University of Idaho's Institutional Review Board (protocol 17—195). Ten panelists were recruited from the Washington State University/ University of Idaho School of Food Science via electronic communication and social media. Panelists were 100% female ranging in age from 25 to 55 yr with an average age of 33.9 yr. They were trained for 11 h before performing formal evaluations over a total of 8 h.

Thirteen textural attributes were introduced to the panelist for describing acid milk gel textures (Table 2) according to previous related studies (Saint-Eve et al. 2004; Pascua et al. 2013; Joyner (Melito) et al. 2014). Panelists also verbally agreed on reference products and intensity scores for the references. In each training session, panelists profiled each training sample individually using a 15-cm line scale to indicate the intensity of each attribute present in the samples. Hard copies of the descriptions of the 13 attributes and reference samples were provided. During the last two training sessions, panelists practiced with the sensory software (Compusense

Table 2 Texture attributes and reference products used for sensory evaluation of yogurts[a]

Attribute	Definition	Reference (scale 0 to 15)
Visual terms		
Spoon lumpiness	Presence of lumps observed in yogurts after being stirred	Yoplait vanilla yogurt = 1 Jell-O chocolate tapioca pudding = 15
Spoon viscosity	Thickness of food after being stirred back and forth for 10 times	Water = 1 Jell-O chocolate pudding = 10.5
Mouthfeel terms		
Grainy	Perception of food granules (small particles) on tongue after food is swallowed or expectorated	Reddi Wip whipped cream = 1 Gerber baby rice cereal = 12
Mouthcoating	Force required to clear sample adhered to the mouth with the tongue during eating	Philadelphia cream cheese = 10 ReddiWip whipped cream =1
Mouth viscosity	Force needed to draw food from a spoon over the tongue	Water = 1 Jell-O chocolate pudding = 12
Firmness	Firmness of food in the mouth when food is compressed against the palate via tongue motions	ReddiWip whipped cream =1 Philadelphia cream cheese = 14
Mouth lumpiness	Feeling of lumps in the mouth during eating	Yoplait yogurt = 1 Jell-O tapioca pudding = 15
Smooth	Lack of individual food particles, opposite of grainy and lumpy attributes	Yoplait yogurt = 13 Gerber baby rice cereal = 1
Low-melting	Food does not spread out quickly in the mouth during eating	Reddi Wip whipped cream =1 Jell-O pudding = 10
Grittiness	Feeling of gritty/chalky particles in the oral cavity during eating	WalMart non-fat Greek yogurt =10 Reddi Wip whipped cream =1
After-feel mouth terms		
Astringent	Astringent/dry sensation in the mouth after food is swallowed or expectorated	Atkins strawberry protein drink = 10 Reddi Wip whipped cream =1
Chalky/gritty after-feel	Feeling of chalk-like particles in the mouth after food is swallowed or expectorated	WalMart non-fat Greek yogurt =10 Reddi Wip whipped cream =1
Slimy	Difficulty of clearing the mouth after food is swallowed or expectorated	Gerber banana baby food = 7 Reddi Wip whipped cream = 1

[a] Sensory terms, definitions, and references obtained from (Saint-Eve et al. 2004; Pascua et al. 2013

Cloud, Guelph, Ontario, Canada) to familiarize themselves with its operation before formal sample evaluation.

Formal sample evaluations were carried out in individual sensory facility booths under white light. Six acid milk gels with their duplicates (12 samples in total) were evaluated per session by the panelists in a completely randomized balanced design. All 24 samples from Table 1 were evaluated in duplicate. Samples were served in 4 oz. plastic soufflé cups and randomly coded with 3-digit numbers. All samples were prepared the day before evaluation. During evaluation, panelists were provided the references upon request. To minimize fatigue, panelists were asked to rinse their mouths with filtered water, expectorate samples after each evaluation, and cleanse their palate with unsalted crackers after evaluation of each sample. Additionally, a 5 min enforced rest period was held after finishing 6 samples to minimize fatigue and errors during evaluation. All samples were evaluated on a 15-cm line scale with anchors at 1.5 cm for low intensity and 13.5 cm for high intensity. The results of the evaluations were collected from Compusense software.

2.2 Rheological and Tribological Results Used for Correlations

Data from rheometry and tribometry performed on acid milk gels in a previous study (shown in Table 3, from Chapter 10,"The Impact of Formulation on the Rheological, Tribological, and Microstructural Properties of Acid Milk Gels") were used for correlation with the sensory attribute data collected in this study. Viscosity results selected for correlation included zero-shear rate viscosity (η_o, Pa.s) and flow behavior index (n, unitless). Viscoelastic parameters selected included critical strain (γ_c, %), complex modulus (G^*, Pa), and phase angle (tan δ, rad). Selected tribological results included friction coefficients (μ, unitless) at sliding speeds of 10, 15, 20, 25, and 30 mm s^{-1}.

2.3 Data Analysis

Analysis of Variance (ANOVA) followed by Tukey's HSD (Honest Significant Difference) test performed with SAS version 9.1 (SAS; Cary, NC, U.S.A.) was used to determine significant differences for three main variables (panelists, replicates, samples, and their interactions) based on predetermined textural attributes (n = 13) of the sensory results. Partial Least Square (PLS) analysis was used to correlate the rheological, tribological, and sensory results to determine relationships among mechanical–sensory, frictional–sensory, and mechanical–frictional properties of acid milk gels using SAS version 9.1 (SAS; Cary, NC, U.S.A.).

3 Results and Discussion

3.1 Acid Milk Gel Textural Attributes

Formulations, panelists and their interaction had significant influence on all textural attributes of acid milk gels ($p \leq 0.001$, Table 4) but replicate and interaction of panelist and replicate showed no significant influence. These results showed that the major influences on sensory scores were formulation and panelists. Panelist influence can be decreased by additional training. Despite the influence of panelist on

Table 3 Selected rheological and tribological parameters for correlation analysis obtained from Chapter 10, "The Impact of Formulation on the Rheological, Tribological, and Microstructural Properties of Acid Milk Gels" results[a]

	Viscosity parameters				Viscoelastic parameters				Friction coefficients	
Formula	η_o (Pa.s) 25°C, NS	n (Pa.s) 25°C, NS	η_o (Pa.s) 25°C, S	n (Pa.s) 25°C, S	γ_c (%) 25°C, NS	γ_c (%) 25°C, S	G^* (Pa) 25°C, NS	G^* (Pa) 25°C, S	μ, 25°C, (10 mm s^{-1}) NS	μ, 25°C, (10 mm s^{-1}) S
1	380	0.908	0	0.643	0.547	0.555	179	119	0.745	0.592
2	0	0.503	0	0.5	0.975	0.975	94.5	56.6	0.609	0.521
3	0	0.414	0	0.407	0.975	1.300	58.1	38.2	0.152	0.101
4	2241	0.962	0	0.926	0.731	0.411	284	119	0.177	0.091
5	1072	0.907	728	0.816	0.731	0.731	698	503	1.004	0.761
6	42.6	0.604	26.4	0.55	1.74	0.73	64.4	30.4	1.435	0.907
7	517	0.823	290	0.804	0.730	0.730	362	78.3	0.965	0.751
8	105	0.833	52.8	0.427	0.975	0.975	119	37.7	0.662	0.662
9	0	0.679	0	0.422	0.975	0.731	130	76.6	1.328	0.764
10	205	0.822	114	0.783	2.33	2.33	288	185.8	1.320	1.320
11	231	0.855	123	0.853	10.000	13.400	113	61.7	0.305	0.218
12	3447	0.86	787	0.804	0.975	0.976	1178	295	1.767	0.646
13	0	0.584	0	0.35	0.730	0.730	73.3	42.2	1.078	0.878
14	151	0.844	73.9	0.802	10	7.48	112	75.5	0.387	0.530
15	96.7	0.802	34	0.731	12.180	12.180	73.0	45.7	0.556	0.732
16	2298	0.827	1773	0.721	1.3	1.74	2638	879	1.536	0.826
17	467	0.873	120	0.824	5.6	10	250	61	0.927	0.352
18	212	0.792	79.2	0.782	3.120	12.180	315	141	0.722	0.833
19	161	0.805	54	0.746	3.120	12.180	131	45.9	0.705	0.404
20	307	0.748	45.6	0.712	0.41	0.547	87.8	28.3	1.051	0.795
21	190	0.843	103	0.839	7.480	7.480	150	77.1	0.700	0.521
22	75.1	0.778	30.6	0.72	12.18	12.18	64.6	35.2	0.747	0.705
23	143	0.794	43	0.731	2.330	3.120	115	43.6	0.871	0.635
24	136	0.781	49.3	0.705	2.33	2.33	97.9	44.2	0.957	0.595

[a] η_o: zero-shear viscosity; n: flow index; γ_c: critical strain; μ: friction coefficient

results, significant differences in sensory scores among formulations were found for all attributes evaluated, indicating that formulation was the primary factor influencing texture attribute scores.

The control sample (sample 1), samples with added fat (samples 2, 3, and 4), CS (sample 9), or both WPI and CS (sample 13) showed the greatest spoon lumpiness (Table 5). Samples with WPI and gums (samples 10 and 11) and samples formulated with more than three hydrocolloids (samples 19–24) had the least spoon lumpiness. Addition of whey powder has been linked to the formation of lumps, grits, or grains (Morell et al. 2015). This attribute significantly decreased when WPI was used with CMC or other hydrocolloids. Additional proteins from WPI and the charged portions of CMC can form a strong network which minimizes structure

Table 4 Effect of different parameters and their interactions on the values of acid milk gel (n = 24) texture attributes[a, b]

Textural attributes	Formulation	Replicate	Panelist	Formulation × Replicate	Panelist × Replicate	Panelist × Formulation
Spoon viscosity	192.53***	3.14	29.21***	2.35	0.55	1.84***
Graininess	12.98***	0.37	13.75***	0.9	0.41	1.76***
Mouthcoat	91.86***	2.29	24.82***	1.12	1.1	2.11***
Firmness	84.39***	3	28.63***	1.23	0.26	1.83***
Mouth viscosity	195.54***	0.9	76.57***	0.95	1.22	3.99***
Spoon lumpiness	59.34***	4.81	34.5***	2.63	1.55	2.24***
Mouth lumpiness	27.82***	2.32	20.96***	1.41	0.66	2.09***
Smoothness	37.46***	0.86	61.18***	0.96	2.02	3.07***
Low-melting	57.55***	0.01	31.05***	1.69	0.7	3.08***
Grittiness	16.27***	0.36	26.64***	0.78	2.04	2.72***
Astringency	15.69***	1.3	30.14***	0.78	0.63	1.21***
Chalkiness afterfeel	14.5***	2.8	33.39***	0.99	0.79	2.49***
Sliminess	140.84***	5.19	48.87***	0.85	0.69	3.57***

[a] Due to the limitations of the experimental design, there were not sufficient degrees of freedom to evaluate the panelist × formulation × replicate interaction

[b] $^{*}p \le 0.05$; $^{**}p \le 0.01$; $^{***}p \le 0.001$

Table 5 Acid milk gels sensory attributes as evaluated by trained panelists

Formula number	Spoon lumpiness	Spoon viscosity	Graininess	Mouthcoating	Mouth viscosity	Firmness	Mouth lumpiness	Smoothness	Low-melting	Grittiness	Astringency	Chalkiness afterfeel	Sliminess
1	7.93^{ab}	2.81^{k}	$4.08^{abcdefg}$	2.78^{h}	2.45^{h}	2.60^{g}	4.52^{bcd}	5.23^{g}	9.63^{a}	5.12^{ab}	5.86^{a}	4.65^{a}	1.97^{f}
2	7.96^{ab}	3.29^{k}	5.18^{ab}	3.115^{h}	3.04^{gh}	2.64^{g}	5.64^{ab}	5.67^{fg}	8.91^{ab}	$4.20^{abcdefghi}$	5.00^{abc}	4.05^{abc}	1.98^{f}
3	9.42^{a}	3.10^{k}	$3.94^{abcdefg}$	3.15^{h}	2.93^{gh}	2.72^{g}	4.78^{bc}	6.25^{efg}	9.56^{a}	$3.48^{cdefghij}$	5.16^{ab}	3.34^{abcd}	1.94^{f}
4	7.86^{ab}	3.31^{k}	$3.87^{abcdefg}$	3.17^{h}	2.98^{gh}	2.96^{g}	4.52^{bcd}	6.38^{defg}	8.99^{ab}	$3.61^{bcdefghij}$	4.91^{abcd}	3.35^{abcd}	2.000^{f}
5	8.21^{ab}	3.01^{k}	$4.01^{abcdefg}$	2.69^{h}	2.65^{h}	2.47^{g}	4.56^{bcd}	5.26^{g}	9.27^{ab}	4.96^{abcd}	5.69^{a}	4.52^{a}	1.91^{f}
6	5.11^{cdef}	8.30^{cde}	4.33^{abcdef}	6.43^{bcde}	7.16^{bc}	7.79^{bcde}	3.49^{cde}	8.52^{abcde}	3.36^{ef}	3.16^{fghij}	3.61^{cde}	2.84^{cd}	4.78^{bcde}
7	4.32^{defg}	5.02^{hi}	2.57^{fgh}	4.41^{fg}	4.30^{gf}	4.95^{f}	3.17^{cde}	8.68^{abcd}	6.84^{bcd}	3.26^{fghij}	4.7^{bcde}	3.51^{abcd}	4.00^{e}
8	6.90^{bc}	3.48^{jk}	4.47^{abcde}	3.35^{gh}	2.84^{h}	2.98^{g}	4.71^{bc}	6.23^{efg}	7.88^{abc}	4.61^{abcdef}	5.43^{ab}	4.25^{ab}	2.12^{f}
9	10.10^{a}	2.92^{k}	5.39^{ab}	3.01^{h}	2.87^{h}	2.80^{g}	7.37^{a}	4.80^{g}	8.50^{ab}	4.82^{abcde}	5.25^{ab}	4.65^{a}	1.93^{f}
10	2.26^{gh}	6.23^{fg}	4.79^{abcd}	5.38^{ef}	5.72^{de}	6.34ef	2.35^{e}	7.96^{bcdef}	5.34^{cde}	$4.26^{abcdefgh}$	3.72^{cde}	3.78^{abcd}	12.16^{de}
11	3.17^{fgh}	9.51^{ab}	2.35^{gh}	7.31^{ab}	7.85^{ab}	9.02^{ab}	2.16^{e}	10.16^{ab}	3.36^{ef}	2.93^{hij}	3.33^{e}	2.50^{d}	6.02^{a}
12	5.03^{cdef}	4.48^{ij}	5.88^{a}	3.36^{gh}	3.40^{gh}	3.36^{g}	3.17^{cde}	5.64^{gf}	9.09^{ab}	5.19^{a}	4.87^{abcd}	4.59^{a}	2.43^{f}
13	9.57^{a}	3.08^{k}	4.86^{abc}	2.93^{h}	2.705^{h}	2.53^{g}	5.67^{ab}	5.12^{g}	8.21^{ab}	4.82^{abcde}	5.65^{a}	4.47^{a}	2.21^{f}
14	3.61^{efgh}	7.54^{de}	2.33^{gh}	6.11^{bcde}	5.76^{cde}	7.08^{de}	2.16^{e}	9.59^{ab}	12.17^{ef}	2.83^{hij}	3.55^{de}	2.97^{bcd}	4.68^{cde}
15	6.07^{bc}	7.82^{cde}	2.49^{fgh}	6.91^{abc}	7.03^{bcd}	8.36^{abcd}	2.60^{e}	9.40^{ab}	3.84^{ef}	2.64^{ij}	2.84^{e}	2.79^{cd}	5.28^{abc}
16	5.58^{cde}	2.92^{k}	3.13^{cdefgh}	2.45^{h}	2.14^{h}	2.26^{g}	3.34^{cde}	6.79^{cdefg}	10.04^{a}	5.02^{abc}	5.76^{a}	4.525^{a}	1.92^{f}
17	2.96^{fgh}	9.85^{a}	2.10^{h}	7.69^{a}	8.93^{a}	9.79^{a}	2.10^{e}	9.78^{ab}	2.26^{f}	2.72^{hij}	3.04^{e}	2.49^{d}	5.77^{ab}
18	2.29^{gh}	5.88^{gh}	2.94^{defgh}	5.41^{ef}	5.06^{ef}	6.58^{e}	2.90^{e}	8.94^{abc}	5.42^{cde}	$4.52^{abcdefg}$	3.36^{e}	4.05^{abc}	4.54^{cde}
19	3.17^{fgh}	8.13^{cde}	3.11^{cdefgh}	6.23^{bcde}	6.63^{bcd}	7.64^{bcde}	2.00^{e}	9.71^{ab}	12.17^{ef}	$3.39^{defghij}$	3.59^{cde}	2.96^{bcd}	5.24^{abc}
20	1.59^{h}	8.38^{cde}	2.73^{efgh}	6.68^{abcd}	6.66^{bcd}	8.13^{bcd}	1.89^{e}	10.92^{a}	4.52^{def}	3.00^{ghij}	3.20^{e}	2.83^{cd}	5.23^{abc}
21	3.77^{efgh}	8.69^{bc}	2.60^{efgh}	7.15^{ab}	8.01^{ab}	8.83^{abc}	2.36^{e}	10.44^{a}	3.45^{ef}	2.98^{ghij}	3.13^{e}	3.09^{bcd}	5.47^{abc}
22	2.47^{gh}	7.52^{de}	2.33^{gh}	5.69^{de}	5.84^{cde}	7.18^{de}	1.91^{e}	10.02^{ab}	4.23^{ef}	2.62^{j}	3.43^{e}	3.01^{bcd}	5.07^{abcd}
23	2.00^{h}	7.32^{ef}	2.58^{fgh}	5.87^{cde}	5.95^{cde}	7.35^{cde}	2.10^{e}	9.11^{abc}	4.31^{def}	2.87^{hij}	3.27^{e}	2.83^{cd}	4.93^{bcde}
24	4.83^{cdef}	8.49^{bcd}	$3.75^{bcdefgh}$	6.66^{abcd}	6.76^{bcd}	7.47^{cde}	2.88^{de}	9.02^{abc}	2.97^{ef}	$3.46^{cdefghij}$	3.43^{e}	3.36^{abcd}	5.09^{abcd}

Letters that are different in each column indicate significant differences ($p < 0.05$)

irregularities by forming a high number of cross-links and aggregations throughout the system (Ibrahim et al. 2010; van de Velde et al. 2015).

Mouthcoat, spoon viscosity, firmness, and mouth viscosity attributes were higher for samples with a combination of two or more hydrocolloids (samples 19–24) compared to when hydrocolloids were used individually (samples 1–9). These results were attributed to associative interactions between the oppositely charged portions of the polysaccharides and the proteins from the milk, SMP, and WPI. Network stabilization can also occur because of hydrophobic interactions and hydrogen bridging among the polymers in the system (Doublier et al. 2000; Bertrand and Turgeon 2007). Interestingly, addition of fat (samples 2, 3, and 4) did not have a significant effect on these attributes compared to the control sample (sample 1). This result implies that hydrocolloids play a greater role in certain semisolid food texture attributes than fat content.

As expected, mouth lumpiness and smoothness were inversely related. The least smooth samples were the control sample (sample 1), samples with added fat (samples 2, 3, and 4), samples with added starch (samples 8 and 9), and samples with added CS and WPI (sample 13) (Table 4). This result showed that hydrocolloids played a large role in providing a smooth mouthfeel, which is desirable in many semisolid food products, including yogurt.

The intensities for spoon viscosity and mouth viscosity were similar (Table 5), which was unsurprising. Additionally, samples that were prepared with more than two hydrocolloids and had high viscosity, smoothness, and sliminess also had low graininess, chalkiness afterfeel, and grittiness. Hydrocolloids can stabilize the protein network in dairy products through strong interactions with casein micelles, and this phenomenon is more effective at lower pH values (Walstra 1996). This stabilization will decrease casein precipitation and improve viscosity and gel strength (Walstra 1996). Neutral hydrocolloids alter the texture attributes of the system by increasing the viscosity of the continuous phase (Walstra 1996). The mechanism for starches is different: starch granules can swell in the presence of water and heat to alter texture attributes of semisolid foods. These effects appeared to be synergistic, as the blends of hydrocolloids produced samples with significantly different textures than samples prepared with only one or two hydrocolloids.

The control sample (sample 1), samples with fat (samples 2, 3, and 4), samples with added starch (samples 8 and 9), and samples with a combination of starch and protein (samples 12 and 13) had the lowest mouthcoating, mouth viscosity, firmness, smoothness, and sliminess. These samples also had the highest graininess, chalkiness afterfeel, astringency, and grittiness. Addition of milkfat may have caused an incompatibility with SMP due to the solubility level of SMP in the milk when milkfat is added. Furthermore, starches, when used alone, can reduce smoothness and increase graininess, chalkiness, and grittiness due to the retrogradation effect when the gelatinized starch cools (Bird et al. 2000). Addition of milk powders like WPI and SMP can have a similar effect when used alone (Isleten and Karagul-Yuceer 2006).

Milk proteins, mainly those in whey, precipitate at their isoelectric points when mixed with HWS. This effect generally results in increased astringency

(Sano et al. 2005; Andrewes et al. 2011). In addition, the particle size of whey proteins increases upon addition to yogurt due to increased interactions between whey proteins and the binding sites of κ-casein (Beaulieu et al. 1999; Puvanenthiran et al. 2002). Furthermore, the interaction of κ-casein with the larger and irregularly-shaped whey protein particles can cause protein aggregation (Puvanenthiran et al. 2002; Engelen et al. 2005). The aggregates can be felt during oral processing, resulting in a sensation of roughness and dryness (Cayot et al. 2008) on the oral surfaces including the tongue, palate, and surrounding soft oral tissues (Engelen et al. 2007). This effect is known to occur in yogurt (Beaulieu et al. 1999; Puvanenthiran et al. 2002) and was observed in samples 5, 13, and 16, all of which had added WPI. Samples containing fat (samples 2, 3, and 4) and the control sample (sample 1) also had relatively high astringency, likely due to the SMP included in the formulation Conversely, samples formulated with more than two hydrocolloids (samples 14, 15, and 19–24) generally had the lowest amount of astringency, likely because the hydrocolloids prevented HWS from interacting with whey proteins; this interaction is known to cause an astringent sensation (Andrewes et al. 2011). If the whey proteins interact with hydrocolloids, they are more likely to remain as part of the network instead of existing as free particles, reducing astringency.

Overall, addition of gums significantly improved desirable attributes, e.g. firmness, spoon and mouth viscosity, smoothness, and sliminess (manifesting as a ropy texture, which is pleasing to consumers) (van de Velde et al. 2015; Han et al. 2016), and decreased negative attributes such as grittiness, graininess, astringency, and chalkiness afterfeel (Alakali et al. 2008). Addition of gums can significantly change the microstructural, textural, and rheological properties of acid milk gels by two major mechanisms: segregative and aggregative interactions. Aggregative interactions generally involve hydrocolloids with net charges, e.g. CMC. The counterions from protein and charged hydrocolloids create strong aggregation throughout the protein matrix and improve textural attributes such as firmness and smoothness. Segregative interactions describe the interactions between proteins and neutral gums, e.g. LBG. These neutral hydrocolloids improve textural properties by increasing the viscosity of the continuous phase, resulting in increased gel firmness (Thaiudom and Goff 2003).

3.2 *Principal Component Analysis*

Principal Component analysis (PCA) was performed to visualize sensory texture attributes (Fig. 1). Using PCA also helped eliminate descriptor redundancies from textural attributes and obtain possible latent variables by fitting dependent variables into major factor (component) groups. Component 1 explained 85.54% of the variance observed, while component 2 explained 5.87%, indicating that the majority of the variation among the samples was described by these components.

Component 1 was primarily and positively defined by sliminess, spoon viscosity, mouth viscosity, mouthcoat, smoothness, and firmness; and negatively with astringency, low-melting, and graininess. It should be noted that a lower intensity of the low-melting attribute was considered to be more desirable. In other words, products with a low score of low-melting would have a rapid meltaway in the mouth, which is desired for yogurt products. Component 2 was mostly described by spoon and mouth lumpiness, grittiness, and chalkiness afterfeel. Samples prepared with CMC and WPI (sample 11); SMP, WPI, CMC, and PS (sample 14); CMC and PS (sample 17); WPI, LBG, CMC, and PS (sample 19); WPI, CMC, PS, and CS (sample 20); LBG, CMC, PS, and CS (sample 21); LBG, CMC, PS, and WPI (sample 22); and LBG, CMC, PS, and CS (sample 23) were most positively related to component 1. The control sample (sample 1) and samples with low levels of WPI (sample 5) or PS (sample 8) were most negatively related to Component 1. The sample with LBG and CS (sample 18) was most negatively related to Component 2. Overall, the PCA plot showed that samples prepared with more than two hydrocolloids and that included at least one gum (CMC or LBG) were associated with more desirable texture attributes, which was in line with the descriptive sensory results (Sect. 3.1).

Acid milk gels formulations were divided into three large clusters based on the sum of the differences between the initial two object clusters. The first large cluster (green, Fig. 1) consisted of three sub-clusters including (1) samples 14, 19, 20, 22, and 23; (2) samples 11, 17, and 21; and (3) samples 6, 15, and 24. This cluster was closest to smoothness, sliminess, mouth viscosity, spoon viscosity, mouthcoat, and firmness, in agreement with the descriptive analysis data (Table 3). These samples all had PS and CMC in their formulations; most formulations also included WPI. The correlation between CMC and smoothness has been shown in a previous yogurt study (Alakali et al. 2008). CMC can form strong ionic interactions with casein micelles at pH = 4.6. Additionally, PS granules can swell in the continuous phase and improve the evenness and uniformity of the texture (Roller 1996). Furthermore, the combination of WPI and CMC (sample 11) appeared to form a similar texture to when CMC was used with PS (sample 17) as well as when both gums and starches were used without addition of SMP and WPI (sample 21) or when all hydrocolloids were used (sample 24). These results indicated that CMC had a major contribution to textural attributes, regardless of the other hydrocolloids used.

Cluster 2 (red, Fig. 1) included samples 7, 10, and 18. These samples were most positively related to the attributes from Cluster 1, and negatively to the attributes from Cluster 3. The intensity of desirable textural attributes such as smoothness and viscosity were greater than the intensity of the undesirable ones, e.g. graininess and astringency.

The samples in cluster 3 (blue, Fig. 1) included those that contained milk fat and SMP (samples 2, 3, and 4), CS and SMP (sample 9), PS and SMP (sample 8), WPI and CS (sample 13), WPI and PS (sample 12), WPI and SMP (sample 5), and WPI (sample 16). This cluster was broken into five sub-clusters comprising samples (1) 12 and 16, (2) 9 and 13, (3) 3 and 4, (4) control (1) and 5, and (5) 2 and 8. Texture attributes most closely related to this cluster included chalkiness afterfeel, grittiness, astringency, low-melting, and both mouth and spoon lumpiness. Addition of SMP and WPI is known to increase these attributes (Isleten and Karagul-Yuceer

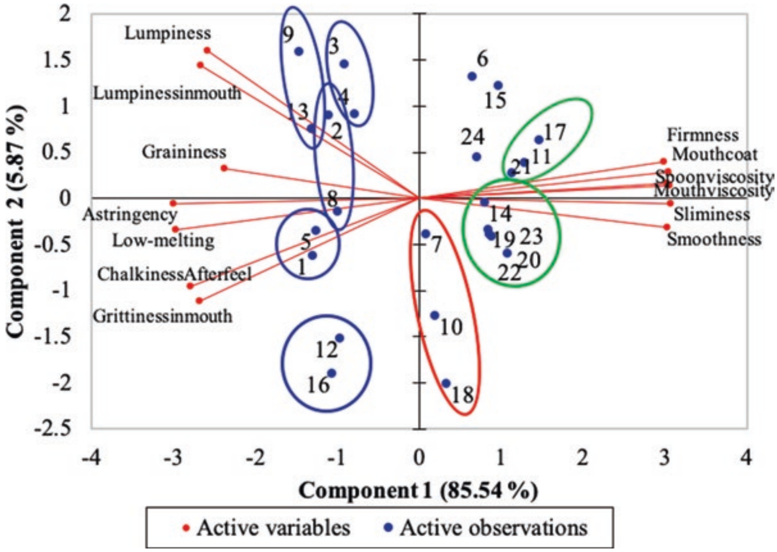

Fig. 1 Principal Component Analysis (PCA) biplot for acid milk gels. In this plot, the 24 formulations correspond to those shown in Table 1. Clusters have been circled based on cluster analysis

2006); the presence and large particles size of PS may have also contributed to these attributes, particularly in sample 8.

Overall, PCA results showed that specific hydrocolloids and their combinations can dramatically impact the intensity of texture attributes in acid milk gels. These results can be used for targeted formulation of yogurts and other semisolid foods with desirable textures and for troubleshooting products with textural issues.

3.3 Correlations among Acid Milk Gel Textural Attributes

The correlation matrix of textural attributes (Table 6) showed that spoon viscosity was positively correlated with mouthcoating, mouth viscosity, firmness, smoothness, and sliminess, and negatively correlated with low-melting and astringency. Similarly, mouthcoating was positively correlated with mouth viscosity, firmness, smoothness, and sliminess but negatively correlated with low-melting and astringency. Mouthcoating correlations with firmness and sliminess were also found in previous studies on yogurts (Janiaski et al. 2016). Additionally, measurements of mouthcoating in custards showed that its intensity can be related to thickness, spoon and mouth viscosity, smoothness, and graininess (Prinz et al. 2006), which is in agreement with the results of this study.

Table 6 Correlation matrix for acid milk gel textural attributes[a, b]

Attribute	Mouthcoat	Mouth viscosity	Firmness	Smoothness	Low-melting	Astringency	Chalkiness afterfeel	Sliminess
Spoon viscosity	0.989***	0.988***	0.986***	0.923***	−0.973***	−0.934***		0.979***
Mouthcoat		0.995***	0.990***	0.925***	−0.980***	−0.957***		0.981***
Mouth viscosity			0.988***	0.934***	−0.976***	−0.961***		0.989***
Firmness					−0.968***	−0.933***		0.965***
Smoothness						−0.928***		0.953***
Low-melting						0.937***		−0.970***
Astringency								−0.960***
Grittiness							0.967***	

[a] Coefficients that were not statistically significant (p > 0.05) and repetitive correlations were removed

[b] $^{*}p \leq 0.05$; $^{**}p \leq 0.01$; $^{***}p \leq 0.001$

Firmness was positively correlated with sliminess. This result was likely due to microstructural features that promoted strong but flexible intermolecular interactions. Sliminess has also been related to the use of exopolysaccharide-producing lactic acid bacteria during yogurt production (van de Velde et al. 2015). Exopolysaccharides produced by lactic acid bacteria can have neutral or negative charges, similar to certain hydrocolloids (van de Velde et al. 2015). The strong interaction of negatively charged polysaccharides produced from lactic acid bacteria with positively charged casein micelles at $pH < 4.6$ results in a stronger protein network with longer chains. This is similar to the structure produced by CMC interactions with milk proteins. CMC is an anionic polysaccharide that can form strong interactions with casein micelles, creating a structure that is similar to that produced by the interaction of exopolysaccharides and casein. This structure can improve the texture of yogurts (van de Velde et al. 2015), as the longer polysaccharide chains contribute to a slick, potentially slimy mouthfeel that often manifests as a long, ropy texture, which is often desirable. Accordingly, samples in this study that had formulations that included CMC tended to have higher sliminess scores (Sect. 3.1).

Smoothness was positively correlated with sliminess and negatively correlated with low-melting and astringency. Grittiness was positively correlated with chalkiness afterfeel, which was not surprising as both of these attributes can be attributed to particle size. Perception of bigger particles on the tongue, especially in samples formulated with WPI, SMP, starch, or a combination of these (Puvanenthiran et al. 2002; Engelen et al. 2005), would increase both chalkiness and grittiness attributes.

Astringency was negatively correlated with sliminess and positively correlated with low-melting. This positive correlation between low-melting and astringency was in agreement with the findings of Morell et al. (2016). According to the American Society for Testing of Materials, the sensory definition of astringency is "the complex of sensations due to shrinking, drawing or puckering of the epithelium as a result of exposure to substances such as alums or tannins" (Materials 2004). Astringency is a common defect in dairy products due to interactions among whey proteins, caseins, and calcium phosphates, or whey proteins with astringent compounds. These interactions result in aggregation that disrupts the salivary film and reduces lubricity in the mouth (Josephson et al. 1967; Andrewes et al. 2011; Gibbins and Carpenter 2013). Astringency has also been attributed to the production of γ-caseins from β-casein by breaking of the peptide bonds between amino acids 28 and 29, 105 and 106, and 107 and 108 in the β-casein chain (Harwalkar et al. 1993; Lemieux and Simard 1994). Another explanation for the astringency perception was proposed to be the aggregation and precipitation of salivary proteins, which results in loss of saliva lubricity (Jöbstl et al. 2004). The dry sensation is therefore due to precipitation of salivary proteins after complexation with astringent molecules from alums, tannins, and polyphenols (Green 1993), which causes direct contact of two oral surfaces (Gibbins and Carpenter 2013). This contact would be exacerbated by low melting and low sliminess; melting and sliminess would provide a thin lubricating layer of material between the oral surfaces that is easy to move, reducing the sticking between oral surfaces.

3.4 Correlations among Acid Milk Gel Sensory Attributes and Rheological Properties

Viscosity parameters with statistically significant correlations to sensory attributes were η_o and n (Table 7). The greatest number of correlations for η_o were at 8 °C when no HWS was added; n showed the most correlations when HWS was added at both 25 °C and 8 °C. These correlations were not surprising based on the results of a previous study (Chapter 10, "The Impact of Formulation on the Rheological, Tribological, and Microstructural Properties of Acid Milk Gels"). F-values showed that HWS had significant impact on acid milk gel n values, but HWS showed no significant effect on η_o and c values. However, formulation did have a significant effect on η_o values.

η_o at 8 °C without HWS was positively correlated with low-melting, grittiness, and astringency, and negatively correlated with mouthcoat, mouth viscosity, and sliminess. Temperature may have influenced the correlations between η_o and astringency, mouthcoat, and sliminess, as they were not found at 25 °C. Interestingly, addition of HWS resulted in fewer correlations for η_o at 8 °C: only grittiness and chalkiness showed correlations. This result implied that melting, mouthcoat, viscosity, and sliminess were assessed immediately after putting the sample in the mouth and before significant saliva–sample interactions. The other sensory terms were likely assessed after the sample had interacted with saliva. The correlations between grittiness and chalkiness with instrumental data when HWS was added to the sample can be explained by the microstructural differences caused by HWS, particu-

Table 7 Correlations between sensory and viscosity results for acid milk gels (n = 24 formulations)[a, b, c]

Attribute	η_o (Pa.s) 8°C, NS	n (Pa.s) 8°C, S	η_o (Pa.s) 8°C, S	η_o (Pa.s) 25°C, NS	η_o (Pa.s) 25°C, S	n (Pa.s) 25°C, S
Spoon lumpiness		-0.553^{**}				
Mouth lumpiness		-0.667^{***}				-0.614^{**}
Spoon viscosity						0.438^{*}
Mouthcoat	0.435^{*}					
Mouth viscosity	-0.407^{*}					0.445^{*}
Firmness						
Smoothness		0.471^{*}				0.500^{*}
Low-melting	0.491^{*}			0.464^{*}		
Grittiness	0.440^{*}		0.442^{*}	0.414^{*}		-0.520^{*}
Graininess		-0.543^{**}				
Chalkiness			0.416^{*}		0.410^{*}	
Astringency	0.418^{*}					
Sliminess	-0.408^{*}					0.460^{*}

[a] Non-significant coefficients and repetitive correlations were removed from the table

[b] $^{*}p \leq 0.05$; $^{**}p \leq 0.01$; $^{***}p \leq 0.001$

[c] NS: no HWS added; S: HWS added

larly the presence or absence of aggregates. Addition of HWS at 8 °C would result in HWS-induced depletion flocculation of protein aggregates in acid milk gels, promoting a grittier mouthfeel. The aggregates may also have increased the resistance to flow, as they would not move smoothly past each other in a shear field.

n at 8 °C with HWS was negatively correlated with graininess, spoon lumpiness, and mouth lumpiness and positively correlated with smoothness. This result indicated that as graininess and lumpiness increased, the extent of acid milk gel shear-thinning behavior decreased, which may also have been related to increased smoothness since the material would not necessarily become thin but would maintain a constant layer over the oral surfaces. At 8 °C, n was negatively correlated with spoon and mouth lumpiness and graininess, and positively correlated with smoothness. However, at 25 °C, n was negatively correlated with mouth lumpiness and grittiness, and positively correlated with spoon viscosity, mouth viscosity, smoothness, and sliminess. These results implied that the temperature plays a key role in the relationships between instrumental and sensory data.

It should be noted that, in general, more correlations were found for parameters with added HWS than without. In fact, n was not correlated with any flow behavior parameter when HWS was not added. This result implied that HWS application is important for understanding the effects of shear-dependent behaviors on oral texture attributes. This finding was supported by significant effects of HWS (for n) and interaction of HWS by formulations (for n, c, and η_o) with viscosity parameters in a previous study (Chapter 10, "The Impact of Formulation on the Rheological, Tribological, and Microstructural Properties of Acid Milk Gels").

A large number of correlations were found between acid milk gel viscoelastic properties and textural attributes (Table 8). Among viscoelastic parameters, γ_c and tan δ had the highest numbers of correlations with sensory attributes. γ_c values at 8 °C and 25 °C with or without HWS were correlated with all sensory attributes. The same correlations were observed for tan δ except at 8 °C without HWS: tan δ was not correlated with graininess. Most γ_c and tan δ correlations were positive for ideal acid milk gel attributes such as spoon viscosity, firmness, mouth viscosity, and smoothness. Some of these correlations were also found by Joyner (Melito) et al. (2014) for a different set of acid milk gels. One potential reason for these results is that high γ_c values indicate a stronger intermolecular structure that requires greater force to make it flow or break. This would likely manifest as increased viscosity and firmness. tan δ indicates the degrees of elastic- versus viscous-type behavior, with larger values indicating more viscous-type behavior. Samples with less elastic-type behavior (i.e. higher tan δ values) would likely be perceived as smoother and with a greater degree of mouthcoating due to increased viscous flow.

G^* had a lower number of correlations with sensory attributes compared to γ_c and tan δ. G^* with and without HWS at 8 °C and with HWS at 25 °C was positively correlated with low-melting, grittiness, and astringency, and negatively correlated with mouthcoat, mouth viscosity, and firmness. At 25 °C and without HWS, G^* was positively correlated with low-melting, grittiness, and chalkiness afterfeel, and negatively correlated with sliminess. The similarity between the correlations for data obtained with and without addition of HWS during testing indicated that strain

Table 8 Correlation between sensory results and viscoelastic parameters for acid milk gels (n = 24 formulations)[a, b, c]

Attribute	γ_c (%) 8 °C NS	γ_c (%) 8 °C S	γ_c (%) 25 °C NS	γ_c (%) 25 °C S	G^* (Pa) 8 °C NS	G^* (Pa) 8 °C S	G^* (Pa) 25 °C NS	G^* (Pa) 25 °C S	tan δ (rad) 8 °C NS	tan δ (rad) 8 °C S	tan δ (rad) 25 °C NS	tan δ (rad) 25 °C S
Spoon lumpiness	-0.438^{*}	-0.485^{*}	-0.469^{*}	-0.498^{*}					-0.625^{**}	-0.604^{**}	-0.628^{**}	-0.589^{**}
Spoon viscosity	0.659^{***}	0.674^{***}	0.669^{***}	0.695^{***}					0.747^{***}	0.619^{**}	0.731^{***}	0.723^{***}
Graininess	-0.530^{**}	-0.627^{**}	-0.605^{**}	-0.632^{***}						-0.412^{*}	-0.466^{*}	-0.408^{*}
Mouthcoat	0.649^{***}	0.669^{***}	0.673^{***}	0.693^{***}	-0.437^{*}	-0.456^{*}		-0.454^{*}	0.763^{***}	0.615^{**}	0.752^{***}	0.732^{***}
Mouth viscosity	0.643^{***}	0.671^{***}	0.667^{***}	0.697^{***}	-0.405^{*}	-0.423^{*}		-0.421^{*}	0.769^{***}	0.640^{**}	0.762^{***}	0.747^{***}
Firmness	0.657^{***}	0.680^{***}	0.660^{***}	0.704^{***}	-0.412^{*}	-0.433^{*}		-0.429^{*}	0.730^{***}	0.596^{**}	0.718^{***}	0.724^{***}
Mouth lumpiness	-0.485^{*}	-0.532^{**}	-0.539^{**}	-0.554^{**}					-0.629^{***}	-0.550^{**}	-0.630^{***}	-0.578^{**}
Smoothness	0.585^{**}	0.622^{**}	0.632^{***}	0.630^{***}					0.722^{***}	0.581^{**}	0.724^{***}	0.669^{***}
Low-melting	-0.605^{**}	-0.637^{***}	-0.645^{***}	-0.649^{***}	0.479^{*}	0.486^{*}	0.441^{*}	0.482^{*}	-0.814^{***}	-0.671^{***}	-0.803^{***}	-0.781^{***}
Grittiness	-0.518^{**}	-0.567^{**}	-0.574^{**}	-0.547^{**}	0.503^{*}	0.503^{*}	0.477^{*}	0.535^{**}	-0.629^{***}	-0.565^{**}	-0.634^{***}	-0.601^{**}
Astringency	-0.540^{**}	-0.574^{**}	-0.595^{**}	-0.595^{**}	0.431^{*}	0.460^{*}		0.463^{*}	-0.793^{***}	-0.665^{***}	-0.791^{***}	-0.743^{***}
Chalkiness afterfeel	-0.576^{**}	-0.592^{**}	-0.591^{**}	-0.609^{**}	0.461^{*}	0.469^{*}	0.440^{*}	0.498^{*}	-0.644^{***}	-0.589^{**}	-0.640^{***}	-0.634^{***}
Sliminess	0.640^{***}	0.658^{***}	0.661^{***}	0.687^{***}	-0.397	-0.412^{*}	-0.357	-0.411^{*}	0.775^{***}	0.642^{***}	0.768^{***}	0.735^{***}

[a] Non-significant coefficients and repetitive correlations were removed from the table

[b] $*p \leq 0.05$; $**p \leq 0.01$; $***p \leq 0.001$

[c] NS: no HWS added; S: HWS added

sweep data can be used to predict texture attributes of semisolid foods. Additionally, HWS improved the strength of the correlations found for G^*, in agreement with the significant impact of HWS and its interaction with formulation for G^* (Chapter 10, "The Impact of Formulation on the Rheological, Tribological, and Microstructural Properties of Acid Milk Gels"). Overall the correlation analysis of rheological and sensory data supports the use of HWS during rheological testing if the end goal is to correlate instrumental data with sensory texture attributes.

3.5 Correlations among Acid Milk Gel Sensory Attributes and Tribological Behaviors

Multiple correlations were found between acid milk gel sensory attributes and tribological behaviors (Table 9). Graininess, grittiness, and chalkiness afterfeel were positively correlated to friction coefficients (μ) at 10 mm s^{-1} and 15 mm s^{-1}. These attributes have been shown to be perceived in the boundary regime (Cassin et al. 2001; Dresselhuis et al. 2008), which is in agreement with the friction profiles observed for these samples (Chapter 10, "The Impact of Formulation on the Rheological, Tribological, and Microstructural Properties of Acid Milk Gels"). A negative correlation of smoothness to friction coefficient was observed at sliding speeds of 20, 25, and 30 mm s^{-1}, which was not surprising: higher friction would result in a less smooth feeling in the mouth. Additionally, this result points to development of an interfacial film at these speeds. As friction coefficient decreases with increased sliding speed, increased perception of attributes such as smoothness, mouth viscosity, mouthcoating, low-melting, and sliminess may occur. These attri-

Table 9 Correlations between sensory results and friction coefficients of acid milk gels without HWS addition at 25 °C (n = 24)[a, b]

Sensory attribute	μ at 10 mm s^{-1}	μ at 15 mm s^{-1}	μ at 20 mm s^{-1}	μ at 25 mm s^{-1}	μ at 30 mm s^{-1}
Graininess	0.428^{*}	0.529^{**}	0.570^{**}	0.560^{**}	0.590^{**}
Mouthcoating					-0.438^{*}
Mouth viscosity					-0.419^{*}
Mouth lumpiness					0.404^{*}
Smoothness			-0.420^{*}	-0.446^{*}	-0.491^{*}
Low-melting					0.402^{*}
Grittiness	0.454^{*}	0.540^{**}	0.597^{**}	0.618^{**}	0.655^{***}
Astringency				0.434^{*}	0.493^{*}
Chalkiness afterfeel	0.428^{*}	0.524^{**}	0.590^{**}	0.611^{**}	0.642^{***}
Sliminess					-0.436^{*}

[a] Non-significant coefficients and repetitive correlations were removed from the table

[b] $^{*}p \leq 0.05$; $^{**}p \leq 0.01$; $^{***}p \leq 0.001$

butes are related to a smoother mouthfeel (De Wijk et al. 2006b). The correlation strengths of chalkiness afterfeel, grittiness, and graininess to friction coefficient increased with increasing sliding speed, potentially because the more rapid movement of the oral surfaces would make any particulates more noticeable. Friction coefficient was also positively correlated with astringency at speeds of 25 and 30 mm s^{-1}, as well as mouth lumpiness at a sliding speed of 30 mm s^{-1}.

The number of correlations found between friction and sensory data indicated that a sliding speed range of 10–30 mm s^{-1} was appropriate for indicating acid milk gel friction-related textural attributes with instrumental measurements. Additionally, correlating sensory attributes with tribological results with added HWS showed notable differences (Table 10) compared to when HWS was not used in tribometry. No correlations were found for friction coefficients at sliding speeds of 10 mm s^{-1}. However, friction coefficients at 25 and 30 mm s^{-1} were correlated to most sensory attributes. A correlation for graininess did not appear for friction coefficients at 10 and 15 mm s^{-1} for samples with added HWS, whereas graininess was correlated with friction coefficients at all selected sliding speeds when samples were tested without HWS. These results suggested that HWS resulted in a decrease of granules or food particles that would increase friction coefficients at those speeds. This may have been due to the lubrication effect of salivary proteins, mainly proline-rich mucins (Chen and Stokes 2012). However, it was more likely due to the breakdown of the acid milk gel structures in the presence of HWS, which would reduce the tiny lumps perceived as grains in the mouth.

Mouthcoating and mouth viscosity were correlated to friction coefficient at 25 mm s^{-1} and 30 mm s^{-1} for samples tested with HWS (Table 10), showing that these attributes can be perceived at lower sliding speeds when mixed with HWS. Spoon viscosity and mouth lumpiness were not correlated with tribological data for samples tested without HWS but were for samples tested with HWS. Smoothness correlations occurred at lower sliding speeds when samples were tested without HWS. The appearance of correlations between friction coefficients and low-melting, grittiness, astringency, chalkiness afterfeel, and sliminess were not affected by addition of HWS during tribological analysis. However, the correlation coefficients were higher for friction coefficients for samples tested with added HWS. Overall, these results point to the importance of adding saliva during tribological testing if the goal is to relate friction and sensory texture attributes.

3.6 Correlations among Acid Milk Gel Rheological and Tribological Behaviors

The only correlations found between friction coefficients and viscosity parameters η_o, n, and c were between (1) η_o at 8 °C and friction coefficient at a sliding speed of 30 mm s^{-1} when HWS was not added to the samples, (2) η_o at 8 °C and friction coefficient at a sliding speed of 30 mm s^{-1} when HWS was added to the samples and (3) n at 8 °C and friction coefficient at sliding speeds of 25 and 30 mm s^{-1} when HWS was added to the samples (results not shown in tables). These results indicated

Table 10 Correlations between sensory results and friction coefficients of acid milk gels with HWS addition at 25 °C (n = 24)[a, b]

Sensory attribute	μ at 15 mm s^{-1}	μ at 20 mm s^{-1}	μ at 25 mm s^{-1}	μ at 30 mm s^{-1}
Spoon viscosity			-0.418^{*}	-0.509^{**}
Graininess		0.407^{*}	0.481^{*}	0.542^{**}
Mouthcoating			-0.439^{*}	0.541^{**}
Mouth viscosity			-0.413^{*}	-0.518^{**}
Firmness			-0.434^{*}	-0.526^{**}
Mouth lumpiness				0.432^{*}
Smoothness			-0.460^{*}	-0.569^{**}
Low-melting				0.444^{*}
Grittiness	0.497^{*}	0.555^{**}	0.631^{*}	0.709^{***}
Astringency			0.443^{*}	0.570^{**}
Chalkiness afterfeel	0.518^{**}	0.588^{**}	0.656^{**}	0.730^{***}
Sliminess				-0.504^{*}

[a] Non-significant coefficients and repetitive correlations were removed from the table

[b] $^{*}p \leq 0.05$; $^{**}p \leq 0.01$; $^{***}p \leq 0.001$

that viscosity and friction were not strongly related for these samples. However, incorporation of HWS during instrumental testing may improve viscosity and friction coefficient correlations.

No correlations were found between friction coefficient at 10–30 mm s^{-1} and tan δ (rad) at 8 °C or 25 °C with or without addition of HWS. On the other hand, γ_c showed significant negative correlation with friction coefficient at sliding speeds between 15 and 30 mm s^{-1} for samples without addition of HWS (Table 11), and at all sliding speeds for samples with added HWS (Table 12). These negative correlations implied that increased acid milk gel resistance to permanent deformation resulted in decreased friction coefficients, and that HWS promoted this effect at lower sliding speeds. Interestingly, the number of correlations between friction coefficients and G^* decreased when HWS was added to the samples before testing. Correlations between friction coefficients and G^* were positive, indicating that increased friction coefficients were related to increased structural stiffness.

Based on the correlation results, γ_c showed the best correlation to friction coefficients measured at sliding speeds of 10–30 mm s^{-1} among all viscoelastic parameters evaluated, the same range found for best correlations between friction coefficients and sensory attributes. In general, viscoelastic parameters were better-correlated to tribological results compared to viscosity parameters, and correlations differed based on sliding speed and HWS application.

Table 11 Correlations between viscoelastic results and friction coefficients of acid milk gels with no HWS added ($n = 24$)[a, b]

Attribute	μ at 10 mm s^{-1} at 25 °C	μ at 15 mm s^{-1} at 25 °C	μ at 20 mm s^{-1} at 25 °C	μ at 25 mm s^{-1} at 25 °C	μ at 30 mm s^{-1} at 25 °C
γ_c (%) at 8 °C		-0.423^{*}	-0.427^{*}	-0.442^{*}	-0.422^{*}
γ_c (%) at 25 °C		-0.480^{*}	-0.489^{*}	-0.503^{*}	-0.486^{*}
G^{*} (Pa) at 8 °C	0.493^{*}			0.437^{*}	0.475^{*}
G^{*} (Pa) at 25 °C	0.516^{**}		0.411^{*}	0.440^{*}	0.470^{*}

[a]Non-significant coefficients and repetitive correlations were removed from the table
[b]$^{*}p \leq 0.05$; $^{**}p \leq 0.01$; $^{***}p \leq 0.001$

Table 12 Correlations between viscoelastic results and friction coefficients of acid milk gels with addition of HWS ($n = 24$)[a, b]

Attribute	μ at 10 mm s^{-1} at 25 °C	μ at 15 mm s^{-1} at 25 °C	μ at 20 mm s^{-1} at 25 °C	μ at 25 mm s^{-1} at 25 °C	μ at 30 mm s^{-1} at 25 °C
γ_c (%) at 8 °C	-0.429^{*}	-0.430^{*}	-0.471^{*}	-0.483^{*}	-0.429^{*}
γ_c (%) at 25 °C	-0.466^{*}	-0.476^{*}	-0.510^{*}	-0.522^{*}	-0.466^{*}
G^{*} (Pa) at 8 °C				0.442^{*}	
G^{*} (Pa) at 25 °C			0.407^{*}	0.489^{*}	

[a]Non-significant coefficients and repetitive correlations were removed from the table
[b]$^{*}p \leq 0.05$; $^{**}p \leq 0.01$; $^{***}p \leq 0.001$

4 Overall Conclusions from This Chapter and Chapter 10, "The Impact of Formulation on the Rheological, Tribological, and Microstructural Properties of Acid Milk Gels"

Formulation changes and addition of HWS to acid milk gels showed significant impact on their microstructures and rheological, tribological, and sensory behaviors. Addition of hydrocolloids produced thicker chains and larger aggregates in acid milk gel microstructures, with the specific effect being dependent on the hydrocolloid added. HWS application resulted in a higher number of aggregates with larger serum pores and fat coalescence in samples with fat.

All samples showed shear-thinning behaviors regardless of formulation or addition of HWS. However, the extent of shear thinning increased with HWS application and increasing temperature. Acid milk gels and yogurt samples with added WPI had the greatest viscosity, and samples with LBG had the lowest. Samples containing CMC or all hydrocolloids showed similar viscosity profiles. This similarity in behavior was reflected in the results for confocal imaging, tribology, and sensory evaluation. Stribeck curve profiles from tribometry showed mostly boundary and mixed regimes for all samples, but curve shapes changed notably for different formulations. Acid milk gel samples with high levels of added WPI (sample 16) showed the greatest friction coefficients, while full-fat acid milk gels showed the lowest. Friction coefficient decreased with addition of HWS for most samples due to enzymatic breakdown and lubrication effects of HWS. The most notable decrease in friction coefficient among the samples occurred when HWS was applied to the sample with PS (sample 8) due to the enzymatic breakdown of PS with salivary α-amylase. However, this effect was not observed for the samples with CS, which was attributed to differences between CS and PS amylose content and granule structure. Strain sweep results showed similar trends to viscosity and friction behaviors. The resistance to deformation under shear strain increased with addition of hydrocolloids in the formulations and decreased with HWS and increased temperature.

Samples made with CMC or more than two hydrocolloids showed the greatest number of desirable textural attributes, i.e. smoothness, firmness, and mouth viscosity. These samples were also least related to negative attributes, i.e. grittiness, graininess, astringency, and chalkiness afterfeel. The opposite results were found for samples containing SMP, WPI, and starches either individually or in combination (samples 1–5, 8, 9, and 13). These differences were attributed to variation in the samples' microstructures.

Rheological and tribological results were well-correlated with sensory results. Correlating sensory evaluation results with the parameters from viscosity models showed a strong correlation between flow index and zero shear viscosity. On the other hand, the textural attributes of grittiness, graininess, and astringency were positively correlated with acid milk gel friction coefficients at 5 different sliding speeds (10–30 mm s^{-1}). Friction coefficients at 25 and 30 mm s^{-1} had the most correlations with sensory attributes. Not surprisingly, mouth viscosity, firmness, smoothness, and low-melting were negatively correlated with acid milk gel friction coefficients. Friction coefficients were also correlated with viscosity and viscoelastic parameters of acid milk gels. Addition of HWS increased the number of correlations found among these parameters. These results showed that HWS application during instrumental testing (rheometry and tribometry) can result in better prediction of semisolid food texture perception from instrumental data. In general, the results from this study are beneficial for food manufacturers who wish to use instrumental testing in combination with sensory testing during formulation of new semisolid products with desirable textures similar to their full-fat counterparts.

Acknowledgements Funding for this project was provided by the USDA National Institute of Food and Agriculture (grant #2015-67018-23069).

Appendix A: Supplemental Table

Table 13 HWS composition[1]

HWS samples	α-amylase	Protein concentration
1-morning	32.1^{a}	1.26^{a}
2-afternoon	31.8^{a}	1.24^{a}
3-morning	31.7^{a}	1.18^{ab}
4-afternoon	31^{a}	1.15^{ab}
5-morning	30.8^{a}	1.06^{abc}
6-afternoon	30.4^{a}	0.991^{bcd}
7-morning	29.4^{a}	0.905^{dc}
8-afternoon	27.4^{a}	0.816^{d}

[1] Different letters in a given column indicate significant differences among HWS for protein concentration and α-amylase at $p \leq 0.05$

References

Alakali, J., Okonkwo, T., & Iordye, E. (2008). Effect of stabilizers on the physico-chemical and sensory attributes of thermized yoghurt. *African Journal of Biotechnology, 7*, 2.

Andrewes, P., Kelly, M., Vardhanabhuti, B., & Foegeding, E. (2011). Dynamic modelling of whey protein–saliva interactions in the mouth and relation to astringency in acidic beverages. *International Dairy Journal, 21*(8), 523–530.

Beaulieu, M., Pouliot, Y., & Pouliot, M. (1999). Composition and microstructure of casein: Whey protein aggregates formed by heating model solutions at 95 C. *International Dairy Journal, 9*(3–6), 393–394.

Bertrand, M.-E., & Turgeon, S. L. (2007). Improved gelling properties of whey protein isolate by addition of xanthan gum. *Food Hydrocolloids, 21*(2), 159–166.

Bird, A. R., Brown, I. L., & Topping, D. L. (2000). Starches, resistant starches, the gut microflora and human health. *Current Issues in Intestinal Microbiology, 1*(1), 25–37.

Cassin, G., Heinrich, E., & Spikes, H. (2001). The influence of surface roughness on the lubrication properties of adsorbing and non-adsorbing biopolymers. *Tribology Letters, 11*(2), 95–102.

Cayot, P., Schenker, F., Houzé, G., Sulmont-Rossé, C., & Colas, B. (2008). Creaminess in relation to consistency and particle size in stirred fat-free yogurt. *International Dairy Journal, 18*(3), 303–311.

Chen, J. (2015). Food oral processing: Mechanisms and implications of food oral destruction. *Trends in Food Science & Technology, 45*(2), 222–228.

Chen, J., & Engelen, L. (2012). Food oral processing: Fundamentals of eating and sensory perception. John Wiley & Sons: Ames, IA. 320 p.

Chen, J., & Stokes, J. R. (2012). Rheology and tribology: Two distinctive regimes of food texture sensation. *Trends in Food Science & Technology, 25*(1), 4–12.

Chojnicka-Paszun, A., De Jongh, H. H. J., & De Kruif, C. G. (2012). Sensory perception and lubrication properties of milk: Influence of fat content. *International Dairy Journal, 26*(1), 15–22.

de Wijk, R. A., & Prinz, J. F. (2005). The role of friction in perceived oral texture. *Food Quality and Preference, 16*(2), 121–129.

De Wijk, R., Prinz, J., & Janssen, A. (2006a). Explaining perceived oral texture of starch-based custard desserts from standard and novel instrumental tests. *Food Hydrocolloids, 20*(1), 24–34.

De Wijk, R., Terpstra, M., Janssen, A., & Prinz, J. (2006b). Perceived creaminess of semi-solid foods. *Trends in Food Science & Technology, 17*(8), 412–422.

Doublier, J.-L., Garnier, C., Renard, D., & Sanchez, C. (2000). Protein–polysaccharide interactions. *Current Opinion in Colloid & Interface Science, 5*(3–4), 202–214.

Dresselhuis, D., De Hoog, E., Stuart, M. C., & Van Aken, G. (2008). Application of oral tissue in tribological measurements in an emulsion perception context. *Food Hydrocolloids, 22*(2), 323–335.

Engelen, L., de Wijk, R. A., Prinz, J. F., Janssen, A. M., van der Bilt, A., Weenen, H., & Bosman, F. (2003). A comparison of the effects of added saliva, α-amylase and water on texture perception in semisolids. *Physiology & Behavior, 78*(4), 805–811.

Engelen, L., de Wijk, R. A., van der Bilt, A., Prinz, J. F., Janssen, A. M., & Bosman, F. (2005). Relating particles and texture perception. *Physiology & Behavior, 86*(1), 111–117.

Engelen, L., van den Keybus, P. A., de Wijk, R. A., Veerman, E. C., Amerongen, A. V. N., Bosman, F., Prinz, J. F., & van der Bilt, A. (2007). The effect of saliva composition on texture perception of semi-solids. *Archives of Oral Biology, 52*(6), 518–525.

Gibbins, H., & Carpenter, G. (2013). Alternative mechanisms of astringency–what is the role of saliva? *Journal of Texture Studies, 44*(5), 364–375.

Green, B. G. (1993). Oral astringency: A tactile component of flavor. *Acta Psychologica, 84*(1), 119–125.

Han, X., Yang, Z., Jing, X., Yu, P., Zhang, Y., Yi, H., & Zhang, L. (2016). Improvement of the texture of yogurt by use of exopolysaccharide producing lactic acid bacteria. *BioMed Research International, 2016*, 7945675.

Harwalkar, V., Cholette, H., McKellar, R., & Emmons, D. (1993). Relation between proteolysis and astringent off-flavor in milk1. *Journal of Dairy Science, 76*(9), 2521–2527.

Ibrahim, N. H., Man, Y. B. C., Tan, C. P., & Idris, N. A. (2010). Mixture design experiment on flow behaviour of O/W emulsions as affected by polysaccharide interactions. *World Academy of Science, Engineering and Technology, 67*, 1000–1006.

Isleten, M., & Karagul-Yuceer, Y. (2006). Effects of dried dairy ingredients on physical and sensory properties of nonfat yogurt. *Journal of Dairy Science, 89*(8), 2865–2872.

Janiaski, D., Pimentel, T., Cruz, A., & Prudencio, S. (2016). Strawberry-flavored yogurts and whey beverages: What is the sensory profile of the ideal product? *Journal of Dairy Science, 99*(7), 5273–5283.

Janssen, A. M., Terpstra, M. E., De Wijk, R. A., & Prinz, J. F. (2007). Relations between rheological properties, saliva-induced structure breakdown and sensory texture attributes of custards. *Journal of Texture Studies, 38*(1), 42–69.

Jöbstl, E., O'Connell, J., Fairclough, J. P. A., & Williamson, M. P. (2004). Molecular model for astringency produced by polyphenol/protein interactions. *Biomacromolecules, 5*(3), 942–949.

Joyner, H. S., Pernell, C. W., & Daubert, C. R. (2014). Impact of formulation and saliva on acid milk gel friction behavior. *Journal of food science, 79*(5), E867–E880.

Josephson, R., Thomas, E., Morr, C., & Coulter, S. (1967). Relation of heat-induced changes in protein-salt constituents to astringency in milk systems1. *Journal of Dairy Science, 50*(9), 1376–1383.

Krzeminski, A., Tomaschunas, M., Köhn, E., Busch-Stockfisch, M., Weiss, J., & Hinrichs, J. (2013). Relating creamy perception of whey protein enriched yogurt systems to instrumental data by means of multivariate data analysis. *Journal of Food Science, 78*(2), S314–S319.

Lee, W., & Lucey, J. (2010). Formation and physical properties of yogurt. *Asian-Australasian Journal of Animal Sciences, 23*(9), 1127–1136.

Lemieux, L., & Simard, R. (1994). Astringency, a textural defect in dairy products. *Le Lait, 74*(3), 217–240.

Malone, M., Appelqvist, I., & Norton, I. (2003). Oral behaviour of food hydrocolloids and emulsions. Part 1. Lubrication and deposition considerations. *Food Hydrocolloids, 17*(6), 763–773.

Materials, A. S. f. T. a. (2004). *ASTM E112–96 (2004) e2: Standard test methods for determining average grain size*. ASTM.

Morell, P., Hernando, I., Llorca, E., & Fiszman, S. (2015). Yogurts with an increased protein content and physically modified starch: Rheological, structural, oral digestion and sensory properties related to enhanced satiating capacity. *Food Research International, 70*, 64–73.

Morell, P., Chen, J., & Fiszman, S. (2016). The role of starch and saliva in tribology studies and the sensory perception of protein-added yogurts. *Food & Function, 8*, 545.

Ozcan, T. (2013). Determination of yogurt quality by using rheological and textural parameters. In *Proc. 2nd international conference on nutrition and food sciences*. IPCBEE.

Pascua, Y., Koç, H., & Foegeding, E. A. (2013). Food structure: Roles of mechanical properties and oral processing in determining sensory texture of soft materials. *Current Opinion in Colloid & Interface Science, 18*(4), 324–333.

Peng, X., & Yao, Y. (2017). Carbohydrates as fat replacers. *Annual Review of Food Science and Technology, 8*, 331–351.

Prinz, J., Huntjens, L., & de Wijk, R. (2006). Instrumental and sensory quantification of oral coatings retained after swallowing semi-solid foods. *Archives of Oral Biology, 51*(12), 1071–1079.

Puvanenthiran, A., Williams, R., & Augustin, M. (2002). Structure and visco-elastic properties of set yoghurt with altered casein to whey protein ratios. *International Dairy Journal, 12*(4), 383–391.

Roller, S. (1996). Starch-derived fat mimetics: Maltodextrins. In *Handbook of fat replacers* (p. 99). Boca Raton: CRC Press.

Saint-Eve, A., Kora, E. P., & Martin, N. (2004). Impact of the olfactory quality and chemical complexity of the flavouring agent on the texture of low fat stirred yogurts assessed by three different sensory methodologies. *Food Quality and Preference, 15*(7), 655–668.

Sano, H., Egashira, T., Kinekawa, Y., & Kitabatake, N. (2005). Astringency of bovine milk whey protein. *Journal of Dairy Science, 88*(7), 2312–2317.

Sonne, A., Busch-Stockfisch, M., Weiss, J., & Hinrichs, J. (2014). Improved mapping of in-mouth creaminess of semi-solid dairy products by combining rheology, particle size, and tribology data. *LWT- Food Science and Technology, 59*(1), 342–347.

Stokes, J. R., Boehm, M. W., & Baier, S. K. (2013). Oral processing, texture and mouthfeel: From rheology to tribology and beyond. *Current Opinion in Colloid & Interface Science, 18*(4), 349–359.

Thaiudom, S., & Goff, H. (2003). Effect of κ-carrageenan on milk protein polysaccharide mixtures. *International Dairy Journal, 13*(9), 763–771.

van de Velde, F., de Hoog, E. H., Oosterveld, A., & Tromp, R. H. (2015). Protein-polysaccharide interactions to alter texture. *Annual Review of Food Science and Technology, 6*, 371–388.

Walstra, P. (1996). Dispersed systems: Basic considerations. In *Food science and technology* (pp. 95–156). New York: Marcel Dekker.

Using Human Whole Saliva to Better Understand the Influences of Yogurt Rheological and Tribological Behaviors on Their Sensory Texture

Maryam Baniasadidehkordi and Helen S. Joyner

1 Introduction

Yogurt, a popular semisolid food in many countries, is produced by fermentation of milk using the lactic acid bacteria *Streptococcus salivarius* ssp. *thermophilus* and *Lactobacillus delbrueckii* ssp. *bulgaricus*. The demand for reduced- or non-fat yogurts has increased during recent years due to health concerns. However, reduction or removal of fat from yogurts can compromise their texture attributes, since fat plays a major role in creating a smooth, creamy texture in dairy products (De Wijk et al. 2006; Chojnicka-Paszun et al. 2012). Application of hydrocolloids has been an effective solution to improve the textural properties of reduced-fat yogurts. There are a wide range of hydrocolloids used in dairy products as fat replacers (Ognean et al. 2006; Peng and Yao 2017), including carboxymethyl cellulose (CMC), locust bean gum (LBG), and starch (Cho and Prosky 1999; Peng and Yao 2017). CMC is an anionic hydrocolloid that is used widely in dairy products as a fat replacer to enhance their textures (Cho and Prosky 1999). This gum is not only an effective stabilizer in dairy systems but also a dietary fiber with health benefits such as reduction of blood cholesterol and improvement of digestion and absorption (Cho and Prosky 1999). LBG is a galactomannan with a 1:4 ratio of galactose:mannose, and its mannan part is made soluble by side chains of single galactoses. LBG is a neutral (non-ionic) hydrocolloid that is stable at a pH range of 3.5–11 (Cho and Prosky 1999). Corn starch and potato starch with modified structures are usually used as fat mimetics in dairy products (Cho and Prosky 1999; Peng and Yao 2017).

When evaluating the use of hydrocolloids in dairy products, rheometry and tribometry are typically applied in conjunction with sensory analysis to evaluate the

---

M. Baniasadidehkordi · H. S. Joyner (✉)
School of Food Science, University of Idaho, Moscow, ID, USA
e-mail: hjoyner@uidaho.edu

H. S. Joyner (ed.), *Rheology of Semisolid Foods*, Food Engineering Series,
https://doi.org/10.1007/978-3-030-27134-3_12

impact of the hydrocolloids on food texture attributes (Janssen et al. 2007; Sonne et al. 2014; Morell et al. 2016). However, the specific hydrocolloid selected as a fat replacer in dairy products may affect texture not only through its functional properties, but also through hydrocolloid–saliva interactions. Thus, human whole saliva (HWS) has been incorporated during rheological and tribological measurements in multiple studies because of its important role in food texture perception (Guinard et al. 1997). During the initial stages of oral processing, rheological properties are the dominant influence on oral behaviors because they are related to the deformation and change in particle size of foods due to the mastication. After the food is mixed with HWS, broken into small pieces, and formed into a bolus (a mix of food and HWS) in the later stages of oral processing, food tribological behaviors become more important than rheological behaviors. The importance of food tribological behaviors continues with swallowing the food and sensing the remaining food residue on the tongue and palate (Stokes et al. 2013). Because different textural attributes may be perceived during different stages of oral processing, correlating rheological, tribological, and sensory behaviors along with incorporation of HWS during instrumental evaluation of food products can provide a more accurate indication of semisolid food texture attributes for targeted design of nutrient-dense foods that have textures as close as possible to their full-fat counterparts. Thus, the objective of this study was to determine the effects of HWS on the relationships among yogurt microstructures, functionalities, and textures.

2 Materials and Methods

2.1 Materials

Skim milk was purchased from a local supermarket (WinCo Foods, Moscow, ID, USA). Whey protein isolate (WPI) (Provon 190, 89.4% protein) was donated by Glanbia Nutritionals (Fitchburg, WI, USA). Low heat skim milk powder (SMP) and heavy cream (Darigold, 40% fat) were provided by the WSU Creamery (Pullman, WA, USA). Corn starch (CS) and modified potato starch (PS) were donated by Ingredion (Bridgewater, NJ, USA). Locust bean gum (LBG) and carboxymethyl cellulose (CMC) (pre-hydrated Ticalose CMC 2500 powder) were donated by TIC Gums (TIC Gums, Inc., Belcamp, MD, USA). Glucono-delta-lactone (GDL) was donated by Jungbunzlauer (Jungbunzlauer, Inc., MA, USA). The protein assay kit (Quick Start Bradford) used for measuring the protein concentration of HWS was obtained from Bio-Rad laboratories (Bio-Rad laboratories, Inc., CA, USA). Teflon balls (6 mm) for tribometry were purchased from McMaster-Carr (Atlanta, GA, USA). GluconoFluorescein Isothiocyanate (FITC) dye and cavity slides for confocal imaging were purchased from Sigma (Sigma-Aldrich, St. Louis, MO, USA), and Nile red dye was purchased from TCI America (Portland, OR, USA).

2.2 Yogurt Preparation

Twelve yogurts were prepared using skim milk (89.15–97.2% w/w), SMP (0–2.8% w/w), cream (0–3.5% w/w), WPI (0–2.8% w/w), and hydrocolloids, including corn starch (0–1% w/w), potato starch (0–0.7% w/w), LBG (0–1.8% w/w), and CMC (0–1% w/w) (Table 1). These yogurts were selected from 24 previously-studied formulations of acid milk gels based on their significant differences in rheological and tribological properties (Chaps. 10 and 11). Dry powders and cream were added to the skim milk at room temperature (22 ± 2 °C). To disperse the powders, the mixture was stirred with a spatula for 3 min in a water bath (Precision, Thermo Fisher Scientific, Waltham, MA, USA) at 85 °C. Samples were held at 85 °C for 30 min to both ensure pasteurization and complete hydrocolloid dissolution. Samples were then homogenized at 5000 rpm for 1 min using a stand homogenizer (Polytron, Kinematica AG, NY, USA). GDL (1.1–1.55% w/w, see Table 1) was added to samples after cooling to 42.2 °C on the benchtop. Samples were then incubated at 42.2 °C for 4–6 h to reach a pH of 4.55–4.6. The gel was broken with a metal laboratory spatula, then the samples were stored in a refrigerator at 4 °C overnight. Yogurts were blended at 350 rpm for 10 s before testing. Each sample was made in duplicate, and samples were tested the day after preparation.

2.3 Proximate Analyses

All proximate analyses were performed in duplicate. Protein contents were determined with a Leco FP-528 nitrogen analyzer (Leco Corp., St. Joseph, MI, USA) according to the manufacturer's instructions (Kjeldahl conversion factor = 6.38).

Table 1 Experimental design for yogurts

Formula number	SMP (w/w)	Sweet WPI (w/w)	LBG (w/w)	CMC (w/w)	Potato starch (w/w)	Corn starch (w/w)	Skim milk (w/w)	Cream (w/w)	Starter culture (w/w)
1	2.8	0	0	0	0	0	97.2	0	0.04
2	2.83	0	0	0	0	0	95.96	1.21	0.04
3	2.89	0	0	0	0	0	92.26	4.85	0.04
4	2.95	0	0	0	0	0	89.15	7.9	0.04
5	1.8	1	0	0	0	0	97.2	0	0.04
6	1.8	0	1	0	0	0	97.2	0	0.04
7	1.8	0	0	1	0	0	97.2	0	0.04
8	2.1	0	0	0	0.7	0	97.2	0	0.04
9	2.1	0	0	0	0	0.7	97.2	0	0.04
10	0	2.8	0	0	0	0	97.2	0	0.04
11	0	0	1.8	0	0	1	97.2	0	0.04
12	0.2	0.8	0.45	0.45	0.45	0.45	97.2	0	0.04

Fat contents were determined only for samples with added cream using Mojonnier method 989.05 (AOAC 1995a). Moisture contents were determined with a DKN 400 oven (Yamato Scientific America, Inc., Santa Clara, CA, USA), according to the method of the AOAC (1999). Ash contents were determined by using the method from AOAC (1995b) based on dry basis weight. Carbohydrate contents were determined by difference.

2.4 HWS Collection

HWS collection procedure were approved by the University of Idaho Institutional Review Board (protocol 17–196). HWS was collected from five healthy people (three females and two males, ages 20–35) with normal saliva flow according to the method of Bongaerts et al. (2007). Panelists were asked to refrain from eating and drinking anything except water for 2 h prior to collection. At the beginning of collection, they were required to rinse their mouth twice with deionized water and expectorate into a waste cup. They were then asked to chew on the bulb-shaped end of a disposable plastic pipette to stimulate saliva flow and expectorate into a 2 oz. cup. Fresh HWS was collected every 2 h and used for both rheological and tribological testing within 2 h of collection for testing.

2.5 Rheometry

Yogurt rheological behaviors were measured with an Anton Paar MCR 302 rheometer (Anton Paar, Graz, Austria) using a 50 mm diameter parallel plate with a gap height of 1 mm. All tests were carried out at 25 and 8 °C with and without addition of HWS (collected per Sect. 2.4). Samples were equilibrated at the testing temperature for 60 s prior to the test, and all samples were evaluated in triplicate. Shear rate sweeps (0.01–100 s^{-1}) were carried out to measure yogurt viscosity profiles. Oscillatory tests including strain sweeps (0.01–100%, 1 Hz) and frequency sweeps (0.1–100 rad s^{-1} and 0.75% strain) were performed to measure yogurt viscoelastic behaviors. Frequency sweeps were performed at 75% of the lowest critical strain to ensure samples remained in the linear viscoelastic region (LVR). Critical strain was calculated by determining the strain at which G^* deviated by >1% for this study.

2.6 PDMS Plate Production

Polydimethylsiloxane (PDMS) plates were manufactured for tribometry using the method reported by Bongaerts et al. (2007). A curing agent and a base (Dow Corning Corporation, Midland, MI, USA) were used to prepare the plates. The mixture was poured into an aluminum mold (4 mm height, 60 mm diameter). Air bubbles were removed by a cabinet vacuum desiccator (Bel-Art Products, Wayne, NJ, USA) under a pressure of −90 kPag. Vacuum was applied cyclically up to 10 times until all bubbles were removed. PDMS plates were cured in the mold at 55 °C for 2 h in a DKN 400 oven (Yamato Scientific America, Inc., Santa Clara, CA, USA), then stored overnight at room temperature (22 ± 2 °C) to complete curing. The plates were removed and stored at room temperature (22 ± 2 °C) until used for testing.

2.7 Tribometry

Tribometry was performed using an Anton Paar MCR 302 (Anton Paar, Graz., Austria) with a three-ball (Teflon, 6 mm diameter) geometry on a 60-mm diameter PDMS plate. The materials of the plate and balls were selected to mimic the oral surfaces (tongue–palate) (Johnson et al. 1993; Prakash et al. 2013). A 1 N normal force used was used to mimic the in-mouth force during swallowing, which is between 0.01 and 10 N (Miller and Watkin 1996). The PDMS plate was placed on top of the rheometer base plate and pressed firmly to adhere the two surfaces. A line was marked on both the PDMS plate and rheometer plate using an indelible laboratory pen to provide a visual indicator that the PDMS plate did not move during testing. Friction coefficient was measured at sliding speeds of 0.01–1000 mm s^{-1}. Samples were tested at 25 °C with and without addition of HWS. For samples tested with HWS, 0.5 mL of HWS was added to 3 g of sample and held at room temperature (22 ± 2 °C) for 5 min for complete digestion (Joyner (Melito) et al. 2014). At least three replicates for each sample duplicate were performed with and without HWS. The PDMS plate was cleaned after each run with 70% ethanol and laboratory wipes for non-fat samples; 70% ethyl ether was used for cleaning the surfaces after testing the samples with fat to prevent fat film buildup on the surface of PDMS plates and balls, followed by a rinse with 70% ethanol. Plates and balls were changed after every 6 runs to prevent wear of the tribo-surfaces from impacting the results.

2.8 Textural Evaluation of Yogurts

Sensory evaluation of yogurts was performed with the approval of the University of Idaho's IRB (protocol 17–195). Panelists (*n* = 10) were recruited from Washington State University (20 min away) and University of Idaho by email and social media. Participants (100% female; ages 25–55 years, mean age of 34 years) were trained for 11 h before evaluating all samples in two sessions. Total training and evaluation of samples was completed over 2 months. Textural attributes (*n* = 13) were introduced to the participants for describing the texture of the yogurts (Table 2); texture attributes and reference samples were selected from previous related studies (Saint-Eve et al. 2004; Pascua et al. 2013). During training, panelists profiled each yogurt

Table 2 Texture attributes and reference products used for sensory evaluation of yogurts (Saint-Eve et al. 2004; Pascua et al. 2013)

Attribute	Definition	Reference (scale 0–15)
Visual terms		
Lumpiness	Presence of lumps observed in yogurts after being stirred	Yoplait vanilla yogurt = 1 Jell-O tapioca pudding = 15
Spoon viscosity	Thickness of food after being stirred back and forth for 10 times	Water = 1 Jell-O pudding = 10.5
Mouthfeel terms		
Grainy	Feeling of small particles on the tongue after food is swallowed or expectorated	Reddi Wip whipped cream = 1 Gerber baby rice cereal = 12
Mouthcoating	Force required to clear sample adhered to the mouth/with the tongue during eating	Philadelphia cream cheese = 10 Reddi Wip whipped cream = 1
Mouth viscosity	Force needed to draw food from a spoon over the tongue	Water = 1 Jell-O chocolate pudding = 12
Firmness	Firmness of food in the mouth when food is compressed against the palate via tongue motions	Reddi Wip whipped cream = 1 Philadelphia cream cheese = 14
Lumpiness in-mouth	Feeling of lumps in the mouth during eating	Yoplait yogurt = 1 Jell-O tapioca pudding = 15
Smooth	Lack of individual food particles, opposite of grainy and lumpy attributes	Yoplait yogurt = 13 Gerber baby rice cereal = 15
Low-melting	Food does not spread out quickly in the mouth during eating	Reddi Wip whipped cream = 1 Jell-O chocolate pudding = 10
Grittiness	Feeling of gritty/chalky particles in the oral cavity during eating	WalMart non-fat Greek yogurt = 10 Reddi Wip whipped cream = 1
After-feel mouth terms		
Astringent	Astringent/dry sensation in the mouth after food is swallowed or expectorated	Atkins strawberry protein drink = 10 Reddi Wip whipped cream = 1
Chalky/Gritty after-feel	Feeling of chalk-like particles in the mouth after food is swallowed or expectorated	WalMart non-fat Greek yogurt = 10 Reddi Wip whipped cream = 1
Slimy	Difficulty of clearing the mouth from food in the mouth after food is swallowed or expectorated of clearing	Gerber banana baby food = 7 Reddi Wip whipped cream = 1

individually using a 15 cm line scale to indicate the intensity of each attribute present in the samples. Hard copies of descriptions of the 13 attributes along with a 15 cm line scale for each attribute were provided for each training session. Panelists were allowed to practice with the sensory data collection software (Compusense Cloud, Guelph, Ontario, Canada) for the last two training sessions to familiarize themselves with the software for the formal evaluations. Formal sensory evaluation of the 12 yogurt samples was performed in duplicate in separated sensory booths under white light. Samples were coded with 3-digit numbers and evaluated at 8 °C within 48 h of preparation. Six samples were evaluated in duplicate per session. 4 oz. plastic soufflé cups were used for serving the samples. Panelists were asked to rinse their mouths with filtered water, expectorate the samples after each evaluation, and cleanse their palates with unsalted crackers after evaluation of each sample to prevent fatigue. After evaluation of six samples, a 5 min break was required to minimize fatigue and errors. Attribute intensity was marked using a 15 cm line scale with anchors at 1.5 cm for low intensity and 13.5 cm for high intensity. Attribute data were collected from Compusense software for further analysis.

2.9 Confocal Imaging

Confocal laser scanning microscopy (CLSM) was used to image yogurt microstructures. GluconoFluorescein isothiocyanate (FITC) and Nile red dyes were applied to stain yogurt proteins and fat globules, respectively. 8 mg of FITC was added to 500 μL of ethanol in a 1 mL vial and vortexed for 10 s. 500 μL of deionized water was then applied to the FITC solution and vortexed for another 10 s. Nile red solution was prepared similarly, except 5 mg of Nile red was used. FITC and Nile red were used for samples with fat, but only FITC was used for the non-fat samples. Concentrations were adjusted for 120 g yogurt samples. Dyes were added to the yogurt mix before incubation. Samples were incubated, stirred, and stored as described in Sect. 3.2; microscopy analysis was done the next day. For testing, 500 μL of each sample was transferred to a cavity slide and covered with a glass coverslip. Samples were imaged at 20× and 4–8 °C. The wavelengths of Nile red and FITC were excited at 488 nm and 559 nm, respectively.

2.10 Data Analyses

Statistical analyses were performed using SAS version 9.1 (SAS, Cary, NC, USA) and XLSTAT (version 16.11; Addinsoft, Boston, MA, USA). Rheological and tribological graphs were plotted with Origin 8 software (OriginLab, Northampton, MA, USA). Error bars on graphs represent standard deviations of duplicate samples (6 data points total). Viscosity profiles were fitted to four models: Cross-Williams

(Eq. 1), Cross (Eq. 2), Herschel-Bulkley (Eq. 3), and power law (Eq. 4) using TRIOS software version 4.4.0 (TA Instruments; New Castle, DE, USA).

$$\eta = \frac{\eta_o}{\left[1+\left(c\dot{\gamma}\right)^{1-n}\right]} \tag{1}$$

$$\eta = \eta_\infty + \frac{\eta_o - \eta_\infty}{1+\left(k\dot{\gamma}\right)^{n}} k\dot{\gamma}^{n-1} \tag{2}$$

$$\sigma = \sigma_o + k\dot{\gamma}^{n} \tag{3}$$

$$\sigma = k\dot{\gamma}^{n-1} \tag{4}$$

In all equations, η is apparent viscosity (Pa.s) and $\dot{\gamma}$ is shear rate (s^{-1}). In Eq. (1), η_o is the zero-shear rate viscosity (Pa.s), c is the time constant (s), and n is the flow behavior index (unitless). In Eq. (2) η_o is the zero-shear rate viscosity (Pa.s), η_∞ is infinite shear rate viscosity (Pa.s), c is the time constant (s), and n is flow behavior index (unitless). In Eq. (3), σ_o is the yield stress (Pa), k is the consistency coefficient ($Pa.s^{1-n}$) and n is the flow behavior index (unitless). In Eq. (4), k is the consistency coefficient ($Pa.s^{1-n}$) and n (unitless) is the flow behavior index. Friction coefficients between 1 and 100 mm s^{-1} sliding speeds were selected for correlation analysis to mimic oral sliding speed (Malone et al. 2003). These values were used for correlation analysis between tribological–sensory and tribological–rheological results.

ANOVA was used to determine significant differences in sensory results considering three main variables (panelists, replicates, and samples), as well as significant differences among yogurt proximate analysis results and rheological and tribological parameters. Tukey's HSD (Honest Significant Difference) test was used for mean separations. Principal Component Analysis (PCA) was used to determine drivers behind variation of yogurt sensory attributes. Partial Least Square (PLS) analysis was performed to correlate rheological–tribological, rheological–sensory and tribological–sensory results.

3 Results and Discussion

3.1 Formulation Effects on Yogurt Proximate Composition

Significant differences were observed for yogurt protein contents (Table 3). Differences in protein content were attributed to the reduction of SMP for adjustment of other ingredients in the formulation. Sample 11 (added LBG and CS) had the lowest amount of protein, as expected since no SMP powder was added to this formulation. Sample 10 (high WPI level) had the highest protein concentration due to the use of WPI as the only hydrocolloid. There were also significant differences in moisture content among the samples. Yogurts with higher amounts of hydrocolloids may have retained more water in their microstructure and reduced the availability of the surface water for evaporation. The amount of carbohydrate increased by increasing CS, PS, CMC, and LBG, and decreased with addition of fat and protein, mainly WPI, which was expected. This effect was observed in samples 12 (all hydrocolloids added) and 9 (added CS), which had the highest carbohydrate content, and samples 4 (full-fat) and 10 (high WPI level), which had the lowest carbohydrate content. There were no significant differences in yogurt ash contents, which was not surprising considering the bulk of the minerals in yogurt are from the milk, not the texture-modifying ingredients.

3.2 *Formualtion and HWS Effects on Yogurt Microstructures*

Overall, CLSM results showed the conformation of protein network microstructure (green) was dependent on yogurt formulation, and the size of serum pores increased with addition of hydrocolloids (black areas in Figs. 1, 2, and 3). Pores size in samples with gums (samples 6, 7, and 12, Fig. 2d, g; 3g) were significantly bigger than those in the control sample (sample 1, Fig. 1a). LBG, used in sample 6, is a neutral hydrocolloid, so there would be minimal electrostatic interaction between LBG and caseins at the pI of casein (4.6, close to the pH of all samples, which was ~4.5), causing a weaker network. However, LBG can increase viscosity by increasing the continuous phase viscosity, which would likely result in the smaller, more weakly aggregated protein network in these samples (Perrechil et al. 2009).

Table 3 Yogurt proximate compositions[1]

Formula number	Protein (%)	Moisture (%)	Fat (%)	Ash (%)	Carbohydrate (%)[2]
1	5.61 ± 0.075^{bc}	85.12 ± 0.092^{abc}	0	0.78 ± 0.028^{a}	8.8^{abc}
2	5.36 ± 0.249^{dc}	83.54 ± 0.922^{c}	0.50 ± 0.022^{a}	0.65 ± 0.006^{a}	9.9^{ab}
3	4.64 ± 0.129^{efg}	86.00 ± 0.406^{a}	1.98 ± 0.008^{b}	0.70 ± 0.048^{a}	7.26^{de}
4	4.62 ± 0.006^{fg}	85.01 ± 0.496^{abc}	3.52 ± 0.142^{c}	0.62 ± 0.008^{a}	6.99^{e}
5	6.07 ± 0.094^{b}	85.86 ± 0.132^{abc}	0	0.79 ± 0.017^{a}	7.90^{dc}
6	4.65 ± 0.015^{efg}	86.61 ± 0.207^{a}	0	0.69 ± 0.003^{a}	8.77^{bc}
7	4.56 ± 0.075^{fg}	85.21 ± 0.084^{abc}	0	0.74 ± 0.09^{a}	9.73^{ab}
8	5.04 ± 0.053^{de}	85.68 ± 0.394^{ab}	0	0.70 ± 0.024^{a}	9.1^{abc}
9	4.82 ± 0.035^{efg}	85.06 ± 0.612^{bc}	0	0.76 ± 0.069^{a}	9.45^{a}
10	6.79 ± 0.153^{a}	86.07 ± 0.363^{abc}	0	0.73 ± 0.088^{a}	7.06^{de}
11	4.48 ± 0.034^{g}	86.62 ± 0.061^{a}	0	0.67 ± 0.082^{a}	8.83^{abc}
12	4.96 ± 0.024^{def}	84.43 ± 0.162^{bc}	0	0.65 ± 0.025^{a}	10.03^{a}

[1] Different letters in a given column indicate significant differences at $p \leq 0.05$

[2] Carbohydrates were calculated by difference

The greater amount of serum observed in the microscopy images for sample 6 (added LBG, Fig. 2d) was in line with its higher moisture content (Table 3). Also, the moisture content of the sample containing all hydrocolloids (sample 12) was significantly lower than that of samples 6 (added LBG) and 7 (added CMC, Fig. 2g), which may be related to differences in their pores sizes. The protein network in the sample with added CMC (sample 7) was shown to be thicker and more compact than that of the sample with added LBG (sample 6). This was attributed to casein–CMC interactions, which occurred due to the opposite charges on CMC and milk proteins at yogurt pH and resulted in a stronger protein network. The denser protein matrix of sample 5 (Fig. 2a) compared to the control sample (sample 1) was attributed to higher protein content (Table 3). Addition of WPI can increase the level of casein–casein and casein–whey interactions and result in greater cross-linking and a denser microstructure with more protein chains. Addition of fat in samples 2 and

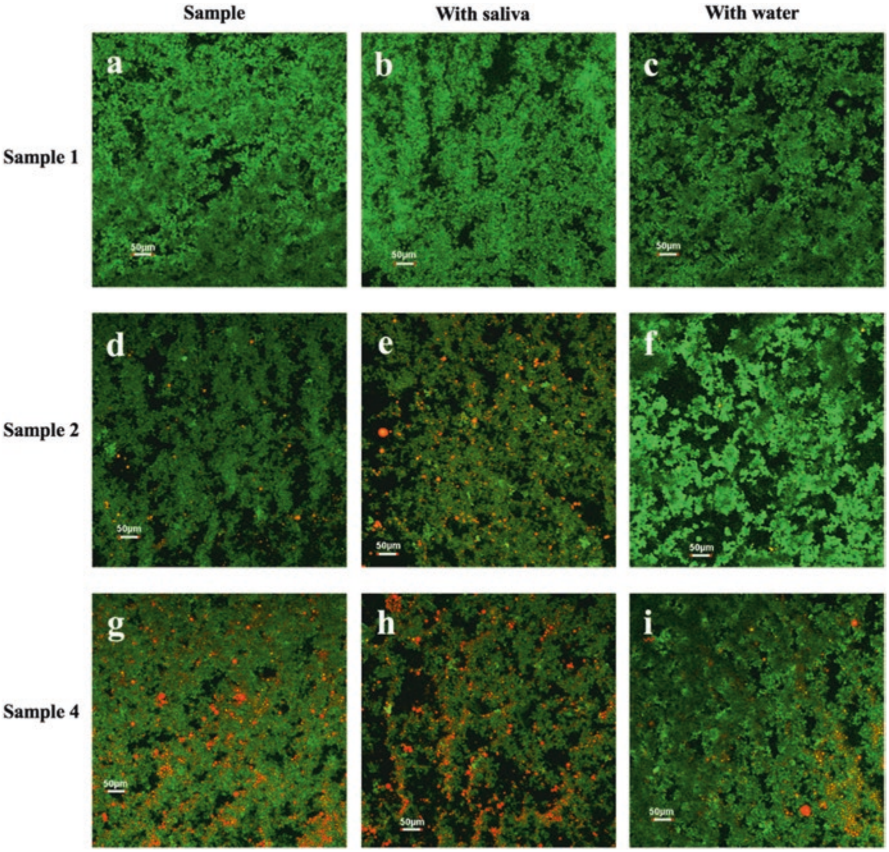

Fig. 1 CLSM results of yogurts; (**a**) sample 1; (**b**) sample 1 with HWS; (**c**) sample 1 with water; (**d**) sample 2; (**e**) sample 2 with HWS; (**f**) sample 2 with water; (**g**) sample 4; (**h**) sample 4 with HWS; (**i**) sample 4 with water. The protein network, fat globules, and serum pores are shown in green, red, and black, respectively

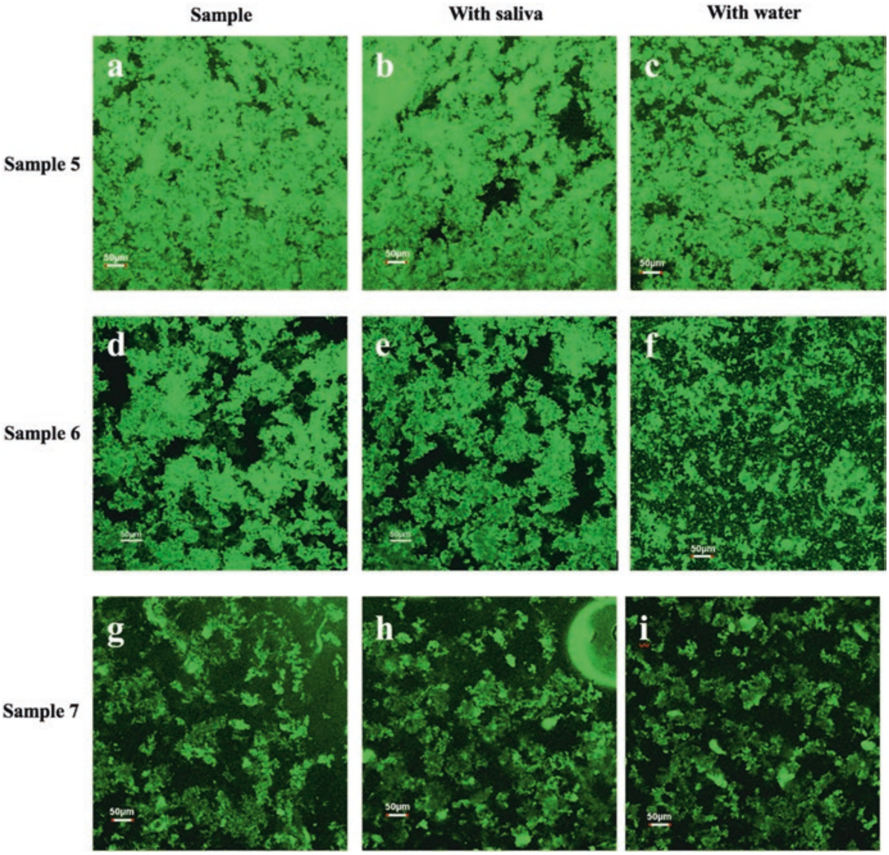

Fig. 2 CLSM results of yogurts; (**a**) sample 5; (**b**) sample 5 with HWS; (**c**) sample 5 with water; (**d**) sample 6; (**e**) sample 6 with HWS; (**f**) sample 6 with water; (**g**) sample 7; (**h**) sample 7 with HWS; (**i**) sample 7 with water. The protein network and serum pores are shown in green and black, respectively

4 caused a denser protein microstructure compared to the control sample (sample 1). This result was in agreement with other studies of microstructural features of yogurts produced by homogenized milk (Serra et al. 2007).

In general, addition of HWS caused greater protein aggregation regardless of formulation. This effect was most clearly illustrated for the control sample (sample 1, Fig. 1b), and samples with added PS (sample 8, Fig. 3b) and CS (sample 9, Fig. 3e) when HWS was added. The greater effect of HWS on the starch-containing samples was likely because amylase breaks down amylose in starch to smaller sugars (Janssen et al. 2007). This would cause disruption of the starch embedded in the casein network and result in a larger serum phase. In addition, HWS caused fat coalescence in samples 2 and 4 (Fig. 1e, h). This observation was attributed to depletion flocculation created by the osmotic pressure from salivary proteins

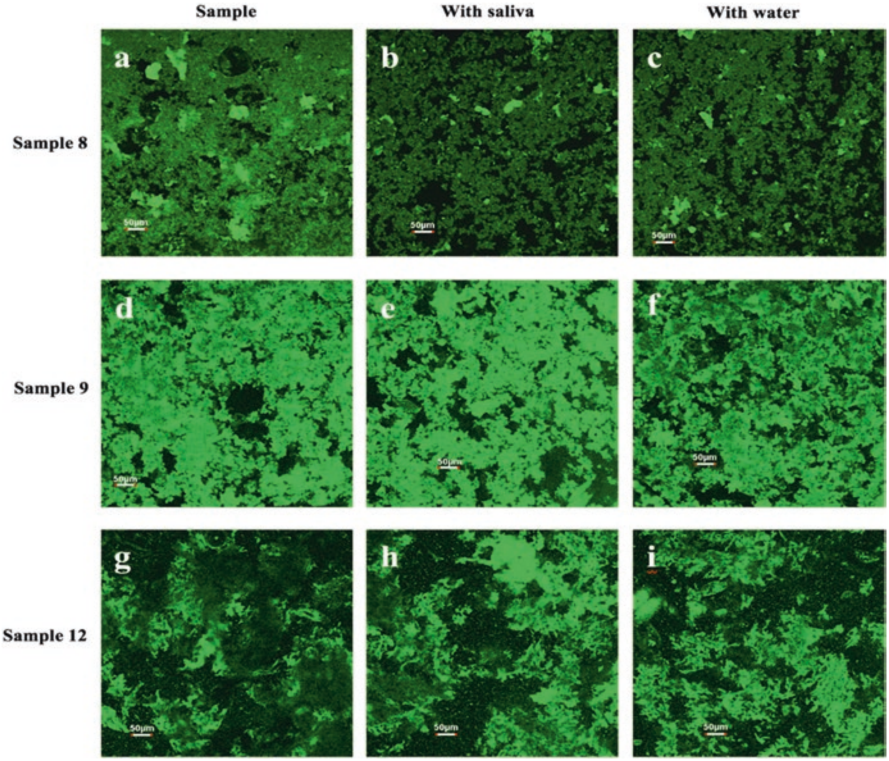

Fig. 3 CLSM results of yogurts; (**a**) sample 8; (**b**) sample 8 with HWS; (**c**) sample 8 with water; (**d**) sample 9; (**e**) sample 9 with HWS; (**f**) sample 9 with water; (**g**) sample 12; (**h**) sample 12 with HWS; (**i**) sample 12 with water. The protein network and serum pores are shown in green and black, respectively

Table 4 Main sources of variation of flow properties of yogurts (n = 12) determined by F-values obtained from three-way ANOVA[a]

Source of variation	η_o (Pa.s)	n	k (Pa.s^{1-n})
Formulations	16.4***	1.2	1.8
HWS	12.5***	1.3	0.4
Temperature	9.7***	1	1.2
HWS × temperature	1.9	1	0.1
Formulation × HWS	6.1**	1	1.2
Formulation × temperature	4.8**	1	0.8

[a] *, **, and *** indicate significant differences at $p \leq 0.05$, $p \leq 0.01$, and $p \leq 0.001$, respectively

(Chen 2015). However, the effect of HWS was not notable on the microstructures of samples prepared with gums (samples 6, 7, and 12, Fig. 2e, h, Fig. 3h), indicating that saliva had little interaction with the gums, as expected.

Overall, addition of HWS had different effects on yogurt microstructures, particularly the protein network, than the effects from the addition of water. Addition of water to the samples notably increased the porosity in all yogurts due to the dilution effect of water and its integration into the serum pores. The dilution effect of water was shown most clearly for the sample containing LBG (sample 6, Fig. 2f). This results was attributed to the weaker microstructure of LBG in the continuous phase due to disrupted weak interactions, e.g. hydrogen and non-covalent bonds, upon addition of water (Murray and Phisarnchananan 2014) compared to the samples with stronger interactions, such as covalent bonds and hydrophobic interactions with casein micelles.

3.3 Formulation and HWS Effects on Yogurt Rheological Behaviors

3.3.1 Yogurt Viscosity Behaviors

Three-way ANOVA was used to determine the effects of formulation (hydrocolloids), HWS, and temperature on the flow parameters from non-Newtonian models of yogurts including η_0, n, and c (Table 4). For η_0, formulation, HWS, and temperature showed significant effects at $p \leq 0.001$, as well as significant effects at $p \leq 0.01$ for the interaction of formulation with each of the other two parameters. Interaction of HWS with temperature for η_0 was not significant. Surprisingly, no significant effects were observed for n or k for any combination of parameters. These results might have been caused by the dominant role of η_0 in the non-Newtonian viscosity models compared to n or k (see subsequent discussion).

The significant impact of hydrocolloids can be mainly explained by (1) the electrostatic interactions between counterions of anionic hydrocolloids with casein micelles, (2) swelling of starch granules in the presence of water and heat in the yogurt system, and (3) dispersion of large, neutral hydrocolloid particles in the continuous phase and their depletion flocculation effects. These factors can also significantly change the microstructure of protein network and overall conformation of yogurts (Figs. 1, 2, and 3). The significant effects from HWS were attributed to the digestive, dissolving, and coalescence properties of HWS resulting mostly from the enzymes, salivary proteins, and electrolytes present in HWS. Temperature can weaken the intermolecular bonds in a semisolid food system, decrease resistance to flow, and lower the viscosity (Berk 2018). Based on these results, the importance of hydrocolloids, HWS, and temperature on yogurt flow properties as a model system for semisolid foods can be helpful in designing semisolid foods with specific rheological properties.

All yogurts showed shear-thinning behavior (Tables 5, 6, 7, and 8). Shear-thinning behavior in a yogurt system is typically due to alignment of entangled protein molecules with the shear field. The viscosity curves of all samples were fit to Cross-Williams, ($R^2 > 0.935$) Cross ($R^2 > 0.748$), Herschel-Bulkley ($R^2 > 0.74$), and power law ($R^2 > 0.985$) models. The best-fit model varied by formulation. Formulations with added fat tended to fit best to the Cross model, while formulations incorporating hydrocolloids tended to fit better to the Herschel-Bulkley and Cross-Williams models. While all the models used for fitting are suitable for shear-thinning materials, there are a few key differences among them. The main difference between the Cross model and the Cross-Williams model is the presence of η_∞ (Pa s) in the Cross model; η_∞ is indicative of shear-independent flow behavior under high-shear conditions. The primary difference between the power law and Herschel-Bulkley models is the yield stress in the Herschel-Bulkley model. The differences in best-fit model results were likely due to the more complex microstructures in samples containing hydrocolloids. The presence of hydrocolloids can result in a yield stress and persistent shear-thinning behavior even at very high shear rates due to polymer entanglements that break down with increasing shear. Without these entanglements, such as in samples 2, 3, and 4 (fat-containing samples with no added gums or starches), there is less structure to break down under shear, resulting in little to no yield stress and a viscosity plateau at higher shear rates.

Generally, η_0, η_∞, n, and σ_o decreased with increasing temperature and addition of HWS. Addition of hydrocolloids increased the viscosity, except for the sample with LBG (sample 6). This sample was also the only one fitted to a power law model, which is mostly applicable to weak gels, although the protein microstructure was shown to be highly entangled (Fig. 2) compared to the control sample (sample 1, Fig. 1). These entanglements have been observed previously (Murray and Phisarnchananan 2014). LBG is a neutral hydrocolloid that increases the viscosity of the system by increasing the continuous phase, not through interactions with protein network (Hansen 1993). Another mechanism for the viscosity increase

Table 5 Viscosity profiles for yogurts ($n = 12$) at 8 °C without added HWS

Formula	Model	η_o (Pa.s)	η_∞ (Pa.s)	n	c (s)	k (Pa.s^{1-n})	σ_0 (Pa)	R^2
1	Herschel-Bulkley	–	–	0.955	–	0.177	14.9	0.740
2	Cross	2190	0.212	0.935	31.2	–	–	0.891
3	Cross	693	0.222	0.930	19.8	–	–	0.895
4	Cross	627	0.214	0.926	19.7	–	–	0.919
5	Cross	532	0.020	0.966	65.5	–	–	0.820
6	Power law	56.1	–	0.286	–	–	–	0.985
7	Cross-Williamson	1358	–	0.928	13.0	–	–	0.935
8	Herschel-Bulkley	–	–	0.902	–	0.157	26.0	0.806
9	Herschel-Bulkley	–	–	0.772	–	0.682	19.5	0.856
10	Cross	13,476	0.02	0.971	19.5	–	–	0.748
11	Cross-Williamson	370	–	0.697	8.80	–	–	0.999
12	Cross-Williamson	416	–	0.834	10.33	–	–	1.000

Table 6 Viscosity profiles for yogurts (n = 12) at 8 °C with added HWS

Formula	Model	η_o (Pa.s)	η_∞ (Pa.s)	n	c (s)	k (Pa.s^{1-n})	σ_0 (Pa)	R^2
1	Cross-Williamson	254	–	0.891512	64	–	–	0.999
2	Cross	637	0.101	0.914	25.5	–	–	0.938
3	Cross	418	0.122	0.908	28.2	–	–	0.965
4	Cross	531	0.174	0.911	37.8	–	–	0.922
5	Cross	461	0.010	0.949	52.1	–	–	0.917
6	Power law	29.3	–	0.324	–	–	–	0.992
7	Cross-Williamson	232	–	0.805	11.3	–	–	1.000
8	Herschel-Bulkley	–	–	0.746	–	0.176	6.61	0.975
9	Herschel-Bulkley	–	–	0.387	–	3.05	5.71	0.962
10	Cross	3976	0.09	0.961	34.5	–	–	0.961
11	Cross-Williamson	184	–	0.699	5.13	–	–	0.999
12	Cross-Williamson	141	–	0.755	11.3	–	–	1.000

Table 7 Viscosity profiles for yogurts (n = 12) at 25 °C without added HWS

Formula	Model	η_o (Pa.s)	η_∞ (Pa.s)	n	c (s)	k (Pa.s^{1-n})	σ_0 (Pa)	R^2
1	Herschel-Bulkley	–	–	0.856	–	0.199	7.39	0.871
2	Cross	1177	0.054	0.928	19.9	–	–	0.881
3	Cross	364	0.109	0.920	22.6	–	–	0.924
4	Cross	344	0.086	11.6	0.916	–	–	0.948
5	Cross	471	0.013	0.957	55.8	–	–	0.952
6	Power law	29.5	–	0.358	–	–	–	0.993
7	Cross-Williamson	454	–	0.825	12.6	–	–	0.998
8	Herschel-Bulkley	–	–	0.776	–	0.289	15.3	0.924
9	Herschel-Bulkley	–	–	0.841	–	0.322	11.0	0.880
10	Cross	4712	0.01	0.957	79.691	–	–	0.970
11	Cross-Williamson	223	–	0.649	7.49	–	–	0.999
12	Cross-Williamson	219	–	0.776	10.6	–	–	1.000

observed for neutral hydrocolloids is depletion flocculation. The large LBG molecules would create an increased osmotic pressure between the casein micelles, which would push the caseins together and cause flocculation (Thaiudom and Goff 2003). Samples with LBG (sample 6) and LBG and CS (sample 11) also showed the least decrease in their viscosity upon addition of HWS, which was expected based on the confocal images (Fig. 2). Similar results were shown with LBG solutions and HWS (Zinoviadou et al. 2008).

The viscosity of sample 11 slightly increased compared to the control due to inclusion of LBG and CS, which was expected because addition of CS and LBG together in a system can make a stronger gel than when LBG is used individually (Murray and Phisarnchananan 2014). The viscosity of sample 7 increased notably from the control due to addition of CMC. CMC is an anionic gum that interacts with

Table 12.8 Viscosity profiles for yogurts ($n = 12$) at 25 °C with added HWS

Formula	Model	η_o (Pa.s)	η_∞ (Pa.s)	n	c (s)	k (Pa.s^{1-n})	σ_0 (Pa)	R^2
1	Cross-Williamson	84.4	–	1	19.2	–	–	0.999
2	Cross	305	0.047	0.910	23.7	–	–	0.964
3	Cross	226	0.061	0.907	26.5	–	–	0.975
4	Cross	345	0.083	0.909	33.2	–	–	0.943
5	Cross-Williamson	214	–	0.946	33.1	–	–	0.900
6	Power law	15.5	–	0.391	–	–	–	0.996
7	Cross-Williamson	106	–	0.755	10.6	–	–	1.000
8	Herschel-Bulkley	–	–	0.601	–	0.272	4.89	0.954
9	Herschel-Bulkley	–	–	0.532	–	0.830	3.69	0.961
10	Cross	648	0.01	0.908	11.5	–	–	0.760
11	Cross-Williamson	106	–	0.624	6.96	–	–	0.999
12	Cross-Williamson	79.9	–	0.693	13.7	–	–	1.000

positively charged casein micelles through aggregative phase separation to create a strong matrix (van de Velde et al. 2015). The yield stress of sample 8, which contained PS, was higher than that of sample 9, which contained CS. PS can increase viscosity due to the large size of its swollen starch granules in the dispersed phase. CS is a neutral polysaccharide that can increase viscosity through weak interactions in the continuous phase (Dang et al. 2009). The network formed by CS and milk protein is not as strong as the PS–milk protein network; hence, the force (σ_o) that was needed for sample 8 (added PS) to flow was greater than that for sample 9 (added CS) due to the increased size of the starch granules.

Sample 10, which incorporated WPI, had the highest viscosity of all samples, likely because of its high protein content (Table 2). Denaturation of whey proteins occurs due to heat treatment above 70 °C. High concentration of denatured whey proteins results not only in increased interactions with casein micelles but also in interactions among non-associated whey proteins. These interactions yield a stronger protein gel network with more cross-linking and a more aggregate microstructure (Lucey and Singh 1997). Sample 5, which also contained WPI but at a lower concentration, showed similar results, although its viscosity was lower than sample 10 likely due to its lower protein content (Table 2). Interestingly, the viscosity of sample 12 was not similar to that of the other samples even though it contained all hydrocolloids. This result was attributed to the conflicting contributions of hydrocolloids in this sample.

Addition of fat notably increased viscosity (samples 2, 3, and 4), likely due to the embedded fat globules throughout the protein matrix creating a resistance to flow (Chojnicka-Paszun et al. 2012; Nguyen et al. 2017). Full-fat yogurt (sample 4) showed higher viscosity than samples 2 and 3, supporting this hypothesis.

Yogurt viscosity and n values decreased with addition of HWS and increased temperature (Tables 5, 6, 7, and 8). Samples evaluated with added HWS at 25 °C showed the lowest viscosity (Table 8), which was expected. Increasing temperature weakens the intermolecular bonds in a yogurt system, decreasing resistance to flow and lowering the viscosity (Berk 2018). The effect of HWS varied based on the type(s) of hydrocolloids used in the formulations. Salivary proteins, enzymes, and other HWS components can disrupt semisolid food microstructures (Janssen et al. 2007). For example, HWS has been shown to cause protein flocculation when mixed with yogurt (Vingerhoeds et al. 2009; Sarkar and Singh 2012). These effects can be observed in the microstructural images (Figs. 1, 2, and 3). Samples containing PS (sample 8) and CS (sample 9) showed the greatest decrease in yield stress upon addition of HWS. Similar results were reported for starch-based custards (Janssen et al. 2007). Amylase in the HWS would break down the amylose in the starches into simple sugars like maltose and glucose (Humphrey and Williamson 2001). Although this effect was not clearly observed in the confocal images of sample 8 (added PS) in this study, the digestion of PS by amylase was visually shown by another study (Janssen et al. 2007).

3.3.2 Yogurt Viscoelastic Behaviors

The effects of formulation (hydrocolloids), HWS, and temperature on yogurt viscoelastic properties, including critical strain (γ_c, %), G^* (complex modulus at γ_c, Pa), and tan δ (phase angle at γ_c, rad), were determined using F-values from three-way ANOVA (Table 9). Formulation and temperature showed significant effects at $p \leq 0.001$ for tan δ and γ_c.; HWS also showed significant effects on tan δ ($p < 0.001$) and γ_c ($p < 0.01$). Additionally, significance at $p < 0.01$ was observed for the interaction of formulation with temperature on tan δ and γ_c. HWS was the only parameter that had a significant effect on G^* ($p \leq 0.05$). However, temperature was borderline for significance ($p \leq 0.07$). This finding might explain the significant differences of G^* values from Tukey's HSD with different temperatures (Table 10). The significant changes in G^* may have been due to the increased stability and resistance to permanent deformation observed in yogurts with added hydrocolloids compared to the control sample. For example, starches (PS and CS) and gums (CMC and LBG) can improve gel stability by increasing the number of internal molecular interactions as well as by creating stronger bonds through different mechanisms. HWS effects were also likely due to structural changes upon its addition. As previously

Table 9 F-values for sources of variation of viscoelastic properties of yogurts ($n = 12$) obtained from three-way ANOVA[a]

Source of variation	γ_c	G^*	tan δ
Formulations	45^{***}	2.5	418^{***}
HWS	10.8^{**}	4.6^{*}	121^{***}
Temperature	75.1^{***}	4	72.4^{***}
HWS × temperature	1.5	1.8	0.4
Formulation × HWS	2.3	1.2	38.7^{***}
Formulation × temperature	5.1^{**}	1.2	4.4^{**}

[1] $\gamma_{c:}$ critical strain, G^*: complex modulus at γ_c, tan δ: phase angle at γ_c

[a] *, **, and *** indicate significant differences at $p \leq 0.05$, $p \leq 0.01$, and $p \leq 0.001$, respectively

Table 10 Viscoelastic parameters of 12 yogurts measured by strain sweep at 1 Hz[1]

	γ_c (%)	γ_c (%)	γ_c (%)	γ_c (%)	G^* (Pa)	G^* (Pa)	G^* (Pa)	G^* (Pa)	tan δ (rad)	tan δ (rad)	tan δ (rad)	tan δ (rad)
	8 °C	8 °C	25 °C	25 °C	8 °C	8 °C	25 °C	25 °C	8 °C	8 °C	25 °C	25 °C
Formula number	NS	S	NS	S	NS	S	NS	S	NS	S	NS	S
1	1.74^{a}	1.30^{a}	3.12^{a}	2.33^{a}	66.2^{e}	43.6^{h}	56.4^{e}	33.2^{f}	0.313^{cd}	0.345^{e}	0.3475^{c}	0.355^{d}
2	0.731^{d}	0.976^{b}	1.74^{b}	1.30^{b}	448^{b}	249^{c}	178^{c}	171^{c}	0.298^{cde}	0.317^{fg}	0.336^{cd}	0.334^{g}
3	0.411^{f}	0.547^{e}	0.731^{e}	0.730^{e}	230^{d}	103^{gf}	133^{d}	63.8^{e}	0.296^{cdef}	0.320^{f}	0.320^{de}	0.336^{fg}
4	0.731^{d}	0.411^{f}	0.547^{f}	0.730^{e}	323^{bcd}	133^{e}	168^{c}	67.1^{e}	0.314^{cd}	0.329^{ef}	0.327^{cd}	0.349^{ef}
5	0.548^{e}	0.731^{c}	0.976^{d}	0.976^{c}	415^{b}	278^{b}	245^{b}	205^{b}	0.319^{c}	0.333^{ef}	0.341^{cd}	0.332^{g}
6	0.548^{e}	0.411^{f}	0.547^{f}	0.411^{g}	380^{bc}	206^{d}	187^{c}	102^{d}	0.571^{a}	0.591^{b}	0.665^{a}	0.639^{b}
7	1.30^{b}	0.976^{b}	1.74^{b}	1.30^{b}	257^{cd}	125^{ef}	128^{d}	63.1^{e}	0.502^{b}	0.555^{c}	0.588^{b}	0.626^{bc}
8	0.548^{e}	0.411^{f}	0.976^{d}	0.547^{f}	360^{bcd}	90.0^{g}	231^{b}	39.1^{f}	0.287^{def}	0.340^{e}	0.295^{f}	0.352^{e}
9	0.411^{f}	0.411^{f}	0.411^{g}	0.547^{f}	253^{cd}	122^{ef}	134^{d}	65.8^{e}	0.280^{ef}	0.300^{g}	0.287^{f}	0.3137^{h}
10	0.547^{e}	0.548^{d}	0.976^{d}	0.976^{c}	3410^{a}	516^{a}	499^{a}	329^{a}	0.268^{f}	0.300^{g}	0.298^{ef}	0.301^{h}
11	0.961^{c}	0.731^{c}	1.29^{c}	0.975^{d}	327^{bcd}	198^{d}	245^{b}	115^{d}	0.553^{a}	0.861^{a}	0.595^{b}	0.984^{a}
12	0.411^{f}	0.411^{f}	0.731^{e}	0.730^{e}	347^{bcd}	136^{e}	184^{c}	67.3^{e}	0.502^{b}	0.532^{d}	0.595^{b}	0.621^{c}

[1] $\gamma_{c:}$ critical strain, G^*: complex modulus at γ_c, tan δ: phase angle at γ_c
Letters in each column that are different indicate significant differences

discussed, HWS can disrupt semisolid food microstructures through digestion, osmotic pressure, dilution, or net charge alteration. Similarly, increasing temperature allows internal molecules to move more easily and quickly from the additional heat energy, which can decrease molecular bond strength. As a result, the yogurts can lose their original microstructures and become more susceptible to external shear when mechanical force is applied.

Overall, there were significant differences in γ_c, G^*, and tan δ among the 12 yogurt formulations (Table 10). γ_c increased or remained constant with increasing temperature except for sample 4 (full-fat yogurt). The decrease in γ_c value for sample 4 was unexpected but may have been due to increased thermal energy of the oil-in-water emulsion in sample 4 at increased temperature, which would decrease the viscosity of the fat globules, resulting in fat coalescence. The molecules would then deform more easily when shear stress is applied, yielding a smaller γ_c. The increasing γ_c values for the other samples can be explained by thermodynamics. At higher temperatures, molecular mobility increases, resulting in more fluid-like behavior and requiring a greater force to induce nonlinear behavior. Fluids are less likely to show nonlinear viscoelastic behavior at lower strains because nonlinear viscoelastic behavior indicates irreversible structural changes. Since fluids tend to have less complex microstructures, it is more difficult to induce irreversible change to that structure. γ_c values of fat-containing samples (samples 2, 3, and 4) increased with addition of HWS. This could be due to fat flocculation resulting from the osmotic pressure of salivary proteins throughout the sample (Huc et al. 2016), decreasing structural complexity and resulting in more resistance to permanent deformation from applied strain.

HWS had a different impact on critical strain values compared to that of temperature. γ_c decreased for most samples with added hydrocolloids. This result may have been due to the destabilization of the original protein microstructure after incorporation of HWS. HWS has the largest effect on the sample with PS (sample 8) compared to the other yogurt samples. This result was attributed to enzymatic breakdown of the starch granules by the amylase in HWS. However, the changes in the microstructure of semisolid food upon addition of HWS can also be explained by other mechanisms, e.g. depletion flocculation. The non-adsorbing molecules in HWS can create an osmotic pressure that forces the aggregation of the emulsion droplets and results in microstructural disruption (Chen 2015).

Overall, G^* decreased with increasing temperature and HWS addition to the samples. G^* values of samples with added PS (sample 8) drastically decreased with the addition of HWS, but this effect was not shown for samples with CS (sample 9). This result was probably due to the high degree of PS–salivary amylase interactions. A similar effect for samples 8 and 9 was also seen in the shear rate sweep results (Sect. 3.3.1). This result can be explained by the higher amount of amylose in CS (Singh et al. 2003). PS has more highly branched amylopectin and lower amylose content compared to large proportion of linear amylose in CS. Saliva can more easily pass through large, open starch granules than highly compacted microstructures (Bird et al. 2000). As a result, amylose is more difficult to digest compared to highly branched amylopectin since the linear amyloses can pack tightly because of their shape. This results in less accessible area on high-amylose starch granules for digestion. Additionally, the compact microstructure of CS results in an increase in gelatinization temperature; when gelatinized, a high proportion of amylose in the starch granules promotes rapid retrogradation (Bird et al. 2000; Singh et al. 2003). Retrogradation is the molecular interaction of starch chains via hydrogen bonds when a gelatinized starch paste is cooled (Hoover 2001). This phenomenon results in the formation of small, insoluble amylose crystallites that move to the available spaces between the amylopectin branches and increase resistance to enzymatic digestion (Bird et al. 2000).

tan δ values increased with added HWS and increased temperature, indicating increased viscous-type behavior. Sample 10, containing WPI, showed the lowest tan δ values, and samples containing LBG (samples 6 and 11) had the highest. Sample 11 (added LBG and CS) showed tan $\delta = 0.99$, indicating approximately equal viscous and elastic moduli with added HWS at 25 °C. Addition of CS, PS, or high levels of WPI (samples 9, 8, and 10, respectively) resulted in smaller tan δ values compared to those of the samples containing fat (samples 2, 3, and 4). As expected, the addition of HWS resulted in greater tan δ values for starch-containing samples (samples 8 and 9) due to starch breakdown by salivary α-amylase. tan δ values for the sample with CMC (sample 7) and the sample with all hydrocolloids (sample 12) were similar. These results may have been indicative of the similar matrix conformation of these two samples, which can be observed in the confocal images of these two samples (Figs. 2 and 3).

Frequency sweep results (Fig. 4) showed that formulation had a notable impact on frequency-dependent behavior. Samples with high levels of WPI (sample 10), full-fat samples (sample 4), and added PS (sample 8) had low dependence of frequency as indicated by the small slope of the viscoelastic moduli. These results were attributed to the presence of covalent bonds in the protein matrix for this sample (Laverse et al. 2011). G' values for samples with LBG (sample 6) and LBG and CS (sample 11) showed high frequency dependence. These samples were weak gels with non-covalent linkages such as hydrogen bonds rather than electrostatic bonds (Laverse et al. 2011; Tang and Liu 2013). The weak molecular structure in samples 6 and 11 can be easily disrupted as the frequency increased from 0.1 to 100 rad s^{-1}. This resulted in an increased slope compared to samples 4, 8, and 10. Another notable difference among formulations was the gap between G' and G''. Samples 4, 8, and 10 had a greater gap between the two moduli, indicating a stronger microstructure compared to samples with a smaller gap between G' and G'', such as samples 6 and 11. The weaker microstructure in samples 6 and 11 was likely caused by destabilization of protein network caused by dispersion of neutral LBG molecules in the continuous phase and depletion flocculation resulting from the altered osmotic pressure within the protein network. Furthermore, it has been shown that a combination of LBG and milk proteins can result in a weak gel due to the thermodynamic incompatibility of LBG (Thaiudom and Goff 2003).

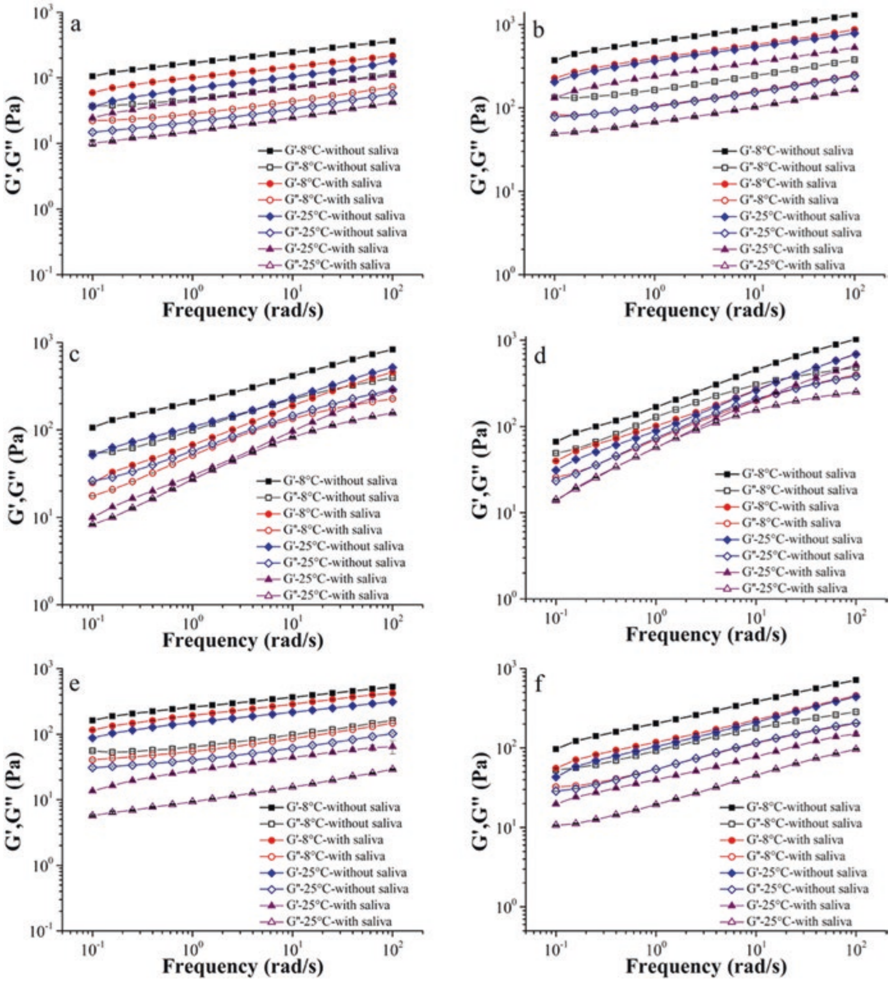

Fig. 4 Frequency sweep results of yogurts; (**a**) sample 4; (**b**) sample 10; (**c**) sample 6; (**d**) sample 11; (**e**) sample 8; (**f**) sample 12

3.4 Effect of Formulation and HWS on Yogurt Friction Profiles

Three-way ANOVA was performed to determine the impact of formulation (hydrocolloids), HWS, and different rates of sliding speeds on yogurt friction coefficients (Table 11). A range of sliding speeds between 10 and 100 mm s^{-1} were selected to mimic oral sliding speeds experienced during consumption of yogurts and other semisolid products (Malone et al. 2003). The effects of formulation, sliding speed, and the interaction of formulation with the other two parameters were all significant

Table 11 Effect of main sources of variation of frictional properties of yogurts ($n = 12$) determined by F-values obtained from three-way ANOVA[a]

Source of variations	Friction coefficient
Formulation	377^{***}
Sliding speed	26.6^{***}
HWS	710^{*}
Sliding speed × HWS	6.6^{**}
Formulation × HWS	131^{***}
Formulation × sliding speed	2.8^{***}

[a] *, **, and *** indicate significant differences at $p \leq 0.05$, $p \leq 0.01$, and $p \leq 0.001$, respectively

at $p \leq 0.001$. HWS was significant at $p \leq 0.05$, and the interaction of sliding speed with HWS was significant at $p \leq 0.01$. Salivary proteins, mainly high molecular weight and proline-rich proteins, e.g. mucins, are the main source for the high lubricity of HWS (Bongaerts et al. 2007). HWS has been shown to have friction coefficients that were two orders of magnitude lower than those of water in its boundary regime. The significant impact of formulation was likely due to the addition of hydrocolloids with significantly different functionalities due to their different electrostatic charges, molecular size, and adhesive properties. This can result in significantly different network microstructures, number of intermolecular interactions, bond strength, and aggregate size, all of which can dramatically alter the frictional behaviors of the yogurt formulations. For instance, addition of WPI can lead to a larger particle size that can increase friction coefficients. Additionally, sliding speed can change the position of food between the two surfaces (balls and PDMS plate) and impact the friction coefficient.

Stribeck curves for the yogurt samples showed an increase in friction coefficient at the beginning of the curve up to approximately 0.1 mm s^{-1} (Fig. 5). This increase was not a hydrodynamic regime, but was due to elastic deformation of the PDMS plate because the rotational speed of the double-ball attachment was not high enough to allow slip (Zinoviadou et al. 2008). This start-up behavior typically disappeared at a sliding speed of ~0.1 mm s^{-1} and was minimal in full-fat yogurt (sample 4). During testing, fat globules form an interfacial film between the sliding surfaces, acting as a lubricant and resulting in a notable decrease in friction coefficient, which would promote sliding rather than stretching of the PDMS plate (Prakash et al. 2013; Huc et al. 2016).

The profile shape of Stribeck curves significantly changed for various hydrocolloids (Fig. 5). The length of the boundary regime for samples with PS (sample 8), CS (sample 9), and high WPI levels (sample 10) was similar to that of the control sample (sample 1). This result was likely due to the larger size of the WPI, SMP, and starch molecules. These molecules would not be able to fit between the PDMS surface and balls when the gap between these contacting surfaces was small at low siding speeds, resulting in similar friction behavior to that of the control sample at

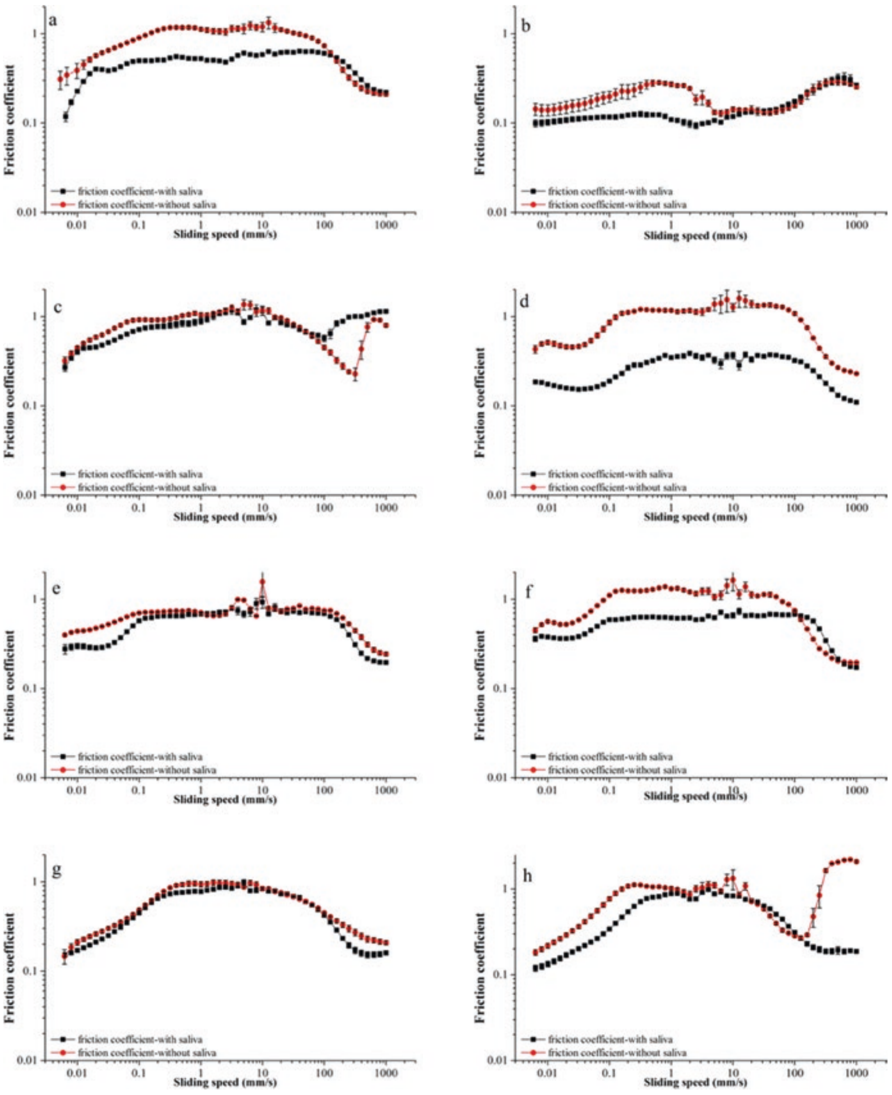

Fig. 5 Tribological results of yogurts; (**a**) sample 1 (control); (**b**) sample 4; (**c**) sample 6; (**d**) sample 7; (**e**) sample 8; (**f**) sample 9; (**g**) sample 10; (**h**) sample 12

those speeds. Sample 4 (full fat sample) showed a friction curve shape that was distinctly different from those of the other samples, likely due to its milkfat content. Part of hydrodynamic region can be seen at the end of the mixed regime for this sample when HWS was not added to the sample. Samples containing CMC (sample 7) and all hydrocolloids (sample 12) had similar friction curves, as did the control sample (sample 1) and samples containing PS (sample 8), CS (sample 9), and high levels of WPI (sample 10). Samples 7 and 12 also had similar phase angles (Table 7) and microstructures (Figs. 2 and 3). The friction curves for samples 6 and 7 were notably different in their shape. Addition of LBG (sample 6) caused higher friction coefficients than addition of CMC (sample 7). This result was likely due to the type of microstructures that LBG and CMC formed in the yogurt systems. The small, aggregated LBG molecules dispersed throughout the protein network would have been easier to deform and made a more particulate microstructure compared to the cohesive microstructure formed with addition of CMC. Samples with added LBG (sample 6), CMC (sample 7), and all hydrocolloids (sample 12) transitioned to the mixed regime at lower sliding speeds compared to the control sample (sample 1) and the samples with added PS (sample 8) or CS (sample 9). Among all samples, the full-fat sample (sample 4) showed a transition to the mixed regime at the lowest sliding speed. Samples with added LBG (sample 6), CS (sample 9), and all hydrocolloids (sample 12) had the least changes in their friction profiles after addition of HWS, which was in agreement with microscopy and rheological results. LBG, used in sample 6, is a neutral polysaccharide that has been shown to be less affected by HWS than other hydrocolloids (Zinoviadou et al. 2008). The effect of HWS on the friction behavior of CMC was greater than that for LBG. Addition of HWS to samples containing PS (sample 8) resulted in a drastic decrease in friction coefficients compared to samples made with CS (sample 9). This effect was attributed to the lower amylose content and larger granule size and branched microstructure of PS compared to CS, as discussed in the previous section (Sect. 3.3.2). However, these samples showed similar friction profile shapes.

Overall, the friction behaviors of yogurts changed with formulation and addition of HWS. Correlation of these observations with sensory results can be helpful to decide whether using HWS is necessary in tribometry to determine relationships between friction behaviors and sensory texture. These correlations will be discussed in Sect. 3.7.

3.5 Effect of Formulation and HWS on Yogurt Texture Attributes

Formulation, panelist, and their interaction showed significant influence on most yogurt textural attributes at $p \leq 0.001$. Panelist affected sliminess at $p \leq 0.01$, the interaction of panelist and formulation affected chalkiness afterfeel at $p \leq 0.05$, and none of these factors had a significant effect on spoon viscosity (Table 12). These results indicated that all factors evaluated contributed significantly to the variance in sensory scores. There were no significant differences between replicates or for any interaction term containing replicates, indicating that replicates did not contribute significantly to the variations in scores.

Significant differences among samples for texture attributes were found for every texture attribute measured (Table 13), which was not surprising given the variation in the samples' microstructural, rheological, and tribological results. Samples without gums and starches (samples 1–5) showed the highest spoon lumpiness. These samples contained SMP (sample 1), low levels of WPI (sample 5) and different fat ratios (samples 2, 3, and 4). Spoon lumpiness intensity significantly decreased when WPI was used in a higher ratio and without addition of SMP (sample 10), as well as when LBG (sample 6), CS (sample 9), or a combination of all hydrocolloids (sample 12) were used. Addition of milk-based additives can cause unpleasant texture attributes in yogurts (Morell et al. 2015). This has been attributed to protein aggregation and a possibility of two different protein matrices, one formed by the native milk proteins and the second by the added proteins (Morell et al. 2015). Using polysaccharide-based hydrocolloids, on the other hand, can provide a smoother texture. Unsurprisingly, lumpiness in mouth followed similar trends as spoon lumpiness.

Samples with added LBG (sample 6), CMC (sample 7), and all hydrocolloids (sample 12) had the highest degree of mouthcoat. Mouthcoating was significantly lower in the sample with high levels of WPI (sample 10), the low-fat sample (sample 2) and the sample with added PS (sample 8). Samples 1, 3, 4, and 5 were not significantly different from samples 2 and 8 for intensity of mouthcoat. The lack of mouthcoating in samples containing starches was likely due to the role of amylase in starch breakdown. This effect was noted by De Wijk et al. (2009). The low mouthcoating for the sample containing high levels of WPI may be due to its high melting attribute, which would remove the feeling of a coating on the oral surfaces due to rapid meltaway. Attribute scores for samples 1–5 (control sample, samples containing fat, and sample with low levels of WPI) showed that the effects of SMP were

Table 12 Main sources of variation of textural attributes of yogurt ($n = 12$) determined by F-values obtained from three-way ANOVA[a]

Sources	Formulation	Replicate	Panelist	Formulation × Replicate	Panelist × Replicate	Panelist × Formulation
Spoon viscosity	73.39***	13.01	17.96***	1.23	1.3	1.23
Graininess	85.45***	3	40***	0.69	1.02	4.34***
Mouthcoat	33.06***	2.36	18.73***	0.65	1.03	2.83***
Firmness	74.73***	2.37	29.12***	2.84	2.23	4.66***
Mouth viscosity	98.19***	0.13	22.13***	0.59	1.08	5.2***
Lumpiness	161.4***	3.48	40.37***	1.8	0.69	4.8***
Lumpiness in mouth	178.91***	0.04	56.11***	2.72	1.24	5.45***
Smoothness	119.99***	0.06	42.71***	1.74	0.68	4.61***
Melting	29.94***	1.98	38.3***	1.74	1.05	4.45***
Grittiness	21.74***	0.41	22.76***	2.08	0.8	2.51***
Astringency	16.36***	1.41	58.82***	1.15	0.98	2.48***
Chalkiness afterfeel	13.13***	0.08	13.82***	0.72	0.85	1.79*
Sliminess	83.7***	2.3	6.97**	1.9	1.07	4.72***

[a] *, **, and *** indicate significant differences at $p \leq 0.05$, $p \leq 0.01$, and $p \leq 0.001$, respectively

Table 13 Yogurt sensory attributes as evaluated by trained panelists[1]

Formula number	Attribute number[2]												
	1	2	3	4	5	6	7	8	9	10	11	12	13
1	10.0^{a}	4.05^{d}	7.28^{b}	3.79^{c}	3.16^{cd}	3.81^{bc}	8.53^{a}	3.49^{d}	7.00^{bc}	5.09^{a}	5.94^{a}	4.16^{ab}	1.78^{c}
2	10.6^{a}	3.82^{d}	6.96^{b}	3.53^{cd}	2.94^{cd}	3.48^{bc}	8.49^{a}	3.45^{d}	7.12^{bc}	4.69^{ab}	5.85^{a}	3.98^{ab}	1.88^{c}
3	10.5^{a}	3.68^{d}	6.18^{b}	3.84^{c}	3.02^{cd}	3.47^{bc}	8.38^{a}	3.77^{d}	7.58^{b}	4.46^{ab}	5.76^{a}	4.13^{ab}	1.91^{c}
4	9.82^{a}	4.07^{d}	5.91^{bc}	3.98^{c}	3.33^{cd}	3.45^{bc}	7.85^{a}	4.00^{d}	7.61^{ab}	4.52^{ab}	5.32^{ab}	4.40^{ab}	1.97^{c}
5	10.4^{a}	3.86^{d}	6.48^{b}	3.75^{c}	3.06^{cd}	3.49^{bc}	8.15^{a}	3.71^{d}	7.51^{bc}	4.7^{ab}	5.80^{a}	4.21^{ab}	1.98^{c}
6	4.67^{c}	7.30^{b}	9.64^{a}	6.28^{a}	6.67^{a}	5.76^{a}	4.54^{b}	3.31^{d}	4.40^{e}	4.31^{ab}	4.32^{bcd}	3.68^{bc}	3.39^{b}
7	2.53^{d}	7.63^{ab}	2.51^{d}	5.38^{ab}	6.70^{a}	5.52^{a}	1.93^{d}	10.1^{a}	5.23^{cde}	2.19^{c}	3.77^{cd}	2.38^{c}	4.58^{a}
8	6.97^{b}	3.37^{de}	3.79^{d}	3.29^{cd}	2.92^{cd}	2.8^{dc}	4.07^{bc}	6.94^{c}	9.00^{ab}	3.57^{bc}	5.69^{a}	3.60^{bc}	1.82^{c}
9	5.5b^{c}	5.69^{c}	4.15d^{c}	4.45^{bc}	4.92^{b}	4.16^{b}	2.95^{bcd}	7.66^{bc}	6.80^{bcd}	4.76^{ab}	5.60^{ab}	4.51^{ab}	2.38^{c}
10	4.58^{c}	2.44^{e}	2.66^{d}	2.39^{d}	2.13^{d}	2.03^{d}	2.21^{d}	8.99^{ab}	9.93^{a}	2.75^{c}	5.56^{ab}	2.40^{c}	1.65^{c}
11	2.53^{d}	3.86^{d}	9.40^{a}	4.03^{c}	3.61^{bc}	2.94^{dc}	2.73^{cd}	3.31^{d}	8.21^{ab}	5.60^{a}	4.96^{abc}	5.36^{a}	3.30^{b}
12	3.77^{cd}	8.46^{a}	3.95^{d}	5.84^{a}	6.91^{a}	6.15^{a}	2.36^{cd}	9.07^{ab}	4.56^{de}	2.51^{c}	3.49^{d}	2.56^{c}	4.44^{a}

[1] Letters in each column that are significantly different indicate significant differences

[2] Attributes include: (1) Spoon lumpiness; (2) Spoon viscosity; (3) Graininess; (4) Mouthcoat; (5) Mouth viscosity; (6) Firmness; (7) Lumpiness in mouth; (8) Smoothness; (9) Melting; (10) Grittiness; (11) Astringency; (12) Chalkiness afterfeel; (13) Sliminess

dominant to those of the milkfat content in perceived sensory texture. SMP is a popular additive that is used to alter yogurt texture (Karam et al. 2013) through short chains of proteins in the system. The bonds between these chains can easily break once the product is in the mouth, resulting in a low mouthcoat; longer protein chains are needed to provide a more substantial mouthcoat.

Increased astringency, grittiness, and graininess due to addition of SMP and WPI in the yogurt samples may have been due to increased particle size when these proteins were added to the yogurt system, resulting in a higher sensation of astringency, grittiness, and graininess (Sano et al. 2005; Andrewes et al. 2011). Another reason for the increased astringency, grittiness, and graininess could be aggregation of milk proteins with themselves or with saliva. Sliminess and ropiness are attributes that can be caused by exopolysaccharide- (EPS-) producing bacteria. The EPS can have negative or neutral charges based on the strains of bacteria (van de Velde et al. 2015). Thus, EPS can form long chains with milk proteins, resulting in a long, stringy texture. The mechanism of EPS interaction with milk proteins has been shown to be similar to the interaction mechanism of milk proteins with added hydrocolloids. Samples containing CMC (sample 7) and all hydrocolloids (sample 12) showed the highest intensity of sliminess, probably due to the presence of CMC, which has an opposite charge to that of milk proteins. These electrostatic interactions, as well as hydrophobic interactions, can form longer chains of proteins and cause a slimier texture. It appeared that the presence of strong interactions was required for this attribute in the yogurt samples since samples with LBG (sample 6), a neutral hydrocolloid with weak bonds to protein, had significantly lower sliminess than sample 7 or 12.

Overall, samples 7 (CMC) and 12 (all hydrocolloids) showed similar attribute trends. For instance, spoon viscosity, firmness, and viscosity in mouth had the greatest intensity and graininess, chalkiness, and grittiness had the lowest intensity for both samples. These results suggest that yogurts formulated with either CMC or a combination of all hydrocolloids used in this study had the most positive combination of texture attributes. The suitability of these combinations have also been shown in other studies (Alakali et al. 2008; Murray and Phisarnchananan 2014).

3.6 Principal Component Analysis of Sensory Results

Principal component analysis (PCA) was performed to visualize the relationships between the samples and their textural attributes (Fig. 6). The first two principal components accounted for 59.9% and 26.3% of the variance, respectively, in the 13-variable system. The attributes most negatively correlated with PC1 were mouth viscosity, spoon viscosity, sliminess, and firmness. The most positive correlations to PC1 were for astringency and low-melting. PC2 was positively correlated with graininess and negatively correlated with smoothness. The results from this plot were in accordance with the results for the sensory attributes (Table 13).

A cluster analysis of the 13 textural attributes of all yogurts showed the yogurts fit into one of three groups, designated by the colors of the circles in the PCA plot (Fig. 6). The first cluster (green) had two main subgroups: (1) samples 7, 9, and 12, and (2) samples 8 and 10. Samples 7, 9, and 12 were positively described by smoothness, sliminess, both viscosity-related attributes, firmness, and mouthcoating but negatively related to astringency and low-melting. Samples 8 and 10 showed the opposite relationships. As explained in Sect. 3.5, the CMC in sample 7 and all hydrocolloids in sample 12 had the greatest contribution to these attributes due to a higher number of electrostatic and hydrophobic interactions, as well as covalent bonds formed by CMC and PS, which are negatively charged hydrocolloids (Alakali et al. 2008). Additionally, samples 7 and 12 showed the highest intensities of ideal texture attributes (see Sect. 3.5), which was attributed to the addition of CMC. The palatability of the yogurt produced with CS (sample 9) was likely caused by its structural features (Alakali et al. 2008). CS granules are small compared to PS granules, and they can reduce the sensation of dryness in the mouth. Alakali et al. (2008) suggested that the residual corn oil in CS may also be partially responsible for the palatability of CS-containing yogurts.

The second cluster (red) included samples 6 (containing LBG) and 11 (containing LBG and CS). Sample 6 was positively related to most of the attributes that were positively related to the first cluster (green) and negatively related to lumpiness-related attributes, graininess, low-melting, and astringency. In the LBG-containing samples, the neutral LBG would increase the viscosity of the continuous phase,

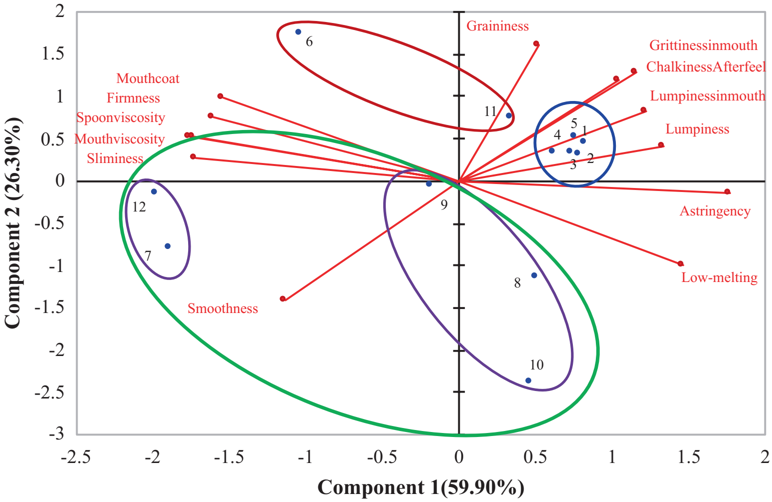

Fig. 6 Principal Component Analysis (PCA) biplot for texture attributes of yogurts (n = 12) analyzed by descriptive sensory panelists (n = 10). Clusters have been circled based on cluster analysis

promoting these attributes (Thaiudom and Goff 2003). Sample 11 was positively related to lumpiness-related attributes, graininess, low-melting, and astringency. However, the intensity of these undesirable defects was significantly lower than those of samples 8 and 10 in the green cluster. The presence of CMC was hypothesized to be the reason for this result.

The third cluster (blue) consisted of samples 1, 2, 3, 4, and 5 (control, fat-containing samples, and low-level WPI-containing sample, respectively). These samples were mostly related to grittiness, chalkiness afterfeel, both lumpiness attributes, graininess, and astringency. SMP was the common additive in these samples. Addition of milk powders, e.g. SMP and WPI, is known to increase the intensity of these attributes (Isleten and Karagul-Yuceer 2006). Overall, the combination of PCA and cluster analysis helped illustrate significant attributes as well as trends among samples.

3.7 Correlations Among Yogurt Rheological, Tribological, and Texture Behaviors

3.7.1 Correlations Among Yogurt Textural Attributes

Multiple significant correlations were found among textural attributes (Table 14). There were two major groups of attributes in this matrix. The first group included negative texture attributes: spoon and mouth lumpiness, low-melting, grittiness, astringency, and chalkiness afterfeel. As expected, these negative attributes showed negative correlations with the second group of more palatable attributes: spoon viscosity, mouthcoat, mouth viscosity, firmness, smoothness, and sliminess. The overall drivers behind these attributes included particle size, structural features, and changes to structural features, upon contact with HWS.

As expected, the highest correlations were between spoon lumpiness and mouth lumpiness, as well as spoon viscosity and mouth viscosity. This result was likely due to the fact that appearance may highly affect other senses; i.e., the appearance of the sample impacted its in-mouth perception, or the intensity of these attributes in the mouth remained similar to those of their appearance. Viscosity-related attributes had the highest number of correlations to other attributes. In terms of the undesirable attributes, astringency and lumpiness had the highest correlation. These results emphasize that yogurt textural attributes can be related to each other, potentially due to structural features that have a variety of effects. Therefore, care must be taken in formation of new yogurt products so that formulation changes to address issues with one textural attribute does not cause undesirable changes in a second attribute.

Table 14 Correlation matrix for yogurt textural attributes[a]

Attribute	Spoon lumpiness	Spoon viscosity	Graininess	Mouthcoating	Mouth viscosity	Firmness	Lumpiness in mouth	Smoothness	Melting	Grittiness	Sliminess
Spoon viscosity	-0.534^{*}	1.00			0.991^{***}				-0.942^{***}		
Mouthcoat		0.953^{***}		1.00					-0.961^{***}		
Mouth viscosity	-0.609^{*}	0.991^{***}		0.958^{***}	1.00				-0.920^{***}		
Firmness		0.975^{***}		0.958^{***}	0.953^{***}	1			-0.986^{***}		
Lumpiness in mouth	0.955^{***}										
Smoothness	-0.602^{*}		-0.893^{***}				-0.761^{**}			-0.878^{**}	
Low-melting		-0.942^{***}		-0.961^{***}	-0.920^{***}	-0.986^{***}					
Grittiness			0.814^{**}				0.548^{*}	-0.878^{**}	1.00	1.00	
Astringency	0.740^{**}	-0.884^{***}		-0.822^{**}	-0.896^{**}	-0.809^{**}	0.628^{*}		0.750^{**}	0.562^{*}	-0.964^{***}
Chalkiness afterfeel			0.727^{**}					-0.785^{**}		0.960^{***}	
Sliminess	-0.745^{**}	0.884^{***}		0.829^{**}	0.900^{***}	0.808^{**}	-0.614^{*}		0.761^{**}		1.00

[a] Only significant correlations at $^{*}p \leq 0.01$$^{**}p \leq 0.001$; $^{**}p \leq 0.0001$ are shown

Table 15 Correlation among yogurt flow and viscoelastic parameters[a]

Formula	η_o at 8 °C no HWS	η_o at 25 °C no HWS	c at 25 °C no HWS	n at 8 °C no HWS	η_o at 8 °C HWS	η_o at 25 °C HWS	c at 8 °C HWS	n at 25 °C HWS
G^*, 8 °C, no HWS	***0.985	***0.980	*0.817					
G^*, 25 °C, no HWS	*0.892	**0.900	*0.855					
tan δ, 8 °C, no HWS				*-0.676				
tan δ, 25 °C, no HWS				*-0.650				
G^*, 8 °C, HWS					*0.864	*0.780		
G^*, 25 °C, HWS					*0.844	*0.791		
γ_c, 25 °C, HWS							*0.712	*0.628

[a] Only significant correlations at $^{*}p \leq 0.05$; $^{**}p \leq 0.01$; $^{***}p \leq 0.001$, are shown

3.7.2 Correlations Among Yogurt Viscoelastic and Flow Behaviors

Correlations were found among yogurt viscosity and viscoelastic behaviors for samples with and without added HWS (Table 15). G^* was significantly correlated with η_o and c at 8 and 25 °C, and tan δ was only correlated to G^* and η_o at 8 °C without HWS application. These results showed with increasing G^*, η_o also increased. These correlations were reflected in the viscosity and strain sweep results: samples with higher tan δ had lower η_o values. Thus, the greater the values of η_o, the more solid-like behavior the material exhibited. When samples were tested with addition of saliva, G^* was correlated to η_o at both 8 and 25 °C, but tan δ showed no significant correlation with any other parameter. Critical strain correlated to n and c from viscosity parameters: samples with increased critical strain also had higher n and c values. Overall, addition of HWS did have some impact on the correlations found among rheological parameters, suggesting that incorporation of HWS may impact relationships among sample rheological behaviors. This was not surprising considering the impact of HWS on yogurt microstructures (Sect. 3.2).

Tribological results were negatively correlated to yogurt viscosity parameters, including n when HWS was not added and both c and n with added HWS (Table 16). The correlations were found at all selected sliding speeds (10–100 mm s^{-1}) for n with added HWS and all selected sliding speeds but 1 mm s^{-1} for c with added HWS and n when HWS was not added.

In general, increased shear-thinning behavior, potentially due to weaker microstructures, resulted in higher friction coefficients. The correlations of c with tribological results when HWS was added suggested that addition of HWS to samples for testing can strengthen the correlations between flow properties and friction

Table 16 Correlations among yogurt friction coefficients and flow parameters[a]

Friction coefficients (μ) with HWS												
Viscosity parameters	μ at 1 mm s^{-1}	μ at 5 mm s^{-1}	μ at 10 mm s^{-1}	μ at 15 mm s^{-1}	μ at 20 mm s^{-1}	μ at 25 mm s^{-1}	μ at 30 mm s^{-1}	μ at 40 mm s^{-1}	μ at 50 mm s^{-1}	μ at 60 mm s^{-1}	μ at 80 mm s^{-1}	μ at 100 mm s^{-1}
n with HWS	−0.702*	−0.701*	−0.675*	−0.66*	−0.655*	−0.652*	−0.65*	−0.648*	−0.647*	−0.647*	−0.646*	−0.645*
c (s) with HWS		−0.609*	−0.592*	−0.583*	−0.581*	−0.58*	−0.58*	−0.578*	−0.577*	−0.577*	−0.577*	−0.577*
n no HWS		−0.797**	−0.852***	−0.878***	−0.888***	−0.891***	−0.893***	−0.894***	−0.9***	−0.9***	−0.9***	−0.9***

[a] Only significant correlations at $^*p \leq 0.05$; $^{**}p \leq 0.01$; and $^{***}p \leq 0.001$ are shown

coefficients. However, there were no correlations between η_o and friction coefficients at any sliding speed. In addition, no significant correlations were found among yogurt viscoelastic and friction behaviors. This result was not expected as some viscoelastic properties, e.g. viscoelastic moduli or tan δ, have been found to be related to friction behavior in other studies (Chen and Engelen 2012). The lack of correlation in this study implied that structural features that control viscoelastic properties in these samples may not have significant impact on friction behaviors and vice versa.

3.7.3 Correlations Among Yogurt Flow Parameters and Textural Behaviors

Viscosity parameters and sensory results showed few correlations. However, η_o was positively correlated with firmness at 25 °C ($R^2 = 0.87$) and n was negatively correlated with sliminess at 8 °C ($R^2 = 0.88$) when HWS was added. Firmer yogurts showed higher instrumental viscosity, since a greater force was needed to induce flow. Firmer materials would have stronger bonds and other intermolecular interactions, making their microstructures more resistant to flow. As previously discussed, sliminess is the result of strong interactions between milk proteins and hydrocolloids. Slimy materials typically show shear-thinning behavior; this behavior can be intensified by addition of long-chain, proline-rich mucins and other salivary proteins. c was negatively correlated with low-melting ($R^2 = 0.930$), grittiness ($R^2 = 0.822$), and astringency ($R^2 = 0.844$) at 8 °C when HWS was not added. The parameter c is the time needed for a material to flow and is known to be increased by protein aggregations or larger particle sizes (Genovese et al. 2007). Therefore, more time is needed to disrupt stronger microstructures or larger molecules through shear.

3.7.4 Correlations Among Yogurt Viscoelastic and Textural Behaviors

Viscoelastic parameters that correlated with yogurt texture attributes included only tan δ at γ_c obtained from strain sweep data. Neither γ_c nor G^* at γ_c showed significant correlations with sensory terms (Table 17). tan δ was positively correlated with viscosity-related attributes, mouthcoat, firmness, and sliminess. It was also negatively correlated with low-melting, lumpiness, and astringency. As tan δ increases, materials show more viscous-type behavior; i.e., they flow more readily under their own weight. A potential explanation for the correlation of tan δ with firmness and viscosity is that panelists may have interpreted the increased fluid-like behavior as increased viscosity, sliminess, and mouthcoat. Correlations at different temperatures were not significantly different. This was attributed to the short time semisolid foods are held in the mouth before swallowing.

Table 17 Correlations among yogurt viscoelastic parameters and sensory attributes[a]

Viscosity parameters	Spoon lumpiness	Spoon viscosity	Mouth-coat	Mouth viscosity	Firmness	Low-melting	Astringency	Sliminess
tan δ (rad) at 8 °C, no HWS	−0.695*	0.702*	0.783*	0.750*	0.656*	−0.663*	−0.832**	0.860**
tan δ (rad) at 8 °C, with HWS	−0.698*						−0.626*	0.706*
tan δ (rad) at 25 °C, no HWS	−0.690*	0.748*	0.807*	0.787*	0.710*	−0.710*	−0.870**	0.886**
tan δ (rad) at 25 °C, with HWS	−0.708*						−0.654*	0.734*

[a]Only significant correlations at $^{*}p \leq 0.05$; $^{**}p \leq 0.01$; and $^{***}p \leq 0.001$ are shown

3.7.5 Correlations Among Yogurt Frictional and Textural Behaviors

Friction coefficients of yogurts at 1–100 mm s^{-1} sliding speeds were correlated with sensory results at 25 °C (Table 18). These sliding speeds were selected since oral sliding speeds have been reported to be in the range of 10–100 mm s^{-1} (Malone et al. 2003). The lower sliding speeds were selected to account for some of the slower movements used while evaluating food texture.

Spoon lumpiness was positively correlated to friction coefficient at all sliding speeds, excluding 1 and 5 mm s^{-1} for friction coefficients measured without HWS, and excluding 1 mm s^{-1} for friction coefficients measured with added HWS. Friction coefficients with and without saliva at 1 mm s^{-1} were correlated with mouth viscosity and smoothness. Negative correlation of smoothness with friction coefficient were expected: smoother yogurts would have lower friction coefficients due to the lack of large particles or lumps. Mouth viscosity was positively correlated with friction coefficients at 60, 80, and 100 mm s^{-1} when no HWS was added during tribological testing. This result was opposed to the findings for model hydrocolloid solutions (De Vicente et al. 2006). However, the positive correlation between viscosity and friction has been found in a more recent study on semisolid dairy products (Sonne et al. 2014). The conflicting results may be due to the larger particle sizes in semisolid foods with higher protein content compared to that of oil-in-water emulsions, particularly if WPI is used as the protein source (Krzeminski et al. 2011). The protein molecules might be trapped between or adhere to the two sliding surfaces, increasing the friction during sliding.

Table 18 Correlations among sensory attributes and friction coefficients of yogurts with and without HWS addition at 25 °C ($n = 12$)[a]

Sensory attributes	μ at 1 mm s^{-1}	μ at 5 mm s^{-1}	μ at 10 mm s^{-1}	μ at 15 mm s^{-1}	μ at 20 mm s^{-1}	μ at 25 mm s^{-1}	μ at 30 mm s^{-1}	μ at 40 mm s^{-1}	μ at 50 mm s^{-1}	μ at 60 mm s^{-1}	μ at 80 mm s^{-1}	μ at 100 mm s^{-1}
Correlations with HWS												
Lumpiness		0.615*	0.990***	0.997***	0.999***	0.999***	0.999***	0.999***	0.999***	0.999***	0.999***	1.00***
Spoon viscosity	−0.840**	−0.692*										
Smoothness	−0.902***	−0.684*										
Low-melting	0.617*											
Mouth viscosity												
Correlations without HWS												
Lumpiness			0.914***	0.967***	0.992***	0.996***	0.998***	0.998***	0.999***	0.999***	0.999***	0.999***
Spoon viscosity	−0.840**											
Smoothness	−0.902***											
Low-melting	0.616*											
Mouth viscosity										0.577*	0.579*	0.581*

[a] Only significant correlations at $^{*}p \leq 0.05$; $^{**}p \leq 0.01$; and $^{***}p \leq 0.001$ are shown

4 Comparison of Yogurt and Acid Milk Gel Microstructures, Rheological and Tribological Behaviors, and Texture Attributes

Acid milk gels are often used as an analog for yogurts since controlling the final pH and time to reach final pH is easier with a chemical acidifier, e.g. GDL, compared to using live bacteria. However, using different methods of chemical and biological acidification may result in notable differences in gel microstructure and physicochemical, functional, and textural behaviors of the products. Therefore, this section compares the microstructural features and rheological, tribological, and sensory behaviors of acid milk gels (full data set presented in Chapter 11) and yogurts to determine the differences between these two systems and assess the suitability of acid milk gels as an analog for yogurts. Table 19 presents the acid milk gel formulations used for comparison with the yogurts.

Table 19 Acid milk gel formulations used for comparison to yogurts

Formula number used in this chapter	Formula number used in Chap. 11	SMP (w/w)	WPI (w/w)	LBG (w/w)	CMC (w/w)	Potato starch (w/w)	Corn starch (w/w)	Skim milk (w/w)	Cream (w/w)	GDL (w/w)
1	1	2.8	0	0	0	0	0	97.2	0	1.1–1.55
2	2	2.83	0	0	0	0	0	95.96	1.21	1.1–1.55
3	3	2.89	0	0	0	0	0	92.26	4.85	1.1–1.55
4	4	2.95	0	0	0	0	0	89.15	7.9	1.1–1.55
5	5	1.8	1	0	0	0	0	97.2	0	1.1–1.55
6	6	1.8	0	1	0	0	0	97.2	0	1.1–1.55
7	7	1.8	0	0	1	0	0	97.2	0	1.1–1.55
8	8	2.1	0	0	0	0.7	0	97.2	0	1.1–1.55
9	9	2.1	0	0	0	0	0.7	97.2	0	1.1–1.55
10	16	0	2.8	0	0	0	0	97.2	0	1.1–1.55
11	18	0	0	1.8	0	0	1	97.2	0	1.1–1.55
12	24	0.2	0.8	0.45	0.45	0.45	0.45	97.2	0	1.1–1.55

4.1 Microstructural Comparison

Comparing the microstructural images of acid milk gels to their yogurt counterparts showed only slight differences. The protein network of yogurts showed slightly more open and larger strands, chains, and clusters for most of the formulations compared to their acid milk gel analogues. This result was attributed to rate of acidification from lactic acid bacteria (LAB) versus GDL to form the protein matrices in these systems. During acidification, GDL is hydrolyzed to gluconic acid to lower the pH in acid milk gels. On the other hand, LAB consume lactose as a source of sugar to produce lactic acid. Both acids lower the pH, resulting in aggregation and gelation of milk proteins. However, LAB typically produce lactic acid at a slower rate than GDL dissociation, resulting in a longer gelation time for yogurt compared to that for acid milk gels (Lucey et al. 1998). Gelation time was considered to be the time needed to reach a pH between 4.55 and 4.6 (casein's isoelectric point). Acid milk gels had a 4 h gelation time; yogurts had a 4–6 h gelation time. Gelation time was optimized based on the control sample formation for acid milk gels. However, gelation time differed among the various formulations of yogurts due to variations in LAB activity and different amount of starter culture added to account for formulation differences per the manufacturer's instructions.

At pH between 4.55 and 4.6 for both acid milk gels and yogurts, electrostatic and protein–protein attractions occurred through hydrophobic interactions to form the protein matrix throughout the gel (Lee and Lucey 2004). In this protein network, casein micelles are linked by protein clusters and chains that are distributed in a serum phase with void pores or pores in which the aqueous phase is trapped (Lee and Lucey 2010). This matrix was shown to be similar in acid milk gels and yogurts.

4.2 Rheological and Tribological Behavior Comparison

Overall, there were no significant differences ($p > 0.05$) among the zero shear viscosity values of the yogurts and acid milk gels at 8 and 25 °C based on the results of a two-tailed t-test. Both acid milk gels and yogurts showed shear-thinning behavior, but their viscosity curves were best fit to different flow behavior models. The differences in the flow behavior results can be explained by microstructural differences and longer yogurt gelation time. Slow acidification can provide better conditions for protein interaction, strengthening the gel network and increasing viscosity (Martin et al. 1999; Lee and Lucey 2006), as well as promoting structural features that are slower to break down under shear. Accordingly, most yogurt formulations had moderately larger protein clusters and more even protein–protein crosslinking compared to their acid milk gel analogues. Additionally, the comparison of n values of yogurts and their acid milk gel analogues obtained from the flow behavior models showed no significant differences at 8 and 25 °C ($p > 0.05$). This result was reflected in the similar shapes of the yogurt and acid milk gel viscosity profiles (examples shown in

Fig. 7). Yogurt and acid milk gel strain sweep data also showed similar patterns (examples shown in Fig. 8). Additionally, yogurt viscoelastic properties, including γ_c, G'', and G^*, were not significantly different from their acid milk gel analogues at both 8 and 25 °C ($p > 0.05$). Similarly, no significant differences were observed in acid milk gel and yogurt friction coefficients at selected sliding speeds at 25 °C ($p > 0.05$), and their friction profile shapes were similar (examples shown in Fig. 9).

4.3 Textural Attribute Comparison

Of all the textural attributes evaluated for the yogurts and acid milk gels, only graininess scores showed significant differences between similar yogurt and acid milk gel formulations ($p \leq 0.05$). Acid milk gels showed significantly lower graininess compared to yogurts. Interestingly, the longer yogurt gelation time did not appear to alter graininess intensity in yogurts versus acid milk gels. The most notable difference was shown for samples containing both LBG and CS (sample 11), which was

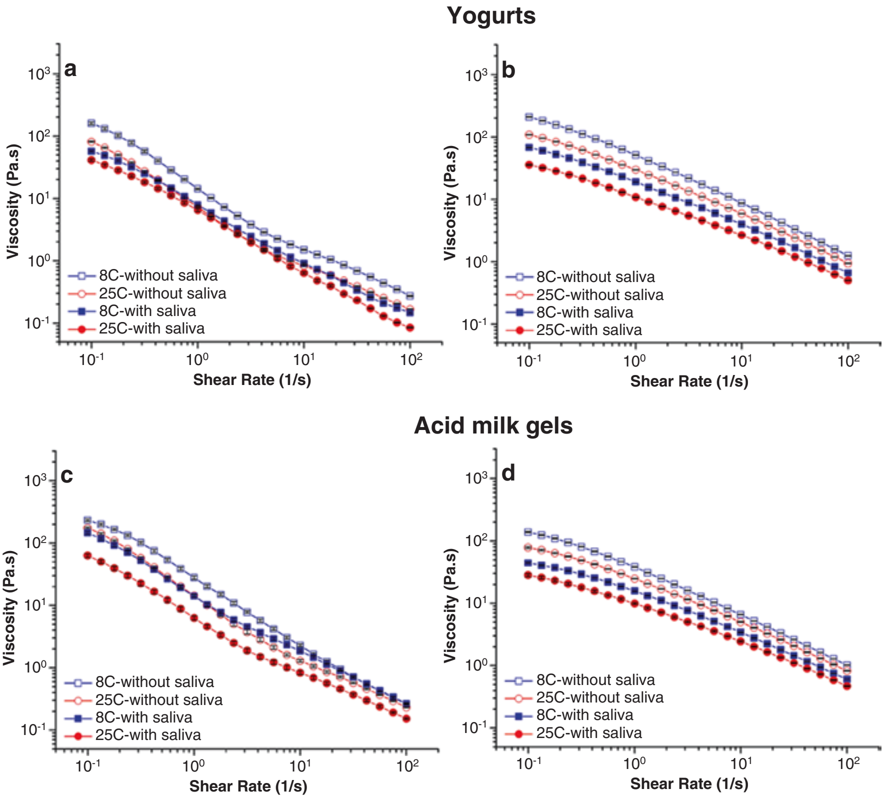

Fig. 7 Shear rate sweep results of two formulations of each of yogurts and acid milk gels. (**a**) sample 1; (**b**) sample 12; (**c**) sample 1; (**d**) sample 24. Formulations for acid milk gel samples are provided in Chap. 10

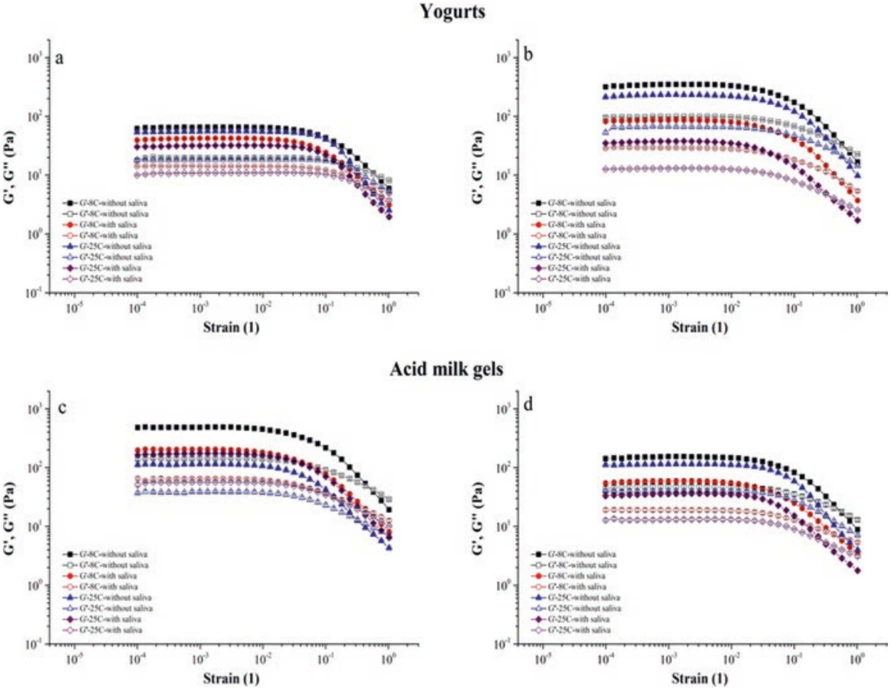

Fig. 8 Strain sweep results of two formulations of each of yogurts and acid milk gels. (**a**) sample 1; (**b**) sample 8; (**c**) sample 1; (**d**) sample 8. Formulations for acid milk gel samples are provided in Chap. 10

also reflected in the differences between the acid milk gel (Fig. 10) and yogurt (Fig. 6) PCA biplots.

Considering the sensory data for both acid milk gels and yogurts, samples 12 (all hydrocolloids added), 7 (added CMC), 6 (added LBG), and 11 (added LBG and CS) were the samples most related to the positive texture attributes, including mouthcoat, sliminess, spoon viscosity, firmness, mouth viscosity, and smoothness, for both acid milk gels and yogurts. The presence of at least one gum was hypothesized to be the main reason for improving the positive textural attributes. Samples formulated with CMC and all hydrocolloids had the lowest amount of astringency, likely because the hydrocolloids prevented HWS from interacting with whey proteins and causing an astringent sensation (Andrewes et al. 2011). Adding fat to samples 2, 3, and 4, and PS and CS to samples 8 and 9, respectively did not improve the textural attributes compared to the control (sample 1) in either yogurts and acid milk gels. Sample 8 (added PS) had high astringency and low-melting scores in both yogurts and acid milk gels. Sample 1 (control), and 5 (added WPI) were closest to lumpiness-related attributes along with chalkiness afterfeel, grittiness, and graininess. The least smooth samples were the control sample (sample 1), samples with added fat (samples 2, 3, and 4), and samples with added starch (samples 8 and 9) for both

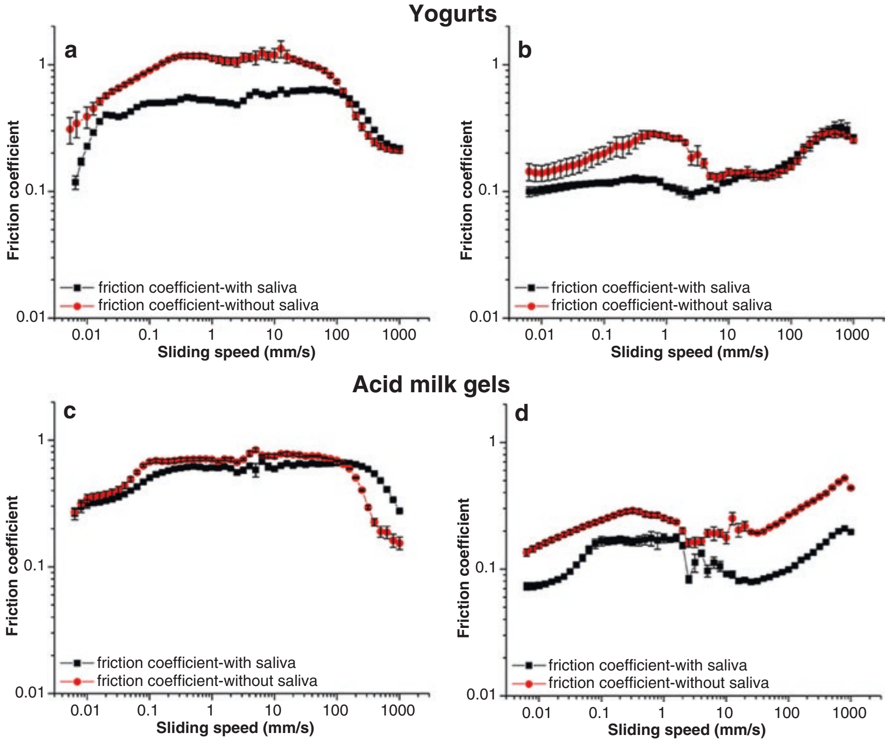

Fig. 9 Tribology results of two formulations of each of yogurts and acid milk gels. (**a**) sample 1; (**b**) sample 4; (**c**) sample 1; (**d**) sample 4. Formulations for acid milk gel samples are provided in Chap. 10

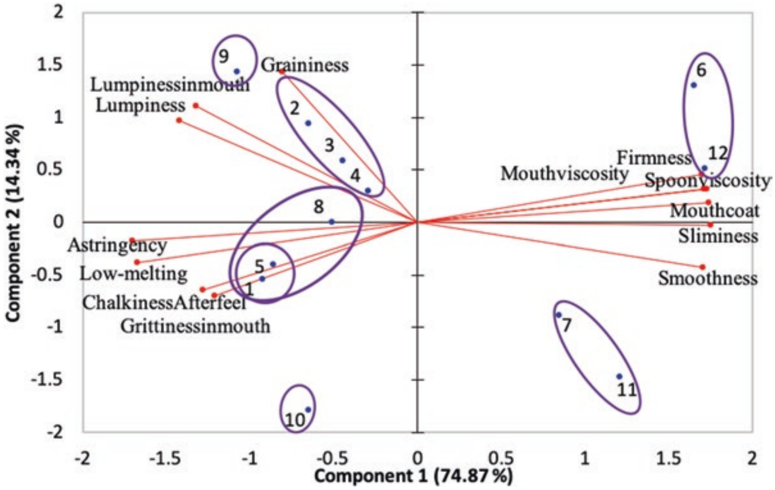

Fig. 10 Principal Component Analysis (PCA) biplot for texture attributes of acid milk gels ($n = 12$) analyzed by descriptive sensory panelists ($n = 10$). Clusters of samples determined from cluster analysis have been circled

yogurts and acid milk gels. Overall, the PCA plots showed that samples prepared with at least one gum (CMC or LBG) were associated with more desirable texture attributes, which was in line with the descriptive sensory results for both yogurts and acid milk gels.

5 Conclusions

Overall, the combination of rheology, tribology, sensory, and confocal imaging were found to be useful techniques for a deeper understanding of drivers of different yogurt textures. Addition of different hydrocolloids to the yogurt formulations significantly changed flow, viscoelastic, friction, and textural behaviors in yogurts. Microstructural images were a beneficial tool for determining protein network conformations, which showed relationships with multiple instrumental parameters and texture attributes. HWS had significant influence on all instrumental parameters and can be used to determine some of the mechanisms of food disruption when used during instrumental testing. However, correlations among yogurt rheological, tribological, and sensory behaviors did not significantly change for samples tested with or without HWS. More work is needed to understand the impact of HWS effects during oral processing and how HWS affects relationships between yogurt structures, mechanical behaviors, and sensory texture attributes.

The comparison of selected rheological parameters, tribological parameters, and sensory properties of acid milk gels and yogurts showed no significant differences, excluding the intensity of graininess in the textural attributes. Additionally, the patterns of their flow behavior, viscoelastic behavior, and friction profiles were also similar. However, small differences were observed for their sensory graininess and microstructures. This result was attributed to a longer gelation time for the LAB starter cultures compared to GDL. Therefore, acid milk gels can be considered an appropriate analog for yogurts that offers better control over final pH and gelation time.

Acknowledgements Funding for this project was provided by the USDA National Institute of Food and Agriculture (grant #2015-67018-23069).

Appendix

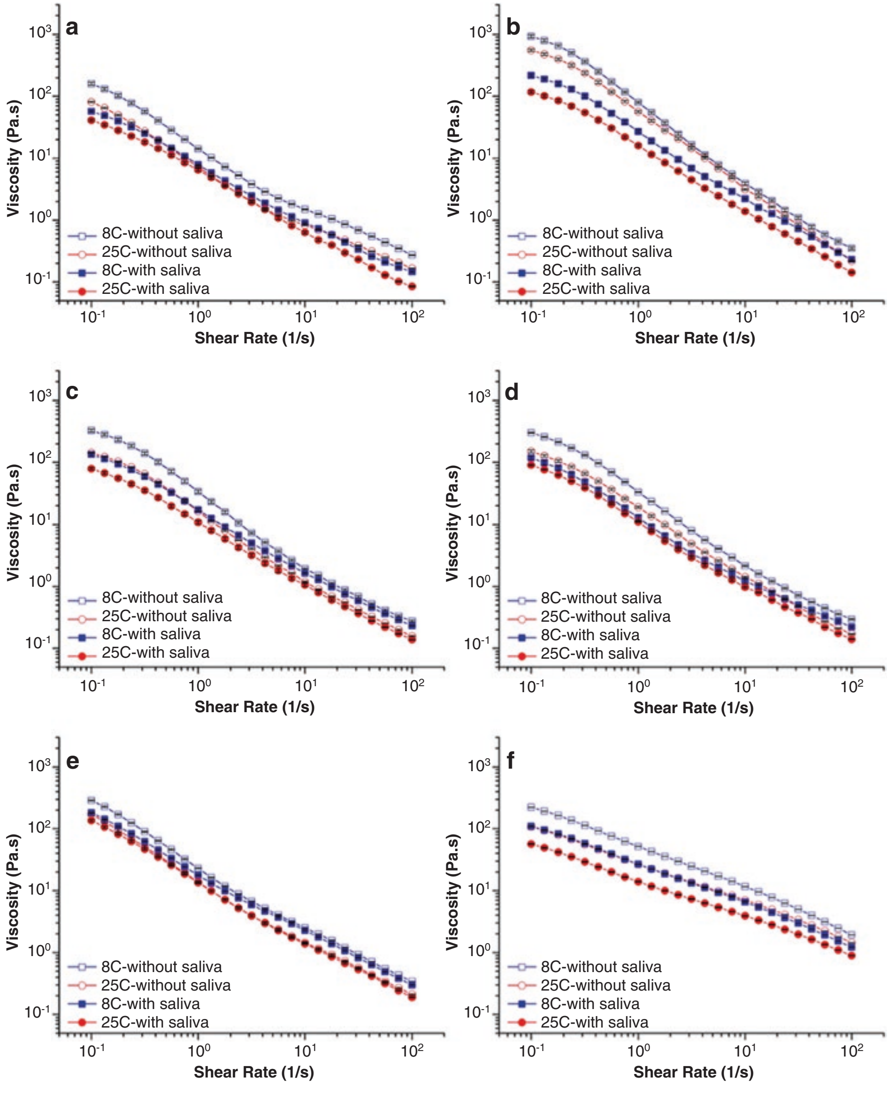

Fig. 11 Yogurt shear rate sweep results; (**a**) sample 1; (**b**) sample 2; (**c**) sample 3; (**d**) sample 4; (**e**) sample 5; (**f**) sample 6; (**g**) sample 7; (**h**) sample 8; (**i**) sample 9; (**j**) sample10; (**k**) sample 11; (**l**) sample 12

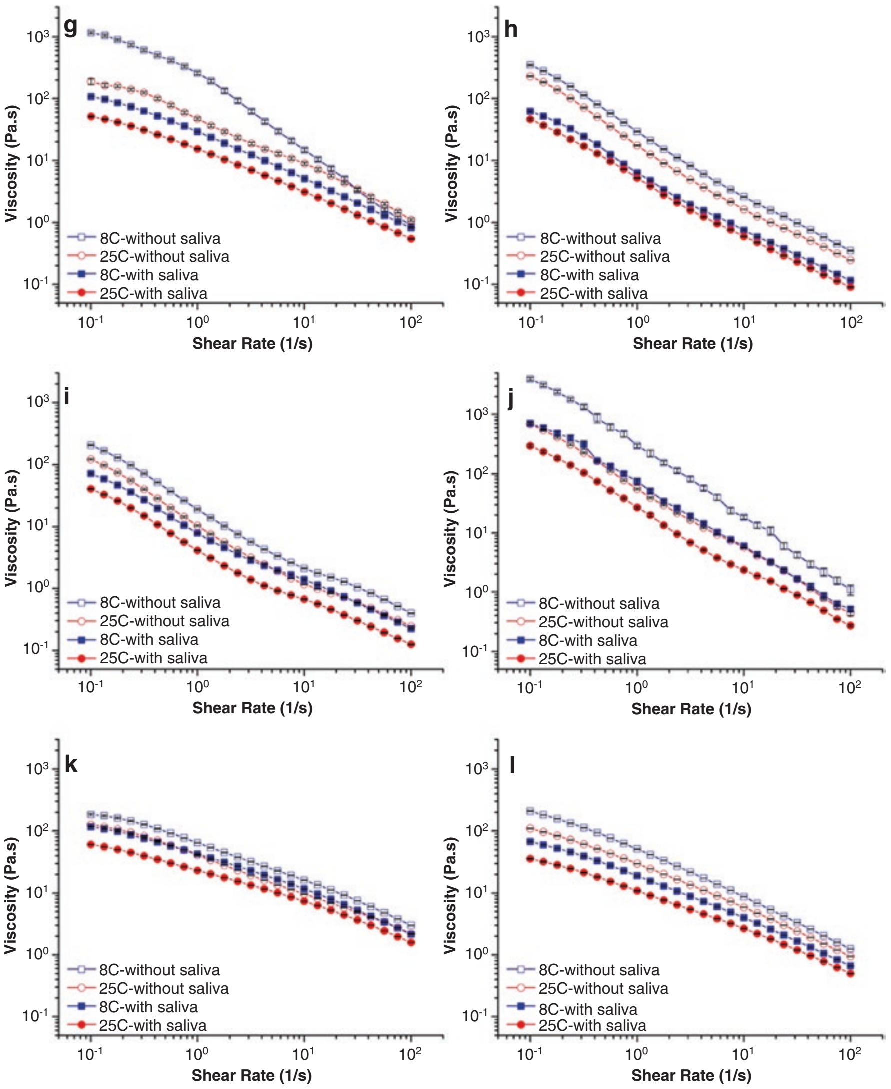

Fig. 11 (continued)

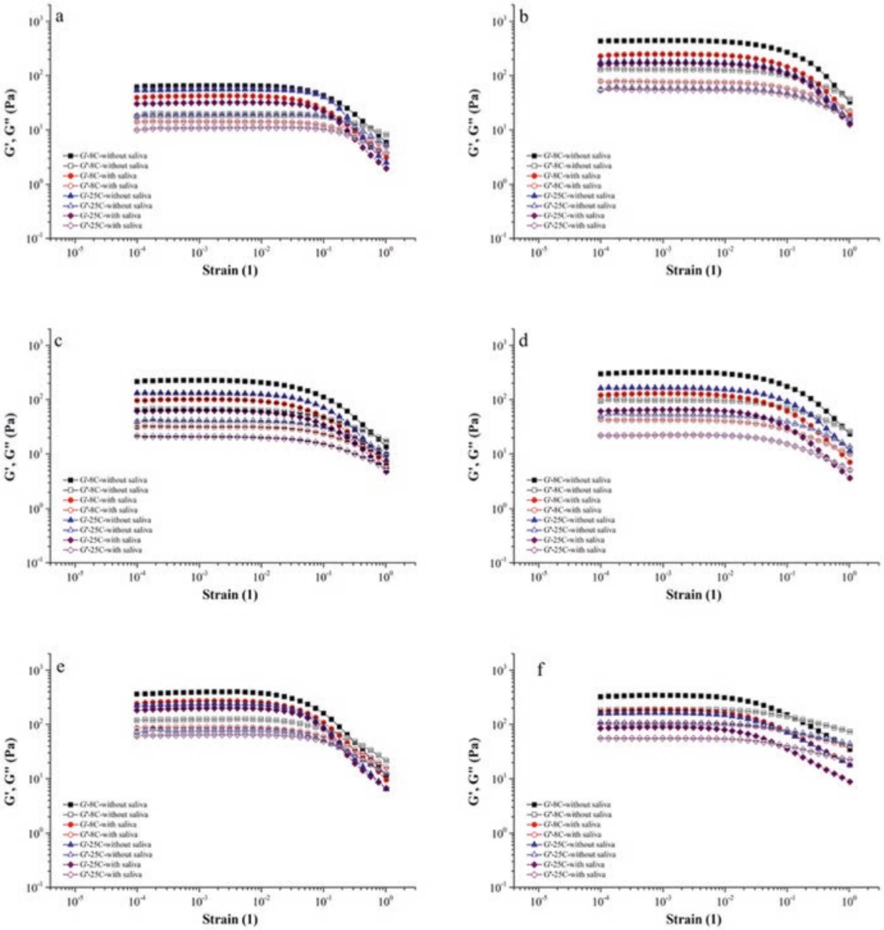

Fig. 12 Yogurt strain sweep results; (**a**) sample 1; (**b**) sample 2; (**c**) sample 3; (**d**) sample 4; (**e**) sample 5; (**f**) sample 6; (**g**) sample 7; (**h**) sample 8; (**i**) sample 9; (**j**) sample10; (**k**) sample 11; (**l**) sample 12

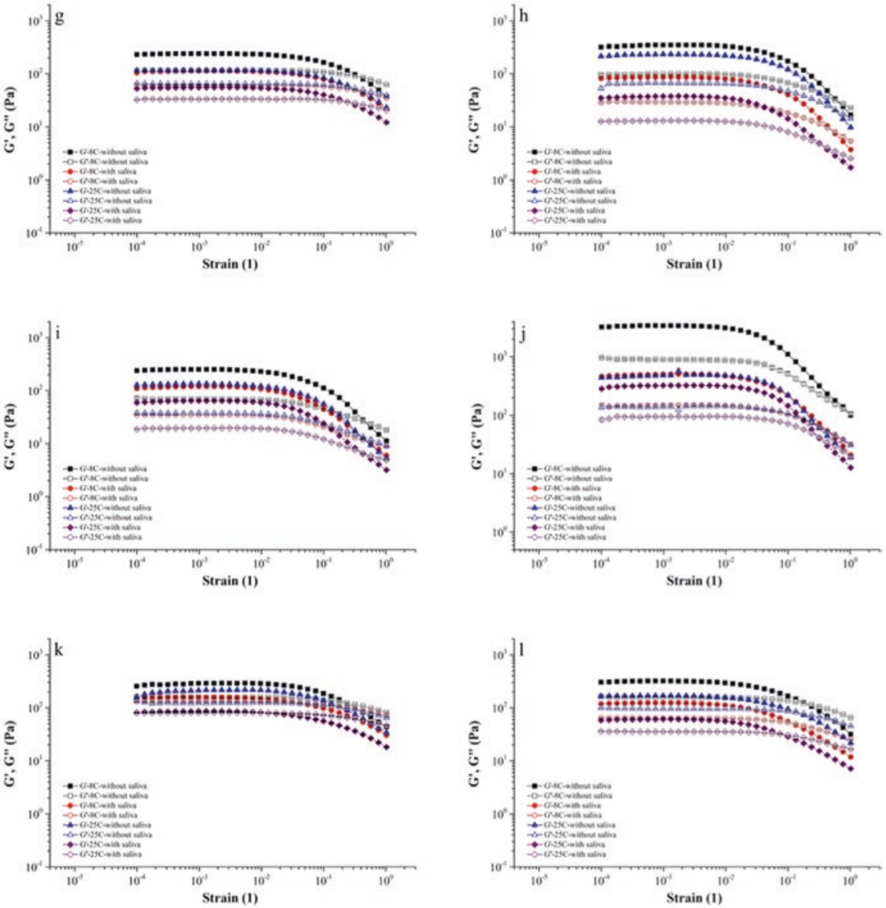

Fig. 12 (continued)

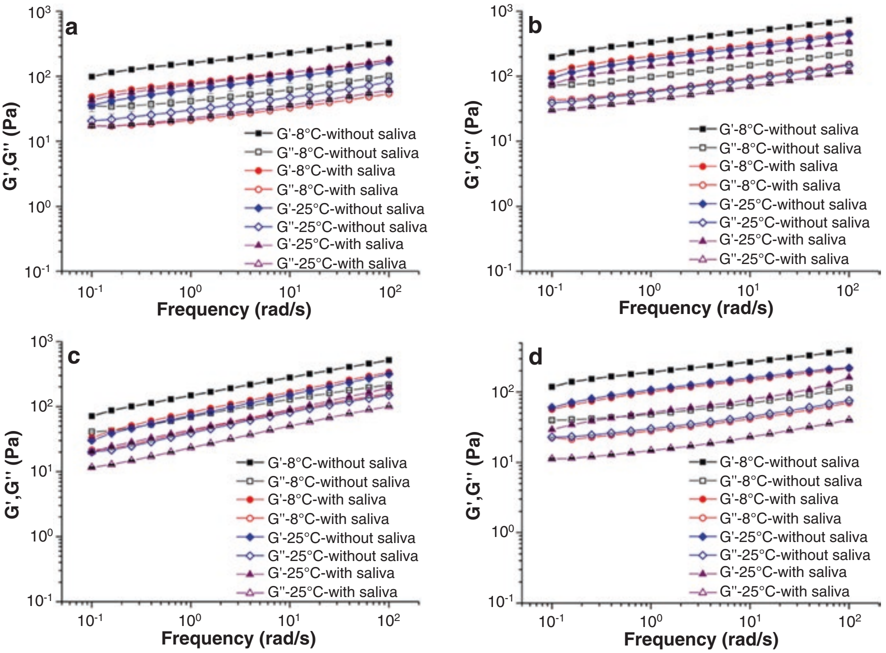

Fig. 13 Yogurt frequency sweep results; (**a**) sample 3; (**b**) sample 5; (**c**) sample 7; (**d**) sample 9

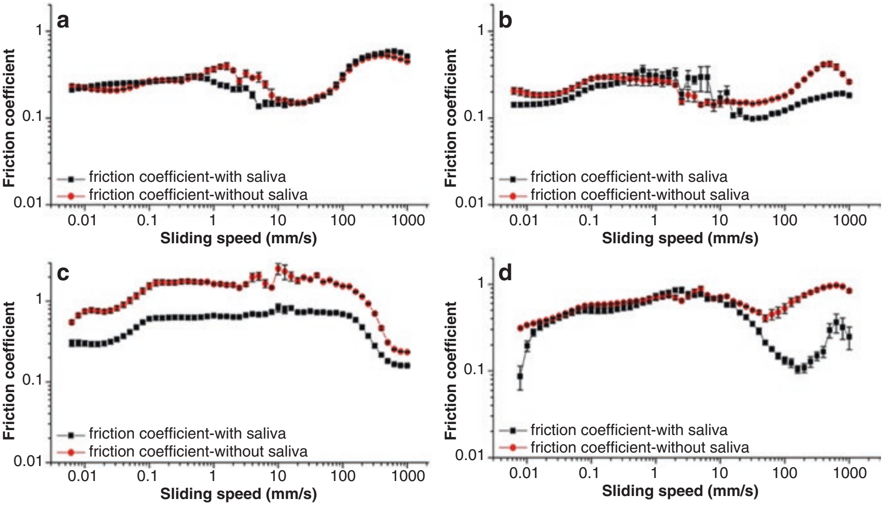

Fig. 14 Yogurt tribological profiles; (**a**) sample 2; (**b**) sample 3; (**c**) sample 5; (**d**) sample 11

References

Alakali, J., Okonkwo, T., & Iordye, E. (2008). Effect of stabilizers on the physico-chemical and sensory attributes of thermized yoghurt. *African Journal of Biotechnology, 7*(2), 158–163.

Andrewes, P., Kelly, M., Vardhanabhuti, B., & Foegeding, E. (2011). Dynamic modelling of whey protein–saliva interactions in the mouth and relation to astringency in acidic beverages. *International Dairy Journal, 21*(8), 523–530.

Berk, Z. (2018). *Food process engineering and technology*. London: Academic Press.

Bird, A. R., Brown, I. L., & Topping, D. L. (2000). Starches, resistant starches, the gut microflora and human health. *Current Issues in Intestinal Microbiology, 1*(1), 25–37.

Bongaerts, J., Fourtouni, K., & Stokes, J. (2007). Soft-tribology: Lubrication in a compliant PDMS–PDMS contact. *Tribology International, 40*(10), 1531–1542.

Bongaerts, J., Rossetti, D., & Stokes, J. (2007). The lubricating properties of human whole saliva. *Tribology Letters, 27*(3), 277–287.

Chen, J. (2015). Food oral processing: Mechanisms and implications of food oral destruction. *Trends in Food Science & Technology, 45*(2), 222–228.

Chen, J., & Engelen, L. (2012). *Food oral processing: Fundamentals of eating and sensory perception*. Chichester: Wiley.

Cho, S. S., & Prosky, L. (1999). Application of complex carbohydrates to food product fat mimetics. In *Complex carbohydrates in foods* (Food science and rechnology) (Vol. 93, pp. 411–430). New York: Marcel Dekker.

Chojnicka-Paszun, A., De Jongh, H., & De Kruif, C. (2012). Sensory perception and lubrication properties of milk: Influence of fat content. *International Dairy Journal, 26*(1), 15–22.

Dang, H. V., Loisel, C., Desrumaux, A., & Doublier, J. (2009). Rheology and microstructure of cross-linked waxy maize starch/whey protein suspensions. *Food Hydrocolloids, 23*(7), 1678–1686.

De Vicente, J., Stokes, J., & Spikes, H. (2006). Soft lubrication of model hydrocolloids. *Food Hydrocolloids, 20*(4), 483–491.

De Wijk, R., Terpstra, M., Janssen, A., & Prinz, J. (2006). Perceived creaminess of semi-solid foods. *Trends in Food Science & Technology, 17*(8), 412–422.

De Wijk, R. A., Kapper, C., Borsboom, P., & Prinz, J. F. (2009). Persistence of oral coatings of CMC and starch-based custard desserts. *Food Hydrocolloids, 23*(3), 896–900.

Genovese, D., Lozano, J., & Rao, M. A. (2007). The rheology of colloidal and noncolloidal food dispersions. *Journal of Food Science, 72*(2), R11–R20.

Guinard, J.-X., Zoumas-Morse, C., & Walchak, C. (1997). Relation between parotid saliva flow and composition and the perception of gustatory and trigeminal stimuli in foods. *Physiology & Behavior, 63*(1), 109–118.

Hansen, P. (1993). *Food hydrocolloids: Structures, properties and functions. Food hydrocolloids in the dairy industry*. New York: Plenum Press.

Hoover, R. (2001). Composition, molecular structure, and physicochemical properties of tuber and root starches: A review. *Carbohydrate Polymers, 45*(3), 253–267.

Huc, D., Michon, C., Bedoussac, C., & Bosc, V. (2016). Design of a multi-scale texture study of yoghurts using rheology, and tribology mimicking the eating process and microstructure characterisation. *International Dairy Journal, 61*, 126–134.

Humphrey, S. P., & Williamson, R. T. (2001). A review of saliva: Normal composition, flow, and function. *The Journal of Prosthetic Dentistry, 85*(2), 162–169.

Isleten, M., & Karagul-Yuceer, Y. (2006). Effects of dried dairy ingredients on physical and sensory properties of nonfat yogurt. *Journal of Dairy Science, 89*(8), 2865–2872.

Janssen, A. M., Terpstra, M. E., De Wijk, R. A., & Prinz, J. F. (2007). Relations between rheological properties, saliva-induced structure breakdown and sensory texture attributes of custards. *Journal of Texture Studies, 38*(1), 42–69.

Johnson, S., Gorman, D., Adams, M., & Briscoe, B. (1993). The friction and lubrication of human stratum corneum. *Tribology Series, 25*, 663–672. Elsevier.

Joyner, H. S., Pernell, C. W., & Daubert, C. R. (2014). Impact of formulation and saliva on acid milk gel friction behavior. Journal of food science, 79(5), E867–E880.

Karam, M. C., Gaiani, C., Hosri, C., Burgain, J., & Scher, J. (2013). Effect of dairy powders fortification on yogurt textural and sensorial properties: A review. *Journal of Dairy Research, 80*(4), 400–409.

Krzeminski, A., Großhable, K., & Hinrichs, J. (2011). Structural properties of stirred yoghurt as influenced by whey proteins. *LWT-Food Science and Technology, 44*(10), 2134–2140.

Laverse, J., Mastromatteo, M., Frisullo, P., Albenzio, M., Gammariello, D., & Del Nobile, M. (2011). Fat microstructure of yogurt as assessed by X-ray microtomography. *Journal of Dairy Science, 94*(2), 668–675.

Lee, W., & Lucey, J. (2004). Structure and physical properties of yogurt gels: Effect of inoculation rate and incubation temperature. *Journal of Dairy Science, 87*(10), 3153–3164.

Lee, W., & Lucey, J. (2010). Formation and physical properties of yogurt. *Asian-Australasian Journal of Animal Sciences, 23*(9), 1127–1136.

Lee, W.-J., & Lucey, J. (2006). Impact of gelation conditions and structural breakdown on the physical and sensory properties of stirred yogurts. *Journal of Dairy Science, 89*(7), 2374–2385.

Lucey, J., & Singh, H. (1997). Formation and physical properties of acid milk gels: A review. *Food Research International, 30*(7), 529–542.

Lucey, J., Tamehana, M., Singh, H., & Munro, P. (1998). A comparison of the formation, rheological properties and microstructure of acid skim milk gels made with a bacterial culture or glucono-δ-lactone. *Food Research International, 31*(2), 147–155.

Malone, M., Appelqvist, I., & Norton, I. (2003). Oral behaviour of food hydrocolloids and emulsions. Part 1. Lubrication and deposition considerations. *Food Hydrocolloids, 17*(6), 763–773.

Martin, N., Skokanova, J., Latrille, E., Beal, C., & Corrieu, G. (1999). Influence of fermentation and storage conditions on the sensory properties of plain low fat stirred yogurts. *Journal of Sensory Studies, 14*(2), 139–160.

Miller, J. L., & Watkin, K. L. (1996). The influence of bolus volume and viscosity on anterior lingual force during the oral stage of swallowing. *Dysphagia, 11*(2), 117–124.

Morell, P., Chen, J., & Fiszman, S. (2016). The role of starch and saliva in tribology studies and the sensory perception of protein-added yogurts. *Food & Function, 8*(2), 545–553.

Morell, P., Hernando, I., Llorca, E., & Fiszman, S. (2015). Yogurts with an increased protein content and physically modified starch: Rheological, structural, oral digestion and sensory properties related to enhanced satiating capacity. *Food Research International, 70*, 64–73.

Murray, B. S., & Phisarnchananan, N. (2014). The effect of nanoparticles on the phase separation of waxy corn starch+ locust bean gum or guar gum. *Food Hydrocolloids, 42*, 92–99.

Nguyen, P. T., Kravchuk, O., Bhandari, B., & Prakash, S. (2017). Effect of different hydrocolloids on texture, rheology, tribology and sensory perception of texture and mouthfeel of low-fat pot-set yoghurt. *Food Hydrocolloids, 72*, 90–104.

Ognean, C. F., Darie, N., & Ognean, M. (2006). Fat replacers: Review. *Journal of Agroalimentary Processes and Technologies, 12*(2), 433–442.

Official Methods of Analysis of AOAC INTERNATIONAL (1995a) AOAC INTERNATIONAL, Gaithersburg, MD, USA, Official Method 989.05

Official Methods of Analysis of AOAC INTERNATIONAL (1995b) AOAC INTERNATIONAL, Gaithersburg, MD, USA, Official Method 923.03

Official Methods of Analysis of AOAC INTERNATIONAL (1999) , AOAC INTERNATIONAL, Gaithersburg, MD, USA, Official Method 934.01

Pascua, Y., Koç, H., & Foegeding, E. A. (2013). Food structure: Roles of mechanical properties and oral processing in determining sensory texture of soft materials. *Current Opinion in Colloid & Interface Science, 18*(4), 324–333.

Peng, X., & Yao, Y. (2017). Carbohydrates as fat replacers. *Annual Review of Food Science and Technology, 8*, 331–351.

Perrechil, F., Braga, A., & Cunha, R. (2009). Interactions between sodium caseinate and LBG in acidified systems: Rheology and phase behavior. *Food Hydrocolloids, 23*(8), 2085–2093.

Prakash, S., Tan, D. D. Y., & Chen, J. (2013). Applications of tribology in studying food oral processing and texture perception. *Food Research International, 54*(2), 1627–1635.

Saint-Eve, A., Kora, E. P., & Martin, N. (2004). Impact of the olfactory quality and chemical complexity of the flavouring agent on the texture of low fat stirred yogurts assessed by three different sensory methodologies. *Food Quality and Preference, 15*(7), 655–668.

Sano, H., Egashira, T., Kinekawa, Y., & Kitabatake, N. (2005). Astringency of bovine milk whey protein. *Journal of Dairy Science, 88*(7), 2312–2317.

Sarkar, A., & Singh, H. (2012). Oral behaviour of food emulsions. In *Food oral processing* (pp. 111–137). Oxford: Wiley-Blackwell.

Serra, M., Trujillo, A. J., Quevedo, J. M., Guamis, B., & Ferragut, V. (2007). Acid coagulation properties and suitability for yogurt production of cows' milk treated by high-pressure homogenisation. International Dairy Journal, 17(7), 782–790.

Singh, N., Singh, J., Kaur, L., Sodhi, N. S., & Gill, B. S. (2003). Morphological, thermal and rheological properties of starches from different botanical sources. *Food Chemistry, 81*(2), 219–231.

Sonne, A., Busch-Stockfisch, M., Weiss, J., & Hinrichs, J. (2014). Improved mapping of in-mouth creaminess of semi-solid dairy products by combining rheology, particle size, and tribology data. *LWT-Food Science and Technology, 59*(1), 342–347.

Stokes, J. R., Boehm, M. W., & Baier, S. K. (2013). Oral processing, texture and mouthfeel: From rheology to tribology and beyond. *Current Opinion in Colloid & Interface Science, 18*(4), 349–359.

Tang, C.-H., & Liu, F. (2013). Cold, gel-like soy protein emulsions by microfluidization: Emulsion characteristics, rheological and microstructural properties, and gelling mechanism. *Food Hydrocolloids, 30*(1), 61–72.

Thaiudom, S., & Goff, H. (2003). Effect of κ-carrageenan on milk protein polysaccharide mixtures. *International Dairy Journal, 13*(9), 763–771.

van de Velde, F., de Hoog, E. H., Oosterveld, A., & Tromp, R. H. (2015). Protein-polysaccharide interactions to alter texture. *Annual Review of Food Science and Technology, 6*, 371–388.

Vingerhoeds, M. H., Silletti, E., De Groot, J., Schipper, R. G., & Van Aken, G. A. (2009). Relating the effect of saliva-induced emulsion flocculation on rheological properties and retention on the tongue surface with sensory perception. *Food Hydrocolloids, 23*(3), 773–785.

Zinoviadou, K., Janssen, A., & De Jongh, H. (2008). Tribological properties of neutral polysaccharide solutions under simulated oral conditions. *Journal of Food Science, 73*(2), E88–E94.

Index

A

Acid milk gels, 153, 156–159, 213, 233, 351, 384–389
  α-amylase and protein concentration, 277
  amylose hydrolysis, 276
  boundary regime, 275
  CLSM results, 286–288
  confocal imaging, 282
  correlations
    rheological and tribological behaviors, 341, 342
    sensory attributes and rheological properties, 337–339
    sensory attributes and tribological behaviors, 340, 341
    textural attributes, 334, 336
  data analysis, 283, 327
  descriptive sensory analysis, 323
  descriptive sensory evaluation, 325, 326
  flow behaviors
    cross model, 289
    formulation and temperature, 293
    non-Newtonian behavior, 293
    pseudoplastic behavior, 289
    rheological properties, 294
    semisolid food system, 293
    viscoelastic properties, 295
    viscosity parameters, 290, 295
    viscosity profiles, 290
  food friction behaviors, 324
  food system, 323
  food texture attributes, 275
  frequency sweep results, 299
  friction-related attributes, 324
  HWS
    analyses, 281
    collection, 279
    composition, 345
  hydrocolloids, 276, 323
  hydrodynamic regime, 276
  instrumental friction measurements, 324
  materials, 277
  mechanical and frictional properties, 276
  microstructural
    comparison, 385
    imaging, 276
    properties, 285, 286
  microstructure–function–texture relationships, 277
  mixed regime, 275
  PCA, 332–334
  PDMS plate production, 280
  proximate analysis, 278
  proximate compositions, 284, 285
  rheological
    and tribological behavior comparison, 385, 386
    and tribological results, 327
  rheometry, 280
  saliva composition, 285
  sample preparation, 278
  semisolid foods, 276, 323
  shear rate sweep results, 305
  shear-thinning properties, 323
  strain sweep results, 309
  temperature change, 277
  textural attributes
    comparison, 386
    influences, 327

H. S. Joyner (ed.), *Rheology of Semisolid Foods*, Food Engineering Series,
https://doi.org/10.1007/978-3-030-27134-3

Acid milk gels (*cont.*)
    κ-casein, 332
    mechanism, starches, 331
    network stabilization, 331
    parameters and interactions, values, 329
    rheological and tribological parameters, 328
    segregative and aggregative interactions, 332
    starch and protein, 331
    trained panelists, 330
    viscosity, 331
    WPI and CMC, 328
  textural optimization, 323
  tribological properties, 301–303
  tribological results, 316
  tribology, 275, 302
  tribometry, 281
  viscoelastic behaviors
    CMC, 294, 295
    crossover frequencies, 300
    frequency sweep, 296
    HWS and temperature, 300
    hydrocolloids, 301
    internal molecular interactions, 294
    semisolid foods, 294
    solid behavior, 296
    strain sweeps, 294, 296
    temperature and formulation, 294
    thermodynamics, 295
    viscous-dominant behavior, 295, 300
  viscosity, 275
Agitating/stirring, 34, 54, 88, 89, 178, 187, 188, 222, 278
American Society for Testing of Materials, 336
Amphiphilic proteins, 183
Amplitude sweeps, 14–16
Analysis of Variance (ANOVA), 283, 327, 356, 360, 361, 365, 369, 373
Apparent viscosity, 5, 38, 39, 44, 46, 66, 89, 136, 150, 192, 205, 209, 212, 213, 217–219, 222, 249, 261, 356
Astringency, 144, 153, 154, 157, 223, 239, 258, 275, 276, 324, 329, 331–334, 336–338, 341, 344, 375–377, 381, 387
Astringency−friction relationships, 153

B
Behavior models, 10, 19, 21, 32, 71, 72, 385
Bernoulli equation, 4
Beta-lactoglobulin, 154
Biaxial extension flow, 65
Bingham model, 6, 22, 41
Bingham plastics, 40, 41, 72
Bovine serum albumin (BSA), 170, 281
Brightfield microscope images, 210
Brookfield viscometers, 66
Bulk modulus, 47, 48
Bulk viscosity, 38, 152, 262
Burger's model, 5, 50, 51

C
Calcium, 55, 56, 174, 185, 186, 189
Calcium-fortified fruit yogurt, 44
Capillary viscometers, 4
Carbohydrates, 83, 175, 184, 214, 264–265, 278, 284, 285, 352, 357
Carboxymethyl cellulose (CMC), 214, 277, 278, 285–287, 291, 294–296, 300, 303, 328, 332, 333, 336, 344, 349–351, 357, 358, 363, 365, 368, 371–373, 375–377, 387, 389
Carrageenans, 39, 84, 147, 174, 175, 185, 213, 214, 224, 264
Carrageenan-supplemented yogurts, 213
Carreau model, 43
Casein, 16, 37, 39, 44, 49, 51, 52, 82, 84, 88, 92, 146, 158, 169, 170, 174, 178, 185, 186, 189, 190, 206, 210, 211, 220–223, 261, 264, 266, 291, 336, 357
Caseinates, 185, 204, 209, 210
Casson model, 6, 43
Charged food polymers, 155
Chebyshev coefficients, 100, 101, 105, 106, 121, 125, 126, 128
Chebyshev harmonics, 109
Chebyshev polynomials, 98, 100
Chemical composition, 124, 210, 213
Coalescence, 21, 22, 34, 36, 86, 146, 155, 157, 172, 174, 184, 192, 263, 289, 303, 304, 343, 359, 361, 367
Colloidal calcium phosphate (CCP), 44, 46, 174, 186, 222, 266
Complex modulus, 13, 14, 52, 54, 70, 126, 183, 283, 327, 365, 366
Compliance, 18, 49–51, 71, 78, 85
Concentric cylinder geometry, 12, 67–69, 76, 78
Cone-and-plate geometry, 67, 68, 78
Cone-with-needle-tip geometry, 66, 67
Confocal imaging, 262, 276, 282, 304, 344, 350, 355, 363, 365, 368, 389
Confocal laser scanning microscopy (CLSM), 262, 282, 286–288, 355, 357–360

Contact surface–food interactions, 150, 151
Controlled shear rate tests
  parallel plates, 76
  viscosity
    function of temperature, 77, 78
    function of time, 76, 77
    series of shear rates, 76, 77
Controlled strain tests, 79, 80
Controlled-stress rheometer, 91, 211
Controlled stress tests, 78, 79
Corn starch (CS), 87, 277, 278, 349–351
Correlation analysis, 142, 143, 328, 340, 356
Creaminess, 23, 32, 52, 53, 55, 144, 145, 153, 156, 157, 175, 180, 192, 194, 211, 224, 237, 250, 252, 258, 262, 263, 265, 275, 323
Creep, 7, 16–18, 22, 49–52, 78
  compliance, 49, 71
  tests, 71, 78, 87
Creep-recovery behavior
  applying and removing force, 49
  Burger's model, 50, 51
  creep compliance, 49
  Kelvin model, 50
  Maxwell model, 50
  modification, 51, 52
  zero shear viscosity, 49
Creep-relaxation tests, 16–18
Crosslinked tapioca starch (CTS), 109, 127
Cross model, 43, 283, 289, 291, 362
Cross-Williams model, 283, 289, 362
Cupuassu (*Theobroma grandiflorum*), 209

D
Dairy lactic acid bacteria, 46
Dark chocolate shear-thinning behavior, 125
Depletion flocculation, 185, 289, 293, 295, 300, 303, 338, 359, 361, 363, 367, 368
Descriptive sensory methodology, 90
Destabilization of emulsions, 36, 37, 55
Deutsches Institut für Normung (DIN), 7
Dietary fibers, 37, 44, 48, 56, 177, 178, 217, 219, 349
Digestion, food, 23, 24, 177, 211
Direct acidification, 88
Direct physiological analysis, 253, 260
Direct strain oscillation (DSO), 103
Doughs, 47, 49
  buckwheat flour, 126
  development, 127
  samples, 106
  wheat flour, 110–114, 125, 126, 128
Droplet interfaces, 21
Ductile fat crystals, 127
Dynamic mechanical analysis (DMA), 12, 206
Dynamic viscosity, 20, 38, 54, 99, 261

E
Egg protein, 171–173, 185
Egg white foams, 106, 124, 125, 184
Einstein equation, 5, 6
Elastic Lissajous-Bowditch curves, 102–104, 111, 119, 120
Electronically-commutated motor (EC motor), 103
Electrostatic interactions, 147, 174, 191, 213, 300, 357, 361, 375
Empirical tests, 242, 256, 257
  description, 65
  flow on inclines, 65, 66
  geometric configurations, 65
  penetrometry, 66, 67
  spindle viscometry, 66, 67
Emulsion-based, 21, 167, 172, 182, 263
Emulsion droplets, 20–22, 24, 35, 36, 192, 367
Emulsions, 5, 6, 21, 22, 24, 56, 82, 84, 86, 127, 146, 152, 155–157, 171–173, 175, 176, 182–185, 191–193, 236, 260, 262, 263
  amphiphilic properties, 35
  destabilization, 36, 37, 55
  oil-in-water, 36, 46, 180, 181, 187, 367, 382
  and protein–polysaccharide networks, 35
  in semisolid food, 34
  stability, 34, 35, 323
  structures, 34
  time-dependent destabilization, 55
  water-in-oil, 36, 110
Emulsion system, 20–22, 24, 182, 183, 185, 262
Enhanced rheometer inertia correction (ERIC), 108
Exopolysaccharides (EPS), 34, 46, 178, 186–188, 192, 214–217, 266, 336, 375
Extensional flow, 64, 65

F
Falling-ball experiments, 4
Fat content, 33, 36, 43, 55, 88, 93, 118, 145, 146, 154, 155, 169, 172, 180, 203, 206, 207, 259, 260, 262–263, 265, 278, 284, 285, 331, 352

Fat globules, 37, 42, 49, 51, 114, 115, 155, 169, 187, 189, 193, 194, 209, 282, 286, 289–291, 303, 355, 358, 364, 367, 370
Fermentation, 20, 43, 48, 88, 92, 115, 127, 174, 186, 192, 204, 206–208, 210, 212, 216, 217, 220–222, 265, 266, 349
Fiber enriched yogurt, 46, 47
Fibrillar proteins, 146
Firmness, 6, 18, 32, 43, 52, 53, 90, 174, 176, 180, 190, 192, 205, 207, 209–211, 215, 216, 218–224, 232, 237, 243, 255, 258, 264, 266, 331–339, 342, 344, 375–377, 381, 387
First-order Chebyshev and Fourier coefficients, 100
Fish protein, 172, 173
Fixed time period, 74, 75
Flexible plastic layer, 85
Flocculation, 21, 22, 34, 36, 156, 167, 176, 178, 185, 191, 192, 194, 214, 264, 289, 293, 295, 300, 303, 338, 359, 361, 363, 365, 367, 368
Flow behaviors, 3–6, 8, 9, 19–21, 24, 102, 151, 212, 215, 217, 219, 237, 241, 242, 256, 283, 289–294, 338, 362, 379–381, 385, 389
  assessment, 10–12
  Herschel-Bulkley, 43
  and material's viscosity, 38
  model, 385
  Newtonian, 39, 72, 86
  non-Newtonian, 41
  observation, 54
  semisolid foods, 63
  shear rate, 71
  shear-thinning, 86
  and texture, 31, 32
  and viscosity, 53, 174
  viscous, 72
  yogurt, 43, 89, 90
Flow dynamics, 4
Flow fields, 64, 65, 67, 68, 74, 75
Fluid film, 149
Fluid foods, 8, 31, 39, 133, 180, 231, 232, 236, 237
Food consumption, 231, 239
Food digestion, 23, 24, 177
Food emulsions, 6, 21, 24, 35, 82, 175, 182
Food foams, 83, 87, 184
Food friction–texture relationships, 153
Food gels, 33, 83, 146
Food ingredients, 84, 169, 172, 276
Food microstructure, 82–83, 86, 127, 146, 155, 157, 167–169, 194, 242, 245, 249–267, 277, 365, 367
Foods, 3–25
  components, 109, 110
  instability, 86
  phase separation, 86
Food−saliva interactions, 152, 153, 239, 240
Food–saliva mixtures, 154, 238, 250
Food sensory texture attributes, 253, 254
Food structure design, 6, 22, 23, 237
Food suspensions, 6, 82, 83
Food texture, 23, 52, 55, 133, 143, 145, 181, 231–235, 237, 238, 241, 245, 253–255, 260, 275, 323, 331, 344, 350, 382
  back extrusion test, 242
  instrumental assessment, 241, 242
  sensory evaluation, 243, 244
  TPA, 243
Force-displacement curve, 243
Formal sample evaluation, 252, 326
Fourier coefficients, 100
Fourier decomposition, 99
Fourier series, 99
Frequency, 12, 14, 15, 47, 70, 80, 81, 92, 93, 97–99, 101–103, 106–109, 111, 113, 114, 124, 126, 211, 221, 239, 240, 257, 261, 280, 300
Frequency sweeps, 16, 17, 80, 81, 87, 93, 98, 257, 280, 296, 299
Friction and sensory behaviors, 145, 157
Friction behavior, 23, 135–138, 140, 141, 144–158, 238, 239, 242, 259, 263, 301, 303, 324, 344, 370, 372, 381
Friction coefficients, 19, 134–136, 138, 141–143, 145–148, 150–157, 258, 259, 263, 275, 276, 281, 283, 301–304, 327, 328, 340–344, 353, 356, 369, 370, 372, 379–383, 386
Fundamental rheological tests, 7
  concentric cylinder geometry, 68, 69
  cone-and-plate geometry, 68
  measuring geometries, 67, 68
  parallel plate geometry, 68
  properties, 67

G
Gelatin, 8, 48, 84, 147, 169, 171–173, 204, 207, 213, 224
Gelation time, 221, 222, 385, 386, 389

Gel cure, 80
Gelled foods, 11, 16, 43, 86
Gelling agents, 83, 84, 86, 171
Gel matrix, 89, 155, 193, 236, 237
Gels, 33, 34, 39, 43, 47–49, 51, 52
Geometry counterrotation, 150
Glucono-delta-lactone (GDL), 192, 212, 277, 350, 222, 278, 282, 351, 384, 385, 389
Gluten, 110, 111, 113, 114, 125, 126, 128
Gluten-free dough samples, 106, 110, 127
Glutenin, 110, 114, 126
Gluten network, 110, 113, 125
Gold standard, 251, 253
Greek-style yogurt, 207, 211–212
Greek yogurt, 11, 43, 53, 88, 89, 207
Guar gum solutions, 106, 147
Gums, 37, 83, 115, 171, 173, 174, 177, 241, 266, 276, 285, 294, 295, 328, 332, 333, 357, 361, 365, 373

H
Hagen-Poiseuille equation, 4, 6
Hard particle suspensions, 82, 83
Harmonics, 99–101, 109, 110, 112, 116, 126–128
Heat-induced interactions, 220
Heat treatment, 16, 51, 88, 188–191, 193, 204, 210–212, 220, 222, 266, 290, 296, 364
Hencky strain, 6
Herschel-Bulkley flow behavior, 42, 43
Herschel-Bulkley models, 6, 42, 43, 205, 215, 218, 219, 283, 291, 292, 362
High (hydrostatic) pressure processing (HHP), 190, 191
High temperature short time (HTST), 188
History of rheology, 3–7
Hookean solids, 7, 8
Human whole saliva (HWS), 276, 277, 279–283, 285–296, 299–304, 318, 331, 332, 337–345
  collection, 352
  flow behavior parameter, 338
  friction coefficients, 382
  friction profiles, 324
  rheological and tribological measurements, 350
  sensory attributes, 338, 341
  viscosity, 324, 363
  yogurt friction profiles, 369, 370, 372
  yogurt microstructures, 357
  yogurt viscoelastic properties, 365
Hydrocolloids, 6, 16, 20, 36, 42, 46, 115, 146, 147, 157, 174, 204, 207, 209, 212–214, 224, 276, 278, 284–287, 289, 293–295, 299–304, 323, 328, 331–334, 336, 343, 344, 351, 358, 362, 364, 365, 367–373, 375, 376, 381, 382, 387, 389
  application, 349
  depletion flocculation, 363
  food texture attributes, 350
  LBG, 357
  significant impact, 361
Hydrodynamic cavitation, 4
Hydrogen bonds, 146, 147, 190, 214, 368
Hydrophobic regions, 173, 263
Hysteresis loops, 53, 90, 91, 215

I
Inertia corrections, 107, 108
Infinite-shear viscosity, 6, 43
In-phase and out-of-phase stress response, 70
Insoluble fibers, 177–179
Instrumental analyses, 90, 133, 223, 244
Instrumental assessments, 241–244
Instrumental testing, 3, 6, 11, 23, 239, 242, 244, 250, 251, 277, 289, 324, 342, 344, 389
Interfacial stabilizers, 84
Intracycle shear-thinning behavior, 105, 118, 122

J
Johnson-Kendall-Roberts (JKR) contact theory, 143

K
κ-carrageenan, 174, 175, 214
Kelvin model, 50
Kelvin-Voigt model, 5, 50
Kinematic viscosity, 38, 74

L
Lactic acid bacteria (LAB), 46, 207, 220, 336, 349, 385, 389
Lactobacillus delbrueckii ssp. *bulgaricus*, 46, 48, 158, 168, 169, 186, 203, 349
LAOS behavior, 127
  fat levels and yogurt samples
    linear viscoelastic behavior, 115
    Lissajous curves, 119

LAOS behavior (*cont.*)
        national brand and store brand, 117
        raw stress waves, 117
        SAOS tests, 117
        3D un-normalized Lissajous-Bowditch curves, 118
    mayonnaise, 124
    tomato paste, 124
    wheat flour dough, 110–114
    yogurt (*see* Yogurts)
LAOS measurements, 102
    applications, 109, 110
    inertia corrections, 107, 108
    wall slip, 108, 109
    wheat flour dough, 111–113
    yogurt samples and fat levels, 121
Large amplitude oscillatory shear (LAOS)
    Chebyshev coefficients, 125, 126
    chemical composition, 124
    debranching, 125
    dimensionless characterization, 105, 106
    dough development, 127
    first-order viscoelastic moduli, 127
    frequency, 106, 107
    intrinsic region, 126
    Lissajous-Bowditch curves, 102, 103, 106
    measurements (*see* LAOS measurements)
    nonlinear viscoelastic behaviors, 125
    parameters, 104, 105
    pectin, 125
    strain stiffening behavior, 126
    theory
        amplitude and phase, 101
        Chebyshev polynomials, 100
        complex fluids and soft solids, 98
        critical strain value, 98
        definition, 98
        first-order Chebyshev and Fourier coefficients, 100
        Fourier coefficients, 100
        Fourier decomposition, 99
        Fourier series, 99
        intracycle stiffening/softening, 101
        intracycle stress-strain plots, 99
        linear material functions, 101
        SAOS tests, 97
        sinusoidal wave function, 99
        strain- and shear-related behavior, 101
        stress response, 99
        thickening/thinning behaviors, 101
    transition region, 126
    type I/strain thinning, 127
    type II/strain hardening, 127
    type III/weak strain overshoot, 127
    type IV/strong strain overshoot, 127
Large strain modulus, 104
Linear material functions, 101
Linear viscoelasticity, 72, 73, 126
Linear viscoelastic region (LVR), 14–16, 18, 73, 79, 80, 87, 92, 97–100, 102–105, 110, 112–116, 118, 120–122, 124–127, 266, 280, 352
    properties, 98
Lipids, 37, 56, 83, 114, 167, 176–181, 187, 194, 236, 237
Liquids, 5, 6, 12, 22, 24, 34, 39, 64, 66, 71, 79, 83, 102, 140, 155, 180, 231–234, 236, 261
Lissajous-Bowditch curves, 98, 99, 104, 110, 114, 118–120, 124, 125, 128
    elastic, 103, 111
    frequency sweep measurement, 102
    graphical descriptions and definitions, 105
    strain-controlled and stress-controlled rheometers, 102
    stress *vs.* strain plots, 103
    systematic evaluation, 106
    tomato paste, 103, 106
    viscous, 103, 111, 112
Lissajous curves, 102, 114, 116, 118, 119, 121, 123, 125
Locust bean gum (LBG), 16, 109, 147, 169, 173–175, 185, 194, 213, 277, 278, 284–288, 294, 295, 300, 301, 303, 304, 332, 333, 344, 349–351, 356–358, 361–363, 365, 368, 372, 373, 375, 376, 386, 387, 389

M
Macromolecular gels, 83, 84
Mashed potato paste, 106
Maxwellian behavior, 5
Maxwell model, 5, 50
Mayonnaise, 11, 32, 33, 36, 39, 41, 54, 55, 87, 109, 124, 126, 128, 144, 155, 167, 171, 172, 174, 176, 180, 192, 264
Measurement challenges, 82, 85, 86, 89, 90
Measurement protocol, 148–151, 156
Mechanoreceptors, 239–241
Micellar casein concentrate (MCC), 211
Microbial transglutaminase, 209
Microstructures, 5, 24, 31, 37, 44, 46, 47, 52, 63, 78, 82, 83, 86, 88, 118, 122, 127, 146, 147, 155, 157, 167–173, 175, 177–181, 186–194, 205, 209–211, 213–215, 219, 221, 222, 233, 234, 241, 242, 244, 245, 249–267, 277, 285, 287, 289, 294–296, 300, 301, 304, 343, 344,

350, 355, 357–362, 364, 365, 367, 368, 370, 372, 379, 381, 384–389
Microtubes, 282
Milkfat droplets, 180
Milk processing, 193
Milk protein concentrate (MPC), 158, 210
Minimum strain modulus, 104
Mini-Traction Machine (MTM), 138
Modulus, 13, 14, 16, 38, 47–49, 51, 52, 54, 55, 70, 73, 75, 79–81, 85, 89, 92, 97, 99, 101, 104, 108, 110, 126, 135, 139, 176, 183, 192, 205, 210, 243, 257, 261, 264, 283, 327, 365
Molten polymers, 106
Motor-transducer design, 108

N

Newtonian behavior, 8, 39–41, 76, 87
Newtonian fluids, 7–9, 41, 42, 75
Nile red dyes, 277, 282, 350, 355
Non-destructive test, 98
Nonfat dry milk (NDM), 204
Nonlinear rheology
  LAOS (*see* Large amplitude oscillatory shear (LAOS))
  SAOS (*see* Small amplitude oscillatory shear (SAOS))
Nonlinear stress *vs.* shear rate profile, 71
Nonlinear viscoelastic behaviors, 14, 73, 98, 100–103, 105, 106, 110, 112, 116, 124–128, 266, 367
Nonlinear viscoelasticity, 72, 73, 126
Non-Newtonian behavior, 89, 135, 151, 218, 293
  shear-dependency, 41–44
  time dependency, 44, 46
  yield stress, 40, 41
Non-Newtonian fluids and semisolids, 71, 72
Non-Newtonian food systems, 22
Non-sinusoidal stress response, 99, 108
Non-sinusoidal stress waveforms, 108
Nuclear magnetic resonance (NMR), 210

O

Oil-in-water (o/w) emulsions, 20, 35, 36, 46, 171, 180–183, 187, 193–194, 262, 367, 382
  destabilization, 34
Oral viscosity, 52–54, 145, 222, 239, 256, 294
Orange fibers, 48
Oscillatory measurements, 54, 92
Oscillatory shear frequency sweep test, 81
Oscillatory shear stress/strain sweep test, 80
Oscillatory shear temperature sweep test, 81
Oscillatory shear tests, 73, 80, 81, 87, 89, 93, 98, 107
Oscillatory shear time sweep test, 80, 81
Oscillatory strain, 14, 70, 108, 120
Oscillatory stress/strain tests, 73, 92
Oscillatory tests, 5, 7, 23, 78, 80, 81, 206, 280, 352
  amplitude sweeps, 14, 15
  complex modulus, 14
  complex viscosity, 13, 14
  DMA, 12
  frequency sweeps, 16, 17
  LVR range, 14
  phase angle, 13
  sinusoidal deformation, 12
  tan δ, 13
  viscoelastic moduli, 13
Osmotic pressure, 289, 294, 295, 300, 301, 359, 363, 367, 368

P

Parallel plate geometry, 67–69, 71, 78, 85, 107–109
Parameter sweeps, 65, 69, 72, 74, 82, 85, 92
Partial least square (PLS), 23, 327, 356
Pectin, 20, 37, 44, 46, 84, 86, 110, 116, 124, 125, 169, 171, 178, 179, 183, 219, 264
Penetration force, 75, 214
Penetration tests, 66, 85, 89
Penetrometry, 65–67
Phase angle, 13–15, 47, 48, 70, 81, 85, 92, 101, 107, 108, 125, 283, 300, 327, 365, 366, 371
Phase separation, 3, 20, 85, 86, 155, 172, 182, 183, 303, 364
Physical properties, 31, 210, 235, 237
Planar extensional flow, 65
Plant/vegetable oils, 180
Polydimethylsiloxane (PDMS), 139, 140, 150, 151, 280, 281, 302, 352, 353, 370
Polymer-clay suspensions, 106
Polymers, 39, 41, 44, 46, 56, 81, 106, 147, 149, 155, 177, 283, 289, 300, 331
Polyphenols, 153, 219, 324, 336
Polysaccharides, 20, 22, 34, 37, 41, 48, 49, 55–56, 82, 84, 116, 146, 147, 155, 157, 167, 169, 171, 182–184, 194, 213, 214, 218, 264, 291, 299, 331, 336, 372
  carrageenans, 174
  dietary fiber, 177, 178
  gums, 173
  starch, 175, 176

Post-acquisition corrections, 108
Potato protein and chitosan, 183
Potato starch (PS), 124, 176, 276–278, 349–351
Power law-based models, 19
Power law equation, 42
Power law model, 6, 11, 42, 362
Prandtl number, 20
Prebiotics, 157, 204, 209, 217, 224
Predictive models, 63, 94
Principal component analysis (PCA), 23, 332–334, 356, 375–377, 387–389
Process engineering, 4, 19, 20
Product stability, 20–22, 56
Protein and polysaccharide networks, 37
Protein gels, 8, 16, 92, 93, 109, 173, 259, 264, 364
Proteins, 37, 39, 42, 43, 45, 49, 52, 56, 83, 86, 88, 122, 146, 152, 153, 173, 174, 182–185, 187–190, 194, 210–213, 216, 218–221, 261, 263, 264, 266, 277, 282, 285, 288–290, 293, 294, 296, 301, 303, 324, 328, 331, 332, 336, 341, 355, 358, 359, 361, 364, 365, 367, 368, 370, 373, 375, 381, 385, 387
    casein, 169
    egg, 171
    fish, 172
    gelatin, 171
    whey, 84, 170
Pseudoplastic, 41–43, 53, 72, 76, 205, 211–213, 215, 219, 283, 289
Punch tests, 65, 66

R
Reynolds number, 5, 19
Rheological behaviors, 7, 9, 18, 20–24, 31, 33, 54, 56, 64, 85, 86, 97, 106, 110, 111, 115, 123, 124, 126, 144, 148, 149, 151, 155–156, 158, 174, 180, 190, 217, 224, 225, 232, 235, 239, 242, 249–267, 275, 289, 324, 350, 352, 361–369, 379
    creep-recovery behavior, 49, 50, 52
    viscoelasticity, 47, 48
    viscoelastic properties, 48, 49
    viscosity (*see* Viscosity)
Rheological parameters, 3, 6, 13, 19, 22, 23, 65, 74, 85, 92, 98, 205, 250, 379, 389
Rheological terms
    flow fields, 64, 65
    materials, 64
    test and geometries, 65, 67, 69
    variables, 69–71
    viscoelastic behavior, 72, 73
    viscous behavior, 71, 72
Rheological and rheology tests, 19, 22, 82, 85, 86, 97, 126, 128, 324, 340
    behaviors, 7
    controlled shear rate tests, 76–78
    controlled strain tests, 79, 80
    controlled stress tests, 78, 79
    creep-relaxation, 16, 18
    deformation, 7
    empirical, 65, 67
    flow behaviors, 8
    fluid foods, 8
    foods, 7
    fundamental, 67, 69
    measurements of torque, 7
    oscillatory (*see* Oscillatory tests)
    oscillatory shear tests, 80, 81
    rotational, 9, 10, 12
    semisolid foods, 8, 9
    two-plate model, 8
    uncontrolled parameters, 74–76
    viscoelastic profiles, 8
Rheological variables
    compliance, 71
    modulus, 70
    phase angle, 70
    strain, 69
    stress, 69
    viscosity, 70
Rheology, 205, 206, 213, 223–225, 232, 238, 261, 275, 283, 301, 324, 389
    applications, 6
    Burgers model, 5
    capillary viscometers, 4
    Casson model, 6
    description, 3
    Einstein equation, 5, 6
    flow dynamics, 4
    flow resistance and velocity, 4
    in food industry
        digestion, 23, 24
        process engineering, 19, 20
        product stability, 20–22
        structure design & sensory prediction, 22, 23
    framework, 3
    Hagen-Poiseuille equation, 4
    Hencky strain, 6
    Herschel-Bulkley model, 6
    hydrodynamic cavitation, 4

- infinite-shear viscosity, 6
- instruments, 6, 7
- Kelvin-Voigt model, 5
- Maxwellian behavior, 5
- methodology, 3
- and microstructure, 63
- parameters, 3
- research, 3, 4
- Reynolds number, 5
- shear-thinning flow behavior, 5
- Stokes' Law, 4
- theory of elasticity, 4
- viscoplastic liquids, 6
- zero-shear viscosity, 6

Rheology–texture relationships
- carbohydrate content, 264
- complexity, 267
- conceptualizing oral sensations
  - food product, 249
  - instrumental rheological measurements, 250
  - parameters, 250
  - semisolid and non-Newtonian food products, 249
  - semisolid foods, 250
  - stages, 250
- fat content, 262, 263
- flavor and aroma perception, 265
- force *vs*. time, 254
- friction tester, 259
- instrumental evaluation
  - direct physiological analysis, 260
  - empirical tests, 256, 257
  - food properties/behaviors, 253
  - fundamental methods, 257
  - imitative techniques, 253–255
  - tribological methods, 258, 260
- instruments and testing methodologies, 267
- measurement, 267
- multi-discipline collaborations, 267
- protein content, 263, 264
- rheological and sensory data, 260–262
- sensory evaluation
  - of food, 251–253
  - yogurt, 265, 266

Rheometers, 7, 15, 20, 52, 85, 91, 94, 102, 104, 107, 108, 138, 149, 150, 211, 235, 251, 259, 266, 280, 281, 352, 353

Rheopectic, 44, 45, 77, 78

Rigid interfaces, 21

Rigid structures, 85

Ropiness, 53, 89, 375

Ropy cultures, 48, 49, 188, 215

Rotational tests, 14, 16, 24
- controlled strain mode, 9
- controlled stress mode, 9
- flow behavior assessment, 10–12
- shear-dependent materials, 9, 10
- shear rate/shear stress, 9

S

Saliva, 53, 141, 148, 152–159, 211, 233, 235–240, 242, 244, 245, 250, 266, 279, 280, 285, 289, 295, 300, 303, 304, 324, 336, 341, 349–394

Scanning electron microscopy, 190, 206, 211, 219

Semisolid dairy products, 87, 91, 179, 263, 382

Semisolid food rheology, 22, 52, 54, 232
- measurement challenges, 85, 86
- microstructures, 82, 83
- texturants, 83, 84
- viscoelastic properties, 87, 88
- viscous properties, 86–87

Semisolid foods, 6, 8–10, 13–16, 19–23, 63–94, 133–159, 205, 206, 220, 224, 225, 231, 232, 241–244, 249–267, 275–277, 281, 283, 293, 294, 301, 323, 324, 331, 334, 340, 344, 349, 350, 361, 365, 367, 381, 382
- behaviors
  - rheological, 33
  - separation, 34, 35
  - slumping, 33
  - spreading, 33, 34
  - structural features, 33
  - texture attributes, 33
- bolus swallowing, 234
- chewing behavior, 235
- classification, 63
- cocoa butter, 168
- elastic/viscous behaviors, 31
- flow behaviors and texture, 31, 32
- food bolus, 235
- food microstructure, 167
- food property assessment, 235
- healthy and dysphagic adults, 234
- homogenization, 193, 194
- human physiology, 235
- indirect assessment, 235
- ingredient strategies
  - emulsions, 182
  - foams, 183, 184
- LAOS (*see* Large amplitude oscillatory shear (LAOS))

Semisolid foods (*cont.*)
  microstructure, 31, 168, 170–173, 175, 177
  oil-in-water emulsion system, 182
  oral behaviour
    consumption, 236
    effect, surface and bulk properties, 238
    emulsion gel, 236
    food structure design, 237
    food types, 236
    lipid droplets, 236
    structural and physicochemical properties, 237
    temporal attribute sensations, 237
    texture, 236
  oral processing research, 234
  processing strategies
    adjusting pH, 191
    adjusting storage time, 192
    exopolysaccharides, 186, 187
    external shear forces, 187
    homogenization parameters, 193
    HPP, 190, 191
    manipulating ionic strength, 185
    thermal treatments, 188, 189
  properties, 31
  protein/polysaccharide emulsion, 183
  rheological behaviors (*see* Rheological behaviors)
  sensory attributes, 52–54
  structural variety
    crystallization, triacylglycerols, 37, 38
    emulsions, 35–37
    protein and polysaccharide networks, 37
    stabilization, 35
  texture modification, 54–56
  viscosity, 260
  whip cream, 187
  yogurt microstructure, 189
Sensory and oral processing, 231–245
  food–saliva interactions and impacts, 240
  food texture, 231–233
  force-displacement curve, 243
  mechanoreceptors, 239, 241
  role of saliva, 238, 239
  solid and semisolid food, 233
  structural changes and texture sensation, 234
  tongue movement, 238, 239
Sensory assessments, 244
Sensory attributes, 3, 4, 6, 13, 18, 22, 23, 35, 38, 55, 90, 141, 143–146, 154, 157, 192, 194, 204, 222, 231, 237, 238, 240, 241, 244, 249–267, 276, 294, 323, 324, 327, 330, 337–342, 344, 356, 374, 375, 382, 383
  creaminess, 53
  firmness, 52, 53
  ropiness, 53
  smoothness, 54
  thickness, 54
  viscosity, 53, 54
Sensory evaluation methods, 22
Sensory panel, 52, 223, 251, 252, 257, 261, 264
Sensory testing, 22, 222, 242, 251, 252, 257, 324, 344
Sensory texture, 18, 87, 88, 156, 168, 177, 190, 194, 224, 232, 253, 257, 258, 262, 263, 265, 267, 301, 324, 332, 340, 341, 349–394
Set-style yogurt, 85, 219, 223
Set yogurt, 88, 93, 168, 214, 215, 219, 222, 224
Shared databases, 94
Shear compliance, 71
Shear-dependency, 41–44, 71, 151
Shear-dependent behaviors, 5, 9–11, 42, 43, 260, 338
Shear-dependent materials, 9, 10, 42, 71–72
Shear flow, 64, 65, 87
Shear modulus, 14, 47, 48, 70, 257
Shear rate-shear stress curve, 72
Shear strain, 8, 14, 69, 73, 100, 205, 344
Shear stress, 6, 8, 9, 11, 14, 18, 19, 22, 34, 38–41, 49, 54, 69, 71, 72, 74, 80, 90, 91, 205, 206, 250, 261, 367
Shear-thickening behaviors, 44, 45, 71, 72, 87, 101, 106, 112, 113, 122, 126
Shear thickening ratio, 105, 123
Shear-thinning, 5, 9, 41, 72, 76, 87, 103, 106, 119, 121, 125, 126, 205, 261, 283, 323
Shear-thinning behavior, 42, 44, 71, 86, 87, 102, 105, 113, 118, 122, 123, 125, 126, 192, 211, 214, 239, 261, 289, 292, 338, 343, 362, 379, 381, 385
Shear-thinning flow behavior, 5, 6, 10, 86
Shear-thinning materials, 5, 72, 90, 205, 283, 362
Single-culture strains, 220
Single-mode Giesekus model, 126
Sinusoidal deformation, 12
Sinusoidal stress response, 70, 116
Sinusoidal wave function, 99
Skim milk, 49, 51, 203, 211, 221, 223, 266, 277, 278, 350, 351
Skim milk powder (SMP), 204, 209–211, 213, 277, 278, 285, 296, 331–333, 336, 344, 350, 351, 356, 370, 373, 375, 377
Slumping, 33

Small amplitude oscillatory shear (SAOS), 73, 111, 117, 123
  applications, 126
  to LAOS, 101
  Lissajous-Bowditch curves, 102
  measurements, 97, 106, 110
  methods or fundamental, 128
  non-destructive, 98
  sinusoidal oscillatory stress responses, 116
Smoothness, 23, 52–55, 139, 144, 156, 157, 190, 193, 194, 213, 222, 224, 232, 237, 238, 240, 258, 263, 264, 266, 275, 323, 331–342, 344, 375–377, 382, 387
Sodium caseinate (NaCN), 191, 208–210, 213
Softer cheeses, 85
Soft particle suspensions, 82, 83, 86
Solid content, 55, 169, 207, 208, 278, 284, 296, 300
Solid-like behavior, 13, 16, 64, 81, 87, 90, 220, 221, 300, 379
Solids, 4, 5, 7, 8, 13, 31, 33, 34, 43, 55, 64, 69, 79, 86, 98, 125, 146, 167, 169, 203, 204, 207–212, 231–234, 249, 278, 284, 295, 296, 300
Soluble fibers, 177, 178
Soluble proteins, 83
Somogyi-Nelson assay, 281
Spindle viscometry, 65–67, 85
Spoon viscosity, 53, 54, 331–334, 338, 341, 372, 375, 377, 387
Spreading, 33, 34, 54
Stability and viscoelastic moduli values, 214
Stabilized emulsion, 35, 36, 171
Standardization of the specific rheological tests, 94
Standardized sample preparation techniques, 94
Starch, 5, 10, 16, 20, 37, 83, 84, 86–88, 109, 110, 113, 115, 124, 125, 127, 146–148, 152, 154–156, 158, 169, 171, 173, 175–177, 188, 204, 211, 213, 214, 224, 263–265, 276, 277, 281, 282, 285, 292–295, 300, 324, 331, 333, 336, 344, 349, 359, 361, 362, 364, 365, 367, 368, 370, 373, 387
Steady shear test, 89
Steric stabilization, 173, 182, 185, 191, 214
Stirred yogurt, 11, 19, 20, 53, 55, 65, 88–93, 168, 188, 192, 207, 213, 215, 222, 224, 266
Stokes' Law, 4, 5, 20, 21, 37, 39
Storage moduli values, 221
Storage modulus, 13, 38, 48, 49, 55, 70, 80, 92, 97, 99, 176, 192, 205, 210, 261, 264
Strain, 6–9, 12–18, 47, 49, 51, 69–71, 73–75, 80, 81, 87, 89, 92, 93, 97–116, 118–128, 186, 187, 206, 215, 216, 220, 231, 255, 257, 266, 280, 295, 296, 327, 328, 338, 352, 365, 367, 375, 379
  function of time, 78, 79
Strain-controlled rheometers, 102
Strain (γ) sweep, 14, 15, 18, 80, 81, 87, 102, 115, 116, 124, 257, 280, 294, 296, 338, 340, 344, 352, 366, 379, 381, 386, 387, 392
Strain rate (shear rate), 6, 69–71, 73, 99, 100, 103–107, 112, 113, 116, 118, 120–125, 128
Strain-softening, 105, 106, 112, 114, 125, 126
Strain-stiffening behavior, 105, 106, 112, 121, 122, 125, 126, 128
Strain-stiffening ratio, 105, 123
Strain sweep tests, 80, 102
Streptococcus salivarius ssp. *thermophilus* (*S. thermophilus*), 48, 158, 168, 186, 203, 208, 209, 215, 216, 221, 349
Stress, 3, 7, 9, 11–16, 18, 22, 33, 41, 43, 46, 47, 49–51, 64, 69–73, 76–81, 87, 89–93, 98, 99, 101–103, 105–107, 109, 110, 113, 114, 116–119, 122, 124, 127, 128, 149, 205, 206, 223, 231, 241, 255, 257, 266, 292, 295
Stress relaxation test, 73, 79, 80
Stress (τ) sweep, 11, 14, 15, 18, 78, 80, 81
Stress *vs.* shear rate profiles, 71
Stress *vs.* strain plots, 99, 103, 107
Stress-controlled rheometers, 102
Stress–strain behavior, 99
Stress–strain rate behavior, 99
Stress-versus-strain-rate curve, 71
Stribeck curves, 134–137, 140, 143, 275, 276, 301, 303, 344, 370
Structure, 4, 11, 15–18, 22, 24, 31, 33, 35, 44, 46, 56, 63, 66, 73, 76, 79, 82–90, 92–94, 97, 103, 106, 107, 110, 113–116, 118, 122, 125, 127, 146, 158, 167–170, 172–178, 183, 187, 188, 190, 192–194, 205–208, 210, 211, 215, 216, 218, 219, 222, 223, 225, 231, 233, 236, 242, 250, 254, 256, 261–267, 285, 286, 288, 289, 292–296, 301, 304, 323, 328, 336, 338, 341, 344, 349, 362, 367, 368, 389

Structure (*cont.*)
  dispersed phase, 41
  elastic, 51
  emulsions, 34
  fundamental shift, 45
  ice and fat crystals, 38, 56
  lipid depends, 37
  stabilization, 35
Structure–function relationships, 82, 222
Surface layer, 55, 140, 150, 152, 153, 173
Surface separation, 135, 148, 276, 301
Surfactants, 21, 84, 182, 183, 239
Suspension-based systems, 20
Syneresis, 13, 34, 52, 53, 55, 86, 204, 208, 210, 212, 213, 219, 221, 223, 224, 265, 266

T
Temperature, 10, 15, 16, 20, 33, 34, 39, 40, 43, 74–76, 78, 80, 81, 88, 92, 103, 134, 148, 158, 167, 168, 170, 171, 176, 180, 188, 189, 192, 194, 204, 215, 216, 220, 222–224, 244, 251, 262, 263, 265, 277, 278, 280–283, 289, 290, 292–296, 300, 301, 337, 338, 343, 344, 351–353, 361, 362, 364, 365, 367, 368, 381
  ramp tests, 77
  sweeps, 87
  and test duration, 140
Temporal changes, 154
Temporal dominance of sensations (TDS), 235
Textural attributes, 6, 22, 23, 31, 54, 63, 89, 94, 136, 139, 156, 157, 231, 237–241, 253–260, 275–277, 323, 325, 327–336, 338, 341, 344, 350, 353, 372, 373, 375–378, 386–389
Textural characterization, 178, 187, 231, 232, 237, 245
Textural modification, 54, 55
Texturants
  classification, 84
  gelling agents, 84
  interfacial stabilizers, 84
  thickeners, 84
Texture, 18, 22, 32, 204–206, 231–238, 241–244, 253–258, 349–394
  attributes, 33, 156–157
  ice cream emulsion controls, 36
  modification, 54–56
  perception, 39
  and physicochemical properties, 37
  and rheological behavior, 31
  sensory attributes, 52–54
  stringy, 48
Texture modification, 54
  calcium, 55
  fat content, 55
  polysaccharides, 55
  solid content, 55
  storage time, 55
Texture perception, 39, 233, 235, 237, 241, 244, 245, 258, 276, 277, 281, 324, 344, 350
Texture profile analysis (TPA), 219, 235, 243, 254, 255
Texturizers, 6, 20, 82, 84
Theory of elasticity, 4
Thermal treatments, 35, 188, 189
Thickeners, 20, 84, 86, 87
Thickness, 23, 52–56, 85, 90, 109, 143, 188, 210, 213, 224, 237, 238, 241, 242, 250, 252, 256, 258, 260, 261, 265, 266, 275, 294, 301, 323, 334
Third-order harmonics, 112, 126–128
Thixotropic fluid behavior, 44, 45
Thixotropy, 11, 12, 19, 44–46, 76–78, 90, 91, 107, 124, 125, 188, 215, 217
Three-dimensional un-normalized Lissajous-Bowditch curves, 116, 118
Time-dependency, 14, 44, 46, 90
Tomato paste, 41, 87, 103–106, 109, 124, 126, 128, 256
Tomato salad dressing viscosity, 39, 40
Treated milk protein concentrate powder (TMPC), 212
Triacylglycerols, 36–38
Tribology, 23, 206, 223, 224, 232, 238, 242, 253, 258, 259, 261, 275, 283, 302, 323, 344, 388, 389
  acid milk gels, 159
  attributes, 144
  ball-on-plate testing setup, 139
  factors impacting friction, 137, 138
  food friction behavior, 136
  formulation
    boundary and mixed behavior, 145
    bound fat droplets, 146
    fat deposition, 146
    fat-related friction behaviors, 145
    fat-related sensory behaviors, 145
    fibrillar proteins, 146
    food friction behaviors, 145
    food microstructures, 146
    high solid fat content, 146
    lubricating properties, 145
    polysaccharides, 146

    proteins, 146
    sensory attributes, 145
    solutions and emulsion-filled gels, 146
  friction behaviors, 144
  friction, lubrication and wear behaviors, 133
  lubricated sliding
    friction coefficient, 134
    stribeck curve, 134–136
  measurement
    data analysis, 141, 143
    parameters, 140, 141
    protocol, 148, 150
    testing geometry, 138
    testing surfaces, 139, 140
  relationships
    to rheological behaviors, 155
    to structural features, 154, 155
    to texture attributes, 156
  saliva, 152, 154
  sample stick-slip behaviors, 142
  screening procedure, 144
  sliding countersurfaces, 134
  Stribeck curve, 135, 137
  viscosity behaviors, 143
  viscosity profile, 151
  yogurt, 157, 158
Tribometry, 133, 158, 242, 275, 277, 280, 281, 301, 327, 341, 344, 349, 350, 352, 353, 372
Triglycerides, 167, 168, 179
Type I nonlinearity, 124
Type III nonlinearity, 124

U

Ultra-high temperature (UHT), 188
Uniaxial extensional flow, 65
Universal Dynamic Spectrometer, 211
U.S. Food and Drug Administration Code of Federal Regulations, 203

V

Viscoelastic behaviors, 5, 8, 9, 12–14, 16, 18, 24, 47, 50, 51, 64, 72, 81, 82, 87, 89, 98, 103, 110, 152, 153, 158, 218, 294–301, 352, 365–368, 379, 389
  linear viscoelasticity, 73
  nonlinear viscoelasticity, 73
  viscoelasticity, 48
Viscoelastic fluid, 7, 8, 13, 103, 296
Viscoelastic food materials, 6
Viscoelasticity, 21, 47, 48, 69, 72, 89, 126, 152, 214, 232
Viscoelastic liquids, 5, 102
Viscoelastic materials, 8, 47, 79, 103, 109, 125, 126, 206
Viscoelastic moduli, 13, 15, 16, 47, 48, 55, 92, 109, 114, 127, 156, 213, 214, 217, 219, 224, 256, 257, 276, 296, 300, 304, 368, 381
Viscoelastic properties, 5, 47, 83, 87–88, 92–93, 97, 98, 211, 213, 241, 280, 295, 300, 301, 303, 304, 323, 338, 365, 381, 386
  dietary fibers, 48
  formula/physical treatments, 48
  yogurts, 48, 49
Viscoelastic solid, 7, 8, 13, 16, 83, 101–103, 172, 295, 296
Viscometers, 4, 7, 54, 66, 67, 75, 76, 89, 212
Viscoplastic liquids, 6
Viscosity, 4–14, 19, 20, 22, 24, 31, 33, 34, 36, 45, 49, 51, 52, 55, 56, 66–68, 72, 74, 84–86, 88, 90, 99, 104, 105, 107, 121, 128, 135–138, 140, 143, 145, 149, 150, 152, 153, 155–158, 173, 174, 176, 177, 180, 183–185, 188, 190, 192, 193, 205, 207, 209–214, 216–219, 221–224, 232, 238, 239, 241, 242, 249, 256–257, 260–266, 275, 276, 280, 283, 289–295, 300, 303, 304, 323, 324, 326, 327, 331–334, 337, 338, 340–342, 344, 352, 355–357, 361–365, 367, 372, 375–377, 379, 381, 382, 385, 387
  apparent, 38, 39, 89
  bulk, 38
  complex modulus, 183
  definition, 70
  dynamic, 38
  function of
    rotation speed at constant temperature, 75
    temperature, 77, 78
    temperature at constant rotation speed, 76
    time, 76, 77
    time constant rotation speed, 75
  kinematic, 38
  measurements, 38
  Newtonian behavior, 39–41
  non-Newtonian behavior
    shear-dependency, 41–44
    time dependency, 44, 46
    yield stress, 40, 41

Viscosity (*cont.*)
  oil and mobility, 34
  oral, 53, 54
  profile, 151
  reversible/irreversible, 39
  series of shear rates, 76, 77
  series of stresses, 78, 79
  spoon, 53
  vs. strain rate, 70, 71
  tomato salad dressing, 39, 40
Viscous behavior, 5, 8, 13, 15, 31, 47, 48, 86, 87, 90, 101, 107, 111
  Newtonian fluids, 71
  non-Newtonian fluids and semisolids, 71, 72

W

Wall slip, 68, 100, 108, 109, 116, 123, 126
Washington State University and the University of Idaho School of Food Science, 325
Water, 4, 8, 33–37, 41, 42, 56, 82, 83, 86–88, 109, 110, 113, 146, 147, 152, 167, 172, 176–182, 184, 190, 194, 205, 206, 210, 212, 214, 263, 264, 278, 279, 282, 285, 287–289, 301, 303, 304, 327, 331, 351, 352, 355, 357–361, 370
Water-in-oil emulsions, 36, 110, 180
Waxy rice starch gels, 124
Wheat flour dough, 110–114, 125, 126, 128
Whey protein, 5, 8, 16, 17, 39, 42, 43, 49, 51, 52, 55, 84, 146, 153–155, 157, 169–171, 183–185, 189–191, 210–212, 220, 221, 224, 261, 263, 264, 266, 276, 290, 294, 296, 299, 324, 332, 336, 364, 387
Whey protein concentrates (WPCs), 43, 49, 157, 169, 170, 204, 208–212, 215
Whey protein isolate (WPI), 8, 17, 51, 139, 170, 204, 208, 211, 213, 263, 277, 278, 284, 285, 289–292, 294–296, 300, 301, 303, 304, 328, 331–333, 336, 343, 344, 350, 351, 356–358, 364, 368, 370, 371, 373, 375, 377, 382, 387

X

Xanthan gum, 55, 100, 103, 110, 124, 125, 127, 147, 169, 173, 174, 183–185, 188, 204, 213, 214, 224

Y

Yield point, 6, 9, 11, 15, 16, 21, 236
Yield stress, 6, 9–11, 15, 31, 33, 40–44, 46, 53, 55, 71, 72, 87, 90, 91, 151, 158, 174, 176, 205, 206, 210, 211, 215, 218, 220, 223, 261, 266, 283, 292, 356, 362, 364, 365
Yogurt rheology, 88–91, 205–206, 210, 212, 216, 217, 224, 266, 349–394
  viscoelastic properties, 92, 93
Yogurts, 63, 65, 83, 86, 87
  CLSM results, 358–360
  confocal imaging, 355
  correlations
    flow parameters and textural behaviors, 381
    frictional and textural behaviors, 382, 383
    textural attributes, 377
    viscoelastic and flow behaviors, 378, 379
    viscoelastic and textural behaviors, 381
  data analyses, 355, 356
  food tribological behaviors, 350
  formulation effects, 356, 357
  frequency sweep results, 369, 394
  friction profiles, 369, 370, 372
  HWS collection, 352
  hydrocolloids, 349
  materials, 350
  measurement challenges, 89, 90
  microstructures, 357
  PCA, 375, 376
  PDMS, 352
  preparation, 351
  proximate analyses, 351
  rheometry, 352
  samples and fat levels
    elastic and viscous Lissajous-Bowditchcurves, 123
    elliptical trajectories, 118
    linear viscoelastic behavior, 114
    Lissajous curves, 118
    national brand, 114–116, 121
    nonlinearities, 120
    raw stress waves, 116
    SAOS tests, 116
    stess–strain rate projection, 116
    store brand, 114–116, 122, 123
    stress response, 116
    structural changes of materials, 116
    3D un-normalized Lissajous-Bowditch curves, 116

- semisolid food, 349
- sensory analysis, 349
- shear rate sweep results, 386, 390
- strain sweep results, 387, 392
- structural features, 88
- textural evaluation, 353, 355
- texture attributes, 349, 372, 373, 375
- tribological profiles, 394
- tribological results, 371
- tribology, 388
- tribometry, 353
- types, 88
- viscoelastic behaviors
  - fluids, 367
  - frequency sweep results, 368
  - frictional properties, 370
  - molecular structure, 368
  - oil-in-water emulsion, 367
  - semisolid food microstructures, 367
  - strain sweep, 366
  - tan δ values, 368
  - temperature, 365
  - thermodynamics, 367
- viscoelastic properties, 92, 93
- viscosity behaviors
  - HWS, 362, 363
  - hydrocolloids, 361
  - intermolecular bonds, 364
  - microstructure of, 361
  - non-Newtonian models, 361
  - osmotic pressure, 363
  - power law model, 362
  - semisolid food microstructures, 365
  - shear-thinning behavior, 362
  - sources of variations, 360
  - starch-based custards, 365
  - temperature, 361
  - WPI, 364
- viscous properties, 90, 91

Yogurt styles
- base processing, 220, 221
- cream-top, 207
- cup-set yogurt, 206
- custard, 207
- definition, 203
- drinkable, 207
- EPS, 214–216
- fermentation, 221, 222
- food science literature, 204
- frozen, 208
- fruits, vegetables/herbs, 217
- functional ingredients, 217, 218, 220
- Greek, 207
- health benefits, 204
- hydrocolloids, 212–214
- Icelandic, 207
- improvement, 204
- manufacturers and food scientists, 204
- non- and low-fat, 204
- opportunities, 224
- optional additional dairy ingredients, 209, 211, 212
- popularity of, 204
- probiotic bacteria, 208
- research-based recommendations, 204
- rheological properties, 205, 206
- storage, handling and sensory evaluation, 223, 224
- sundae, 207
- swiss, 207
- use of milk, 208, 209
- whipped, 207
- whole milk yogurt, 203

Young's modulus, 47, 48, 135, 257

Z

Zero-shear viscosity, 6, 10, 11, 22, 43, 49, 151, 289, 344, 385